Impact and fatigue properties of natural fibre composites.

Shahzad, Asim

Impact and Fatigue Properties of Natural Fibre Composites

Asim Shahzad

Submitted to the University of Wales in fulfilment of the requirements for the Degree of PhD

Swansea University
Prifysgol Abertawe

2009

ProQuest LLC.
789 East Eisenhower Parkway
P.O. Box 1346
Ann Arbor, MI 48106 – 1346

ABSTRACT

Low velocity impact and fatigue properties of hemp fibre reinforced polyester composites have been studied. The specific tensile properties and impact damage tolerance of hemp fibre composites were found to be very low compared to CSM glass fibre composites. However hybridisation of hemp with glass fibres even at low concentrations improved their tensile and impact properties considerably.

Despite having poorer absolute fatigue strength, hemp fibre composites exhibited better fatigue sensitivity than CSM glass fibre composites in tension-tension fatigue. This correlated well with the lower stiffness degradation observed during fatigue of hemp fibre composites than glass fibre composites at the same normalised stress level. Also, images taken during fatigue loading showed that hemp fibre composites were better at resisting crack formation and growth than glass fibre composites.

Alkalisation pre-treatment of hemp fibres at low concentrations of 1% and 5% NaOH solution resulted in improvements in tensile and fatigue properties of composites made from these fibres but no such improvements were observed for 10% alkalised fibre composites. The improvements were attributed to improvement in fibre/matrix bonding following this treatment which was also confirmed by SEM images. No improvement in impact damage tolerance was observed for any of these three alkalised fibre composites.

Immersion of undamaged and impact damaged hemp fibre composites in water produced a degradation in tensile properties, particularly stiffness, and made them more ductile and susceptible to failure by shear. Most degradation occurred within the first 100 hours of immersion and longer immersion in water for up to 400 hours did not result in any further degradation, although there was some evidence of further reduction in strength over much longer periods. However, there was no deterioration in fatigue strength and fatigue sensitivity of hemp fibre composites following immersion in water, reinforcing the good fatigue properties of these composites.

DECLARATION

This work has not previously been accepted in substance for any degree and is not being concurrently submitted in candidature for any degree.

Signed .

Date.....11/09/2009.....

STATEMENT 1

This thesis is the result of my own investigations, except where otherwise stated. Where correction services have been used, the extent and nature of the correction is clearly marked in footnotes. Other sources are acknowledged by footnotes giving explicit references. A bibliography is appended.

Signed

Date.....11/09/2009.....

STATEMENT 2

I hereby give consent for my thesis, if accepted, to be available for photocopying and for inter-library loan, and for the title and summary to be made available to outside organisations.

Signed

Date.....11/09/2009.....

ACKNOWLEDGEMENTS

I would like to start off by expressing my deep gratitude to my supervisor, Dr. D.H. Isaac, for his constant guidance, technical expertise and support throughout this research.

Thanks are also due to Dr. C. Arnold for valuable advice whenever it was required and to P. Davies for helping with microscopic work.

Last, but not least, I am indebted to my beloved wife Sumiata for her patience and selfless support, and my three lovely daughters, Nabeeha, Yumna and Aleena, who were always there to cheer me up after a hard day at work.

CONTENTS

1. INTRODUCTION

Global warming, environmental pollution, greenhouse gases, sustainability, recycling – these are all vital issues of our modern age which have gained increasing importance in the last decade or so. Read any newspaper on any given day and there is expected to be some reference to these issues in one way or the other. The award of the 2007 Nobel Peace Prize to the Intergovernmental Panel on Climate Change (IPCC) and the American politician A.A. Al Gore "for their efforts to build up and disseminate greater knowledge about man-made climate change, and to lay the foundations for the measures that are needed to counteract such change" underlines the importance these issues have acquired in this age. As the Nobel Peace Prize citation correctly stated, whereas in the 1980s global warming seemed to be merely an interesting hypothesis, the 1990s produced firmer evidence in its support. In the last few years, the connections have become even clearer and the consequences still more apparent. Indeed these issues have become so important that they form an integral component of manifestos of political parties (both Labour and Conservative in UK).

The much publicised Stern Report [1] in 2006 put the issue in perspective by concluding that the concentration of greenhouse gases could reach double its pre-industrial level as early as 2035, virtually committing us to a global average temperature rise of 2°C. It estimated that the overall costs and risks of climate change will be equivalent to losing at least 5% of global GDP each year. One of the remedial measures it suggested was that the support for energy Research and Development should at least double, and support for the deployment of new low-cost technologies should increase up to five fold.

According to The King Review of Low Carbon Cars [2], in 2000, cars and vans accounted for 7% of global carbon dioxide emissions. Under a business-as-usual scenario, global road transport emissions are projected to double by 2050.

The invention of polymers in early 20th century laid the foundation of a revolution in materials. This revolution had an inherent drawback with respect to the environment because of poor biodegradability of these materials. This meant that disposal of this material put extra burden on already dwindling landfill resources in most countries. The annual global disposal of millions of tonnes of plastics, especially from packaging, has raised the demands for looking for new means of managing this non-biodegradable waste. The perfect example of this is the polyethylene shopping bag. In developing countries like Pakistan, which lack the basic infrastructure for proper disposal of these materials, these bags have become a nuisance and a major source of pollution in cities and even in villages.

These environmental issues have resulted in considerable interest in the development of new composite materials based on biodegradable resources, such as natural fibres, as low-cost and environment-friendly alternative for synthetic fibres. Hemp, sisal and flax are some examples of the natural fibres being used in composite materials. Synthetic polymers have been conventionally used as matrices in composite materials which are not eco-friendly. Now new matrix materials are also being developed, based on natural and renewable resources, for the development of 'green' biocomposites. Polyactic acid, soy oil, and lignophenolic resins are some examples of such biodegradable matrix materials.

Making chemical products and new material from renewable and biodegradable resources in not a new idea [3]. Most of the chemical products and materials were made from renewable resources until the early part of the 20th century. The tremendous success and growth of the petrochemical industry in the 20th century slowed the growth of bio-based products. Increase in environmental awareness over the last couple of decades has resulted in a renewed interest in natural materials, and issues such as sustainability, recyclability and environmental safety are becoming increasingly important. This has necessitated the introduction of new materials and products based on natural materials. It is estimated that about two-thirds of $1.5 trillion world chemical industry can be based on renewable resources [3]. Environmental legislation and consumer pressure are forcing manufacturers of materials and end-products to consider the environmental effects of their products at all stages of their life cycle. This has resulted in a 'cradle-to-grave' approach, which encompasses recycling and ultimate disposal in the production process [4].

A directive by the European Union (2000/53/EC) has stipulated that by 2015 vehicles must be made of 95% recyclable materials, of which 85% can be recovered through reuse or mechanical recycling and 10% through energy recovery or thermal recycling.

All member states are required to transpose the directive into national laws by April 2012. According to the Environment Agency, around 2 million vehicles reach the end of their lives in the UK each year. Currently between 74-80% of the weight of a typical end-of-life vehicle is re-used or re-cycled. The directive aims to reduce the amount of waste from vehicles and includes requirements for member states to introduce strict standards for the treatment of the end-of-life vehicles at authorised treatment facilities [5]. The directive is of particular concern to composite materials [6] since economically feasible recycling and re-use of these materials is relatively difficult to achieve. Hence it is vitally important to develop new environment friendly and easily recyclable materials.

As a consequence, the use of natural fibre composites in automotives has increased in the last two decades. Interior automobile parts (headrests, seat backs, armrests, door panels, front and rear panels, trunk liners, headliners, etc.) are the primary market for natural fibre composites, which are expected to continue rapid market penetration. In 2000, the European car industry used 28,300 tons of natural fibres of which flax made up 20000 tons, jute 3700 tons and hemp fibre 3500 tons [7]. According to the Business Communications report, the global market for natural fibre composites is growing at 9.9% per year [8].

In automotive parts, natural fibre-composites can reduce the energy needed for production by 80%. DaimlerChrysler have introduced flax fibre reinforced polyester composites in engine and drive train covers of buses and Mercedes passenger cars. They are also using sisal fibre in the production of various car components. Interior parts from natural fibre-polypropylene and exterior parts from natural fibre-polyester resin are being made. About 30 different natural fibre reinforced materials are being currently used in the vehicle interior of Mercedes-Benz C-Class model [9]. The Toyota Motors have made a commercial vehicle with door trim panels made of kenaf-PP composite and a cover for a spare tyre made of kenaf-PLLA composite. Araco Corporation, Japan, has made an electrical vehicle with a body totally made of natural fibre-based composite (kenaf fibre plus lignin based matrix extracted from kenaf) [10].

Further applications are becoming evident in the building and construction industry and beyond. It has been estimated that construction and post-construction activities consume 50% of all material resources globally and 70% of global timber products. In addition 45% of all energy generated is used to heat, ventilate and light buildings and 40% of water is used for sanitation and other uses in buildings. The current population increase rate of 73 million per year worldwide will obviously place higher demands on the consumption of raw and natural materials. So there is greater need to turn to renewable, sustainable and recyclable materials for use in the construction industry.

In the US, Canada and Australia, wood fibre based composite materials have been developed for use in construction industry for some time. The Council for Scientific and Industrial Research (CSIR), South Africa, is investigating the applications of these composites in construction, with the aim of producing construction materials that are less harmful, recyclable and made mainly from renewable materials (www.csir.co.za). Significantly their studies have confirmed that natural fibre composites fall within the targeted mechanical properties range for tensile strength, flexural strength, and impact strength for load-bearing elements in buildings.

The developing countries are also not lagging behind in this field. In India and South America, jute and sugar cane fibres are used in low cost housing. In India, composites made from jute and sisal fibres are being explored for their potential use as panels, doors, roofing sheets, and shuttering [11]. In China husk based composites have recently been developed for planking. Projects for manufacturing natural fibre composites are already underway in countries like India, Guatemala, Vietnam, Brazil, Sri Lanka, and Madagascar. Spider silk has recently emerged as an important material to be used as fibre because of its very high strength and toughness [12]. Novel nano-composites are being made by combining organic biopolymers and nanoscopic inorganic particles on a molecular scale. The new nano-composites offer new opportunities in advanced biomedical applications since they are biodegradable and biocompatible. All these exciting developments point to a promising future of natural fibre composites.

Food and Agriculture Organisation (FAO) of the United Nations has identified natural fibre composites as a vital source of achieving sustainability in rural areas in developing countries in its comprehensive report "Applications of Natural Fibre Composites in the

Development of Rural Societies" [13] . The report identifies the following applications of natural fibre composites for development in developing countries: roofing panels, fluid containers, constructive bridge parts, and small boats. The fact that most developing countries still strongly depend on their rural sector, which supplies the raw materials for natural fibre composites, gives a good link to transfer the technology, the so-called natural fibre link. The link is strongest when making natural fibre composites part of the rural industry. A sustainable development approach is pursued, meaning that after the introduction of the technology, the receiving country is capable of independent further development.

FAO has also designated 2009 as the International Year of Natural Fibres (www.naturalfibres2009.org). The objectives have been listed as raising awareness and stimulating demand for natural fibres, promoting the efficiency and sustainability of the natural fibres industries, encouraging appropriate policy responses from governments to the problems faced by natural fibre industries and fostering an effective and enduring international partnership among the various natural fibres industries.

However all this development brings its own challenges. The economic success of these materials is not obvious at present. Factors such as land fill tax, agricultural land use and high costs of recycling make the economic viability of these materials much more complex. Consumer demand is not yet sufficient to drive market forces. The energy involved in harvesting and treating the fibres should not be more detrimental to the environment than the glass processing or the waste disposal. Using a non-recyclable thermosetting matrix may also nullify the advantages of using natural fibres. Then there are the critical issues of fire/matrix interfacial adhesion, reduction of moisture absorption, reduction of undesirable odours during processing, fire and creep resistance, durability, and inconsistent mechanical properties of natural fibre composites.

Taking all factors into account, the evidence points towards a promising future of these materials, and hence the need of ample investment and research to explore their potential to replace conventional materials. This project is also a step in this direction.

1.1 AIMS OF THE PROJECT

The aims of this project are to address some of the issues of hemp fibre reinforced polyester composites by carrying out a series of mechanical tests, particularly a study of the performance following impact, i.e., assessing the residual properties including tensile and fatigue characterisation. Similar testing of CSM glass fibre composites will also be done and the results will be compared. The effects of hybridisation of hemp fibres with glass fibres on their mechanical properties will be studied. The study also aims to assess the impact of various pre-treatments of fibres prior to incorporation in the matrix to improve fibre-matrix bonding. Additionally, it aims to consider the effects of environmental conditions such as water immersion, UV radiation, etc, on the performance of hemp fibre reinforced polyester composites.

2. LITERATURE REVIEW

2.1 COMPOSITE MATERIALS

There are a number of possible definitions of composite materials but, broadly speaking, a composite material can be defined as "a heterogeneous mixture of two or more homogenous phases which have been bonded together" [14]. In order to qualify as a composite material, the constituent phases should be present in reasonable proportions, they should have different properties from each other and from the resultant material, and they should be intimately mixed and combined to give the resultant composite material [15].

Like many other scientific inventions, man has learnt from Mother Nature how to use the synergistic effects of two or more constituent materials to increase the strength and stiffness of the resultant material. Many natural materials designed for load-bearing are composites in structure, wood and bone being the best examples. Wood is made up of fibrous chains of cellulose molecules in a lignin matrix, while bones are essentially composed of hard inorganic crystals in a matrix of tough organic constituent called collagen. Typical tensile strengths and tensile modulus values of wood and bone are 100 and 140 MPa, and 14 and 28 GPa respectively [16].

All materials, in general, are at their strongest when in fibre form compared to bulk form. This is because the defects found in the bulk material are reduced to virtually zero in the fibre form because of the small cross sectional dimensions of the fibre. For example, carbon in monolithic form has elastic modulus of 10 GPa and flexural strength of 20 MPa. But in fibrous form the same material has elastic modulus of 290 GPa and tensile strength of 3100 MPa [15]. This increased strength of fibres can be utilized by stacking them together in some way. For maximum utilization, a matrix for embedding these strong fibres is required to provide a strong and stiff material for engineering purposes. The properties of the matrix should complement the properties of fibres. The matrix serves to bind the fibres together, transfer loads to the fibres, and protect them

against environmental attack. The resulting composite material combines very strong and stiff fibres within a matrix to form a material of much greater strength, stiffness and toughness than the fibres and the matrix acting alone. The fibres are also termed as the reinforcement in the composite material.

2.1.1 A Brief History of Composite Materials

Composite materials have been is use since pre-historic times. The oldest reference is found in the Bible, Book of Exodus, about difficulty of making bricks without straw. In the beginning of the 20th century, the invention of polymers was the catalyst for the development of composite materials. It was soon realised that polymers could be used efficiently as matrices for composite materials. The first such composites were phenolic resin reinforced with asbestos fibres. The invention of fibreglass (glass fibre reinforced polyester composites) resulted in a big surge in the use of these materials in various applications. The first fibreglass boat was made in 1942. By this time reinforced plastics were also being used in aircraft and electrical components. The first boron and high strength carbon fibres were introduced in early 1960s and were soon used in high-performance applications in aircraft components. Metal matrix composites were introduced in 1970. Dupont developed aramid fibres (Kavlar®) in 1973. By late 1970s, composites were being widely used in aircraft, automotive, sports, and biomedical industries. In 1980 a complete composite bicycle was made. The 1980s saw a significant increase in high modulus fibre utilisation in composites (new metal-matrix, ceramic-matrix, carbon-carbon composites) for high temperature applications. In 1990s increasing concerns about the environmental pollution shifted the focus to biodegradable composites made of natural fibre reinforced by either synthetic or natural biodegradable matrix. Concurrently, more high performance composite materials were developed which found applications in micro-light (man-powered) aircraft, Formula 1 car chassis, un-stayed masts, racing sails, vaulting poles, squash and tennis rackets, fishing rods, golf clubs, helicopter rotor blades, commercial and military aircrafts, and light weight construction in civil engineering [17]. According to one estimate [17], the proportion of weight of composite materials in the airframe of large international airliners was about to pass the 50% mark in 2008.

The largest static composite structures are bridges which are made of decking material composed of fibreglass [18]. In 2008 a full-size locomotive pulling 26 heavy axle load

coal cars crossed the first composite railroad bridge in the world, produced by HC Bridge Company, USA [19].

Among big mobile composite structures is the B-2 stealth bomber which is made of graphite-epoxy composite. The gradual replacement of metals by composite materials is best epitomised in the world's largest aeroplane Airbus A380, "the most spacious and efficient airliner ever conceived" [20]. A twin-deck airliner with 555 seat capacity, A-380 made its first flight in April 2005 and is now operating successfully. Composite materials make up 25% of the A380's airframe by weight. The reduced weight by using composites means that the plane burns 17% less fuel per seat and operating costs are 15% lower per passenger than today's largest aircraft. Carbon-fibre reinforced plastic, glass-fibre reinforced plastic and quartz-fibre reinforced plastic are used extensively in wings, fuselage sections, tail surfaces and doors. It is the first commercial airliner with a central wing box made of carbon fibre reinforced plastic, and it is the first to have a wing cross-section that is smoothly contoured.

Within the last 50 years, there has been a rapid increase in the production and use of composites. There are now numerous applications where composite materials have replaced traditional materials, mostly in automotive, aerospace, marine, and process applications. The total worldwide usage of polymer composites is over 8 million tonnes per annum, while their market value is between 10 and 15 billion pounds and the market is growing at a rate of 5-10% per annum [21]. Predictions suggest that the demand for composites will continue to increase with metal, ceramic and natural materials based composites making a more significant contribution.

2.2 CONSTITUENTS OF COMPOSITE MATERIALS

Composites consist of one or more discontinuous phases embedded in a continuous phase. The discontinuous phase is usually harder and stronger than the continuous phase and is called the reinforcement, whereas the continuous phase is termed the matrix. In addition, composite materials also have a third phase on a microscopic scale, called the interface or interphase.

Properties of composites are strongly influenced by the properties of the constituents, their concentration and the interaction between them. Concentration of the constituents is usually measured in terms of volume or weight fraction. The contribution of a

constituent to the overall properties of the composite is determined by this parameter. It is generally regarded as the single most important parameter influencing the composite properties [22]. It is also an easily controllable manufacturing variable used to alter the properties of the composite.

2.2.1 Reinforcements

The role of the reinforcement in a composite material is fundamentally one of providing the main strength and stiffness to the composite material. A wide range of reinforcements, mostly in the form of fibres, is now available commercially. A high fibre aspect ratio (length/diameter) permits very effective transfer of load via matrix to the fibres, thus making fibres a very effective and attractive reinforcement material. All of the different fibres used in composites have different properties and so affect the properties of the composite in different ways. Other forms of reinforcements used in composites are particles, whiskers and flakes. All reinforcements have high strength and stiffness and relatively low density.

Glass, carbon and aramid fibres are the principal reinforcements used in polymer matrix composites. The most important reinforcement fibre is E-glass fibre because of its low cost. Carbon, graphite and aramid fibres are exceptional because of their high stiffness. Ceramic fibres, whiskers and particles are used to reinforce metal and ceramic matrices. Natural fibres are now being increasingly used in composites. The orientation of the reinforcement affects the isotropy of the composite. Equi-axed, uniformly dispersed particles or randomly oriented short fibres make isotropic composites whose properties are independent of the direction. The hemp fibres used in this research were in the form of non-woven randomly oriented mat, and hence the composites made from them were expected to have isotropic properties. Using continuous fibres in composites generally result in anisotropic material whose properties vary in different direction within the material, but they are optimum in the fibre direction. Anisotropy is also one of the main advantages of using composite materials since the direction of the fibres in the composite can be tailored to coincide with the loading direction.

2.2.2 Matrices

The matrix comprises approximately 30% to 40% of the composite and fulfils a variety of functions in addition to simply maintaining the shape of the composite and aligning the reinforcements [23]. These functions are:

- The matrix binds the composite constituents; therefore the thermal behaviour of the composite is generally determined by its thermo mechanical stability.
- The matrix protects the reinforcements, typically rigid and brittle, from premature wear such as abrasion and environmental attack.
- More importantly, the matrix distributes the applied load and acts as stress transfer medium so that when an individual fibre fails, the composite does not lose its load-carrying capability.
- For compressive loading, the matrix also plays a critical role in preventing the fibres from buckling.
- Durability, interlaminar toughness, and shear, compressive, and transverse strengths are also provided by the matrix.

Matrices may be polymers, metals or ceramics. The choice of matrix is related to the required properties and intended applications of the composite and the method of manufacture. Physical and chemical characteristics of the matrix such as melting or curing temperature, viscosity, and reactivity with fibres influence the choice of the fabrication process.

2.2.2.1 Polymer matrices

Polymers matrices are the most widely used matrix material for fibre composites. Their main advantages are low cost, easy processibility, good chemical resistance, and low specific gravity. Their disadvantages are low strength, low modulus, low operating temperatures, and degradation by prolonged exposure to UV light and some solvents.

Polymers are composed of long chain-like molecules consisting of many simple repeating units. Synthetic polymers used for making composites are generally called

resins. Polymers can be classified into two types, thermoplastics and thermosets, according to the effect of heat on their properties.

Thermosets:

Thermosets have cross-linked or network structures with covalent bonds between all molecules. They do not melt but decompose on heating. Once solidified by cross-linking (curing) process, they can not be reshaped. Thermoset resins fulfil most of the functions detailed in the start of this Section and it is not surprising that the first commercial composites were based on unsaturated polyester resins, a thermoset. However, they have many disadvantages as well, including a relatively low resistance to elevated temperatures, poor toughness, and the inability to undergo large-scale plastic deformation. Thermosets typically have specific gravity of 1.1-1.46, a tensile strength of up to 100 MPa, and a tensile modulus of 2-4 GPa [23]. Over three quarters of all matrices used in polymer matrix composites are thermosets.

Thermosets are formed from a chemical reaction in situ, where the resin and hardener or resin and catalyst are mixed and then undergo a non-reversible chemical reaction to form a hard, infusible product. Chemical cross-links between polymer chains are formed during the curing process, contributing to rigidity, high strength, solvent resistance, and good oxidative and thermal stability. Important examples of thermosets include epoxies, unsaturated polyesters, and phenolics.

Unsaturated Polyester Resin:

In this research unsaturated polyester resin was used as matrix. First developed in 1942, it is the most widely used thermoset resin because it is easy to use (low viscosity), cures at room temperature, has good mechanical properties as a composite constituent, is resistant to chemical attack, and is relatively cheap. It has good dimensional stability and is relatively easy to handle. Its main disadvantages are poor impact and hot/wet mechanical properties, limited shelf life, emission of styrene, flammability, and relatively high shrinkage during curing.

It is used in basic hand lay-up manufacture to complex mechanised moulding processes. It is manufactured by reacting together dihydric alcohols (glycols) and dibasic organic acids, either or both of which contain a double-bonded pair of carbon atoms. By elimination of water between acids and glycols, ester linkages are formed, producing a

long chain molecule comprising alternate acid and glycol units. Processing will largely determine the length of the polymer chain. Other influential factors are monomer content and filler addition.

In polyesters, the curing process is started by using organic peroxides as catalysts which initiate a free radical copolymerisation reaction. The free radicals are provided by the peroxide catalyst as it decomposes and it is the rate at which these free radicals are produced which governs the gel and cure times of the resin. Polyester resin begins to cure as soon as the catalyst has been added. The reaction is exothermic and the heat evolved can raise the temperature to above 150°C very quickly [24]. The reinforcement has to be mixed with the resin before the resin cures completely. The possibility of cold-curing of polyester resin from liquid state is one of the key reasons for widespread use of these systems. For curing of unsaturated polyester resin, methyl ethyl ketone peroxide was used as catalyst in this research. It is used for room temperature cure of polyester resin in conjunction with a cobalt accelerator over the temperature range 15-25 °C. An accelerator assists the speed of cure by increasing the rate at which the catalyst breaks down into free radicals and is added in advance to the polyester resin.

Styrene is usually used as the diluent for polyester resin in order to reduce viscosity of the resin. It is also used to assist the escape of trapped air, permit greater use of reinforcements, increase the heat distortion point, improve quicker wetting of the fibres, reduce costs, and increase the resistance to water in the finished product [25].

The most common reinforcements for polyesters are glass fibres. The construction industry accounts for the greatest usage of reinforced polyesters, followed by the marine, transportation, electrical and sanitary ware industries.

Thermoplastics:

Thrmoplastics soften or melt on heating. They consist of linear or branched-chain molecules having strong intramolecular bonds but weak intermolecular bonds. They are either semi-crystalline or amorphous in structure. Thermoplastics consist of high molecular weight polymer chains which display a linear or slightly branched topology and are formable at elevated temperatures and pressures. Thermoplastics, like metals, soften with heating and eventually melt, hardening again with cooling. This process of crossing the softening or melting point on the temperature scale can be repeated as often

as desired without any appreciable effect on the material properties in either state. Typical thermoplastics include polyethylene, polystyrene, nylon, polypropylene, and polyether-ether ketone (PEEK).

2.2.3 Interface/ Interphase

Interface is the surface forming the common boundary between matrix and reinforcement where these two are bonded together. It is through interface that the stress is transferred from the matrix to the reinforcement. It also provides resistance to crack propagation and chemical attack. Hence the interface is vitally important in determining the mechanical properties of composite materials.

In some cases, the contiguous region between matrix and reinforcement is a distinct added phase, called an interphase. Examples are the coatings on glass fibres and the adhesive that bonds the layers of a laminate together. When an interphase is present, there are two interfaces, one between each surface on the interphase and its adjoining constituents.

Interfacial bonding is sometimes improved by physical or chemical treatment of fibres. The main aim is to modify the surface energy to allow better wetting between matrix and the fibre, to provide chemical groups that will bond to reacting thermosets, and to increase the surface roughness of fibres to improve the interlocking between the matrix and the fibre. Coupling agents (generally organosilanes) are the most important types of modifications for synthetic fibres, followed by plasma treatments.

2.2.3.1 Effect of Interface on Composite Properties

The mechanism of load transfer through the interface becomes more important in the discontinuous fibre reinforced composites and in the continuous fibre reinforced composites when the individual fibres fracture prior to ultimate failure of the composite [22]. The interfacial bond controls the mode of propagation of microcracks at the fibre ends. In case of a strong bond, the cracks do not propagate along the length of the fibres. Thus the fibre reinforcement remains effective even after the fibre breaks at several points along its length. A strong bond also results in higher transverse strength and good environmental properties of the composites. Harris et al [26] showed that poor interfacial bonding results in improved fracture toughness but poorer shear strength in

composites. Favre and Merienne [27] observed that shear strength of composites was roughly proportional to square root of the interface strength while Ying [28] observed approximately linear increase of shear strength with increase in interface strength.

Interfacial bonding is of particular concern in natural fibre composites. Natural fibre surfaces are irregular which should theoretically enhance the fibre-matrix interfacial bonding. However this is offset by chemical incompatibility between the fibre and polymer matrix. The fibres have an outer waxy layer, typically 3-5 μm thick, of fatty acids which are long chain aliphatic compounds not compatible with common resins such as polyester. Natural fibres are polar in nature which also makes them incompatible with inherently non-polar polymer matrices. This problem may be solved by exposing the fibre surface to physical and chemical treatments.

2.2.3.2 Measurement of Interfacial Strength

In order to get a measure of the strength of fibre/matrix interfacial bonding, standard tests have been devised. Four methods are generally used for measuring the interfacial strength [29]: pull-out, micro-tension, micro-compression, and fragmentation. The pull-out method has been found to be the best from the point of view of understanding how the interface affects composite properties and this method has been used in determining the interfacial shear strength of hemp fibres in polyester resin in this research.

2.2.3.3 Wettability, Contact Angle and Surface Energy

Interlinked with the fibre/matrix interfacial strength are the important parameters of wettability, contact angle and surface energy. Good interfacial strength requires proper wetting of the fibre surface by the liquid matrix. Wettability is the measure of spread of a liquid over solid surface. Good wettability means that the liquid matrix can flow over the fibre covering every part of the rough surface of the fibre and displacing the air at the same moment. Good wettability requires low viscosity of liquid matrix and a decrease in the free energy of the system.

Surface energy of a solid or liquid is a manifestation of unbalanced molecular forces at the surface [30]. Because of this imbalance, they possess additional energy at the surface. In liquids this excess energy tends to reduce the surface area to a minimum, resulting in surface tension. In solids, due to the lack of mobility at the surface, this energy is not directly observable and must be measured by indirect methods. These

methods involve exposing the solid to various liquids, whose surface tensions are known, and measuring the contact angle.

Fig. 2.1 shows a thin film of liquid matrix spread over the solid fibre surface where γ_{SG}, γ_{LG} and γ_{SL} represent the solid-gas, liquid-gas and solid-liquid surface energy per unit area respectively and θ is the contact angle. The gas is normally air. The work of adhesion, W_a, as the liquid matrix spreads over the solid fibre surface is given by the Dupre equation,

$$W_a = \gamma_{SG} + \gamma_{LG} - \gamma_{SL} \quad \text{.....(2.1)}$$

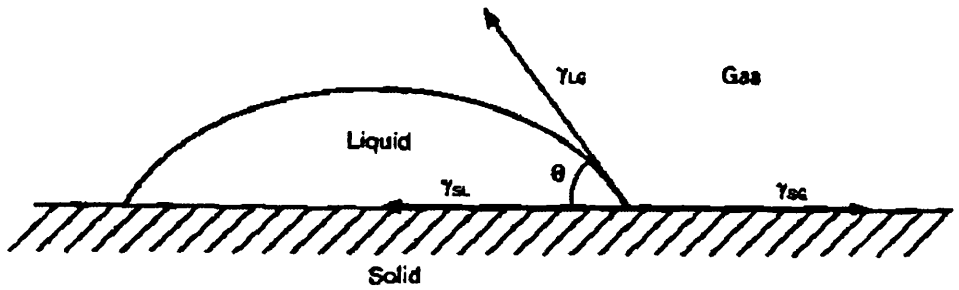

Fig. 2.1: A liquid in equilibrium with a solid surface [15]

Surface energies γ_{SG} and γ_{LG} are positive because these are the energies required for new covering areas of solid-gas and liquid-gas interfaces, and γ_{SL} is negative because this energy is recovered as the solid surface is covered. Thus wetting is more favourable when surface energies of the solid and the liquid are large and their interfacial energy is small. However large values of surface energies of liquids inhibit the spreading of a liquid droplet. Contact angle is then used to represent the measure of degree of attraction of the liquid for the solid.

Resolving equation (2.1) into its horizontal components in equilibrium conditions,

$$\gamma_{SG} = \gamma_{SL} + \gamma_{LG} \cos\theta \quad \text{.....(2.2)}$$

If the contact angle is 0° or less than 90°, the liquid is said to spread on or to wet the solid. If it is greater than or equal 90°, the liquid/solid interaction is termed to be non-wetting.

Equation (2.2) shows that for complete wetting to occur (θ=0°), the surface energy of the solid should be equal to or greater than the sum of the liquid surface energy and the

interface surface energy. Interface surface energies are frequently small enough than the solid and the liquid surface energies to be ignored. Therefore fibres with higher surface energies than liquids are likely to wet very easily. Therefore, glass fibres (γ_{SG}=560 mJ/m^2) are easily wetted by polyester (γ_{LG}=35 mJ/m^2) and epoxy (γ_{LG}=43 mJ/m^2) resins [21].

Surface energy in terms of dispersive and polar components:

Fowkes suggested that various molecular attractive forces on the surface can be assumed to be linearly additive [31]. Therefore total surface energy of the solid surface and the liquid can be written as

$$\gamma_S = \gamma_S^d + \gamma_S^p \quad \text{and} \quad \gamma_L = \gamma_L^d + \gamma_L^p$$

where the superscript *d* refers to the contribution due to London dispersive forces (Van der Waal's bonding), common to all materials, and *p* refers to contribution due to polar forces, mostly made up of hydrogen bonding and dipole-dipole interactions.

Owens and Wendt [32] proposed that the interfacial interaction between the solid and the liquid is the geometric mean of the individual surface energies. This is expressed as

$$\gamma_{SL} = \gamma_S + \gamma_L - 2(\gamma_S^d \gamma_L^d)^{1/2} - 2(\gamma_S^p \gamma_L^p)^{1/2} \quad \text{.....(2.3)}$$

Substitution of equation (2.1) in equation (2.3) and ignoring polar terms gives Fowkes equation, which expresses work of adhesion in terms of solid and liquid surface energies,

$$W_a = 2[(\gamma_S^d \gamma_L^d)^{1/2} + (\gamma_S^p \gamma_L^p)^{1/2}] \quad \text{.....(2.4)}$$

Substitution of equation (2.2) in equation (2.1) gives another expression for work of adhesion in terms of surface energy and contact angle,

$$W_a = \gamma_L (1+\cos\theta) \quad \text{.....(2.5)}$$

Substitution of equation (2.5) in equation (2.4) gives

$$\gamma_L (1+\cos\theta) = 2[(\gamma_S^d \gamma_L^d)^{1/2} + (\gamma_S^p \gamma_L^p)^{1/2}] \quad \text{.....(2.6)}$$

For a non-polar substance, $\gamma_S^p = \gamma_L^p = 0$, and equation (2.6) is reduced to

$$\gamma_S^d = \gamma_L^d (1+\cos\theta)^2/4 \quad \text{.....(2.7)}$$

Equations (2.6) and (2.7) are used in the calculation of the surface energy of solid by immersing the solid in a non-polar liquid.

Methods for determining surface energy of fibres:

Over the years various techniques have been developed to determine the surface energies and wettability of fibres. These include sessile drop, capillary rise in a power bed or fibre assemblies, air-pressure techniques, Wilhelmy plate, sedimentation volume film rotation, inverse gas chromatography, and vapour probe techniques [33]. Wilhelmy technique has been widely used in the determination of surface energy of natural fibres and this technique will be used in this research for determining the surface energy of hemp fibres.

Wilhelmy related the downward force exerted on a vertical plate when it is brought into contact with a liquid to the contact angle between them. This method has obvious limitations for use with natural fibres because of their rough, heterogeneous, non-uniform and absorbent surfaces. However at the moment, this is the best method available for determining the surface energy of natural fibres.

2.3 TYPES OF COMPOSITE MATERIALS

Composite materials can be classified into three broad categories according to the type, geometry, and orientation of the reinforcement phase [34] as shown in Fig 2.2. **Particulate composites** contain particles of various sizes and shapes randomly dispersed in within the matrix. **Discontinuous or short fibre composites** contain short fibres or whiskers as the reinforcement which can be either all oriented in one direction or randomly oriented. **Continuous fibre composites** contain long continuous fibres as reinforcement which can all be parallel (unidirectional), or oriented at right angles to each other (cross ply or woven fabric), or oriented along several directions (multidirectional).

Fibre-reinforced composites can be further subdivided into four main groups according to the matrix used. These are polymer matrix composites, metal matrix composites, ceramic matrix composites and carbon/carbon composites.

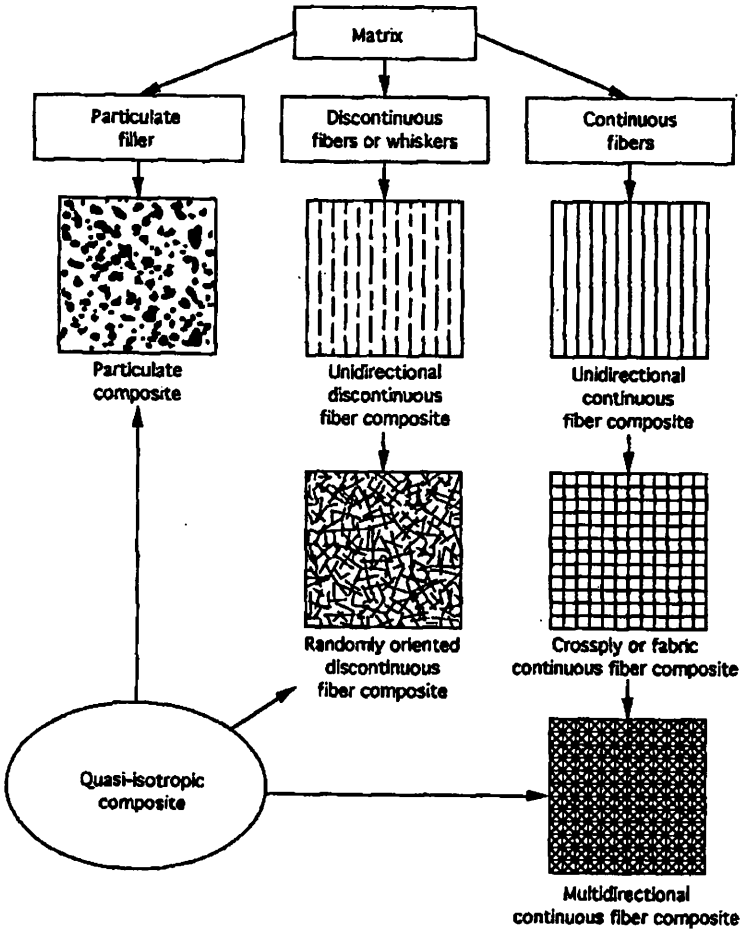

Fig. 2.2: Classification of composite materials [34]

2.3.1 Polymer Matrix Composites (PMCs)

These are the most common of all composites used. These materials use a polymer thermoset or thermoplastic resin as the matrix, and a variety of fibres such as glass, carbon, aramid, boron, and natural fibres as the reinforcement. They are primarily used in low temperature applications. They commonly exhibit marked anisotropy since the matrix is much weaker and less stiff than the fibres. Their main advantages are high specific strength and stiffness, design flexibility, higher damping factors than metals and better environmental resistance.

2.3.2 Metal Matrix Composites (MMCs)

Increasingly found in the aerospace industry, these materials use a metal such as aluminium as the matrix, and reinforce it with fibres such as silicon carbide. These are mostly used for applications where high temperature performance or good tribological properties are important. Their commercial usage is quite limited compared to PMCs.

2.3.3 Ceramic Matrix Composites (CMCs)

Used in very high temperature environments, these materials use a ceramic as the matrix and reinforce it with short fibres, or whiskers such as those made from silicon carbide and boron nitride. These materials are still in early stages of development.

2.3.4 Carbon/carbon composites

Carbon-carbon composites consist of carbon or graphite matrix reinforced with graphite yarn or fabric. They have unique properties of relatively high strength at high temperatures coupled with low thermal expansion and low density.

2.3.5 Hybrid Composites

One purpose of this research was to study the properties of hemp/glass fibre hybrid composites. A brief review of hybrid composites follows.

Hybrid composites use more than one kind of reinforcements in the same matrix and hence the idea is to get the synergistic effect of the properties of reinforcements on the overall properties of composites. With hybrid composites it may be possible to have greater control of the properties, achieving a more favourable balance between the advantages and disadvantages inherent in any composite material.

Hybrid composites offer three main advantages over composites made from one kind of reinforcement. First, they provide designers with new freedom of tailoring composites to achieve required properties. Second, a more cost effective utilisation of expensive fibres such as carbon and boron can be obtained by replacing them partially with less expensive fibres such as glass and aramid. Third, they provide the potential of achieving a balanced pursuit of strength, stiffness and ductility. Hybrid composites have also demonstrated weight savings, reduced notch sensitivity, improved fracture toughness, longer fatigue life and excellent impact resistance [35].

The earlier attempts at hybridisation were made by combining stiffer fibres (carbon, boron) with more compliant fibres (glass, Kevlar) to increase the strain to failure of composite and hence enhanced impact properties. The effect is greater when the proportion of stiffer fibre is small and it is finely dispersed in the composite. Besides improving the impact performance, the incorporation of glass fibres also reduced the cost.

The following variables influence the behaviour of the hybrid composite [22]: volume and weight fraction of each component fibre; lay-up sequence and orientation; relative properties of resin and fibres and interlaminar shear strength between plies; and extent and nature of voids and any other quality defects.

The properties of hybrid composites may not follow from a direct consideration of the independent properties of individual components by rule of mixtures. Therefore, a positive or negative hybrid effect is defined as a positive or negative deviation from a certain mechanical property from the rule of mixture behaviour. It is commonly agreed that the elastic moduli follow the rule of mixture behaviour [36]. The ultimate strength is reported to exhibit a negative hybrid effect.

The hybrid effect is explained by assuming that the weakest low elongation fibres that break first form cracks that are bridged by the surrounding high elongation composite, thus allowing the stronger low elongation fibres to reach their ultimate strength [37].

Aveston and Kelly [38] have suggested the following equation for the ultimate tensile strength of unidirectional hybrid composites

$$\sigma_c = \sigma_{Lu} V_{LE} + \varepsilon_{Lu} E_{HE} V_{HE} \quad \text{.....(2.8)}$$

where σ_{Lu} is the ultimate tensile strength of low elongation fibres, V_{LE} is the volume fraction of low elongation fibres, ε_{Lu} is the strain to failure of low elongation fibre, and E_{HE} and V_{HE} are the tensile modulus and volume fraction of high elongation fibres. For low volume fraction of high elongation fibres, the failure of low elongation fibres leads to the fracture of the hybrid and there is no multiple fracture. As the concentration of high elongation fibres increases, a transition in failure modes occurs because there is sufficient amount of these fibres to carry the load on the fracture of low elongation fibres. The fracture mode then is the multiple fracture of brittle fibres and the ultimate tensile strength is given by:

$$\sigma_c = \sigma_{Hu} V_{HE} \quad (2.9)$$

The hybridisation of low strain to failure fibres with high strain to failure fibres results in an increase in energy absorption capacity and hence improved impact resistance of the hybrid composite. A number of studies (e.g., [39], [40], [41], [42]) have shown the improved impact properties of hybrid composites. Charpy impact test, Izod impact test and drop weight method have been utilised in these studies.

The hybridisation of glass fibres with carbon fibres also improves the fatigue resistance of the hybrid composite [43]. This is attributed to the increased stiffness of the composite because of carbon fibres.

2.4 NATURAL FIBRES

Natural fibres are classified according to their source: plants, animals, or minerals. Mostly plant fibres are used to reinforce polymers in composites, and hereafter in this thesis, the term natural fibres will refer to plant fibres.

Natural fibre crops are the earliest known cultivated plants. They were used as the raw materials for making ropes and textiles. Hemp and linen fragments have been found in Neolithic sites in Syria, Turkey, Mesopotamia (present day Iraq) and Iran, carbon dated back to 8000-6000 B.C. [44]. The ancient Egyptians wrapped their corpses in linen cloth (fabric made from flax fibres) for thousands of years. In central Europe there is evidence of Swiss lake dwellers cultivating flax and making linen more than 4000 years ago. More recently, fibre crops like flax, hemp and nettle were used extensively for the production of textile fibres until the late 19^{th} century. The growing demand for and production of cheap synthetic textile fibres led to reduction in the importance of natural fibre crops in 20^{th} century.

As early as 1896, natural fibres were being used in composite materials for making aeroplane seats and fuel tanks [45]. Natural fibres are perhaps the oldest additives used in plastics. Their use dates back to the original plastic, Bakelite, in which they were used to provide impact resistance, reduce cost, and control shrinkage. In 1908, the first natural fibre reinforced composites were made by reinforcing sheets of phenol- or melamine- formaldehyde resins with paper or cotton [45]. Their higher cost and poor performance compared to standard plastics inhibited any further development. With the

introduction of thermoplastics in the mid-1900s, natural fibres and fillers were replaced by mineral products and glass fibres to reinforce polymer matrices.

2.4.1 Classification

Natural fibres are classified according to the part of the plant they are extracted from. Some fibres, like cotton, are part of the seeds of the plants. Some fibres, like hemp and flax, are contained within the tissues of the stems of dicotyledonous plants and referred to as bast fibres. Some fibres, like sisal and banana, are part of the leaves of monocotyledonous plants. Some fibres, like coconut, are part of the fruit of the plants. The term fruit here is used in its botanical rather than everyday use. The natural fibres used as reinforcements in composites are shown in Table 2.1.

Of these fibres, jute, ramie, flax, sisal, and hemp are the most commonly used fibres for composites. According to the Food and Agriculture Organisation (FAO), about 30 million tons of natural fibres (both plant and animal origin) are produced annually. The worldwide production of major fibres is shown in Table 2.2.

Table 2.1: Natural fibres used as reinforcement in composites [46]

Bast (stem) fibres: Flax, Hemp (and Sunhemp), Kenaf, Jute, Mesta, Ramie, Urena, Roselle, Papyrus, Cordia, Indian Malow, Nettle
Leaf fibres: Pineapple, Banana, Sisal, Pine, Abaca (Manila hemp), Curaua, Agaves, Cabuja, Henequen, Date-palm, African palm, Raffia, New Zealand flax, Isora
Seed (hairs) fibres: Cotton, Kapok, Coir, Baobab, Milkweed
Stem fibres: Bamboo, Bagasse, Banana stalk, Cork stalk
Fruit fibres: Coconut, Oil palm
Wood fibres: Hardwood, Softwood
Grasses and Reeds: Wheat, Oat, Barley, Rice, Bamboo, Bagasse, Reed, Corn, Rape, Rye, Esparto, Elephant grass, Cannary grass, Seaweeds, Palm, Alpha

Table 2.2: Current worldwide production of major fibres [47]

Fibre	Production (1000 tons)
Jute	2300-2800
Flax	1000
Coir	500
Kenaf	340
Sisal	300
Ramie	280
Hemp	90

Bast fibres:

Because of their superior mechanical properties, bast fibres are the most widely used fibres for composite manufacture of all the natural fibres. The estimated worldwide production of bast fibre raw materials is about 25 million tons of which about 6 million tons are pure fibres [48]. Bast fibres form the fibrous bundles in the inner bark of the stems which helps to hold the plant erect. In doing so, these fibres offer strength and stiffness to the tree. Therefore all the bast fibres have high strength and stiffness. These fibres are grown in the temperate and sub-tropical regions of the world. The bast fibres mostly used in reinforcing composites are flax, hemp, kenaf, jute, and ramie.

2.4.2 Advantages and Disadvantages

The main advantages and disadvantages of using natural fibres in composites are listed in Table 2.3. The environmental advantages of natural fibres seem to override their disadvantages. Perhaps the biggest drawback of natural fibres is the variability in their physical and mechanical properties. Diameters and properties of natural fibres vary significantly depending upon factors such as source, age, retting and separating techniques, geographic origin, rainfall during growth, and constituents' content.

Nishino [10] has identified the following factors that can cause the variability in the physical and mechanical properties of natural fibres.

Materials: Microscopic: crystallinity; microfibril angle; crystal modifications

Macroscopic: fineness; porosity; size and shape of lumen;

History: source; age; retting and separating conditions; geographical origin; rainfall during growth

Measurement conditions: tensile speed; initial gauge length; moisture; temperature; different cross-section of fibres at different points.

Morvan et al [49] showed that fibre diameter of flax fibres is greater in the middle part of the stem than in the bottom or top regions. The diameter was also found to vary depending on the development stage of the plant, the diameter being smaller during flowering /capsulation stage than mature capsule or seed maturation stages. It is natural to expect that this variability in diameter will also impart variability to the mechanical properties of the fibres.

Catling and Grayson [50] measured the diameters of hemp fibres and found the average to be 30 μm with a range of 11.68-31.96 μm. The average hemp fibre length was found to be 8.46 mm with a range of 1-34 mm. Olsen and Plackett [51] found the average hemp fibre diameters to be 25 μm and average hemp fibre length was found to be 25 mm with a range of 5-55 mm.

Another important factor is price. The price of fibres varies a lot depending on the economy of the countries where such fibres are available. The price of the fibre depends on availability, the fibre preparation process, and the pre-treatment of the fibre. In recent years, prices of natural fibres have been fluctuating, especially for flax fibres. Flax fibres are highest strength fibres and are marginally more expensive than glass fibre.

Table 2.3: Advantages and Disadvantages of Natural Fibres

Advantages	Disadvantages
Low cost	High moisture absorption
Renewable resource	Poor dimensional stability
Low density	Poor microbial resistance
High specific properties	Low thermal resistance
High Young's modulus	Discontinuous fibre
Good tensile strength	Anisotropic fibre properties
Non-abrasive to tooling and moulds	Low transverse strength
No skin irritations, no respiratory issues	Low compressive strength
Low energy consumption in production	Local, seasonal quality variations
CO_2 neutral	Demand and supply cycles
No residues when incinerated	Production efficiency dependent on environmental conditions
Biodegradable	Fibre preparation time, labour intensive
Unlimited availability	Large areas required for cultivation
Acoustic abatement capability	Use of pesticides in some cases
Thermal incineration with high energy recovery	
Can be stored for long periods of time	
Fast absorption/desorption of water	

2.4.3 Composition and Structure

Natural fibres themselves are cellulose fibre reinforced materials as they consist of crystalline cellulose micorfibrils in an amorphous matrix of lignin and/or hemicelluloses. These fibres consist of several fibrils that run all along the length of the fibre. The hydrogen bonds and other linkages provide the necessary strength and stiffness to the fibres.

With the exception of cotton all natural fibres are made of cellulose, hemi-cellulose, lignin, pectin, waxes and water soluble substances. Cellulose, hemi-cellulose and lignin are basic components that define physical properties of fibres. Cellulose is the stiffest and the strongest organic constituent in the fibres. Generally, the fibres contain 60-80% cellulose, 10-20% hemicelluloses, 5-20% lignin, and up to 20% moisture. The chemical compositions of some common natural fibres are given in Table 2.4. However there is considerable variation in the chemical composition reported by different authors, depending upon the quality of the extraction method. Therefore the data given in this table should be viewed with caution with the understanding that there can be variation in results.

A high cellulose content and low microfibril angle (to be defined later) are desirable properties for a fibre to be used as reinforcement in polymer composites. In general, bast fibres have higher cellulose content and a few, such as ramie and hemp, have very low lignin content. Wood fibre is the richest in lignin. Wood and bamboo have lower cellulose content than bast fibres. Different chemical and physical characteristics of natural fibres result in wide range of different properties and, consequently, in their applications.

2.4.3.1 Cellulose

Cellulose, a semi-crystalline polymer, is the principal component of all plant fibres. In 1838 Anselme Payne discovered that the cell walls of large numbers of plants consist of the same substance which he named cellulose [45]. It is a linear condensation polymer consisting of β-D-anhydroglucopyranose units ($C_6H_{12}O_5$) joined together by β-1, 4-glycosidic bonds to form a long and thin filament structure, as shown in Fig. 2.3. Linkages between anhydroglucopyranose units occur through condensation reactions between adjacent carbon 1 and 4 positions. It is thus a β-1, 4-D glucan. Two

anhydroglucopyranose units are linked to form a 'cellobiose unit' that has a length of 1.03 nm [45].

For plant cellulose the Degree of Polymerisation (DP) range is 7000-15000. For hemp the cellulose DP is 4800 [52]. Compared to this, the DP of flax and jute cellulose is 4700, while that for ramie cellulose is 5800. A similar DP range of these fibres suggest that they contain cellulose molecules of approximately the same average molecular weight.

Covalent bonds join anhydroglucose units together giving strength to the length of the chain. Hydroxyl groups along the cellulose polymer can form two different hydrogen bonds depending on the location of the glucose monomers. First type of bonds, which occur within a cellulose molecule, are called intramolecular linkages. The other types of bonds which occur between adjacent cellulose polymers are called intermolecular linkages. Intramolecular linkages help stiffen the chain while intermolecular linkages give rise to supra-molecular structures. Thus the molecular structure of cellulose is responsible for its supra-molecular structure and this, in turn, determines many of its chemical and physical properties.

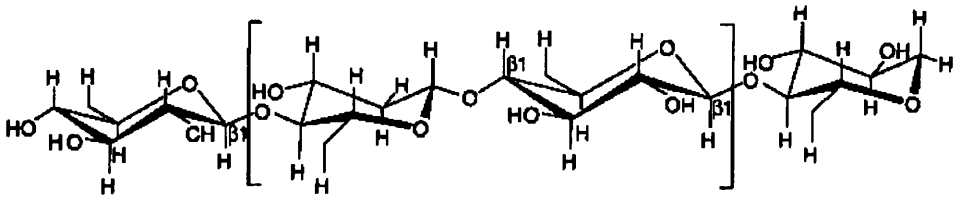

Fig. 2.3: Cellulose molecular structure [44]

Intermolecular linkages form cellulose molecules into sheets that can pack together to create a crystalline structure. These cellulose chains create the reinforcement structure called microfibrils. There are 48 molecular chains of crystalline cellulose at the core of microfibrils in the secondary cell wall that have cross section of 5x3 nm. Microfibrils themselves have cross section of 10x5 nm. The cellulose surrounding the core of microfibril is in non-crystalline state (amorphous cellulose) as well as other molecules such as hemicellulose and lignin. Thus chemically, cellulose is a semi-crystalline polymer composed of long linear packed chains embedded in a hemicellulose and lignin matrix. In general, primary cell walls contain 10-20% cellulose, and secondary cell

walls up to 50% cellulose. The cellulose crysatllinities have been determined at 90-100 g/100 g cellulose in plant-based fibres and 60-70 g/100 g cellulose in wood-based fibres [53]. At 60% crystallinity, the amorphous regions in the chain have a length of about 120°A, implying that there are short alternating crystalline and amorphous regions in cellulose chains.

The crystal structure of naturally occurring (native) cellulose is called cellulose I. Cellulose I crystallises in monoclinic spherodic structures. The structures of regenerated cellulose is called cellulose II. The mechanical properties of natural fibres also depend on the cellulose type because each type of cellulose has its own cell geometry and the geometrical conditions determine the mechanical properties [45]. Most of the studies undertaken have found higher characteristic values of elastic modulus for cellulose I than for cellulose II [54]. Flax and hemp fibres have cellulose I which have been found to have elastic modulus of 74-103 GPa. Overall stiffness of cellulose is in the range 130-165 GPa [55] and is independent of moisture content.

Cellulose Studies done on cellulose content of hemp bark by Keller et al. [56] showed that the cellulose content of the bark increased continuously until the harvest. The content increase was different for different parts of the stem. Smallest increase was observed in the bottom part, followed by the middle and the top part. The cellulose content of the male plants was found to increase more than that of the female plant. At the harvest time of 274 days the cellulose content of the hemp bark was about 79%. Since the tensile properties of the fibre are dependent on the cellulose content, the study found that the tensile strength of the fibres of the two most advanced growth stages were significantly higher that those of lowest growth stages. However, the differences in tensile strength between different stem sections (top, middle, bottom) were not significant for fibres at same growth stage.

Table 2.4: Chemical Composition, Moisture Content, and Microfibrillar Angle of Natural Fibres [45]

Fibre	Cellulose (wt%)	Hemicellulose (wt%)	Lignin (wt%)	Pectin (wt%)	Moisture Content (wt%)	Waxes (wt%)	Microfibrillar Angle (degrees)
Bast Fibres							
Hemp	70-74	17.0-22.4	3.7-5.7	0.9	6.2-12	0.8	2-6.2
Flax	71	18.6-20.6	2.2	2.3	8-12	1.7	5-10
Jute	61-71.5	13.6-20.4	12-13	0.2	12.5-13.7	0.5	8
Kenaf	45-57	21.5	8-13	3-5	-	-	-
Ramie	68.6-76.2	13.1-16.7	0.6-0.7	1.9	7.5-17	0.3	7.5
Leaf Fibres							
Sisal	66-78	10-14	10-14	10	10-22	2	10-22
Henequen	77.6	4-8	13.1	-	-	-	-
Pineapple	70-82	-	5-12.7	-	11.8	-	14
Banana	63-64	10	5	-	10-12	-	-
Abaca	56-63	-	12-13	1	5-10	-	-
Seed Fibres							
Cotton	85-90	5.7	-	1	7.85-8.5	0.6	-
Coir	32-43	15-31	12-20	8	-	-	-

2.4.3.2 Hemicellulose

Hemi-cellulose is not a form of cellulose at all and the name is a misnomer. They represent a class of heteropolymers with a selection of sugar molecules as monomeric units. The monomeric units consist of D-glucose, D-galactose, D-mannose, D-xylose and L-arabinose with glucuronic and glacturonic units present. These are group of poly-sacchrides that remain associated with the cellulose after lignin has been removed. Hemicellulosic polymers are non-linear, branched, fully amorphous, and have significantly lower molecular weight than cellulose. The degree of polymerisation of hemicellulose is between 150-200 monomers in each molecule which is 10 to 100 times less than that of native cellulose. Unlike cellulose, the constituents of hemicellulose differ from plant to plant.

Hemicellulose is found in the middle lamella, primary wall and the secondary cell wall where it is bonded with cellulose and lignin to from the thickest cell wall layer. The mechanical properties of the fibres are often determined by the structure and quantities of the chemical constituents of the secondary cell wall region. The hydrophilic nature of the surface of cellulose is not compatible with hydrophobic lignin thus limiting hydrogen bonding. Hemicellulose acts as a coupling agent between crystalline cellulose and lignin creating a lignin-polysacchride complex (LPC). Hemicellulose can covalently bond to lignin and hydrogen bond to cellulose. The imperfect bond that occurs between cellulose and lignin via hemicellulose allows stress transfer to the microfibrils but creates a weak interface in the structure that allows failure to occur giving the overall structure the toughness required. Because of its open structure containing many –OH and acetyl groups, hemicellulose is partly soluble in water and can absorb relatively large amount of water. The stiffness of hemicelluloses is dependent on content of moisture and can vary from 8 GPa at low moisture content to 0.01 GPa at 70% moisture content [55].

2.4.3.3 Lignin

During the biological synthesis of plant cell walls, lignin fills the spaces between the cellulose and hemicellulose fibres cementing them together. This lignification process causes a stiffening of cell walls and the carbohydrates are protected from physical and chemical damage. Lignin is a biochemical polymer that acts a structural support material in a plant and is generally resistant to microbial degradation. Lignin is

complex, highly cross-linked, non-crystalline, high molecular weight, hydrocarbon polymer with both aliphatic and aromatic components.

The exact chemical structure of lignin is still obscure but most of the functional groups and units which make up the lignin molecule have been identified. The high carbon and low hydrogen content of lignin suggest that it is highly unsaturated or aromatic in nature. The constituents of lignin are p-coumaryl, coniferyl and synapyl alcohols that are formed by dehydrogenative radical polymerisation. Their chief units are various ring substituted phenyl-propanes linked together in ways, which are not fully understood. Lignin is believed to be linked with cellulose through two types of linkages, one alkali sensitive and the other alkali resistant. The alkali sensitive linkage forms an ester type combination between lignin hydroxyls and carboxyls of hemicellulose uronic acid. The ether type linkage occurs through the lignin hydroxyls combining with the hydroxyls of cellulose. Lignin, being poly-functional, exists in combination with more than one neighbouring chain molecules of cellulose and /or hemicellulose, forming a cross-linked structure.

Lignin content in wood is 20-40% but in hemp it ranges from 3-13%. Lignin levels are believed to decrease during fibre processing. Its mechanical properties are distinctly poorer than those of cellulose. The stiffness is moisture dependent and can vary from 6.5 GPa at 4% moisture content to 3 GPa at 20% moisture [55].

Lignin can be removed by using chemical or chemo-mechanical processes to release individual fibres from fibre bundles. Lignin is softened when fibres are heated to temperature above the glass transition temperature of lignin. Glass transition temperature of lignin varies for different fibres and increases with decrease in moisture content [57]. Lignin starts to degrade at about 214 °C and hence heating the fibres up to 200 °C may cause some softening of fibre.

2.4.3.4 Pectin

Pectin is a collective name for hetero-polysacchrides, which consist essentially of polygalacturonnic acid with high molecular weight. It is found in the middle lamella and primary cell walls. It has a linear main chain of 1-4 linked α-D-galacturonic acid. Regular intervals of α- 1-2 and α- 1-4 bonded rhamnose units branch from this chain. Arabinose and galactose molecules are present as side chains with small amounts of

xylose and glucose monomers. Pectin along with hemicellulose binds cell wall layers. Removal of pectin facilitates the separation of fibre bundles from the stem. Therefore, the removal or degradation of pectin is very important during the retting process. Its composition in hemp ranges from 0.8-1.3%. Pectin is soluble in water only after a partial neutralization with alkali or ammonium hydroxide.

Waxes make up the part of fibres that can be extracted with organic solutions. These waxy materials consist of different types of alcohols, which are insoluble in water.

2.4.3.5 Bast fibre structure

Having identified the chemical constituents of natural fibres, we are now in a position to describe the structure of the bast fibre. Natural fibres extracted from the bast of the plant are bundles of individual cells. A schematic of the typical structure of a bast fibre is shown in Fig. 2.4. Bast fibres transport water and nutrients in the plant and thus have a hollow central canal called the lumen. The walls of the cells in each fibre are built of smaller structural units called fibrils. In turn each fibril is made up of microfibrils and elementary fibrils of cellulose. Microfibrils constructed from crystalline cellulose act as a reinforcement bound within a matrix of lignin with amorphous cellulose, hemicellulose and pectin acting as a binder between the two phases. The fibrils can be 5-10 nm in diameter, made up of 50 to 100 cellulose molecules and can have lengths of 100 nm to several micrometers depending on the source of cellulose. Microfibrils are oriented at an angle to the longitudinal fibre axis called microfibrillar or spiral angle. The cell walls differ in their composition (ratio between cellulose and hemicellulose/lignin) and in their orientation (spiral angle) between different fibres. Chemical processes such as alkalisation and acetylation can also result in variations in these structural parameters within the same fibre.

The cellulose content and the spiral angle generally determine the mechanical properties of natural fibres. The characteristic values of these structural parameters for different bast fibres are shown in Table 2.5.

Table 2.5: Structural Parameters of different bast fibres [58]

Fibre	Cellulose content (%)	Microfibrillar angle (°)	Cross-sectional area ($x10^{-2}$ mm^2)	Cell length (mm)	Cell length/ cell diameter ratio
Hemp	78	6.2	0.06	23.0	960
Flax	71	10.0	0.12	20.0	1687
Jute	61	8.0	0.12	2.3	110
Ramie	83	7.5	0.03	154.0	3500

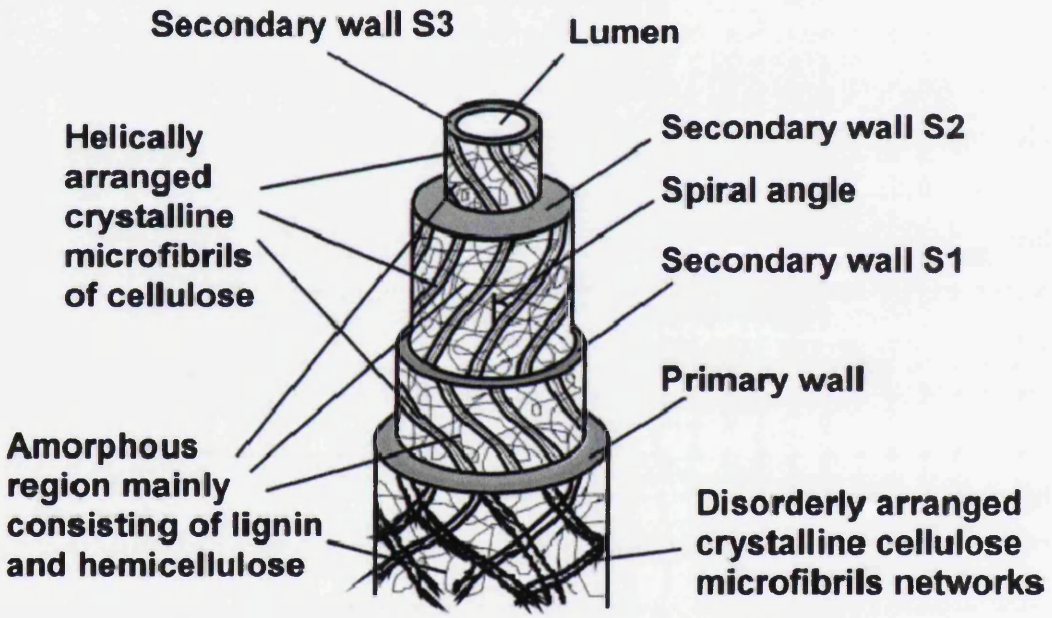

Fig. 2.4: Schematic representation of bast fibre structure [44]

There are four distinct layers in the cell wall: the middle lamella, and the primary, secondary, and tertiary cell walls. Each layer has a characteristic variation in morphology and composition. The middle lamella at the exterior of the cell is composed primarily of pectin that binds the fibres together into a bundle. Adjacent to the middle

lamella is the thin primary cell wall that consists of a disorganised arrangement of cellulose fibrils embedded in a matrix of pectin, hemicellulose, lignin and proteins. Further in, the secondary cell wall, with the largest proportion of cellulose within the wall, consists of three layers of cellulose fibrils, referred to as the outer layer (S_1), middle layer (S_2), and the inner layer (S_3), with varying axial orientation that are bound by lignin and hemicelluloses.

Microfibrils in the S_1 layer run parallel to one another in two distinct spirals with an angle between 50° and 70° to the vertical axis. The S_1 layer accounts for about 10% of cell wall thickness. The S_2 layer is the thickest layer in the cell wall accounting for about 85% of cell volume. Microfibrils in the S_2 layer also lie parallel to each other in a spiral formation.

The S_3 layer is similar to the S_1 layer but it only accounts for 1% of the thickness of the cell wall. The longitudinal strength and stiffness of fibres correlates with the microfibrillar angle. A smaller angle results in higher mechanical properties. The microfibril angles of hemp, flax and sisal fibres are 6.2°, 10° and 20° respectively. Not surprisingly the tensile strength and stiffness is greatest in hemp fibres followed by flax and sisal fibres. The structure, cell dimensions and defects, and the chemical composition contribute to the mechanical properties of the fibres but a small microfibrillar angle also plays a crucial part. However, at some locations the angle between the longitudinal direction of the fibre and that of the microfibrils differ from the angle found in the bulk fibre wall. These local misalignments are known as dislocations, kink bands, micro-compressions or slip planes and are a major reason for reduction in properties of fibres. Thygesen [59] has reported the successful use of hydrolysis method for quantification of dislocations in hemp fibres.

Fig. 2.5 shows the composition and structure of a typical bast fibre, flax in this case. As we go on decreasing the fibre diameter, the strength of the fibre increases as does the cost of the fibre. Unfortunately, despite various attempts to separate the fibre cells from fibre bundles, most of the fibres used in composite applications are fibre bundles. The fibre bundles have relatively low strength of 600-700 MPa compared to that of 1500 MPa of individual fibre cell [4]. The theoretical value of tensile modulus of native cellulose has been calculated at 167.5 GPa [60]. Cellulose microfibrils with diameters of 50-5000nm have been separated [60]. Some research has shown the promising

properties of composites made from microfibrils. However the use of microfibrils as reinforcement in composites is still in its infancy and needs more research.

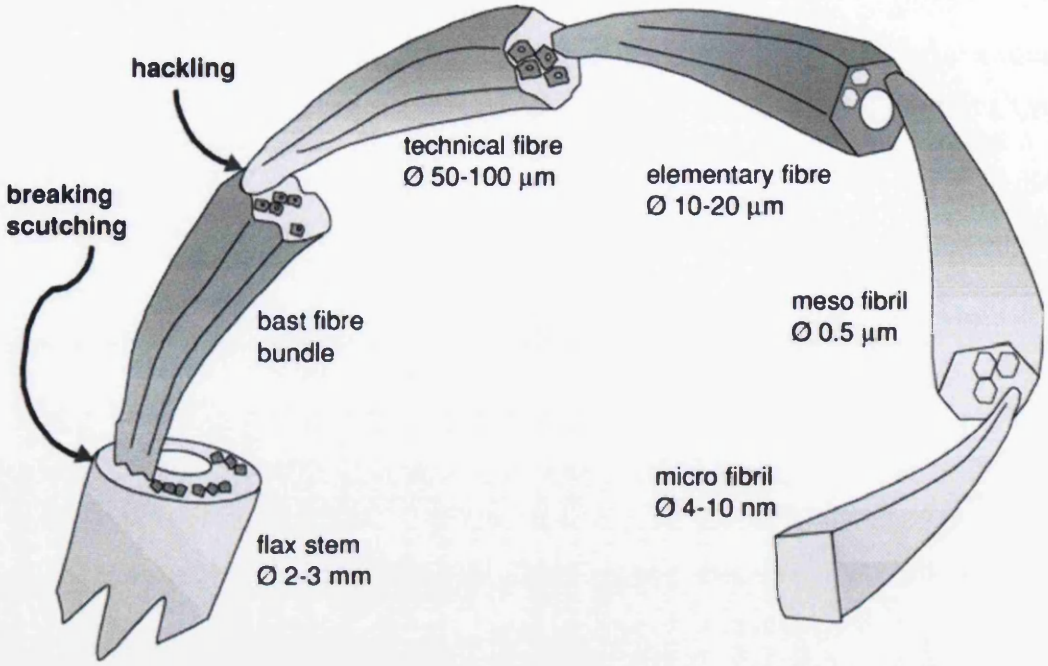

Fig. 2.5: Composition and built of a typical bast fibre (flax) [61]

2.4.4 Mechanical Properties of Natural Fibres

The mechanical properties of natural fibres as compared to conventional synthetic fibres are shown in Table 2.6. It can be seen that the natural fibres compare well with glass fibres, but are not as strong as either aramid or carbon fibres. However the density of E-glass fibres is higher than those of natural fibres. Therefore, in terms of specific properties, some natural fibres are comparable to E-glass fibres on a stiffness basis. They however have lower specific tensile strength than E-glass fibres.

Table 2.6: Mechanical properties of natural fibres as compared to conventional synthetic fibres [45]

Fibre	Density (g/cm^3)	Elongation (%)	Tensile Strength (MPa)	Tensile Modulus (GPa)
Hemp	1.48	1.6	690	70.0
Cotton	1.5-1.6	7.0-8.0	287-597	5.5-12.6
Jute	1.3	1.5-1.8	393-773	26.5
Flax	1.5	2.7-3.2	345-1035	27.6
Ramie	1.5	3.6-3.8	400-938	61.4-128.0
Sisal	1.5	2.0-2.5	511-635	9.4-22.0
Coir	1.2	30.0	175	4.0-6.0
E-Glass	2.5	2.5	2000-3500	70
S-Glass	2.5	2.8	4570	86
Aramid	1.4	3.3-3.7	3000-3150	63-67
Carbon	1.4	1.4-1.8	4000	230-240

In natural fibres a range of mechanical properties can be obtained by using different ways of processing. Retting of hemp fibres increases their tensile strength and modulus. In one study, the tensile strength of hemp fibres was found to be 490 MPa for unretted fibres, 560 MPa for less retted fibres and 620 MPa for retted fibres. Similarly tensile modulus was found to be 30-50 GPa for unretted fibres and 40-60 GPa for retted fibres [48]. The retting process followed by decortication, increases the fineness of fibres, loosening up the fibre bundles into thinner bundles or elementary fibres, thus increasing their mechanical properties. The higher specific properties are the biggest advantage of using natural fibre composites where the desired property is predominantly weight reduction.

Overall the mechanical properties of natural fibres are dependent on the following factors [62]: fibre diameter, size of crystalline fibrils and non-crystalline regions, spiral angle of fibrils, degree of crystallinity, degree of polymerisation, type of cellulose, orientation of chains, and void structure.

2.4.5 Hemp

Hemp is naturally one of the most ecologically friendly fibres and also the oldest. The Columbia History of the World states that the oldest relics of human industry are bits of hemp fabric discovered in tombs dating back to approximately 8,000 BC [63]. The flowering tops and, to a lesser extent, leaves of hemp produce resin secretions containing the narcotic 9-Δ tetrahydrocannabinol (THC) for which marijuana and hashish are famous. Since industrial hemp produces less than 0.2% THC, it can not be used as a narcotic.

Hemp is an annual plant native to central Asia and known to have been grown for more than 12000 years. It probably reached central Europe in the Iron Age and there is evidence of its growth in the UK by the Anglo-Saxons (800-1000 AD). It is now grown mostly in the EU, Central Asia, Philippines, and China. According to FAO, almost half of the world's industrial hemp supply is grown in China, with most of the remainder being cultivated in Chile, France, the Democratic People's Republic of Korea and Spain [47].

There has been an exponential increase in the use of hemp for various applications in recent years. According to FAO, world production of hemp fibre grew from 50,000 tonnes in 2000 to almost 90,000 tonnes in 2005 [47]. Hemp currently accounts for less than 0.5 percent of total world production of natural fibres. A Google search on hemp returns about 9,200,000 web links. Most of these websites are devoted to the promotion of hemp for medicinal and industrial applications. The number of books written on hemp has also increased. The experts on hemp prefer to call themselves 'hempologists'.

As Annie Kelly wrote in the Guardian in 2006 [63], only fifteen years ago, any farmer trying to grow hemp in Britain could be arrested. But in 2006, grown under license, more than 3,500 acres of hemp was harvested as an industrial crop, processed, and made into a plethora of natural products, including insulation, horse bedding, fabric, biodiesel and paper. "Hemp is back and is throwing off its 'hippy' shackles to emerge as one of

the UK's fastest growing sustainable industries", she wrote. The National Non-Food Crops Centre (www.nnfcc.co.uk) recognizes hemp as an established minor crop.

The ban on hemp cultivation, imposed in 1971 under the Misuse of Drugs Act, was finally overturned in 1993. Campaigners successfully argued that although industrial hemp was a variety of the cannabis plant, it could be grown as a legitimate crop as it contained practically no THC.

Still permission of the Home Office is required to grow hemp. Only one company in Britain has the license to grow hemp. Hemcore, the UK's first large-scale hemp company, has seen rapid growth over the last few years. It now owns the only hemp processing plant in the UK and currently contracts 40 farmers to grow 3,500 acres of hemp a year, which it converts into industrial materials. It currently provides all BMW 5 Series cars with hemp door panels, as well as making high-quality horse bedding.

(a) **(b)**

Fig. 2.6: Hemp crop (a) and hemp leaves and stem (b)

2.4.5.1 Structure of Hemp Plant

Hemp, botanically known as *cannabis sativa*, is an annual plant belonging to the family of Cannabidaceae. When mature, hemp develops a rigid woody stem, ranging in height from 1 to 5 metres. It produces long stalks which can grow to a height of 150 to 300 cm. A view of fully grown hemp crop, hemp leaves and hemp stem are shown in Fig. 2.6. Stalks of hemp are hexagonally shaped and are 4 to 26 mm in diameter depending on the plant spacing during growth and sex of the plant. Hemp is dioecious, that is, it carries male and female flowers on different plants. Hemp male plants can be 10 to 15% taller than female plants but have thinner stalks and often grow fewer branches. Male plants ripen earlier and must be harvested earlier. Monoecious varieties, where male and

female plants grow on the same plant, have also been developed by breeding. Dioecious varieties yield better textile fibres while monoecious fibres are preferred by the pulp and paper industry. Strands of hemp fibres may be 1.8 m or longer. The individual or elementary fibres are on average 13-25 mm long [64] .

Leaves of hemp plants are fine pinnate shaped containing several pinnations (the number of pinnations depends on variety of plant). After retting and decortication processes, fibres are obtained in the form of bundles that can be up to 2 meters in length. Hemp grows best where the temperature range between 13 and 22 °C. It requires plentiful supply of moisture during its growth, ideally 125 mm per month. Hence the fibres extracted from the plant are very hydrophilic in nature. It grows best in a deep, well-drained clay-loam soil containing considerable organic matter.

2.4.5.2 Composition of Hemp Stem

The cross-section of hemp stem consists of pith, xylem, cambium, phloem, cortex, and finally the protective layer of epidermis as shown in Fig. 2.7. The pith is composed of thick woody tissues that support the plant. After harvesting, it produces hurds or shives which make up 60 to 75% of the total mass. Cambium is the differentiating layer. Pith produces bast fibre cells from the inside and bark does that from outside. Short chlorophyll containing cells and long bast fibre cells make up the phloem. Cortex is a thin wall of cells that contains chlorophyll but produces no fibres. Epidermis is the outer protective layer.

Just like physical and mechanical properties, there is considerable variation in the composition of hemp fibres reported by different authors as shown in Table 2.7. Various factors contributing to variation in composition and properties of natural fibres have already been discussed in Section 2.4.2.

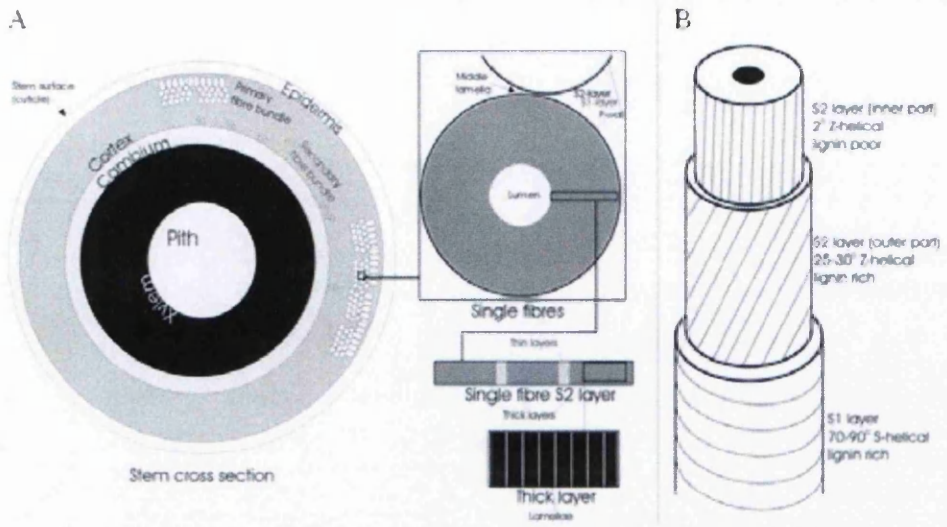

Fig. 2.7: Cross-sectional view of hemp stem and hemp fibre [65]

Table 2.7: Chemical composition of hemp fibres as reported by different authors

Cellulose (%)	Hemicellulose (%)	Pectin (%)	Lignin (%)	Other (%)	Reference
67	16.1	0.8	3.3	2.8	[66]
74.4	17.9	0.9	3.7	0.8	[67]
74	18	1	4	-	[68]
55	16	18	4	7	[69]
76	11.5	1.3	3.2	-	[7]
57-77	-	-	9-13	-	[70]
75.1	<2.0	-	8	-	[71]
70-74	17.9-22.4	0.9	3.7-5.7	0.8	[6]
75.6	10.7	-	6.6	-	[72]
78.3	-	-	2.9	-	[52]
76.1	12.3	1.6	5.7	3.3	[73]

2.4.5.3 Properties of Hemp Fibres

Table 2.8 shows typical physical and mechanical properties of hemp fibre. Again these are representative values for these properties with considerable scope for variation. The mechanical properties were derived in tension. Apart from their high tensile strength and stiffness, their high aspect ratio (length/diameter ratio) and lower density make hemp fibres a good material to be used as reinforcements in composite materials. They have high tenacity (about 20% higher than flax) but low elongation at break. Their disadvantages for use in composite materials, like most other natural fibres, are their non-uniform and non-smooth surfaces, variability of properties, and low resistance to water absorption and decay.

Table 2.8: Typical physical and mechanical properties of hemp fibre [22]

Properties	Values
Length (ultimate) (mm)	8.3–14
Diameter (ultimate) (μm)	17–23
Aspect ratio (length/diameter)	549
Specific apparent density (gravity)	1500
Microfibril angel (θ)	6.2
Moisture content (%)	12
Cellulose content (%)	90
Tensile strength (MPa)	310–750
Specific tensile strength (MPa)	210–510
Young's modulus (GPa)	30–60
Specific Young's modulus (GPa)	20–41
Failure strain (%)	2–4

Variability in tensile properties of hemp fibres

Perhaps the biggest disadvantage of hemp fibres for use as reinforcement in composites is the variability in their mechanical properties. This variability will inevitably be transferred to the composites made from them. Even when large number of fibres are tested, the variability in their properties can be very high as shown in Table 2.9.

Table 2.9: Tensile Properties of hemp fibres as reported by different authors

Tensile Strength (MPa)	Tensile Modulus (GPa)	Elongation at break (%)	Reference
690	-	1.6	[74]
1235	-	4.2	[66]
310-750	30-60	2-4	[75]
550-900	70	1.6	[76]
690	-	1.6	[77]
895	25	-	[68]
500-1040	32-70	1.6	[7]
920	70	-	[78]
690-1000	50	1-1.6	[79]
920	70	1.7	[80]
270-900	20-70	1.6	[81]

Pickering et al [82] studied the effect of growth period on tensile properties of hemp fibres. During the flowering stage of male plants (99-124 days of growth) the tensile strength of fibre increased gradually. Changes in chemical composition of the fibres as the plant aged were attributed to the increase in tensile properties. They also found that

fibres with gauge length of 1.5 mm had higher tensile strength than fibres with gauge length of 10 mm.

2.4.6 Fibre Surface Modification Methods

A strong degree of adhesion is needed for effective transfer of stress from matrix to fibres in composite materials. This requires surface modification of fibre surfaces. Strongly polarized cellulose fibres are not inherently compatible with the hydrophobic non-polar polymers matrices. Also the poor resistance to moisture absorption makes natural fibres less attractive for making composites to be used in outdoor applications. Additionally for several technical oriented applications, the fibres have to be specially prepared or modified regarding homogenisation of the fibres' properties, degrees of elementarisation and degumming, degrees of polymerisation and crystallisation, moisture repellence, and flame retardant properties [45].

There are two methods of improving the fibre-matrix interface: physical methods and chemical methods. Physical methods do not change chemical composition of fibres, but improve mechanical bonding to polymers. Commonly used methods are stretching, clantering, thermotreatment, production of hybrid yarns, electric discharge, corona treatment, cold plasma treatment and alkalisation.

Chemical modification is defined as a chemical reaction between some reactive constituents of the natural fibres and chemical reagent, with or without catalyst, to form a covalent bond between the two. In chemical methods, coupling agents are used to bring about compatibility between strongly polarized cellulose fibres that are inherently incompatible with hydrophobic polymers [83]. These coupling agents react with the hydroxyl groups of cellulose and the functional groups of the matrix. General methods used are change of surface tension, impregnation of fibres, and chemical coupling. The surface modifications due to coupling agents cause noticeable improvements of the characteristic values of composites. The most commonly used chemical methods are liquid ammonia, esterification, silane coupling method, isocynates, permengnates and graft copolymerisation. In this research, plasma, alkalisation and acetylation were used for surface treatments of hemp fibres.

2.4.6.1 Plasma Treatment

Plasma is a partially ionised gas which contains ions, electrons, atoms and neutral species. The process acts under vacuum conditions to ionise the gas in a controlled and qualitative way. So a vacuum vessel is pumped down to a pressure in the range of 10^{-2} to 10^{-3} mbar with the use of high vacuum pumps. The gas introduced in the chamber is ionised with the help of a high frequency generator. The environment formed, plasma, is also known as the 4^{th} state of matter. This environment interacts with the surface of the material being treated to make it more reactive.

The main advantage of plasma is that it is a well controlled and reproducible technique. Another advantage is that it only reacts with the surface of the material, so the bulk of material being treated remains unaltered. Surface activation takes place by the replacement of weak bonding by high reactive hydroxyl, carbonyl and carboxylic groups. The type of functional group formed is dependent on the type of gas used.

There are three important components of a plasma system: the material being treated, the vacuum pump, and a high frequency generator for generating plasma. The following sequence follows in a plasma process: 1) Evacuation of the chamber by using vacuum pumps, 2) inletting the process gas inside the chamber and ignition of plasma, and 3) venting of chamber and removal of material.

The ionisation of the process gas starts with the collision of an electron produced by an electrode with a molecule of the process gas. A further electron is shot out from the molecule. The molecule becomes a positive ion and goes to the cathode. The electron goes to the anode and strikes further molecules. The accelerated cations release numerous electrons from the cathode. This process continues like an avalanche until the gas is completely ionised.

Plasma technology chemically and physically modifies the top molecular layers of the surface of a material. As a result, the surface is chemically cleaned and the surface energy rises sharply. The surface becomes activated and new and highly reactive chemical groups are created on the surface. This allows complete wetting and spreading of a liquid on the surface, leading to robust adhesion of thin films and coatings. A thin film of another material can be applied on the activated surface due to excellent adhesion of the treated surface.

2.4.6.2 Alkalisation/ Mercerisation

The standard definition of mercerisation proposed by ASTM D1695 is: "the process of subjecting a vegetable fibre to the action of a fairly concentrated aqueous solution of a strong base so as to produce great swelling with resultant changes in the fibre structure, dimension, morphology, and mechanical properties". The definition does not mention the alkali concentration to be used or the treatment temperature.

Mercerisation is an alkali treatment method and depends on the type and concentration of the alkaline solution, its temperature, time of treatment, tension of the material as well as the additives used. Most of the non-cellulosic components and part of the amorphous cellulose are removed by this process. It results in the removal of hydrogen bonding in the network structure. Normally sodium hydroxide (NaOH), also called caustic soda, is used in this process.

Native cellulose, also called cellulose I, is a semi-crystalline polymer consisting of short alternating crystalline and amorphous regions in the cellulose chains [84]. It shows a monoclinic crystalline lattice which can be changed into different polymorphous forms through chemical or thermal treatments. The important ones are alkali-cellulose and cellulose II, as shown in Fig. 2.8 [85]. As a result of sodium hydroxide penetration into crystalline regions of cellulose I, alkali cellulose is formed. After unreacted NaOH is leached, regenerated cellulose (cellulose II) is formed. The transformation is an irreversible exothermic process resulting in the modification of elementary cells. The reaction equation is shown below.

$$\text{Fibre-OH} + \text{NaOH} \rightarrow \text{Fibre-O-Na}^{+} + \text{H}_2\text{O}$$

The effect of alkali on a cellulose fibre is a swelling reaction, during which the natural crystalline structure of the cellulose relaxes. The type of alkali (KOH, LiOH, NaOH) and its concentration will influence the degree of swelling, and hence the degree of lattice transformation into cellulose II. Experiments have shown that Na+ has got a favourable diameter, able to widen the smallest pores in between the lattice planes and penetrate into them. Therefore sodium hydroxide results in a high swelling. After removal of surplus NaOH the new Na–cellulose-I (alkali cellulose) lattice is formed, a lattice with relatively large distances between the cellulose molecules, and these spaces are filled with water molecules. The OH-groups of the cellulose are converted into

ONa-groups, expanding the molecules dimensions. Subsequent rinsing with water removes the linked Na-ions and converts the cellulose to a new crystalline structure: cellulose II. This lattice is thermodynamically more stable than cellulose I. Thus sodium hydroxide can cause a complete lattice transformation from cellulose I to cellulose II, in contrast to other alkalis. Thus this process depolymerises cellulose I molecular structure producing short length crystallites.

By removing the natural and artificial impurities, alkali treatment leads to fibrillation of the fibre bundle into smaller fibres. It reduces the fibre diameter thereby increasing the aspect ratio. This treatment increases surface roughness, resulting in better mechanical interlocking and the amount of cellulose exposed on the fibre surface. This increases the number of possible reaction sites and allows better fibre wetting.

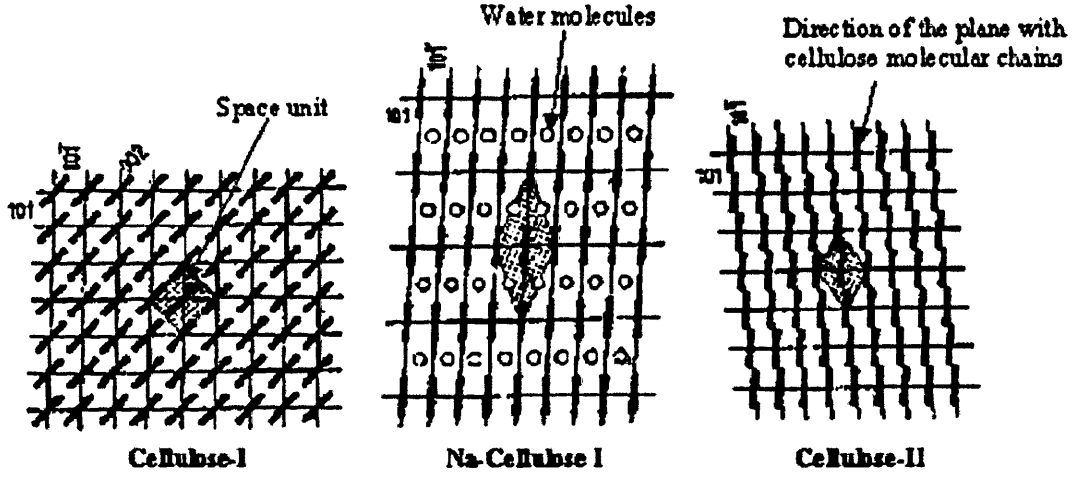

Fig. 2.8: A schematic representation of the crystalline lattices of cellulose I, Na-cellulose I and cellulose II [85]

Moreover alkali treatment influences the chemical composition of fibres, the degree of polymerisation, and molecular orientation of the cellulose crystallites, due to removal of cementing substances such as lignin and hemicellulose [81]. Hemicellulose has been shown to be very sensitive to caustic soda which exerts only slight effect on lignin or cellulose. With the removal of hemicellulose because of alkalisation, the interfibrillar region is likely to be less dense and rigid and thereby makes the fibrils more capable of rearranging themselves along the direction of tensile deformation. When natural fibres are stretched, such rearrangement amongst fibrils results in better load sharing in them

and hence results in higher stress development in the fibre. As lignin is removed gradually, the middle lamella joining the ultimate cells is expected to be more plastic as well as homogenous due to gradual elimination of microvoids. The treatment also results in decrease in spiral angle and increase in molecular orientation and crystallinity index , which result in increase in the stiffness of fibres.

It has been reported [86] that the alkaline boiling process is a very effective method of removing pectin and lignin from hemp fibres for textile applications.

2.4.6.3 Acetylation

Acetylation has been used for years to improve the properties of wood cellulose like moisture repellency, dimensional stability and environmental degradation [84]. Their use in improving the properties of natural fibres has increased in the last decade or so. The method is based on the reaction of lignocellulosic material with acetic anhydride at elevated temperature, with or without a catalyst. Acetic anhydride reacts with the more reactive hydroxyl groups according to the equation [84],

$$\text{Fibre-OH} + 3(CH_3CO)_2 \rightarrow \text{Fibre-O-CO-}CH_3 + 3\ CH_3COOH + 54\text{Kcal}$$

The acetylation of hydroxyl groups reduces hydrophilicity, causes bulking of cell wall and renders the materials less susceptible to biological decay.

2.4.7 Natural Fibre Reinforced Composites

The first natural composite material known in history was made in ancient Egypt some 3000 years ago, which was clay reinforced with straw to build walls. With the development of more durable materials like metals, the interest in natural fibres was lost.

2.4.7.1 A brief history

The use of natural composite materials by human kind is almost as old as the species itself, notably through animal and plant fibres reinforced with other materials. The Egyptians invented papier-mache and there is evidence of the use of natural fibres by the Inca and Maya civilisations in making clay pottery to improve toughness ([87], [88]). In the USA in 1850s, shellac was compounded with wood floor to mould union

cases to display early photographs. In France at the same time, Lepage worked in France with albumen and wood flour to produce his decorative Bois Durci plaques.

The history of 'modern' natural fibre reinforced composites can be traced back to the advent of synthetic polymers in the early part of the 20th century [89]. With the invention of Bakelite phenolic resin in 1909, natural fibre in the form of wood flour or waste strings and rags, were added to form the earliest forms of composites. These composites were used in radio and speaker cases [89].

Much of the early work on natural fibre reinforced synthetic resins was spurred on by the search for lighter materials for use in aircraft primary structures. In 1924, Caldwell and Clay carried out research into the use of fabric reinforced synthetic resins for airscrews. In 1930s a composite called Gordon Aerolite was developed by reinforcing phenolic resin with unidirectionally aligned flax thread [88]. It was used in the fabrication of a wing spar for the Bristol Blenheim and an experimental fuselage for the Spitfire fighter because of concerns regarding shortage of aluminium during World War II. The research had to be discontinued because the shortage of material did not materialise. Cellulose reinforced composites were also used in making aircraft drop tanks and aircraft pilot seats for Spitfire during the war. The hygroscopic nature of these materials and the high moulding pressures required in their fabrication inhibited their further development. Further details about the development of these earlier green composites can be seen in the excellent article written by Hughes [89].

On display in the Science Museum, London, is a coffin made in 1938 of phenolic resin reinforced with wood flour (www.sciencemuseum.org.uk/ accessed on 10/01/2008). This coffin is believed to be the largest phenolic moulding in the world. The coffin did not go into large scale production because of the inventor's death in 1944 during World War II. It was discovered in the attic of the Bakelite Company, London, in 1985.

In 1941, hemp fibres (and flax) were used in resin matrix composites for the bodywork of a Henry Ford car which was able to withstand ten-times the impact on an equivalent metal panel [90]. Unfortunately the car did not make into general production due to economic limitations at the time. By the mid 1940s, the use of cellulosic fibre, either as a fabric or in paper form, reinforced polymers was well established. They were used for making seats, bearings, and fuselages in aircraft during WWII due to shortage of aluminium at that time. One example of this, the Gordon-Aerolite, has already been

described above. Another example was a cotton-polymer composite which was reportedly the first fibre-reinforced plastic used by the military for aircraft radar. In Europe, the body of the East German "Trabant" car, made between 1950 and 1990, was one of the first to be built from material containing natural fibres (cotton fibres embedded in a polyester matrix).

As late as 1947, Brown [91] was optimistic enough to predict about the "great extension in the application of this material". However these predictions were short-lived. The commercial success of glass fibre, having superior properties than natural fibres, and concurrent development of synthetic resins such as unsaturated polyester resins and epoxies during and just after the Second World War led to the mass production of synthetic composites, and corresponding decline in use of natural fibres in these composites.

2.4.7.2 Contemporary applications

Ecological concerns of society in issues such as sustainability, recyclability, and environmental safety in 1990s resulted in renewed interest in natural fibre composites. Two principal drivers have contributed to this surge in interest in natural fibre composites – environment and cost. Driven by increasing environmental awareness, automakers in the 1990s made significant advancements in the development of natural fibre composites, with end-use primarily in automotive interiors. A number of vehicle models, first in Europe and then in North America, featured natural fibre-reinforced thermosets and thermoplastics in car components, as described in the Introduction chapter. Indeed a company in Japan went to the extent of making a complete car body of natural fibre composite components [10].

In recent years, the demand for natural fibre composites has increased for such products as decking, window/door profiles, fencing/siding/railings, furniture, flooring, and automotive parts, pallets/crates/boxes, and marine components. The components made from natural fibre composites for automotive applications are: head rest, seat back, roof liner, back covering, parcel shelf, rear hatch, trunk base, sub-floor covering, door covering, bonnet insulation, and roof reinforcement.

Daimler-Benz has been working on replacement of glass fibres with natural fibres in automotive components since 1991. Mercedes-Benz used coconut fibres in their

vehicles over a nine year period. Mercedes first used jute-based door panels in its E-class vehicles in 1996. In 2000, DaimlerChrysler started using sisal fibres for vehicle production.

Promoted as low-cost and low-weight alternatives to fibreglass, natural fibre composites signalled the start of a "green" industry with enormous potential. In 2000, the North American market for these natural fibre composites exceeded $150 million. In the same year the European car industry consumed 28,300 tons natural fibre, including 20,000 tons of flax, 3700 tons of jute and 3500 tons of hemp fibres [7].

Germany has been at the forefront of using natural fibres in composite materials for automobile applications. A recent survey [92] found that the use of natural fibres (excluding wood and cotton) in automotive composites almost doubled from 9,600 tonnes in 1999 to 19,000 tonnes in 2005. Flax fibres had the biggest market share at 65%, followed by hemp fibres at 10%. According to authors the market share of hemp fibres can be increased by establishing further processing capacities or by reduction in hemp insulation material market. Similarly the use of natural fibre reinforced composites doubled from 15,000 tonnes in 1999 to 30,000 tonnes in 2005. On average the 5.4 million passenger cars produced in 2005 used 18 kg of natural fibres per car.

The consumption of hemp fibres in European Union also increased in this time. Another survey [93] found the market share of hemp fibre in automotive industry in EU countries increased from 1% in 1996 to 15% in 2002.

In 2008, the British company Lotus (www.lotuscars.com) unveiled its environment friendly car Eco Elise. The car uses hemp, sisal and wool fibres in the manufacture of interior trim, roof, seat covers and hard top. The car has received the thumbs-up from drivers of TV programme on automotives Top Gear.

Window frames and floor coverings made of hemp fibre reinforced polymer composites were used during the 2008 Beijing Olympics [94].

A consortium of European companies is working on a project called BioCompass (www.biocompass.org.uk) assessing the environmental credentials of naturally derived construction materials. The project is focusing on key issues such as raw material supply, energy requirement, durability of naturally derived materials compared to conventional alternatives, and end-of-life issues.

Another project called COMBINE (www.combineproject.org.uk) is doing research on developing high performance bio-derived composites for structural applications by using innovative combinations of natural fibres and bio-plastics. The technology will be demonstrated by manufacturing and testing three case study components – a marine bar top lid, a marine wheelhouse roof and a mobile baby incubator. The project started in November 2006 and will take 30 months to complete. The total value of the project is one million pounds.

BioComp (www.biocomp.eu.com) is a project being run by 25 European companies and research institutions. The main objective of this project is to obtain a breakthrough for SMEs on the development and use of engineering thermoplastic and thermosetting materials mainly from natural resources, like lignin from the paper industry and from the High Pressure Hydrothermolyses (HPH) process, other biopolymers, furan resins, woven and non-woven cellulose fibres and fibre mats to final model products.

Sustainable Composites Ltd. (www.suscomp.com) is a British company that was established in 2003 to develop a range of eco-friendly manufacturing materials made from sustainable crops such as hemp and castor oil. The company has successfully made surfboard and a dinghy from these materials. They have also developed a linseed oil based resin that contains 96% vegetable oil.

A Dutch company NPSP Composieten BV (www.npsp.nl) is manufacturing diverse products using hemp and flax fibres. Examples of products are mushroom-shaped guideposts for bicycle paths, housings of radar units (glass fibres disturb the radar rays), boats, furniture and loudspeakers.

Research done by the German Aerospace Centre, DLR, has resulted in successful manufacture of industrial safety helmet, train seat panels, and CD holder based on natural fibre composites [95]. Pipes, slabs and car door interior panelling have also been developed from natural fibre-biodegradable polymer composites [96]. Four German companies, sponsored by the German government, have launched an internet portal, www.n-fibrebase.net, which contains databases of the properties and markets of natural fibre composites.

Eureka Factory Ecoplast (www.eureka.be/ecoplast) project has successfully developed natural fibre reinforced thermoplastic composites which are being used as parts in vacuum cleaners, lawn mowers, storage boxes, and speaker boxes.

Milliken, a Belgium-based company, has developed Halo, a natural fibre thermoplastic composite. Halo utilizes advanced non-woven fabric formation technology to achieve a performance level with natural fibres that can compete with fibreglass-reinforced products (www.netcomposites.com, accessed on 9/4/2008).

The Council for Scientific and Industrial Research (CSIR), South Africa (www.csir.co.za), is investigating the use of natural fibre composites in construction. Their research has confirmed that the properties of natural fibre composites fall within the range of those required for load-bearing elements.

Use of natural fibres with cement matrix has been used to make low cost building materials, like panels, claddings, roofing sheets and tiles, slabs and beams. Door shutters, door frames, roofing sheets, and shuttering plates from sisal and jute composites have been successfully developed in India [11].

One estimate [97] puts the present production volume of natural fibre composites in Europe at 100,000 tons, half of which are consumed by the European automotive industry.

2.4.7.3 Future outlook

On display in the Science Museum in London is the model of a futuristic car made of kenaf fibre reinforced lignin matrix composite (www.sciencemuseum.org.uk/ accessed on 10/01/2008). Full of revolutionary technology, this one-Unit concept car, designed by Toyota, Japan, uses plant-based materials instead of oil-based plastics and metals for its body. This is one example of the potential of natural fibre composites to replace conventional materials in future.

The technology road map for plant/ crop based renewable resources 2020, developed by the U.S. Department of Agriculture and the U.S. Department of Energy, has set a target of 10% of basic chemical building blocks to be made from plant-based renewable resources by 2020, with developed concepts in place by then to achieve a further increase to 50% by 2050 [3].

The 4th International Conference of the European Industrial Hemp Association (EIHA), held in November 2006 in Germany, revealed a globally increasing interest in hemp raw materials due to worldwide raw material shortages [94]. It was also pointed out that because of increasing wood prices worldwide, manufacturers have started to use hemp as a replacement material in lightweight chip boards. The conference concluded that the demand of hemp fibre was bound to increase in coming years.

On the other hand, a workshop on natural fibre reinforced plastics organised by German Federation of Reinforced Plastics (www.avk-frankfurt.de) in February, 2007, concluded that natural fibre reinforced plastics needed to be made more competitive through innovation. It also concluded that while natural fibres had established their market share in the automotive industry, biopolymers were unlikely to tap into the industrial market in the near future.

In the comprehensive 2008 research report "European Markets for Naturally Reinforced Plastic Composites" [98], the analysts note that the current penetration of wood plastic composites in decking and natural fibre composites in the automotive segment remains below 10 per cent, with further potential to increase. However, users of natural fibre composites have concerns over the available capacity and the effect of a drastic reduction in European agricultural subsidies. Still, both the environmental benefits and cost competitiveness of natural fibre composites give these materials the capacity to replace plastic or non-renewable reinforcements. The main market segments for natural fibre composites in 2008 were automotive, building and technical parts. However, while the natural fibre composites automotive market is developed in Europe, other regions could provide more growth. Growth opportunities abound for natural fibre composites in Europe. "Ultimately, however, suppliers will have to concentrate on raising public awareness and product development to boost market penetration in existing segments and open up new opportunities", the report concludes.

2.4.7.4 Suitability of natural fibres for use in composites

The mechanical properties of composite material are largely dependent on the properties of the fibres and the ratio of the load carried by the fibres. The ratio of the total load carried by fibres is given by [22]:

$$\frac{P_f}{P_c} = \frac{(E_f/E_m)}{(E_f/E_m)+(V_m/V_f)} \quad \text{.....(2.10)}$$

where P_f is the load carried by the fibres, P_c is the total load on the composite, and E_f, E_m, V_m and V_f are fibre modulus, matrix modulus, matrix volume fraction and fibre volume fraction respectively. Thus to use high strength fibres most efficiently, the fibre modulus should be much greater than matrix modulus. The percentage of load carried by the fibres will be higher for higher E_f/E_m ratio and a higher volume content of fibres. Thus for a given fibre-matrix system, the fibre volume fraction must be maximised if the fibres are to carry a higher proportion of the composite load.

The excellent strength of glass fibre reinforced composites is a result of high strength of the fibres and a high E_f/E_m ratio of approximately 20. Considering the maximum reported modulus value of 70 GPa of hemp fibres and that of polyester (3.7 GPa), the E_f/E_m of hemp fibres in polyester matrix is also approximately 20. Using a typical fibre volume fraction value of 50%, the fraction of the total load P_c carried by the fibres is

$$P_f = \frac{20}{20+1} = 0.95\ P_c$$

It is thus seen that the natural fibres can carry as much as 95% of the total load on the composites. This suggests that natural fibres can carry the load vey efficiently in a composite material and hence are good contenders to replace glass fibres.

Another important parameter for efficient transfer of the load from matrix to fibre is the aspect ratio which should be at least in the range 100-200 [46]. Most of bast fibres have aspect ratio in the range 500-1000. The high aspect ratio of natural fibres means they can transfer the stress very efficiently because of good surface area for adhesion and makes them suitable for use in composites. Low density and higher specific mechanical properties of natural fibres also make them attractive as reinforcements in polymer matrix composites.

The critical length of fibre is an important parameter for short fibre composites. The length of the fibres should be greater than the critical length for them to effectively carry the load. The value of critical length of a fibre is given by

$$l_c = \sigma_f D / 2\tau \quad \text{.....(2.11)}$$

where σ_f is the fibre fracture strength, D is the diameter of the fibre and τ is the interfacial shear strength or the matrix shear strength. Using typical values of 500 MPa for σ_f, 50 μm for D, and 5 MPa for τ, the values of l_c for natural fibre composites comes out to be about 2.5 mm. Therefore a fibre of length 12.5 mm (five times the critical length) can carry an average fibre stress of 90% of fibre fracture stress. Most of the bast fibres have lengths greater than this and hence can effectively bear the stress.

These arguments point at the good potential of natural fibres to be used as reinforcement in polymeric composites.

2.4.7.5 Advantages and Disadvantages of Natural Fibre Composites

The main advantages of natural fibre composites are:

Low density, which results in comparable, if not higher, specific strength and stiffness compared to glass fibre composites; low cost; less tool wear; and good thermal and acoustic insulating properties.

The main disadvantages of natural fibre composites are:

Lower strength properties, in particular impact strength; variable properties; moisture absorption leading to degradation of mechanical properties and dimensional instability; limited maximum processing temperature; lower durability; and poor fire resistance.

2.4.7.6 Fabrication

Most commonly used processing methods for fabrication of synthetic fibre reinforced polymers can also be applied to natural fibre composites. Hand lay-up is the most widely used and convenient method to make natural fibre reinforced thermosetting matrix composites. Other methods used for making natural fibre composites with either thermosetting or thermoplastic matrix, are injection moulding, vacuum injection, filament winding, resin transfer moulding (RTM), pultrusion, bulk and sheet moulding and film stacking. In this research a combination of hand lay-up and compression moulding will be used for making laminates. A brief description of the hand lay-up process is given below.

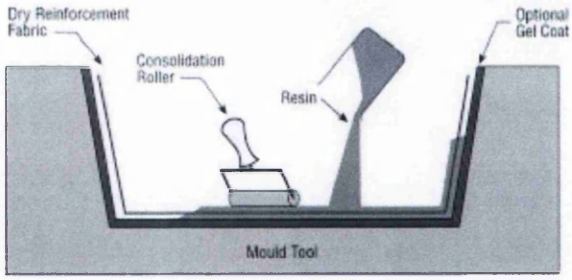

Fig. 2.9: A schematic diagram of hand lay-up process [99]

As shown in Fig. 2.9, resins are impregnated by hand into fibres which are in the form of woven, knitted, stitched, bonded fabrics or non-woven mats. This is usually accomplished by rollers or brushes, with an increasing use of nip-roller type impregnators for forcing resin into the fabrics by means of rotating rollers and a bath of resin. Laminates are left to cure under standard atmospheric conditions for the duration as recommended by the resin manufacturer. For some resins, post-curing is recommended to get optimum properties.

It is a low/medium volume method for making large, relatively simple parts. The most common applications are boat hulls, tanks, equipment housings, building panels, standard wind turbine blades. This process is low in investment costs and extremely flexible in production. The main disadvantage is the difficulty of removing all the trapped air in the laminate.

2.4.7.7 Matrix Materials

Matrix materials most commonly used in natural fibre composites are shown in Table 2.10.

Table 2.10: Matrix materials used in natural fibre composites [70]

Thermosets: Phenolic, Epoxy, Polyester, Polyimide, Polyurethane

Thermoplastics: Polypropylene, Polyamide, Polyethylene, Polystyrene, Polyvinyl chloride

Rubber and Natural Polymers: India rubber, Modified starch, Polyactide, Cellulose ester, Tannin, Polyhydrooxybutivic acid, lignin based epoxy, soy-based resins.

2.4.7.8 Natural Fibre Reinforced Thermoplastics

Thermoplastics offer many advantages over thermoset polymers for use with natural fibres like low processing cost, design flexibility, and ease of moulding complex parts. Their biggest disadvantage is that their processing temperature is restricted to below 230 °C to avoid thermal degradation of natural fibres. Only those thermoplastics are useable for natural fibres whose processing temperature does not exceed 230 °C, for example, polyethylene and polypropylene. Other thermoplastics like polyamides, polyesters and polycarbonates, that require processing temperatures of greater than 250 °C, can not be used with natural fibres.

Natural fibres generally have higher modulus than thermoplastics, thus resulting in higher modulus composites [100]. Natural fibre reinforced thermoplastic composites are flexible, tough and show good mechanical properties. However the fibre orientation in these composites is random and accordingly property improvement is not as high as in thermoset composites. Thermoplastics have significant viscosity and therefore their good wetting with natural fibres is difficult to achieve. Increasing their temperature to reduce viscosity could damage the natural fibres.

Polypropylene (PP) is the most extensively used thermoplastic in natural fibre composites owing to its low density, excellent processibility, good mechanical properties, high temperature resistance, good dimensional stability and good impact strength. Mutje et al [101] determined polarities of hemp fibres, glass fibres and polypropylene and observed hydrophobic behaviour of glass and PP in contrast to very hydrophilic nature of hemp fibres. However it was found that irregular surface morphology of hemp could still improve the fibre-matrix adhesion. The tensile strength of hemp-PP composites was 50% of that of glass-PP composites and tensile modulus was 80% of glass-PP composites at 40% fibre weight fraction. Using maleated polypropylene (MAPP) as a compatibility agent resulted in considerable increase in tensile properties of hemp-PP composites. Mechanical properties of some selective natural fibre-PP composites and glass fibre-PP composites are shown in Table 2.11.

Wambua et al. [102] studied the mechanical properties of natural fibre/ polypropylene composites, using kenaf, coir, sisal, hemp and jute fibres, all at 40% fibre weight fraction. Hemp fibre composites showed the highest tensile strength of 52 MPa while coir showed the lowest (10 MPa). The strengths of kenaf, sisal and jute composites were

approximately 30 MPa. Similar results for flexural properties of these composite were achieved. Hemp composites showed the best flexural strength properties (54 MPa) which is comparable with glass fibre composites with propylene matrix (60 MPa). But, more importantly, the specific flexural strength of hemp composite (36.5) was higher than that of glass fibre composite (24). Similarly tensile and flexural moduli also showed similar trends. Hemp and kenaf composites registered highest tensile modulus of 6.8 GPa, which was comparable to that of glass fibre composites (6.2 GPa). It was lowest for coir composites with 1.3 GPa. Again the specific moduli of hemp and kenaf composite (4.6) were higher than that of glass fibre composite (2.5). The flexural modulus was again highest for hemp composite at 5 GPa and it was lowest for coir composite at 0.5 GPa. Finally, the Charpy impact strength of these composites was investigated. The impact strength of these composites was found to be quite low compared to glass fibre composites. The maximum impact strength was registered for hemp and sisal composites which was 25 kJ/ m^2 whereas it was 54 kJ/ m^2 for glass fibre composites. The mechanical properties of hemp composites proved them as a promising candidate to replace glass fibre. The specific properties of natural fibre composites were better than those of glass. It was concluded that natural fibres composite have potential to replace glass in many applications that do not require very high load bearing capabilities.

Table 2.11: Mechanical Properties of (untreated) Natural fibre Reinforced Polypropylene Composites

Fibre/ Fraction(%)	Tensile Strength (MPa)	Tensile Modulus (GPa)	Flexural Strength (MPa)	Flexural Modulus (GPa)	Impact Strength (J/m^2)	Reference
None	20-40	1.0-1.4	42.1	1.1	16	[21]
Woodflour/ 50(wt)	38	5.5	44	5.3	22(J/m)	[100]
Newsprint/40(wt)	32.3	3.22	57.4	3.53	30.3(J/m)	[103]
Kenaf/ 50(wt)	65	8.3	98	7.3	32	[100]
Banana /30(wt)	38	3.06	56	3.2	-	[104]
Bamboo/20(wt)	20.3	2.1	27	3.1	-	[105],[106]
Hemp /30(wt)	22.1	10.2	-	-	-	[107]
Hemp /40(wt)	40.2	3.55	73.3	4.1	29	[103]
Hemp / 50(wt)	50	6.5	85	4	53(kJ/m^2)	[108]
Hemp/ 30(wt)	32.3	1.53	48.5	1.67	15.1(kJ/m^2)	[109]
Hemp/ 30-70(wt)	55	6.7	85	4.7	46(kJ/m^2)	[110]
Hemp/ 64(wt)	42	-	63	-	152	[111]
Hemp/ White rice husk ash/ 40(wt)	34 22.48	2.7 2.03	41.5	2.3 2.3	3.89(kJ/m^2) 180	[112] [113]
Sisal/	30	1.09	49.2	2.44	106(J/m)	[114]
Glass/22(vol)	88.6	6.2	60.0	4.4	54.12(kJ/m^2)	[115]

2.4.7.9 Natural Fibre Reinforced Thermosets

Although the use of thermoplastics in natural fibre composites is increasing, natural fibre reinforced thermosets still constitute the majority of the composites made from natural fibres. The most commonly used thermosets are polyester, epoxy, and vinylester. The natural fibre composites made with thermosets are highly solvent resistant, tough, and creep resistant. The fibres can carry as much as 80% of the load in these composites [116].

The mechanical properties of thermoset biocomposites depend on the mechanical properties of the matrix and the fibre as well as the interfacial bonding between the two. Interfacial bonding between the matrix and the fibre depends on three factors: mechanical anchoring, physical attractive forces (van der Waals force and hydrogen bond), and chemical bonding between the matrix and the fibre. The surface of the natural fibre contains many hydroxyl groups in its chemical structure which make hydrogen bonds with the hydroxyl groups in the main backbone chain of the matrix. The polyester resin, having no hydroxyl group in its backbone chain, has generally the weakest bonding with the natural fibre compared to epoxy and vinylester resins [117]. Considerable shrinkage (up to 8%) during curing of polyester resin also weakens this bonding.

Unsaturated polyester resin is by far the most widely used thermoset for natural fibre composites. Table 2.12 shows the summary of mechanical properties of various natural fibre composites with unsaturated polyester resin reported by various researchers.

Early attempts to investigate the mechanical properties of sunhemp fibre reinforced polyester composites were made by Sanadi et al. [118]. They found that tensile strength of these composites varied from 50 MPa to 150 MPa depending on fibre volume fraction of 5% to 40%. Young's modulus varied from 5 GPa to 13 GPa and the Izod impact strength ranged from 6 kJ/m^2 to 20 kJ/m^2. It should be pointed out the composites were made by using unidirectional fibres; hence these values are higher than for the fibres used as randomly oriented mats.

Hepworth et al. [119] studied the properties of flax fibre/ epoxy composites. With 80% fibre volume fraction, composites with stiffness of 26 GPa and strength of 378 MPa

were made. However composites of flax fibre made with phenolic resin produced poor composites with stiffness of only 3.7 GPa and strength of 27 MPa.

Hautala et al [120] fabricated plywood-type composites from hemp fibre strips and epoxy resin. The flexural strength was found to be comparable to that of traditional plywood. The appearance, manufacturing properties and workability was also found to be suitable for floor and furniture applications. By using 48 layers of hemp or flax fibres, composites of even greater strength were manufactured. The flexural strength of the composites at 50-60% fibre weight fraction was determined at 140 MPa and flexural modulus at 6 GPa.

Aziz and Ansell [121] studied the mechanical properties of hemp and kenaf -fibre reinforced polyester composites, untreated and with alkali treatment. The alkali-treated fibres of both types of composites showed superior flexural strength and flexural modulus values compared to untreated fibres. The improvement in properties was observed for short, long and random mat fibres.

They also studied the effect of using specially formulated polyester resins for natural fibres. These resins are more polar in nature, making them hydrophilic so that they can bond better with the OH-groups on the surface of natural fibres. It was observed that these polyesters made a positive impact to the strength of the composites. The flexural stiffness of these composites was found to be close to that of glass fibre composites. A considerable improvement was also observed in flexural strength of these composites.

Richardson and Zhang [122] studied the effects of non woven hemp on mechanical properties of phenolics and their micro structural features. They found a significant increase in flexural strength and modulus in phenolics with the introduction of non-woven hemp. Impact toughness was substantially improved. This improvement was attributed to two factors. First that hemp is tougher and stronger mechanically than the phenolic matrix and this leads to increase in mechanical properties. The second is that the presence of hemp has the capability of reducing void (defect) numbers and dimensions, which significantly contributes to improvement in mechanical properties.

Rouison et al [123] also studied the optimization of RTM process in manufacturing hemp fibre composites and their mechanical properties. The tensile strength of hemp fibre/ polyester composites increased linearly with increasing fibre content above 11%

fibre volume fraction. A maximum tensile strength of 60 MPa was achieved for fibre volume fraction of 35%. The results for tensile modulus also showed a similar trend. Again a maximum elastic modulus of 1.7 GPa was achieved for fibre volume fraction of 35%. The flexural strength and flexural modulus also increased linearly with increasing fibre volume fraction. The highest values attained for flexural strength and flexural modulus were 113 MPa and 6.4 GPa respectively. The impact strength of these composites also increased with increasing fibre content. The highest impact strength of 14.2 kJ/ m^2 was achieved again for fibre volume fraction of 35%. Finally flexural creep properties of 21% fibre content were investigated. It was found that these materials are not suitable for use under high fatigue load conditions.

Sebe et al. [124] studied the flexural and impact properties of hemp fibre-reinforced polyester composites made by Resin Transfer Moulding technique. Flexural stress at break and flexural modulus showed an increasing trend with increasing fibre content. Impact strength was found to decrease at low fibre content, and then gradually increase with further addition of fibres.

Yamamoto et al. [125] studied the processing and mechanical properties of natural fibre composites. They used three kinds of kenaf-hemp non-woven materials impregnated with acrylic matrix. The mixing ratio of kenaf/hemp was 50:50. The prepregs were compression moulded. The tensile strength of these composites varied from 28 MPa to 75 MPa for moulding pressure of 1.5 MPa to 6 MPa. The tensile modulus varied form 3.9 GPa to 11 GPa. Elongation to fracture varied from 0.8% to 1.4%. The fractographic study of fractured samples was carried out which showed good adhesion between fibre and matrix.

Khoathane et al [126] studied the mechanical and thermal properties of hemp fibre reinforced 1-pentene/polypropylene copolymer composites. At fibre weight fraction of 30%, tensile strength was measured at 25 MPa, tensile modulus at 2.5 GPa, flexural strength at 3.3 GPa, and impact strength at 1.3 kJ/m^2. The thermal stability of the composites was found to be better than that of the fibres or the matrix as individual entities.

Table 2.12: Mechanical Properties of (untreated) Natural Fibre Reinforced Unsaturated Polyester Composites

Fibre	Fibre wt/vol fraction (%)	Tensile Strength (MPa)	Tensile Modulus (GPa)	Strain to failure (%)	Flexural Strength (MPa)	Flexural Modulus (GPa)	Impact Strength (kJ/m^2)	Reference
Jute	60 (vol)*	250	35	-	-	-	22	[127]
	44±2 (wt)	59.2	6.5	-	89	9	-	[117]
	60 (wt)	132.4	2.9	5.83	140.4	13.85	-	[128]
	45 (vol)	60	7	-	92.5	5.1	29	[129]
	36 (vol)	69.4	9	-	104.4	7.36	14.3	[130]
	63(vol)	61.1	5.6	0.89	116	-	-	[131]
	30(wt)	66	4.42	2.3	93.8	-	-	[11]
Sunhemp	24 (vol)*	125	11.2	-	-	-	21.5	[118]
	54 (wt)	60	-	-	-	-	-	[132]
Coir	25 (wt)*	26	-	-	61.3	-	0.97	[133]
		144	4.7	14.2	-	-	-	[134]
	30(wt)	20.4	2	1	41.5	-	-	[11]
	45(wt)	39.8	3.6	5.2	43.7	4.11	16.5	[134]
Oil palm		129	3.6	9.7	-	-	-	[134]
	45(wt)	35.1	3.29	3.75	41.6	3.85	16.7	[134]
Flax	55 (wt)*	157	42.5	0.97	-	-	-	[135]
Sisal	50 (vol)	29.7	1.15	9.52	59.6	11.9	-	[136]
	30 (wt)	68.3	-	-	107.8	-	163.6(J/m)	[137]

	54 (wt)	50	-	-	-	-	-	[132]
	43(vol)	67	2.19	6	84	3.5	-	[138]
	50(wt)	40	2.13	4-6	77	-	-	[11]
Isora	45(vol)	190	7.5	-	240	14	440(J/m)	[139]
Pineapple	30 (wt)	43.4	-	-	85.8	-	-	[140]
	30 (wt)	52.9	2.3	-	80.2	2.76	24.2	[141]
Wheat straw	40 (wt)	-	8	-	56	7.3	7	[142]
Elephant grass	31 (vol)	118	2.17	-	-	-	-	[143]
Banana	10(vol)	-	-	-	57	2	54	[144]
	51 (wt)	60	-	-	-	-	-	[132]
Pandanus	10(vol)	-	-	-	43	1.8	24	[144]
Hemp	35(vol)	60.2	1.74	-	112.9	6.4	14.2	[123]
	36(wt)	-	-	-	110	7.5	13	[108]
	30(vol)	38	6	-	100	6.5	20(J/m)	[145]
	20(vol)	33	1.42	-	54	5	4.8	[146]
Glass (CSM)	7 (vol)	-	-	-	108	5.6	34	[108]
	20 (vol)	73.4	7.9	-	233.8	9.28	80.4	[130]

* unidirectional composites

2.4.7.10 Natural Fibre Reinforced Biodegradable Polymers

The natural fibres reinforced with biodegradable polymers result in completely 'green' composites. The advantages of using such composites with respect to environmental pollution are obvious and the research in such composites has increased substantially in recent years. Examples of biodegradable polymers are thermoplastic starch, polyhydroalkanoates (PHA), polyactides (PLA), lignin based epoxy, soy based resins, and epoxidised linseed and soyabean oil.

Table 2.13: Natural fibre reinforced biodegradable polymer composites

Fibre	Matrix	Reference
Hemp	Cashew nut shell liquid (epoxy)	[147]
Flax, hemp and wool	Epoxidised soy bean oil	[148]
Kenaf	Polylactic acid	[10]
Flax, jute, ramie, oil palm, regenerated cellulose	Polyester, polysaccharides, thermoplastic Starch	[149]
Flax, hemp, ramie	Starch, lactic acid	[96]
Manila hemp	Starch	[150]
Hemp, flax	Soy oil	[151]
Hemp	Cellulose ester	[152]
Flax, cellulose, pulp, hemp	Acrylated epoxised soyabean oil	[153]
Hemp	Polylactic acid	[154]
Hemp	Euphorbia oil	[155]
Sisal	MaterBi-Z	[156]
Sisal	MaterBi-Y	[157]
Jute	Polyesteramide	[158]

Although produced from natural sources, these polymers are not necessarily biodegradable because it depends mainly on the chemical structure (degree of cross linking) of the polymers. One of the major drawbacks of these polymers is their cost. Most biodegradable resins currently cost three to five times the cost of commonly used resins such as PP, LDPE, HDPE, and PVC [74]. Some examples of studies done on these composites are shown in Table 2.13. These studies have shown promising properties of these composites, although in most cases these properties are lower than those of natural fibre reinforced thermosets and thermoplastics.

2.4.7.11 Natural Fibre Hybrid Composites

One method of increasing the mechanical properties of natural fibre composites is by hybridising them with another synthetic or natural fibre of superior mechanical properties. The synthetic fibre mostly used for this purpose is glass fibre. Although the biodegrability of the composite is reduced, this can offset the advantages gained by the increase in mechanical properties. Table 2.14 shows some examples of the studies done on natural fibre hybrid composites.

Some researchers have also used two natural fibre reinforcements in hybrid composites as shown in Table 2.14. Two natural fibres with different microfibrillar angle, and hence different mechanical properties, can result in improved properties of composites.

Santulli [159] has identified the following factors that can be helpful in successful development of glass/ natural fibre hybrid composites: larger fibre volume fraction; improved effectiveness of interfaces in dissipating impact damage; and modification of the configuration to improve impact properties.

Table 2.14: Natural Fibre Hybrid Composites

Fibres	Matrix	Reference
Natural fibre/synthetic fibre		
Jute/ glass	Epoxy, Polyester	[160], [161], [8], [162]
Hemp/glass	Polypropylene	[163], [164]
Coir/ glass	Polyester	[165]
Sun-hemp/ carbon	Polyester	[13], [99]
Banana/ glass	Polyester	[166]
Oil palm/ glass	Polyester, Epoxy	[167], [168]
Sisal/ glass	Polyester	[169]
Flax/ glass	Polypropylene	[170]
Bamboo/ glass	Polypropylene	[105], [106]
Natural fibre/natural fibre		
Banana/ sisal	Polyester	[171]
Jute/ cotton	Novolac	[172]
Sisal/ oil palm	Natural rubber	[173]
Cotton/ kapok	Polyester	[174]
Ramie/ cotton	Polyester	[175]
Flax/ cellulose	Polypropylene	[170]

2.4.7.12 Effects of Fibre Surface Treatments

Sebe et al [124] modified the surface of hemp fibre composites, with polyester as the matrix, via esterification of hemp hydroxyl groups using mathacrylic anhydride. Increased bonding between fibre and matrix due to this treatment did not vary the flexural stress at break but was detrimental to toughness. This behaviour was ascribed to a change in the mode of failure, from fibre pull-out to fibre fracture, resulting in a marked reduction in the energy involved in the failure of the composite, leading to a more brittle material.

Rouison et al. [146] studied the effect of various surface modifications on the mechanical properties of hemp fibre/ polyester composites. Chemicals used for paper sizing (AKD, ASA, Rosin Acid and SMA) as well as silane compound and sodium hydroxide were used to modify the fibres' surface. The tensile, flexural and impact properties were investigated. All the chemicals, except alkali solution, improved substantially the hydrophobic behaviour of fibres. The paper sizing chemicals decreased the flexural and tensile properties by creating a weaker fibre-matrix interface. But the silane, SMA, and alkali treatments improved these properties slightly. These improvements were attributed to better interface interaction due to enhanced hydrophobic behaviour of fibres and, for alkali treatment, to better strength properties of fibres. The lack of strong adhesion between fibre and matrix was confirmed by the slight increase in impact strength of these samples as well as the analysis of their tensile fracture surface. A slight improvement in mechanical properties was observed for SMA, silane and alkali treated specimens. However close examination of these tests and of the fracture surface of the samples showed no improvement in fibre-matrix adhesion.

Hill et al [134] undertook extensive studies to observe the effect of acetylation on the properties of coir, palm, flax and jute fibres. The rate of acetylation was found to be proportional to the lignin content of the fibres. The effect of acetylation at reaction temperature of 120°C on the tensile properties of palm and coir fibres was found to damage the fibre structure resulting in poor mechanical properties, whereas at 100° C the modified fibres showed improved performance. Also the modified fibres showed a high degree of decay resistance over a five month test period.

Abdul Khalil and Hill [134] studied the mechanical properties of oil palm- and coir fibre-reinforced polyester composites. Composites made of fibres acetylated at 120 °C showed lower tensile properties than untreated fibres due to cell wall damage. However for treatment at 100 °C, the cell wall damage was reduced and improvements in tensile properties were observed. However the impact strength did not improve significantly following the treatment.

Bogoeva-Gaceva et al. [81] studied the effect of dewaxing, alkali treatment, cyanoethylation and acetylation on kenaf fibres. All treatments resulted in improvement of surface morphology as well as changes in crystalline structure of cellulose.

Tserki et al. [176] studied the impact of acetylation and propionylation treatments on flax, hemp, and wood fibres. The highest effect of esterification was achieved for woof fibres due to their high lignin/ hemicellulose content, followed by flax and hemp fibres. Crucially, both the acetylation and propionylation treatments reduced water adsorption in fibres, rendering them more hydrophobic. The SEM examination showed the surfaces of the esterified materials to be smoother than untreated material.

Oujai and Shanks [177] studied the effect of solvent extraction, alkalization and AN grafting of hemp fibres on surface properties and mechanical properties of hemp fibres. Spectroscopic studies and diffraction techniques showed slight decrease of crystallinity index. The structural transformation of fibres from cellulose 1 to cellulose 2 was observed at high NaOH concentration of 10-20% wt/v. The AN grafted fibres had no transformation of crystalline structure as observed after mercerization. Only a variation of X-ray crystallinity index with grafting amount was observed. Moisture regain of pre-treated and modified fibres depended on the structure of the fibre and amount of grafting.

Mwaikambu [174] also used alkalisation and acetylation techniques for hemp, sisal, jute and kapok fibres. Both treatments successfully modified the structure of natural fibres as well as increase in the crystallinity index of the fibres. A high crystallinity index resulted in stiff, strong fibres and hemp fared the best in this respect. By observing the first exothermic peak (DSC), hemp had the highest stability after acetylation. This implied that acetylation did not result in degradation of the crystalline cellulose. Fourier Transform Infrared (FT-IR) spectroscopy showed hemp to be not much reactive. But SEM results indicated that after chemical treatment, all the fibres except kapok possessed rough surfaces which increased mechanical interlocking with resins. It was concluded that hemp had the highest crystallinity index and thermal stability when alkalised and acetylated with and without acid catalyst, followed by jute, sisal, and kapok fibres.

Mwaikambo and Ansell [178] undertook a thorough analysis of physical and fine structure of hemp fibre bundles, namely surface topography, diameter, cellulose content and crystallinity index. The fibre bundles were alkalised and their physical and mechanical properties analysed. Alkalisation was found to change the surface topography of fibre bundles and the diameter decreased with increased concentration of

caustic soda. Cellulose content increased slightly at lower NaOH concentrations and decreased at higher NaOH concentrations. The crystallinity index decreased with increase in caustic soda concentration up to 0.24% NaOH beyond which, it decreased with increase in NaOH concentration.

It was also found that the tensile strength and stiffness increased with increase in the concentration of NaOH up to a limit. Tensile strength and Young's modulus increased with decrease in cellulose content, while crystalline cellulose decreased slightly but with improved crystalline packing order resulting in increased mechanical properties. Similar observations were elucidated by the crystallinity index. Alkalised hemp fibre bundles were found to exhibit a similar specific stiffness to steel, E-glass and Kevlar 29 fibres. The results also showed that crystallinity index obtained following alkalisation had a reverse correlation to the mechanical properties. Stiffer alkalised hemp fibre bundles were suitable candidates as reinforcements to replace synthetic fibres. The improvement in mechanical properties of alkali treated hemp fibre bundles confirmed their use as reinforcement.

Kostic et al [73] studied the effect of alkalisation of varying concentrations at different temperatures on hemp fibres. The treated hemp fibres were finer, with lower lignin content, increased flexibility, and in some cases tensile properties were improved.

FTIR analysis of 8% wt/vol NaOH treated hemp fibres by Ouajai and Shanks [179] indicated the removal of pectin and hemicellulose by this treatment. The IR lateral crystallinity index exhibited slight decrease following this treatment indicating the presence of less ordered cellulose structure. X-ray diffraction studies of untreated hemp fibres showed the characteristics of cellulose I. Following NaOH treatment of up to 20% wt/vol, the crystalline transformation to cellulose 2 was observed which resulted in decrease of crystallinity.

It is generally accepted that interfacial adhesion can be best described in terms of dispersion forces and acid–base interactions. Therefore, there is a need for quantitative determination of acid–base character of natural cellulosic fibres. In their study, Gulati and Sain [180] determined acid base characteristics and dispersion component of surface energy of hemp fibres using inverse gas chromatography. Effect of alkalization and acetylation on acid–base characteristics was also examined. The results indicated that alkalization and acetylation made the hemp fibre amphoteric, thereby improving

their potential to interact with both acidic and basic resins. A parallel was drawn between the changes in fibre-matrix acid–base interactions and the actual improvement in the mechanical properties of the composites manufactured using resin transfer moulding process.

Wang et al [72] exposed hemp fibres of nano-scale (30-100 nm width) to 12% NaOH solution. The cellulose content was found to increase significantly from 76% for untreated fibres to 94% for treated fibres. There was corresponding decrease in hemicelluloses of 10.7% for untreated fibres to 1.9% for treated fibres. X-ray crystallography of fibres showed that the crystallinity of fibres increased after the treatment, thus affirming the increase in cellulose content.

The FTIR analysis of 5% alkalised hemp, kenaf, flax ad henequen fibres by Sgriccia et al [181] showed complete removal of hemicellulose and partial removal of lignin following the treatment. Pietak et al [182] observed that hemp fibres treated to 18% alkali solution for only 30 minutes resulted in removal of non-cellulosic components and more cellulose rich surface.

The removal of hemicellulose and lignin following 5% alkalisation was also confirmed by Sinha and Rout [183] for jute fibres. The crystallinity index of the fibre was also found to increase following the treatment. The mechanical testing of the fibres showed that they were stiffer and more brittle than non-alkalised fibres. Taha et al [184] also confirmed the removal of hemicellulose from date palm fibres following treatment with 5% NaOH solution.

Beckermann and Pickering [185] used 10% NaOH and 5% NaOH/2% Na_2SO_3 solutions for treatment of hemp fibres. NaOH treatment was more effective in removal of lignin and increased the crystallinity index of fibres following the treatment. The treated fibres were also more thermally stable than untreated fibres. Both the treatments resulted in increase in tensile properties of hemp-PP composites.

Mwaikambo and Ansell [147] also observed increase in tensile properties of hemp fibre reinforced cashew nut shell liquid (CNSL) composites following alkalisation of fibres. The increase was observed for both unidirectional and non-woven fibre composites.

Bledzki et al [186] used 22% NaOH solution on hemp fibres and studied the properties of unidirectional hemp yarn-epoxy composites. The flexural strength was increased by

45% and flexural modulus was increased by 100% following the treatment. The use of MAH-PP coupling agent was also studied for unidirectional hemp-PP and flax-PP composites. The transverse tensile strength of hemp-PP composites increased by 75% but there was no increase in longitudinal strength following the treatment. Flax-PP composites showed 150% increase in flexural strength and 65% increase in transverse tensile strength following the treatment.

Towo and Ansell [187] studied the effect of 0.06M alkalisation on mechanical properties of sisal fibre reinforced polyester and epoxy composites. The treatment resulted in 28.5% increase in tensile strength of polyester composites but only marginal increase in tensile strength of epoxy composites.

Mehta et al [145] studied the effect of various fibre surface treatments on the mechanical properties of hemp/polyester composites. The surface treatments used were: 5% alkalisation, silane, and acrylonitrile. All treatments resulted in increase in mechanical properties of the composites. The only exception was impact strength which was found to decrease following alkalisation treatment, and there was only marginal increase in impact strength for other treatments. This was consistent with the fact that improved fibre/surface adhesion will reduce the impact strength of the composites.

Thygesen et al [188] studied the effects of steam explosion, wet oxidation, and enzymatic defibration on chemical composition, crystallinity and cellulose chain length of hemp fibres. The degree of crystallisation of cellulose decreased slightly by enzymatic defibration but not by other treatments. The cellulose chain length decreased significantly only by steam explosion. The cellulose content was highest in the fibre bundles after wet oxidation.

Couto et al [114] studied the effects of oxygen plasma treatment on sisal fibres and polypropylene and their composites. No improvements in tensile or flexural properties were observed but there was some improvement in impact resistance following the treatment.

Yuan et al [189] reported an improvement in tensile properties of woodfibre-polypropylene composites following air plasma and argon plasma treatments, with air plasma being more effective in improving the properties.

Marais et al [135] studied the effect of plasma treatment on mechanical properties of flax fibre- and flax/PET fibre-reinforced polyester composites. It was found that the tensile strength decreased from 115 MPa to 102 MPa while tensile modulus increased from 11.5 GPa to 13.4 GPa for flax fibre composites. The improvement in modulus was attributed to improvement in interfacial adhesion while the decrease in strength was attributed to damage to fibres during the treatment. For flax/PET fibre composites, the tensile strength decreased from 79 MPa to 78 MPa while the modulus increased from 8.7 GPa to 9.7 GPa following the treatment.

George et al [190] reported a reduction in tensile properties of pineapple leaf- LDPE composites at higher concentrations of NaOH. Mishra et al. [137] reported a reduction in tensile, impact, and flexural strengths of sisal fibre reinforced polyester composites after exposing fibres to 10% NaOH solution. The same composites showed increase in tensile and flexural strengths when fibres were treated to 5% NaOH solution compared to non-surface treated fibres. This decrease in properties was attributed to increase in brittleness of fibres at higher concentration of NaOH. Mukherji et al [191] reported that the use of more than 1% NaOH solution on cellulose fibres weakens the fibres resulting in poorer mechanical properties.

From their studies on the effect of chemical modification on sisal-oil palm (hybrid) fibre reinforced natural rubber composites, John et al [192] reported that the tensile strength of the composites increased with increase in alkali solution concentrations of up to 4%. The tensile strength was found to decrease at alkali concentration of 8% which was attributed to the degradation of sisal and oil palm fibres following treatment at this concentration.

Mehta et al [145] exposed hemp fibres to 5% NaOH solution for one hour. They reported an increase in thermal stability of hemp fibres after treatment. After the treatment, the carbon content within the fibres was found to increase while oxygen and nitrogen contents were found to decrease.

A survey by Santulli [159] of various research papers on the effects of various fibre surface treatments on impact properties of natural fibre composites found that fibre treatments other than alkalisation did not appear to lead to a substantial improvement in impact properties.

This comprehensive review shows that considerable improvements can be gained in the mechanical properties of natural fibre composites by using the suitable surface treatment. The choice of treatment will depend on the range of improvement required and the applications of the composites following the treatment.

2.4.7.13 Natural Fibre Composites in Comparison to Glass Fibre Composites

The performance of natural fibre composites will inevitably be judged against the performance of glass fibre composites because the primary reason of using natural fibres is their potential to replace glass fibres. Various studies have been undertaken in this regard.

Fig. 2.10 shows a stiffness comparison of natural fibre and glass fibre composites. The figure shows that natural fibre composites can attain the same stiffness per unit weight at lower fibre weight fraction than glass fibre composites, albeit at slightly higher cost.

Table 2.15 shows the values of different environmental parameters in the production of 1 kg of hemp fibres and 1 kg of glass fibres. The lower power consumption and lower emission of greenhouse gases gives natural fibres a clear edge compared to glass fibre.

Table 2.15: Environmental Parameters in production of 1 kg of fibres [7]

Parameters	Hemp fibre	Glass fibre
Power consumption (MJ)	3.4	48.3
CO_2 emission (kg)	0.64	20.4
SO_x emission (g)	1.2	8.8
NO_x emission (g)	0.95	2.9
BOD (mg)	0.265	1.75

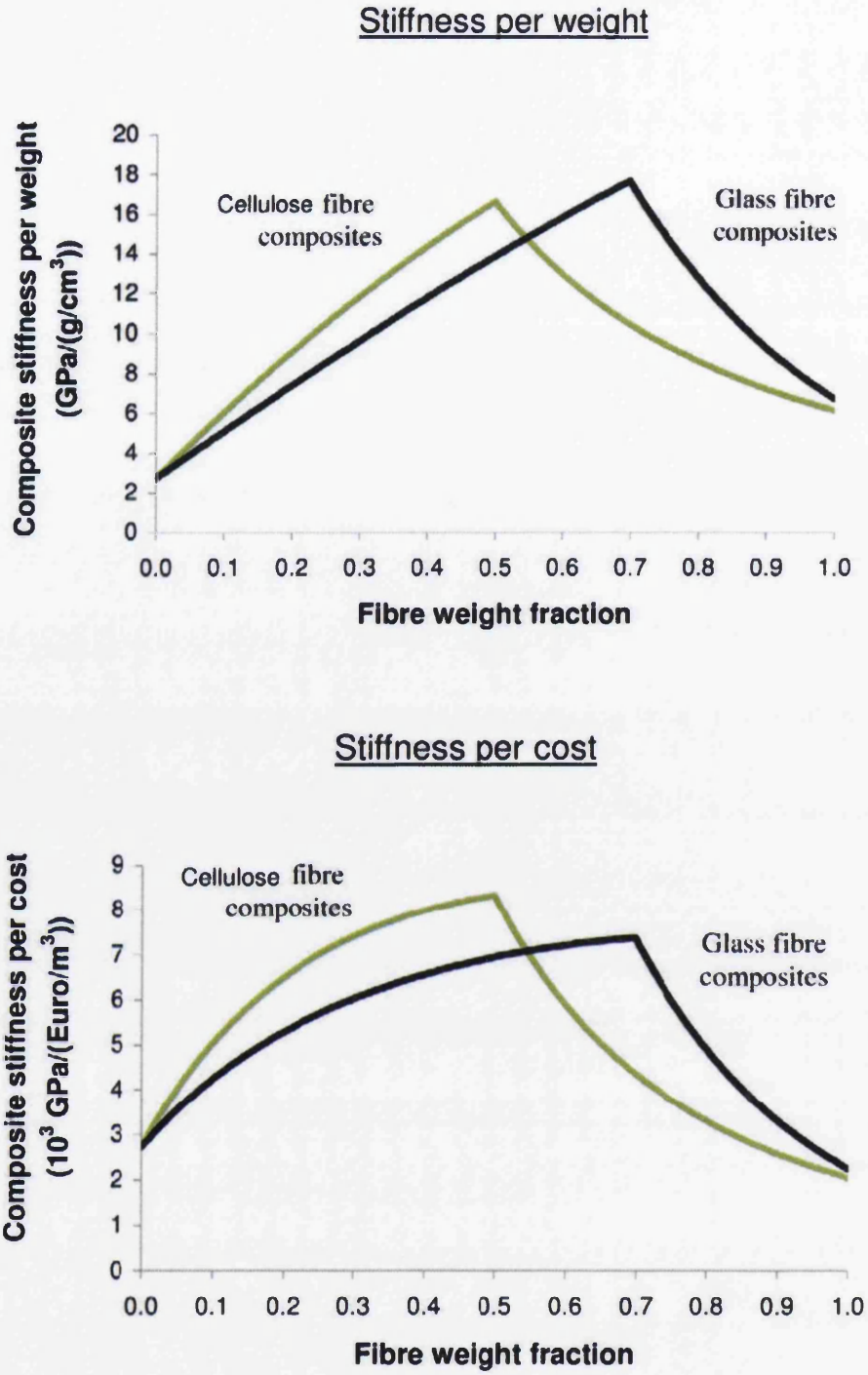

Fig. 2.10: Comparison of stiffness of natural fibre composites with glass fibre composites per unit weight and cost [193]

2.5 IMPACT PROPERTIES

The increase in the applications of composite materials has made it essential for them to perform well under various types of impact loading. Composite materials have to be designed to withstand impact during service life, like a dropped tool or flying debris. Stones hitting the under-shield of a car, a lifeboat hitting rocks, a fork-lift truck nudging the side of a portable building, are other possible examples of composite structures undergoing impact [194]. It has therefore become essential to understand the impact behaviour of composite materials.

Composite materials are very sensitive to out-of-plane (transverse) loading because they are much weaker in the thickness direction than in the plane of lamination. Consequently composite materials subjected to transverse impact may suffer significant damage, resulting in deterioration in their overall load-bearing capacity.

An attempt to improve the tensile properties of a composite frequently results in a deterioration of impact properties [22]. For example, high modulus carbon fibre composites have greater tensile strength but poorer impact strength than low modulus glass fibre composites. It is therefore important to have a good understanding of impact behaviour of composites for safe and efficient design and to develop new composites having good impact properties as well as good tensile properties.

Impact resistance of a material can refer to quite different aspects of a material's behaviour [194]. The impact resistance of a composite may refer to the ability of the composite to withstand a given blow without any damage (resilience); the maximum force necessary to rupture or separate a composite structure (impact strength); the amount of energy absorbed by a given mass of the composite (crush resistance); or the level of damage that a composite can sustain during impact loading without undue reduction to some primary structural function (damage tolerance). In the aerospace industry, the residual compressive strength of an impact damaged composite component is the design-limiting factor. Damage tolerance is defined in the aircraft industry as "the ability of a structure to sustain anticipated loads in the presence of fatigue, environmental deterioration (corrosion), or accidental damage until such damage is detected through inspections or malfunctions and repaired" [195]. Other industrial sectors also adopt similar damage-tolerant design philosophies. The present study will

be mostly concerned with studying the impact damage tolerance of hemp fibre composites.

Impact is defined as a relatively sudden application of an impulsive force to a limited volume of material or part of a structure. There has been considerable variation in interpretation of low-velocity. Sjoblom et al [196] defined low velocity impact as events which can be treated as quasi-static, the upper limit of which can vary from one to tens of m/s. Cantwell and Morton [197] and Hogg and Bibo [194] classified low velocity as up to 10 m/s. In contrast Abrate [198] stated that low velocity impact occurs for impact speeds of less than 100 m/s. Liu and Malvern [199] suggested that the type of impact can be classified according to the damage incurred. Robinson and Davies [200] defined a low velocity impact as being one in which the through thickness stress wave played no significant part in the stress distribution. Impacts in the speed range greater than 100 m/s are termed ballistic events, while those at speeds greater than 1000 m/s are termed hypervelocity events [194]. Agarwal and Broutman [22] defined low-velocity impacts as the ones that do not cause through-the-thickness fracture. Low velocity impact is also defined in context of low energy impact, e.g., less than 136 J [201].

The results of an impact are largely elastic at low impact energies, with some energy dissipated as heat, sound, internally in the material. At high impact energies, there is deformation, permanent damage, complete perforation, or fragmentation of the impacting or impacted body, or both. The ability of composites to undergo plastic deformation is quite limited with the result that energy is frequently absorbed in creating large areas of fracture with ensuing reductions in both strength and stiffness [197]. Damage due to impact loading in a composite is a function of velocity, mass, hardness, and the shape of the impactor. The nature and extent of impact damage are function of impact parameters such as impact energy, impact angle, laminate material (and fibre volume fraction and lay-up), and laminate geometry. For composites, impact tests are considered to be a more useful method for measuring overall toughness, compared to conventional fracture toughness analysis.

2.5.1 Energy Absorption and Failure Modes

Upon impact loading, a solid can absorb energy by two basic mechanisms: creation of new surfaces and material deformation. If the impact energy is large enough, a crack

initiates and propagates, thus actuating the second energy-absorbing mechanism. The material deformation continues in advance of the crack during crack propagation. In brittle materials, only a small amount of deformation takes place and the energy absorbed is also small, so brittle materials exhibit low energy-absorption capability. In ductile materials, large plastic deformation takes place and therefore large energies are absorbed during their fracture.

The total energy absorbing capability or toughness can be increased by increasing either the path of the crack during separation or the material deformation capability. In composites this can be achieved by replacing low energy absorbing constituents with greater energy absorbing constituents and this is one of the major advantages that composite materials have over monolithic materials like metals.

There are five basic mechanical failure modes that can occur in composite materials after initial elastic loading. These mechanisms account for the total energy absorbed in the fracture process. These are fibre failure and fracture, resin cracking and fracture, debonding between fibre and matrix, delamination of adjacent plies in a laminate, and fibre pull out.

2.5.1.1 Matrix Deformation and Cracking

Matrix damage is the first type of failure induced by low velocity impact and usually takes the form of matrix cracking but also debonding between fibre and matrix. Brittle resins such as polyesters and epoxies undergo little deformation prior to fracture and hence have low energy absorbing capability. Most of the energy is absorbed in creation of new surface during matrix fracture. Thus the contribution of polymer matrices to the total impact energy may be insignificant. Matrix cracks also occur due to property mismatching between fibre and matrix and are usually oriented in plane parallel to the fibre direction in unidirectional layers [202]. The degree of matrix cracking can be used as an indicator of the degree of impact and the degree of damage.

The energy required for matrix fracture per unit area of the composite is given by [22]

$$U=\frac{(1-V_f)^2 d\,\sigma_m\,U_m}{4V_f\tau} \qquad \text{.....(2.12)}$$

where σ_m is the tensile strength of the matrix, d is the fibre diameter, U_m is the work done in deforming the matrix to rupture per unit volume, and τ is the interfacial shear strength. For brittle polymer matrices U_m is small and thus the energy required for matrix deformation may only be a negligible fraction of the total energy.

2.5.1.2 Fibre/Matrix Debonding

During impact the fibres become separated from the matrix material by cracks running parallel to the fibres, thus breaking the chemical or secondary bonds between the fibre and the matrix. This type of cracking occurs when fibres are strong and the interface is weak. A debonding crack runs at the fibre-matrix interface or in the adjacent matrix, depending on their relative strengths. In either case a new surface is produced. An increase in impact energy is observed with a decrease in interface strength because it promotes extensive debonding or delamination. This may have important implications in natural fibre composites where the interfacial bonding is relatively poor.

There is no expression for theoretically estimating the debonding energy. However values of the work of debonding have been calculated to be ≤ 500 J/ m^2 which is of the order of the interface shear strength times the failure strain of the resin [22].

2.5.1.3 Fibre Pullout

Fibre pullouts occur when brittle or discontinuous fibres are embedded in a tough matrix. The fibres break at their weak cross sections, thus producing stress concentration in the matrix which is relieved by matrix yielding. The fracture may proceed by the broken fibres being pulled out of the matrix rather than fibres fracturing again at the plane of the composite fracture. This is particularly true for short fibres. Fibre pullouts are usually accompanied by extensive matrix deformation.

An expression derived for the energy dissipated during extraction of discontinuous fibres of length l is given by [22],

$$U = \frac{V_f \sigma_f l}{12} \quad \text{.....(2.13)}$$

where σ_f is the fibre tensile strength.

2.5.1.4 Delamination

A crack propagating through a ply in a laminate may get arrested as the crack tip reaches the fibres in the adjacent ply. Because of the high shear stress in the matrix adjacent to the crack tip, the crack may branch off and start running at the interface parallel to the plane of the plies. This is called a delamination crack. A delamination is a crack which runs in the resin rich area between plies of different fibre orientation and not between lamina of same ply group [202].

Delamination cracks are responsible for absorbing a significant amount of fracture energy. They occur frequently when laminates are tested in Charpy or Izod impact tests. It has also been shown [22] that matrix cracking and delamination are associated phenomena in low-velocity impact. It may be possible to estimate the internal delamination by investigating the external matrix cracking patterns.

Liu [203] concluded that delamination was a result of bending stiffness mismatch between adjacent layers, i.e. different fibre orientations between layers. He also concluded that it is the bending-induced stresses that which are major cause of delamination.

Dorey [204] provided a simple expression for the elastic strain energy absorbed at the point of delamination failure which suggested that the damage mode is more likely to occur for short spans and thick laminates with low interlaminar shear strength.

$$E = \frac{2\tau^2 w L^3}{9 E_f t} \qquad \text{.....(2.14)}$$

Where τ is interlaminar shear strength, w is width, L is unsupported length, E_f is flexural modulus and t is the thickness of the sample.

Delamination due to transverse impact only occurs after a threshold energy has been reached and it only occurs in the presence of a matrix crack. It has also been shown that delaminations do not always run precisely in the interface region, but can run slightly either side. Matrix cracks which lead to delamination are known as critical matrix cracks.

2.5.1.5 Fibre Failure

This damage mode occurs much later in the fracture process. Fibre failure is due to locally high stresses and indentation effects, governed by shear forces, and on the non-impacted face due to high bending stresses [202]. Fibre failure is precursor to catastrophic penetration mode. Fibres will fracture when their fracture strain is reached. Brittle fibres such as graphite have low fracture strain and hence low energy-absorbing capability.

Dorey [49] has derived a simple equation for the energy required for fibre failure due to back surface flexure,

$$E = \frac{\sigma^2 w\, t\, L}{18E} \qquad \text{.....(2.15)}$$

where σ and E are flexural strength and modulus respectively, and w, t and L are specimen width, thickness and length respectively.

The energy required per unit area of the composite for fracture of fibres in tension is given by [22],

$$U = \frac{V_f \sigma_f^2 l}{6 E_f} \qquad \text{.....(2.16)}$$

where V_f is the fibre volume fraction, σ_f is the ultimate tensile strength of the fibres, l is the fibre length and E_f is the fibre modulus. It has been shown that fracture of fibres accounts for only a small fraction of the total energy absorbed. However the presence of fibres strongly influences the failure modes thus the total impact energy.

2.5.1.6 Penetration

Penetration is a macroscopic mode of failure. It occurs when fibre failure reaches a critical extent, enabling the impactor to completely penetrate the material [202]. Cantwell and Morton [205] showed that the impact energy penetration threshold rises rapidly in the specimen thickness for Carbon fibre reinforced plastics. They also showed that shear-out is the major form of energy absorption (50-60% depending on plate thickness) in the penetration process. For glass fibre reinforced plastics, El-Habak [206] showed that glass fibre treatment played a key role in determining the perforation load

and polyester resin performed better than epoxy. Dorey [204] again came up with a simplified equation for the energy absorbed in penetration as

$$E = \pi \gamma t d \quad \text{.....(2.17)}$$

where γ= fracture energy, d= diameter of impactor, and t= sample thickness.

2.5.1.7 Damage Modes in Randomly Oriented Fibre Laminates

The damage modes in randomly oriented laminates, like the ones used in the present research, are less easy to establish and less search has been carried out on this topic. Most of the research has concentrated on sheet moulding compound (SMC) panels and continuous filament mats (CFM) used in pultrusion.

In their research on SMC panels, Liu and Malvern [199] found that matrix cracks on the impacted surface were short and formed a series of rings away from the point of contact. They also defined three types of impact-induced damage for SMC composites: indentation (crushing of matrix under the impactor), bending fracture, and perforation (damage resulting from penetration and associated fracture).

2.5.2 Constituents' Influence on Impact Properties

All the three constituents of composite materials, namely, fibre, matrices and the interface, play their parts in the impact response of composite materials. Their roles are now discussed.

2.5.2.1 Fibre

For resistance to low-velocity impact, the ability to store energy elastically in the fibres is the basic parameter with respect to their impact performance. This corresponds to the area under stress-strain curve, which is dictated by the fibre modulus and strain to failure. E-glass fibres have higher strain to failure than carbon fibres. Therefore they have better impact response than carbon fibres. The same is true for aramid fibres.

Higher fibre failure strains, with same elastic modulus, result in higher energy absorption, since the strain energy absorbed by the matrix represents a large portion of the total strain energy. For the same impact energy, higher capacity to absorb energy result in less fibre breakage and higher residual tensile strength. Also matrix damage, which occurs after initial fibre failure, will also be reduced so that residual compressive

strength is also increased. So the ability of fibres to store energy elastically appears to be the fundamental parameter in determining impact resistance.

Fibre orientation also has significant influence on the impact behaviour of the composites. Research done by Agarwal and Narang [207] showed that in Charpy impact testing of unidirectional fibre composites, the impact energy continuously decreased with increasing fibre orientation. Minimum impact energy was observed at fibre orientation angle of 90°. For cross-ply composites, Mallick and Broutman [208] showed that the lowest impact energy was observed at fibre orientation angle of 45°.

2.5.2.2 Matrix

The properties of the matrix used in the composite material play a significant part in the response of the composite material to impact. A ductile matrix will have improved residual strength after impact due to better resistance to delamination and matrix cracking. Teh and Morton [209] compared damage resistance of nine composites and showed that brittle matrix systems have lower threshold velocities and higher damage area growth rate than toughened matrix systems.

Epoxy, one of the most widely used thermoset resins, is brittle and has poor resistance to crack growth [202]. Plasticizing modifiers, rubber and thermoplastic particles have been used in the resin to reduce matrix damage and improve interlaminar fracture toughness. However increased interlaminar fracture toughness invariably reduces mechanical properties. The inclusion of a thin discrete layer of very tough, high shear strain resin has also been used to minimize delamination.

Most of thermoplastic resins give better fracture toughness compared to thermoset composites. But thermoplastic resins have their limitations, like low thermal stability and chemical resistance, poor fibre-matrix interfacial bonding and poor creep properties, which prevent extensive use of these resins.

2.5.2.3 Interface/interphase

Like all other mechanical properties, the interface/ interphase plays a vital role in the composite response to impact. Interphase region affects the failure mode which occurs at a given load. Poor adhesion results in failure at low transverse stress, leaving clean fibres. The bond strength can be used to improve the toughness by absorbing energy in

fibre-matrix debond. However this leads to reduction in the mechanical properties of the composite material [202]. Usually the surfaces of the fibres are chemically treated to improve the level of adhesion between matrix and fibre. Carbon fibres are treated with oxidative process whereas glass fibres are treated with a coupling agent.

Yeung and Broutman [210] studied the effect of different surface treatments on interfacial strengths of glass fabric reinforced polyester and epoxy composites. For polyester laminates, interfacial strength was found to vary over a large range by changing the coupling agent on the fibre surface. The interfacial strength of epoxy laminates was found to be independent of surface treatments because epoxy resin can form strong bonds with glass surface even in the absence of a coupling agent.

For polyester laminates, total impact energy appeared to have a minimum. Crucially, it was found that the total impact resistance can be maximised by reducing the interfacial bonding. The greatest value of impact strength occurred when the shear strength was lowest. This is because the initiation of failure requires less energy when the interfacial bond is poor and a large value of total impact energy is achieved during the delamination phase occurring after failure initiation. The sample supports less load during propagation but absorbs more energy because of large deflections that the sample can sustain. This is going to be crucial with respect to the fibre surface treatments of hemp fibres.

In general, impact on composites with low levels of fibre surface treatment generated large areas of splitting and delamination with severe effect on residual compressive properties of the material. While impact loading on highly treated composites results in a smaller, more localised damage zone, a lower perforation threshold, and improved compressive properties. However, the increased notch sensitivity associated with fibre surface treatment results in a reduction in the post-impact tensile strength of the material.

2.5.3 Measurement of Impact Strength

2.5.3.1 Impact testing techniques

The impact test fixture should be designed to simulate the loading conditions to which a component is subjected in service and then reproduce the failure modes and

mechanisms likely to occur. In simple terms, the impact problem can be divided into two separate conditions: low velocity impact by a large mass (e.g. dropped tool), and high velocity impact by a small mass (e.g. runaway debris, small arms fire). The former is generally simulated using a falling weight or a swinging pendulum and the latter using a gas gun or some other ballistic launcher.

The Izod and Charpy impact tests have been traditionally used to assess the impact performance of metals. For polymers the Izod test is preferred, while for composites, the Charpy test is preferred. In either test, specimen geometries are not representative of component dimensions and so these tests are suitable only for ranking the impact resistance of composites. Also they give no indication of residual properties after impact. In either test, the impact energy may be over estimated because energy is stored elastically in the specimen prior to failure, or is dissipated acoustically, thermally, or in the kinetic energy of the failed parts. To overcome this effect, a notch is machined in the sample. The purpose of the notch is to reduce the sources of error due to stored energy. When the sample is impacted, the failure starts at the notch before significant energy storage occurs elsewhere in the specimen. The notch produces a high stress concentration and thus minimises the energy required for initiation of failure. The total measured energy required for fracture is then essentially the energy required for propagation of failure [22]. Notches are also used to determine if the material is notch-sensitive, for example, due to a scratch or a surface flaw.

It has been shown that composites exhibit a reduced modulus and, hence greater energy storage, in impact loading. It is therefore considered that while a place exists for these tests in a laboratory context for the purpose of material development, the tests can not be considered suitable for predicting the response of thin composite structures [194]. In this research some Izod tests will be carried out to compare results with other tests.

Another popular method of assessing impact energy is the drop weight test, and is more representative approach for assessing the impact response of composite materials, and this type of test will be used extensively in this research. Again there is a large variety of specimen shapes used in this test. The steel striker has a polished hemispherical head up to 20 mm in diameter, and is allowed to fall from a height of up to 2m (corresponding to a maximum velocity of 6.3 m/s) onto the specimen. It has been noted that pyramidal and hemispherical indenters give different results so these different test

methods are not comparable. To increase the impact velocity, the projectile may be fired at the specimen. This may involve a conventional bullet, an anti-tank shell, a small ball fired by a gas gun, or a liquid drop. The impact velocity can range from 20-100 m/s to 6000 m/s.

2.5.3.2 Impact Testing Parameters

For composites, a variety of test parameters have been used. A summary of these parameters is given below.

Impactor shape and dimension:

Mostly hemisphere steel noses with diameter of 12.7 mm have been used in impact tests. The size and shape of the impactor directly influence the impact event. The stress during the impact will be more localized with the small impactor. Therefore the damage threshold energy for a certain specimen will be lower compared to a large one.

Impact velocity and energy:

For fibre reinforced polymer composites, the impact behaviour is dependent on the velocity of impactor when striking the sample [22]. The impact energy can be changed by either changing the impact velocity or impactor mass. The degree of damage in a sample is dependent on the impact energy. Low velocity impact loading by a heavy object induces an overall target response, whereas high velocity impact by a light projectile induces localized mode of target deformation resulting in energy being dissipated over a small region immediate to the point of impact. For impact velocities up to 50 m/s, the target impact response and the amount of resulting damage are found to be a function of the impactor mass. However for impact velocities of 1 to 5.5 m/s, the range mostly used in drop weight tests, the effects of impact velocity are so small that they are hardly noticed or measured, even for the strain sensitive glass-fibre composite materials. This was confirmed by Rydin et al [211] for low velocity impact testing of woven and non-woven glass fabric reinforced vinylester composites. For impact velocity of less than 7 m/s, impact energy and contact force, rather than impact velocity, were the determining factors of the extent and type of damage.

From their studies on low velocity impact testing of graphite/epoxy and graphite/PEEK laminates, Sjoblom et al [196] concluded that low-velocity impact testing of composites

should be instrumented; total impact energy is not a very good parameter to use for direct material characterization, impact force history is a much more relevant measure; and the energy loss during impact is a more direct measure of the damage formed during impact than is the impact energy.

Specimen dimensions and clamp mode:

The geometry of a specimen is a fundamental parameter in determining the impact response of composite materials. The failure process in the specimen can be changed by the geometry of the specimen and the support conditions. Delamination is more likely with short spans, thick laminates whereas flexural failures are more likely with large spans or thin skins. Penetration is most likely for small projectiles which are moving at such a high velocity that the laminate cannot respond quickly enough in flexure and high stresses are generated close to the point of impact.

In their studies on the effects of impact on laminate thickness of carbon fibre reinforced epoxy composites, Matemilola and Stronge [212] found that the ratio of missile nose radius to laminate thickness r/h was important in determining the side of the plate where damage first occurred. Damage developed first on the impact side of the laminate for r/h <1, while for r/h >1 damage developed first on the distal side.

In their studies on low velocity impact testing of woven E-glass/epoxy laminates, Datta et al [213] observed that for a constant impact energy level, as the laminate thickness increased the number of drops to failure also increased. However it was found that a thinner laminate can be chosen in place of a thicker one when its usage mainly calls for only the impact resistance of the material, thus providing an economical design for the composite structures.

In their studies on impact properties of woven-roving and CSM glass reinforced polyester composites, Sutherland and Soares [214] found that the effect of laminate thickness variation was more important for CSM laminates than woven roving laminates. Hence the data for thin laminates of CSM composites may not be applicable for thick laminates.

Finally, it should be mentioned that the impact data generated using a particular test geometry and specimen size may not necessarily represent the results generated using of striker, specimen, span and support conditions influence the distribution of tensile,

compressive and shear stresses throughout the thickness of samples and thus influence the values obtained for various test parameters.

2.5.4 MECHANICS OF IMPACT LOADING

Impact energy of a plastic or composite is given by:

$$U=\frac{E}{b\,(d-c)} \qquad \text{.....(2.18)}$$

where U is the impact energy and E is the energy registered in the test, for a specimen of breadth *b* and depth *d*, containing a notch of depth *c*. The fracture energy can be expressed as:

$$U=\frac{E}{\emptyset\, b\,(d-c)} \qquad \text{.....(2.19)}$$

where Ø is a calibration factor dependant on specimen and crack dimensions and compliance [215].

An impact test gives a load history curve of the type shown in Fig. 2.11 [22]. The load history is divided into two distinct regions, a region of fracture initiation and a region of fracture propagation. In the fracture initiation phase, elastic strain energy is accumulated in the sample with the increase in the load and no gross failure takes place. In this phase some failure mechanisms on a microscale, for example, microbuckling of the fibres on the compression side or interfacial debonding, can take place. As the critical load is reached at the end of this phase, the sample may fail either by a tensile or a shear failure depending on the relative values of the tensile and interlaminar shear strengths. At this stage the fracture may propagate either in brittle manner or a progressive manner continuing to absorb energy with reduction in loads. By integrating the area under the load displacement curves, and noting the value up to the maximum load or the load at first failure, the energy required to start or initiate damage can be deduced and related to energy required to propagate damage and the total energy involved. The ratio of the propagation energy, E_p, to the initiation energy, E_i, is known as the ductility index D [215]. Values range from zero upwards. The zero value indicates a completely brittle material. A large value of D means more energy is used in propagating failure compared with that to cause initiation.

The total impact energy is then the sum of the initiation energy and propagation energy and is equal to the area under the curves in the load-time graph as shown in Fig. 2.11. The energy absorbed by the sample at any time is given by:

$$E = \int Pv\, dt \quad \text{.....(2.20)}$$

where P and v are the instantaneous load and velocity respectively.

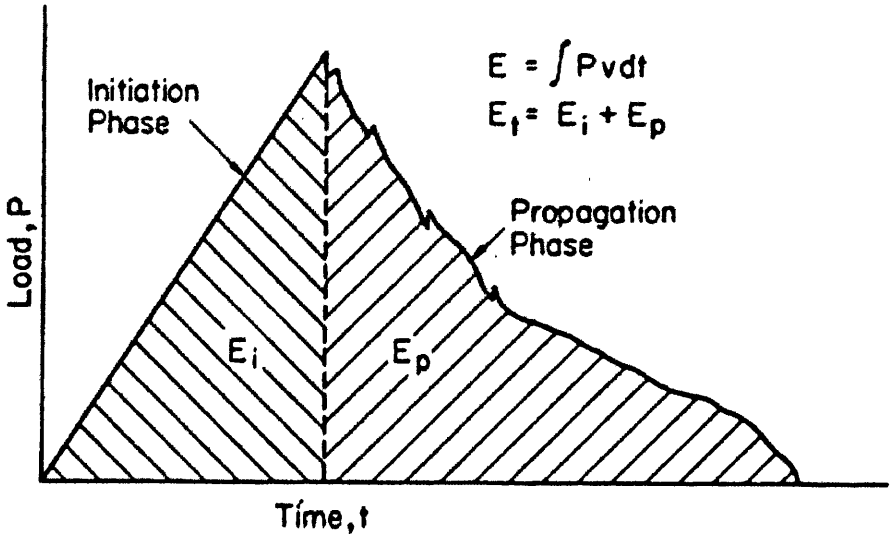

Fig. 2.11: Total impact energy absorbed by a composite during low velocity impact [22]

2.5.5 Post Impact Residual Properties

A significant loss in residual strength and structural integrity results in composite materials due to impact damage. Low velocity impact is potentially dangerous because it can produce extensive subsurface delaminations that may not be visible on the surface. Even barely visible impact damage (BVID) can cause strength reductions of up to 50% [215]. High velocity impact produced by projectiles, shock waves, and fragments from exploding ammunition is a highly dynamic event leading to penetration or perforation of composites. All impact damage is detrimental to mechanical and structural properties of composites. Residual strengths in tension, compression, bending and fatigue are reduced to varying degrees depending on the dominant damage modes. In general impact damage has greater effect on residual strength than on stiffness. It has

also been shown that impacts at higher energy levels produce more degradation than a number of lighter impacts.

2.5.5.1 Residual Tensile Strength

There appears to be a threshold impact energy required to cause a reduction in tensile strength of a laminate. This threshold is different for different laminates and is dependent on material parameters such as laminate thickness, fibre type, and matrix material. Residual tensile strength normally follows a curve of the form shown in Fig. 2.12 [216]. In region I no damage occurs as the impact energy is below the threshold value for damage initiation. Once the threshold has been reached, the residual tensile strength reduces sharply as shown in region II. In Region III the minimum value of residual tensile strength is reached just before complete perforation. Region IV results from a constant value of residual tensile strength because perforation has occurred in the material leaving a neat hole. In this region, the residual tensile strength can be estimated by considering the damage to be equivalent to a hole the size of the impactor. In region IV the hole diameter becomes practically independent of impact velocity.

In their studies on impact properties of graphite/epoxy and Kevlar/epoxy composites, Cairns and Lagace [217] observed that a threshold damage size existed below which no strength degradation was found to occur.

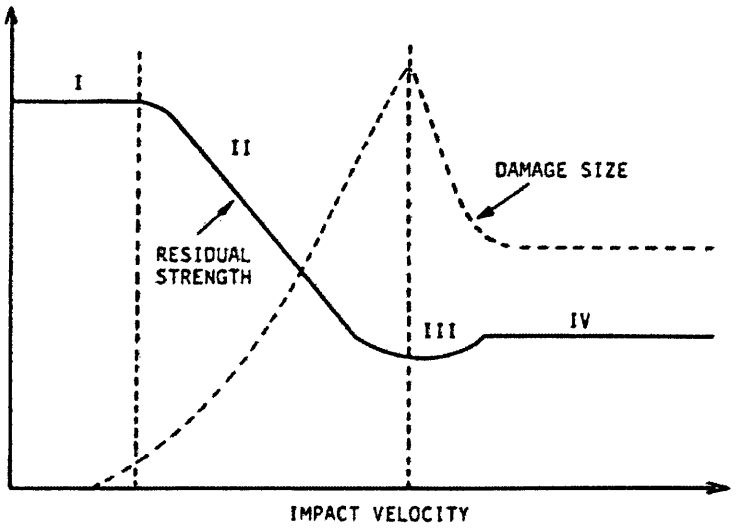

Fig. 2.12: Schematic diagram of the residual strength and damage size after impact [216]

2.5.5.2 Residual Compressive Strength

The residual compressive strength also decreases with increasing impact energy and is significant for even very light impacts. Poor post impact residual compressive strength is the greatest weakness of composite laminates [202]. This is mainly due to local instability resulting from delamination causing large reduction in compressive strength. Under a compressive load, delamination can cause buckling in one of three modes: global instability/ buckling of the laminate, local instability, or a combination of both. The mode of failure changes from global, to local to mixed mode as the delamination length increases. However post-impact compressive strength testing is often avoided due to the difficulty in providing a large enough gauge section to accommodate the damage.

2.5.5.3 Residual Flexural strength

It has been reported that both flexural strength and flexural modulus decrease with increasing low-velocity impact energy for ductile specimens (glass/ epoxy) while brittle specimens (graphite/ epoxy) showed no losses until complete failure occurred [202]. Because of complex stress patterns in the material, a detailed analysis of damage on residual flexural strength is still to be carried out.

2.5.5.4 Residual Fatigue Life

The post-impact fatigue behaviour of composites is important, especially because of the presence of barely visible damage and internal damage. It has been found that the ability of composites to withstand cyclic loading is far superior to their static strength when they are damaged or have defects [218]. In one study on graphite-epoxy laminates [204] it was found that the S-N curve for 3J impact damaged laminate was very flat and after one million cycles, the fatigue strengths of the damaged and undamaged laminates were similar.

It has been reported that compression-compression and tension-compression are the critical fatigue loading cases, with compression being the worst case static loading condition [202]. The maximum residual compressive load divided by the static failure

load (S) typically decreases from 1.0 to 0.6 in the range 1 to 10^6cycles. In compression, the rate of degeneration is at its highest up to 100 cycles and after 10^6 cycles no further degradation occurs. So S=0.6 can be taken as the fatigue threshold. Therefore, it is believed that fatigue loading is not a good method of characterising residual properties.

2.5.5.5 Modelling post-impact residual strength

Various attempts have been made to model the post-impact strength of composites. Amongst the most prominent was the one proposed by Caprimo [219] who considered that the damage at the impact site could be modelled as an equivalent hole and calculated residual strengths based on fracture mechanics concepts using the following relationship

$$\frac{\sigma_r}{\sigma_o} = \left[\frac{U_o}{U}\right]^{\alpha} \qquad \text{.....(2.21)}$$

where σ_r is the residual strength, σ_o is the undamaged strength, U_o is the threshold impact energy, and U is the impact energy, and α is a constant dependent on the geometry and the material. Work done on low velocity impact behaviour of carbon/epoxy laminates by Found and Howard [220] showed that this equation gave a good approximation of residual tensile and compressive strengths of the laminates following low velocity impact.

2.5.6 Impact Properties of Natural Fibre Composites

The impact properties of natural fibre composites are poorer than their synthetic fibre counterparts because of their poor mechanical properties. Santulli [221] has outlined the characteristics of impact behaviour of natural fibre composites as follows. The measurement of impact damaged area can be difficult as an effect of fibres suffering early debonding around the impact point even at low stress. The variability of properties of natural fibres will also have an effect on their impact properties. The presence of defects in natural fibres reduces the possible effect of bridging from the fibres during impact loading. As a result, the fibres are likely to bend and pull out of the matrix rather than fracture under impact loading.

The natural fibre composites are expected to possess superior impact properties because of their ability to absorb tremendous amount of energy during impact fracture [222].

Since natural fibres themselves are cellulose fibril based composite materials, their fracture modes include uncoiling of fibrils, fibril pull out, plastic deformation of fibrils, fibril splitting and diversion of the crack at fibril-fibril interface. These fracture mechanisms are expected to contribute to high toughness of natural fibre composites [222]. However in practice the impact strength of natural fibre composites has been found to be quite low compared to glass fibre composites as shown in Table 2.12. The following factors can be ascribed for the poor impact properties of natural fibre composites: lower fibre strength; micro-compressive defects along fibre length causing stress concentrations; defects induced during manufacture; poor interfacial bonding; non-uniform cross-section of fibres limiting fibre pull-out. A selection of studies undertaken so far on this subject are summarised below.

The work of fracture increases linearly with fibre volume fraction for natural fibre reinforced polyester composites. This has been shown to be true for sunhemp fibres [118] and for jute fibres [127]. The Izod impact strength of sunhemp/polyester composites at 24% fibre volume fraction was reported to be 21 kJ/m^2 [118] which is 15 times greater than that for polyester resin alone.

Santulli [131] investigated damage due to low velocity impact on jute fibre reinforced polyester composites. A number of post-impact mechanical tests, including tensile tests, three-point bending and indentation, were carried out. On all these tests acoustic emission activity (AE) was monitored. The results showed that AE gave reliable measurement of the level of post-impact damage.

Wambua et al. [223] studied the response of flax, hemp and jute fibre reinforced polypropylene composites to ballistic impact by fragment simulating projectiles. They found that flax composites exhibited better energy absorption than hemp and jute composites.

Pavithran et al. [165] determined the fracture energies for sisal-, pineapple-, banana- and coconut-fibre–polyester composites (fibre content approximately 50 vol.%) in Charpy impact tests. They found out that, except the coconut-fibre–polyester composites, an increase in fracture energy was accompanied by an increasing fibre toughness (determined by the stress–strain diagram of the fibres). Natural fibre reinforced plastics with fibres which show a high spiral angle of the fibrils, indicated a higher composite-fracture-toughness than those with small spiral angles. That is why

composites with sisal fibres (spiral angle=25°) show an optimum of impact properties. They also investigated the specific toughness of sisal–UHMPE composites, which is approximately 25% below that of comparable glass-fibre based composites (same fibre-volume-content).

Fracture toughness is another parameter which can be used to assess the damage tolerance properties of composites materials. Hughes et al [130] used linear elastic fracture mechanics to study the fracture toughness properties of jute-polyester and hemp-polyester composites and compared them with CSM glass-polyester composites. The fracture toughness of natural fibre composites was found to be almost three times lower than that of glass fibre composites at same fibre volume fraction. The values of critical strain energy release rate were also five to ten times lower that those of glass fibre composites. The estimation of crack tip plastic zone radii of natural fibre composites were up to five times lower than that of glass fibre composites. Since the volume of damage zone (proportional to crack tip radius) gives a measure of energy absorbing capacity of the material, this again pointed at the poor toughness properties of natural fibre composites. The use of linear elastic fracture toughness thus reaffirmed the poor toughness properties of natural fibre composites.

Yuanjian [86] reported that hemp fibre reinforced polyester composites exhibited greater reduction in strength and stiffness than glass fibre composites in low velocity impact. These studies have thus pointed at generally poor impact properties of natural fibre composites.

2.5.7 Impact Properties of Natural Fibre Hybrid Composites

One way of increasing the relatively poor impact properties of natural fibre composites is to combine them with stronger and tougher glass fibres and make hybrid composites. It has been shown for E-glass/flax hybrid epoxy composites [224] that hybrid laminates were much more impact resistant (up to four times for the same laminate thickness) when impacted on the glass side. It was thus suggested that the sandwich configurations with glass fibre skin and natural fibre core can be considered the most suitable configuration for higher impact resistance.

Table 2.16 summarises the results of impact strength of E-glass/ natural fibre composites reported by various researchers. In their studies on damage tolerance

properties of jute-glass/ polyester hybrid composites, Ahemd et al [225] observed that jute composites had better energy absorption capacity compared to jute-glass hybrid composites. However they had poor damage resistance and tolerance capability compared to hybrid composites.

Table 2.16: Impact strength of E-glass/ natural fibre hybrid composites

Natural fibre	Matrix	Natural fibre wt. fraction (%)	Glass fibre wt. fraction (%)	Impact strength (kJ/m^2)	Reference
Bamboo	Polyester	6.2	18.8	32	[160]
Coir	Polyester	15	30	40	[226]
		30 (vol)	5 (vol)	24	[165]
Jute	Polyester	6	8	44	[227]
Sisal	Polyester	2 (vol)	6 (vol)	5.8 (J/m)	[187]
Flax	Polypropylene	30	20	43.2	[170]
	Polypropylene	30	20	43.2	[228]
	Soybean oil	16	25	33.6	[229]
Hemp	Polypropylene	30	10	75 J/m	[230]
Oil palm	Polyester	3.5	31.5	17	[167]
	Epoxy	Variable	Variable	Max. 95	[168]
Jute	Polyester	-	-	29	[231]

From their studies on impact properties of flax/glass epoxy hybrid composites, Santulli et al [224] observed that composites containing 2/3 glass and 1/3 flax fibres had penetration energy of 56J compared to 18J for flax only composites.

2.6 FATIGUE PROPERTIES

Fatigue is defined as a process which causes damage in a material and structure under fluctuating loads of a magnitude much less than the static failure load. The accumulated damage results in a gradual and significant decline of mechanical properties such as strength and stiffness, in crack growth and finally into complete failure or collapse. Fatigue loads are almost unavoidable for materials in service. The fatigue strength of all materials including metals, plastics and composites is lower than their static strength [22].

The total number of load cycles that can be endured by the material or structure before failure is called fatigue life. The number of cycles to failure depends on a number of factors: stress levels, stress state, mode of cycling, process history, material composition, dimension and geometry, loading conditions and load history, environmental conditions, and lastly, by the mutual influence of all these parameters. The maximum cyclic load or stress range a material or structure can withstand for a given fatigue life is called fatigue strength.

Composite materials are generally regarded as having good fatigue strength. Therefore they find applications in aircraft and other vehicles which experience significant amount of fatigue [232]. Unidirectional continuous fibre-reinforced composites are especially known to possess excellent fatigue resistance in the fibre direction [22]. This is because load in unidirectional composites is primarily carried by the fibres which generally exhibit excellent fatigue resistance. Laminated composites may have lower fatigue resistance than unidirectional composites because some plies are weaker than others in loading direction and may show physical evidence of damage much before the final fracture. The damage may be in the form of the failure of fibre-matrix interface, matrix cracking or crazing, fibre fracture or delamination.

In composite materials subjected to fatigue, although initial damage may appear early, its propagation may be arrested by the internal structure of the composite. In this respect composite materials have clear advantage over metals subjected to fatigue where a crack may rapidly grow to final fracture. In composites subjected to fatigue loading, damage takes the form of numerous micro-cracks predominantly in the matrix material or at the fibre-matrix interface [17]. The damage is sustained and spreads throughout the bulk

material. Unlike metals in fatigue, there is no dominant crack and so it is difficult to assess the nature of future damage by present knowledge.

Salkind [233] argued that although the initial imperfections in composite materials (broken fibres, delamination, matrix cracking, fibre debonding, voids) can be much larger than corresponding imperfections in metals (cracks) , the growth of damage in a metal in fatigue is typically much more abrupt and potentially more dangerous than in a composite material. Accordingly the typical S-N curves in a composite are much flatter than that for a metal [234]. The composite materials are also less susceptible to the effects of stress concentrations like notches, holes, etc, than metals. The specific endurance limit of composite materials subjected to cyclic tensile loading is greater than that of metals [235]. Cyclic compressive loads lead to significant damages in composites. The damage mechanisms of composites do not develop only on the surface, as with metals, but inside the material as well.

The inhomogeneous and anisotropic nature of composite materials means that fatigue processes in these materials are generally very complex, involving accumulation of many damage modes. The fatigue behaviour of composites has been studied extensively ever since the introduction of composite materials. However, because of the complexity of composite materials, the knowledge of their fatigue behaviour is still far from enough.

Hertzberg and Manson [236] summarised the results of research on fatigue of fibrous composites by various researchers in the following five points:

- Failure criteria vary widely. Fatigue damage is progressive but physical integrity can be maintained for many decades of cycles.
- Many individual processes are involved in the failure of fibres, matrix, and interfacial regions.
- The nature of damage is complex, depending on the mode of loading, the relative orientation of the stress and the fibre axes, the coupling of stress fields, constraints due to in-plane and through-thickness elements in continuous fibre systems and the presence and nature of flaws.
- The concept of cracking needs redefining.

- While strength and fracture toughness generally decrease on cycling, the occurrence of certain combinations of individual failure processes with certain fibre arrays may result in effective crack blunting so that fracture toughness may increase, at least over part of the fatigue life.

2.6.1 Fatigue Testing Methods

Fig. 2.13 shows a typical stress-strain-time diagram in a fatigue test. A cyclic load is applied between predetermined maximum and minimum limits of stress, σ_{max} and σ_{min}, or strain. The ratio of minimum to maximum stress is called R ratio. The mean stress, stress amplitude, and cyclic frequency are also important parameters. The cyclic stress mode can be sinusoidal, triangular, or whatever is most appropriate for the end application in mind.

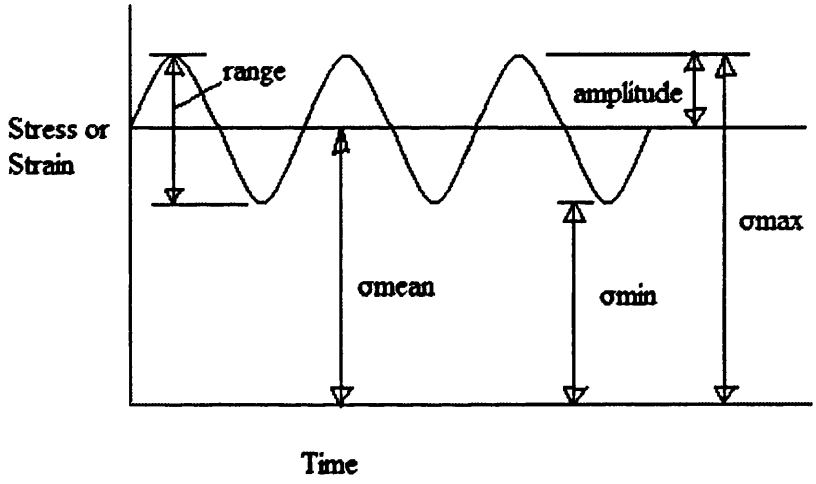

Fig. 2.13: Typical stress-strain-time diagram in fatigue testing [232]

There are six main types of fatigue test methods: tension-tension, tension-compression, flexural, interlaminar shear, torsion and compression-compression fatigue. The majority of fatigue tests on fibre reinforced polymer composites have been performed with axial tension-tension cycling. Tension-compression and compression-compression cycling are not commonly used since failure by compressive buckling may occur in thin laminates. Completely reversed tension-compression cycling is achieved by flexural fatigue tests. In addition limited numbers of interlaminar shear fatigue and in-plane shear fatigue tests have been performed.

The relationship between the fatigue strength (S) and the fatigue life (N) is mostly presented in diagrams by means of S-N or Wöhler curves for constant amplitude loading. The ordinate is generally the stress amplitude or the maximum stress in a cycle and is plotted on a linear scale. The abscissa is the number of cycles to failure for a particular stress cycle and is plotted on a logarithmic scale. This is the most widely used form of data presentation and provides a simple-to-interpret indication of how material properties are degraded by constant amplitude fatigue. The S-N curves for all materials including metals, polymers and composites have negative slope. The exact shape of the curve differs from material to material.

2.6.2 Damage Development

Fig. 2.14 shows a schematic representation of a typical S-N curve with damage development and residual strength variations superposed [237]. The cyclic loading amplitude is represented as 60% of the static ultimate strength, which is a typical value for long term behaviour.

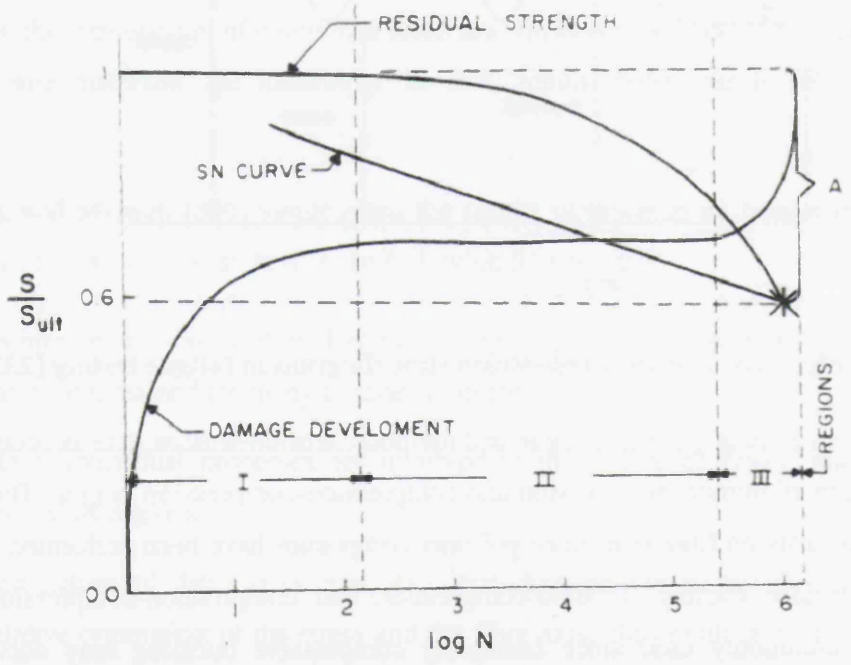

Fig. 2.14: Three stages of damage development during fatigue loading of composite materials [237]

As shown in the figure, the damage process can be considered in three stages. Stage I occurs during the first 10-15% of life and is characterised by a rapid (and rapidly decreasing) rate of damage development. For laminates that have off-axis plies, Stage I usually involves matrix cracking through the thickness of off-axis plies parallel to the fibres and perpendicular to dominant load axis. The matrix cracks cause a reduction in the stiffness of the laminate since cracked laminae carry less load than they did prior to cracking. However these stiffness changes are of small order and are generally not of great engineering consequence [237]. During this stage there is small but measurable effect on residual strength of the laminate.

Stage II corresponds to the next 70-80% of life, during which damage continues to initiate and grow, but at a slower rate than during Stage I. During this stage matrix cracks couple and grow, especially along interfaces, and delaminations (if present) may grow. However the cracks quickly stabilise to vary nearly constant pattern with a fixed spacing. Similar behaviour is observed for off-axis plies. The stability of the crack pattern is the reason for sudden decrease in the damage rate. During this stage, the interface separation (delamination and debonding) mechanisms dominate the damage development. The strength reduction is of the order of 30 to 40% [237]. The reduction is stiffness during this stage is relatively small.

But at the end of Stage II, the laminate is severely damaged to the level where continued cyclic loading accelerates the damage process during Stage III, the final 10-15% of life. The decrease in the stiffness during this stage is quite sudden and sharp. Final failure, and the events immediately preceding it, is dominated by fibre fracture, which is also the reason for sudden drop in stiffness. The accumulation of damage of all types results in the fracture of the laminate.

Fig. 2.15 traces the damage process as a function of percentage of life of composite laminates which contain 0° plies (principal load direction) and off-loading axis plies subjected to cyclic loading [238]. Although the number of possible damage modes and combination of damage modes is large, the number of failure modes is comparatively small.

2.6.2.1 Matrix Cracking

The major damage mode during Stage I is matrix cracking. Matrix cracks initiate in plies which experience tensile stress perpendicular to fibres in those plies if those stresses exceed amplitudes sufficient to cause failure of matrix material between fibres or separation of fibres and the matrix phase. These cracks generally occur in composites which have brittle matrix materials, but also occur under cyclic loading in composites which have ductile matrix components such as metal matrix components. Primary matrix cracks are the source of subsequent damages development under cyclic loading, and form the basis not only for damage development localization under tensile loads, but also for the development of localized buckling and the growth of delamination under compressive loads. Matrix cracking is observed to occur at similar load or strain levels in cyclic loading as is observed for quasi-static loading situations.

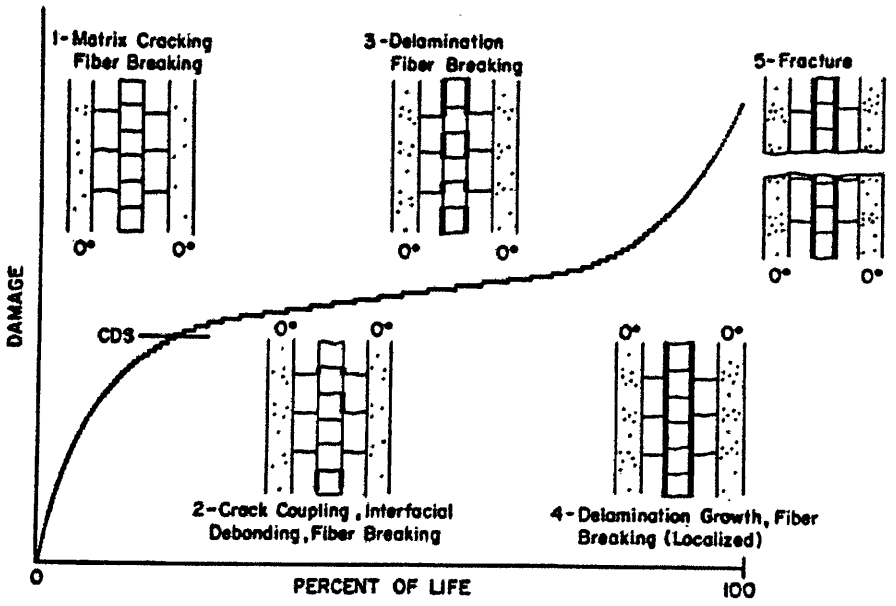

Fig. 2.15: Damage development during fatigue of composite materials [238]

Throughout Stage I, the number and density of matrix cracks increases until a uniform, saturation spacing is reached. This state of damage is known as the Characteristic Damage State (CDS). It is a laminate property and is completely defined by the properties of individual plies, their thickness, and the stacking sequence of the variously oriented plies. It is independent of extensive variables such as load history and

environment, and internal affairs such as residual or moisture related stresses. It is achieved near the end of Stage I as shown in Fig. 2.14.

2.6.2.2 Interfacial Debonding

As the loading history continues, Stage II damage begins whereby matrix cracks grow along the interfaces between plies. Crack coupling produces interfacial debonding which is confined to the material near the edge of the laminate. Debonding occurs in the fibre-rich regions of the plies in which the fibres lie perpendicular or at a large angle to the loading direction [22]. Large stress and strain concentrations at the fibre-matrix interface are responsible for initiation of debonding. After initiation the cracks usually propagate along the fire-matrix interface. With more cycles, the interfacial debonds on interfaces with high interlaminar shear stress begin to grow in the plane of the laminate to form delaminations. The remainder of Stage II is taken up by initiation and growth of delaminations and additional fibre fractures.

For randomly oriented fibrous composites also, the first stage of the damage is the formation of debonding cracks along the fibres lying perpendicular or at the largest angles to the direction of load. In their studies on fatigue properties of chopped strand mat polyester resin laminates, Owen and Smith found the first signs of damage to occur at about 30% of the ultimate tensile strength [22].

2.6.2.3 Fibre Fracture

The locally high stress fields associated with crossing matrix cracks and the intersection of matrix cracks and ply interfaces is one of the factors responsible for fibre fracture. Fibre fracture is the major damage mode in laminates subjected to tensile and compressive cyclic loads. Fibre fracture occurs during all three stages of fatigue life. Some failures are random fractures of statistically weak fibres but most fibre fractures are associated with matrix cracks in adjacent plies.

The consequences of fibre fracture depend on the state of the matrix [239]. There are three possible states:

1. The matrix is intact. In this case fibre failure would cause a shear stress concentration in the interface which may lead to fibre-matrix debonding.

2. The matrix has cracked in a dispersed failure mode. In this case fibre failure increases the matrix crack length leading to enhanced stress in the neighbouring fibres.

3. The matrix has cracked fully in a cross-section and the fibres have bridged the crack. In this case the load shed by the cracked matrix is shared equally by the bridging fibres. The weakest fibres fail first and the load shared by the broken fibres is shared equally by the surviving fibres.

When a fatigue crack in the matrix approaches a fibre, it may grow in three ways. With a weak interface and strong fibres, the crack can bypass the fibre by an antiplane-strain mode of crack growth. When the interface is strong, high stresses ahead of the crack tip affect the fibres. In ductile fibres the crack growth is rapid. Brittle fibres fail abruptly because of the large crack-tip stresses. Fatigue crack growth in fibres results in poor fatigue resistance of composites.

2.6.2.4 Delamination

Delamination cracks are responsible for final fracture of the material. The onset of stage III is characterised by an increase in the damage rate caused by damage localisation and delamination growth. The presence of delamination cracks prevents load distribution between plies and the composite is essentially reduced to a number of independent plies acting in parallel to support the load. The weakest of these plies fails and triggers failure of the remaining individual plies. Broutman and Sahu [240] found that delamination cracks are clearly marked out only at a late stage (after about 90%) of fatigue life. Under cyclic tensile loads, laminate fracture is coincident with the catastrophic fracture of the major load-bearing plies. Under cyclic compressive loads, failure occurs when laminate stiffness degrades to such an extent that the laminate can not support the applied loads. Failure is usually due to buckling or micro-buckling and subsequent shear crippling.

Laminates subjected to both tensile and compressive loads may exhibit either tensile or compressive fracture modes, depending on the response of competing damage modes to the magnitude of loads and the material system. Delaminations may produce a great reduction in the laminates life subjected to reversed cyclic loads than in the life of similar laminates subjected to either tensile or compressive cyclic loads of the same

amplitude. When loads are reversed, delaminations are subjected to a cyclic shear stress range twice as large as the range under either cyclic tensile or compressive loads alone.

Fatigue life diagrams:

Talreja [239] proposed fatigue damage mechanisms in polymer matrix composites based on the so-called fatigue life diagrams, as shown in Fig. 2.16. The horizontal band centred about the composite static failure strain shows the dominant region of catastrophic damage while the sloping band corresponds to progressive damage. The horizontal line below the sloping band shows the fatigue strain limit of the matrix. The relations between fatigue damage and fatigue loading are apparent. At low cycles, catastrophic fibre damage is dominant resulting in failures within the tensile static strength scatter band. For intermediate cycles, progressive damage mechanisms become dominant, while at high cycles, below the matrix limit, only matrix microcrack nucleation is seen. Thus that the fatigue performance of fibre reinforced composites is bounded by two limiting factors, fibre strength and fatigue limit of the matrix material. The relative magnitude of their values determines the slope of the fatigue life curve, which is one measure of the fatigue resistance of composite materials.

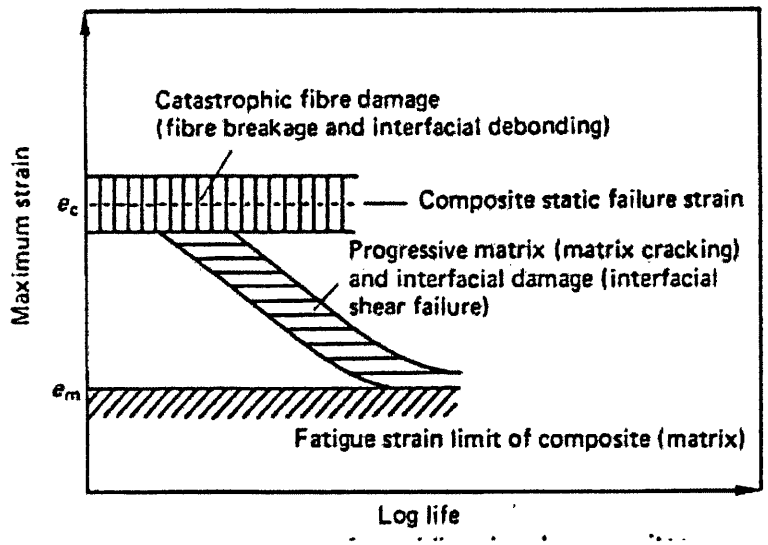

Fig. 2.16: Fatigue life diagram of composites [63]

2.6.3 Factors Affecting the Fatigue Behaviour

The fatigue behaviour of composites is dependent on the properties of the constituents, the matrix and the reinforcing fibre, and their interaction. Such dependencies include the

type of matrix and fibre, the interface between the matrix and fibre, volume fraction of the fibres, and stacking sequence. For a particular structure, however, the fatigue loading parameters will also largely affect the performance during the cyclic loading. The fatigue loading parameters include test method, maximum loading stress or strain, the loading control mode, the mean stress or strain, R ratio, fatigue loading frequency and the test environment.

2.6.3.1 Matrix

The damage due to fatigue usually begins with matrix cracking for fibre reinforced polymer composites. The resins most commonly used as matrices for PMCs are polyesters and epoxy resins. The fatigue behaviour in these composites is similar to fatigue in metals and is cycle dependent rather than time dependent. Epoxy resins are slightly superior to phenolic, polyester and silicone resins in terms of fatigue properties. The better behaviour of epoxy resins is attributed to their greater strength, better bonding to the fibres, lower shrinkage resulting in smaller residual stresses and inherent toughness [241]. Despite great chemical differences, the influence of the resin on the fatigue strength of PMCs is rather small when compared with the influence of the different reinforcements. In her studies on fatigue properties of thermosetting glass fibre composites, Dyer [242] observed that composites made with polyurethane-vinylester resin showed better fatigue performance than those made with polyester resin.

2.6.3.2 Fibre

Various studies have shown that a ranking of materials from best to worst in fatigue performance is high modulus carbon fibre, high strength and low modulus carbon, aramid/carbon hybrid, glass/ aramid hybrid, s-glass, and E-glass. Glass fibre suffers the maximum degradation in fatigue and its endurance limit is about one third of its static strength, which is comparable to its counterpart in the case of steel and aluminium [218]. The better performance of carbon and aramid fibre as compared to E-glass can be attributed partly to their higher ultimate strength. However their better behaviour under fatigue loading is, above all, the result of the considerably greater modulus, almost three times that of glass fibres, which also results in a much greater modulus of the laminate. A laminate with a greater modulus of elasticity needs a higher cycling stress level to reach the critical strain level. This is especially the case under tensile loading conditions, as the resin is far less sensitive to cracking under compression. However,

under compression load, the buckling strength of the fibres dominates the fatigue behaviour, especially in the case of aramid but somewhat less with high modulus carbon fibres. The higher thermal conductivities of carbon and boron, which tend to reduce hysteretic heating, also contribute to their superior fatigue performance.

Mandell [243] studied the general trends of tensile fatigue sensitivity of unidirectional composites loaded parallel to different fibres. The high modulus materials graphite, boron, and aramid were found to be very fatigue resistant. Both E- and S-glass composites lost on the order of 10% of their static strength per decade of cycles. However in off-axis loading directions and in compression, the higher modulus materials tend to approximate the glass fibre trend line.

Tanimoto and Amijima [244] studied the effect of glass fibre content on fatigue properties of laminated glass fibre-polyester composites. Their results showed that the fatigue strength increased with increasing glass content in both axial fatigue and rotating bending fatigue. This increase was attributed to increase in static strength of the composites as a result of increased fibre content.

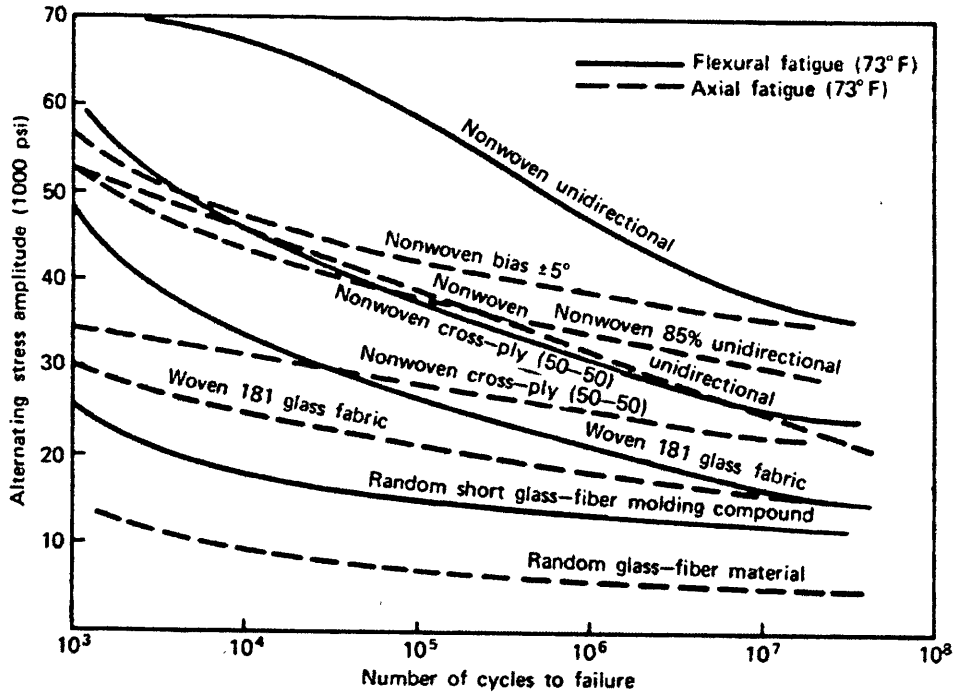

Fig. 2.17: Effect of fibre orientation on fatigue strength of composite materials [241]

Boller [245] studied the influence of fibre orientation on fatigue strength and found that unlike static tensile strength, unidirectional composites do not have optimum fatigue strength and isotropic fibres show better fatigue resistance. Davis et al [241] also studied the influence of different laminate constructions on the fatigue strength as shown in Fig. 2.17. Non-woven materials were found to be superior to woven materials in fatigue because the fibres do not get crimpled as in the fabric construction. Thus non woven materials were found to possess optimum fatigue properties.

2.6.3.3 Interface

The influence of interfacial properties on the fatigue behaviour of composites is complex, and has been studied by many researchers. It is now widely accepted that an improved interfacial adhesion between high strain fibres and high strain matrices results in improved fatigue performance for various polymer matrix composites.

Studies done by Hofer et al [246] on untreated and organosilane surface treated glass fibre reinforced composites showed that untreated glass exhibited the highest fatigue strength in a dry environment but lowest strength in a humid environment. The research was inconclusive regarding the effectiveness of various surface treatments on fatigue strength.

2.6.3.4 Test Parameters

Fatigue test parameters include load control mode, test frequency, mean stress, stress ratio R, etc. All these affect the fatigue response of composite materials to some degree.

The viscoelastic nature of polymers causes a phase difference between cyclic stresses and strains in polymeric matrix composites exemplified by hysteresis loops even at low stress level. This results in energy accumulation in the form of heat within the material. Owing to the low thermal conductivities of the material, the heat is not easily dissipated, which in turn creates a temperature difference between the centre and the surfaces of a polymeric laminate. At a constant stress amplitude level the temperature difference due to viscoelastic heating increases with increasing frequency of cycling.

Dally and Broutman [247] have shown that the magnitude of the test frequency affects the internal heating of composites in tension-tension axial fatigue. As the frequency of fatigue loading increases, internal heating of the composite increases and fatigue life

decreases. Frequencies of fatigue load under 5 Hz have been reported to produce negligible internal heating in glass fibre reinforced polymer composites. However frequency effects have been found to have negligible effect on fatigue lives of both cross-ply and isotropic composites.

The influence of mean stress in fatigue tests is usually presented through a plot of permissible stress amplitude as a function of mean stress for a fixed cyclic life. It has been found that the influence of mean stress on the fatigue behaviour of composites is similar to that of metallic materials [22]. For a fixed cyclic life the permissible stress amplitude decreases as the mean stress increases. For a negative mean stress, the stress amplitude is larger than for a zero mean stress. For a given mean stress, cyclic life decreases as the stress amplitude increases.

The stress ratio R, which is defined as the ratio of minimum stress and the maximum stress during fatigue loading, is also an important fatigue parameter. A wide range of R values have been used in the fatigue testing of composite materials. Generally, when the stress ratio increases the fatigue strength decreases. For tension-tension fatigue test, R of 0.1 is usually used to ensure no compressive load to the specimen.

Mandell and Meier [248] studied the effects of stress ratio, frequency and loading time on the tensile fatigue of 0/90° E-glass epoxy laminates. It was observed that the S-N curves were influenced by waveform and frequency even in the absence of heating effects. The initial strength and the rate of loss of initial strength were greater for waveforms with less time at maximum stress. At low cyclic stresses, the S-N curves for various waveforms tended to converge to a lifetime determined solely by the number of cycles. The degradation rate was generally much higher under cyclic loading than under constant load but the cyclic lifetime converged to the static lifetime as the amplitude of the cyclic stress approached zero.

Stress concentrators such as notches, holes, fasteners, impact damage and other imperfections have less effect on tensile fatigue strength than on static strength. Depending on the laminate configuration, these concentrators can reduce static tensile strength by up to 50%.

The fatigue behaviour may also be affected by the production process and quality control. The curing and hardening process can affect the properties of the resin and the

interface. During the laminating process air bubbles may be entrapped in the fabric weave or in the surface layer. Such voids may result in a fatigue strength reduction factor up to 1.3 to 1.4 for the onset of resin cracking. The distribution of the resin, the saturation of the reinforcement and the stretching of the fibres are determined by the laminating process. Inhomogeneous distribution of the resin and slack of the fibres may result in an overall or local influence on stiffness and fatigue strength.

The effects of increasing ambient temperature on fatigue life of composites are usually detrimental; the higher the temperature, the greater the damage, though the degradation is not necessarily linear with respect to temperature [236].

2.6.3.5 Moisture

It is well known that some polymeric materials may absorb moisture when exposed to humid environments. The absorbed moisture lowers the glass transition temperature of polymeric resins and their composites, and also causes a degradation of mechanical properties, especially in shear and compression. Cyclic loading of composites may accelerate the diffusion of moisture into the composites due to matrix cracking. Fatigue life may be reduced considerably due to environmental conditions, as in seawater, especially if the surrounding medium can penetrate into the laminate along surface cracks and along debonded fibres. The reduction of the fatigue strength is considerable at higher load amplitudes, whereas the effect will be small at lower stress levels.

Studies undertaken on the effect of water on fatigue life of composites ([249], [250]) observed that fatigue life was inversely proportional to the initial water absorption of the matrix resin. However some researchers have reported little specific effects of moisture on the behaviour of graphite fibre- and graphite/glass hybrid-composites [251].

2.6.4 Mechanical Properties Degradation

The post-fatigue performance of a fibre-reinforced composite is studied by measuring its static modulus and strength after cycling for various fractions of its total life to fracture. Both static modulus and strength are reduced with increasing number of cycles. The actual shape of residual strength and stiffness versus cycles varies with material, stacking sequence, loading history and environment.

2.6.4.1 Strength Reduction

In general, the tensile and compressive residual strengths of composite laminates decrease throughout the fatigue lives. In their studies on glass fibre-epoxy composites, Broutman and Sahu [240] found that most of the strength reduction occurred in the first 25% of the fatigue life beyond which the rate of decrease in static strength was reduced. The shape of residual strength degradation curve can be related to fatigue damage mechanisms. Matrix cracks and early fibre fracture, which develop during the first 10% to 15% of fatigue life and are widely scattered throughout the laminate, have a small, but measurable, effect on stiffness and strength, particularly residual tensile strength. After the Characteristic Damage State (CDS) of regularly spaced matrix cracks forms and as stage II damage develops, residual strength decreases at an increasing rate. Residual strength continues to decrease throughout stage II and into stage III where delamination and fibre fracture greatly influence response. This has been shown in Fig. 2.14 above.

2.6.4.2 Stiffness Reduction

The use of stiffness change as a quantitative indicator of fatigue damage has received considerable attention because it is generally accepted now that the strength degradation does not always reflect the fatigue damage [252]. Stiffness is a well-defined engineering property, routinely measured, clearly interpreted, and directly involved in mechanics calculations. Stiffness changes are directly related to internal stress redistributions, and where strength reductions are large, the attending stiffness changes are also large [237].

One major difference between the behaviour of composites and metals in fatigue is the change in stiffness which can occur continuously over a large portion of fatigue life to fracture. Several experimental studies on composite materials in late 1960s and early 1970s observed reduction in stiffness in the loading direction during fatigue. Until mid-1970s, this phenomenon had been observed in fatigue testing of glass, graphite, and boron reinforced epoxy, glass reinforced polyester and polypropylene, and boron reinforced aluminium [253].

Hahn and Tsai [254] formulated a gradual failure model that attempted to relate the modulus degradation to the interior damage. Hahn and Kim [255] proposed another model that suggested a fatigue failure criterion based on longitudinal modulus

degradation. On the basis of studies done on stiffness changes in boron-epoxy laminates, Reifsnider and O'Brien [256] argued that the nature of fatigue damage in composites is anisotropic and therefore all fatigue properties would be affected.

Determining the change in stiffness of composites under cyclic loading is important for two other reasons [257]. First, many engineering structures made of composite materials, for example aerospace components, are deformation-limited structures. The compressively loaded columns and shell structures are also designed to have high stiffness to carry load without buckling. Any change in stiffness during fatigue loading will alter the response of the component to loads and reduce the performance level of the structure. In designing stiffness-critical composite structures, therefore, fatigue failure criteria based on stiffness changes, rather than fracture, is used.

Secondly, change in stiffness provides a good non-destructive technique for monitoring change throughout a loading history. Stiffness changes are directly related to the severity of damage by the mechanics associated with the subsequent response of the material. The stiffness change in composites during cyclic loading is greater than the change in residual strength. Thus stiffness change can be used to anticipate and predict remaining strength and life of the structure.

The stiffness decreases monotonically during cyclic loading, as has been shown for [0/90°] graphite-epoxy laminates [258], [±45°] glass-epoxy laminates [253], and [±45/0/±45/0°] glass/graphite-epoxy laminates [253]. It has been shown experimentally [259] that the magnitude of stiffness degradation increases as the maximum cyclic stress level decreases. However the stiffness degradation rate is not strictly linear.

The stiffness change because of cyclic loading depends on the specific material and loading. However a general relationship of stiffness change-expended cycles has been established and verified for many composite materials, including metal matrix composites [257]. This relationship identifies three distinct stages of stiffness reduction. First stage is characterised by initial rapid decrease in stiffness caused by matrix cracking and some early fibre fracture. The second stage is an intermediate but long period of stiffness reduction which results from additional matrix cracking, crack coupling along ply interfaces, and delaminations. The third stage is again short and is characterised by rapid decrease in stiffness resulting from increase in damage growth rates.

The three-stage stiffness reduction regime was confirmed by Kim and Elbert [260] for unidirectional E-glass/polyester composites. They were also successful in relating these stages to the micro-mechanisms of failure by examining the fractured specimens. During stage I, the fibre surface flaws apparently coalesce and result in interfacial failure and the onset of transverse and shear cracking in the matrix. During stage II, the static modulus remains nearly steady but the hysteresis energy rapidly increases. During stage III, the matrix cracks coalesce and fibres on a plane fail, causing delamination through the specimen cross-section. The three stages of stiffness reduction were also confirmed for [0,0,±45°] woven carbon fibre/polyester composites by Khan et al [261].

In his studies on stiffness degradation of composites in fatigue, Yuanjian [262] observed the same three stages of stiffness reduction for $[\pm 45^\circ]_4$ glass fibre reinforced polyester and $[\pm 45^\circ]_4$ glass fibre reinforced polyvinylester composites. However $[0/90^\circ]_{2s}$ glass fibre reinforced polyester composites were observed to show much lesser reduction in stiffness with increase in fatigue cycles compared to $[\pm 45^\circ]_4$ glass fibre reinforced composites.

Dyer [242] also reported same three stages of stiffness reduction for $[90/0^\circ]_{2s}$ and $[90/0/\pm 45_2/0/90^\circ]$ glass fibre reinforced-polyester and –polyurethane composites. However the composites made with lay-ups of $[\pm 45^\circ]_4$ showed only two stages of stiffness reduction in both matrices.

Setiadi et al [263] compared the performance of continuous randomly oriented glass fibre reinforced composites in polyester and polyurethane matrices under zero-tension fatigue loading. The polyurethane-based composites showed better fatigue resistance than the polyester-based composites in terms of mild modulus degradation and high energy dissipation rate when tested at 50% of UTS. The good fatigue resistance of the polyurethane-based composites mainly came from the tough polyurethane resin, which resisted the development of matrix cracks. This suggests that polyurethane has a better fatigue resistance than polyester.

Beaumont [264] proposed a model for stiffness reduction during fatigue loading of composite materials. The relationship between the modulus and the number of fatigue cycles for glass fibre reinforced polymer composites is given by the following equation:

$$\frac{E}{E_o} = 1 - \{25(\frac{\sigma_{max}}{E_o}) N^{0.25}\} \quad \text{.....(2.22)}$$

where E is the current (damaged) modulus, E_o is the undamaged modulus, σ_{max} is the maximum applied stress, and N is the number of cycles. This equation has been applied successfully to 0/90 glass fibre-epoxy laminates and Kevlar-epoxy laminates.

Most of the studies have concentrated only on observing the effect of fatigue on the longitudinal stiffness. Talreja [252] devised an experiment to observe the effect of tension-tension fatigue on the four elastic constants of unidirectional glass fibre reinforced polyester composites: longitudinal elastic modulus, transverse elastic modulus, the two Poisson's ratios ν_{12} and ν_{21}, and in-plane shear modulus. The longitudinal elastic modulus remained essentially constant with increase in the number of cycles. The Poisson's ratio ν_{12} showed slight increase. The in-plane shear modulus and the Poisson's ratio ν_{21} showed significant changes which were attributed to matrix damage. It was concluded that fatigue damage characterisation of composites can not be based on the measured changes in longitudinal modulus alone because they do not reflect all damage events in fatigue of composites.

2.6.5 Fatigue Life Prediction Models

Various models have been developed to predict the fatigue life of composite materials. They fall into four main categories: empirical, residual strength degradation, stiffness degradation and actual damage state based theories [259].

Empirical fatigue theories are used to characterise the S-N curves of the materials. The equations mostly used to characterise the S-N data are given below.

$$\sigma_{ult}/\sigma_a = N^s \quad \text{.....(2.23)}$$

$$\sigma_a = \sigma_{ult} - b \log N \quad \text{.....(2.24)}$$

$$\sigma_a/\sigma_{ult} = 1 - b \log N \quad \text{.....(2.25)}$$

$$\sigma_{range} = a + b/N^x \quad \text{.....(2.26)}$$

$$\sigma_{range} = a + b/N^x - c/A^y \quad \text{.....(2.27)}$$

$$\sigma_a/\sigma_{ult} = a + b/(\log N)^x \quad \text{.....(2.28)}$$

where A= (1-R)/(1+R) = σ_{range} / σ_{mean}, a and b are experimentally determined material constants, σ_{ult} represents static strength, σ_a is the maximum or minimum applied stress, and σ_{range} is the stress range.

Equation (2.23) represents a straight line S-N curve on a log-log plot of the fatigue data. Equation (2.24) represents the straight line fatigue data on a stress-log N plot. This equation has been used to characterise a large class of glass fibre reinforced composite materials [265]. Equation (2.25) has been shown to apply to fatigue behaviour of most composite systems. For tension-tension fatigue, b typically has values between 0.06 and 0.12 for laminates of common engineering interest [237]. Even unidirectional composites have values of b usually in the 0.08-0.1 range. Equation (2.26) has been shown to be mostly applicable to metals [266]. Equation (2.27) has been used to characterise glass-epoxy fatigue data [267]. Equation (2.28) has been used to characterise a number of composite materials [268].

2.6.6 Fatigue Properties of Natural Fibre Composites

Like other mechanical properties, the fatigue behaviour of natural fibre composites is still not fully studied. Studies into their behaviour were carried out by Gassan et al. with thermoplastics and thermosets [269]. The composites were made with flax and jute used for epoxy, polyester and polypropylene and were tested in tension-tension fatigue. They investigated the influence of type of fibre, textile architecture, fibre-matrix adhesion, fibre mechanical properties and amount of fibre on tension-tension fatigue behaviour. Due to differences in fibre fine structure and surface morphology, significant differences in composite damping were measured between unidirectional flax and jute epoxy composites, with an approximately, two-fold increase in damping for the flax–epoxy composites. Damage propagation was quite similar for both types of composites.

The influence of textile architecture was investigated by use of unidirectional and woven reinforced jute–epoxy composites. Critical load for damage initiation and load at failure was lower and damage propagation was more rapid for the composites based on woven reinforcements. The quality of fibre–matrix adhesion was shown to have a significant effect on the fatigue behaviour of both reinforced brittle polyesters and ductile polypropylene matrices. For both, the critical load for damage initiation was

lower and damage propagation was more rapid for composites with untreated jute wovens.

Fibre strength and modulus were found to influence the critical load for damage initiation, the rate of damage propagation and the load at failure in unidirectional flax–epoxy composites. Increasing mechanical fibre properties increases the critical load and the failure load, while damage propagation was reduced. Composite damping was reduced with increasing fibre fraction below and above the critical load for damage initiation, with comparable rates for damage propagation.

An improved fibre–matrix adhesion due to a coupling agent such as MAH grafted PP leads, for these modified jute–polypropylene composites at comparable fibre contents, to a distinctly higher dynamic strength, i.e. stress at fracture measured in the load increasing test, as for the composites with untreated jute-fibres. Progress of damage for unmodified jute–polypropylene composites is nearly independent of the fibre content, which results in independent maximal stresses, due to the improved fibre–matrix adhesion, caused by the MAH grafted PP coupling agent and the thereby improved force transfer. In contrast to untreated jute–polypropylene composites, a 40% increase of dynamic strength, at comparable fibre contents (ca. 40 vol.%), is attained through the usage of the coupling agent. The damage of the jute polypropylene composites (modified as well as unmodified) does not occur spontaneously, but occurs continuously with the increasing stress.

Thwe and Liao [105] reported remarkable fatigue properties of bamboo fibre reinforced polypropylene composites. For composites tested in tension-tension fatigue (R=0.1, f=5 Hz), they reported that all samples tested at load levels of less than 80% of UTS survived one million cycles. Even the composites tested at 80% of UTS were able to survive 50000-500000 cycles. They also reported gradual decline in residual stiffness of bamboo fibre reinforced polypropylene composites tested in tension-tension fatigue at 80%, 65%, 50% and 35% of UTS. Three stages of stiffness reduction, commonly found in synthetic fibre composites, were reported for these composites. For hybrid composites in which 5% of bamboo fibres were replaced by glass fibres, the reduction in stiffness was lower, indicating superior fatigue resistance of hybrid composites.

Yuanjian [262] studied the fatigue properties of hemp fibre reinforced polyester composites with 44% fibre weight fraction. It was found that at the same relative stress

levels, the fatigue lives of glass fibre composites were better than hemp fibre composites.

2.7 ENVIRONMENTAL PROPERTIES

In order to compete with other materials, composite materials should have good environmental properties. Ambient moisture, water, chemicals, sunlight, heat, and radiation all cause changes in the microstructure and the chemical composition of composite materials. These changes in turn cause changes in properties such as strength, modulus, impact and fatigue.

Many composite materials are seen as being quite resistant to external environments, especially when compared to corrosion properties of ferrous metals. However many chemical and physical processes can combine to result in accelerated failure in composite materials.

Some examples of composite material encountering different environmental conditions are: fibreglass boats exposed to sea water, ultraviolet radiation, sunlight and repetitive wave forces; aircraft parts exposed to fuels, paint strippers, hydraulic fluids, brake fluids and runway de-icers; storage tanks; sewage pipes; and chemical plants' components.

Reactive environments include all reactive substances, whether synthetic or natural, such as water, oxygen, bleach, petrol, lubricants, detergents, cleaning solvents, acids, alkalis, etching and oxidizing agents, and even gases. High or fluctuating temperatures also cause deterioration of properties of composite materials. The whole spectrum of radiation should also be considered, like ultraviolet, infrared, X-rays, and gamma rays. However ultraviolet and visible light are considered to be more harmful to composite materials [270]. For this research the effect of ultraviolet light and moisture on composite materials will be studied.

2.7.1 Ultraviolet Light

Although UV light makes up only about 5% of sunlight, it is responsible for most of the sunlight damage to the materials, especially polymers, exposed outdoors. This is because photochemical effectiveness of light increases with decreasing wavelength. Since polymer matrix forms the outside surface of the composite material, it is important to consider the performance of the polymer matrix to UV light. The energy of

photons of UV light is sufficient to rupture the bonds within polymer molecules. This rupture causes changes in molecular weight, formation of cross-links, and reaction with oxygen. These structural changes lead to gross physical changes such as chalking, cracking, surface embrittlement, discolouring and loss of tensile and impact strength [271]. The solar ultraviolet radiation spectrum is divided into three ranges: UV-A, UV-B and UV-C. UV-A is the energy in wavelength between 400 nm and 315 nm, the former being the boundary between visible light and ultraviolet light. The energy at the 315 nm boundary begins to cause adverse effects on polymers. UV-B is the 315 nm to 290 nm range. It includes the shortest wavelengths found on the earth's surface and is responsible for severe polymer damage. UV-C includes the solar radiation below 290 nm. Due to complete absorption by ozone layer, it is found only in outer space.

The primary degradation processes in a polymer matrix, such as the formation of excited states, radicals, and chain scission, are largely the result of UV radiation. UV radiation is irrelevant to the heating of an irradiated sample [272]. The heating is caused solely by the absorption of visible and infrared radiation. Thus the primary degradation processes are essentially unrelated to temperature. However many secondary degradation processes do depend on temperature. The photochemical effect of sunlight on a plastic material depends on the absorption properties and bond energies of the material. The range of dissociation energies between atoms in polymer molecules is 70-100 Kcal/mol [271]. UV light in the range 290-320 nm has an energy range of 89-98 Kcal/mol, but, fortunately, it accounts for only 0.5% of sunlight. Light in the range 300-360 nm has energy range of 79-89 Kcal/mol and it thus falls within the range of dissociation energies between atoms in polymer molecules. The energy wavelength of UV-A is thus the major contributor to the degradation in polymers.

Polyesters contain chromopores, which are atom grouping in the molecule that react with sunlight [271]. For polyester, the wavelength that has the greatest photochemical effect is 325 nm [273] which falls within the wavelength range of UV-A. Hence polyesters are more susceptible than other polymers to degradation because of interaction with the sunlight. In one study on the effect of weathering on polyester resin, the resin was exposed to actinic rays in a twin arc Fadeometer [25]. An exposure of 400-700 hours was considered equivalent to one year of outdoor exposure. Initially there was no visible change after several hundred hours of exposure. Then the yellowing of the samples suddenly became noticeable. The tensile strength of the resin

deteriorated from 66 MPa to 47 MPa after 2400 hours of exposure. Similarly the flexural strength deteriorated from 90 MPa to 82 MPa after same exposure period.

To simulate the physical damage caused by sunlight it is not necessary to reproduce the entire spectrum of sunlight. In many cases it is only necessary to simulate the short wavelength. UV light causes degradation in polymers through a breakdown of molecular weight [273]. To overcome this problem, ultraviolet absorbers, such as carbon black or aromatic ketones, are added to plastics.

It has also been shown [16] that in composite materials, exposure to sunlight is confined to surface layers down to about 10 μm depth, this being the typical thickness of resin at which the intensity of ultraviolet light is reduced to one half its incident value. Shkorieh and Bayat [274] studied the properties of glass-polyester composites exposed to UV radiation for different intervals of time. The composites showed reduction of 30% in tensile strength, 18% in tensile modulus and 15% in strain to failure following exposure to 100 hours. The composites made with UV absorber showed little degradation following exposure for the same time interval.

2.7.2 Moisture

The amount of moisture absorbed by the polymer matrix composite depends on the matrix type, exposure time, component geometry, relative humidity, temperature, and exposure conditions. Typical consequences of exposure of composite materials to these environments are: matrix swelling, fibre-resin debonding, matrix cracking, and chain scission [270]. In case of natural fibre reinforced composites, additional problems are encountered because of hydrophilic nature of natural fibres.

Diffusion is the major mechanism for moisture penetration into composite material. This involves direct diffusion of water molecules into the matrix and fibres. The other common mechanisms of moisture penetration are capillary flow along the fibre/matrix interface, followed by diffusion from the interface into the bulk resin, and transport by microcracks [275]. Capillary flow is mostly active only after debonding between fibre and matrix has occurred and transport of moisture by microcracks involves both flow and storage of water in micro-damage. A composite material exposed to moisture will absorb moisture at higher rate initially that will slow down with time and eventually reach an equilibrium (saturation) level. The rate at which a composite laminate of a

given thickness attains the equilibrium moisture concentration depends on the temperature and relative humidity of the environment. In general, thermoset matrix composites have saturation limits ranging from 1 to 2%, while thermoplastic matrix composites have lower range of saturation limit, i.e. 0.1-0.3% [218].

The absorption of liquid molecules into polymer matrix or fibre results in significant swelling. The degree of swelling is linked to the solubility and molecular volume of the absorbed liquid, and the stiffness of material also plays a part. Swelling is found most commonly in the polymer matrix, but also for some polymer fibres. The swelling of natural fibres is a well known phenomenon. Swelling interacts with any internal residual stresses formed during processing, for example because of shrinkage of polymer matrix during curing. Unsaturated polyester resin is well known for its shrinkage during curing. If the fibres do not shrink, this leads to compressive stress on the fibres and a tensile stress in the matrix. Swelling of fibres tends to increase the tension in the matrix and put the fibres into tension. Aramid fibres swell with weight gains of as much as 4%.

The possible effects of absorbed moisture on polymeric composites have been summarised as [276]: Plasticisation of matrix, resulting in reduction in glass transition temperature and usable range, changes in dimensions due to matrix swelling, enhanced creep and stress relaxation, resulting in increased ductility, change in coefficient of expansion, reduction in ultimate strength and stiffness, fibre-dominated properties are generally not affected.

2.7.3 Constituents' Influence on Environmental Properties

The matrix, the fibre and the interface all contribute differently to the environmental properties of the composites.

2.7.3.1 Matrix

All organic matrices are permeable to moisture. Most organic matrices are permeable to a whole range of organic liquids with a consequent reduction in matrix modulus. They are also poor at withstanding high temperatures. Most resins withstand dilute acids and alkalis better than light alloys or stainless steels. This is the major reason for the excellent corrosion resistance of composite materials compared to solids. Anions and cations do not diffuse easily through un-cracked resins [270].

The most important type of chemical degradation in matrix materials is hydrolysis, where water, or OH^-, H^+, or H_3O^+ ions attack chemical groups within the matrix. The hyrolysis reaction are more pronounced in acidic or alkaline environments. The more polar groups within polymers are most susceptible to hydrolysis, notably the ester, amide, carbonate, and amide groups. Unsaturated polyester resin, used in this study, is most susceptible to hydrolysis reaction with the eater groups being broken primarily by OH^- ions.

The other important type of chemical degradation in the matrix material is chemical oxidation with oxidizing acids such as nitric and sulphuric, or other oxidizing agents such as peroxides and hypochlorites. Attack occurs via active free radicals, like H_2O and HO radicals, which attack main chain bonds in the polymer. Polyesters have a higher concentration of ester groups than other resins, and so are most susceptible to hydrolysis, especially with alkaline environments. Apicella et al [277] studied the ageing characteristics of commercial grade polyester resins and the composites made from them. The polyester resins studied were: vinyl ester, bisphenol, and isophthalic. The equilibrium uptake of water at 20 °C was lowest at 0.35% for isophthalic resin and highest at 65% for vinylester resin. The corresponding water uptake for E-glass fibre reinforced resins was slightly higher which was attributed to debonding of fibres. The lowest hydrolytic stability was observed for isophthalic resins, which possessed the highest ester content. After 50 days of immersion in water at 20 °C, isophthalic resin lost 32% of its tensile strength, 11% of tensile modulus, and 18% of elongation to break. The E-glass fibre reinforced isophthalic resin composites lost 19% of tensile strength, 4% of tensile modulus, and 14% of elongation to break after same conditions.

As with all chemical reactions, an increase in temperature leads to an increase in degradation rate in the matrix. As the key degradation reaction is main chain scission in most polymers, the activation energies for degradation in a certain environment are strongly dependent on the bond strength of the weakest bond in a polymer, with simple carbon chain polymers having fairly high activation energies. Polyesters that have oxygen bridges in the main chain have lower activation energies.

An increased tensile stress on polymer chains results in increase in rate of degradation. This is either because the stressed chains are more susceptible to scisson reactions or that once broken, chains are less likely to recombine if they are under stress.

It has been shown [22] that the moisture content does not have a significant effect on fibre-dominated properties but may reduce matrix-dominated properties. The matrix strength falls with increasing moisture content, although its failing strain may be increased. It was shown for unidirectional carbon/epoxy laminates that their elastic moduli and strengths in transverse tensile and shear loading were reduced by the presence of moisture while the axial properties were unaffected [278].

In one study, the moisture absorption of glass mat reinforced polyester laminates was found to be 0.28% and the ultimate tensile strength of these laminates was 89.7 MPa in dry conditions and 81.4 MPa in wet conditions [276]. Special grade polyester laminates are excellent at resistance to acids, bases and distilled water for long times at temperatures as high as 210° F. Glass filled polyester laminates are also used for their excellent resistance to ionising radiation exposure.

Dyer [242] reported moisture saturation level of 0.67% for polyester resin immersed in distilled water and sea water. The polyurethane vinylester resin had saturation level of 0.55% in distilled water and 0.54% in sea water, suggesting greater solubility of water in polyester. The tensile strength and tensile modulus of both resins was found to decrease following immersion in both media.

Another important effect of moisture absorption on the polymer matrix is plasticization. Plasticization occurs because of absorption of liquid molecules into a polymeric matrix or fibre. The small solute molecules disrupt the intermolecular bonding between polymer chains, allowing easier chain movement. This leads to a reduction in glass transition temperature (T_g) of the polymer. The lowering of Tg can have serious effect on the properties of the composite [275]. This mechanism primarily occurs in amorphous regions, so it is more important for glassy polymers.

Generally the higher the equilibrium solubility, the greater the degree of plasticization. Plasticization can lead to a significant decrease in stiffness, increase in creep rate, increase in diffusion coefficient, and the potential for environmental stress cracking of the polymer. In the polymer composites it results in reduction in matrix dominated properties such as shear, transverse tension and longitudinal compression [279].

2.7.3.2 Fibre

Glass fibres are resistant to most chemicals but they do not withstand strong alkalis and acids indefinitely [270]. They suffer from corrosion in aqueous environments, especially under acidic conditions. Even hot water causes glass fibres to lose their strength. Carbon fibres are resistant to almost all chemical agents, but they are vulnerable to oxidation and intercalation. Aramid and other thermoplastic fibres absorb moisture, unlike glass and carbon, undergo chemical degradation under certain circumstances, and are affected by ultraviolet light. Natural fibres also absorb moisture because of their hydrophilic nature, and also suffer chemical degradation as discussed in section.

The use of glass fibres does not improve the excellent corrosion resistance of polyester resins; in fact, in strong caustic environments, the use of glass fibres actually reduces the performance of polyester resin. In such cases carbon fibres are preferred over glass fibres.

2.7.3.3 Interface

The interface between fibres and resin can be damaged by liquids and thermal cycling. It is reflected in reduced transverse tensile strength and short beam strength of the composite [270]. Fibre surface treatment is the best method of protecting the interface from environmental damage.

Degradation of either the matrix or the fibre leads to weakening of the interface. Other factors that are important for degradation of the interface are:

- Degradation of fibres always occurs first on fibre surfaces, thereby weakening the interface.
- The level of cure or crystallinity may be lower at the interface leading to easier degradation.
- Water accumulates at the interface, partly due to greater free volume, more hydrophilic nature of the fibres, and location of voids, debonds, and microcracks.

- Elastic or thermal strain mismatch between the matrix and the fibres can cause the matrix to experience the greatest local stress at the interface.

Kawagoe et al [280] studied the effect of water absorption on interfacial strength between glass fibre/polyester. They found that absorbed water collected preferentially at the interface and resulted in reduction of up to 70% in bond strength at elevated temperatures.

In their studies on the effect of moisture on interfacial strength of carbon fibre reinforced epoxy composites, Pratt and Bradley [281] found that the absorption of 1.4% moisture resulted in a reduction of less than 20% in the interfacial shear strength. This reduction was associated with a reduction in the residual compressive stresses at the interface associated with the cool-down from the curing temperature.

2.7.4 Modelling the Moisture Absorption Behaviour

Various researchers have tried to model the moisture absorption behaviour in composites materials. Amongst the first to do so were Shen and Springer [282] who derived expressions for moisture absorption and moisture content as function of time for one dimensional homogeneous and composite materials exposed either on one side or on both sides to humid air or water. They found that when a) the material is exposed to the environment on one side only or on two sides with both sides being parallel, b) initially the temperature and moisture distribution inside the material are uniform, and c) the moisture content and the temperature of the environment are constant, the moisture content of the material during both adsorption and desorption is:

$$M = G\,(M_m - M_i) + M$$

where M_i is the initial moisture content of the material, M_m is the maximum moisture content which can be attained under the given environmental conditions, and G is a time dependent parameter whose value is given by:

$$G = 1 - \frac{8}{\pi^2} \sum_{j=0}^{\infty} \frac{\exp[-(2j+1)^2 \pi^2 (\frac{D_x t}{s^2})]}{(2j+1)^2}$$

This equation may be approximated by the expression:

$$G = 1 - \exp\left[-7.3 \left(\frac{D_x t}{s^2}\right)^{0.75}\right]$$

For a material exposed on both sides to the same environment, *s* is equal to sample thickness, and D_x is the diffusivity of the material in the direction normal to the surface. For fibre reinforced composites in which the orientations of all the fibres with respect to x, y, and z axes are α, β, and γ, the values of D_x is given by:

$$D_x = D_{11} \cos^2 \alpha + D_{22} \sin^2 \alpha$$

where D_{11} and D_{22} are the diffusivities in the directions parallel and normal to the fibres. The value of D_x can also be estimated from the diffusivity of the matrix D_r and the volume fraction of the fibres v_f by using:

$$D_x = D_r \left[(1-v_f) \cos^2\alpha + (1-2\sqrt{v_f}/\pi) \sin^2\alpha\right]$$

This expression is valid for unidirectional and laminated composites. For laminated composites the fibres must be in a plane parallel to the surface.

The time required for a material to attain at least 99.9% of its maximum possible moisture content is given by:

$$t_m = \frac{0.6786 s^2}{D_x}$$

They applied the equations to moisture absorption in 45° and unidirectional graphite T-300 Fiberite 1034 composites. The test data was found to support the analytical results.

2.7.5 Effect of Moisture on Mechanical Properties

The effect of moisture on the mechanical properties of composite materials can be determined in two ways: by measuring the percentage retention of mechanical properties, such as tensile, shear, or flexural strength; and by examination the sample before and after exposure using optical and scanning electron microscopy (SEM). For carbon fibre-epoxy composites, the consequent losses in mechanical properties can be of the order of 50% for interlaminar shear strength, 50% for compressive strength and 10% for tensile strength. Various studies on composite materials have found them to maintain their mechanical properties in moist conditions.

Choqueuse et al [283] studied the effect of moisture absorption on five composites: E-glass fibres reinforced polyester, vinyl ester, epoxy, and prepreg epoxy, and carbon fibre reinforced PEEK composites. The glass fibres were woven with 90% of fibres in 0° (longitudinal) direction and 10% fibres in 90° (transverse) direction. The fibre weight fraction of the composites ranged from 50-60%. The composites were immersed in distilled water at 5, 20, 40 and 60 °C at pressures of 0.1 MPa and 10 MPa. It was found that even after immersion in water for two years, saturation level was generally not reached. For glass fibre-polyester composites, the values of mass of water absorbed were about 0.7% at 5 °C, 1.2% at 20 °C, 1.5% at 40 °C, and 1.7% at 60 °C at 0.1 MPa (atmospheric) pressure. The same values at 10 MPa pressure were 1.4% at 5 °C, 1.5% at 20 °C, 2.3% at 40 °C, and 2.1% at 60 °C. The effect of increasing temperature on water absorption was noticeable but the effect of pressure was negligible. It was found that epoxy composites absorbed more water than other composites (up to 5% after two years at 60°C) and after drying residual weight gain was noted. The epoxy composites were also more sensitive to pressure than other composites, the weight gain being accelerated at 10 MPa. Except for carbon-PEEK composites, for which there was no significant change of mechanical properties, a degradation of mechanical properties of up to 50% was noted for thermoset composites. The degradation was anisotropic and affected both strengths and moduli. However no simple correlation between the loss of mechanical properties and absorption parameters could be made. In general the hydrostatic pressure did not affect the loss in properties.

This was also confirmed by Dewmille and Bunsell [284] in their studies on unidirectional glass fibre reinforced epoxy composites made in the shape of round bars. For the composites immersed in water at temperatures less than 50°C, there was little effect on mechanical properties although the saturation water content was 0.66-0.71% at fibre volume fraction of 48%. The saturation water content was found to increase with increase in temperature. At 100°C the saturation water content was 1.35-1.45. The mechanical properties also started to degrade at immersion water temperatures of 80°C and above.

In their studies on CSM glass fibre reinforced polyester composites, Han and Koutsky [285] found the water saturation level to be 0.6 weight percent of the specimen at fibre weight fraction of 44%. The value of diffusion coefficient was 5.4 x 10^{-6} mm^2/s which is close to the value reported by other researchers. The fracture energy of samples

soaked in water for 22 days was 950 J/m^2 which was higher than that for dry specimens, 800 J/m^2. The smaller elastic modulus of the soaked specimens induced a greater viscoealstic response and hence more energy was absorbed. The critical load for crack propagation was approximately the same before and after soaking (470 N). The crack propagation mode and the fracture surface appeared to be unaffected by the presence of water. This again pointed towards superior performance of composites in water.

Philips [286] undertook environmental stress-rupture (EST) tests on glass fibre reinforced polyester composites in air and in aqueous environments. For composites tested in water at 40°C, the stress-rupture behaviour was unaffected by specific variations in immersion conditions such as distilled water or seawater, and unsealed or sealed edges of the samples.

Jones et al [287] studied the environmental fatigue properties of cross plied 0/90° epoxy based laminates reinforced with glass, carbon and Kevlar fibres. The environments studied were dry, 65% RH, and boiling water. The CFRP laminates were largely insensitive to the effect of moisture. The GFRP were also unaffected by moisture content unless the fibres were damaged by an extreme environment of boiling water. The KFRP laminates showed lower fatigue strength in boiling water but beyond 10^5 cycles the S-N curve for boiling water coincided with those at other conditions. The laminates were also tested in flexural fatigue. The boiling water as observed to have less deleterious effect on flexural fatigue of GFRP than on its axial fatigue. The same was true for KFRP. The CFRP appeared to be marginally strengthened by boiling water in flexural fatigue, which was attributed to the beneficial effect of resin plasticization on interlaminar shear strength.

Loos and Springer [288] also exposed CSM glass fibre-polyester composites to various environmental conditions. Composites with fibre weight fraction of 65% immersed in distilled water at 23°C showed equilibrium moisture gain of 3.5%. Increasing the temperature of water to 50°C did not affect the equilibrium moisture level. The equilibrium moisture level of same composites in saturated salt solution at 23°C was lower at 1.5%. In call cases the moisture absorption followed the Fickian behaviour up to the saturation point. The diffusion coefficient was calculated at 1.1×10^5 mm^2/s for composites immersed in distilled water at 23°C.

Ellyin and Rohrbacher [289] immersed glass fibre-epoxy composites with various fibre configurations in distilled water at room temperature and at 90°C. Composites with cross-ply $[\pm 0_2, 90_3]_s$ configuration showed a moisture saturation level of 1.8% at room temperature, while those at 90°C did not reach their saturation limit after 40 days of immersion.

Sindhu et al [290] studied the properties of CSM glass fibre reinforced polyester composites in different aqueous media. The composites immersed in water for 3 months showed 20% reduction in their tensile strength but 1% increase in tensile modulus. Composites immersed in 10% salt solution again showed 20% reduction in tensile strength and 9% reduction in tensile modulus. Composites immersed in 10% alkali solution showed 40% reduction in tensile strength and 1% reduction in tensile modulus. Dyer [242] also reported a moisture saturation level of 0.7% for $[\pm 45]_4$ glass fibre reinforced polyester laminates immersed in distilled water and sea water. For laminates with same lay-up but in polyurethane matrix, the saturation level was 0.5%.

Pritchard and Speake [291] immersed neat polyester resins and glass reinforced polyester laminates in water for up to three years at temperatures in the range 30-100 °C. The residual mechanical properties were found to be functions of true absorbed water content, both for resins and laminates. Empirical relations describing the relationships were obtained for each property, most of which were of the form

$$P = a\,(1 - e^{-b\,\exp(-cM_t)}) + d$$

where P is the residual property, M_t is the true water absorption, and *a, b, c,* and *d* are empirical constants. Using these equations it was possible to predict residual mechanical properties at 15°C and at temperatures outside the experimental range for a period of 25 years. Experimental data obtained over three years at the lower end of the temperature range appeared to fit the predicted data well.

2.7.6 Environmental Properties of Natural Fibre Composites

Natural fibres are susceptible to environmental degradation because of their structure. Biodegradation by microorganisms occurs because they hydrolyse the carbohydrate polymers, especially hemicelluloses, into digestible units [292]. Photochemical degradation by UV light occurs primarily in lignin which is also responsible for colour

change. Cellulose is less susceptible to UV degradation. Hemicellulose and cellulose are degraded by heat much before the lignin. Lignin also contributes to char formation.

2.7.6.1 Moisture Absorption

Cellulosic fibres are hydrophilic and absorb moisture. The moisture content of fibres can vary between 5 to 10%. This can lead to dimensional variations in composites and also affects mechanical properties of composites. It can also lead to poor processibility and porous products. It can cause fibres to swell and ultimately rot through attack by fungi. A possible solution is to improve fibre-matrix interface by using compatibilizers and adhesion promoters. With better adhesion, the moisture sensitivity is usually reduced [9]. Also surface treatments of fibres with silanes can make the fibres more hydrophobic.

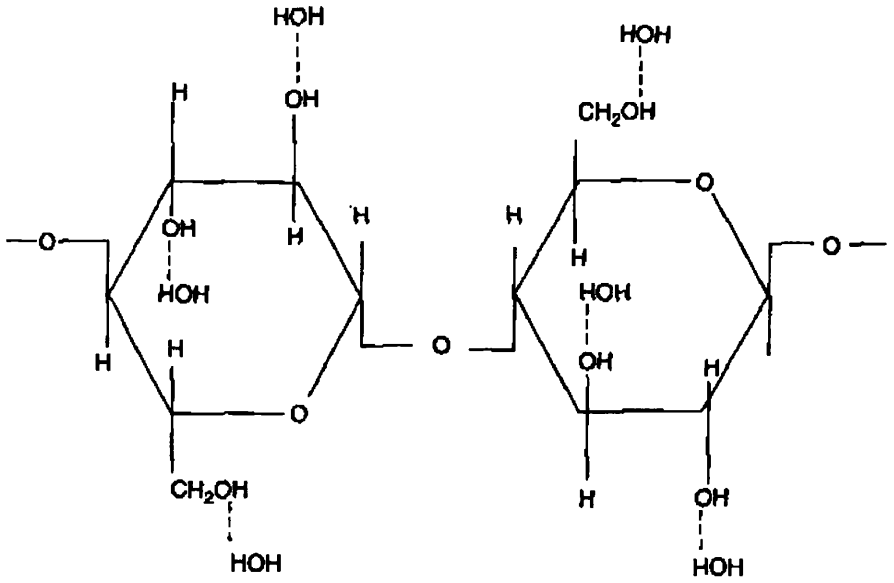

Fig. 2.18: Absorption of moisture in natural fibres [117]

As soon as the natural fibres are exposed to moisture, hydrogen bonds are formed between the hydroxyl groups (-CH_2OH) of the cellulose molecules and water as shown in Fig. 2.18. The first water molecules are absorbed directly into the hydrophilic groups of the fibres and form a relatively strong hydrogen bond. Following this, other water molecules are attracted either to other hydrophilic groups or they form further layers on top of the water molecules already absorbed by weaker hydrogen bonding. Thus the

natural fibres absorb and desorb moisture from atmosphere until they reach the equilibrium stage.

Water uptake in the cell walls causes fibres to swell until the forces of water absorption are counterbalanced by the cohesive forces of the cell walls. The swelling of fibres is found to be directional with the maximum swelling occurring in the lateral direction and minimum in the longitudinal direction. The amorphous part of native cellulose, with all hydroxyl groups accessible to water, contributes more to swelling than the crystalline part, where only the surfaces are available for water sorption [70]. Therefore increasing the crystallinity of the fibre reduces the swelling capacity. The hydrophilic hemicellulose also contributes greatly to fibre swelling. Reducing the amount of hemicelluloses also reduces the swelling capacity of fibres. Thus the swelling of fibres as a result of moisture absorption can affect the dimensional stability and weaken the interfacial bonding of the composite. These can have adverse effects on the mechanical properties of these composites.

Ho and Ngo [293] studied the water sorption characteristics of hemp and coir fibres. Both fibres displayed two-stage water sorption curves: the first stage obeyed Fick's law, whereas the second stage represented non-Fickian diffusion. Hemp fibre displayed saturation water uptake of 66% at 23 °C which increased to 80% at 80 °C. At 23 °C the following sorption parameters for hemp fibres were determined: Diffusion coefficient 0.56×10^{-9} m^2/s, sorption coefficient 0.66, permeability coefficient 3.7×10^{-10} m^2/s.

Jimenez and Bismarck [71] exposed different natural fibre to 100% relative humidity and determined the equilibrium moisture uptake. Cornhusk, hemp and sisal fibres had uptake values of 33% whereas abaca, flax, luffa, henequen, lechuguilla and lyocell fibres had equilibrium moisture uptake of 23-30%.

The moisture absorption in natural fibre reinforced composites is found to increase with increase in fibre content. This was found to be true for the following composites: jute-epoxy [62]; jute-polyester [294]; hemp-polyester [295], pineapple-polyester [296], banana-polyester [297], woodflour-polyester [298], ramie/cotton-polyester [299], sisal-epoxy [300], sisal-polypropylene [301], rice husk-polypropylene [302], pineapple-polyethylene [303], cellulose-polypropylene [304], and rice hull-HDPE [305].

Increasing the water temperature accelerates the water sorption but does not affect the saturation uptake. This has been shown to be true for sisal-PP composites for water temperatures of 50°C and 70°C [301].

In their studies on water absorption behaviour of hemp fibre reinforced polypropylene composites, Hargitai et al [108] found the saturation water uptake to be strongly dependent on fibre weight fraction. Whereas the saturation water uptake for composites with 30% fibre weight fraction was only 7%, the value for composites with fibre weight fraction of 70% was as high as 53%.

Sgriccia et al [181] reported that hemp fibre reinforced epoxy composites had a saturation weight gain of 18.4% following immersion in water for 1500 hours. This is a considerably high value considering that the composites had a fibre weight fraction of 15%. At the same fibre weight fraction, henequen-epoxy composites had the highest weight gain of 28% while flax-epoxy and kenaf-epoxy composites had similar weight gain as hemp-epoxy composites.

In another study, Aghedo and Baillie [306] reported a saturation mass gain of 10% for hemp fibre reinforced recycled linear low-density polyethylene composites following 2000 hours of immersion in water.

In their studies on water absorption properties of banana fibre reinforced polyester composites, Mariatti et al [144] reported a water saturation level of 8.1% at fibre volume fraction of 20%. At same fibre volume fraction, they reported the value for pandanus fibre reinforced polyester composites to be 11%.

Sreekumar et al [138] have shown for sisal fibre reinforced polyester composites that equilibrium water uptake also depends on manufacturing method. Composites made by compression moulding had equilibrium water uptake was 1.2 mole percent for 50% fibre volume fraction whereas for composites with same fibre volume fraction but made by resin transfer moulding, it was 0.75 mole percent.

Mehta et al [307] reported saturation moisture uptake of 0.7% for hemp fibre reinforced polyester composites placed in humidity chamber having 90% RH. For acrylonitrile treated hemp fibre composites, the equilibrium moisture uptake was 0.3%.

Mishra et al [308] reported water uptake of 19.5% after 30 hours of immersion for hemp fibre reinforced novolac composites having fibre weight fraction of 40%. For fibres treated with maleic anhydride, the composites' water uptake was reduced to 14.5% for the same time of immersion.

Thwe and Liao [105] reported a moisture saturation level of 1.2% for bamboo fibre reinforced polypropylene composites at 20% fibre weight fraction. The same authors reported a moisture intake level of 13% for the same composites but at fibre weight fraction of 30% in another paper [106]. No reason was given for the large difference in moisture intake levels, but the latter figure seems more sensible. Singh et al [309] reported a saturation water intake of 45% for jute cloth reinforced phenolic composites containing fibre volume fraction of 70%.

A study [7] showed that composites reinforced with 30% hemp fibres in polypropylene matrix immersed in water absorbed approximately 7% of their weight. On the other hand, under standard hygroscopicity and temperature conditions, after saturation the part released all the water adsorbed, and no hysteresis was observed in the sorption/ desorption curves. The mechanical properties of the composites decreased slightly following the absorption of water, although the original properties were recovered as soon as the water was desorbed.

2.7.6.2 Effects of Surface Treatments on Moisture Absorption

Two processes have been generally used to reduce moisture sensitivity in natural fibres: acetylation and hydrothermal treatment. Experiments have confirmed that equilibrium moisture content decreases with increasing acetyl content in all natural fibre materials which proves the effectiveness of the process.

Hydrothermal treatment increases the crystallinity of cellulose and hence contributes to reduced moisture uptake. Furthermore, part of hemi-cellulose is extracted, further decreasing the moisture uptake. However at higher temperatures, this process leads to deterioration of mechanical properties of the fibres.

Various coupling agents have also been used in to reduce the moisture absorption of natural fibres. The improved moisture resistance of natural fibre composites because of coupling agents can be explained by an improved fibre-matrix adhesion. The coupling

agent builds chemical bonds (silanol) bonds and hydrogen bonds which reduces the moisture caused by fibre-matrix debonding.

Gassan et al. [67] used epoxyfunctional-γ-glycidoxypropyltrimethoxy-silane as coupling agent in jute fibre reinforced epoxy composites. The introduction of coupling agent not only improved the mechanical properties but the moisture uptake was also reduced by about 10-20%.

The investigations on silanised jute–epoxy composites regarding their moisture absorption (in distilled water at 23°C) showed about 20% lowered moisture at equilibrium. However the tensile strength of the silanized composites was found to be independent of the moisture content of the composites [62]. Unmodified jute-epoxy composites reached about 65% of the value of the dry tensile strength at maximum moisture content of 5.2 wt. %.

Singh et al. [309] studied the physical and mechanical properties of jute fibre reinforced phenolic composites under various humidity, hydrothermal and weathering conditions. The results indicated that the loss in properties was considerable and the surface was heavily defaced under high humid/ wet environment.

Wang et al. [305] introduced a new theory for studying the moisture absorption in natural fibre composites. They found that at higher fibre loading when accessible fibre was high, the diffusion process was the dominant mechanism, while at low fibre loading, percolation was the dominant mechanism.

Mishra et al. [308] studied the swelling properties of natural and maleic anhydride esterified fibres of banana, hemp, and sisal reinforced in novolac resin. Amongst all the fibres tested, the maximum absorption of water was found in hemp fibre composite and the minimum in surface treated sisal fibre composite. The surface treatment reduced the water absorption in all the composites. Steam absorption was also found to be maximum for hemp fibre composites. The surface treatment of fibres again reduced the steam absorption in all composites.

The tension-tension fatigue testing of silanized jute-epoxy composites at moisture content of 4.5 wt. % by Gassan and Bledzki [62] showed nearly the same S-N curve as for the unmodified composites at standard humidity. This was again attributed to improved fibre-matrix interfacial bonding.

Rouison et al. [295] studied the water absorption of hemp/ unsaturated polyester composites. The water absorption increased with increasing fibre content. The moisture absorption process was shown to follow the diffusion mechanism and was more prominent in longitudinal than transverse direction. Composite samples immersed in water reached saturation levels after about eight months and showed no signs of cracking due to swelling. Various fibre treatments were tested (sizing, alkali, silane), but none resulted in substantial increase in resistance to water absorption. The most effective technique to increase moisture resistance was to properly enclose all the fibres within the matrix. The samples were immersed in water for one month and then tested for flexural properties. The flexural strength was found to decrease by 11% while flexural modulus was found to decrease by 34%.

2.8 MICROSTRUCTURAL CHARACTERISATION

Microstructural characterisation techniques have been widely used to understand the microscopic and macroscopic behaviour of composite materials. The most common advanced techniques used [310] are optical coherence tomography (OCT), laser Raman spectroscopy (LRS), scanning acoustic microscopy (SAM), X-ray diffraction scanning microscopy, nuclear magnetic resonance (NMR), confocal laser scanning microscopy (CLSM), and electron microscopy. Scanning electron microscopy (SEM) is the most widely used technique for fractography of composite failure analysis and this technique will be used extensively in this research. This technique has proved so successful that there are now books [311] wholly devoted to showing the fracture surfaces of composite materials.

3. EXPERIMENTAL WORK

3.1 MATERIALS

The main materials used in this research were hemp fibre, glass fibre in chopped strand mat (CSM) form, unsaturated polyester resin, and chemicals for fibre surface treatment (acetic anhydride, sodium hydroxide).

3.1.1 Hemp Fibre

In this research, non-woven randomly oriented hemp fibre mat was used. It was provided in the shape of a mat roll by JB Plant Fibres Ltd., UK. The average width of the mat was 1.2 m. Fig. 3.1 shows a close-up of the hemp fibre mat used. Short hemp fibres were randomly dispersed in two dimensions. No technical data was provided by the supplier and tests were undertaken to determine various physical and mechanical properties of fibres, the details of which can be seen in Chapter 4.

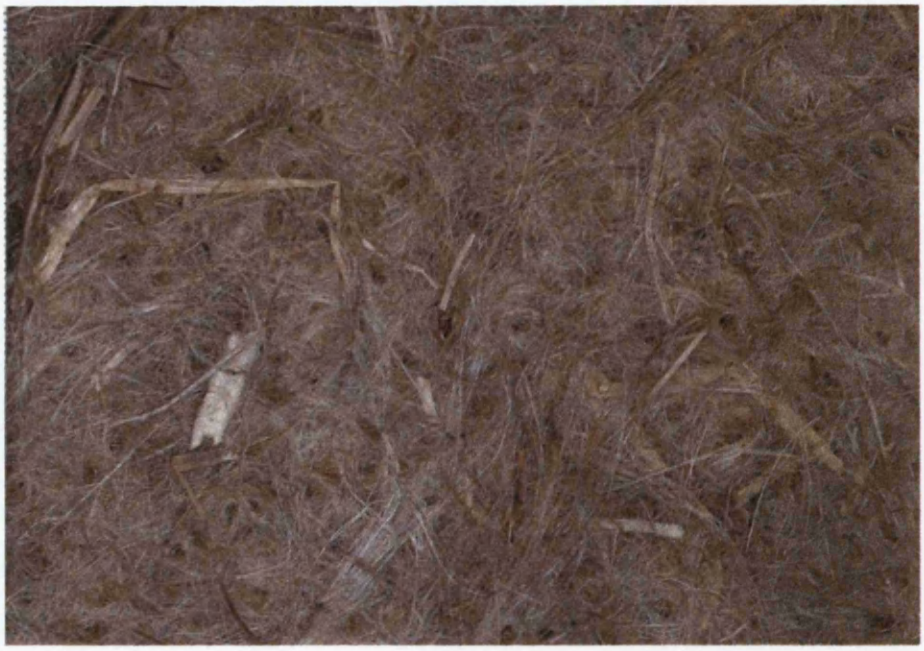

Fig. 3.1: A close-up of hemp fibre mat

3.1.2 Glass Fibre

Glass fibres in chopped strand mat form were supplied by East Coast Fibreglass Supplies, South Shields, UK. Chopped glass strands were bonded in mat form with an emulsion binder. The mat was made of Advantex® glass fibres which combined the electrical and mechanical properties of traditional E-glass with the acid corrosion resistance of E-CR glass. The mat was designed as a reinforcement medium for polyester resins used in contact moulding processes. The properties of the fibres, as given by the supplier, are shown in Table 3.1.

Table 3.1: Properties of chopped strand mat glass fibres

Weight	450 g/m^2
Nominal length of strands	50 mm
Density	2.56 g/cm^3
Tensile strength	2000 MPa
Tensile modulus	76 GPa
Strain to failure	2.6%

3.1.3 Unsaturated Polyester Resin

Unsaturated polyester resin, designated as Resin A by the manufacturers Scott Bader Company Ltd., UK, was used as the matrix. Resin A is a pre-accelerated and low viscosity resin with rapid hardening characteristics. It combines rapid impregnation of reinforcements with very short mould release time, and is ideal for hand lay-up applications. Its properties, as given by the manufacturer, are detailed in Table 3.2.

Resin A required only the addition of a catalyst to start the curing reaction. In this research, the catalyst used was Methyl Ethyl Ketone Peroxide (MEKP), designated as Catalyst M by the manufacturers Scott Bader Ltd, UK. The recommended dosage level of catalyst is 1-2% for laminating resins, and this dosage was used throughout this

research. The typical gel time of catalyst M was 8 minutes with resin A, so it was important to complete the hand lay-up process before this time elapsed.

Table 3.2: Properties of unsaturated Polyester Resin A

Specific gravity at 25°C	1.11
Viscosity @ 25°C, 37.35 sec^{-1}	3.8 poise
Volatile content	42 %
Gel time @ 25°C using 2% catalyst M	8 minutes
Barcol Hardness*	47
Water absorption*, 24 hours @ 23°C	18 mg
Tensile strength*	68 MPa
Tensile Modulus*	3.7 GPa
Elongation at break*	2.5 %

* Properties for fully cured resin

3.1.4 Chemicals for Surface Treatment of Fibres

Two chemicals were used for surface treatment of hemp fibres. Acetic anhydride (≥98% laboratory grade reagent), supplied by Sigma-Aldrich, was used for acetylation treatment. Sodium hydroxide (laboratory reagent grade), supplied by Sigma-Aldrich in the form of pellets, was used in alkalisation treatment.

3.2 SURFACE TREATMENTS OF HEMP FIBRES

3.2.1 Heat Treatment

In order to observe the effect of heat treatment and removal of moisture on mechanical properties of hemp fibre composites, fibres mats of size 250 mm x 200 mm were heat treated in an oven for 30 minutes. Three different temperatures were used: 100°C, 150°C and 200°C. A treatment time of 30 minutes was selected because it was sufficient to remove most of the moisture from the fibres. Also keeping the fibres in an oven for

longer periods of time would not be economically viable in a commercial operation. The fibres heat treated were then used in making laminates immediately after taking out of the oven to prevent any absorption of moisture.

3.2.2 Acetylation

The fibres were treated with acetylation treatment using acetic anhydride. First the fibre mats of size 250 mm x 200 mm were washed and soaked in distilled water for 48 hours at room temperature to remove surface impurities. The fibres were the dried in the oven at 100°C for 4 hours. Then the fibres were soaked in acetic anhydride so that the entire fibre mat was covered in the reagent. The fibres immersed in acetic anhydride were kept in a pre-heated oven at 120°C for 3 hours. However the excessively corrosive nature of acetic anhydride made it difficult to work with this reagent in ordinary laboratory conditions. Nevertheless one laminate was made using this treatment.

3.2.3 Alkalisation

For this research, laboratory reagent grade sodium hydroxide in the form of pellets was used. The fibre mats, of size 250 mm x 200 mm, were soaked in 1%, 5% and 10% NaOH aqueous solution for 24 hours at 23°C. After the treatment, the fibre mats were thoroughly rinsed in cold tap water until the removal of NaOH and then dried in the oven at 100°C for 4 hours. Some mats were also treated with acetic acid following alkalisation to completely remove any traces of NaOH in fibres. The alkalised mats were then used in the fabrication of laminates.

3.2.4 Plasma Treatment

The plasma treatment of hemp fibres was carried out by using Diener Electronic LFG-40 plasma treatment machine as shown in Fig. 3.2. The machine used a high frequency generator of 40 kHz connected to an electrode inside the chamber for providing the energy required to split the neutral process gas atoms, oxygen in this case, into ions and electrons.

First the hemp fibre mat, of size 250 mm x 200 mm, was placed horizontally inside the chamber. A vacuum was generated inside the chamber with the help of a vacuum pump. At a pressure of about 0.4 mbar, the process gas oxygen was introduced into the chamber. The high frequency generator was switched on and the oxygen gas was ionised, producing the plasma. The hemp fibre mat was exposed to the plasma for ten minutes, the recommended time by the manufacturer for surface activation. Fresh oxygen gas was supplied continuously to the chamber.

Fig. 3.2: Plasma treatment machine

After ten minutes of exposure, the hemp fibre mat was inverted to expose the other side of the mat to plasma for 10 minutes. After 10 minutes of treatment to each side of the mat, the chamber was vented and the mat removed from the chamber and immediately used in the fabrication of laminates.

In order to utilise the maximum activation of the fibre mat, the mat was used for making the composite laminate within 5 minutes of exposure to plasma. Unfortunately no method of measuring the activation of hemp mat surface was available. However it was noted that during the compression moulding of the laminate, considerably less amount of polyester resin spilled out, indicating good wetting between fibre and the resin.

3.3 PROPERTIES OF HEMP FIBRES

3.3.1 Surface Energy

For determining the surface properties (surface energy and dynamic contact angle) of untreated and surface treated hemp fibres a KSV Sigma 700 Tensiometer was used as shown in Fig. 3.3. It is a modular high performance computer-controlled tensiometer which can be used for the measurement of various surface properties. Wilhelmy plate

technique was used for determining surface properties in this research. The machine used Win Sigma software for recording and analysing the data.

Fig. 3.3: KSV Sigma 700 Tensiometer

For measuring the contact angle two liquids, one polar and one non-polar, with known surface tension have to be used. For this experiment Hexane and water were used. A sample of hemp fibre approximately 20mm long was cut and hung on the balance hook of the machine by using a tape such that the fibre was perpendicular to the surface of the liquid. The vessel containing the test liquid was placed on the stage. The fibre was immersed in the liquid for a depth of up to 10 mm and taken out. As the fibre was immersed the software recorded the force during advancing and the receding parts of the cycle. The fibre movement speed was 5 mm/min. The data for the first 1 mm of immersion was ignored. As the test progressed the software measured the force per wetted length (F/L) and force per unit wetted length minus buoyancy correction (F/L-B) where buoyancy B was calculated by using volume of the fibre immersed and the liquid density. The equation for measuring contact angle θ is given by:

$$\theta = \cos^{-1}\left(\frac{F/L - B}{\gamma P}\right) \quad \text{.....(3.1)}$$

where γ is the surface tension of the liquid and P is the perimeter of the fibre. The test was repeated for both hexane and water.

Since hexane is a non-polar liquid, its contact angle gave the dispersive component of the surface energy of the hemp fibre by the following equation:

$$\gamma_S^d = \gamma_L^d (1+\cos\theta)^2/4 \quad \text{.....(3.2)}$$

where γ_S^d is the dispersive component of hemp fibre surface energy and γ_L^d is the surface energy of hexane, given by 18.4 mJ/m. Immersion of hemp fibre in water then helped to find the polar component of the surface energy of hemp fibre by using the equation:

$$\gamma_L (1+\cos\theta) = 2[(\gamma_S^d \gamma_L^d)^{1/2} + (\gamma_S^p \gamma_L^p)^{1/2}] \quad \text{.....(3.3)}$$

where γ_L is the surface energy of water and θ is the contact angle of water. Every term in this equation is known except polar component of surface energy of hemp fibre, γ_S^p, which can then be calculated. The total surface energy of hemp fibre is then the sum of dispersive and polar components of surface energy.

There are a number of possible sources of error in this experiment. For measuring the wetting force, the exact perimeter of the fibre surface must be known. The diameter of the fibre was determined by using optical microscope incorporating a graduated eyepiece. This value was then used to determine the perimeter of the fibre. As the diameter of the fibre is not constant, the value of perimeter is also not constant. The irregular shape of hemp fibre thus introduces a major source of error in these calculations. The surface of the fibre has to be perpendicular to the surface of water to give an accurate value of the wetting force. Although every effort was made to make the two surfaces perpendicular some fibres were inclined by small angle to the surface of water. The handling of fibres with hands during preparation of the test can also introduce some contaminations on the surface of the fibres which can affect the wetting force and hence the contact angle.

3.3.2 Thermal Characterisation

Thermal characterisation of hemp fibres was carried out by using a PerkinElmer Simultaneous Thermal Analyser 6000 as shown in Fig. 3.4. The machine gave simultaneous measurement and analysis of weight change and heat flow with the increase in temperature. The machine used "Pyris" software for recording and analysing the data. The machine could be used with both oxygen and nitrogen gases. For these experiments nitrogen gas was used.

Hemp fibres of approximate weight 12 mg were placed in the sample holder and the machine was started. The temperature was increased at a rate of 10°C per minute. The flow of nitrogen gas was 20 ml per minute. As the temperature increased the software recorded the changes in weight and heat flow in hemp fibres. The test was stopped at a temperature of 450°C.

Fig. 3.4: PerkinElmer Simultaneous Thermal Analyser

3.3.3 Tensile Properties

The tensile testing of single hemp fibres was carried out as per ASTM D3379-75, standard tensile test method for tensile properties for high modulus single filament materials. Tensile testing was done for both untreated and alkalised hemp fibres. Hemp strands were taken from different parts of the mat and elementary hemp fibres were separated from the strand by hand. The fibres were mounted on paper cards of dimensions 45 mm x 20 mm. Holes of diameter 11 mm were punched in the centre of the cards and the fibres were mounted on the cards by gluing with epoxy adhesive. Care was taken to mount the fibres in the exact centre of the holes. It was also made sure that each card contained only one fibre. Mounted fibres were inspected in a Reichert Jung MeF3 optical microscope with an Olympus E330 camera attached. Average widths of the fibres were measured by means of a calibrated eyepiece. Five different readings of fibre width were taken along the length of the fibre and their mean value was used in the calculation of tensile properties.

Mounted fibres were placed in the grips of an Instron 1162 tensile testing machine. A load cell of 50 N was used to measure the force. The supporting sides of the cards were cut by a scissor just before the start of the test and the test was performed at a rate of 0.5 mm/min. Since it was not possible to use an extensometer for measuring the strain in the fibres, the fibre extension was measured from the displacement of testing machine

crosshead. Average tensile properties were calculated using the results of at least 20 fibres of each kind.

3.3.4 Interfacial shear strength of hemp/polyester

Interfacial shear strength testing of untreated and alkalised hemp fibres in polyester resin was evaluated by single fibre pull-out test using an Instron 1162 testing machine. The method was similar to that for determining the tensile properties, except that for mounting the fibres on cards, one side of the fibres was fixed by using epoxy and a blob of polyester resin was dropped on the other side of the fibre. After fibre pulled out of the polyester resin, the embedded length was measured by using the travelling microscope. The interfacial shear strength was then determined by using the equation:

$$\tau = \frac{F}{\pi D l} \qquad \text{.....(3.4)}$$

where τ is the interfacial shear strength, F is the force at pull-out, D is the mean width of fibres, and l is the embedded length of fibres. The failure rate of the fibres by breaking rather than pulling out of the resin was high. At least 10 fibres of each kind were tested and their mean values determined. Czigdiny et al [312] have pointed out the inherent drawback of using this method for natural fibres. Since the resin drop is placed on the fibre without any pressure, the resin enters the voids in the elementary fibres to a smaller extent than when the resin impregnates the fibres in compression moulding pressure. The irregular cross section of the fibres is also expected to affect the calculation of shear strength.

3.4 FABRICATION OF LAMINATES

A combination of hand lay-up method, followed by compression moulding, was used in the fabrication of laminates. For the fabrication of a laminate, approximately 150 ml of Resin A was mixed with 3.0 ml of catalyst M in a glass flask. The mixture was stirred to aid the start of the chemical reaction. A steel frame mould of size 300 mm x 210 mm was used in making laminates. The steel frame mould was covered with acetate film for easy removal and smooth surface finish of the laminate.

Hemp fibre mats of nominal size 250 mm x 200 mm were cut from the roll conditioned at 23°C and 50% RH. First coat of the resin was applied on the acetate film with a

brush. The first hemp fibre mat was laid and another coat of the resin was applied and spread with a brush. Then the second hemp fibre mat was laid and the third coat of the resin was applied and spread with a brush. A roller was then applied to help release the trapped air. Then a second acetate film was put on top of the moulding. The second steel frame plate was placed on top and the mould was placed in the compression moulder. The required pressure was applied in the compression moulder as the excess resin squeezed out of the mould. The laminate was then left in the compression moulder to cure at room temperature for 24 hours. After 24 hours, the laminate was taken out of the mould and the laminate was kept in the oven for post-curing for 3 hours at 80°C. Post-curing was required to obtain optimum properties of the resin, as recommended by the manufacturer.

The laminates were then given to the workshop for cutting up into parallel-sided samples of dimensions 125 mm x 20 mm. The edges of the samples were polished using 300-grit paper to remove any stress concentrating defects. Samples were checked by naked eye for obvious defects. Samples with severe defects, such as air bubbles and resin-rich and resin-dry areas, were rejected. The dimensions of the samples were then accurately measured using a vernier calliper and micrometer. Samples deviating too much from the average thickness of the laminate were rejected. The samples were then weighed in a balance to an accuracy of 0.1 mg.

Glass fibre composite laminates were made by the same method but the pressure was applied by using weights of 400 N. The number of fibre layers used in each laminate was six. Hemp/glass fibre hybrid laminates were also made by the same method. Two mats of hemp and glass fibres each were used in laminate.

3.5 EVALUATION OF FIBRE CONTENT

Since it was not possible to evaluate the fibre weight fraction of hemp fibre composites by calcinations method, the fibre content was evaluated indirectly. The values of weights and dimensions of each sample were used in the calculation of the fibre weight fraction of the sample according to the formula:

$$W_{fh} = \frac{nW_h}{W_c} \quad \text{.....(3.5)}$$

where W_{fh} is the fibre weight fraction of the sample, n is the number of hemp fibre mats used which is 2 in this case, W_h is the average weight per unit area of the hemp fibre mat which was calculated to be 847 g/m^2 and W_c is the average weight per unit area of the sample. So for these samples, the formula simplified to:

$$W_{fh} = \frac{1694}{W_c} \quad \text{.....(3.6)}$$

The values of fibre weight fraction of samples from each laminate were averaged to get the average value of fibre weight fraction of that laminate.

The value of fibre volume fraction was calculated by the standard formula:

$$V_{fh} = \left[1 + \frac{W_m \rho_f}{W_f \rho_m}\right]^{-1} \quad \text{.....(3.7)}$$

where W_m is the matrix weight fraction, W_f is the fibre weight fraction, ρ_m is the polyester matrix density (1.22 g/cm^3), and ρ_f is the hemp fibre density (1.48 g/cm^3).

The fibre content of CSM glass fibre reinforced polyester composites was evaluated by using the calcinations method as prescribed by BS EN ISO 1172:1999 (Textile glass-reinforced plastics- prepregs, moulding compounds and laminates- determination of the textile-glass and mineral-filler content- calcinations methods).

The samples were weighed and subsequently calcinated at a defined temperature until all the resin evaporated. The samples were then reweighed and the glass fibre content was obtained by determining the difference in mass of the test specimen before and after calcination. At least four samples from each laminate were used for this purpose. The samples were cut up from the laminates in sizes such that their weight fell in the recommended range of 2-10 grams. A dry crucible was weighed to the nearest 0.1 mg and was designated as m_1. The sample was placed in the crucible, reweighed to the nearest 0.1 mg and designated as m_2. The crucible containing the sample was then placed in a muffle furnace, preheated to a temperature of 625°C and heated to constant mass. The crucible, together with the residue, was allowed to cool to ambient temperature and reweighed, designates as m_3.

The glass fibre content W_f for each specimen was calculated by using the equation:

$$W_f = \left(\frac{m_3 - m_1}{m_2 - m_1} \right) x100\ \% \quad \text{.....(3.8)}$$

The average of the measurements was calculated for all the specimens from the same laminate.

The use of calcinations method was not possible for glass/hemp fibre hybrid composites because of the presence of hemp fibres. The fibre content of glass/hemp hybrid laminates was evaluated by using the following equations:

$$\text{Total fibre weight fraction } W_f = W_{fh} + W_{fg} \quad \text{.....(3.9)}$$

where W_{fh} is the fibre weight faction of hemp fibres and has been defined above, and W_{fg} is the fibre weight fraction of glass fibres and is given by:

$$W_{fg} = \frac{nW_g}{W_c} \quad \text{.....(3.10)}$$

where n is the number of glass fibre mats used (two in this case), W_g is the weight per unit area of glass fibre mat (450 g/m^2), and W_c is the weight per unit area of the hybrid sample.

Fibre volume fraction is then given by the following equation:

$$V_f = \frac{\rho_c W_f}{\rho_f} \quad \text{.....(3.11)}$$

3.6 MECHANICAL TESTING OF COMPOSITES

3.6.1 Tensile Testing

Tensile properties of the composite samples were determined by using Hounsfield testing machine as shown in Fig. 3.5. Parallel-sided samples with length 125 mm and width 20 mm were used. Parallel sided samples is now almost universally the preferred form of test sample for composite materials [313]. For tensile testing, the samples needed tabs on both ends for proper grip and to avoid the failure of samples at the grips. For this purpose, tabs of the size of 20mm x 20mm were cut up from used hemp fibre composite samples, and were glued on to the pre-roughened ends of the samples using

Scotch-Weld 7838 B/A Structural Adhesive, manufactured by 3M. This is a two-part (base/accelerator) epoxy based adhesive which cures at room temperature. However the curing process can be accelerated by heating at 65°C for 2 hours. The base is modified epoxy resin and accelerator is modified amine, and both are mixed in ratio of 1:1 by weight.

Figure 3.5: Hounsfield testing machine

Samples were placed in the bottom set of grips which were then tightened. A set square was used to ensure that the specimens were aligned along the stress direction. The load cell reading was then zeroed before tightening the top set of grips. A mechanical extensometer PS25C-0118 with gauge length of 25mm was used to measure the strain in the samples during tensile tests. The extensometer was attached in the middle of the sample. The test was then conducted with the cross head moving at the rate of 2mm/min. All tensile tests were performed as per BS EN ISO 527: 1996, Plastics-determination of tensile properties, parts 1 and 4. The load and strain data from each test were recorded on a computer. At least five samples were tested for each composite type. Tensile strength was calculated using the following equation:

$$\sigma = \frac{F_{max}}{A}$$

where F_{max} is the maximum force recorded for each sample and A is the cross section area which equals the average width of the tested specimen multiplied by the average thickness. The modulus of the materials, according to BS527, was determined by the slope of the stress-strain curve in the strain range of 0.05% to 0.25%, which was recorded by the extensometer. The strain to failure value was also recorded by the extensometer.

3.6.2 Impact Testing

Low velocity impact tests were performed in the purpose-designed and assembled falling weight impact rig as shown in Fig. 3.6. The impact test rig was adjusted before conducting impact tests by using a plumb line device to ensure that the dropping impactor hit at the centre of each sample. Samples with off-centre impact points were rejected. All the testing was carried out as per EN ISO 6603-1: 2000 (Plastics – Determination of puncture impact behaviour of rigid plastics; Part1: Non-instrumented impact testing).

After setting-up the impact rig, the sample was tightly clamped between two steel rings of internal diameter 18mm by four nuts. By adding steel weights on the impactor, the weight of the impactor was adjusted to obtain the required levels of impact energy. The impact energy is given by E= mgh, where m is the mass of the impactor plus any mass added on, g is acceleration due to gravity, and h is the height of the impactor nose from the sample. For most of the tests the height of the impactor was kept constant at 0.1 m and value of the weight was changed according to required impact energy.

The head of the impactor was a hemispherical steel nose with a diameter of 12.7mm. This is the standard shape and size of impactor used in most low velocity impact tests. The impactor was held and released using an electromagnet. The impactor was captured after impact to prevent secondary strikes.

Fig. 3.6: Low velocity impact testing rig

Izod Impact Testing:

For Izod impact testing, Ray-Ran Universal Pendulum Impact Testing Machine, shown in Fig. 3.7, was used. The machine used the kinetic energy of a falling pendulum hammer to break a test sample and determined the amount of energy required to do so. The pendulum hammer was first calibrated to take into account the windage and friction losses. This was done by releasing the pendulum hammer form a known height and recording the free swing height it reached opposite the release point. Thus when a test sample was broken, the swing height of the pendulum hammer was subtracted from the

calibrated swing height and the resultant height was used to calculate the kinetic energy required to break the sample.

Both notched and un-notched samples were used in this testing. The test sample was placed vertically into a vice fixed to the bed of the machine and with notch positioned central to the top face of the vice and facing the swing path of the pendulum hammer. The pendulum hammer having a known weight and velocity, hence known kinetic energy, was released and the striking point of the pendulum hammer hit the test sample at a pre-determined height above the vice (normally 22 mm). The swing height of the pendulum hammer after breaking the test sample gave the energy absorbed to break the test sample. The test results were expressed as energy per unit area of the sample. All Izod impact tests were performed as per BS EN ISO 180:1997, Plastics- Determination of Izod impact strength. The specimen dimensions used were:

Fig. 3.7: Ray-Ran Pendulum Impact Tester

Length= 80 ± 2 mm

Width = 10 ± 0.2 mm

Notch base radius = 0.25 ± 0.05 mm

Remaining width at notch base = 8 ± 0.2 mm

As recommend in the Standards, notch type A was used. At least ten specimens from each laminate were tested and their average values were used for determining Izod impact strength of each type of composite.

3.6.3 FATIGUE TESTING

Fatigue testing was carried out as per BS ISO 13003:2003 (Fibre-reinforced plastics – Determination of fatigue properties under cyclic loading conditions). Fatigue tests were performed using the pneumatic fatigue machines at a frequency of 1Hz and a stress ratio (R value) of 0.1 for tension-tension fatigue and -1 for tension-compression fatigue. The choice of frequency ensured that the heating effect due to hysteresis was minimal. The R value of 0.1 in tension-tension was chosen to maximise the cyclic effects without invoking the complications of compressive stresses and the likely variations in failure mechanisms. The maximum stresses during cyclic loading were recorded as stress level of fatigue. Tests were carried out until either complete failure of the specimen occurred or until 10^6 cycles, the latter being designated the upper boundary of the low cycle fatigue regime. The number of cycles to failure was recorded for each specimen and these data were plotted in the form of S-N (Wohler) curves.

Parallel-sided samples were set up in the pneumatic fatigue machine as shown in Fig. 3.8. Initially, the maximum load was taken as 60% of the ultimate tensile strength, and adjusted according to the specimen's dimensions. Further tests then took place at a maximum load of lower or higher percentages of the ultimate tensile strength. The grips were serrated to ensure a good grip on the sample.

The machine, being pneumatic, worked by the pressure of compressed air on a piston. After loading the sample in the machine and tightening the grips, air was allowed into the chamber above the piston, which forced the piston downward and thus loaded the sample in tension. The pressure was set corresponding to the maximum load required on the sample. The pressure determined the amount of air available to push the piston downwards and load the sample. The machine was started. Once the voltage from the load cell on the machine reached the set maximum value, which corresponded to the maximum loading, the solenoid valve was switched off automatically so that no more air could enter the piston chamber, an air outlet valve opened, the piston moved upwards, and the stress was reduced. On reaching the minimum loading, the solenoid valve was again switched on allowing compressed air back into the pressure cylinder, forcing the piston downwards. By using this method, the machine only switched on after the pre set load had been reached and so any drop in pressure in the compressed air

supply had no effect on cycle load. The loading was monitored, and adjusted if necessary, during the entire fatigue process. This machine used a trapezoidal waveform.

Fig. 3.8: Fatigue testing machine

Environmental fatigue tests were carried out on the same machines but the samples were immersed in distilled water by using a specially designed Perspex water chamber.

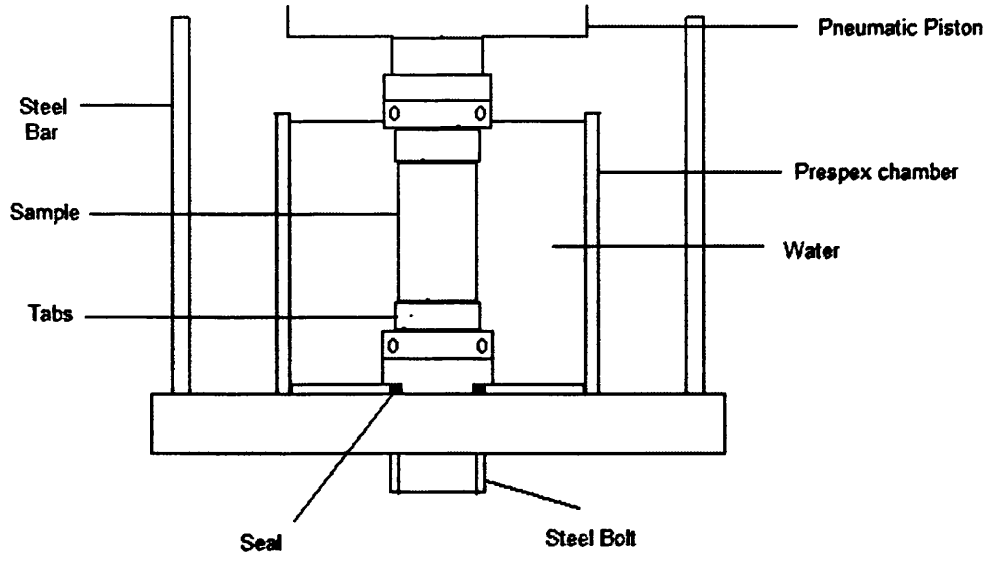

Fig. 3.9: Schematic of fatigue testing set-up in water (not to scale)

The schematic of the environmental fatigue testing rig is shown in Fig. 3.9. The samples were tested in the same manner as for dry samples except that they were now vertically aligned rather than horizontally as in the normal testing. For tension-compression loading, a specially designed anti-buckling device was clamped onto the sample throughout the testing.

3.7 ENVIRONMENTAL TESTING OF COMPOSITES

In order to investigate the environmental properties of hemp fibre reinforced polyester composites, they were subjected to various environmental tests.

3.7.1 Properties in water

The properties of the composites after immersion in water were determined as per BS EN ISO 62:1999, Plastics-Determination of water absorption. Samples of nominal dimensions of 125 mm x 20 mm were immersed in container of either distilled water or 5% salt solution. Before immersion, the samples were first conditioned to a constant mass at 23°C and 50% RH. For determining water absorption, samples were taken out of the container after pre-determined intervals of time, wiped with a clean cloth and weighed in a balance having an accuracy of 0.1 mg. The samples were weighed within one minute of taking out of the container. The samples were tested for their mechanical properties by using the standard methods.

3.7.2 Accelerated Weathering Testing

The samples were exposed to accelerated weathering conditions by using QUV Accelerated Weathering Tester as shown in Fig. 3.10.

Fig. 3.10: QUV Accelerated Weathering Tester

The machine had the facility to simulate the outdoor weathering conditions like sunlight, rain, and dew. It exposed materials to alternating cycles of light and moisture at controlled, elevated temperatures. It simulated the effects of sunlight with fluorescent ultraviolet lamps which are the best way to simulate the damaging effect of sunlight on physical properties. It simulated rain and dew with condensing humidity and water spray. It thus could reproduce the damage to the materials in few days or weeks that actually occurred over months or years of outdoor exposure.

The testing was conducted as per BS EN ISO 4892-1:2001, Plastics-methods of exposure to laboratory light sources-Part1:general guidance, and BS EN ISO 4892-3: 2006, methods of exposure to laboratory light sources-Part 3:flourescent UV lamps. The materials exposed to outdoor conditions are exposed to alternating cycles of UV light

(daytime) and wetness because of dew (night time). The tester had the facility of using both conditions in the cycle and both conditions occurred separately in the machine just as they do in natural weathering. The tester was also used to expose the material to constant UV light.

The tester used UVA 340 lamps for generating UV radiation which is the recommended florescent UV lamp in the British Standards to simulate the UV part of daylight. This lamp is the best available simulation of sunlight in the critical short wavelength UV region between 365 nm and the solar cut off of 295 nm. These lamps have a radiant emission below 300 nm of less than 2% of the total light output, have an emission peak at 343 nm, and are most commonly used for simulation of daylight from 300 nm to 340 nm. The tester had irradiance control system that allowed the selection of exact level of the rate at which light energy fell on a unit area of the sample. For both testing conditions, the irradiance was set at 0.76 $W/m^2/nm$ at 340 nm as recommended by the standards. The temperature was measured by black panel thermometer. This temperature was set at 45°C.

It must be emphasised that it is theoretically impossible to convert the weathering tester exposure hours into months or years of outdoor exposure. The reason is the inherent variability and complexity of outdoor exposure conditions. The amount of sunlight, rain and moisture in one year in London will be different to that in Lahore or Los Angeles. These variables are: the geographical latitude of exposure site (closer to equator means more sunlight); altitude (higher means more UV); local geographical features, such as proximity to a body of water to promote dew formation; random year-to-year variations in the weather in the same city; seasonal variations (winter exposure may only be one seventh as severe as summer exposure); sample insulation (outdoor samples with insulated backing often degrade 50% faster than un-insulated samples); and operating cycle and temperature of the tester.

Thus it is meaningless to talk about a conversion factor between hours of accelerated weathering and months of outdoor exposure. So the data obtained from accelerated weathering testing is relative, not absolute. It gives a reliable indication of the relative ranking of a material's durability compared to other materials.

3.8 SCANNING ELECTRON MICROSCOPY

The scanning electron microscopy of samples was carried out by using Philips XL30CP SEM as shown in Fig. 3.11. This microscope uses controlled pressure which is very useful for non-conducting samples like hemp fibre composites. The microscope uses a tungsten filament for generating the electron beam. For examining the fracture surfaces of tested samples, samples of width of about 5 mm were cut from the fracture surface. They were taped onto the samples holder which was then placed inside the chamber. Vacuum inside the chamber was created. The tungsten electron gun generated an electron beam which was focused into a fine spot less than 4 nm in diameter on the specimen. The beam was scanned over the surface of the sample and the image was seen on the monitor. Magnification was varied to get a clearer image of the sample.

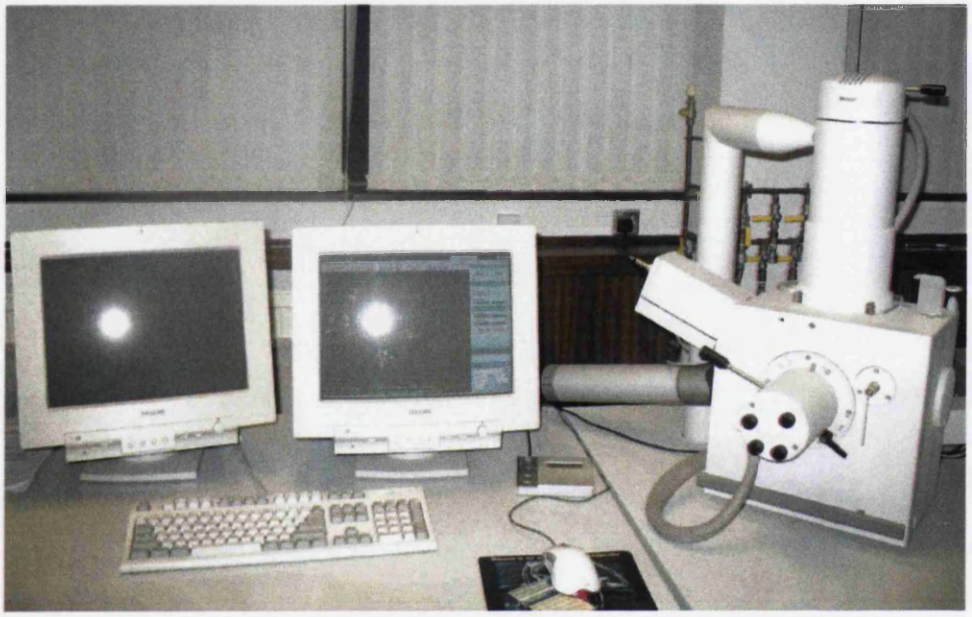

Fig. 3.11: Philips XL30CP Scanning Electron Microscope

4. PHYSICAL AND MECHANICAL PROPERTIES OF HEMP FIBRES

This chapter presents the results of the experiments undertaken to determine various physical and mechanical properties of hemp fibres used in this research. The study of these properties is vital for comparison with similar properties of synthetic fibres and for assessing hemp fibres' suitability for use as reinforcement in composite materials.

4.1 THERMAL PROPERTIES

4.1.1 Moisture loss in a desiccator

Hemp fibres, like all natural fibres, contain moisture because one of their primary functions is to transport moisture and nutrients to different parts of the plant. The purpose of this part of the study was to determine the moisture loss behaviour of hemp fibres when kept in a desiccator and when exposed to elevated temperature, and thus to determine the equilibrium moisture content of the fibres.

The moisture loss behaviour of hemp fibres in a desiccator was observed by keeping a sample of hemp fibres, cut out from hemp fibre mat conditioned at 23°C and 50% relative humidity (RH), in the desiccator containing the desiccant Copper Sulphate and recording weight changes with the passage of time. The results are shown in Fig. 4.1. The moisture loss is quite rapid initially as the moisture in the fibres is absorbed by the desiccant but starts to stabilise after about 1500 minutes as the amount of moisture in the fibres starts to decrease. The fibres have lost almost 4% of their original weight after being kept for 7200 minute (approximately five days) in the desiccator. From the graph, the fibres do not seem to have lost all of their moisture and they can be exposed to elevated temperatures to determine the weight loss behaviour and equilibrium moisture content in the fibres.

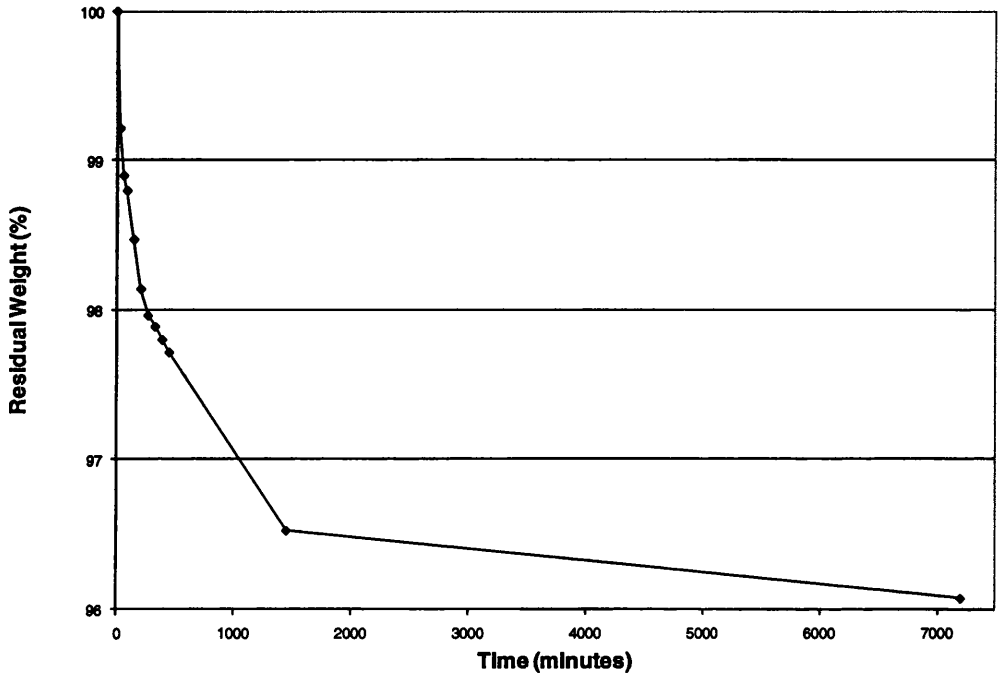

Fig. 4.1: Moisture loss of hemp fibres kept in a desiccator

4.1.2 Elevated temperature weight loss

The elevated temperature weight loss behaviour of hemp fibres was observed by keeping them in an oven at constant temperatures and recording their weight loss at different intervals of time. Four different samples of hemp fibre, each conditioned at 23°C and 50% RH, were kept in the oven at constant temperatures of 50°C, 100°C, 150°C and 200°C, and their weight loss behaviour against time was recorded. The results are shown in Figs. 4.2-4.4.

For the fibres kept at 50°C the moisture loss is much more rapid than that in a desiccator. As shown in Fig. 4.2, the moisture loss at 50°C starts to stabilise after about 200 minutes, when the fibres have lost almost 4% of the moisture, as the amount of moisture in the fibres starts to decrease. After about 1500 minutes of exposure (approximately one day), the fibres have lost almost 4.5% of their original weight. The graph shows that exposing hemp fibres to 50°C does not seem to result in complete removal of moisture after 1500 minutes of exposure. So the next stage was to expose the fibres to higher temperatures to determine the equilibrium moisture content in them.

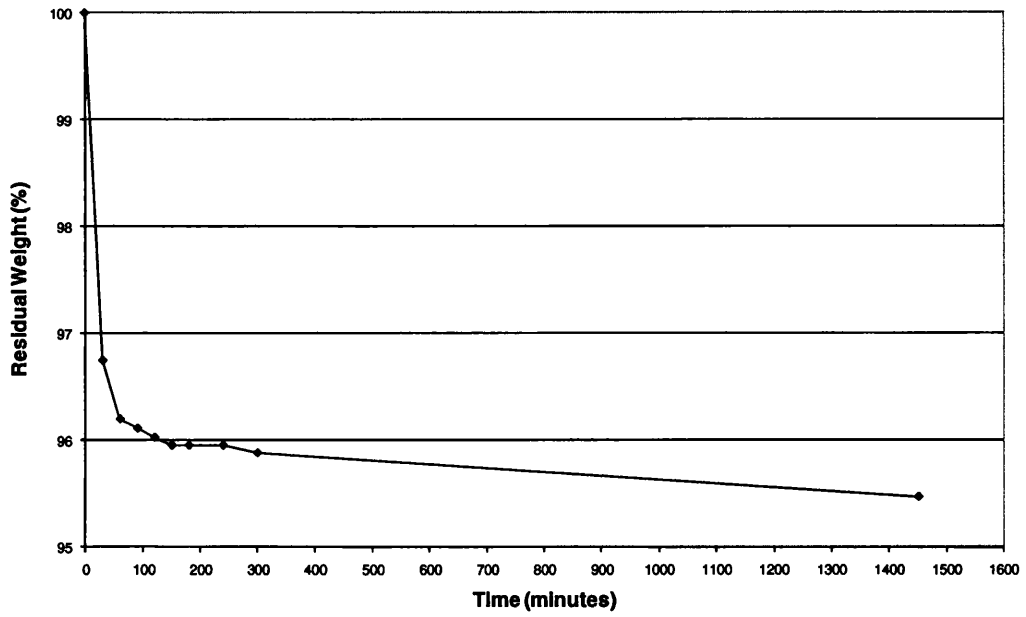

Fig. 4.2: Weight loss of hemp fibres at 50°C

The comparison of weight retention behaviour of hemp fibres exposed to 100°C and 150°C is shown in Fig. 4.3. Exposing the hemp fibres to higher temperatures results in increase in the amount and rate of weight loss. It is clear that the fibres have lost almost all of their equilibrium moisture content within 30 minutes of exposure at 100°C and 150°C. The amount of moisture lost stabilised to an equilibrium value that was different for both temperatures. The fibres exposed to 100°C lost about 8.3% of their initial weight after 300 minutes of exposure, whereas the fibres exposed to 150°C lost about 10.2% of their initial weight after 300 minutes of exposure.

A similar loss in moisture was reported by Gassan and Bledzki [67] for jute fibres dried in a vacuum furnace. The fibres lost about 8% of moisture within the first 45 minutes of exposure at 100°C. The loss of moisture stabilised thereafter and remained constant at around 9% for exposure of up to 240 minutes.

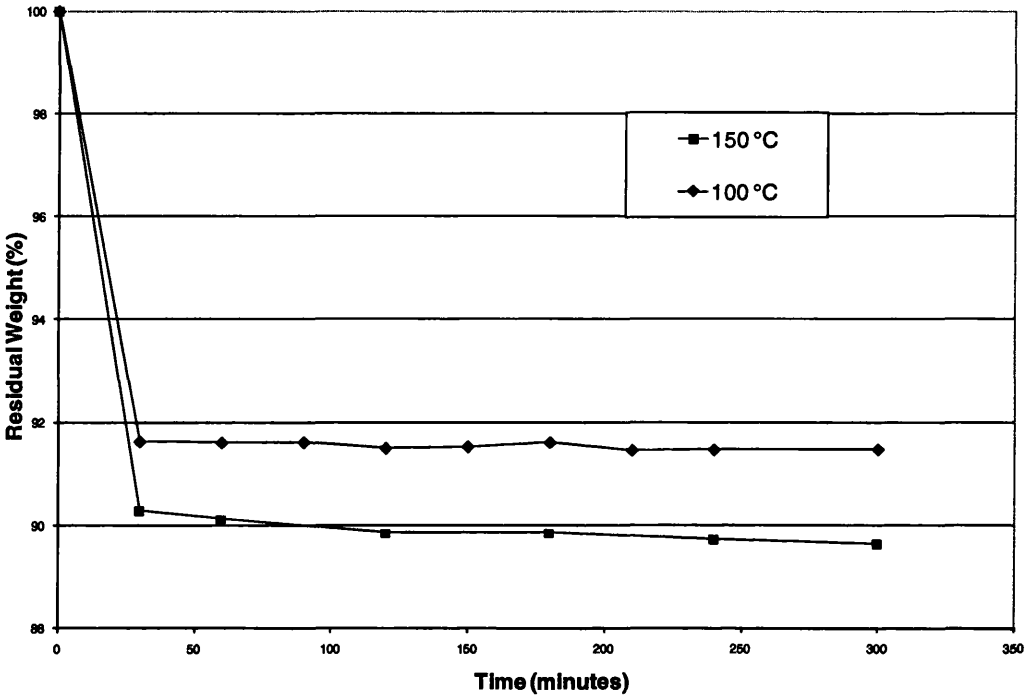

Fig. 4.3: Comparison of weight loss of hemp fibres at 100°C and 150°C

The weight loss behaviour of hemp fibres exposed to 200°C is shown in Fig. 4.4.

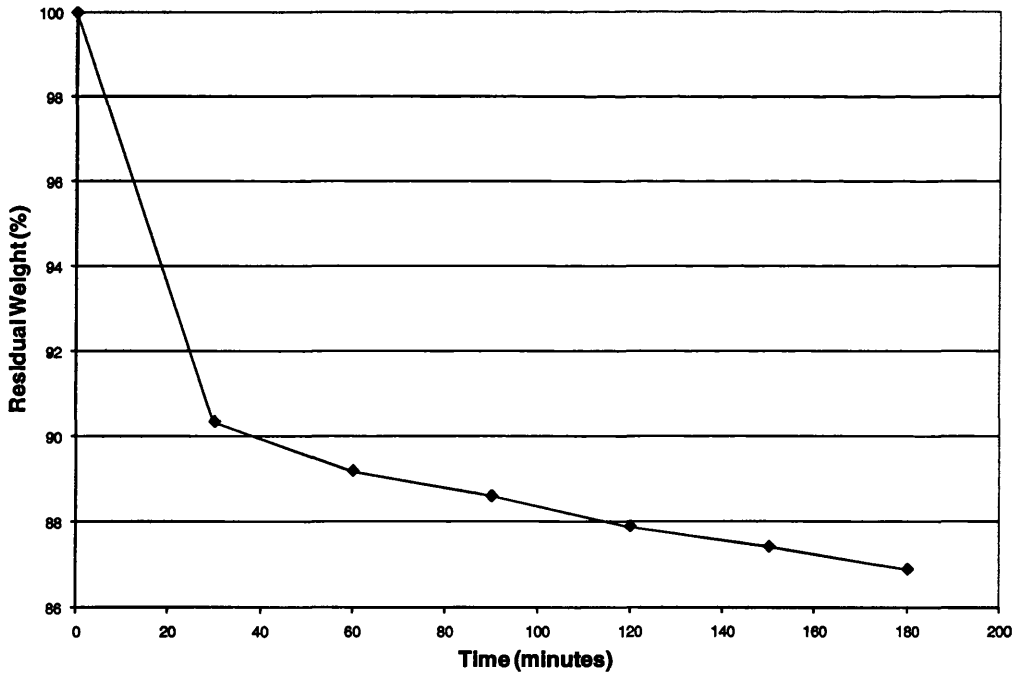

Fig. 4.4: Weight loss of hemp fibres at 200°C

The behaviour of hemp fibres exposed to 200°C is significantly different because between 150°C and 200°C thermal degradation of hemp fibres starts which involves physical and chemical changes within the fibres. It has been shown [314] that heating hemp fibres above 160°C results in softening of lignin, the binding material in the fibres. Therefore the weight loss at this temperature is a combination of the weight loss of moisture plus weight loss due to thermal degradation. The thermal degradation of fibres was evidenced in release of soot and blackening of the colour of hemp fibres due to oxidation. The fibres lost almost 13% of their initial weight after 180 minutes of exposure at 200°C. The continued decrease in weight retention shows that although the fibres have lost almost all of their moisture, they continue losing weight due to thermal degradation of the fibres.

Then a new experiment was set up whereby a hemp fibre sample, conditioned at 23°C and 50% RH, was kept in the furnace at increasing temperatures, starting at 40°C up to 140°C (in 10°C intervals) for a dwell time of one hour and the weight change in the sample was recorded. The dwell time of one hour was chosen because, as shown in Figs. 4.2-3, the fibres were close to their equilibrium weight after heat treatment of about one hour at a particular temperature. The resulting graph is shown in Fig. 4.5.

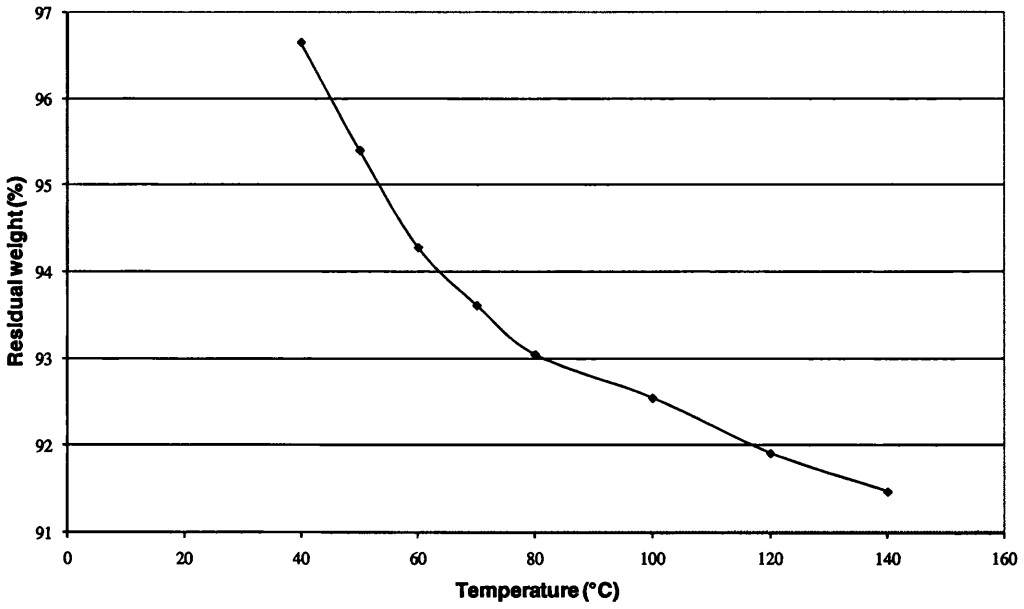

Fig 4.5: Weight loss of hemp fibres, for one hour at increasing temperatures

The graph shows that keeping the hemp fibres at increased temperatures for one hour results in gradual moisture loss of fibres. At 140°C the fibres have lost almost all (9%) of their initial moisture which is consistent with the previous results.

These studies showed that the hemp fibres used in this research had equilibrium moisture content of about 10% when kept at standard conditions of 23°C and 50% RH. This is consistent with the amount of equilibrium moisture content in hemp fibres reported by other authors ([315], [57]). Hemp fibres begin to degrade thermally between temperature range of 150-200°C. Therefore any heat treatment of these fibres should be restricted to about 150°C.

4.1.3 Thermal degradation at elevated temperatures

Natural fibres are heterogeneous mixtures of organic materials and heat treatment at elevated temperatures can result in a variety of physical and chemical changes. The physical changes are related to enthalpy, weight, colour, strength, crystallinity and orientation [316]. The chemical changes relate to the decomposition of various chemical constituents. The decomposition onset temperature is different for different natural fibres. Themogravimetric Analysis (TGA) of jute fibres shows that they start degrading at 240°C [116]. For flax fibres it has been shown [317] that degradation starts at just above 160°C. It has been shown [116] that thermal degradation of natural fibres generally occurs in two stages: one at 220-280°C temperature range, and the other at 280-300°C range. The first range is associated with degradation of hemicellulose whereas the second range is associated with degradation of cellulose and lignin. The cell walls of the fibres undergo pyrolysis with increasing temperature and contribute to char formation. These charred layers help to insulate the lignocellulosic from further thermal degradation. For hemp fibres, Prasad et al [314] have shown that heating the fibres between 160°C and 260°C results in softening of lignin leading to opening of fibre bundles into individual fibres. The effect was more pronounced for fibres heated in air than in inert (nitrogen) environment.

Differential Scanning Calorimetric (DSC) analysis of cellulose by Weilage et al [317] showed a distinct endothermic peak to exist in the temperature range of 303-345°C. This endothermic reaction of cellulose was explained to take place in two competing processes. The first was a depolymerisation process which led to an intermediate

product levoglucosan which further decomposed to various volatile products like aldehydes, ketones, furans and pyrans. The second process was the dehydration process which mainly produced char residue, water and carbon dioxide.

They also showed that in air, the mass of hemp and flax fibres decreased slightly up to 220°C above which irreversible degradation of fibres took place. Flax fibres lost 45% of their original weight following exposure to 260°C for two hours. This correlated well with the decrease in their tensile strength following exposure to these high temperatures.

DSC analysis of hemp fibres by Ouajai and Shanks [179] showed an initial peak to occur between 50 and 160°C which corresponded to mass loss of absorbed moisture of approximately 5%. After that the DTG curve showed three decomposition steps: the first at 250-320°C was attributed to thermal depolymerisation of hemicellulose or pectin (mass loss of 10%); the second at 390-400°C was attributed to cellulose decomposition (mass loss of 55%); and the third at 420°C (mass loss of 30%) was attributed to oxidative degradation of charred residue. The main decomposition temperature (the temperature corresponding to the maximum weight loss) was found to be 397°C.

The thermal degradation of natural fibres results in change in odour and colour and deterioration in mechanical properties of natural fibres. Sridhar et al [318] reported 60% reduction in tensile strength of jute fibres heated under vacuum at 300°C for two hours. Gonzalez and Myers [319] reported deterioration in mechanical properties of wood flour exposed to temperature range of 220 to 260°C for up to 68 hours. In another study, the strengths of flax and ramie fibres were found to decrease by up to 41% and 26% respectively following heat treatment, depending on the temperature applied [45]. Weilage et al [317] reported the tensile strength of flax fibres to decrease gradually following exposure to high temperatures for one hour. From 700 MPa for no heat treatment, the strength was reported to decrease to 530 MPa at 180°C, 380 MPa at 200°C, and 270 MPa at 220°C.

Attempts have been made to improve the thermal stability of natural fibres by grafting the fibres with monomers. Acrylonitrile has been successfully used in improving the thermal stability of jute [320] and sisal [321] fibres.

4.1.3.1 Thermogravimetric Analysis (TGA)

Thermogravimetric analysis is being increasingly used to understand thermal behaviour of natural fibres because it gives an accurate measure of thermal stability of natural fibres. Thermogravimetric analysis of hemp fibres was carried out by using PerkinElmer Simultaneous Thermal Analyser. Hemp fibres were exposed to gradually increasing temperature at the rate of 10°C per minute in the presence of nitrogen gas. The machine software 'Pyris' recorded the changes in temperature and heat flow with increase in temperature. The test was stopped at 450°C.

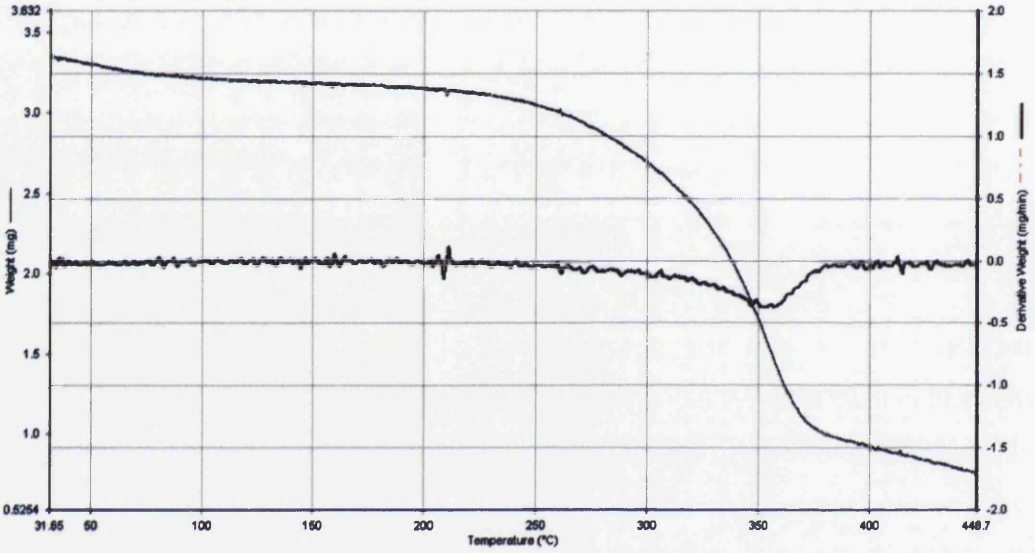

Fig. 4.6: Weight loss curves of hemp fibres with increase in temperature

Fig. 4.6 shows the weight loss and differential weight loss curves for hemp fibres with the increase in temperature. It shows that thermal degradation of hemp fibres starts at around 200°C and becomes rapid at around 300°C. In their studies on thermal degradation of hemp fibres, Beckermann and Pickering [185] reported the degradation onset temperature to be 205°C. On the derivative weight loss curve, the main peak occurred at around 360°C which can be associated with the degradation of cellulose. This was also confirmed in the heat flow curves shown in Fig. 4.7.

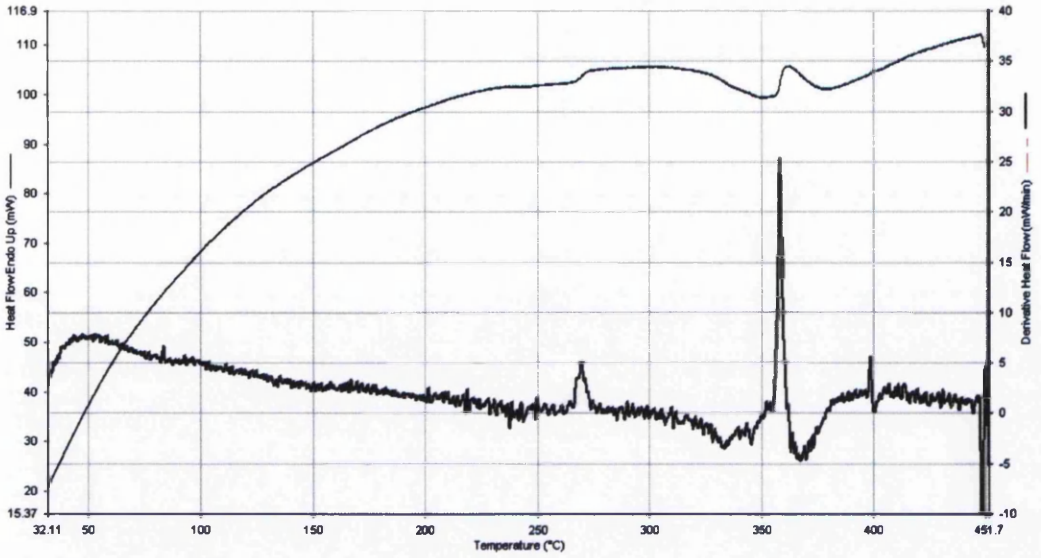

Fig. 4.7: Heat flow curves of hemp fibres with increase in temperature

Fig. 4.7 shows heat flow and derivative heat flow curves of hemp fibres with increase in temperature. The heat flow curve shows gradual increase in heat flow with increase in temperature which stabilises at about 250°C. There is a surge in heat flow at around 270°C and again at around 360°C. The derivative heat flow curve shows an initial peak at about 50 °C which corresponds to mass loss of moisture. The second peak at about 270°C may be attributed to the decomposition of hemicellulose or pectin. The third peak at about 370°C may be attributed to cellulose decomposition and it again corresponds well with the peak in derivative weight loss curve in Fig. 4.5. The small peak at around 400°C may be attributed to oxidative degradation of charred residue.

From their studies on thermal degradation of hemp fibres , Ouajai and Shanks [179] reported the similar four peaks to exist in differential heat flow curves. The temperature corresponding to these four peaks were: 50-160, 250-320, 390-400, and 420°C. From their studies on thermal properties of hemp fibres, Troedec et al [322] reported the temperature corresponding to degradation of hemicellulose and pectin to be 320-370 °C and for degradation of cellulose to be 390-420°C. Aziz and Ansell [323] reported three exothermic peaks for hemp fibres to occur at 255, 352 and 431°C. Mwaikambo and Ansell [324] reported two exothermic peaks for hemp fibres to occur at 357 and 410°C.

These studies have shown that thermal degradation of hemp fibres starts at just above 160°C and becomes rapid at around 250°C. Thermal degradation of hemicelluloses and pectin occurs at around 270°C and thermal degradation of cellulose occurs at around 360°C.

4.2 TENSILE PROPERTIES

The determination of tensile properties of hemp fibres is vital because it gives a measure of how much improvement in mechanical properties can be expected when the fibres are incorporated in a polymer matrix. The sensitivity of hemp fibres to moisture content has been outlined in the previous experiments. The variation in moisture content can affect the tensile properties of fibres. Therefore the fibres tested for tensile properties were equilibrated at 23°C and 50% RH before the testing.

Tensile properties of most of the natural fibres are now well documented. Perhaps the most extensive study on tensile properties of hemp fibres has been undertaken by Prasad and Sain [325] who used hemp fibres of varying diameters, starting from 4 μm up to 800 μm, for tensile testing. The tensile properties were found to be clearly dependent on the diameters of the fibres, decreasing gradually with increase in fibre diameter. This is consistent with the general observation, also applicable to synthetic fibres, that as the fibre diameter decreases, the amount of flaws in the fibres also decreases, thus resulting in increase in tensile properties of fibres. Fibres of diameter 4μm had mean tensile strength and modulus values of 4200 MPa and 180 GPa respectively. These values decreased to 250 MPa and 11 GPa respectively for fibres of diameter 66 μm. For the fibres of diameter 800 μm, the values were as low as 10 MPa for tensile strength and 2 GPa for tensile modulus.

Evaluation of tensile properties of natural fibres is not straightforward because of the variable cross-section of the fibres. The cross-section of one such fibre used in this research is shown in Fig. 4.8 (a). From the figure, it is clear that what appears as a single fibre to the naked eye is in fact a bundle of fibres, consisting of a number of ultimate fibres or cells, five or six in this case. This arrangement of cells makes the cross-section of fibre bundle more polygonal than circular, also shown in Fig. 4.8 (b). For this particular fibre bundle, the average cross section was found to be 20 μm by 80 μm. The bundles of fibres, shown in Fig. 4.8 (c) and (d), also make it clear that the

cross-section of almost all the fibres is polygonal. A similar polygonal cross section has been shown to exist for flax fibres [326], which are also bast fibres like hemp. Therefore taking the average width of the fibres and using it as average diameter can give erroneous results for tensile properties of the fibres.

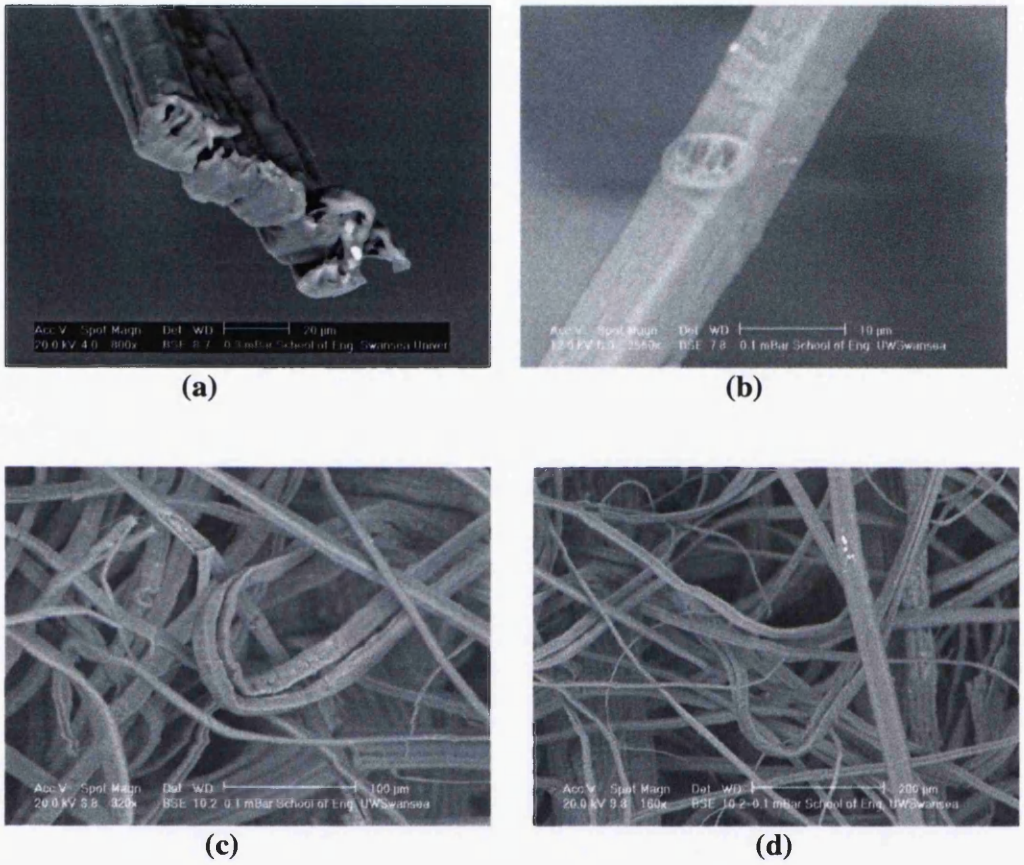

Fig. 4.8: SEM micrographs of a hemp fibre bundle, (a) and (b), and fibre bundles, (c) and (d)

Therefore two different kinds of dimension measurements were used for calculation of tensile properties. In the first, five different measurements of width were taken along the length of fibre bundle and their average was used, assuming it approximated the average diameter of the fibre bundle. In the second, the maximum and the minimum values of the width were used, assuming they approximated the breadth and width of the polygonal cross-section of the fibre bundle. Table 4.1 shows the results for tensile properties for both kinds of cross-sections considered. The mean width of the fibres (circular dimension) was calculated to be 67±26 μm.

The tensile properties of hemp fibres were evaluated according to ASTM D3379-75 as described in Section 3.3.3. A total of 20 fibres were used for evaluation of tensile properties. The results of tensile testing are shown in Table 4.1. The figures in parentheses are standard deviations. These values are lower than those of glass fibres but still good enough to be used as reinforcement in composite materials. Any section of hemp fibre mat will contain fibre of varying cross section and hence different tensile properties. Some of the lower width fibres are expected to approach the tensile properties of glass fibres, as shown by Prasad and Sain [325]. These values are in good agreement with the values for hemp fibres reported by other authors, as shown in Table 4.2. In particular the values reported by Prasad and Sain [325] at a fibre diameter of 66 μm were 250 MPa and 11 GPa for tensile strength and tensile modulus respectively, which are very close to the values calculated in this research.

Table 4.1: Tensile properties of hemp fibres

Fibre Cross-section	Strength (MPa)	Modulus (GPa)	Strain to Failure (%)
Circular	**277 (191)**	**9.5 (5.7)**	**2.3 (0.8)**
Polygonal	**244 (196)**	**8.6 (5.9)**	**2.3 (0.8)**

The calculations showed that, fortunately, the difference in properties for both types of calculations is only about 10%. There is no way to tell which method is more accurate than the other. The variability in tensile properties is evident from the large values of standard deviation, again something to be expected for natural fibres. For future reference, the values for circular cross-section will be used because most of the authors cite properties of natural fibres assuming a circular cross-section.

The calculation of strain did not take into account the compliance within the machine which tends to over-calculate the strain and hence under-calculate the modulus of the fibres. Silva et al [327] showed in their studies on tensile testing of sisal fibres that

taking machine compliance into consideration results in higher values of tensile modulus than the values calculated without taking machine compliance into account.

Despite the dependence of tensile properties on the width of the fibres, most of the authors fail to mention the width at which the fibre tensile properties were calculated, as is evident from Table 4.2. Also, most of the authors cite fibre diameter as the principal dimension, although what they actually mean is fibre width.

Table 4.2: Tensile properties of hemp fibres as evaluated by different researchers

Fibre width (μm)	Strength (MPa)	Modulus (GPa)	Strain (%)	Reference
10.86 (1.6)	2140 (504)	143.2 (26.7)	1.8 (0.7)	[328]
26.5 (6.7)	514 (274)	24.8 (16.3)	-	[185]
68	593 (105)	37.5 (3.4)	1.6 (1.1)	[178]
-	584 (126)	-	-	[56]
-	396 (202)	-	-	[312]
-	619 (373)	-	-	[109]
-	690	-	-	[329]
-	960 (220)	23(5)	-	[65]
-	670	-	-	[330]
-	607 (210)	-	-	[82]
205+65	1178 (231)	68.5 (23.5)	6.4 (0.9)	[331]

The dependence of strength and modulus on fibre width was observed for fibres used for tensile testing in this research, as shown in Fig. 4.9. Both fibre strength and modulus are seen to decrease with increase in fibre width.

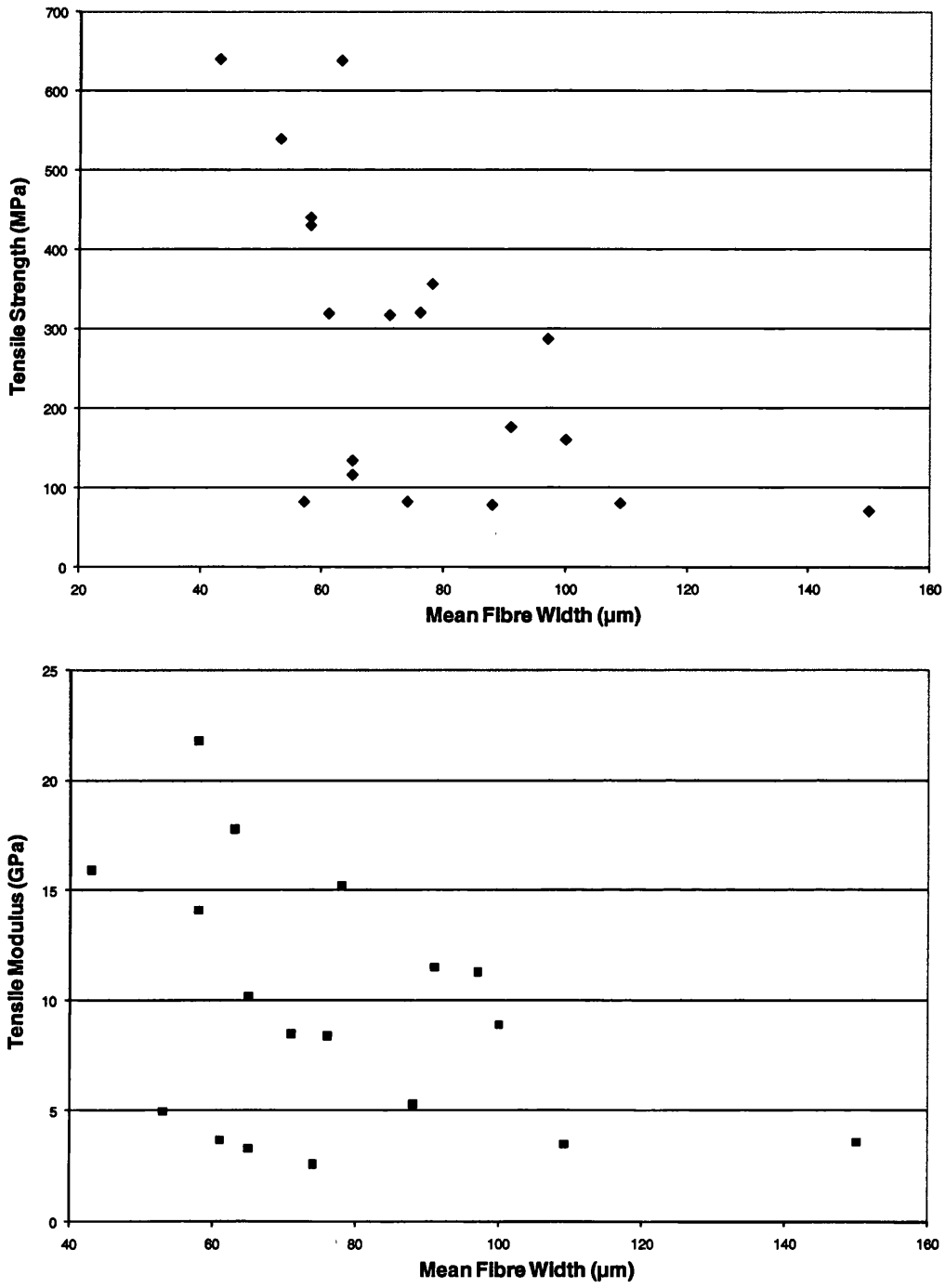

Fig. 4.9: Dependence of hemp fibre strength (top) and modulus (bottom) on fibre width

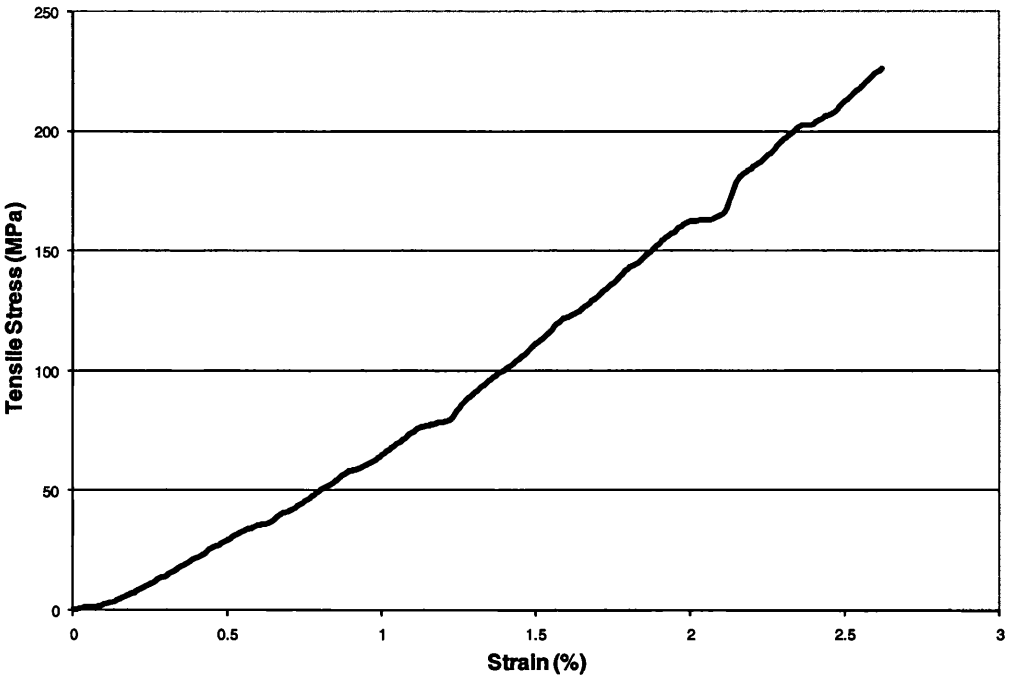

Fig. 4.10: Stress-strain curve of hemp fibre in tensile testing

The typical stress-strain curve of hemp fibre in tensile testing is shown in Fig. 4.10. The curve was found to be almost linear during the whole test. There are a few kinks which can be attributed to compliance in the system because they were found to exist on most of the curves. Pickering et al [82] have reported considerable variation in stress-strain curves for hemp fibres in tensile testing, with some of the fibres showing strain hardening and plastic flow as well as linear elastic behaviour. In this research all the fibres tested showed approximately linear elastic behaviour.

The studies on tensile properties of hemp fibres have shown them to be significantly variable and dependent on the fibre width. A mat consisting of such fibres will have fibres of various dimensions and hence variable tensile properties. The mean tensile properties of the mat will be dependent on the mean tensile properties of the fibres.

4.3 SURFACE ENERGY

The importance of surface energy of fibres in the fibre/matrix interfacial bonding has been discussed in Section 2.2.3.3. It is important to know the surface energy of hemp fibres that will give a good indication of interfacial bonding to be expected between the matrix and the fibre. Surface energy of hemp fibres was determined by using KSV Sigma 700 Tensiometer as described in Section 3.4.4. A total of five fibres were tested.

For comparison, surface energy of CSM glass fibres was also determined. Table 4.3 gives the surface energy of fibres in terms of their polar and dispersive components. The figures in parentheses are standard deviations.

Table 4.3: Surface Energy (mJ/m^2) of hemp and glass fibres

	Polar	Dispersive	Total
Hemp	**20.58 (4.83)**	**12.25 (6.57)**	**32.82 (4.38)**
Glass	**18.44 (6.45)**	**3.05 (1.88)**	**21.49 (7.63)**

The surface energy of hemp fibres is quite similar to that of unsaturated polyester resin (35 mJ/m^2) [21]. This value of surface energy of hemp fibres is similar to the one determined by other researchers. Baltazar-y-Jiminez and Bismarck [71] determined surface tension of hemp fibre to be 31 mJ/m^2. Gulati and Sain [180] determined dispersive component of the surface energy of hemp fibres at 40°C to be 38 mJ/m^2 by using inverse gas chromatography. For unsaturated polyester resin this value was 40 mJ/m^2. Park et al [328] determined surface energies of hemp fibre by using Wilhelmy plate technique similar to the one used in this research. The polar and dispersive components were determined to be 15.2 and 20.0 mJ/m^2 respectively for total surface energy of 35.2 mJ/m^2. For jute fibres, these values were found to be 8.8, 20.7, and 29.5 mJ/m^2 respectively. Van de Velde and Kiekens [332] used the same technique to determine surface energy of flax and glass fibres. The maximum surface energy for flax fibre was found to be 36 mJ/m^2. The maximum value of surface energy for glass fibres was found to be 41.64 mJ/m^2.

These studies showed that the surface energy of hemp fibres is not significantly different from that of glass fibres. Good fibre/matrix interfacial bonding is favoured when the fibre surface energy greatly exceeds the matrix surface energy [21]. The similar values of surface energies of hemp fibre and unsaturated polyester resin imply that a relatively poor interfacial bonding between them can be expected. The polar component of surface energy is greater than the dispersive component, which is

consistent with the polar nature of hemp fibres. This polar nature will also be an impediment in good interfacial bonding with a non-polar polymer matrix. The quantitative measure of fibre/matrix interfacial bonding is the interfacial shear strength which was evaluated next.

4.4 INTERFACIAL SHEAR STRENGTH OF HEMP-POLYESTER

Interfacial shear strength (IFSS) is another important measure of the fibre/matrix interfacial bonding. The interfacial shear strength of hemp fibres in unsaturated polyester resin was evaluated in single fibre pull-out test and the results are shown in Table 4.4. At least 20 fibres were used for testing and the numbers in parentheses are standard deviations.

Table 4.4: Single Fibre Pull-Out Testing Result of Hemp Fibre in Polyester Resin

Interfacial shear strength	**(MPa)**	**1.9 (1.3)**
Force at pull-out	**(N)**	**0.12 (0.07)**
Width of fibres	**(μm)**	**33 (7.5)**
Fibre embedded length	**(mm)**	**0.68 (0.24)**

It has been pointed out [333] that the non-uniform diameter of natural fibres may yield unreliable results for IFSS by using this method, as is evidenced by the large scatter in results (high standard deviations). Therefore any values obtained by using this method should be seen as an approximate measure of the interfacial shear strength rather than highly accurate values.

This value of interfacial shear strength is consistent with the value reported by other authors for natural fibres in a polymer matrix. Czigany et al [312] determined the interfacial shear strength of hemp fibre (mean diameter 113 μm) in polypropylene to be 5.1±1.4 MPa, in biodegradable MaterBi polymer to be 2.9±0.9 MPa and in biodegradable PuraSorb polymer to be 11.3±3.4 MPa. Baltazar-y-Jimenez et al [331] reported interfacial shear strength of 8.4±1.8 MPa for hemp fibres in cellulose-acetate-

butyrate matrix. Hill and Khalil [134] reported interfacial shear strength of 1.39±0.37 for oil palm fibres in polyester resin, and 1.48±0.32 for coir fibres in polyester resin. Sanadi et al [118] reported interfacial shear strength of sunhemp/polyester to be 4.34 MPa.

There is a range of interfacial shear strength values for glass fibres in polyester resin reported in the literature. One study [29] reports IFSS values of 10 and 12 MPa for coated glass fibres in polyester resin. Considering these values, the IFSS of hemp fibres in polyester resin is considerably lower, which is not surprising taking into account their incompatibility with the polymer resins.

5. MECHANICAL PROPERTIES OF UNTREATED HEMP FIBRE AND GLASS FIBRE COMPOSITES

This chapter presents the results of mechanical properties of untreated hemp fibre/polyester, CSM glass fibre/polyester, and hemp-glass/polyester hybrid composites. The properties of hemp fibre composites are compared with those of CSM glass fibre composites. The effect of hybridisation of hemp fibres with glass fibres on the composites' properties is also presented.

5.1 FIBRE CONTENT

There is an inherent problem in calculating fibre weight fraction of natural fibre composites because, unlike glass fibre composites, the resin in natural fibre composite samples can not be burnt off to get an accurate value for the weight of fibre in the sample, the natural fibres having a lower decomposition temperature than the resin. For this reason the fibre weight fraction of the hemp fibre composites was calculated indirectly as explained in Section and converted into fibre volume fraction. The fibre weight fraction of glass fibre composites was calculated by the standard calcination method.

5.1.1 Hemp fibre reinforced polyester composites

5.1.1.1 Weight per unit area of hemp fibre mat

In order to calculate fibre weight fraction of hemp fibre reinforced polyester composites, weight per unit area of hemp fibre mat should be known. No such data was provided by the suppliers of the hemp fibre mat and, therefore, tests were undertaken to calculate the weight per unit area of hemp fibre mat. To do this, patches of different dimensions were cut up from different parts of the mat and were weighed in a balance having the accuracy of 0.1 mg. Since all the laminates were made by using hemp fibre mats of approximately 500 cm^2 area, most of the weight measurements were taken at

this area. The resulting values were plotted on a weight versus area graph as shown in Fig. 5.1. From the graph and from calculating the mean value of the measurements, the value of weight per unit area was found to be 847 ± 66 g/ m^2. Considerably large value of standard deviation is not unexpected because of the variation in fibre concentration in different parts of the mat. This value was used in calculating fibre weight fraction of all the composites made from untreated hemp fibres in this research.

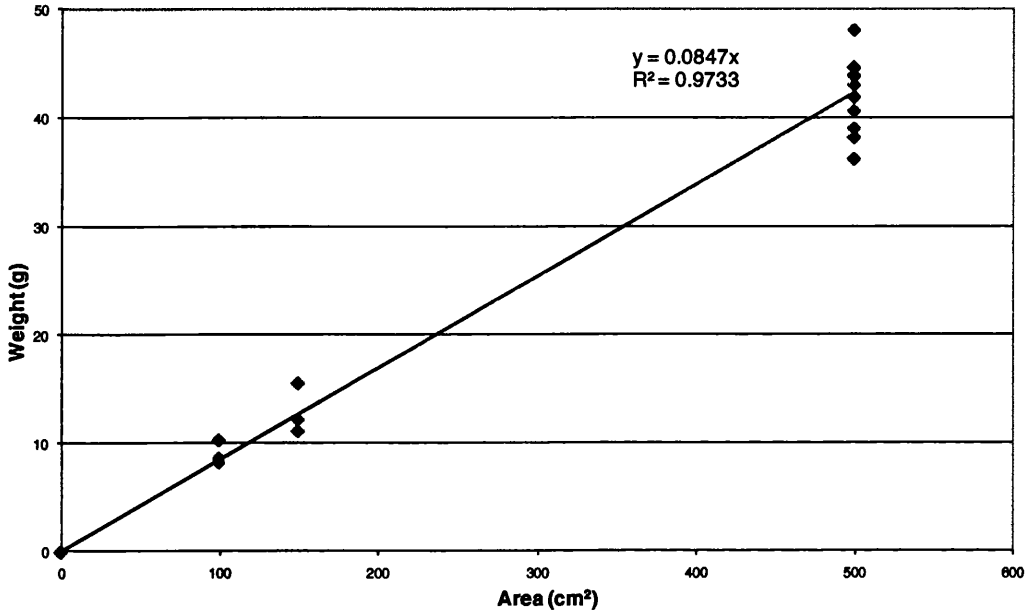

Fig. 5.1: Weight vs. area of hemp fibre mat

5.1.1.2 Fibre weight/volume fraction

Laminates of hemp fibre reinforced polyester composites were made at three different moulding pressures: 1, 2, and 3 MPa. The effect of increasing the moulding pressure on fibre weight fraction and the tensile properties of the composites was evaluated. The results of fibre weight and volume fraction of all composites made at these moulding pressures are summarised in Table 5.1. The calculations for fibre weight and volume fractions have been done as described in Section 3.5. Each value is the mean of all the samples made at a particular moulding pressure (at least 20), and the values in parentheses are standard deviations.

Table 5.1: Fibre weight and volume fraction of composites at different moulding pressures

Moulding Pressure (MPa)	Fibre Weight Fraction (%)	Fibre Volume Fraction (%)
1	47.6 (4.7)	42.8
2	51.3 (3.4)	46.5
3	56.2 (2.8)	51.4

It can be seen that fibre weight fraction of the composites increases approximately linearly with increase in moulding pressure. The composites made at moulding pressure of 3 MPa had the highest fibre weight fraction. It will be shown later in Section 5.3.1 that optimum tensile properties of composites were also obtained for laminates made at moulding pressure of 3 MPa. The considerable variation in fibre weight fraction, represented by standard deviation, can be attributed to variation in hemp fibre concentration in different parts of the hemp fibre mat used. Although all the laminates were made from the same hemp fibre mat, there was appreciable variation in thickness in different parts of the fibre mat because fibres were densely packed at some places and loosely packed at other places. As shown in Section 5.1.1.1, the average weight per unit area of hemp fibre mat was 847 ± 66 g/m^2 which represented a considerable variation in weight per unit area. It is not unexpected, therefore, to observe considerable variation in fibre weight fraction in the laminates made from these fibres. However, the variation in fibre weight fraction decreased, represented by decreasing values of standard deviation, with increase in moulding pressure as the increasing pressure resulted in a more compact laminate. A trial laminate was also made at a moulding pressure of 4 MPa to observe the effect of elevated moulding pressure on fibre weight fraction and mechanical properties of the composites. Although a high average fibre weight fraction of 66% was obtained for this laminate, it did not result in substantial increase in tensile properties of these composites as explained in Section 5.3.1.7. Therefore it was decided to use moulding pressure of 3MPa in making all the hemp fibre reinforced polyester laminates in this research.

The values for fibre volume fraction obtained in this research are considerably higher than the values reported by other researchers who have worked with hemp fibre reinforced polyester composites. Rouison et al [123] reported a 20% fibre volume fraction for composites made by resin transfer moulding. Mehta et al [145] reported fibre volume fraction of up to 30% in their composites made by hand lay-up plus compression moulding process similar to the one used in this research. Sebe et al [124] reported fibre weight fraction of up to 36% for their composites made by resin transfer moulding.

5.1.2 CSM Glass fibre reinforced polyester composites

In order to compare properties of hemp fibre composites with glass fibre composites, laminates of glass fibre reinforced polyester composites were made by using glass fibres in chopped strand mat (CSM) form. CSM glass fibres were used because they have similar geometry (randomly oriented short fibre strands in 2D) as the hemp fibre mat. Laminates of CSM glass fibre reinforced polyester composites with different fibre content were made by using different number of glass fibre layers and different amount of polyester resin, and their fibre weight and volume fractions were evaluated by using the calcination method as described in Section 3.5. The results are shown in Table 5.2. The values in parentheses are standard deviations.

Table 5.2: Fibre fraction of CSM glass fibre reinforced polyester composites

No. of glass fibre layers	Fibre weight fraction (%)	Fibre volume fraction (%)
4	50.8 (1.5)	32
4	45.5 (2.3)	28
6	55.0 (1.9)	37
6	52.8 (1.7)	32

Glass fibre laminates made with six glass fibre layers had similar fibre weight fraction as hemp fibre laminates although the fibre volume fraction was relatively lower than hemp fibre composites because of higher density of glass fibres (2.55 g/cm^3) than hemp

fibres. Therefore all glass fibre laminates were made by using six glass fibre layers. The scatter in the fibre weight fraction is relatively lower than that for hemp fibre composite because of the more regular arrangement of glass fibre mat.

5.1.3 Hemp-CSM glass fibre reinforced polyester hybrid composites

Because of the presence of hemp fibres, it was not possible to use calcination method for evaluation of fibre weight fraction. Instead the indirect method of calculation of fibre weight fraction described in Section 3.5 was used. Because of differences in densities of glass and hemp fibres, it is more meaningful to compare the fibre volume fractions. Therefore the fibre volume fraction for both hemp fibres and glass fibres and total volume fraction have been calculated. The total volume fraction for both configurations is very close to that of hemp fibre composites. Therefore these laminates represent the replacement of about 11% of hemp fibres with glass fibres. The results are shown in Table 5.3. The values in parentheses are standard deviations.

Table 5.3: Fibre fraction of hemp-glass fibre hybrid composites

Fibre Configuration	Fibre weight fraction (%)	Fibre volume fraction (%)		
		Hemp	Glass	Total
Hemp skin, glass core	**61.0 (3.1)**	**35.8**	**11.1**	**46.9 (2.7)**
Glass skin, hemp core	**62.1 (3.1)**	**36.6**	**11.3**	**47.8 (2.8)**

5.2 POSSIBLE SOURCES OF IMPERFECTIONS IN HEMP-POLYESTER COMPOSITES

Hemp fibre reinforced polyester composites are expected to contain a number of possible sources of imperfections that may impede the composites from attaining their optimum mechanical properties. These sources of imperfections are induced during the manufacturing stage or may arise because of the characteristics of hemp fibres. Before

evaluating the mechanical properties, it is important to identify these sources and evaluate their potential effects on the mechanical properties of the composites.

For glass fibre reinforced polymer composites, Johnson and Ghosh [334] have come up with the following list of such possible sources: incomplete impregnation of fibres; incomplete cure of resin; poor wetting and subsequent poor adhesion of fibre to the matrix; the presence of bubbles, voids, delaminations, broken strands, loose ends of fibres, knotted strands, wrinkled strands and crevices; crazing cracks; and local resin rich areas. For natural fibre reinforced polymers composites also, all of these factors may be present and may affect the mechanical properties with varying degrees. However, for hemp fibre reinforced polyester composites, the more significant sources are expected to be incomplete impregnation and poor fibre-matrix adhesion, voids and residual stresses. These imperfections arise from the residual stresses caused by the shrinkage of the polyester resin, porosity and voids induced because of the hand lay-up process used and because of the moisture in the fibres, and poor interfacial bonding between polar hemp fibre and non-polar polyester resin because of their inherent incompatibility.

5.2.1 Porosity and Voids

Porosity and voids in an isotropic solid can have significant effect on its mechanical properties. It has been shown theoretically [16] that the reduction factors for the effective bulk modulus and effective shear modulus introduced into an isotropic elastic solid by a volume fraction V of spherical voids are given by:

$$\frac{E_{eff}}{E} = (1\text{-}3\ V) \qquad (5.1)$$

$$\frac{G_{eff}}{G} = (1\text{-}2\ V) \qquad (5.2)$$

where E and G represent bulk modulus and shear modulus respectively. Hence a 10% volume fraction of spherical voids can result in as much as 30% reduction in bulk modulus and 20% reduction in shear modulus of the solid.

Porosity, defined as air-filled cavities inside an otherwise continuous material, is often an unavoidable component in almost all composite materials. These voids can have significant effect on mechanical properties of composites. For example, it has been

shown that for GRP composites, 10% void content by volume can reduce their compressive strength by about 40% and their interlaminar shear strength by about 50% [15].

Composite materials contain several types of voids. Depending on the fabrication method and matrix type, almost all composite materials contain voids. Most common voids are large cavities formed during the manufacture of the composite as a result of gross defects. Small voids are formed adjacent to the fibres either because of incomplete infiltration during processing or cavitation during deformation. Voids are also formed in resin-rich or fibre-free regions between laminate [21].

Natural fibre composites are expected to have larger void volume fraction than synthetic fibre composites because of the peculiar structure of natural fibres. The factors contributing to voids in natural fibre composites are [335]: existence of luminal cavities of natural fibres, the complex surface chemistry of natural fibres which complicates fibre-matrix compatibility, the heterogeneous shapes and dimensions of natural fibres which restrict matrix impregnation, and low packing ability of natural fibre assemblies which also limits the maximum obtainable fibre volume fraction.

Madsen et al [335] have suggested that the absolute volume of porosity in natural fibre composites can be separated into three main components: Fibre related porosity, which increases linearly with fibre volume fraction and consists of fibre porosity, fibre/matrix interface porosity, and impregnation porosity; matrix related porosity, which again increases linearly with fibre volume fraction and consists of matrix porosity; and structural porosity, which occurs because of insufficient wetting of fibre by matrix. Additionally, the use of thermoset matrices can also be a major cause of porosities in composites.

Mwaikambo and Ansell [336] have determined the inherent porosity content of natural fibres by measuring absolute and bulk densities of fibres. The porosity content of hemp fibres was found to be 2.5% while for sisal and jute fibres, it was as high as 10.9% and 11.4% respectively. This inherent porosity of hemp fibres can contribute to overall porosity content in the laminates.

It was shown in Section 4.1.2 that the hemp fibres used in this research had an equilibrium moisture content of approximately 10%. The curing process of polyester

resin is exothermic, and for unsaturated polyester laminate cured at room temperature, the temperature may rise to 70-100°C [337]. This high temperature can result in the vaporisation of moisture leading to porosity in the laminate.

Madsen et al [335] studied porosity content of four natural fibre composites and suggested a model to predict the volumetric composition and density as a function of fibre weight fraction. It was found that at low fibre weight fractions, the porosity content was low. At regions of high fibre weight fraction, the porosity content started to increase linearly. The transition between these two regions of fibre weight fraction determined the optimal combination of high fibre content and low porosity content. The model predictions were in good agreement with the experimental data. For the unidirectional hemp-PET composites, the transition region was found to exist at about 57% fibre weight fraction with maximum fibre volume fraction of 50.8% and porosity content of 4.6%. For randomly oriented flax fibre reinforced polypropylene composites, the transition fibre weight fraction was found to be 58% with maximum fibre volume fraction of 40.8% and maximum porosity content of 9.1%. For randomly oriented jute fibre reinforced polypropylene composites, the transition fibre weight fraction was found to be 49.3% with maximum fibre volume fraction of 33.7% and porosity content of 8.4%. Their research showed that although high fibre weight fraction is an essential requirement to obtain optimum mechanical properties of natural fibre composites, this would also be accompanied by a high void volume content, thus affecting the mechanical properties.

One of the inherent disadvantages of the hand lay-up process used in this research is the entrapment of air between laminae during manufacturing of the laminates. Although every effort was made to release the air from the laminates, the presence of some voids because of entrapment of air cannot be ruled out.

The percentage void content of the composites made in this research was calculated using the following formula, as given in BS EN ISO 7822:1999 (Textile glass reinforced plastics-Determination of void content):

$$V = \frac{100(\rho_c - \rho_{mc})}{\rho_c} \quad \text{.....(5.3)}$$

where ρ_c is the theoretical composite density and ρ_{ac} is the measured composite density. The measured composite density was calculated by dividing the weight of each sample by its volume. The theoretical density was calculated by using the formula:

$$\rho_c = \frac{100}{\frac{W_f}{\rho_f} + \frac{W_r}{\rho_r}} \quad \text{.....(5.4)}$$

where W_f is the fibre percentage weight fraction, W_r is the resin percentage weight fraction, ρ_f is the density of hemp fibre and ρ_m is the density of polyester resin. For these calculations, the value of hemp fibre density of 1.48 g/cm^3 was used which has been used by most of the researchers. The density of the polyester resin was given by the manufacturer as 1.22 g/cm^3 but was found to be 1.17±0.01 g/cm^3 in actual testing and this value was used in the calculations. The void content in composites made at three different fibre volume fractions was calculated and the results are shown in Table 5.4. These are the mean values of at least 20 samples made at each moulding pressure. The values in parentheses are standard deviations.

Table 5.4 shows quite high values of void volume content in these composites. There are possible sources of error in these calculations which should be appreciated. As the British Standard BS EN ISO 7822:1999 used for these calculations also acknowledges, differences in curing, heating, pressure and molecular forces arising from the reinforcement surface all make the density of the resin in the composite different from the bulk resin density. The value of density of hemp fibre used was taken from literature and it can vary for the fibres used in this research. The indirect method of calculating the fibre weight fraction can also introduce some possible sources of errors.

Table 5.4: Void content in hemp-polyester composites

Moulding pressure (MPa)	Fibre volume fraction (%)	Void content (%)
1	42.8	11.2 (1.5)
2	46.5	11.1 (4.1)
3	51.4	10.2 (3.0)

The void content is more or less similar at all values of fibre volume fraction. It is about 1% lower for composites made at 3 MPa pressure which can be attributed to more compact assembly at higher moulding pressure. However the scatter in the data suggests that differences in void content are not significant.

These void fraction values are similar to the ones reported by Madsen et al [335] and discussed above. Other researchers have also reported similar values for void content for natural fibre composites. Sreekumar et al [138] studied void content of sisal leaf fibre reinforced polyester composites made by resin transfer moulding (RTM) and compression moulding. The void content was found to increase linearly with increase in fibre volume fraction in both methods. In composites made by RTM, the maximum void content was found to be 7% at fibre volume fraction of 50%. Whereas in composites made by compression moulding, a maximum void content of 10% was found at fibre volume fraction of 48%. Their study suggested that compression moulding resulted in higher values of void content in composites compared with those made by RTM. The decrease in void content in RTM composites was attributed to resin flow front. As the resin flow front advanced through the fibres, the size of the entrapped air decreased due to hydrostatic pressure. The tensile properties of the composites made by RTM were also found to be greater than those made by compression moulding. This improvement in tensile properties was attributed to lower amount of voids present in these composites.

Dhakal et al [338] reported void content in hemp fibre reinforced polyester composites to be dependent on fibre volume fraction. The maximum void content was reported to be 18.6% at fibre volume fraction of 26%.

Madsen and Lilholt [339] reported the porosity volume fraction to increase linearly with increase in fibre volume fraction for unidirectional flax yarn reinforced polypropylene composites. It increased from 3.8% for fibre volume fraction of 42.6% to 7.1% for fibre volume fraction of 54.8%.

From their studies on hemp fibre reinforced cashew nut shell liquid (CNSL) composites made by compression moulding, Mwaikambo and Ansell [147] reported the void content to be dependent on moulding pressure. For unidirectional hemp-CNSL composites, the void content increased with increase in moulding pressure, attributed to

delamination due to processing conditions, and the maximum void content of 26% was recorded at a moulding pressure of 9 MPa. For non-woven hemp-CNSL composites, the void content was found to decrease with increase in moulding pressure. For these composites, the void content decreased from 17.5% at 5 MPa pressure to 11% at 9 MPa pressure.

Carpenter [64] reported void volume fraction of 16.7% at fibre volume fraction of 68.5% for woven flax fibre reinforced polyester composites. The woven flax reinforcement were pre-pressed prior to fabrication. A lower void volume fraction was reported for composites made of reinforcement that were not pre-pressed.

It is thus concluded that natural fibre reinforced composites, especially made by compression moulding, can have considerably high volume fraction of voids, sometimes reaching double figures, which can result in considerable degradation in their mechanical properties. It is, of course, difficult to quantify the degradation in properties because of these voids. Therefore while selecting the manufacturing methods for natural fibre reinforced composites this factor should be taken into account.

5.2.2 Poor interfacial adhesion

Poor interfacial adhesion between polar natural fibres and non-polar polymers resin is well documented and may be a significant contributor to reducing the mechanical properties of these composites. As described in Sections 4.3 and 4.4, the lower difference in surface energies of hemp fibres and polyester resin and their relatively poor interfacial shear strength can result in poor mechanical properties of the composites.

However the impact strength of a composite can be increased by poor interfacial bonding because, although less energy is required to initiate a crack, the composite absorbs more energy during propagation of crack through the poorly bonded interface. This has been found to be particularly true for polyester laminates, but not for epoxy laminates which can establish a strong bond with the fibre even in the absence of a coupling agent [22].

5.2.3 Residual stresses

Some laminates made in this research were found to be slightly warped after curing which indicated the presence of residual stresses because of the thermal gradient and shrinkage of polyester resin during the curing stage. These residual stresses can also result in considerable degradation of mechanical properties of the composites.

Residual stresses in composites develop when temperature gradients exist during the curing of thermoset resin and therefore they are sometimes called curing stresses. The shrinkage of polyester resin is about 4-8% after curing. Since this shrinkage is greater than that of hemp fibre, it exerts a stress normal to the surface of the fibre which increases the frictional force against pull-out during fracture and may enhance the toughness. Generally, the residual stresses are detrimental to mechanical properties and the durability of the composites.

5.3 TENSILE PROPERTIES

5.3.1 Hemp fibre reinforced polyester composites

Tensile testing of composites was carried out by using samples from laminates made at moulding pressures of 1, 2 and 3 MPa. The number of samples used for tensile testing at these moulding pressures was 31, 30, and 24 respectively. The results of tensile testing are shown in Table 5.5. These are mean values of the samples tested at each moulding pressure and the values in parentheses are standard deviations. For comparison the tensile properties of un-reinforced polyester resin are also shown.

Table 5.5: Tensile properties of hemp fibre reinforced polyester composites

Fibre Weight Fraction (%)	Tensile Strength (MPa)	Tensile Modulus (GPa)	Strain to Failure (%)
Neat Polyester Resin	**44.8 (7.1)**	**3.7 (0.4)**	**1.35 (0.21)**
47.6 (4.7)	**35.8 (4.2)**	**5.6 (0.7)**	**0.94 (0.19)**
51.3 (3.4)	**40.2 (5.6)**	**6.2 (1.2)**	**1.07 (0.2)**
56.2 (2.8)	**46.4 (4.6)**	**7.2 (0.9)**	**1.03 (0.19)**

5.3.1.1 Tensile Strength

The tensile strength of these composites increases approximately linearly with increase in fibre weight fraction over this region shown in Fig. 5.2. The error bars represent standard deviation. At lower values of fibre weight fraction (up to 51%), the tensile strength of the composites is actually lower than that of un-reinforced polyester resin, suggesting the fibres act as impurities rather than reinforcement at these values. It is only at fibre weight fraction of 56% that these composites have higher tensile strength than un-reinforced polyester resin. The maximum mean value of tensile strength of 46.4 MPa was obtained at a fibre weight fraction of 56% which corresponds to fibre volume fraction of 51%. This strength value is higher than the values reported in the literature for hemp fibre reinforced polyester composites because of higher fibre volume fraction of composites. The reported values are: 33 MPa at a fibre volume fraction of 20% [146], 40 MPa at a fibre volume fraction of 30% [145], and 38 MPa at fibre volume fraction of 20% [130].

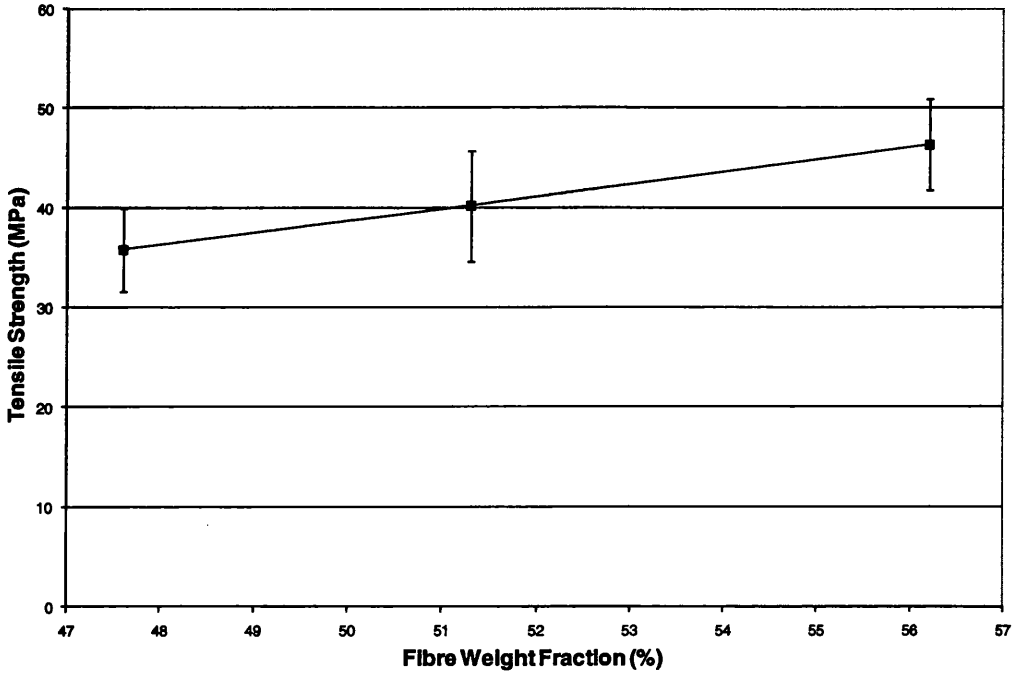

Fig. 5.2: Effect of increasing fibre weight fraction on tensile strength of hemp/polyester composites

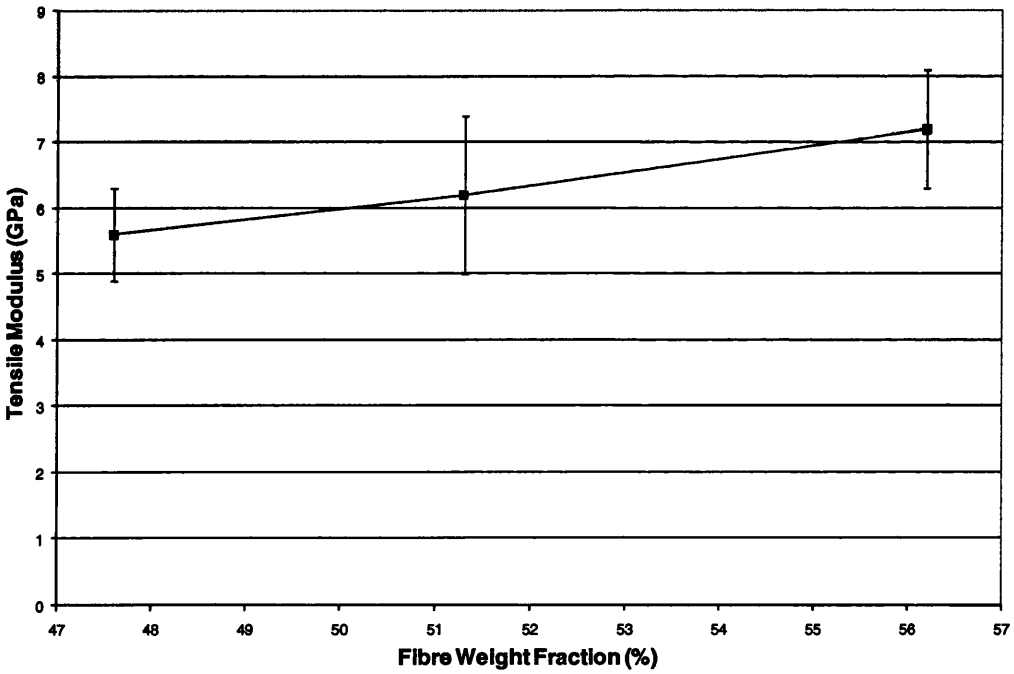

Fig 5.3: Effect of increasing fibre weight fraction on tensile modulus of hemp/polyester composites

5.3.1.2 Tensile Modulus

The effect of increasing the fibre weight fraction on tensile modulus of the composites is shown in Fig. 5.3. Again the tensile modulus of the composites increases approximately linearly with increase in fibre weight fraction. The advantage of using hemp fibres is realised in their much superior tensile modulus values compared to that of un-reinforced polyester resin. Composites with even lower values of fibre weight fraction have resulted in considerable increase in tensile modulus of un-reinforced polyester resin. The value of tensile modulus increased by almost 100% at fibre weight fraction of 56% compared to that of un-reinforced polyester resin. The maximum value of tensile modulus of 7.2 GPa was again attained at fibre weight fraction of 56% corresponding to fibre volume fraction of 51%. This modulus value is higher than the values reported in the literature for hemp fibre reinforced polyester composites. The reported values are: 1.4 GPa at 20% fibre volume fraction [146], 6 GPa at 30% fibre volume fraction [145], and 6.7 GPa at 20% fibre volume fraction [130].

5.3.1.3 Strain to Failure

The effect of increasing fibre weight fraction on strain to failure of the composites is shown in Fig 5.4. Increasing fibre weight fraction does not seem to have any significant effect on strain to failure and these values stay close to the average strain to failure value of about 1%. This value is lower than the strain to failure value of 1.35% for un-reinforced polyester resin which shows that incorporation of hemp fibres in polyester resin results in stiffer and more brittle composites than the polyester resin.

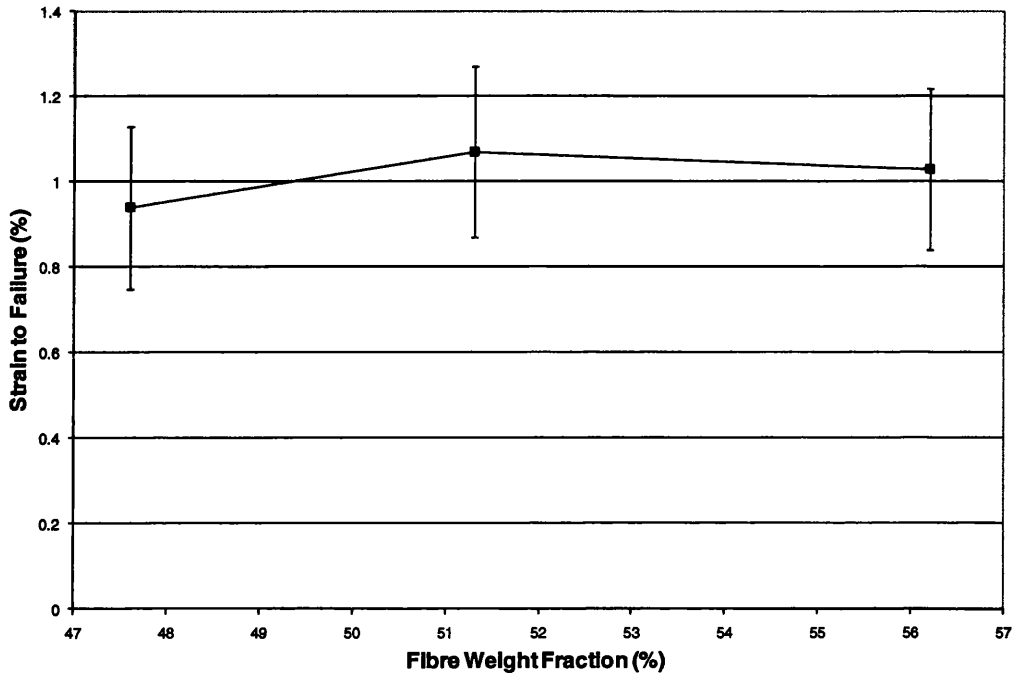

Fig 5.4: Effect of increasing fibre weight fraction on strain to failure of hemp/polyester composites

5.3.1.4 Analysis of tensile properties

The tensile testing of hemp fibre reinforced polyester composites showed that the incorporation of hemp fibres in polyester resin resulted in negligible increase in tensile strength of polyester resin but almost 100% increase in tensile modulus of polyester resin at fibre weight fraction of 56%. This points at the good potential of hemp fibres to be used as reinforcement for polymer composites because the main function of the fibres is to increase the stiffness of the polymer resin. However the real litmus test of hemp fibre composites is their performance in comparison to glass fibre composites.

In one study on non-woven $[\pm 45^{\circ}]_4$ glass fibre reinforced polyester composites [262], the values of tensile strength and tensile modulus were found to be 43 MPa and 5.9 GPa respectively at fibre weight fraction of 42%. The same values for woven $[\pm 45^{\circ}]_4$ glass fibre reinforced polyester composites were found to be 64.2 MPa and 6.21 GPa respectively at fibre weight fraction of 52%. These tensile properties are comparable to the tensile properties of hemp fibre reinforced polyester composites at similar fibre weight fractions. This seems to suggest that hemp fibres have the potential of replacing

glass fibres of particular configurations in terms of their tensile properties. The higher tensile modulus of hemp fibre composites as compared to glass fibre composites at similar fibre weight fractions is noticeable. The comparison of tensile properties of hemp fibre composites with CSM glass fibre composites is undertaken later in Section 5.3.4.

Almost all the samples of hemp-polyester composites used in tensile testing fractured in a completely brittle manner. The crack ran right through the samples almost normal to the loading direction of the samples. This indicated that normal stresses resulting from the tensile forces were the dominant cause for fracture of the samples. Some cracking sound was normally heard just before the eventual fracture of the samples. This sound was most probably due to matrix cracking, which preceded the eventual fracture of the samples, and the fibre/matrix interfacial debonding. The samples fractured mostly in the middle, but some fractures nearer the grips were also observed. A typical fractured sample is shown in Fig. 5.5.

Fig. 5.5: Fracture surface of a hemp-polyester sample in tensile testing

The stress versus strain curves of a typical tensile tested composite sample compared with an unreinforced polyester sample is shown in Fig. 5.6. It is clear that reinforcing the polyester resin with hemp fibres does not result in any appreciable increase in tensile strength but the increase in tensile modulus is quite significant. This increase in modulus means that the strain to failure of the composite is lower than polyester resin. The curve has a noticeable 'knee' which has also been reported to exist for chopped strand mat (CSM) glass fibre- polyester composites [15] and for Sheet Moulding

Compounds (SMC) composites containing E-glass fibres in a polyester resin [340], indicating that mechanical behaviour of short fibre composites is quite similar. The initial slope of the curve is relatively linear and in this phase both matrix and the fibres are expected to carry the load. The curve starts to deviate in strain range of about 0.2-0.5% which may be explained by fracture within fibre strands oriented transverse to load direction and the onset of fibre/matrix debonding because of poor interfacial bonding. A sample was tested at a stress of up to 24 MPa and strain of up to 0.5% and its surface was examined. As shown in Fig. 5.7, the surface of the tested sample showed no signs of matrix cracking and its appearance was quite similar to an untested sample. Therefore the "knee" is most probably due to the damage mechanisms occurring within the material as explained above. The high fibre volume may also inhibit any initiation of matrix cracking at this stage.

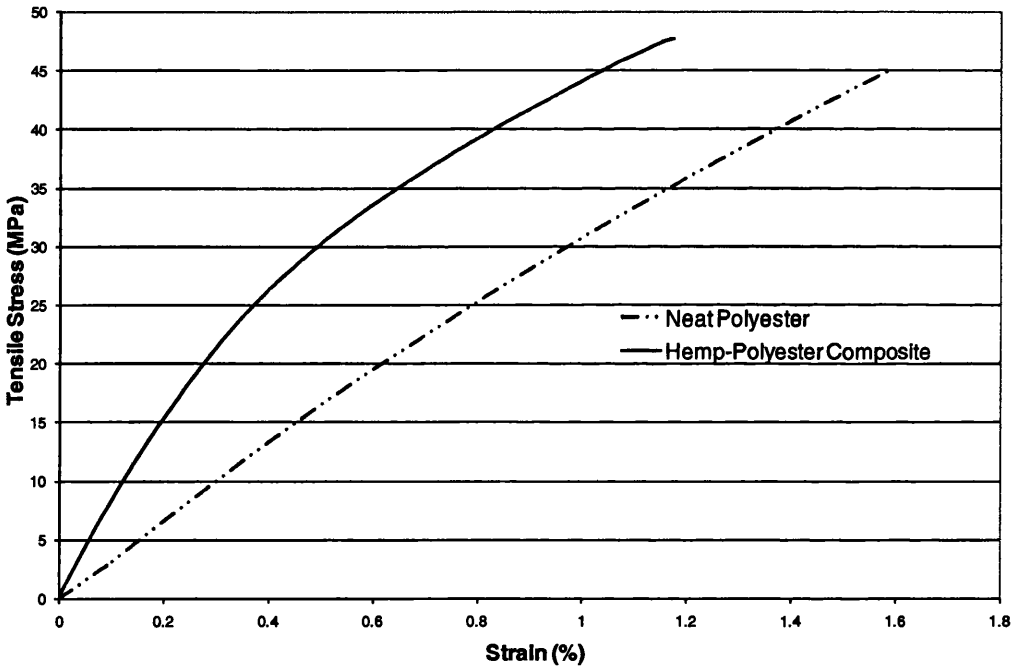

Fig. 5.6: Comparison of stress-strain curves of neat polyester resin with hemp-polyester composites in tensile testing

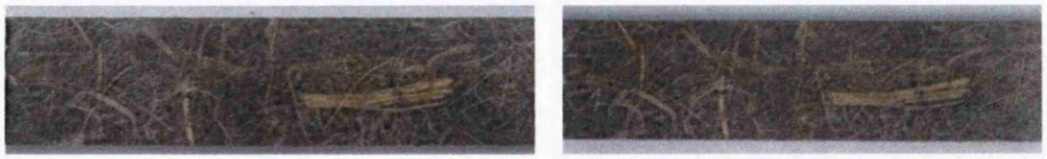

(a) (b)

Fig. 5.7: Surfaces of hemp composite sample before testing (a), and after tensile testing (b), at stress=24 MPa, strain=0.5%

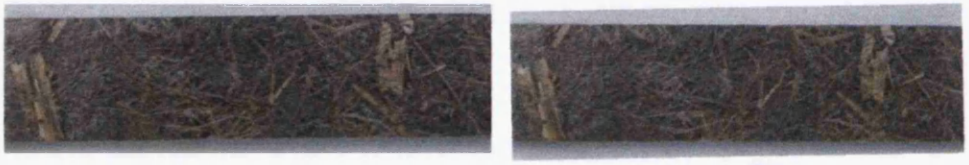

(a) (b)

Fig. 5.8: Surface of hemp composite sample before testing (a), and after tensile testing (b), at stress=37 MPa, strain=0.8%

On increased loading, the debonding is expected to initiate more cracks and as these cracks spread, more of the load is transferred to the fibres. These damage mechanisms result in further change in slope of the curve as the stress is transferred to fibres. Further application of load is expected to result in further debonding and fracture of fibre bundles oriented at other angles to the load. A sample was tested at a stress of up to 37 MPa (about 80% of UTS) and strain of up to of 0.8%. As Fig. 5.8 shows, even at this high stress when the sample is close to fracture, no signs of matrix cracking were visible on the surface and most of the damage is still expected to take place within the sample. The last part of the curve represents when fibres, oriented parallel to the load direction, are expected to carry almost the whole load. The fracture of these fibres results in eventual fracture of the samples in a brittle manner at a strain of about 1%.

In order to ascertain the damage mechanisms of the composites, SEM micrography of fracture surfaces of tensile tested samples was carried out. Fig. 5.9 shows micrographs of fractured surfaces from tensile testing. The figure show that four processes contribute to the fracture of the samples: matrix fracture, fibre-matrix debonding, fibre pull-out and fibre fracture. The poor fibre/matrix interfacial bonding encourages debonding and fibre pull-out, the evidence of which can be seen in the fracture surface.

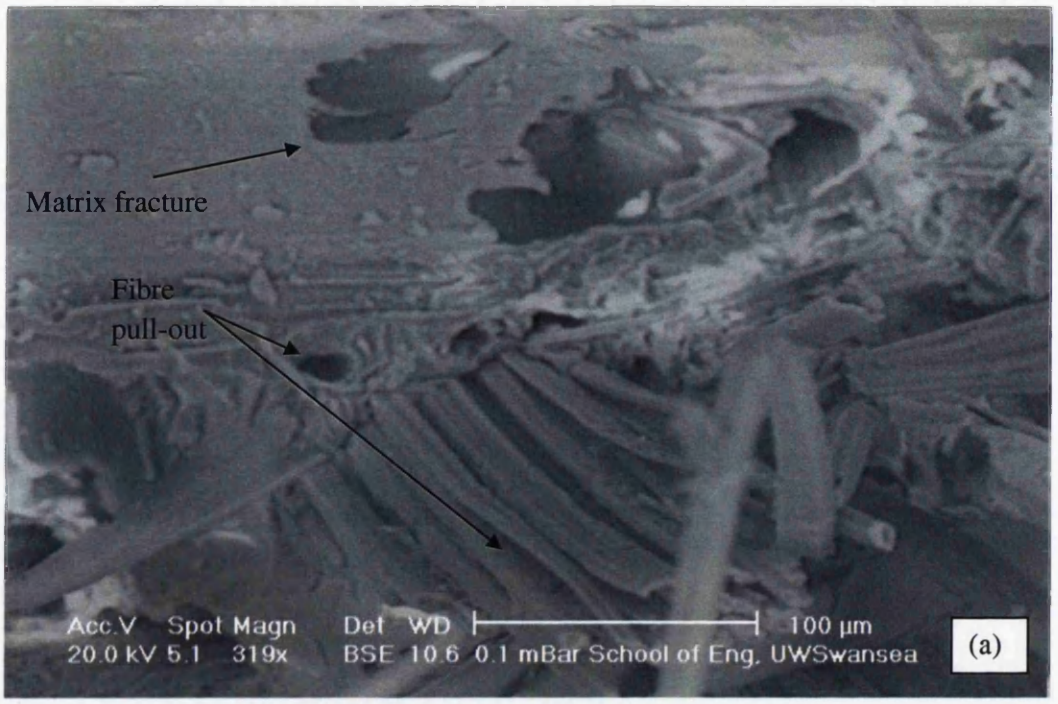

Fig 5.9: SEM micrographs of fracture surfaces of tensile tested hemp fibre reinforced polyester samples

The matrix fracture, which normally occurs in the last phase, and fibre fracture, which normally starts in the initial phase of the fracture, are also evident from the micrographs. Fig. 5.9 (a) shows considerable matrix cracking and some fibre pull-out while Fig. 5.9 (b) shows fibre-resin debonding and fibre fracture.

5.3.1.5 Variability in tensile properties

Due to the inhomogeneous and anisotropic nature of fibre reinforced polymer composites, considerable variation in mechanical properties has been observed for the composites made with the same constituents. For example, coefficient of variation values of 0.079, 0.080, 0.083 and 0.1 were reported by Johnson [341] for tensile modulus measurements for polyester resin reinforced with four different volume fractions of glass fibre. For CSM E-glass polyester composites, Mallick [340] showed that it is not uncommon to observe ± 10% variation in mechanical properties for samples from the same laminate. Owen et al [342] have reported even higher values of variability for sheet moulding compounds. Turner [343] was thus quite justified in commenting, "It seems likely that relatively high coefficients of variation are an inherent characteristic of composite materials in general, probably caused by local variations of fibre volume faction, fibre alignment and void content".

The variability in physical and mechanical properties of natural fibres is an inherent drawback of their use as reinforcement in composite materials. The reasons for this variability have been discussed in detail in Section 2.42. Therefore the use of natural fibres as reinforcement is expected to increase the variability in mechanical properties of composites. This variability is represented by the error bars in the Figs. 5.2-5.4. The composites made at fibre weight fraction of 56% showed a variation of about 10% in tensile strength, about 12% in tensile modulus, and about 18% in strain to failure.

The variation in mechanical properties of hemp fibre composites is well documented. Previous research on hemp-polyester composites in this laboratory by Yuanjian [262] had found that tensile strength of composites decreased from a maximum value of 53.0 MPa at moulding pressure of 2 MPa to 35.8 MPa at moulding pressure of 3MPa, although the fibre weight fraction was reported to be 44% in both cases. It was proposed that this could be due to crushing of fibres at 3 MPa moulding pressure. However, as shown in the present research, it is possible to attain tensile strength for these

composites of up to 50 MPa at moulding pressure of 3 MPa. So this variation can be attributed to variability of properties of natural fibres.

The research undertaken with hemp-polyester composites by Rouison et al. [123] also found considerable variation in mechanical properties for samples containing the same fibre volume fraction. For example, the tensile strength of samples containing 18% fibre volume fraction ranged from 30 MPa to 45 MPa. They also reported tensile modulus values ranged from 1.2 GPa to 2 GPa at 18% fibre volume fraction which again represented considerable variation. So this variation in mechanical properties is not unexpected in natural fibre composites.

Variability in properties of hemp fibres may be the dominant cause of variability in properties of the composites but it is not the only reason. Other reasons such as non-uniform fibre dispersion, local variations in fibre distribution, resin-rich areas, voids, etc. may also contribute, with varying degrees, to the variability in properties.

5.3.1.6 Comparison of theoretical and experimental tensile properties

Over the years a number of models have been developed to predict the theoretical mechanical properties of composites from the constituents' properties. These include the well-known rule of mixtures, the Series model [344], Hirsch model [345], and Halpin-Tsai model [346]. The variability in properties of natural fibres makes it very problematic to apply these models to natural fibre composites because these models assume uniform properties of fibres. Previous attempts at applying these models to predict the properties of natural fibre composites have generally not been very successful. Peponi et al [347] used the Halpin-Tsai model to predict the tensile properties of polypropylene composites reinforced with flax, jute, abaca and sisal fibres. In all four composites, the theoretical values were much higher than experimental values which were attributed to poor fibre/matrix interface which reduced the mechanical properties. In what follows, a model known as modified rule of mixtures has been applied to see if it can predict the tensile properties of hemp-polyester composites accurately.

The hemp fibres used in this research were discontinuous and randomly oriented in the plane of the mat. The composites made from such fibres have the inherent disadvantage of having lower mechanical properties than the properties of composites made from

long, continuous, and aligned fibres in the direction of the fibres. However aligned composites are inherently anisotropic, having maximum stiffness and strength in the direction of alignment and minimum strength in transverse direction to the fibres.

Composites made with randomly oriented fibres, on the other hand, are isotropic. They may have lower mechanical properties but their properties are the same in every direction of the composite. This property may have useful implications in various applications.

The tensile strength of unidirectional composites in the direction of the reinforcement is given by the well-known 'rule of mixtures' as:

$$\sigma_c = V_f \sigma_f + V_m \sigma_m \quad \text{.....(5.5)}$$

where V_f is the fibre volume fraction, σ_f is the tensile strength of the fibre, V_m is the matrix volume fraction, and σ_m is the tensile strength of the matrix.

However equation (5.5) represents an idealistic case and does not take into account imperfections originating in the fabrication stage. For fibres which have greater strain to failure than the matrix, like the one used in this research, the matrix is expected to break before the fibre and the whole load will be transferred to the fibres. Hence the ultimate strength of the composite will be determined by the strength of the fibres. In this case the rule of mixtures is modified to give the composite strength as:

$$\sigma_c = V_f \sigma_f \quad \text{.....(5.6)}$$

Similarly tensile modulus of unidirectional composites in the direction of reinforcement is given by:

$$E_c = V_f E_f + V_m E_m \quad \text{.....(5.7)}$$

where E_f is tensile modulus of the fibre and E_m is the tensile modulus of the matrix.

The tensile strength and tensile modulus values of polyester resin and hemp fibre were evaluated during this research. For polyester resin, these values were 44 MPa and 3.7 GPa respectively, whereas for hemp fibres, these values were 270 MPa and 9 GPa respectively.

For a typical fibre volume fraction of 50%, the tensile strength of hemp fibre reinforced polyester composites is given by:

$$\sigma_c = V_f \sigma_f = (0.5 \times 270) = 135 \text{ MPa}$$

This result assumes that the average tensile strength of hemp fibres used in a laminate is also 270 MPa. This is the theoretical maximum value of tensile strength of unidirectional composites in the direction of fibres. When the reinforcing fibres are discontinuous and randomly distributed, the strength and stiffness of the composite are considerably reduced. To represent this reduction, a factor K, called 'reinforcement efficiency', is used (sometimes also called Krenchel factor). The value of reinforcement efficiency is taken to be unity for an oriented fibre composite in the fibre direction, and zero perpendicular to it. For randomly oriented composites tested in the plane of the fibres, this value is approximately 3/8 the value for unidirectional composites [348].

The modified equation for tensile strength of the composite [15] will then be:

$$\sigma_c = K V_f \sigma_f \quad \text{.....(5.8)}$$

Using the value of 3/8 for reinforcement efficiency for randomly oriented hemp fibre reinforced polyester composites their tensile strength will be reduced to about 50 MPa, which is quite close to the experimental values. The modified rule of mixtures thus gives a reasonable estimate of the tensile strength of hemp-polyester composites.

The modified form of the equation for calculating the tensile modulus of randomly oriented composites is [348]:

$$E_c = KV_f E_f + (1- V_f) E_m \quad \text{.....(5.9)}$$

where K is the Krenchel factor. For a typical fibre volume fraction of 50% and using the value of 3/8 for K, the tensile modulus of the composites is given by:

$$E_c = 3/8 (0.5 \times 9) + (0.5 \times 3.7) \sim 3.5 \text{ GPa}$$

The theoretical value is considerably less than the experimental value of 7.2 GPa. The most probable reason for this is the considerably underestimated value of tensile modulus of hemp fibre because of compliance in the system during tensile testing of the

fibres. A value of hemp fibre modulus of 28.5 GPa will give a composites modulus value close to the experimental value. This value of hemp fibre modulus is closer to the values evaluated by other researchers as shown in Table 4.2. Considering this factor, the rule of mixtures seems to give a reasonable estimate of tensile modulus as well.

Crawford [349] has suggested another modified form of rule of mixtures for estimating the tensile modulus of composite containing randomly oriented short fibres as:

$$E_c = 3/8\ E_L + 5/8\ E_T \quad \text{.....(5.10)}$$

where E_L and E_T are the longitudinal and transverse moduli for aligned fibre composites. Since it was not possible to calculate these moduli experimentally for the composites used in this research, they were estimated by using the equations [349] below,

$$E_L = V_f E_f + V_m E_m \quad \text{.....(5.11)}$$

$$\text{and } E_T = \frac{E_f E_m}{V_f E_m + V_m E_f} \quad \text{.....(5.12)}$$

Using V_f value of 0.5 and hemp fibre modulus value of 9 GPa, the values of E_L and E_T come out to be 6.4 GPa and 5.2 GPa respectively. Using these values in equation (5.10), the value of tensile modulus comes out to be 5.7 GPa which is lower than the experimental value. Using a hemp fibre modulus value of 28.5 GPa, equation (5.10) gives an overestimated value of 10 GPa. In either case, equation (5.10) gives an incorrect estimate of tensile modulus of the composite.

It has been shown that application of modified rule of mixtures is not straightforward for natural fibre composites but it still gives a reasonable estimate of the tensile properties of the composites. There are number of sources of imperfections in natural fibre composites which also contribute to their mechanical properties being different form those predicted by the models.

5.3.1.7 Evaluating optimum fibre content

Section 5.3.1 has shown that increasing the fibre weight fraction results in a proportional increase in the tensile properties of these composites. However for any matrix/ fibre system, there is an optimum value of fibre content beyond which proper

wetting of fibres starts to suffer and it is difficult to get any further increase in the mechanical properties. In fact it is even possible to see some reduction in mechanical properties with the increase in fibre content beyond this optimum value. In order to evaluate the optimum hemp fibre content in these composites, composites were made at higher fibre weight fraction and its effect on their tensile properties was observed.

Various authors have reported a decrease in tensile properties of composites with increase in fibre fraction above a certain threshold value for synthetic fibre composites. In their studies on brittle matrix composites reinforced with glass fibres, Gaggar and Broutman [350] found that the maximum tensile strength occurred at a fibre volume fraction of approximately 50% beyond which there was slight decrease in strength.

Similar optimum fibre content has also been found to exist for natural fibre composites. For jute fibre reinforced polyester composites, Roe and Ansell [127] reported increase in tensile strength and modulus for fibre volume fraction of up to 60%. Further increase in volume fraction resulted in decrease in these properties which was attributed to insufficient wetting of fibres.

A recent study [351] has attributed fibre-fibre interactions as the major cause for decreasing composite strength at high levels of fibre loadings for natural fibre-thermoplastic composites. These fibre-fibre interactions decrease the available fibre stress transfer surface area. The effect was represented by a clustering parameter and a model developed to evaluate the parameter was found to be in general agreement with the experimental results.

In order to observe the effect of increasing fibre content on the tensile properties of hemp fibre composites, three different trial laminates were made and tested for tensile properties. First laminate was made by using four layers of hemp fibre mat rather than the two normally used. It was found that fibre weight fraction in this case was 64%. Second laminate was made at higher moulding pressure of 4 MPa. The fibre weight fraction of the composites thus made was 66%. Third laminate was made by using lower amount of the resin than normally used. The composites thus made had a fibre weight fraction of 66%.

A comparison of tensile properties of standard composites, made at moulding pressure of 3 MPa, with higher fibre content composites is shown in Fig. 5.10. The figure shows

that no improvement in tensile properties was gained by increasing the fibre content beyond that used in standard method of 3MPa pressure. The samples with low resin were found to have poor adhesion even by looking with a naked eye. They are also shown in SEM micrographs in Fig. 5.11 which show relatively lower amount of resin sticking to the fibres, indicating poor interfacial adhesion. These studies have thus shown that increasing fibre weight fraction beyond a certain limit does not necessarily result in increase in tensile properties of the composites. Instead it can sometimes result in degradation in these properties. For hemp fibre composites, the optimum fibre weight fraction was found to be in the range of 50-55% and all the laminates were made with this fibre weight fraction.

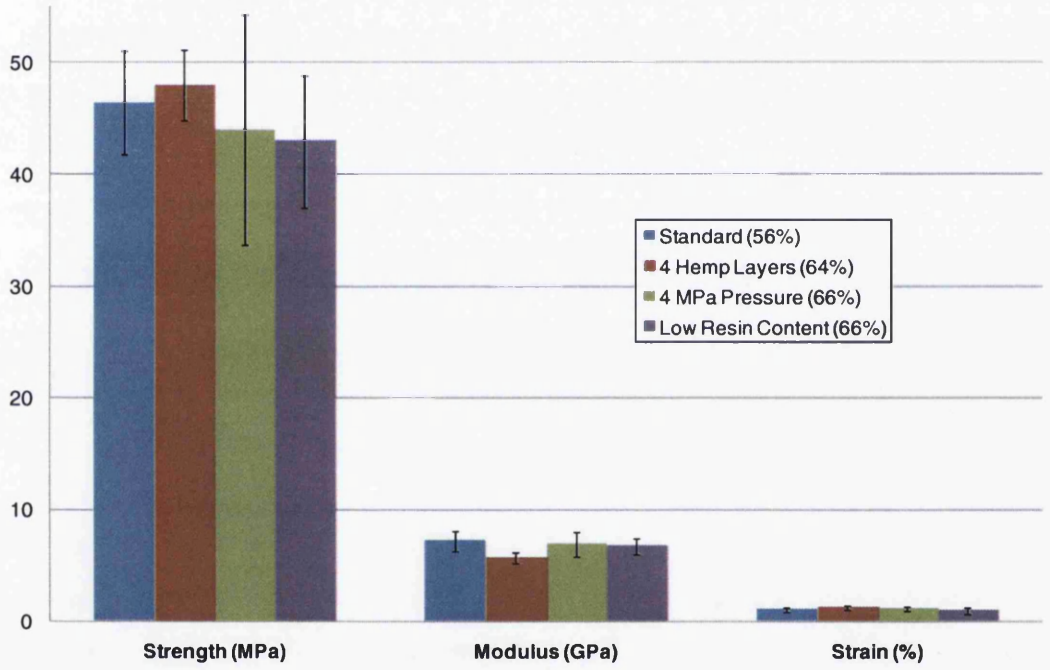

Fig. 5.10: Comparison of tensile properties of standard composites with higher fibre content composites (fibre weight fraction values in parentheses)

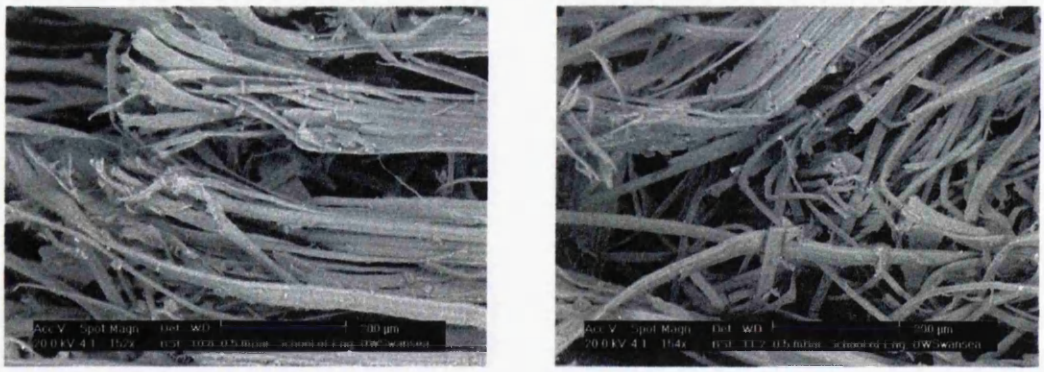

Fig. 5.11: Fracture surfaces of tensile tested samples with low resin content

5.3.2 CSM Glass Fibre Reinforced Polyester Composites

The tensile properties of CSM glass fibre reinforced polyester composite, made at various fibre weight fractions as described in Section 5.1.2, are shown in Table 5.6. These are the mean values of at least five samples tested from each laminate. The values in the brackets are standard deviations.

Table 5.6: Tensile properties of glass fibre reinforced polyester composites

Fibre weight fraction (%)	Tensile Strength (MPa)	Tensile Modulus (GPa)	Strain to Failure (%)
46	165. 0 (12.9)	11.2 (2.0)	2.04 (0.28)
53	200.9 (6.3)	11.3 (0.6)	2.39 (0.30)
55	230.5 (1.3)	12.3 (0.9)	2.50 (0.30)

The tensile strength is seen to increase approximately linearly with increase in fibre weight fraction. The tensile strength is thus seen to be a predominantly fibre dependent property. Unlike hemp fibre composite however, there is only slight increase in tensile modulus with increase in fibre weight fraction. Only 10% increase in tensile modulus was observed for almost 20% increase in fibre weight fraction. Tensile modulus is thus much less dependent on the fibre content.

The strain to failure also increased approximately linearly with increase in fibre volume fraction. The low strain to failure at low fibre fraction for CSM composites are attributed to local strains near weak regions which are higher than the average specimen strain [352]. The composites with 55% fibre weight fraction had the highest strain to failure value of 2.5% which is very close to strain to failure value of 2.6% for glass fibres. This is consistent with the observation of Mandell [352] that the tensile strain to failure for chopped strand materials approaches the strain necessary for fibre-reinforced behaviour (fibre failure). The consistent failure strain in the range 2-2.5% seems to indicate that ultimate failure occurs when fibres fail.

The tensile properties of these composites have been found to be comparable to that of 0/90° glass fibre reinforced polyester composites. At fibre weight fraction of 45.5%, the values reported were [262]: tensile strength: 200.0 MPa, tensile modulus 11.3 GPa, strain to failure: 2%. This seems to suggest that the properties of randomly oriented short fibre composites are similar to cross-ply long fibre laminates with half of the fibres in the loading direction and half of them perpendicular to loading direction.

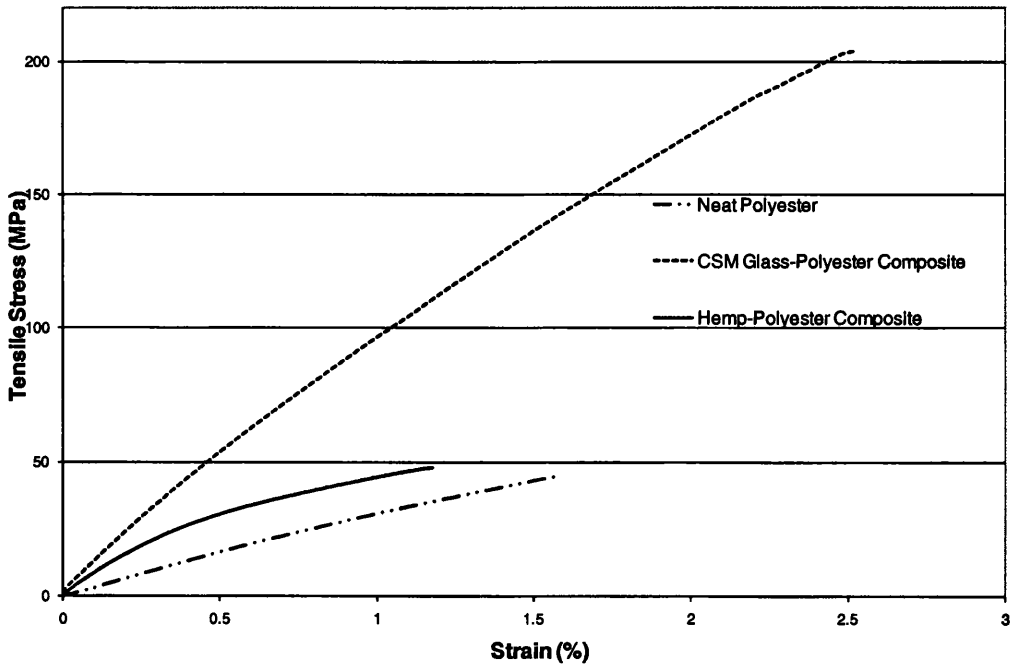

Fig. 5.12: Comparison of stress-strain curves of CSM glass fibre composites with neat polyester resin and hemp-polyester composite

The tensile stress-strain curve of CSM glass fibre composite compared with those of neat polyester resin and hemp-polyester composite is shown in Fig. 5.12. The tensile stress-strain curve of glass-polyester composites has less a discernable "knee" compared to hemp-polyester composites, indicating a more efficient transfer of stress from matrix to fibres. Significantly greater area under the stress-strain curve for glass fibre composites compared to hemp fibre composites also suggests greater impact resistance of the former, a fact verified in actual testing as shown later in Section 5.4.2.

(a) **(b)** **(c)**

Fig. 5.13: Comparison of glass fibre/polyester samples surfaces in tensile testing; (a) no stress (b) stress=113 MPa, strain=1.3% (c) stress=165 MPa, strain=2%

In almost all the glass-polyester samples, there was an audible sound at a stress level of about half of the ultimate tensile strength. The testing of a sample was stopped at this point and its surface was examined. As shown in Fig. 5.13 (b), there was some evidence of matrix cracking and debonding, which resulted in the sample becoming whiter than untested sample, which were responsible for this sound. Further application of stress resulted in further debonding, matrix cracking and fibre fracture as shown in Fig. 5.13 (c) which shows the surface of sample tested at a stress of up to 80% of UTS and strain of up to 2%. The eventual fracture of the samples was brittle and catastrophic.

Fig. 5.14 shows the fracture surface of a tensile tested sample. Compared to the fracture surface of hemp/polyester sample in tensile testing (Fig. 5.5), this fracture surface shows a more violent fracture of glass/polyester samples with considerable evidence of matrix and fibre fracture. The whitening of the sample in and around the fracture zone also indicates considerable delamination/debonding to have taken place before the eventual fracture.

Fig. 5.14: Fracture surface of tensile tested CSM glass-polyester sample

5.3.3 Hemp-CSM Glass Fibre Reinforced Polyester Hybrid Composites

The tensile properties of hemp-CSM glass hybrid fibre reinforced polyester composites are shown in Table 5.7. Two different kinds of fibre configurations were used: hemp skin and glass core, and glass skin and hemp core. Both kinds of configurations represented replacement of about 11% of hemp fibres with glass fibres. Both kinds of configurations showed considerable improvement in the tensile properties of the composites. The tensile properties were seen to be dominated by the fibres which formed the skin of hybrid. The greater strain to failure of glass fibres is more dominant in glass skin composites, hence resulting in more increase in strain to failure and less increase in tensile modulus than hemp skin composites. The hybridisation of a low strain-to-failure fibre with a high strain-to-failure fibres results in enhanced failure strain of the composites. This phenomenon is called the hybrid effect and has been observed for many hybrid composites [37]. The increase in strain to failure of hemp-glass composites can also be attributed to this effect.

Table 5.7: Tensile properties of hemp-CSM glass fibre hybrid composites

Fibre Configuration	Hemp vol. fraction (%)	Glass vol. fraction (%)	Tensile strength (MPa)	Tensile modulus (GPa)	Strain to failure (%)
Hemp only	**51.4**	**-**	**46.4 (4.6)**	**7.2 (0.9)**	**1.03 (0.19)**
Hemp skin, glass core	**35.4**	**10.9**	**70.1 (10.2)**	**8.3 (0.4)**	**1.31 (0.25)**
Glass skin, hemp core	**36.5**	**11.3**	**81.6 (3.7)**	**7.7 (0.3)**	**1.73 (0.08)**

The hybrid effect is quantified as being the percentage increase in the primary failure strain [37]. The hybrid effect has been calculated for many composite systems and its values range from 0% to 100%. The values for hybrid effect in this research were found to be 27% for hemp skin-glass core configuration and 68% for glass skin-hemp core configuration. Hence glass skin-hemp core configuration has been found to be more efficient way of hybridisation in this research.

For hemp skin-glass core composites, the tensile strength is increased by almost 70%, and tensile modulus is increased by about 15%. For glass skin, hemp core composites, the tensile strength is increased by about 75% and tensile modulus is increased by about 7%. Hence in both cases, greater increase in tensile strength was observed than tensile modulus. This is not unexpected considering that the greater strain to failure of glass fibre compared to hemp fibres increased the strain to failure of the composites, thus resulting in negligible increase in tensile modulus. This is also shown in the comparison of stress-strain curves in Fig. 5.15. It is also seen that the 'knee' of the curve for hybrid composites is less prominent than for hemp composites, indicating an improved shifting of stress to fibres because of the presence of glass fibres. The increase in area under the stress-strain curve for hybrid composites compared to hemp fibre composites also suggests that improvement in impact resistance of the former can be expected. This was verified in actual impact testing as shown later in Section 5.4.3.

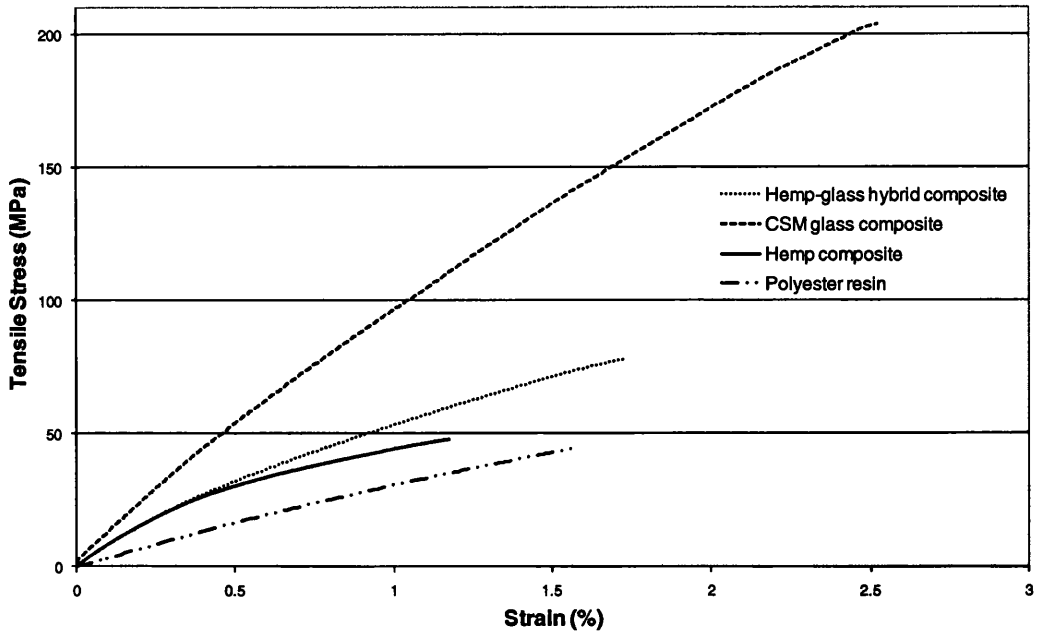

Fig. 5.15: Comparison of stress-strain graphs of composites

Considerable research has shown the positive effects of hybridisation on mechanical properties of natural fibre composites. Examples are coir-glass/polyester [165], sisal-glass/polyester [353], hemp-glass/polypropylene [164], and bamboo-glass/polypropylene [105] composites.

Similar to the fracture of hemp fibre composites, the hybrid samples fractured in a plane perpendicular to the load direction in a brittle manner, as shown in Fig. 5.16. There was no complete separation of the samples as for hemp composites. The hemp fibres were seen to break but the glass fibres were still not separated and it was visible for the samples that had hemp fibres as skin. For samples that had glass fibres as skin, although it was less apparent, it was possible to see separated hemp fibres.

Fig. 5.16: Fracture samples of tensile tested hybrid composites: glass skin-hemp core (top), and hemp skin-glass core (bottom)

5.3.4 Comparison of Specific Tensile Properties

The tensile testing so far has shown that hemp fibre composites do not have comparable strength and stiffness to glass fibre composites at similar fibre weight fraction. However a more realistic comparison can be done by comparing the specific strength and specific stiffness properties of composites. These properties were obtained by dividing the actual strength and stiffness of composites by their densities. The mean density of hemp fibre composites was found to be 1.18±0.03 g/cm^3 at a fibre volume fraction of 50%. Glass fibre composites at a fibre volume fraction of 40% had mean density of 1.61±0.05 g/cm^3. Thus the lower density of hemp fibre composites can counterbalance their lower tensile properties. Table 5.8 shows the comparison of specific tensile properties of hemp, glass and hybrid composites.

Glass fibre composites at 30% fibre volume fraction have greater specific strength and stiffness than hemp fibre composites at 50% fibre volume fraction. Increasing the fibre content up to 40% increases the specific strength but no appreciable increase in specific modulus is observed. Similarly, for glass-hemp hybrid composites, replacing 11% of hemp fibre by glass fibres results in up to 50% increase in specific strength but only marginal increase in specific modulus. Therefore in terms of specific tensile properties, hemp fibre composites do not have comparable properties to glass fibre composites. At low glass fibre content, only the specific modulus of hybrid composites is comparable to hemp fibre composites.

Table 5.8: Comparison of specific tensile properties of composites

Fibre	FVF (%)	Specific Strength [MPa/(Mg/m^3)]	Specific Modulus [GPa/(Mg/m^3)]
Hemp	50	38.1 (4.9)	5.8 (0.6)
Glass	30	108.1 (6.8)	7.4 (1.4)
	33	131.1 (3.8)	7.4 (0.4)
	40	141.2 (2.2)	7.7 (0.4)
Hemp skin-Glass core	46.3 (35.4:10.9)	51.8 (6.8)	6.2 (0.3)
Glass skin-Hemp core	47.8 (36.5:11.3)	61.3 (3.1)	5.8 (0.2)

5.4 LOW VELOCITY IMPACT PROPERTIES

5.4.1 Hemp Fibre Reinforced Polyester Composites

The next phase of this research was focused on investigating the low velocity impact properties of the composites. The non-instrumented impact testing rig used had some obvious limitations. For example, it was not possible to evaluate the energy absorbed by the samples during impact testing. However the testing was still useful in determining the damage tolerance of the materials by evaluating residual tensile and fatigue properties of the composites after impact testing. The data thus obtained is very useful for design and service life requirements of the composites.

5.4.1.1 Izod impact strength

Izod impact strength of un-notched and notched hemp-polyester composites is given in Table 5.9. The samples used in these tests had mean fibre weight fraction of 56% (fibre volume fraction ~ 50%). At least 20 samples were used for each test. The values in brackets are standard deviation figures.

Table 5.9: Izod impact strength of hemp-polyester composites

Mean impact strength of un-notched samples	**(kJ/m^2)**	**17.1 (7.9)**
Mean impact strength of notched samples	**(kJ/m^2)**	**12.7 (2.8)**

Izod impact strength of un-notched samples is higher than that for notched samples since testing with un-notched samples gives an overestimated value of the impact strength. It takes into account the energies required for both initiation and propagation of cracks. Still the values of notched samples are within the standard deviation of the values for un-notched composites. The scatter in the values for notched samples is considerably reduced which can be attributed to the fact that the notch provides a path for the crack to propagate and no energy is required for initiation of the crack.

Comparing with the results available for hemp fibre reinforced polyester composites in the literature, the unnotched impact strength is similar to the value reported by Sebe et al. [124] which is 14 kJ/m^2 at 36% fibre weight fraction. For notched composites, the value is considerably higher than that reported by Rouison et al. [146] of 4.8 kJ/m^2. Their figure is probably lower because of lower fibre volume fraction of 20% of the samples tested. The typical impact strength of neat polyester resin is 2 kJ/m^2 [349]. For CSM glass fibre/ polyester composites, the impact strength is in the range of 100-150 kJ/m^2, the same as for woven roving laminates [349]. Although reinforcing polyester resin with hemp fibres increase their impact strength considerably, the hemp fibre composites have significantly lower impact strength than glass fibre composites.

The impact strength of most natural fibre reinforced polyester composites is quite low compared to glass fibre-polyester composites. A quick glance at Table 2.18 shows that most natural fibre/polyester composites have impact strength in the range 10-30 kJ/m^2.

5.4.1.2 Residual tensile properties

The low velocity impact testing of hemp fibre composites was carried out by using the purpose-built impact testing rig. In this testing it was vitally important to get the impact in the middle of the samples. Problems were encountered in initial stages in getting the

impact point in the middle of the samples. The problem was resolved by using a plumb line device to make the impactor centre coincident with the centre of the samples. All the samples were impacted from a height of about 100 mm so that the impact velocity of all the samples was constant at about 1.4 m/s, well within the range of low velocity impact. Keeping the height constant, the weight of the impactor was varied to get the required impact energy level.

The lowest impact energy level used was 1J and it was gradually increased in increments of 0.5J up to 4J at which point the impactor almost penetrated the samples. All the samples used in low velocity impact testing had an average fibre weight fraction of 55% (fibre volume fraction~50%). The results of tensile tests following the low velocity impact of composites are given in Table 5.10. For comparison the tensile properties of non-impacted composites are also given. The standard deviation figures are in parentheses.

Table 5.10: Residual tensile properties of impact tested composites

Energy Level (J)	Tensile Strength (MPa)	Tensile Stiffness (GPa)	Strain to Failure (%)
0	46.4 (4.6)	7.2 (0.9)	1.03 (0.19)
1	46.0 (5.3)	6.0 (0.9)	1.34 (0.10)
1.5	35.0 (6.1)	4.7 (0.6)	1.23 (0.23)
2	26.2 (5.4)	4.0 (1.4)	1.09 (0.26)
2.5	26.6 (11.5)	4.1 (1.5)	1.24 (0.62)
3	22.7 (1.8)	3.2 (0.5)	0.96 (0.10)
3.5	21.2 (3.6)	3.3 (0.4)	0.93 (0.26)
4	15.2 (2.9)	2.1 (0.3)	1.08 (0.20)

The effect of low velocity impact on the tensile strength of the composites is shown in Fig 5.17. The error bars represent standard deviation results. The figure shows gradual decline in tensile strength of hemp fibre composites with increase in energy level of impact. The effect is negligible up to impact energy of 1 J. However the decline is

much rapid from 1 J up to impact energy of 4. The composites have lost almost 70% of their intrinsic tensile strength after an impact energy of 4 J.

Agarwal and Broutman [22] have shown that there is a threshold impact energy for most composite materials below which they do not show any appreciable reduction in mechanical properties. The value of this energy depends on laminate thickness and matrix and fibre materials. For hemp fibre reinforced polyester composites the value of this threshold energy is seen to be 1J at which they do not show any deterioration in tensile strength. At impact energies higher than 1J, these composites show rapid decline in their tensile strength.

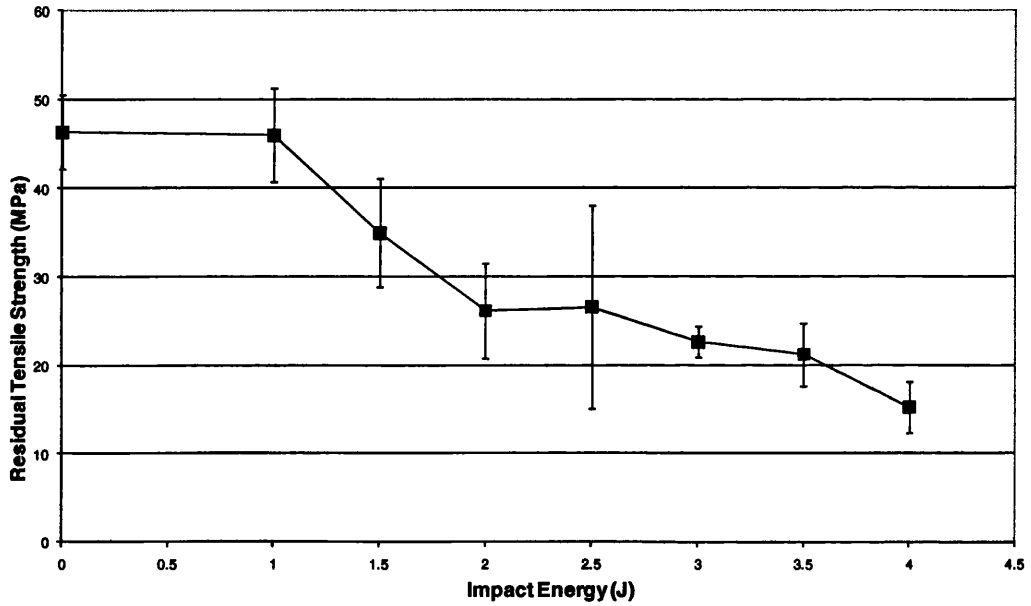

Fig 5.17: Residual tensile strength of composites following low velocity impact

The impact damage tolerance of hemp-polyester composites can be best understood by decline in normalised tensile strength with increasing impact energy as shown in Fig. 5.18. The normalised strength was obtained by dividing actual mean value of strength at particular impact energy by intrinsic tensile strength of the composites. The dashed lines in the figure represent 95% confidence limits of the linear regression line. The figure shows that the composites have lost almost half of their intrinsic strength following impact energy of 3J. Following impact energy of 4J, the composites have lost almost 70% of their intrinsic strength.

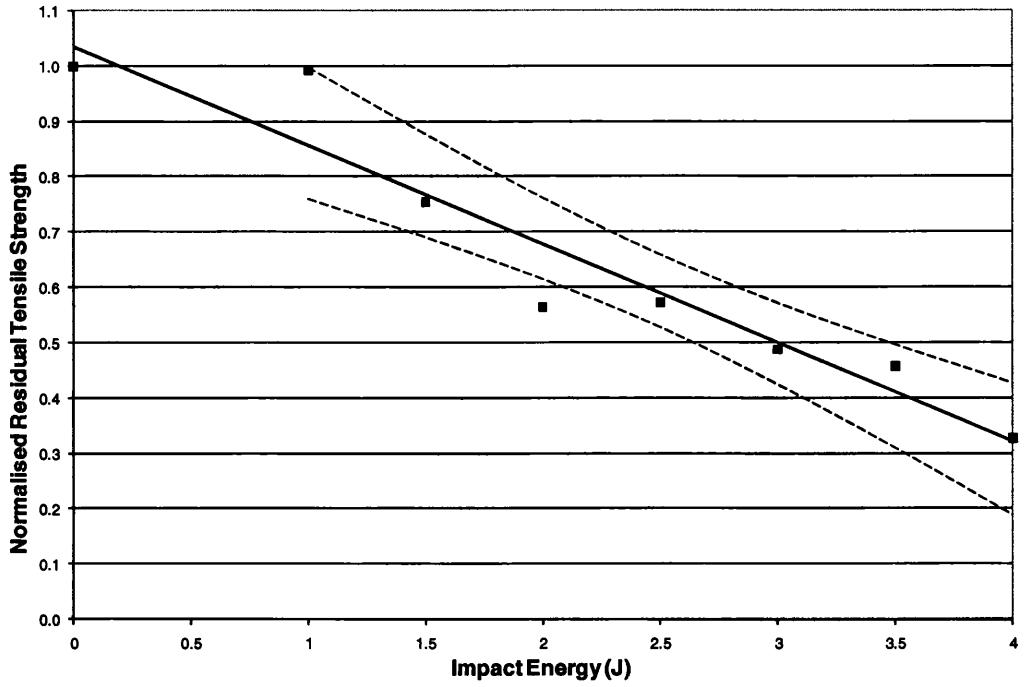

Fig. 5.18: Normalised residual tensile strength of composites following low velocity impact

The effect of low velocity impact on tensile stiffness of hemp fibre composites is shown in Fig 5.19. The term stiffness rather than modulus is used here because what is being measured is the average value of modulus across the impact area. Again the tensile stiffness declines gradually with increase in impact energy level. Following impact energy of 4 J, hemp fibre composites have lost almost 70% of their intrinsic tensile modulus. The damage tolerance of hemp-polyester composites in terms of normalised residual tensile stiffness is shown in Fig. 5.20. The normalised residual tensile stiffness was obtained by dividing actual mean value of residual stiffness at particular impact energy with the intrinsic tensile stiffness of the composites. The dashed lines in the figure represent 95% confidence limits of the linear regression line. The figure shows that composites lose almost 20% of their intrinsic stiffness even at an impact energy of 1J. Further application of impact energy results in a gradual decline of tensile stiffness and at impact energy of 4J, the composites have lost almost 70% of their intrinsic stiffness.

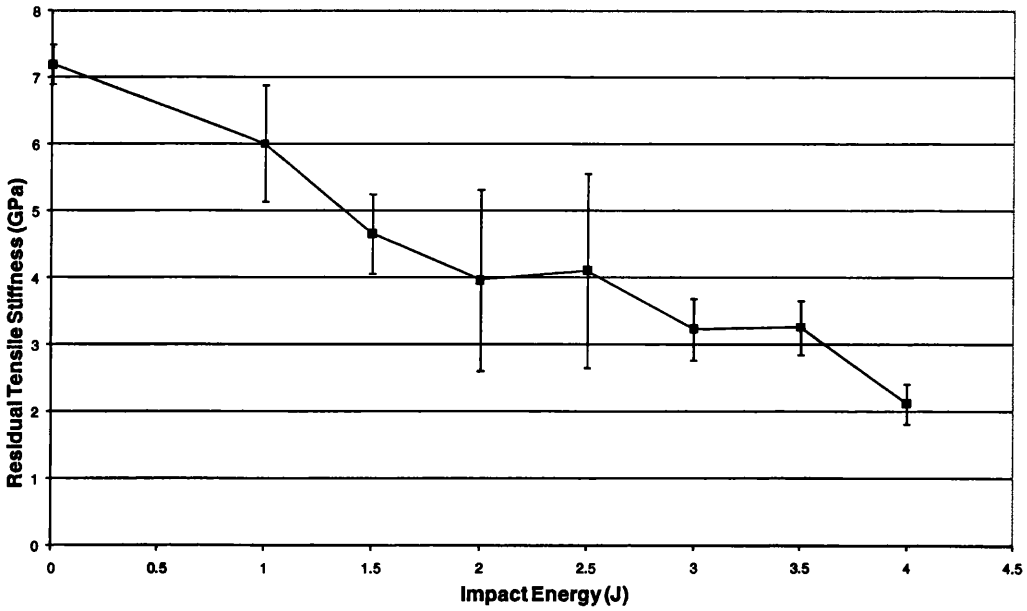

Fig 5.19: Residual tensile stiffness of composites following low velocity impact

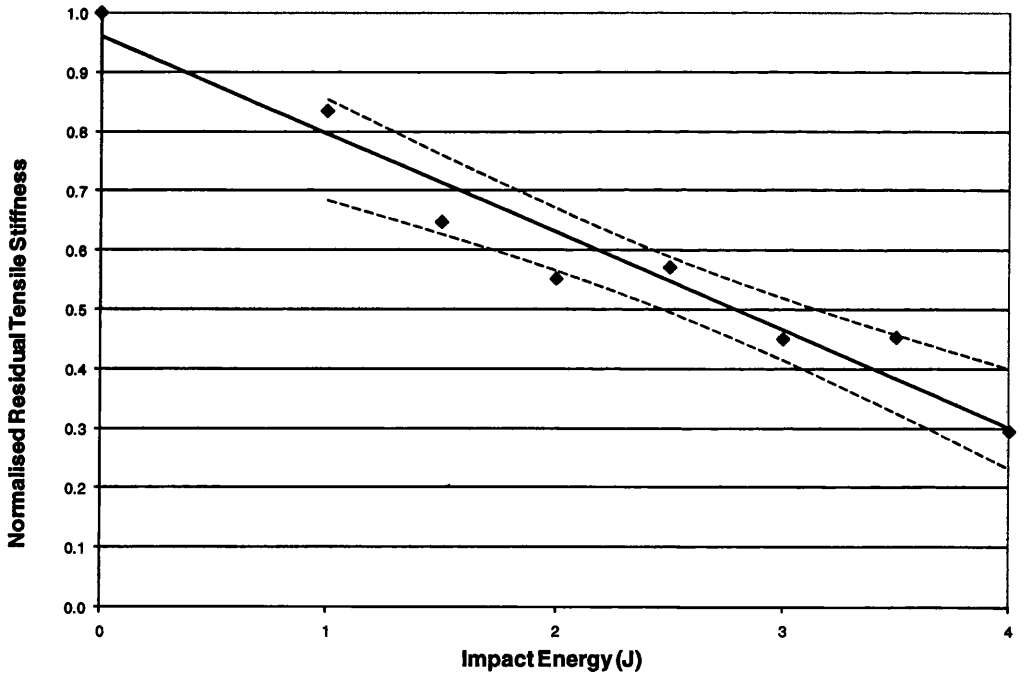

Fig. 5.20: Normalised residual tensile stiffness of the composites following low velocity impact

The effect of increasing impact energy on strain to failure is shown in Fig 5.21. The strain to failure first appears to increase following impact energy of 1J. However

increasing the impact energy does not affect the strain to failure which remains consistent at a value of about 1%. This implies that the impact did not change the fracture behaviour of composites which continued to be brittle.

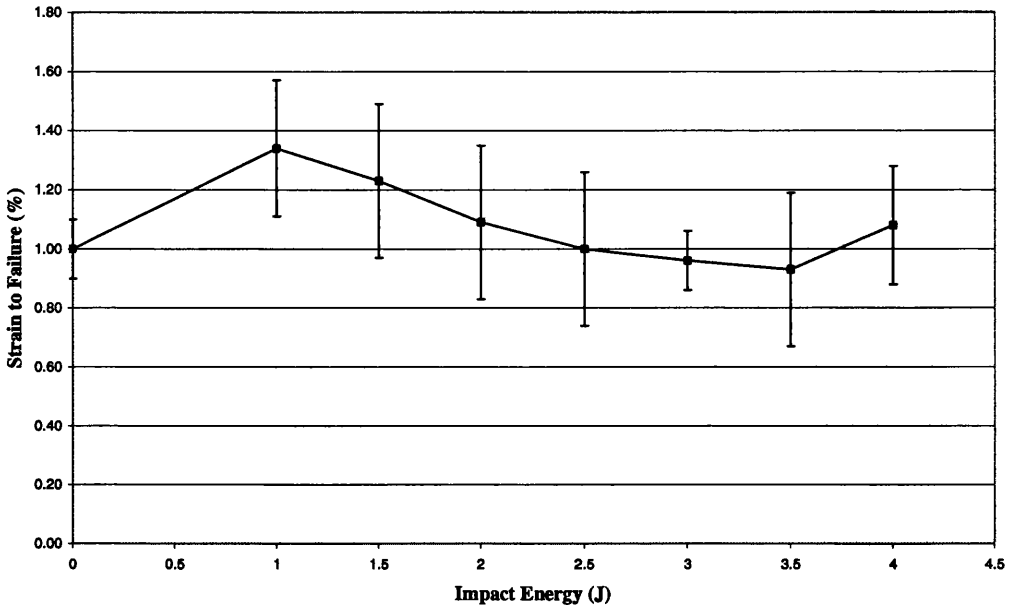

Fig. 5.21: Effect of low-velocity impact on strain to failure of composites

5.4.1.3 Analysis of impact properties

Figs. 5.22-23 show macrographs of the fracture surfaces of impact tested samples. It is evident that impact damage is localised. At an impact energy of 1J, the indentation point is barely visible. At this impact energy level, the coupons have lost only about 1% of their intrinsic tensile strength and almost 17% of their tensile stiffness. However from impact level of 2 J upwards, the indentation point and the damage it creates are clearly visible. At an impact energy of 2J, a crack is seen to be running across the sample as shown by the arrowhead which implies that considerable matrix cracking, interfacial debonding and fibre fracture has occurred. At this energy level, the coupons have lost almost 50% of their intrinsic strength and stiffness. Closer examination by SEM showed considerable evidence of matrix fracture, interfacial debonding and fibre fracture at this energy level as shown in Fig. 5.24. The fibre fracture at this low energy level seems to be the main reason for the poor impact damage tolerance of these composites.

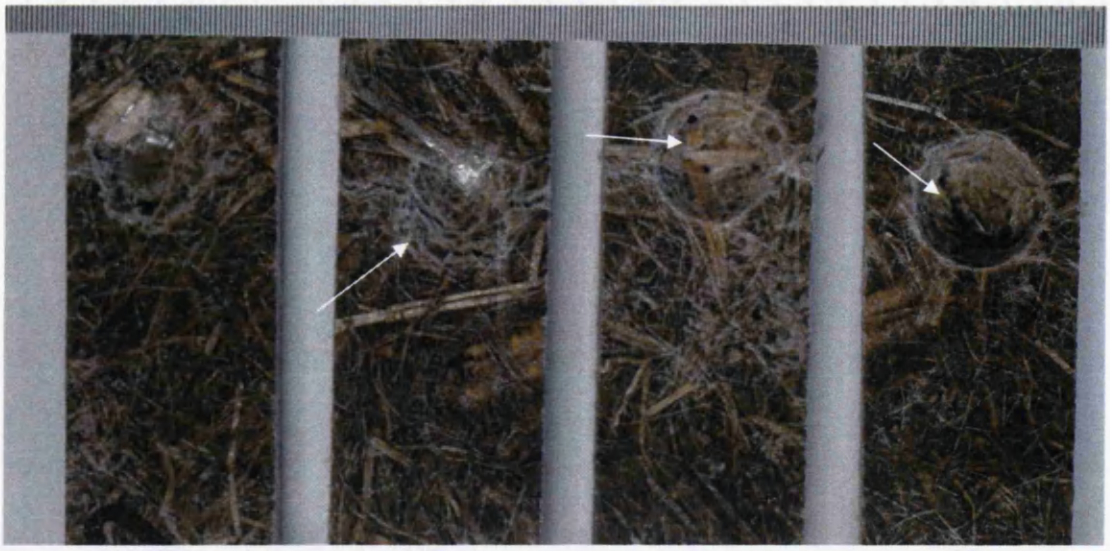

Fig 5.22: The effect of increasing impact energy level, from left to right, on the impacted faces of the samples

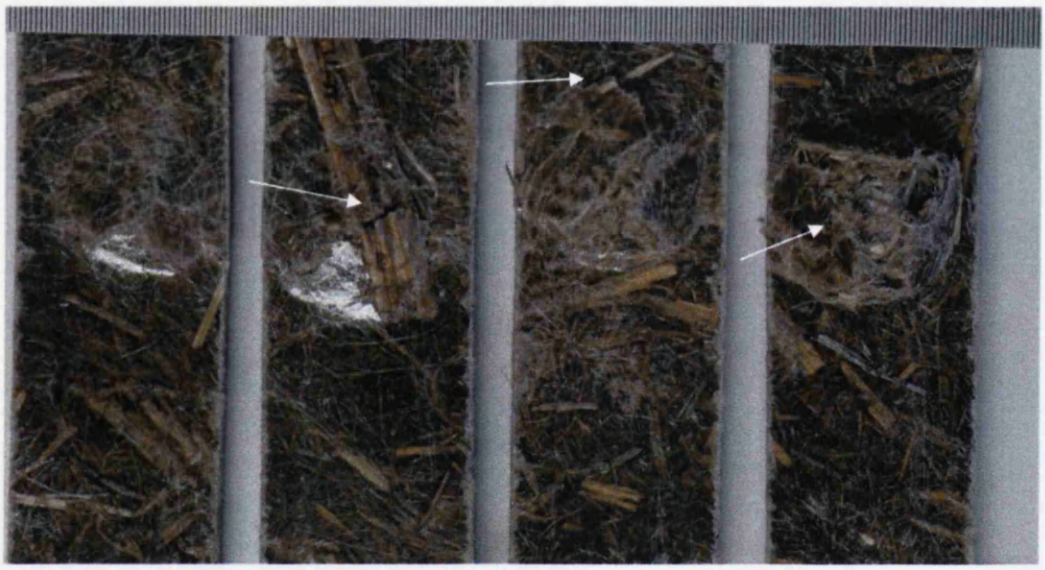

Fig 5.23: The effect of increasing impact energy, from left to right, on the distal faces of the samples

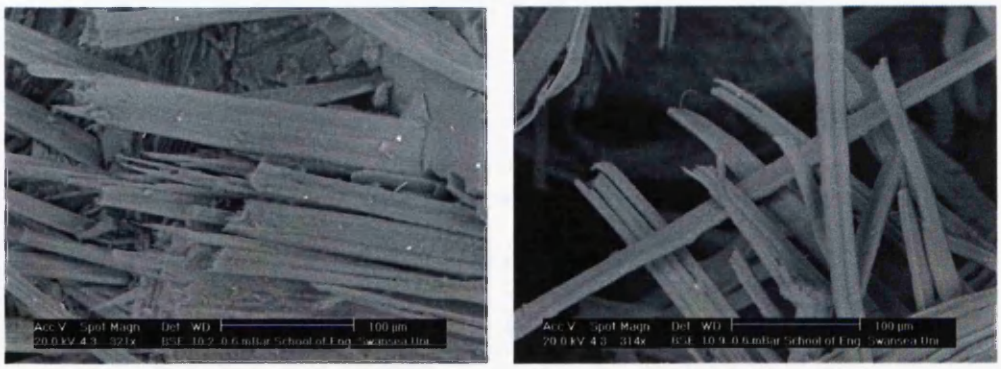

(a) (b)

(c)

Fig. 5.24: SEM micrographs of fracture surface of 2J impacted sample showing evidence of fibre fracture (a) and (b), and matrix fracture and interfacial debonding (c)

The penetration of the impactor into the sample increases with increase in impact energy. At impact energy of 3J, the impactor starts to perforate some coupons, shown by the arrowhead in Fig. 5.23. For impact energy of 4J and above, the samples are in a state of almost complete perforation, again shown by the arrowhead. At this stage, coupons have lost almost 70% of their intrinsic strength and stiffness.

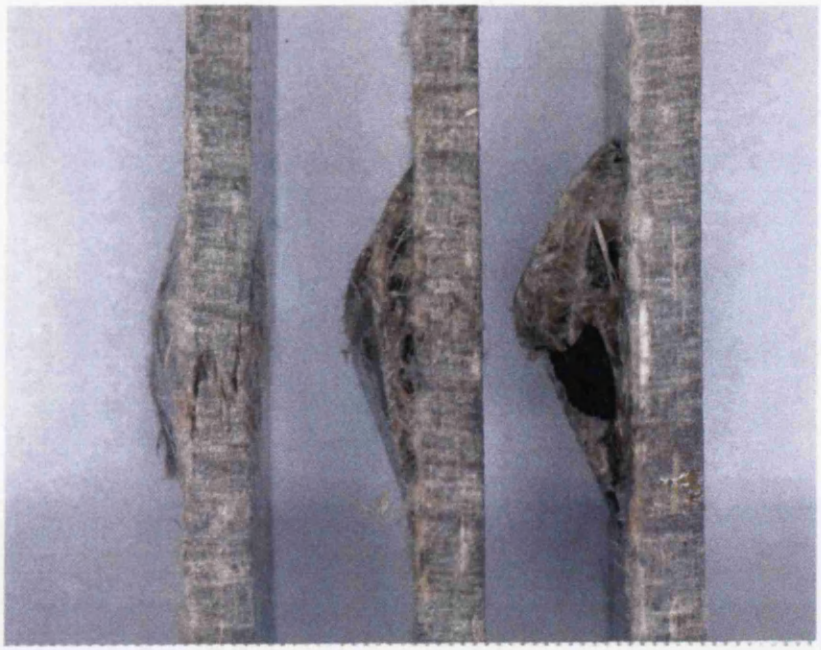

2J **3J** **4J**

Fig. 5.25: Out of plane deformation of hemp/polyester impact tested samples

Fig. 5.25 shows the out-of-plane deformation of impact tested samples with increasing impact energy. It can be seen that the damage increases through the thickness away from the impacted face towards the distal face with increase in the diameter of the crater produced by the damage. The diameter of impact crater was 12.5 mm on the front face, the same as the diameter of the impactor. However on the distal side of coupons, the easily visible damage was about 15 mm for non-perforated coupons and about 18 mm for perforated coupons. An impact energy of 2J is enough to induce cracks in the sample, while at 4J impact, the samples is in the state of almost complete perforation.

Comparison of stress-strain curves of impact tested samples is shown in Fig. 5.26. A relatively similar shape of impact tested samples as that for non-impacted samples shows that the damage development mechanisms during tensile loading are the same for both kinds of samples. The 'knee' of the curves for 3J and 4J impacted sample has become smoother, suggesting a less efficient transfer of stress from matrix to fibres because of the damage to fibres.

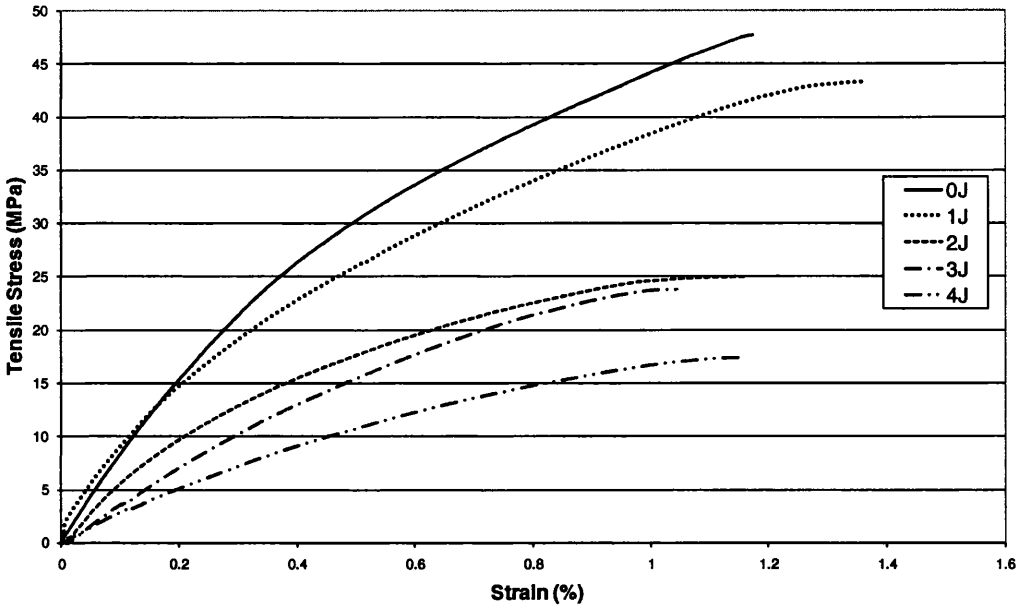

Fig. 5.26: Comparison of stress-strain curves of impact-tested samples

The impact properties of hemp-polyester composites can be understood in terms of the properties of the constituents and various energy absorbing mechanisms.

Brittle nature of hemp and polyester resin:

Perhaps the most important factor in low impact properties of these composites is the brittle nature of both hemp fibres and polyester resin. The strain energy absorbing capacity of the fibres is one of the most important parameters in determining the impact resistance of composites [197]. Thus the composites made from them are also brittle and have low strain to failure of about 1%. This means that they have little capacity to absorb any impact energy through ductile deformation. Even the composites impacted at 4J showed completely brittle fracture in tensile testing. Hence the only mechanism through which these materials can absorb energy is by initiation and propagation of cracks which depends on the toughness of the material. Hughes et al [130] evaluated the fracture toughness of hemp fibre reinforced polyester composites to be 3.51 $MNm^{-3/2}$ at fibre volume fraction of 20%. This was almost three times lower than that of CSM glass fibre-polyester composites (9.01 $MNm^{-3/2}$) at the same fibre volume fraction. The critical strain energy release rate and the crack tip plastic zone radii of hemp fibre composites were also significantly lower than those of CSM glass fibre composites,

implying lower toughness properties of these composites. It was suggested that energy dissipative processes are not stimulated in the crack tip region to the same extent as in glass fibre composites. As shown in Figs. 5.19-21, an impact of 2J energy is enough to initiate and propagate cracks through the materials.

Poor interfacial bonding:

It has been shown for polyester laminates [22] that their total impact resistance can be increased by reducing the fibre/matrix interfacial bonding. The interfacial shear strength of hemp-polyester was found to be 1.9±1.3 MPa in this research. This relatively low value of IFSS would seem to contribute to increased impact resistance. However any positive contribution of low interfacial strength on increased impact resistance seems to have been overridden by low toughness properties of these materials.

Imperfections in laminates:

The contribution of various imperfections introduced during the manufacture of laminates to low impact properties can not be underestimated. It has been shown in Section 5.2 that the laminates contained as much as 11% of voids by weight. Like other mechanical properties, this high void content is expected to have deleterious effect on impact properties as they can act as initiators of cracks, thus reducing the impact resistance of composites.

Energy absorbing mechanisms:

Having determined the low energy absorbing capacity of the composites, the various mechanisms responsible for this energy absorption are now analysed. Various mechanisms involved during crack propagation account for the total energy absorbed in the fracture process. For hemp-polyester composites, the fracture processes are a combination of matrix failure, fibre-matrix debonding, fibre pull-out and fibre fracture, as shown in Fig. 5.9. The effect of these mechanisms on energy absorption is now evaluated.

The contribution of fracture of brittle polyester resin towards total energy absorption will be minimal as explained earlier. The energy required for matrix fracture per unit area of composites is proportional to the work done in deforming the matrix to rupture per unit volume [22]. Since the value of the latter is very small for brittle polyester

matrix, the energy required for matrix fracture is expected to be only a small fraction of total impact energy of these composites.

Fibre/matrix debonding occurs by cracks running parallel to fibres. The relatively poor fibre/matrix interfacial bonding of the composites in this research suggests that most of the impact energy absorbed will be through this mechanism although it is difficult to quantify the proportion of it to the total impact energy. Closely related to debonding cracks are the delamination cracks. These cracks occur due to bending stiffness mismatch in a laminate containing plies of different fibre orientation. Since the composites made in this research contained plies of fibres in same random orientation, the contribution of delamination cracks to total energy absorbed is expected to be minimal, if at all.

Fibre pull-out is another mechanism that occurs because of poor interfacial bonding and contributes considerably to total energy absorption in short fibre composites and their existence has been shown in Fig. 5.9. The fibre pull-out has been found to be extensive for fibres whose length is less than half of the critical fibre length [22] which encourages fibre pull-out rather than fibre fracture to occur. The hemp fibre mat used in these composites is expected to contain a fair share of short fibres of length less than the critical length and hence they can also contribute to total energy absorption.

Fibre fracture contributes to the energy absorption depending on tensile strength and failure strain of the fibres. Hemp fibres were found to have a failure strain of 2.3% in this research, including the compliance in the machine which overestimated the strain. As shown in Fig. 5.24, an impact energy level of as low as 2J was enough to cause fibre fracture which resulted in almost half the reduction in tensile strength of composites. Fibre fracture occurs much later in the fracture process on the non-impacted face due to high bending stresses. Although it has been suggested that fracture of natural fibres involves considerable plastic deformation, hence making significant contribution to total fracture energy, no such evidence of plastic deformation was found in the tensile testing of hemp fibres in the present research.

Another possible reason for poor impact properties of hemp fibre composites is the non-woven random orientation of hemp fibres used in this research. Santulli [131] studied post-impact tensile and flexural properties of woven 0/90 jute fibre reinforced polyester composites with fibre volume fraction of 63%. The laminates impacted at an impact

energy of 5J suffered a loss of 40% in tensile strength but no reduction in tensile modulus was seen. Increasing the impact energy to 15J, no further degradation of tensile properties was observed. Acoustic emission monitoring of impact tested samples was not found to be helpful in quantifying the level of damage. Thus use of woven natural fibres as reinforcement can result in much improved impact properties of composites.

The composites tested for low-velocity impact in this research showed low impact damage tolerance. This seems to suggest that these composites are not suitable for applications where high impact strength of the material is required. In this respect the contention of Hughes et al [130] seems to carry weight in their observation that poor impact properties of natural fibre composites are a significant impediment that will hinder the commercial exploitation of theses composites.

5.4.2 CSM Glass Fibre Reinforced Polyester Composites

Low velocity impact properties of chopped strand mat glass fibre reinforced polyester composites were studied by using the same testing parameters as for hemp fibre composites. Low velocity impact tests were carried out for impact energy of up to 25J.

5.4.2.1 Residual tensile properties

The effect of low velocity impact on the tensile strength of the composites is shown in Fig. 5.27. The graph shows that the decline in tensile strength is gradual with increasing impact energy. After an impact energy of 20J, the graph shows a plateau which suggests that most of the impact damage has occurred by this stage. The graph shows that the composites lost almost half of their intrinsic tensile strength at impact energy of 15J and almost 75% of their intrinsic strength at impact energy of 25J. In similar studies of glass fibre-polyester composites [262], the reduction in intrinsic tensile strength at impact energy of 25J was 90% for ±45° configuration and 55% for 0/90° configuration. Thus although 0/90° glass-polyester composites have similar intrinsic tensile strength as CSM glass-polyester composites, they exhibit superior impact damage tolerance.

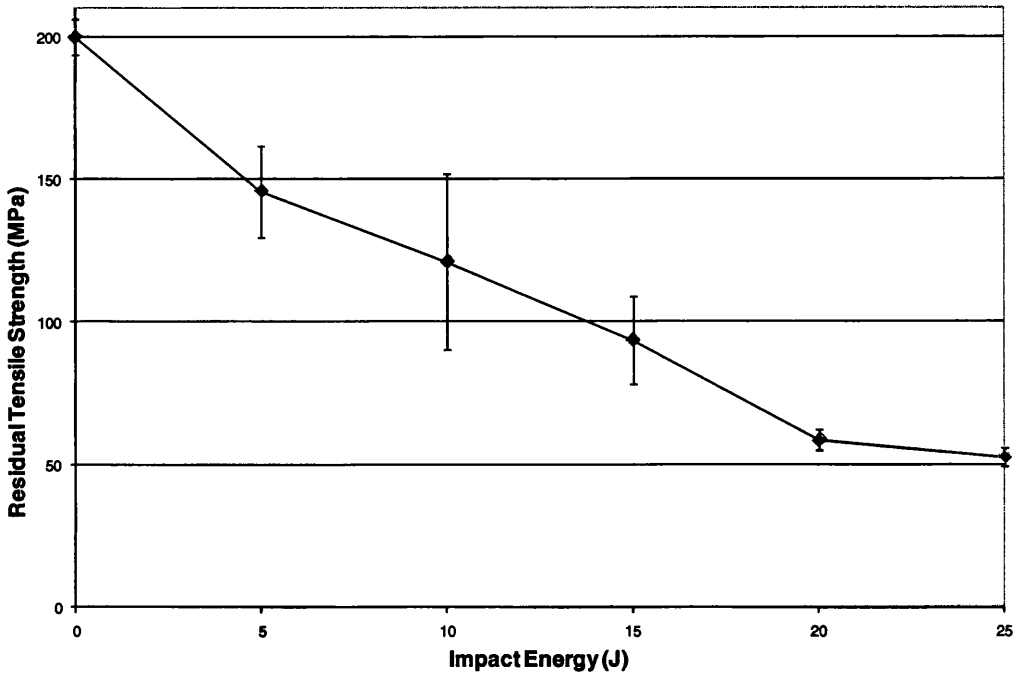

Fig. 5.27: Effect of impact energy on residual tensile strength of CSM glass/polyester composites

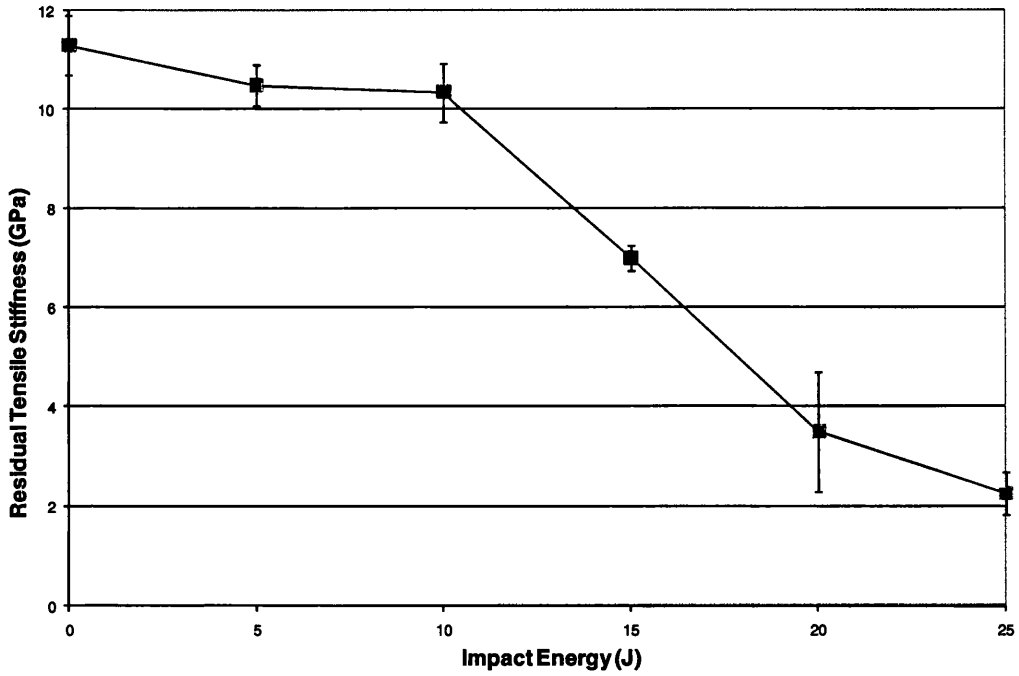

Fig. 5.28: Residual tensile stiffness of composites at increasing impact energy

The effect of low velocity impact on the tensile stiffness of the composites is shown in Fig. 5.28. The impact energy of up to 10J does not seem to have much effect on

intrinsic tensile stiffness. For impact energies of greater than 10J, the decline in tensile stiffness is steady. This behaviour of CSM glass fibre-polyester composites is again similar to that of 0/90° glass-polyester composites [262] which show small reduction in tensile stiffness up to impact energy of 10J but much greater reduction at impact energies of greater than 10J.

The composites lost only 10% of their intrinsic stiffness following impact of up to 10J. The composites lost almost 80% of their intrinsic stiffness at impact energy of 25J. Compared to this the 0/90° glass-polyester composites also lost almost 80% of their intrinsic stiffness at impact energy of 25J.

The macrographs of impacted and distal surfaces of the samples following impact tests are shown in Figs. 5.29-30. The impact testing produced a circular whitened zone on the impacted and the distal sides of the samples. The diameter of the whitened zone was 18 mm on both sides and was independent of the impact energy. The whitened zone has also been reported for other glass fibre configurations like ±45° and 0/90° [262]. The presence of the whitened zone has been attributed to a combination of factors like matrix cracking and debonding/delamination. At impact energy of 5J, cracks formed on the surface of samples due to matrix cracking. The whitening of samples also showed existence of fibre/matrix debonding. This resulted in almost 30% decrease in tensile strength but had little effect on residual modulus. An impact of 10J energy resulted in more matrix cracking and debonding. The strength was reduced by about 40% but it still had little effect on residual modulus. For impact energies of 15J and above, considerable evidence of fibre fracture on the distal side of the sample was observed, shown by arrowhead, which resulted in sudden decrease in tensile stiffness of up to 40%. Further application of impact energy of 20 and 25J resulted in more matrix cracking, debonding and fibre fracture which reduced the properties further.

The comparison of normalised residual tensile properties of hemp and glass fibre composites is shown in Figs. 5.31-32. The residual tensile properties of CSM glass fibre composites were found to be vastly superior to those of hemp fibre composites. Although the fracture of CSM glass fibre composites is also brittle as hemp fibre composites, their superior tensile strength and greater strain to failure means that they have superior damage tolerance than hemp fibre composites. The fracture toughness of CSM glass fibre composites has been reported to be almost three times higher than

hemp fibre composites [130]. This is also a major factor in their better impact properties.

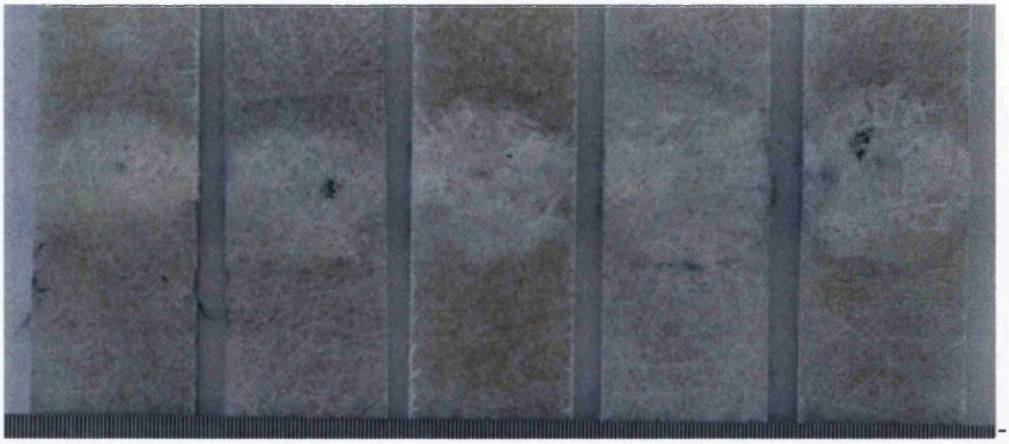

5J 10J 15J 20J 25J

Fig. 5.29: Impacted surface of composites with increasing impact energy

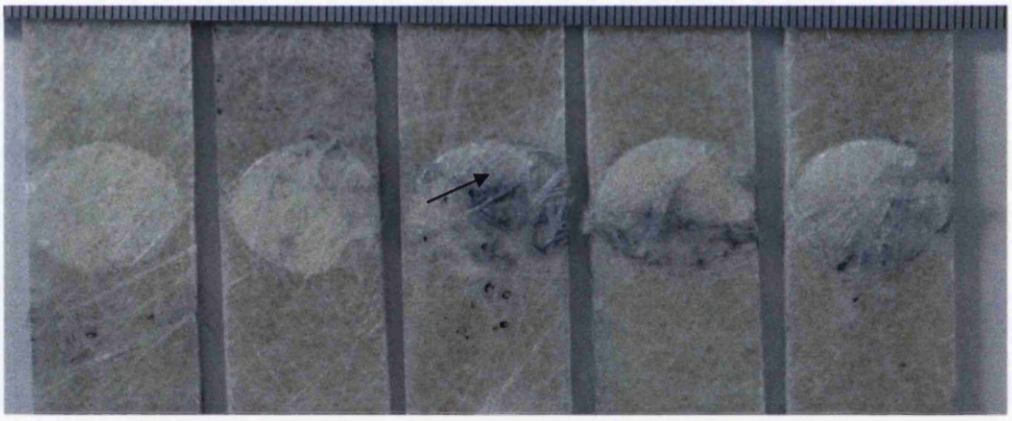

5J 10J 15J 20J 25J

Fig. 5.30: Distal surfaces of impacted samples with increasing impact energy

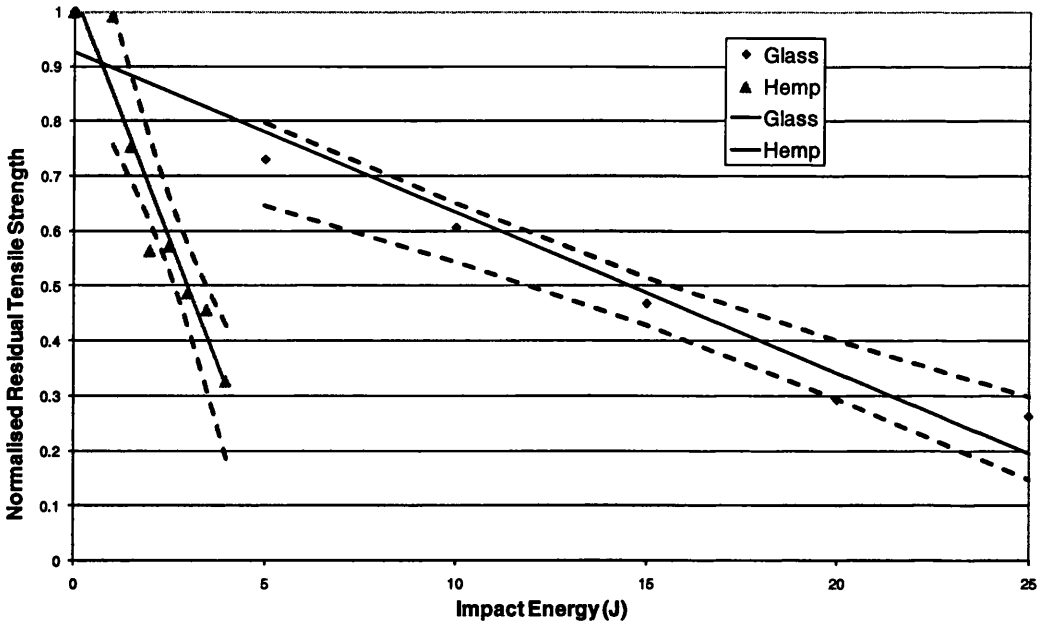

Fig. 5.31: Comparison of normalised residual tensile strength of hemp and glass fibre composites following low velocity impact

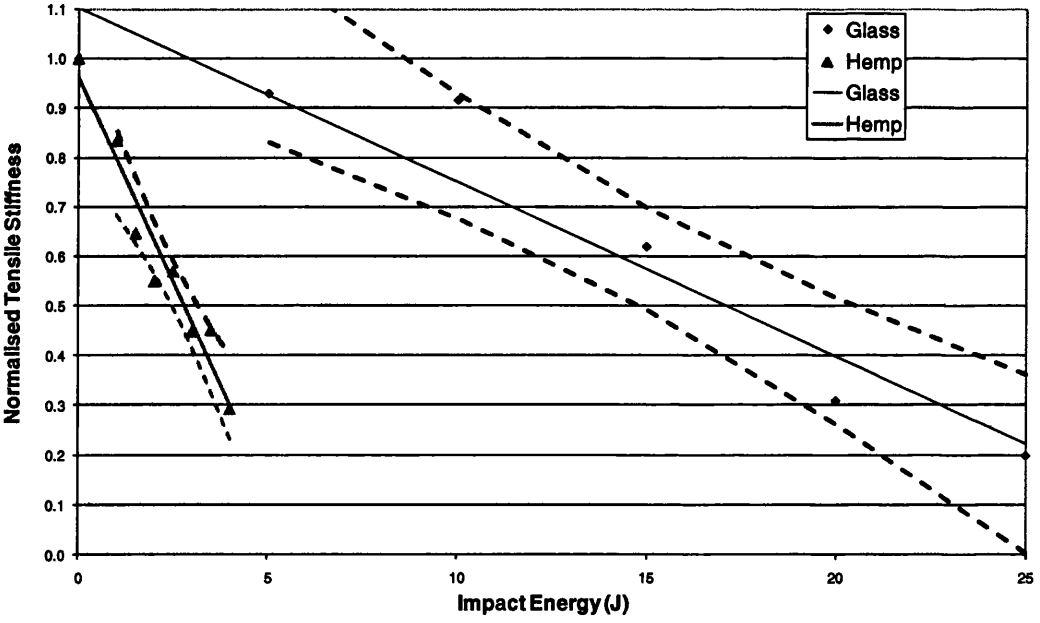

Fig. 5.32: Comparison of normalised residual tensile stiffness of hemp and glass fibre composites following low velocity impact

5.4.3 Hemp-CSM Glass Fibre Reinforced Polyester Hybrid Composites

The previous Section has shown significantly lower impact properties of hemp fibre composites compared to glass fibre composites. However the low velocity impact properties of hemp fibre composites can be improved by incorporating stronger and tougher glass fibres in them. The superior tensile strength and relatively high strain to failure of glass fibres is expected to increase the impact damage tolerance of the hybrid composites. Although the inclusion of glass fibres compromises the biodegradability of the composites, this can compensate the increase in properties obtained by hybridisation.

Two different kinds of hybrid configurations were used for low velocity impact testing: one had glass fibres as core and hemp fibres as skin and the other had hemp fibres as core and glass fibres as skin. Since the distal side of the impacted composites is subjected to bending stresses, the superior tensile properties of glass fibres are expected to result in better impact resistance of composites having glass fibres as skin and hemp fibres as core. In one study the flax-glass fibre hybrid composites have been reported to be as much as four times more impact resistant when impacted on the glass side [224].

5.4.3.1 Residual tensile properties

Figures 5.33-34 show the effect of increasing impact energy level on the residual tensile properties of hybrid composites. Taking into account the scatter in data, the improvement in properties for both kids of hybrid configurations was quite similar.

5.4.3.2 Comparison with hemp fibre composites

In order to compare the effect of impact energy on the residual tensile properties of hybrid composites with hemp composites, normalised residual strength and stiffness were determined and are shown in Figs. 5.35-36. From Fig. 5.35 it is clear that replacement of only 11% by volume of hemp fibres by glass fibres results in considerable improvement in their residual strength. Whereas impact energy of 4J resulted in almost 70% loss of residual strength for hemp composites, the hybrid composites lost only 30% of residual strength at this energy level. The figure also shows that the hybrid composites performed quite similarly irrespective of the configuration and hemp fibres as skin performed as well as glass fibres as skin.

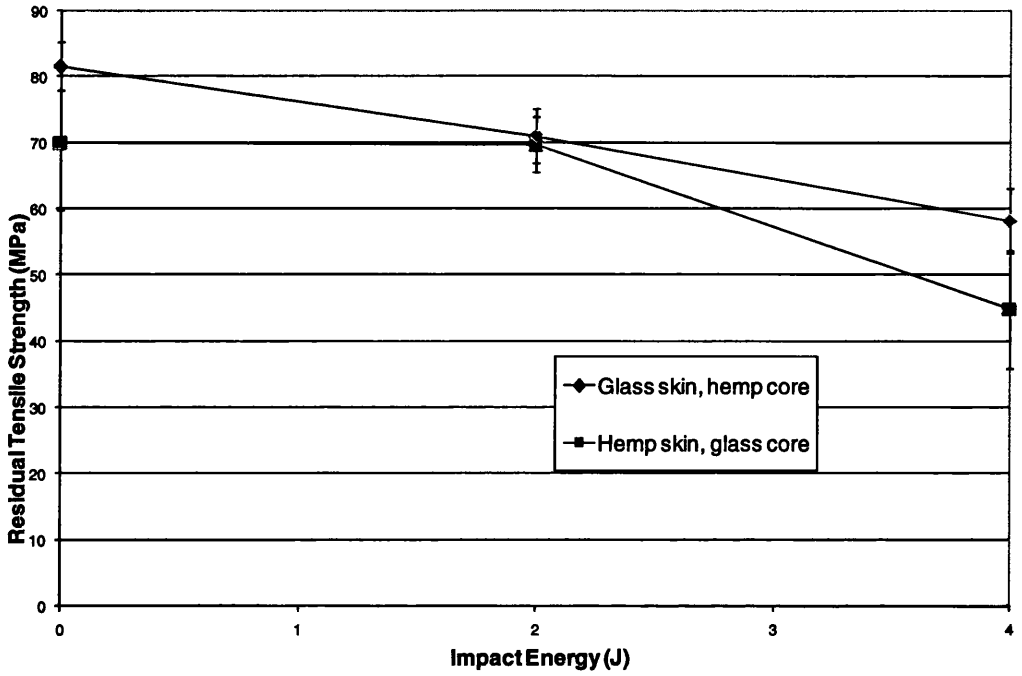

Fig. 5.33: Effect of increasing impact energy on residual tensile strength of hybrid composites

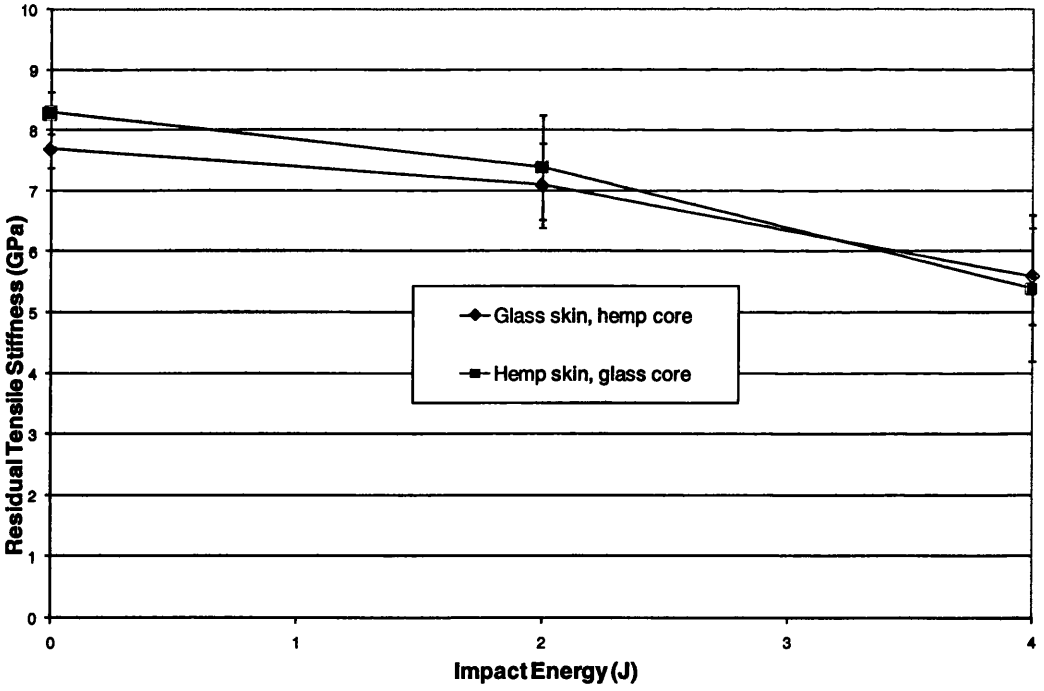

Fig. 5.34: Residual tensile stiffness of hybrid composites with increasing impact energy

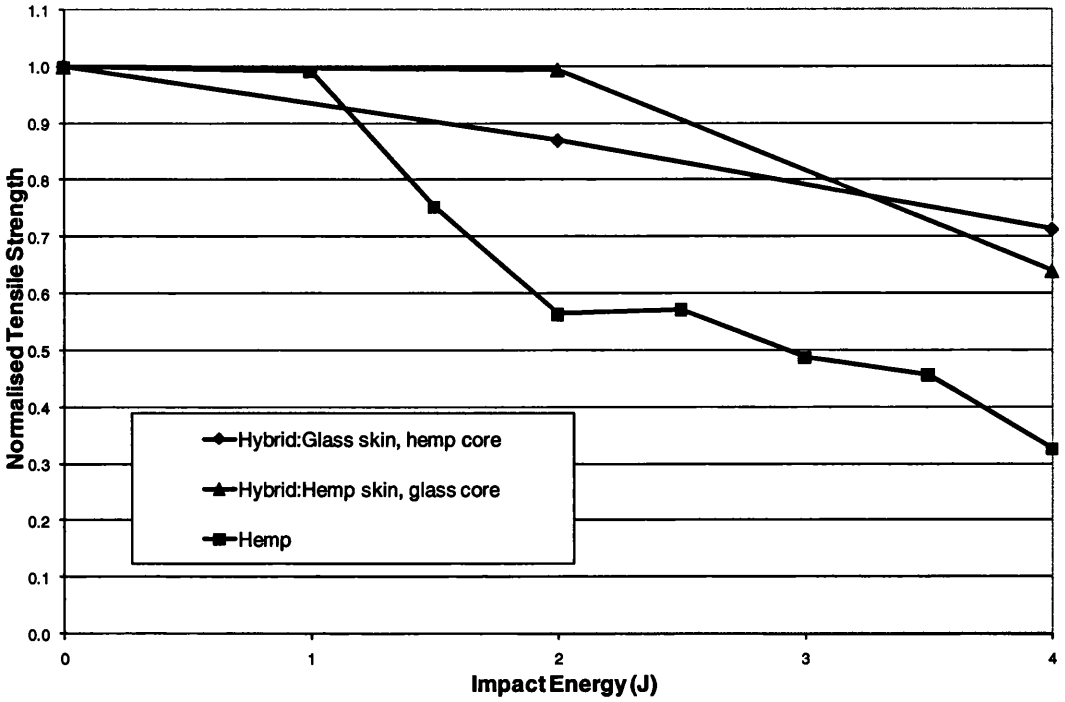

Fig. 5.35: Comparison of normalised residual strength of hybrid composites with hemp composites

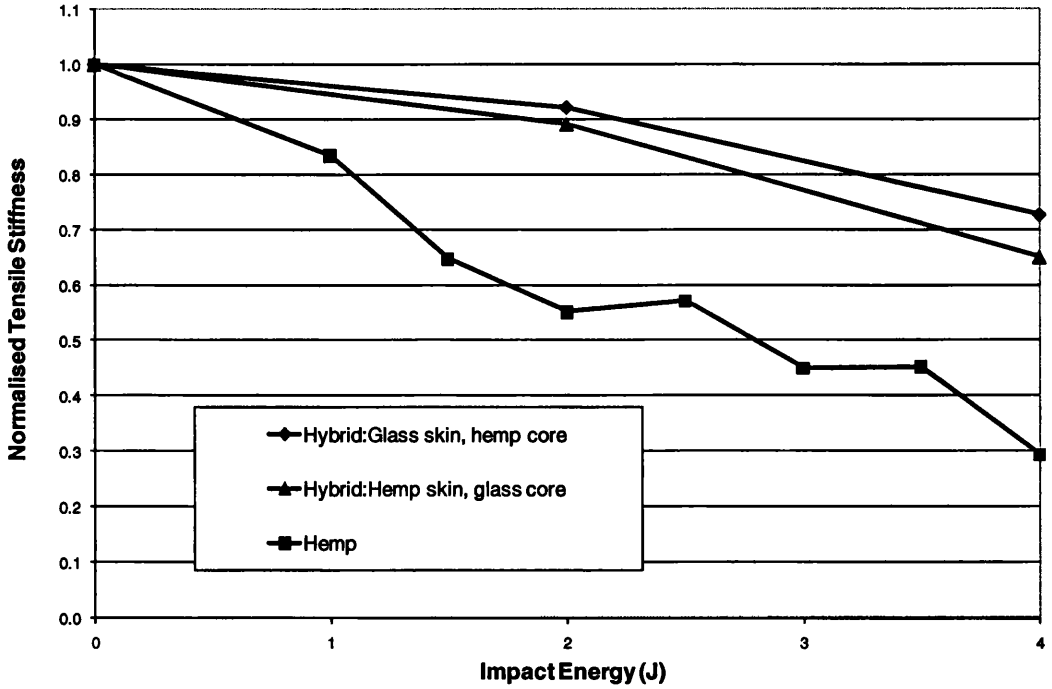

Fig. 5.36: Comparison of normalised residual stiffness of hybrid composites with hemp composites

Fig. 5.36 shows improved residual stiffness of hybrid composites compared to hemp composites. The hybrid composites only lost approximately 30% of their intrinsic modulus, compared to 70% for hemp composites at impact energy of 4J.

5.4.3.3 Comparison with CSM glass fibre composites

The improved impact tolerance of hemp-glass hybrid composites meant they could be subjected to higher impact energies and their impact resistance could be compared to that of CSM glass fibre composites. Therefore hybrid composites with both types of configurations were subjected to impact energies of up to 20J.

Fig. 5.37 shows the residual tensile strength of both hybrid composites at increasing impact energy levels of up to 20J. The advantage of having glass fibre as the skin fibre becomes more obvious at these high impact energy levels as they have higher residual strength than hemp skin composites.

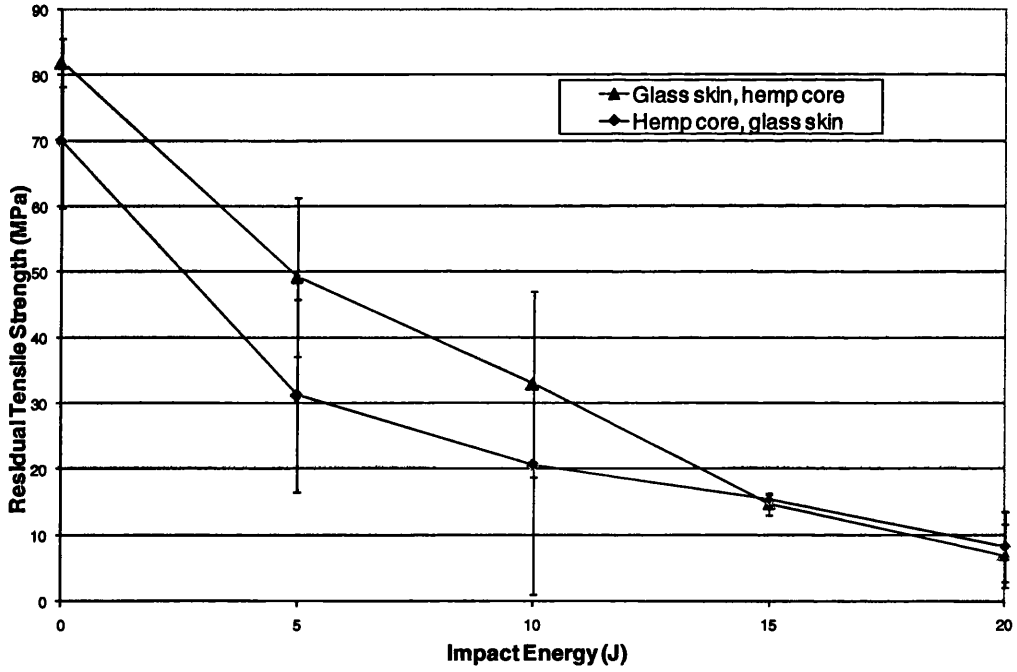

Fig. 5.37: Residual tensile strength of hybrid composites at increasing impact energy

The normalised residual tensile strength of hybrid composites compared with that of CSM glass fibre composites is shown in Fig. 5.38. The decline in tensile strength of hybrid composites is gradual up to impact energy of 20J, by which stage the composites have lost almost 90% of their intrinsic strength. Compared to this the CSM glass

composites have lost almost 70% of their intrinsic strength. Comparing with Fig. 5.30, it is also clear that whereas the hemp fibre composites lose 70% of their strength at impact energy of 4J, the hybrid composites can absorb 10J of impact energy before suffering the same reduction in strength. Hence by replacing just 11% of hemp fibres with glass fibres, the impact damage tolerance can be increased up to 150% in hybrid composites.

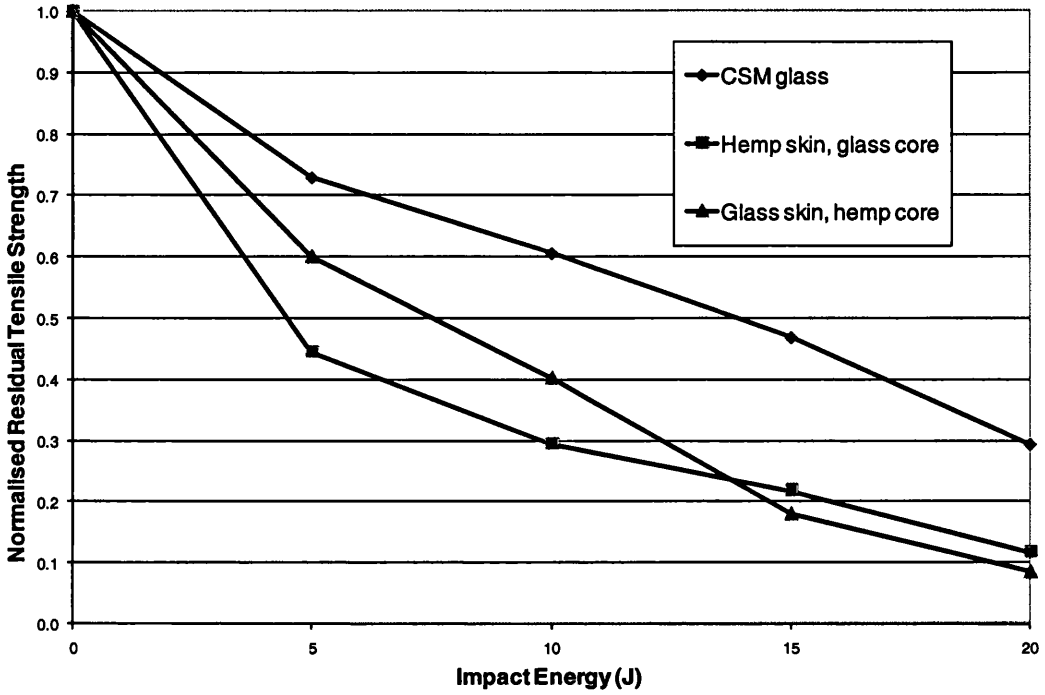

Fig. 5.38: Comparison of normalised residual tensile strength of hybrid and glass fibre composites

Fig. 5.39 shows the residual tensile stiffness of hybrid composites following impact energy of up to 20J. Similar to residual strength, glass skin composites seem to fare better than hemp skin composites. The residual stiffness of both composites is the same at impact energy of 15J at which stage they seem to have lost most of their stiffness. Further impact damage does not result in any increased reduction in stiffness.

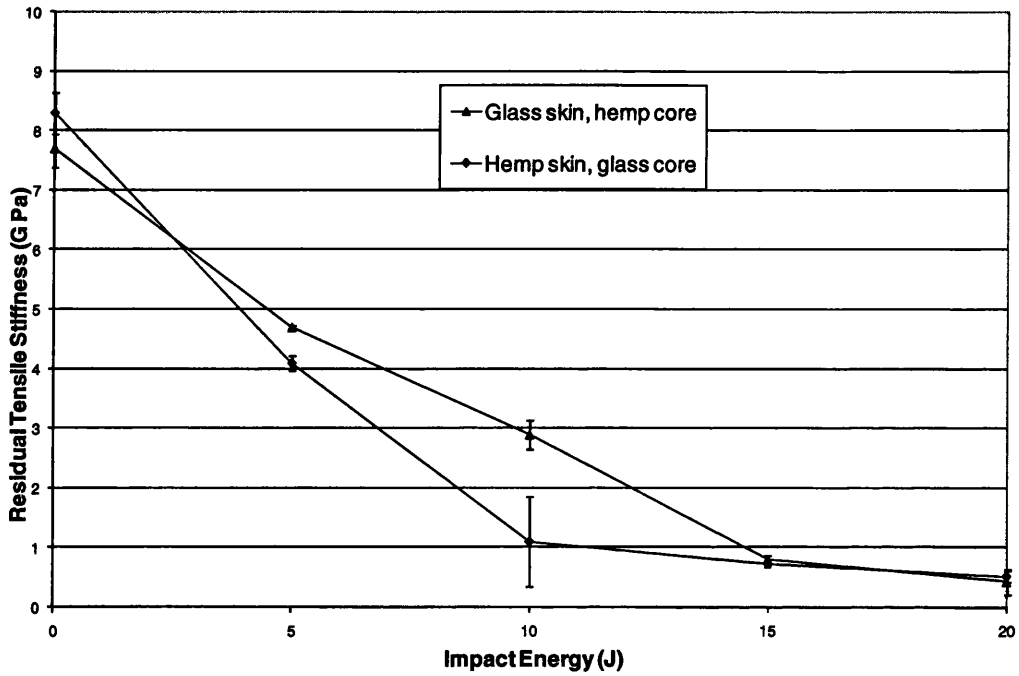

Fig. 5.39: Residual tensile stiffness of hybrid composites at increasing impact energy levels

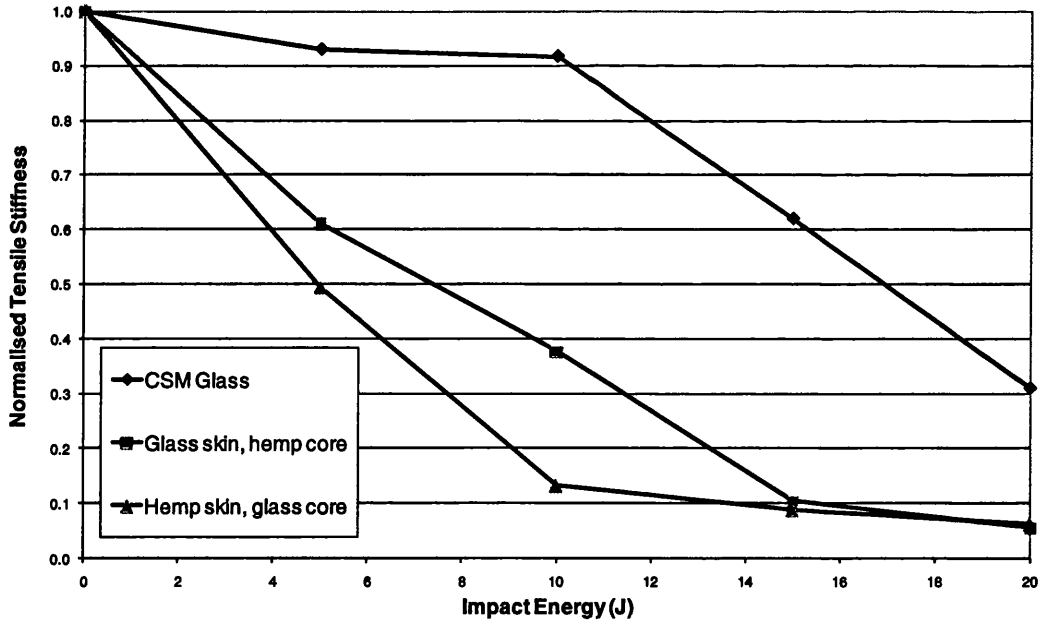

Fig. 5.40: Comparison of normalised residual tensile stiffness of hybrid composites with CSM glass fibre composites

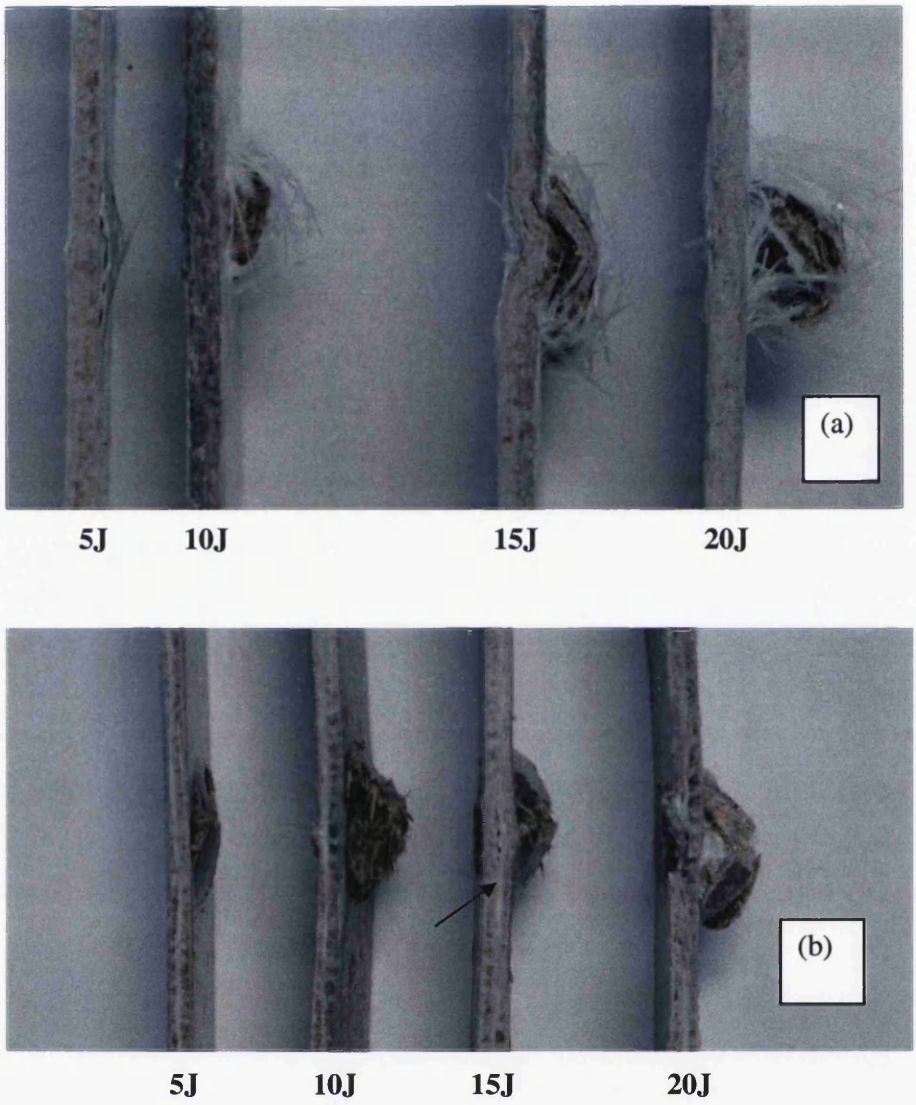

Fig. 5.41: Out-of-plane deformation of glass skin, hemp core (a), and hemp skin, glass core (b) hybrid composites in impact testing

Fig. 5.40 compares the normalised residual stiffness of hybrid composites with those of CSM glass fibre composites at increasing impact energy levels. The figure shows the reduction in tensile stiffness of the hybrid composites is almost 90% following impact energy of 15J for both types of composites. At this energy level CSM composites have lost only 40% of their stiffness. Compared with hemp fibre composites, they lost 70% of their stiffness at impact energy of 4J whereas hybrid composites required impact of up to 10J to suffer the same reduction in stiffness. This again shows improvement in

damage tolerance of hybrid composites. Hence the advantages of using glass fibres in hybrid composites have been underlined in this part of the research.

Fig. 5.41 (a) shows out-of-plane deformation of glass skin, hemp core composites and (b) shows hemp skin, glass core composites following low velocity impact. It is clear that an impact of even 5J can result in visible damage in composites which starts to increase with increase in impact energy. At an impact energy of 10J, there is evidence of considerable matrix and fibre fracture. This correlated well with the reduction in residual properties with increase in impact energy. At an impact energy of 15J, the samples are on the verge of perforation and apart from matrix and fibre fracture, there is some evidence of delamination in hemp skin, glass core composites as shown by the arrowhead. This could be caused by bending stiffness mismatch between hemp and glass fibres. At this stage, the composites had lost most of their strength and stiffness. At an impact energy of 20J, the samples were almost completely perforated.

These studies have shown that hybridisation of hemp fibres with glass fibres results in considerable improvement in their impact properties. The stronger and tougher glass fibres enhance the damage tolerance of the composites and the effect is more pronounced when glass fibres are used as skin.

5.5 FATIGUE PROPERTIES

Fatigue properties of the composites were mainly evaluated in tension-tension mode (R=0.1) at a frequency of 1 Hz. The fatigue stress on the samples was varied and the number of cycles to failure at each stress was recorded. The resulting data was used to draw up the Wohler (S-N) curves. The samples that did not fail after 10^6 cycles (approximately 11 days) of testing were shown on the S-N curve with arrows pointing to the right. The testing was carried out as per BS ISO 13003: 2003: Fibre-reinforced plastics – Determination of fatigue properties under cyclic loading conditions.

5.5.1 S-N Curves

5.5.1.1 Hemp Fibre Reinforced Polyester Composites

The S-N curve of composites with average fibre weight fraction of 52% is shown in Fig. 5.42. The dashed lines in the figure represent the 95% confidence interval of the linear

regression line. The variability of properties of hemp fibres is expected to result in random accumulation of damage in the composites and, therefore, it is not unexpected to see some data points lying outside the 95% confidence limit. It has been reported for glass fibre composites as well that the normal scatter in static strength data is often increased by random damage during fatigue loading [236]. The static strength of the composites is plotted on the curve at 1 cycle (log 1=0). The British Standard BS ISO 13003: 2003 recommends that the value of static strength to be used on S-N curve should be evaluated at the same strain rate as that of fatigue testing. In order to determine the effect of different strain rates on the tensile properties of composites, tensile testing was performed at three different testing speeds and the tensile properties of the composites were evaluated. The results are shown in Table 5.11 and Fig. 5.43.

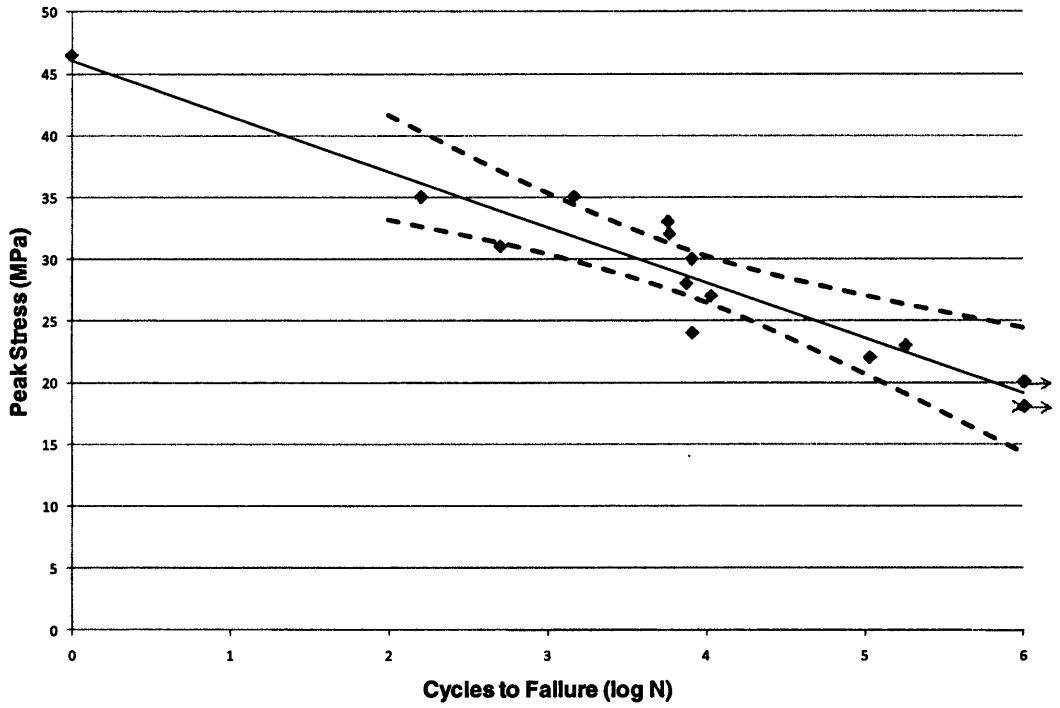

Fig 5.42: S-N curve of hemp fibre composites

The error bars show that the tensile properties were found to lie within the standard deviation at all testing rates and it is reasonable to conclude that these composites are not sensitive to strain rates within this range and it is reasonable to use their static tensile strength values, evaluated at testing rate of 2 mm/min, on the S-N curve.

Table 5.11: Tensile properties of composites at different testing rates

Testing rate (mm/min)	Strain rate (s^{-1})	Tensile strength (MPa)	Tensile modulus (GPa)
2	$2.66x10^{-4}$	37.8 (5.2)	5.6 (0.1)
5	$6.66x10^{-4}$	40.7 (5.5)	5.9 (1.0)
10	$1.33x10^{-3}$	42.0 (0.5)	5.3 (1.0)

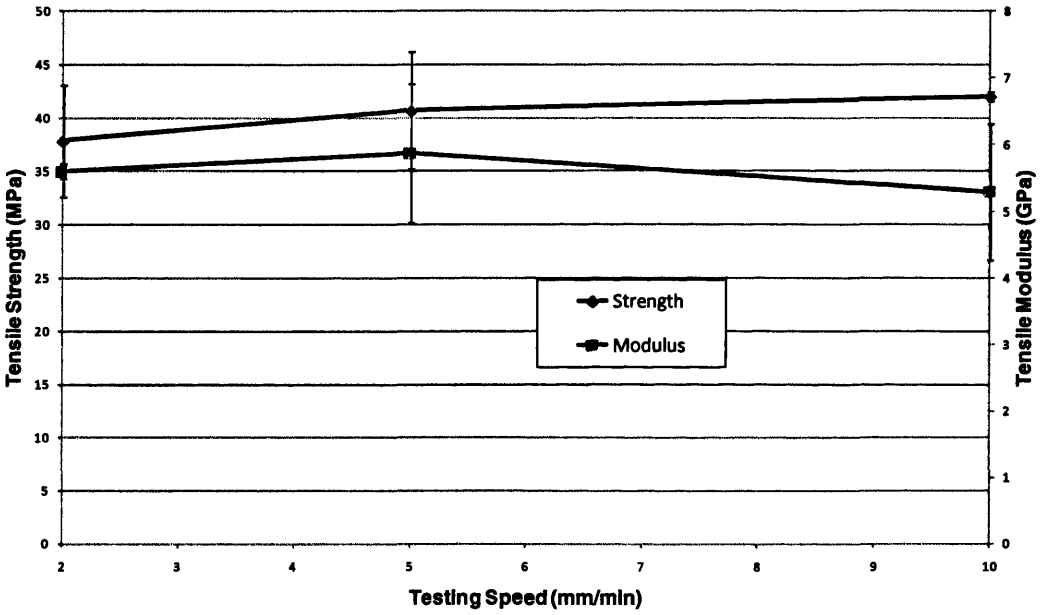

Fig. 5.43: Effect of different testing speeds on tensile properties of composites

The best-fit regression line in Fig. 5.42 shows gradual decline in fatigue strength with increase in the number of fatigue cycles. The regression line predicted endurance limit of about 20 MPa for the composites at 1 million cycles which corresponded well with the experimental data as shown by arrowheads. Hence a stress level of up to 20 MPa (approximately 40% of UTS) can be taken as a safe value for endurance limit for these composites. This correlates well with the stress-strain graph (Fig. 5.6) where the curve starts to deviate at 20 MPa, i.e. damage mechanisms start to become dominant at this stress. For sisal fibre reinforced polyester composites, Towo and Ansell [354] reported the endurance limit to be 35% of static strength in tension-tension fatigue loading.

Of the various fatigue life prediction theories discussed in Section 2.6.5 the following equation can be used to represents the S-N curve for hemp fibre reinforced polyester composites:

$$\sigma_a = \sigma_{ult} - b \log N \quad \text{.....(5.13)}$$

where σ_a is the maximum cyclic loading stress, σ_{ult} is the static tensile strength, N is the number of cycles to failure at a particular value of σ_a, and *b* is a constant depending on the material properties. It represents the gradient of the S-N curve which has a negative slope and hence can be related to the degradation in fatigue strength of the material with increase in number of N. For these materials the value of *b* was found to be about 4.5 MPa.

In order to compare the fatigue sensitivity of these composites with other materials, it is more suitable to use the normalised stress versus cycles to failure curve. The normalised stress (maximum tensile stress divided by ultimate tensile strength) versus cycles to failure curve is shown in Fig. 5.44. The curve shows that the composites lost their static strength by almost 10% per decade of cycles. A similar value of reduction in static strength was reported by Mandell [243] for unidirectional E-glass fibre reinforced composites in the fibre direction. Thus hemp fibre composites are observed to show similar fatigue sensitivity to glass fibre composites.

For normalised S-N curves, equation (5.13) reduces to:

$$\sigma_a / \sigma_{ult} = 1 - b^* \log N \quad \text{.....(5.14)}$$

The constant b^* which represents the slope of normalised S-N curve is called the fatigue sensitivity coefficient and has different value for different materials. The value of b^* was found to be 0.097 for these hemp fibre composites. Mandell [352] collected S-N data for tension-tension fatigue for various chopped E-glass strand composites (both SMC and CSM) available in the literature (64 S-N data sets to be exact) and found that the value of b^* for all the systems were remarkably equal or close to 0.1. This value of b^* was the same for unidirectional continuous glass fibre composites fatigue tested parallel to fibres. A similar value of b^* for hemp fibre composites seems to reinforce the fact that hemp fibres have comparable fatigue sensitivity to that of glass fibre composites.

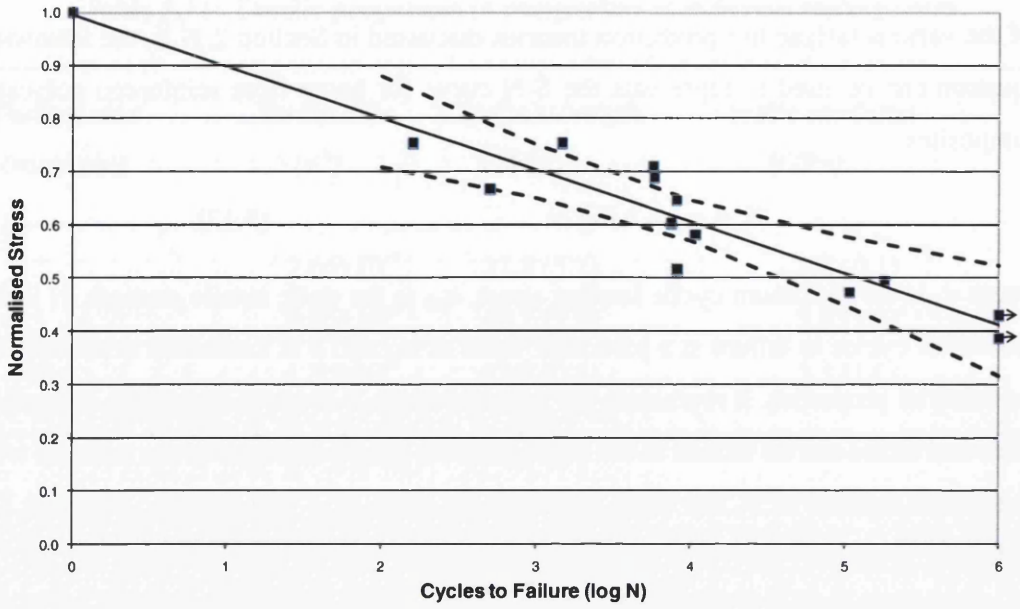

Fig. 5.44: Normalised S-N curve of hemp-polyester composites

Most composites fail in fatigue in the same mode and by the same mechanisms as under static loading [352]. A similar behaviour was observed for hemp fibre composites. As in static tensile testing, the samples tested in fatigue failed in a completely brittle and catastrophic manner, normal to the direction of applied stress. A typical sample fractured in fatigue testing is shown Fig. 5.45.

Fig. 5.45: Fracture surface of a hemp fibre composite sample in fatigue testing

The fatigue fractured sample has quite similar appearance to that fractured in tensile testing. Therefore it can be expected that damage development modes in fatigue were quite similar to those in tensile testing. This is also borne out by the SEM micrographs of the fracture surface as shown in Fig. 5.46. It is clear from the images that, as in

tensile fracture, the principal modes of failure in tension-tension fatigue are matrix fracture, fibre fracture, fibre/matrix debonding, and fibre pull-out.

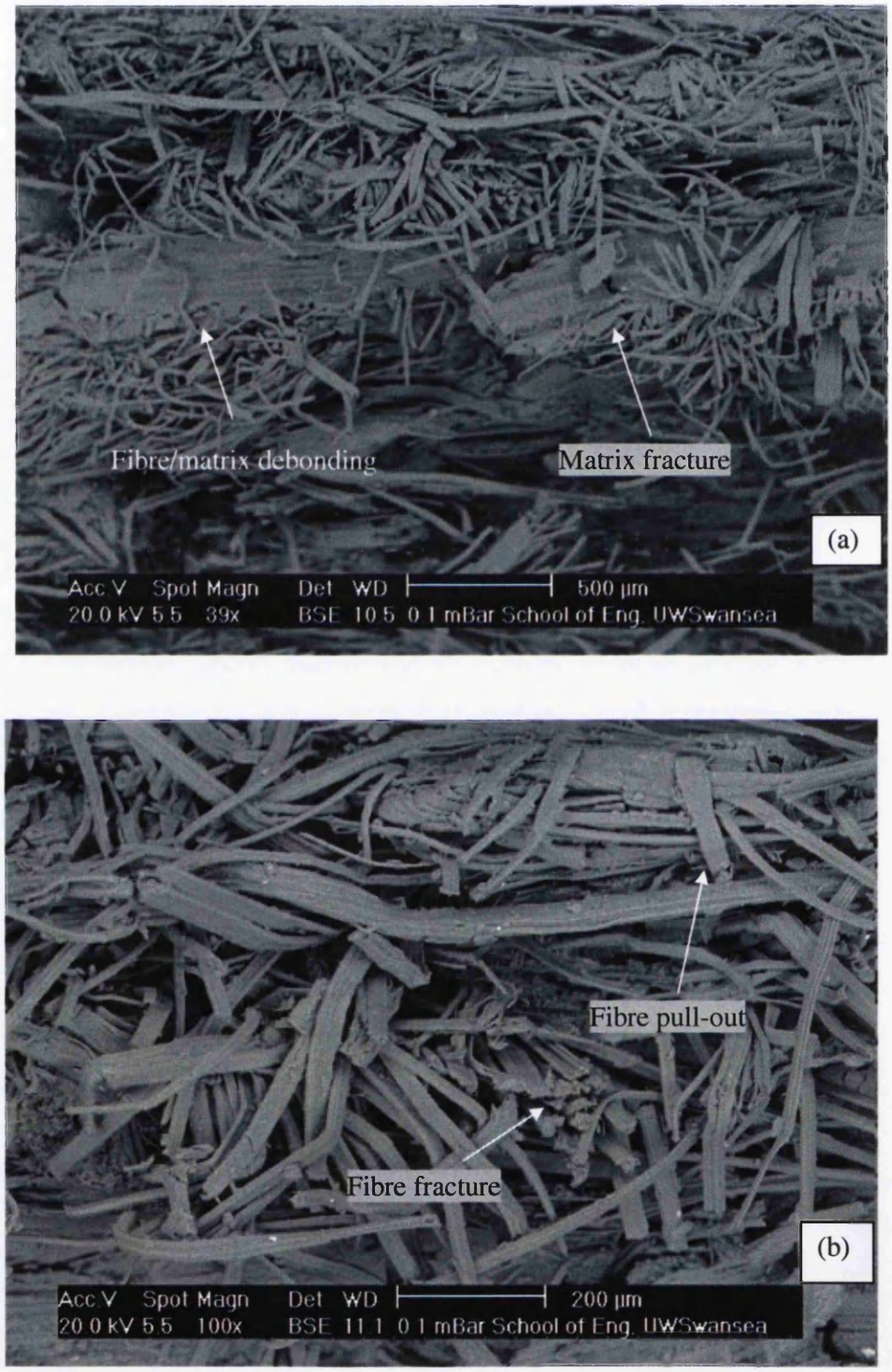

Fig. 5.46: SEM micrographs of fracture surfaces of samples in fatigue testing

It has been established for randomly oriented fibrous composites that in fatigue the damage first initiates by the debonding of fibre strands, lying perpendicular to the loading direction, from the matrix in the fibre rich regions [22]. Owen and Dukes [355] concluded form fatigue testing of CSM glass/polyester composites that the first damage mechanism was debonding of fibres lying normal to tensile axis. A similar damage initiation and development mode can be expected from randomly oriented hemp fibre mat composites. The variability in the tensile strength of hemp fibres means that a few of the weakest fibres are also expected to fail during initial fatigue loading. This will give rise to locally high stresses in the matrix and the fibre-matrix interface. However weak fibre/matrix interface may encourage the growth of the crack along the interface rather than matrix fracture. This may relieve some of the stress concentration in the vicinity of the crack and the weak interfacial bond may even enhance the fatigue life of the composite [22].

The effect of residual stresses on fatigue should not be neglected. These stresses are in addition to the applied stresses in fatigue and can be as high as applied stresses depending on the matrix and fibre characteristics and cure conditions [352]. It has also been suggested that the residual stresses contribute to overestimated value of fatigue sensitivity coefficient because of an increase in applied stress and hence increase in the slope of S-N curve [352].

With the application of more cycles, additional debonding is expected to spread in fibre bundles located in other than normal directions, with the development of matrix cracking in resin-rich areas. These matrix cracks can grow along the weak interface by bypassing the fibre if the fibre is strong. If the fibre is weak and brittle, the matrix cracks can grow by fracturing the fibre. Because of high variability in tensile strength of hemp fibres, both kinds of mechanisms can be expected to exist in these composites. Further application of load is expected to result in interfacial debonding and fracture of fibres oriented in the longitudinal direction. The fibres lying in the loading direction will normally be the last to break. The sample finally breaks in a catastrophic manner when all these damage mechanisms weaken the sample so much that it can no longer sustain the applied load.

5.5.1.2 CSM Glass Fibre Reinforced Polyester Composites

The S-N curve of CSM glass fibre reinforced polyester composites, compared to hemp fibre composites, is shown in Fig. 5.47. The dashed lines represent 95% confidence interval of linear regression lines.

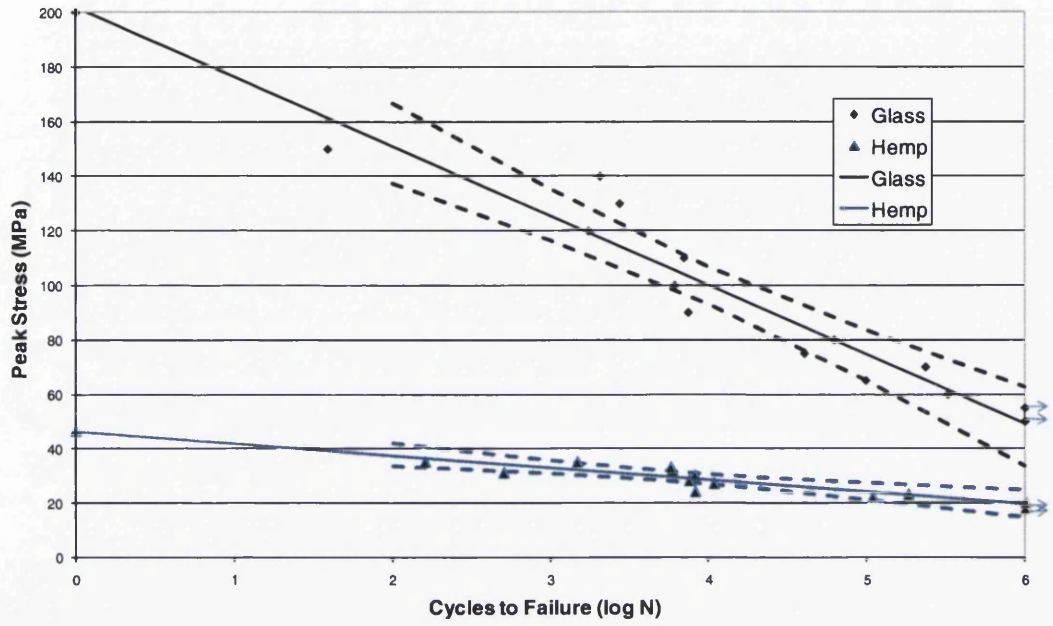

Fig. 5.47: Comparison of S-N curves of CSM glass and hemp fibre composites

CSM glass fibre composites have higher fatigue strength than hemp fibre composites as they require higher fatigue stress to fracture for same number of cycles. However their S-N curve is steeper than hemp fibre composites which can be shown more neatly in normalised S-N curves. The comparison of normalised S-N curves of CSM glass fibre composites with hemp fibre composites is shown in Fig. 5.48. The figure shows better fatigue sensitivity of hemp fibre composites compared with glass fibre composites, also indicated by fatigue sensitivity coefficient value of 0.097 compared to that of 0.127 for CSM glass fibre composites. This value is consistent with the values reported in literature for CSM glass fibre/polyester composites [352] and suggests superior fatigue sensitivity of hemp fibre composites compared to glass fibre composites.

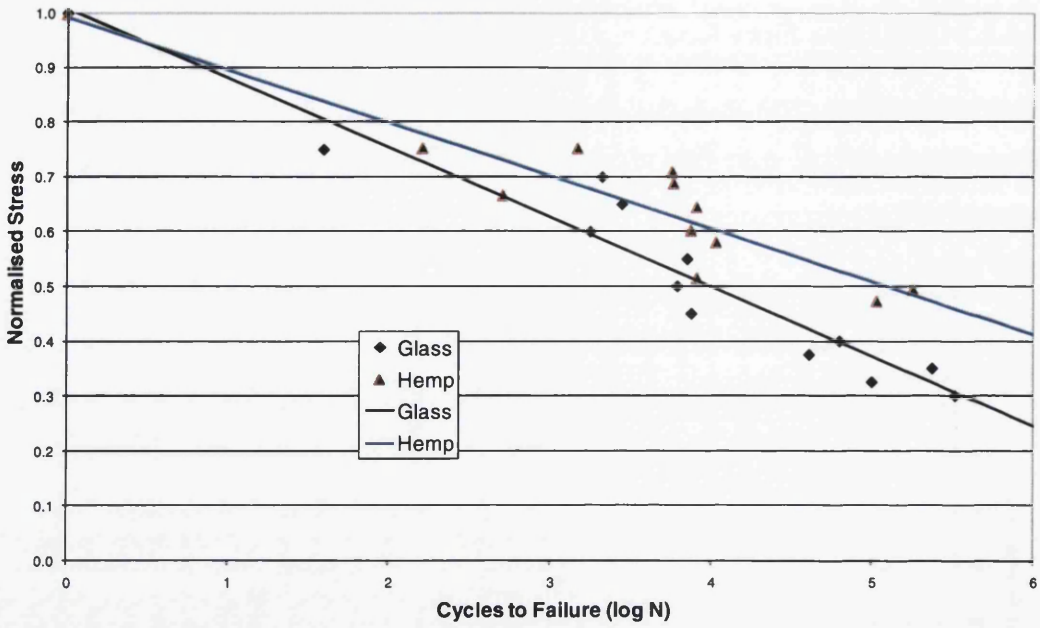

Fig. 5.48: Comparison of normalised S-N curves of hemp fibre and glass fibre composites

5.5.1.3 Hemp-CSM Glass Fibre Reinforced Hybrid Composites

The S-N curve for hemp skin-glass core hybrid composites, compared to S-N curve of hemp composites, is shown in Fig. 5.49. The static tensile strength of hemp skin-glass core composites is about 50% higher than hemp fibre composites. This improvement in tensile strength is also reflected in improved fatigue strength of these composites compared to hemp fibre composites as their S-N curve is observed to lie higher than hemp fibre composites, implying that higher stress is required to fracture the samples at same number of fatigue cycles. The endurance limit of hemp skin-glass core composites also shows an increase to about 30 MPa, almost 50% increase compared to 20 MPa for hemp fibre composites. Thus replacement of about 11% hemp fibres with glass fibres results in significant increase in their fatigue strength.

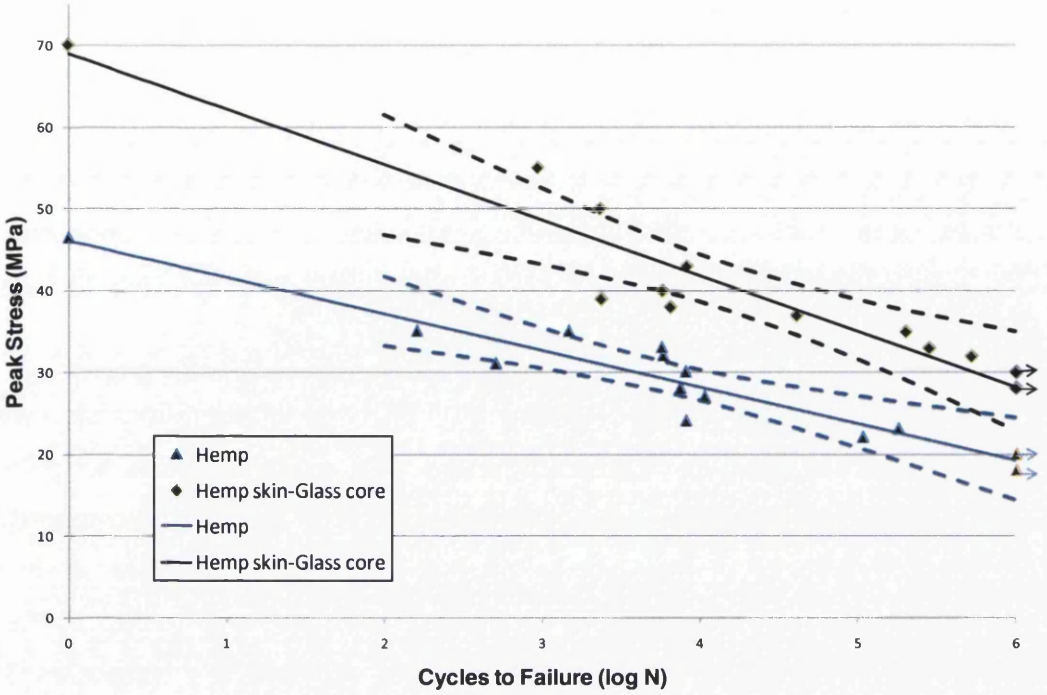

Fig. 5.49: Comparison of S-N curves of hemp skin-glass core hybrid and hemp fibre composites

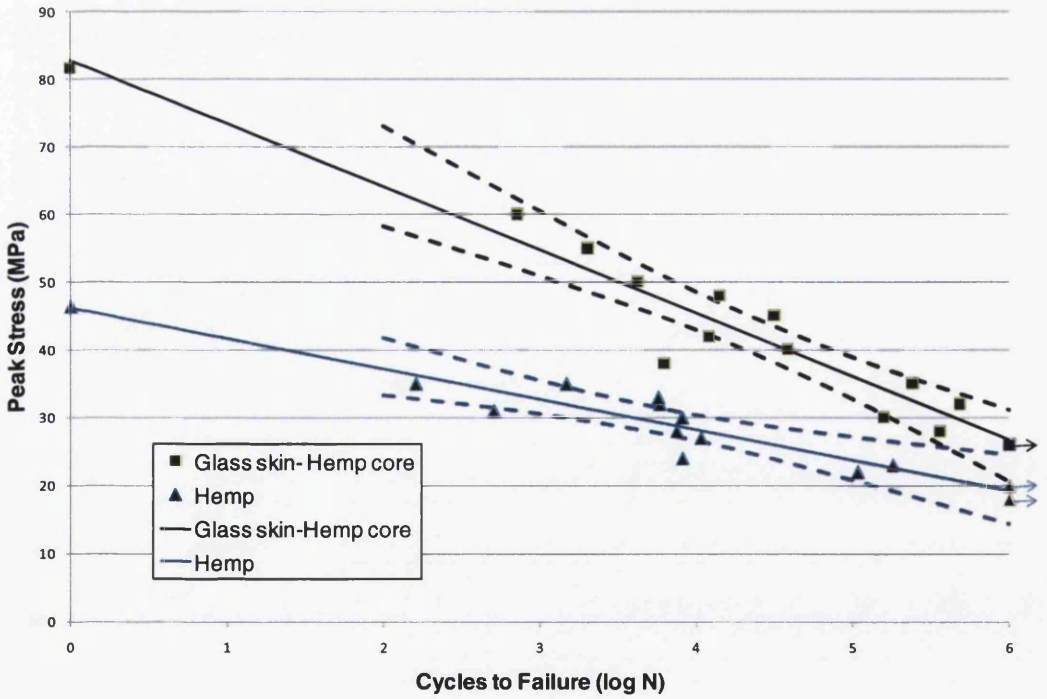

Fig. 5.50: Comparison of S-N curves of glass skin-hemp core hybrid and hemp fibre composites

For glass skin-hemp core hybrid composites, the improvement in static strength compared to hemp fibre composites is about 75% and improvement in fatigue strength is again observed as shown in Fig. 5.50. However the slope of the curve is steeper than hemp skin-glass core composites, suggesting less improvement in fatigue strength. This is also reflected in lower improvement in endurance limit to about 25 MPa, compared to 30 MPa for hemp skin-glass core composites. This suggests that having hemp fibres as skin and glass fibres as core may be a more efficient method of improving the fatigue strength of hybrid composites.

Fig. 5.51 shows the comparison of normalised S-N curves of hemp fibre and hybrid composites. Hemp skin, glass core composites have similar slope as hemp fibre composites whereas the slope of glass skin-hemp core composites is steeper, suggesting less fatigue sensitivity of these composites. The comparison of fatigue sensitivity coefficients of hybrid composites with hemp composites is shown in Table 5.12. There is no change in fatigue sensitivity coefficient of hemp skin-glass core composites. The fatigue sensitivity coefficient of glass skin-hemp core composites is lower than that of hemp fibre composites but the difference between the two does not appear to be significant.

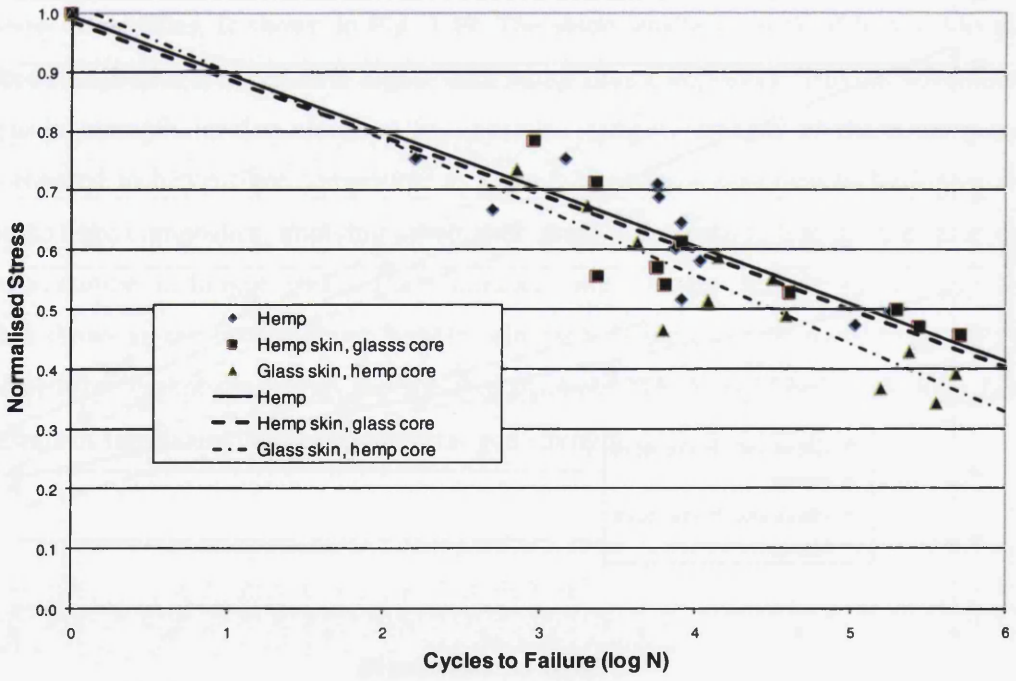

Fig. 5.51: Comparison of normalised S-N curves of hybrid and hemp composites

Table 5.12: Comparison of fatigue sensitivity coefficients of hemp and hemp-glass hybrid composites

Composite configuration	Fatigue sensitivity coefficient
Hemp	**0.097**
Hemp skin-glass core hybrid	**0.097**
Glass skin-hemp core hybrid	**0.115**

Since fatigue strength of composites is primarily strain dependent, the fatigue performance of a hybrid composite is usually dominated by the lower strain phase, which is hemp fibre in this case. Therefore fatigue properties of hybrid composites are expected to be dominated by the fatigue properties of hemp fibres at low concentrations of glass fibres. Having hemp fibres as a core element seems to have resulted in deterioration in fatigue sensitivity as the lower strength and strain of hemp fibres seems to have resulted in greater damage development in fatigue loading than having glass fibres as core element. Overall no improvement in fatigue sensitivity of hybrid composites was observed compared to hemp fibre composites.

5.5.4.1 Overall comparison of S-N Curves

The comparison of S-N curves and normalised S-N curves of hemp fibre, CSM glass fibre and hemp-glass fibre hybrid composites are shown in Figs. 5.52-53. It is clear that although glass fibre composites have higher fatigue strength, they are more fatigue sensitive than hemp fibre composites as shown by the steeper slope of their normalised S-N curve. The endurance limit, which is 40% of the static strength of hemp fibre composites, is seen to be about 25% of static strength for CSM glass fibre composites. The hybridisation of hemp fibres with 11% glass fibres by volume increases their fatigue strength but does not increase their fatigue sensitivity.

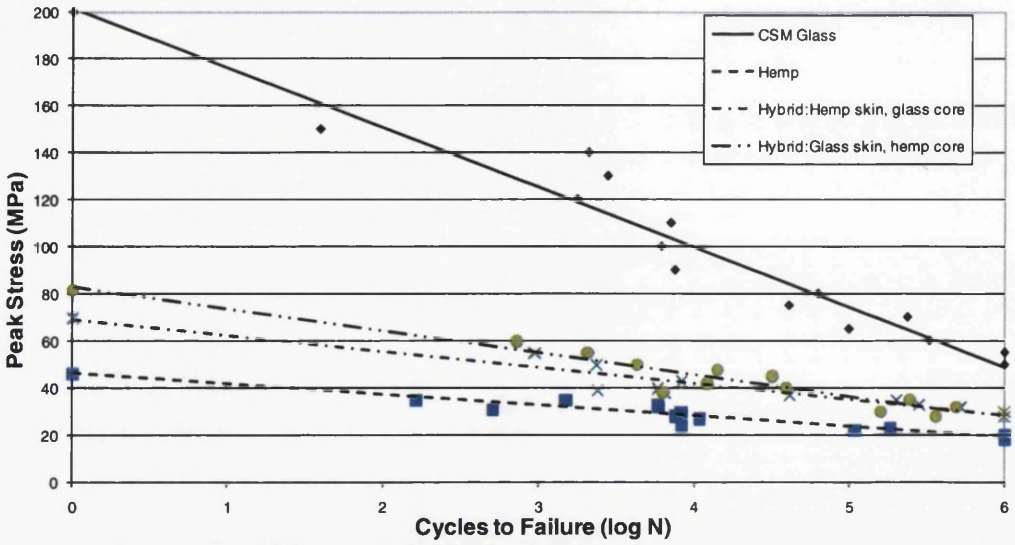

Fig. 5.52: Comparison of S-N curves of composites

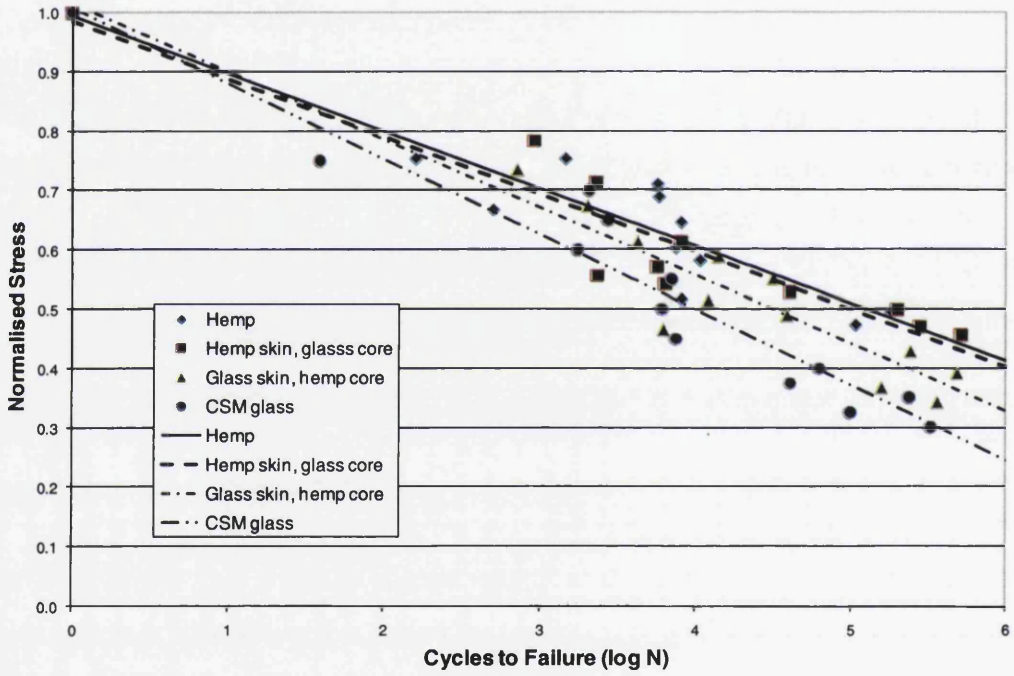

Fig. 5.53: Comparison of normalised S-N curves of composites

5.5.2 Damage Development

5.5.2.1 Hemp Fibre Composites

Stiffness degradation of the composites was monitored periodically during fatigue loading to try to understand the damage development and relate it to fatigue properties of glass and hemp fibre composites. Samples were periodically taken out of the fatigue testing machine following fixed number of cycles and their residual stiffness was determined by using the standard tensile testing method and their surfaces examined.

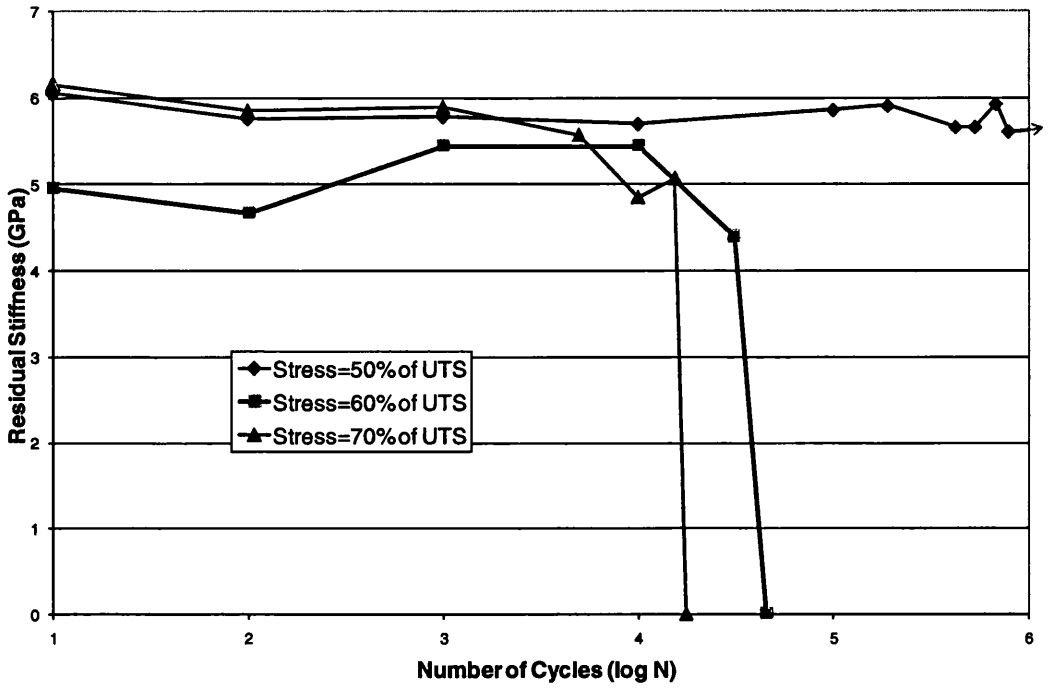

Fig. 5.54: Stiffness degradation of hemp fibre composites at different stress levels

Stiffness degradation of hemp fibre composites at different stress levels is shown in Fig. 5.54. The hemp fibre composites fatigue tested at stress level 50% of their static strength showed negligible reduction in their stiffness throughout the fatigue life. This showed the capability of hemp fibre composites to resist crack initiation and growth during fatigue loading. The sample was inspected after fatigue loading, and no crack was observed to be forming in its surface as shown in Fig. 5.55.

Fig. 5.55: Comparison of sample fatigue tested at stress level 50% of UTS (top) with untested sample (bottom)

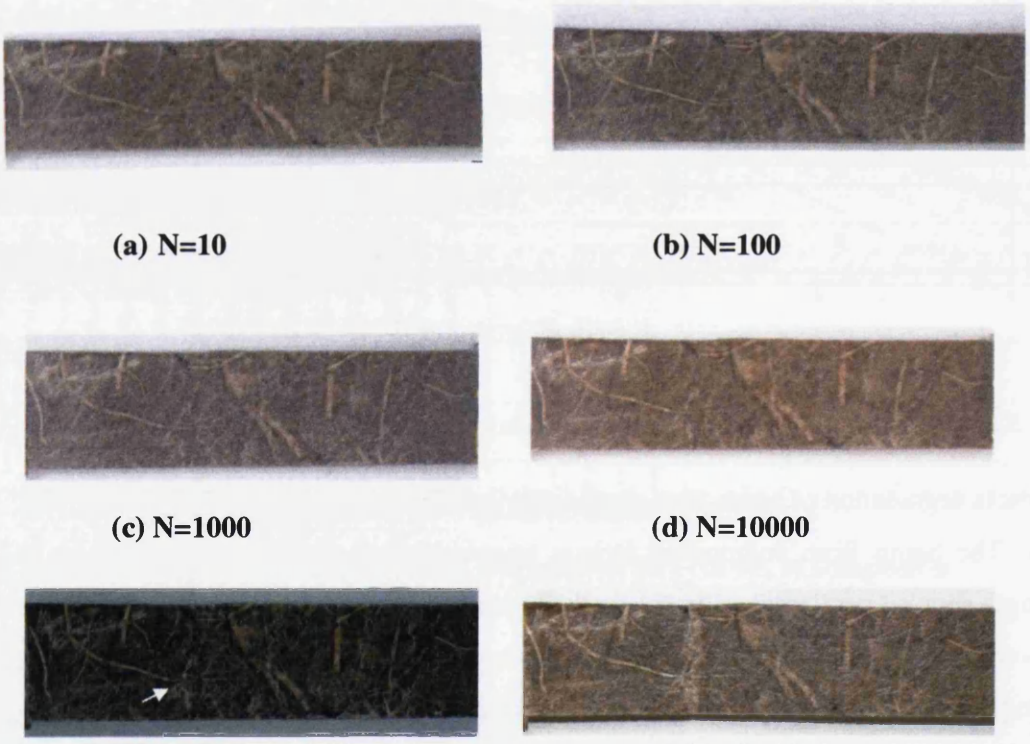

(a) N=10 **(b) N=100**

(c) N=1000 **(d) N=10000**

(e) N=31,000 **(f) N=45500**

Fig. 5.56: Surface of hemp fibre sample fatigue tested at 60% of UTS

Composites fatigue tested at stress level of 60% of their UTS showed some initial improvement in residual stiffness and no change in the surface of the sample was observed as shown in Fig. 5.56. However between 10,000 and 31,000 cycles, a crack was seen to be forming along the edge of the sample, shown by arrowhead in Fig. 5.56 (e), which correlated well with decline in residual stiffness by almost 20% between these two cycles. The sample eventually broke at the same crack site as shown in Fig. 5.56 (f).

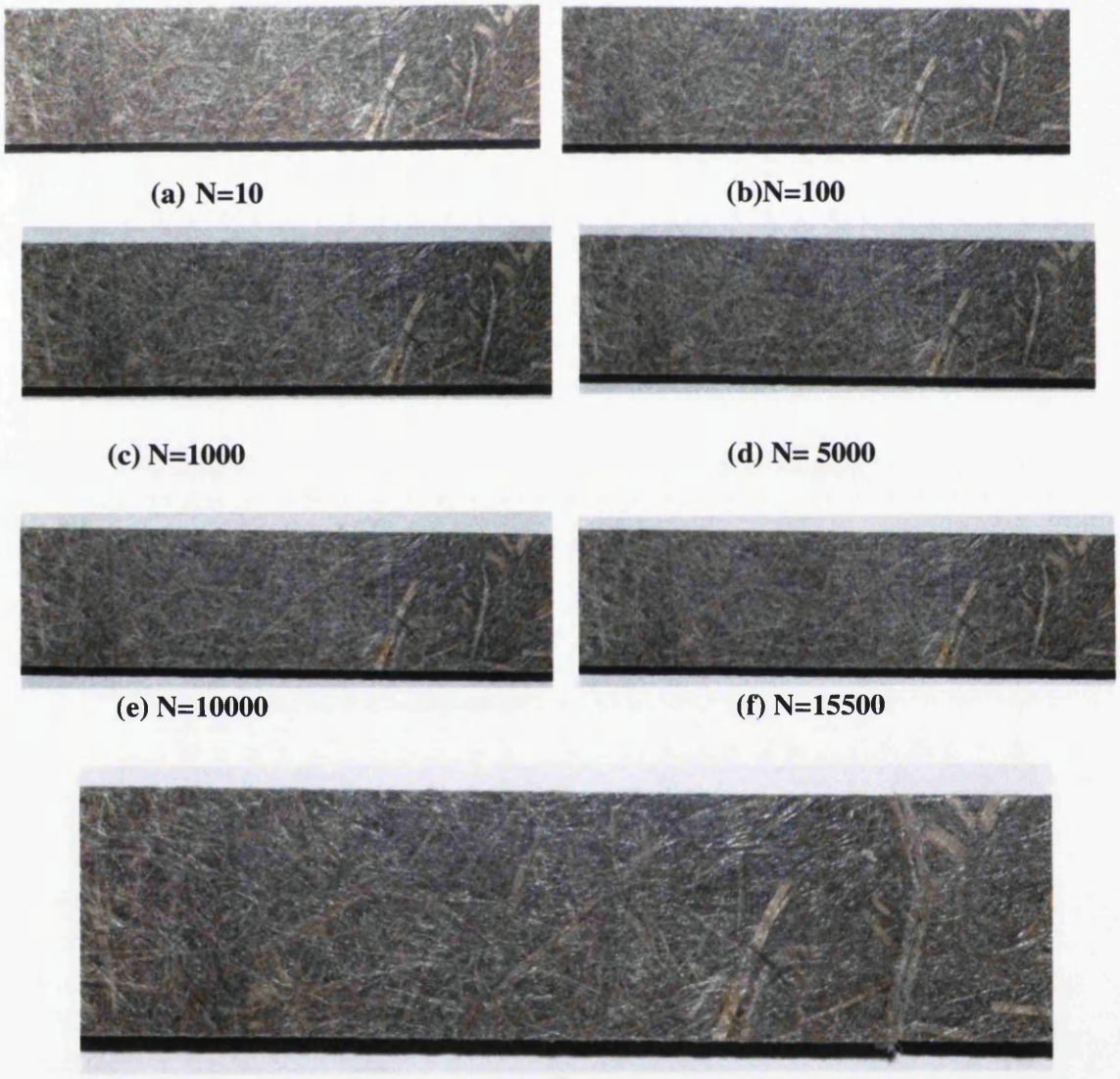

Fig. 5.57: Surface of hemp fibre sample fatigue tested at 70% of UTS

Composites fatigue tested at 70% of their static strength also showed little degradation in residual stiffness at low fatigue cycles. However close to failure, about 15% stiffness degradation was observed. No crack was seen to be forming on the surface, as shown in Fig. 5.57. The reduction in stiffness could be due to fibre/matrix debonding. The sample finally broke along the interface between the resin and fibres located at almost normal to load direction as shown in Fig. 5.57 (g).

Little degradation in residual stiffness even at very high stresses showed good fatigue resistance of these composites and it correlated well with their fatigue sensitivity coefficient.

5.5.2.2 CSM Glass Fibre Composites

Stiffness degradation of CSM glass fibre reinforced polyester composites in fatigue loading is shown in Fig. 5.58. The degradation of stiffness at all stress levels is gradual, the amount of degradation increasing with increase in stress level. This is unlike three stage stiffness degradation that has been reported for continuous glass fibre composites. This is also unlike hemp fibre composites which showed little degradation at similar normalised stress levels.

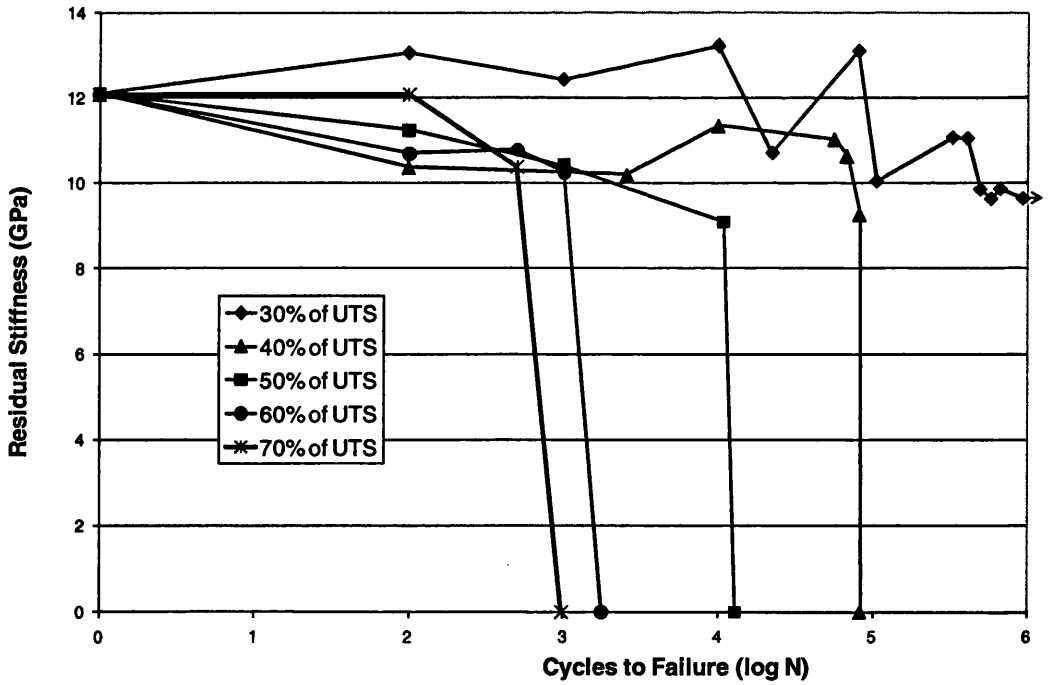

Fig. 5.58: Stiffness degradation of CSM glass fibre composites at different stress levels

The samples tested at 30% of UTS suffered a stiffness degradation of about 20% during its fatigue life. The sample endured 10^6 cycles and the surface of the sample was inspected and compared with an untested sample. As shown in Fig. 5.59, although there was no evidence of crack formation on the surface of the sample, the sample exhibited considerable whitening compared to untested sample. This was consistent with the fact that first damage mechanism in fatigue loading in CSM glass fibre composites is debonding [352] . The stress at this stage was not enough to initiate matrix cracking.

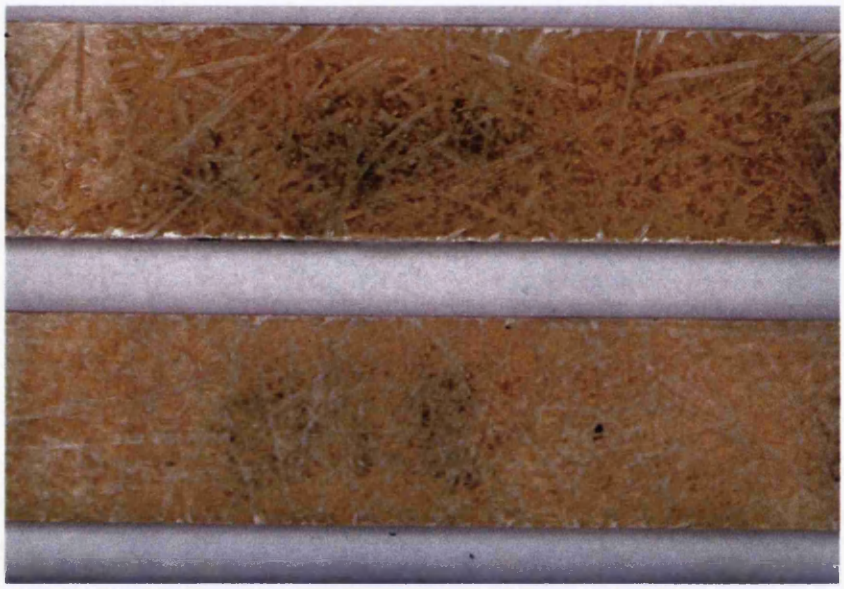

Fig. 5.59: Surfaces of glass fibre composites that endured 10^6 cycles at Fatigue Stress of 30% of UTS (bottom) and untested composite (top)

Samples fatigue tested at stress levels of 40% and 50% of UTS also showed about 20% reduction in modulus before fracturing. Sample fatigue tested at stress levels of 60% of UTS showed immediate decline in modulus. The surface of the sample was monitored and it was observed that a crack formed on the surface of the sample after only 1000 cycles, as shown by arrowhead in Fig. 5.60. Thus the higher stress level induced matrix cracking at early stage of fatigue life. This was also accompanied by fibre/matrix debonding resulting in whitening of the sample. The sample eventually broke at crack site after 1768 cycles. At same normalised stress level, hemp fibre composites resisted formation of crack on the surface until after 10,000 cycles and they were able to endure fatigue cycles of 45,500. This reinforced the better fatigue sensitivity of hemp fibre composites compared to glass fibre composites.

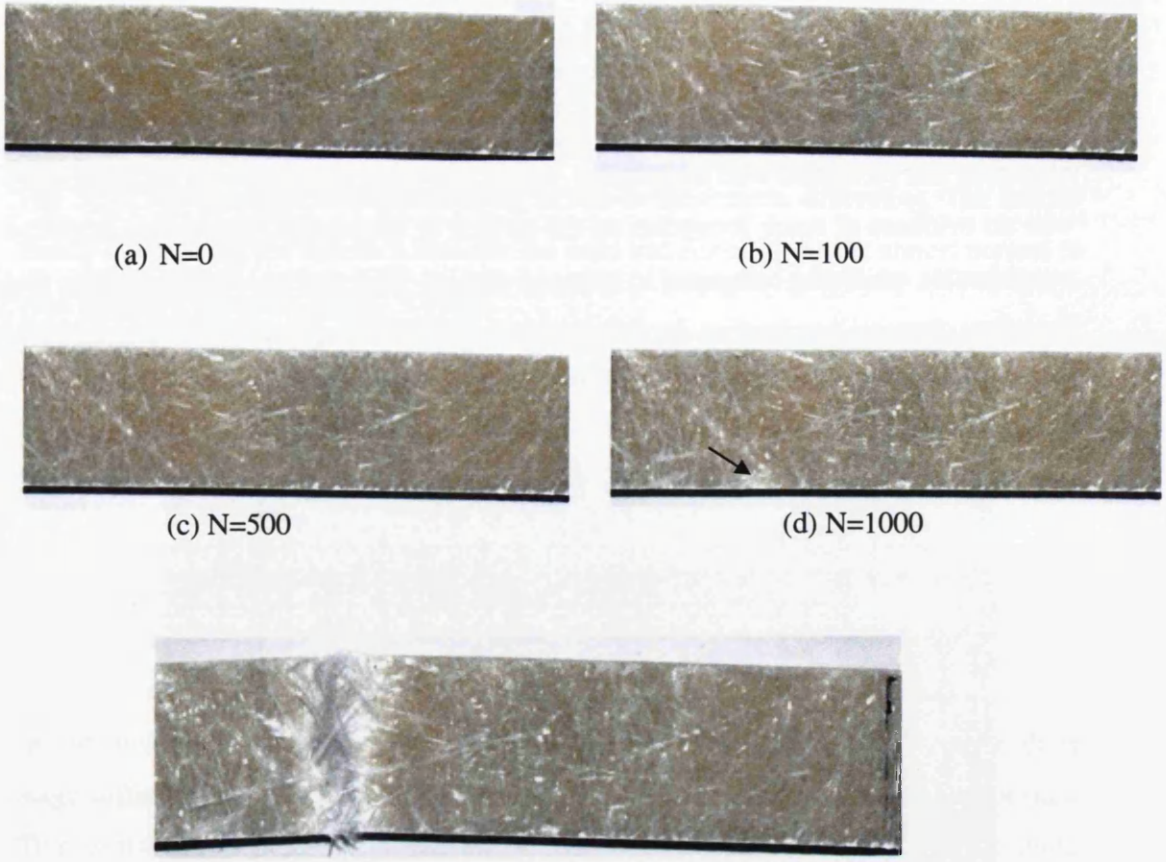

(a) N=0 (b) N=100

(c) N=500 (d) N=1000

(e) N=1768

Fig. 5.60: Surfaces of glass fibre composites after different fatigue cycles fatigue tested at stress level of 60% of UTS

Sample fatigue tested at stress level of 70% of UTS also showed sudden decline in stiffness after 100 cycles of loading, at which point a crack was seen to be forming on the surface as shown in Fig. 5.61 (b). Further application of fatigue stress resulted in rapid propagation of crack and debonding resulting in whitening of the sample. The sample broke after only 982 cycles. At similar normalised stress levels, hemp fibre sample was able to endure 17886 cycles and no crack was seen to be forming on the surface of the sample.

These studies have shown the correlation between fatigue sensitivity and stiffness degradation of hemp and glass fibre composites. At similar levels of normalised stress, hemp fibre composites are more successful at resisting propagation of cracks, thus exhibiting lower degradation in stiffness, compared to glass fibre composites. This results in improved fatigue sensitivity of hemp fibre composites.

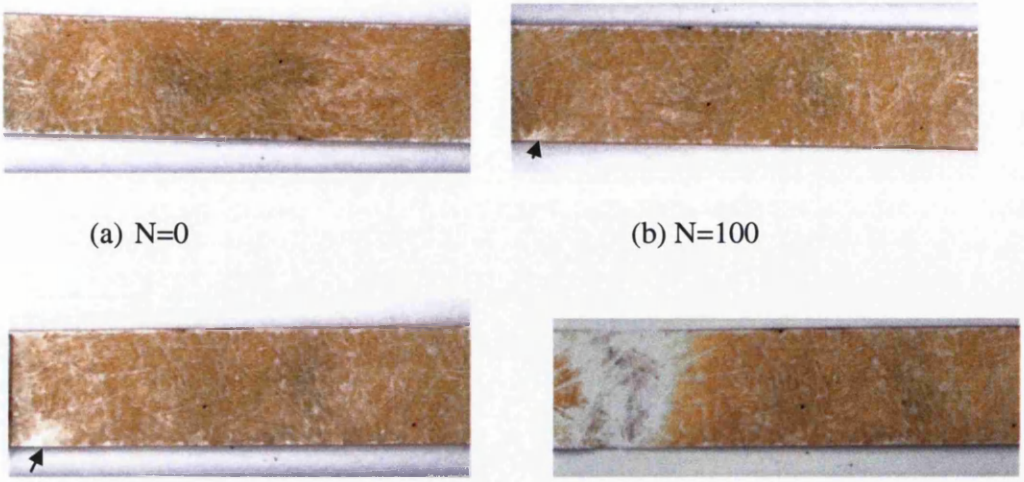

(a) N=0 (b) N=100

(c) N=500 (d) N=982

Fig. 5.61: Surfaces of glass fibre composites after different fatigue cycles fatigue tested at stress level of 70% of UTS

5.5.2.3 CSM Glass-Hemp Hybrid Composites

Fig. 5.62 shows stiffness degradation with increase in the number of cycles at different stress levels for hemp skin-glass core hybrid composites. Similar to hemp fibre composites, the stiffness degradation in composites is minimal with increase in number of cycles. This is consistent with the fact that hemp skin-glass core composites have the same fatigue sensitivity coefficient as the hemp fibre composites.

The effect of cyclic loading on residual stiffness of glass skin-hemp core composites is shown in Fig. 5.63. It is clear that in this configuration also the stiffness degradation is minimal with the increase in number of cycles. The fibre configuration does not seem to have any effect on stiffness degradation of hybrid composites and both kinds of configurations result in similar behaviour as for hemp fibre composites. The replacement of 11% of hemp fibres has not affected their fatigue properties and it continues to be dominated by hemp fibre properties.

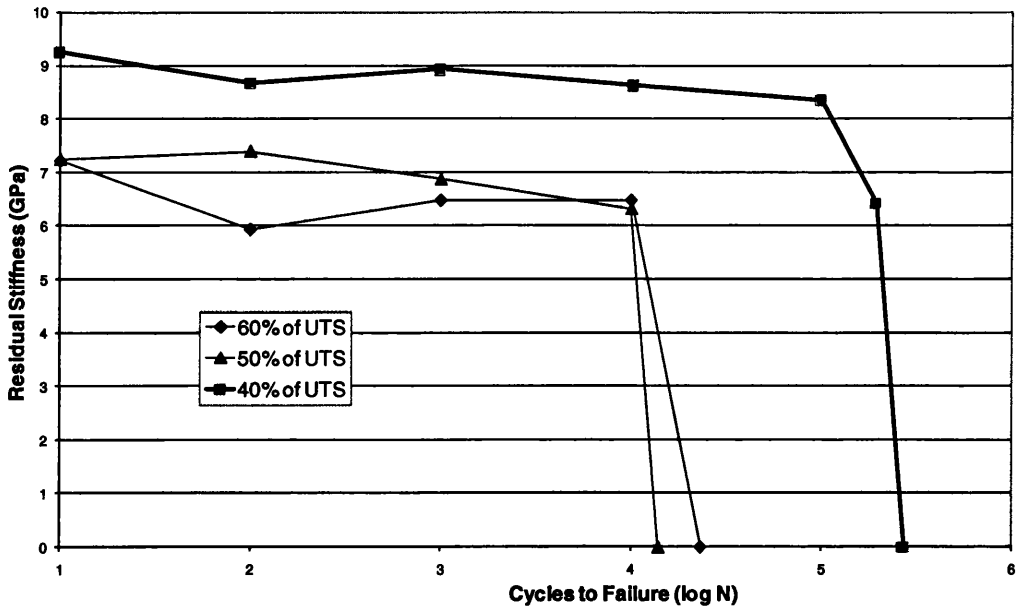

Fig. 5.62: Stiffness degradation of hemp skin-glass core hybrid composites at different stress levels

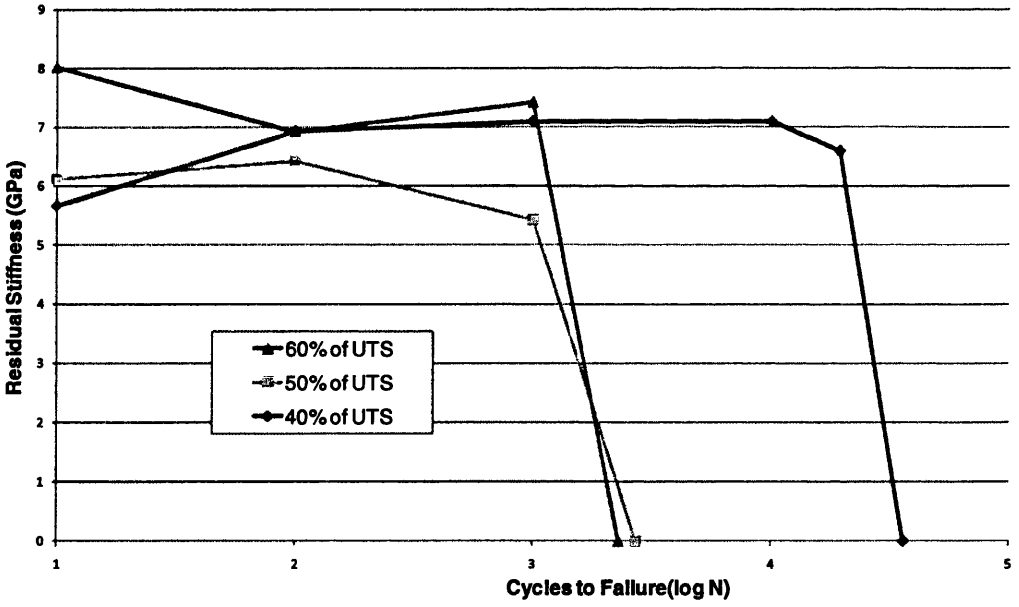

Fig. 5.63: Stiffness degradation of glass skin-hemp core hybrid composites

5.5.3 Fatigue properties following low velocity impact

5.5.3.1 Hemp Fibre Composites

The relatively poor low velocity impact properties of hemp fibre composites can also lead to degradation of their post-impact fatigue properties. It is therefore important to study the effect of low-velocity impact on their fatigue properties.

Samples of hemp fibre reinforced polyester composites that had been subjected to low velocity impact of energy levels of 1, 2, and 3J were subsequently fatigue tested in tension-tension mode at a frequency of 1 Hz (R=0.1). The S-N chart for samples impact tested following an impact energy of 1 J is shown in Fig. 5.64. The dashed lines represent 95% confidence interval of the linear regression line.

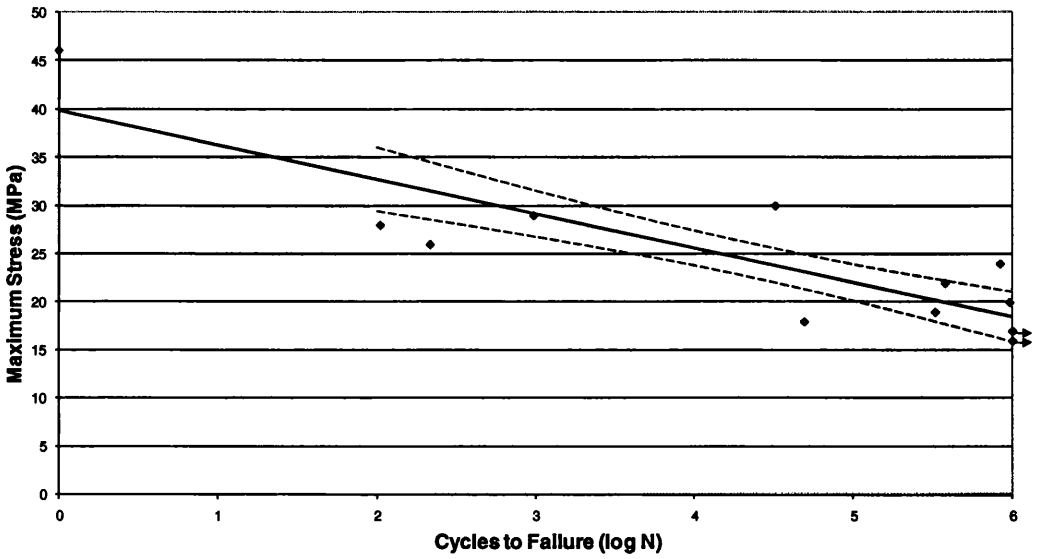

Fig. 5.64: S-N chart of composites following low velocity impact of 1J

The impact of 1J results in gradual decrease in fatigue strength of the samples with increase in number of cycles. It was shown in Section 5.4.1.2 that impact of 1J results in negligible reduction in tensile strength but 17% reduction in tensile stiffness. The deterioration in stiffness seems to have affected the fatigue properties with increase in slope and decrease in endurance limit compared to non-impacted composites. The value of the endurance limit of the samples has gone down to about 17 MPa following impact as against 20 MPa for non-impacted samples as shown by the arrowheads. The scatter in

data is also quite high following low-velocity impact shown by the points lying outside the 95% confidence interval which can be attributed to variation in structural integrity following low velocity impact.

The S-N chart for samples impact tested at 2J is shown in Fig. 5.65. As shown in Section 5.4.1.2, the tensile strength of composites had reduced by almost 45% and tensile stiffness by about 35% following low velocity impact at 2J. This corresponds well with the reduction in fatigue strength following 2J impact. The scatter in the data is again quite high. Fatigue testing of samples impact tested at 2J results in further reduction in fatigue strength, indicated by the reduction in endurance limit to about 11-12 MPa as shown by the arrowheads.

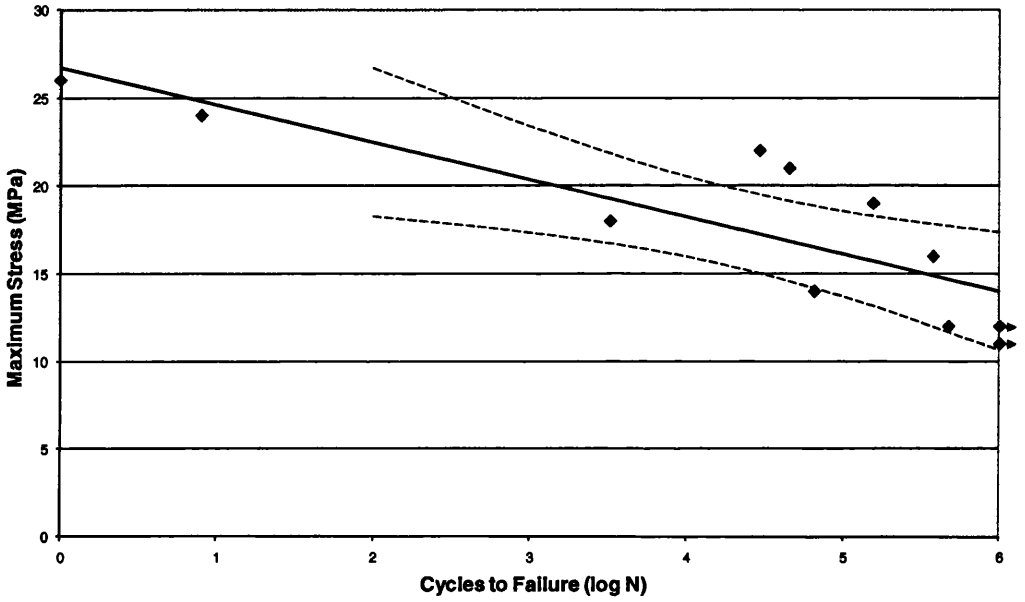

Fig. 5.65: S-N chart of composites following low velocity impact at 2J

The S-N chart for samples impact tested at 3J is shown in Fig. 5.66. Following impact at 3J energy, the tensile strength of these composites had reduced by 50% and tensile stiffness by 55%. This correlated with their reduction in fatigue strength. Fatigue testing of samples impact tested at 3J results in further reduction in fatigue strength of the composites. The endurance limit in this case has gone down to about 11 MPa as shown by arrowheads.

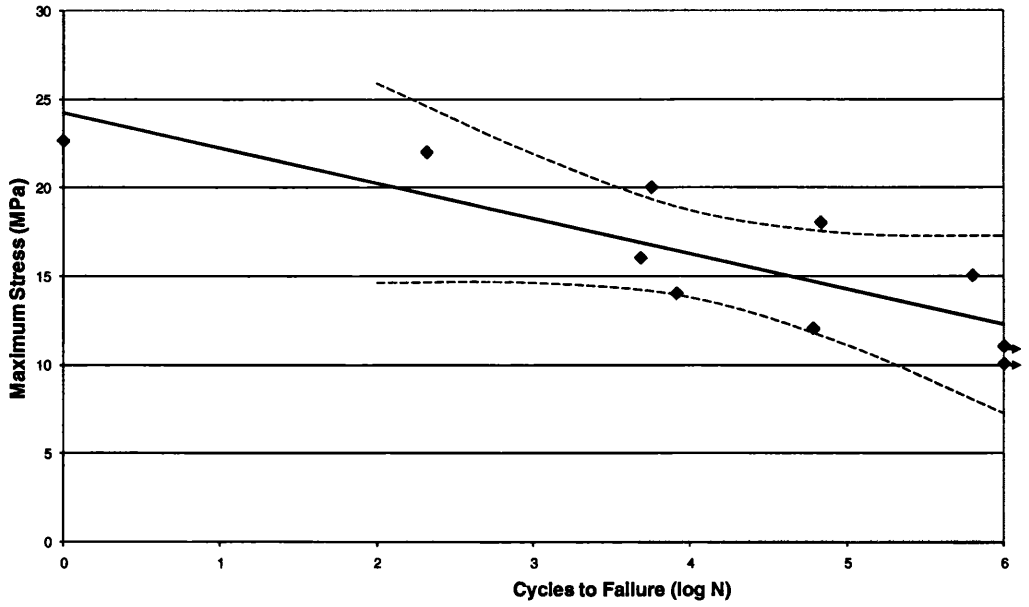

Fig. 5.66: S-N chart for samples impact tested at 3J

The fatigue sensitivity of the composites following low velocity impact can be best understood by comparing the normalised S-N curves and fatigue sensitivity coefficients of the composites following low velocity impact as shown in Fig. 5.67 and Table 5.13. Fig. 5.67 shows that the fatigue sensitivity of non impacted samples and the samples impact tested at 1 J is quite similar and their fatigue sensitivity coefficients are also quite similar. It is possible to draw same 95% confidence limit lines for both of these composites. This is consistent with the fact that an impact of 1J had negligible effect on residual tensile properties of composites.

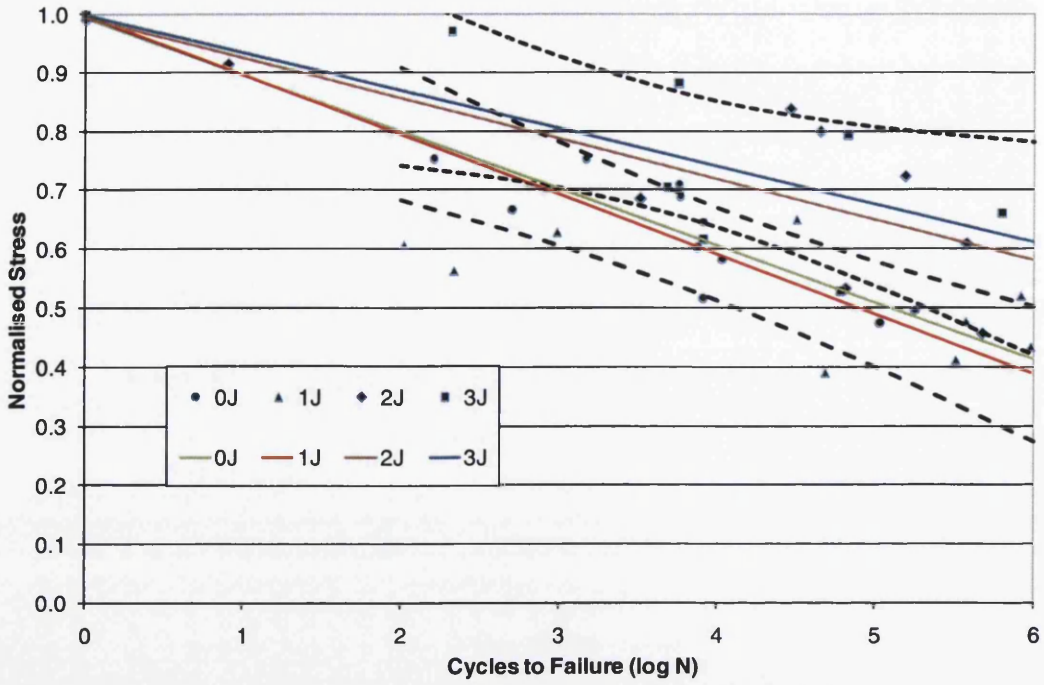

Fig. 5.67: Comparison of normalised S-N curves of impacted and non-impacted composites

Table 5.13: Fatigue sensitivity coefficients at different impact energy levels

Impact Energy (J)	Fatigue sensitivity coefficient
0	0.097
1	0.102
2	0.069
3	0.072

As shown in Section 5.4.1.2, these composites lost almost half of their intrinsic strength following impact at 2J and 3J. The normalised S-N curves of composites impacted at 2J and 3J are similar, resulting in similar values of fatigue sensitivity coefficients. This suggests that their fatigue sensitivity is similar once they have lost almost half of their tensile strength. It is again possible to draw same 95% confidence intervals for both kinds of composites.

Thus fatigue properties of hemp fibre composites following impact can be correlated with their residual tensile properties after impact. When normalised by their respective residual strength, the effect of impact damage becomes more clear and similarities can be drawn between 1J impacted samples with non-impacted samples, and 2 and 3J impacted samples.

5.5.3.2 CSM Glass Fibre Composites

The S-N curve of CSM glass fibre reinforced polyester following impact of 5J is shown in Fig. 5.68. The static strength of 5J impacted samples is reduced by about 25%. The decline is also reflected in poor fatigue resistance following impact and decline in the fatigue limit to about 40 MPa, compared to about 50 MPa for non-impacted composites.

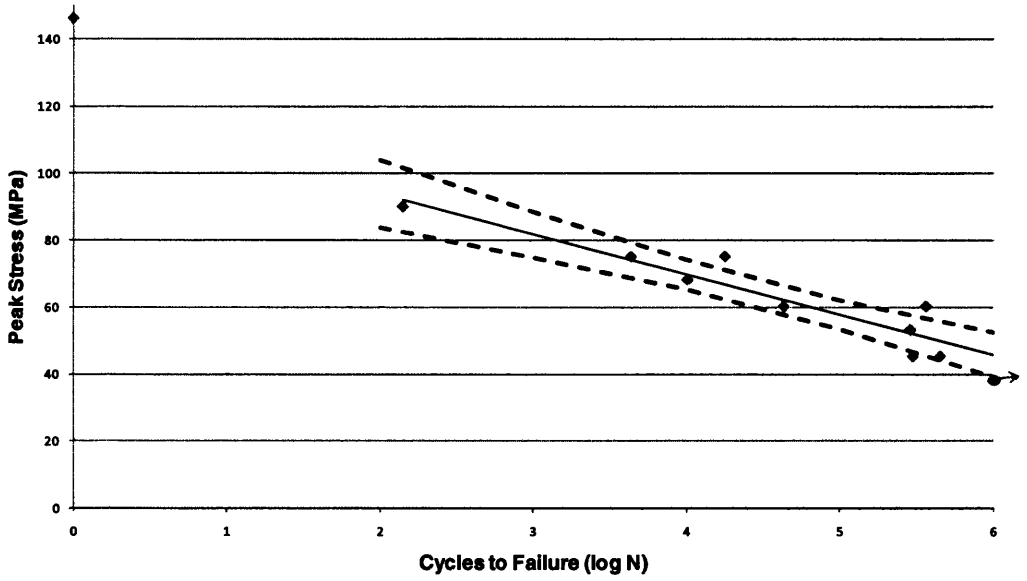

Fig. 5.68: S-N curve of glass fibre composites following 5J impact

The S-N curve of glass fibre composites following impact of 10J is shown in Fig. 5.69. The impact of 10J results in almost 40% reduction in static strength of composites and this is also reflected in the S-N chart with the endurance limit now reduced to about 35 MPa.

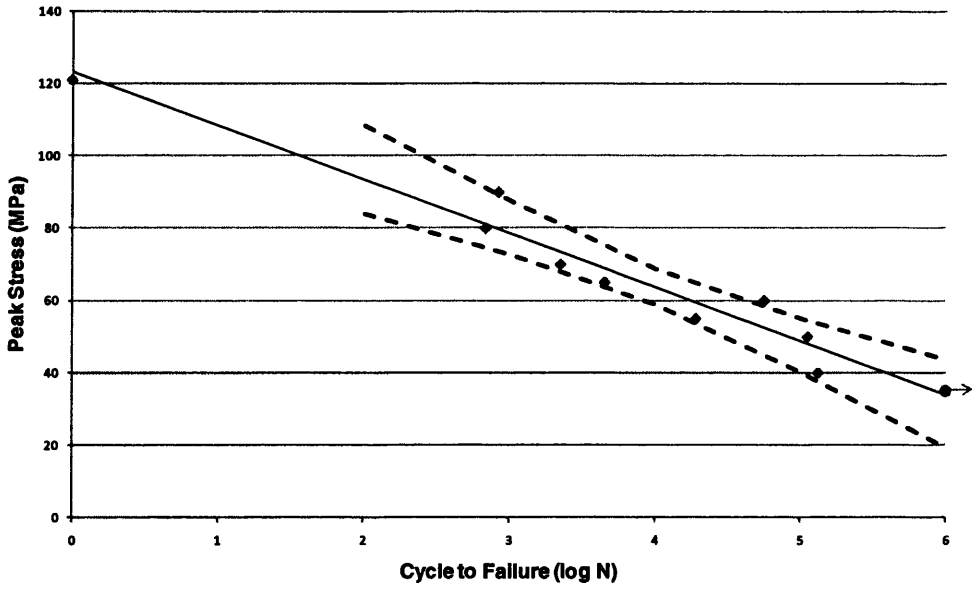

Fig. 5.69: S-N curve of composites following 10J impact

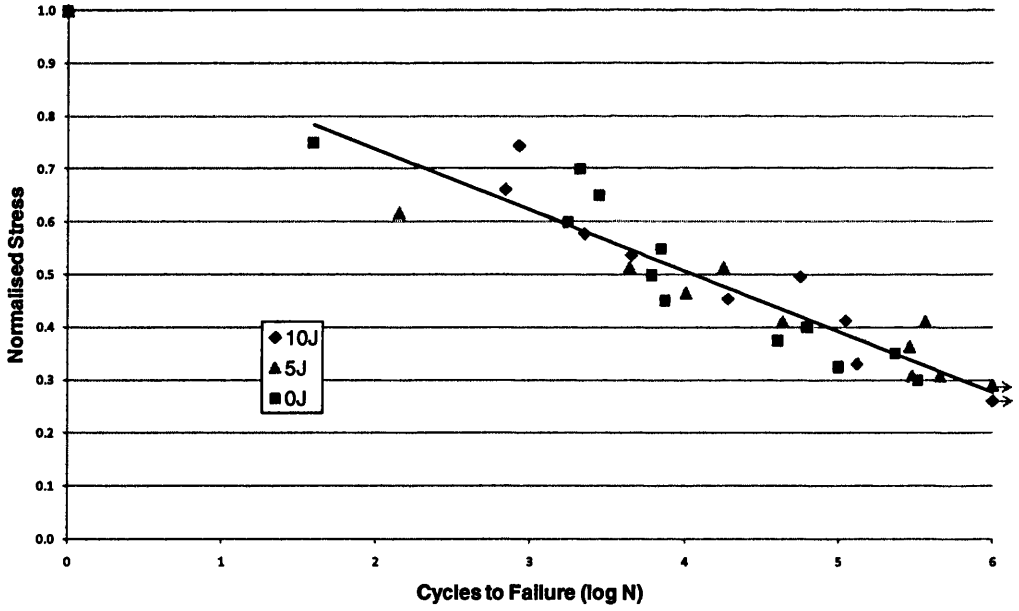

Fig. 5.70: Normalised S-N curve of CSM glass fibre reinforced polyester composites with impact damage

It has been shown [356] that for glass fibre reinforced polyester composites with $[\pm 45°]_4$ and $[0/90°]_{2s}$ fibre configurations, the normalised S-N data following low velocity impact can be represented by a single best fit line, suggesting that the impact induced damage does not significantly affect the fatigue sensitivity. Hence it is possible to

predict fatigue lifetimes of impact damaged composites by determining their residual tensile strength and the S-N curve of non-impacted composites. A similar result for CSM glass fibre reinforced polyester composites was observed in this research as shown in Fig. 5.70.

This seems to suggest that this is an intrinsic property of glass fibres and is independent of the fibre configuration. When normalised by their respective residual tensile strength, hardly any effect of impact damage on fatigue life can be found for glass fibre composites.

5.5.4 Fatigue in tension-compression loading

The compressive behaviour of composite materials has been called their 'Achilles heel' [15] and tension-compression loading is considered to be the worst fatigue loading condition for composite materials. The fatigue lives of synthetic fibre composites are shorter in tension-compression loading than in tension-tension and zero-tension loading. This has been attributed to laminate plies, without fibres in the test direction, developing inter-ply damage and causing local layer delimitation buckling [357]. Because of greater demand on the matrix and the interface in compressive loading, they have greater effect on compressive fatigue behaviour of composite materials than in tensile fatigue. In addition, local resin and interfacial damage lead to fibre instability in compressive loading that is more severe than the fibre fracture that occurs in tensile loading [218]. The tension-compression fatigue loading has been shown to decrease the fatigue strength and increase the slope of S-N curve compared to tension-tension loading for unidirectional and multidirectional graphite-epoxy laminates [218]. The only available example in literature for tension-compression fatigue studies of natural fibre composites is for sisal-epoxy laminates [354].

The comparison of S-N curves in tension-tension and tension-compression fatigue is shown in Fig. 5.71. The S-N curve in tension-tension fatigue is above that of tension-compression fatigue at all points, showing lower fatigue strength in tension-compression fatigue. This is also evidenced by reduction in endurance limit to about 12 MPA in tension-compression as against 20 MPa in tension-tension loading. The fatigue sensitivity coefficient is much higher in tension-compression loading at 0.122 as against 0.097 in tension-tension loading, indicating greater fatigue sensitivity in tension-compression.

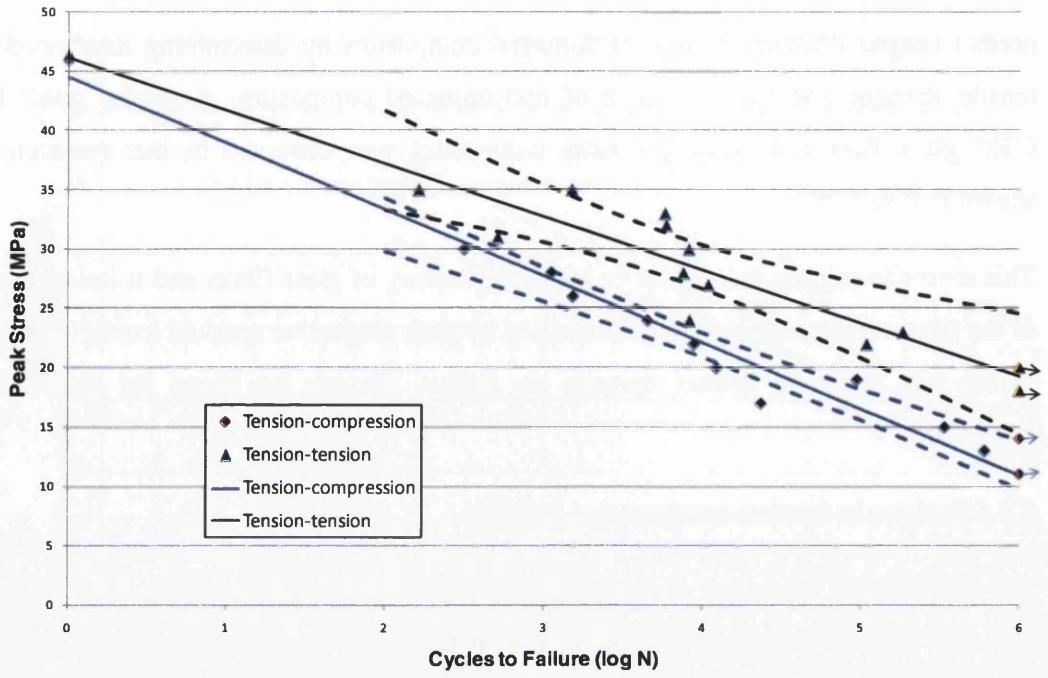

Fig. 5.71: S-N curve of hemp fibre composites in tension-compression fatigue loading

Fig. 5.72: Fractured sample in tension-compression fatigue

The fracture of the samples was still normal to the applied load as shown in Fig. 5.72.

5.6 FLEXURAL PROPERTIES

In many applications, the composite materials are subjected to flexural stresses and it is important to know their flexural properties. The flexural properties of hemp fibre composites was determined by using three point bending tests as described in Chapter 3.

The average fibre weight fraction of these composites was 53%. The results of flexural testing are given in Table 5.14.

Table 5.14: Flexural Properties of hemp fibre composites

Flexural Strength (MPa)	**91.9 (8.6)**
Flexural Modulus (GPa)	**5.9 (0.6)**
Strain to break (%)	**2.7 (0.2)**

These values are consistent with the values reported by other researchers for hemp fibre-polyester composites. Sebe et al [124] reported the flexural strength and modulus at 30% fibre weight fraction to be 115 MPa and 7.5 GPa respectively. Rouison et al [146] reported the values of flexural stress and modulus at 20% fibre volume fraction to be 55 MPa and 5 GPa respectively.

Fig. 5.73: Fracture surfaces of flexural tested sample

The macrographs of flexural tested samples are shown in Fig. 5.73. From the macrographs of the samples, it is evident that the dominant mode of fracture in these samples is the tensile fracture of the outer surface, shown by the arrowhead. No interlaminar shear fracture was observed because of the same fibre geometry in the laminae, which precludes any bending stiffness mismatch which can initiate interlaminar shear fracture. Thus flexural strength of this material seems to be determined by the tensile strength of hemp fibres.

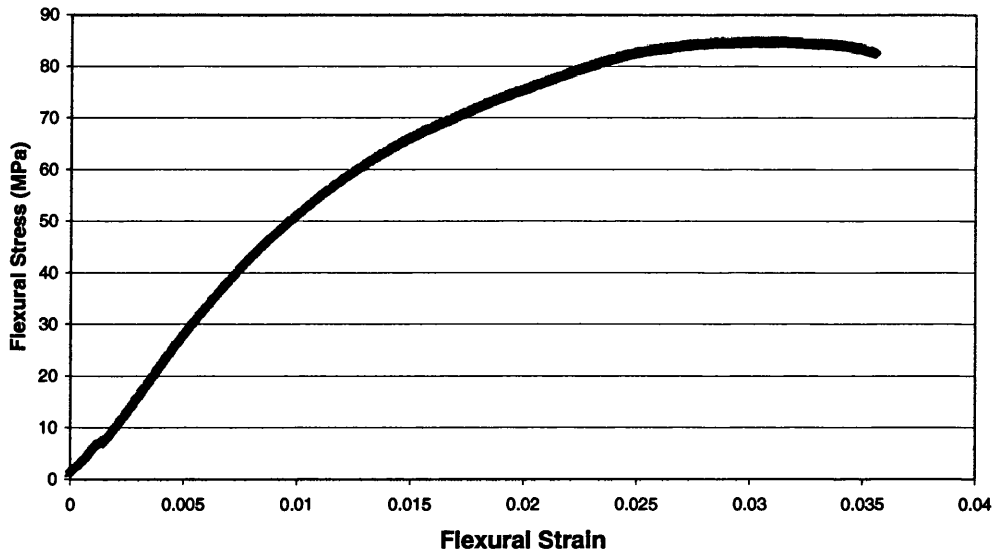

Fig. 5.74: Flexural stress versus strain curve of a typical sample

The flexural stress-strain curve of a typical sample is shown in Fig. 5.74. The initial slope of the curve is relatively constant. At about half of the flexural strength, the slope starts to decrease indicating the onset of fracture in the outer surface. The polymers matrix, with lower strain to failure, is expected to fracture first, transferring the load to fibres. Further application of stress results in fibre/matrix debonding and fracture of the fibres. The slope goes on decreasing until the sample attains its maximum flexural strength at a strain value of about 2.7%.

6. MECHANICAL PROPERTIES OF SURFACE TREATED HEMP FIBRE REINFORCED POLYESTER COMPOSITES

In this part of the research, hemp fibres were subjected to various surface treatments to try to improve the fibre properties and fibre-matrix interfacial bonding and determine their effects on mechanical properties of hemp fibre reinforced polyester composites. Four different kinds of surface treatments were used: heat treatment, alkalisation, acetylation and plasma treatment.

6.1 HEAT TREATMENT

Hemp fibres were subjected to various heat treatments in order to study their effect on the mechanical properties of the composites made from these fibres. Exposing the fibres to elevated temperatures can result in changes in their physical and mechanical properties as discussed in Section 4.1.3. Rong et al [358] reported 37% increase in tensile strength but no change in tensile modulus of sisal fibres following heat treatment at 150°C for 4 hours. The composites made from heat treated fibres in epoxy matrix also showed improvement in tensile and flexural properties compared to non-treated fibre composites. From their studies on jute fibre reinforced epoxy composites, Gassan and Bledzki [67] reported that the tensile strength of composites with maximally pre-dried fibres (moisture content approximately 1 wt. %) increased by about 10% compared to minimally dried fibres (moisture content approximately 10 wt %). The tensile modulus was found to increase by about 20%. The void content in the composites was also found to decrease from 7 volume% at no moisture loss to 0.5 volume % at 10% moisture loss.

The heat treatment can result in three kinds of significant changes in the fibres: increase in surface energy, removal of moisture and changes in microstructure of the fibres. Studies done on hemp fibres by Prasad et al [57] have shown that the non-polar surface

energies of fibres heat treated at 40, 60 and 80°C were higher than those of untreated ones. This indicated a decrease in hydroxyl groups on the fibre surface leading to increased hyrophobicity and less polarity. Higher non-polar surface energy of fibres should result in better interaction between the fibres and the non-polar polymer resin.

As shown in Section 4.1.2, hemp fibres used in this research contained approximately 10% moisture. Removal of moisture can be very useful in improving the interfacial bonding between the fibres and the matrix because water on the fibre surface acts like a separating agent in the fibre-matrix interface [45]. Additionally because of the evaporation of water during the reaction process with thermoset resins (most of which have reaction temperature of over 100°C), voids can form in the composites. Both of these phenomena can result in decrease in mechanical properties of natural fibre reinforced composites. On the other hand removal of moisture can make natural fibres brittle which can decrease their effectiveness as a reinforcement. For cellulose fibres, the tensile strength usually increases with increase in moisture and decreases with increase in temperature [10].

The changes in microstructure of the fibres can also have a significant effect on the mechanical properties of the fibres and hence of the composites made from them. Heat treatment at up to 200°C can result in increase in crystallinity index of fibres due to rearrangement of molecular structure at high temperatures. Natural fibres start to degrade at temperatures of above 150°C which may have an adverse effect on their properties. The oxidation of the fibre surface following heat treatment is another aspect that is crucial with respect to fibre/matrix interfacial bonding and hence the mechanical properties of the composites.

Three different temperatures were selected for heat treatment of hemp fibres: 100°C, 150°C, and 200°C. The fibres were kept in the oven at these temperatures for 30 minutes each. The heat treatment time of 30 minutes was chosen because, as shown in Section 4.1.2, this time was sufficient to remove most of the moisture from the fibres at a particular temperature.

The fibre weight fraction of heat treated fibre composites was lower than that of non-treated fibre composites made at 3MPa pressure. This was expected since, as shown in

Section 4.1.2, heating the fibres to 100°C resulted in almost 8.5% reduction in weight because of removal of moisture. The weight reduction was 9% for fibres heated at 150°C and 10% for fibres heated at 200°C. It was also observed that the laminates made from heat treated fibres showed less spillage of resin following compression moulding than non-treated fibre composites. This indicated improved wetting of fibres by the resin which can be attributed to increase in non-polar surface energy of the fibres following heat treatment. This again may have contributed to reduced fibre weight fraction of composites following heat treatment.

6.1.1 Tensile Properties

The tensile properties of heat-treated fibre composites are shown in Table 6.1 and compared in Figs. 6.1-6.2. The numbers in parentheses are standard deviations.

Table 6.1: Tensile Properties of Heat Treated Fibre Composites

Heat Treatment Temperature	**Room Temperature**	**100°C**	**150°C**	**200°C**
Fibre weight fraction (%)	47	47	46	34
Tensile Strength (MPa)	35.8 (4.2)	40.1 (6.0)	39.8 (5.7)	32.8 (5)
Tensile Modulus (GPa)	5.6 (0.7)	7.2 (0.3)	6.4 (0.9)	6.3 (0.8)
Strain to Failure (%)	0.94 (0.19)	0.80 (0.22)	0.93(0.15)	0.60 (0.13)

Since the fibre weight fraction of heat-treated fibre composites was considerably less than that for untreated fibre composites made at 3 MPa moulding pressure, it is not realistic to compare their properties. Therefore the properties of untreated fibre composites made at moulding pressure of 1MPa, which had similar fibre weight fraction to heat treated fibre composites, have been used in Table 6.1 and Figs. 6.1-6.2.

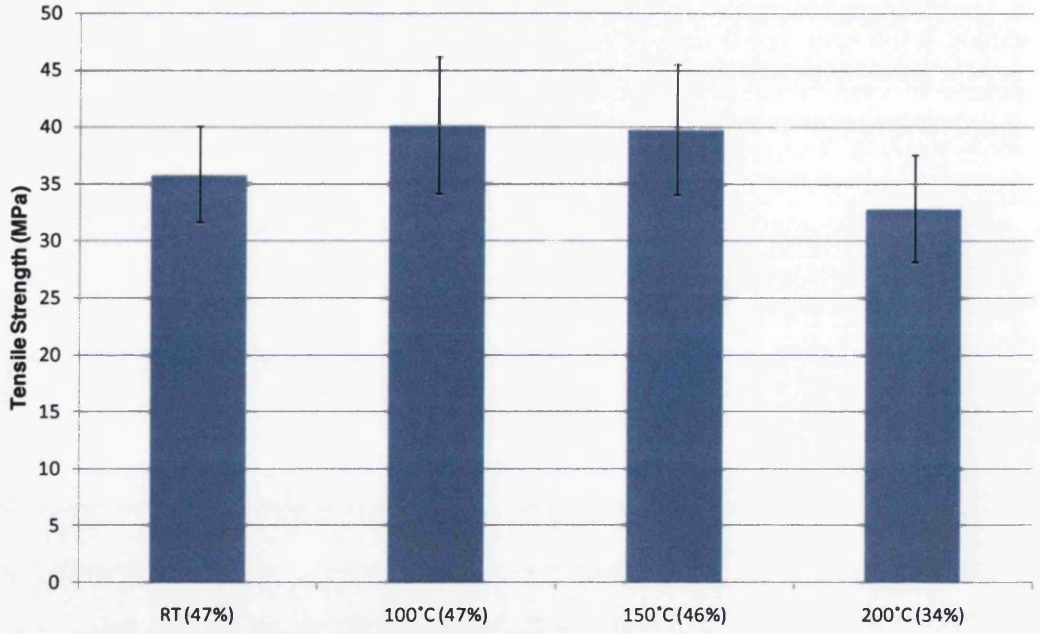

Fig. 6.1: Effects of different fibre heat treatments on tensile strength of composites (fibre weight fractions in parentheses)

Fig. 6.1 shows that tensile strength of composites made from heat treated fibres does show improvement in tensile strength. The increase in strength is approximately 15% compared to untreated fibre composites. However the increase in strength is similar for the fibres heat treated at 100°C and 150°C. This is not unexpected since the amount of moisture removed from fibres at these temperatures is quite similar. Although there was some evidence of oxidation of fibres heat treated at 150°C, this does not seem to have any effect on composites' strength. The composites made from fibres heat-treated at 200°C show considerable decline in tensile strength. The most probable reason for this is that above 150°C considerable changes in the structure of the fibres start to take place. Heat treatment at 200°C leads to increased oxidation, pyrolysis and degradation of fibres. Peters and Still [359] have contended that between 150 and 240°C, gradual degradation of natural fibres occurs which includes depolymerisation, hydrolysis, oxidation, dehydration and decarboxylation, which lead to the decomposition of fibres. The composites made from these fibres have significantly lower fibre weight fraction. This combined with the degradation of the fibres means that the composites made from these fibres have lower tensile strength. Heat treatment at this temperature also results in

embrittlement of fibres which is evidenced in considerable reduction in strain to failure of composites (see Fig. 6.8).

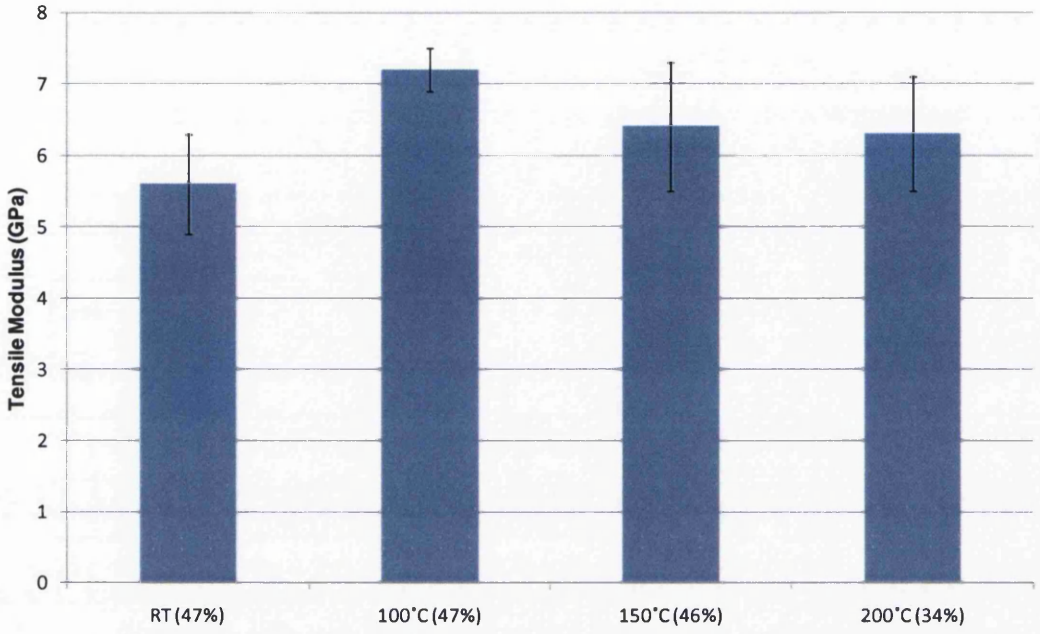

Fig. 6.2: Effects of different fibre heat treatments on tensile modulus of composites (fibre weight fractions in parentheses)

Fig. 6.2 shows the effect of different heat treatments of fibres on tensile modulus of composites made from them. The heat treatment of fibres results in improvement in tensile modulus of composites and the improvement is observed at all three treatment temperatures. The improvement in modulus is approximately 30% for 100°C treated fibre composites and approximately 15% for 150°C treated fibre composites compared to untreated fibre composites. The improved fibre/matrix interfacial bonding because of removal of moisture and increase in surface energy of fibres can be attributed to this increase in modulus. Even degradation of fibres heat treated at 200°C does not seem to have much deleterious effect on the modulus of composites made from these fibres. The probable reason for this is the increase in brittleness of fibres following this treatment which seems to have made the composites stiffer.

The heat treatment of fibres did not result in any changes in fracture behaviour of the samples in tensile testing and they failed in a completely brittle manner. A comparison

of stress-strain curves of heat treated fibre composites with that of non heat treated fibre composites is shown in Fig. 6.3.

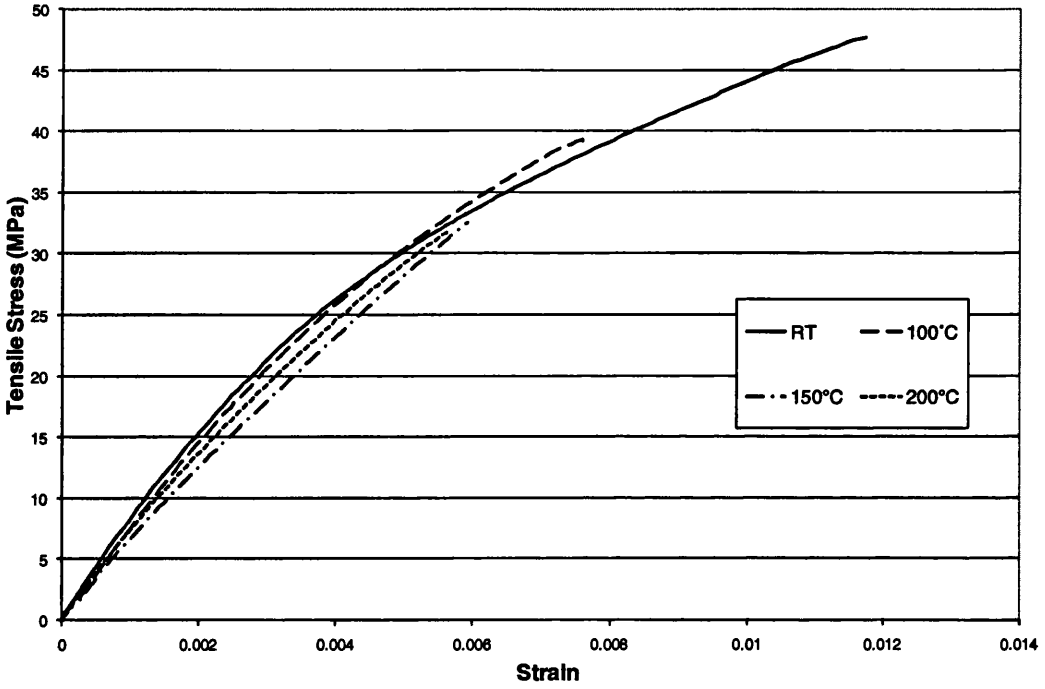

Fig. 6.3: Comparison of stress-strain curves of heat treated fibre composites with untreated fibre composites

This part of the research has shown that heat treatment of fibres does result in some improvement in tensile properties of the composites. However most of the increase in strength and stiffness can be gained by heating the fibres at 100°C. Heating the fibres at higher temperatures does not necessarily result in any further improvement in properties of composites. Heat treatment, therefore, may not be a very efficient method of improving the surface properties of the fibres, as it will also incur extra costs in power consumption. If the fibres are to be pre heat treated for a particular requirement, the heat treatment temperature should be limited to up to 100°C.

6.1.2 Impact Properties

The heat treated fibre composites were tested in low velocity impact to study impact damage tolerance of these composites. The impact testing regime was the same as for untreated fibre composites.

Fig. 6.4 shows the comparison of residual tensile strength of heat-treated and untreated fibre composites following low velocity impact. It is clear from the graph that untreated fibre composites start off by having better tensile strength without impact and maintain their edge in residual strength following impact at all energy levels. The composites with 100°C treated fibres show a threshold impact energy of 1J like untreated fibre composites but then they show gradual decline in residual strength with increase in impact energy. The composites with fibres treated at 150°C and 200°C show decline in strength even at impact energy of 1J indicating their poor impact damage tolerance. The composites from fibres treated at 200°C have the lowest residual strength following impact at all energy levels.

In order to understand the impact damage tolerance of heat-treated fibre composites, their residual strength was normalised at each impact energy level by dividing by their un-impacted strength. The resulting graph is shown in Fig. 6.5. From the figure, it is clear that heat treatment does not result in any improvement in impact damage tolerance of heat treated fibre composites. The composites made from 200°C treated fibres show considerable degradation in their impact damage tolerance which can be related to degradation in the fibre properties following heat treatment at 200°C. The composites made from untreated fibre composites lost almost 70% of their strength following impact at 4J. For composites made from fibres heat treated at temperatures of 100°C and 150°C the loss in strength is about 80% at same energy level. The composites made from fibres treated at 200°C lose almost all of their strength at impact energy of 4J.

Fig. 6.6 shows the comparison of residual tensile stiffness of the heat-treated and untreated fibre composites following low velocity impact. All the heat treated fibre composites show gradual decline in stiffness with increase in impact energy level. The composites made from fibres heat treated at 200°C are again the least damage tolerant in terms of residual stiffness.

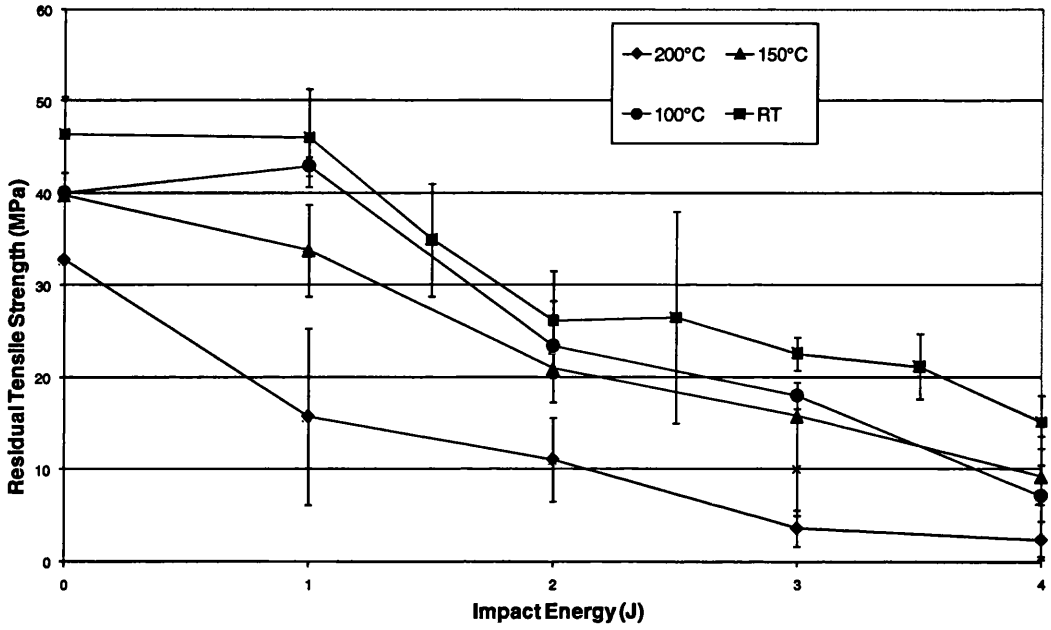

Fig. 6.4: Comparison of residual tensile strength of heat-treated and untreated fibre composites following low velocity impact

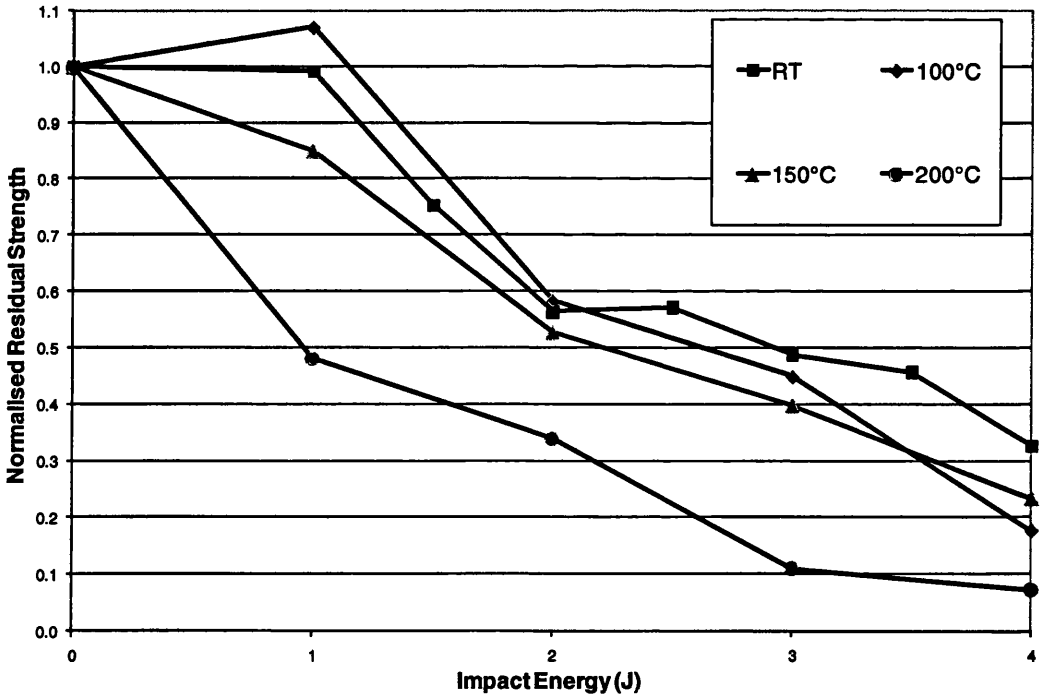

Fig. 6.5: Comparison of normalised residual strength of heat-treated and untreated fibre composites

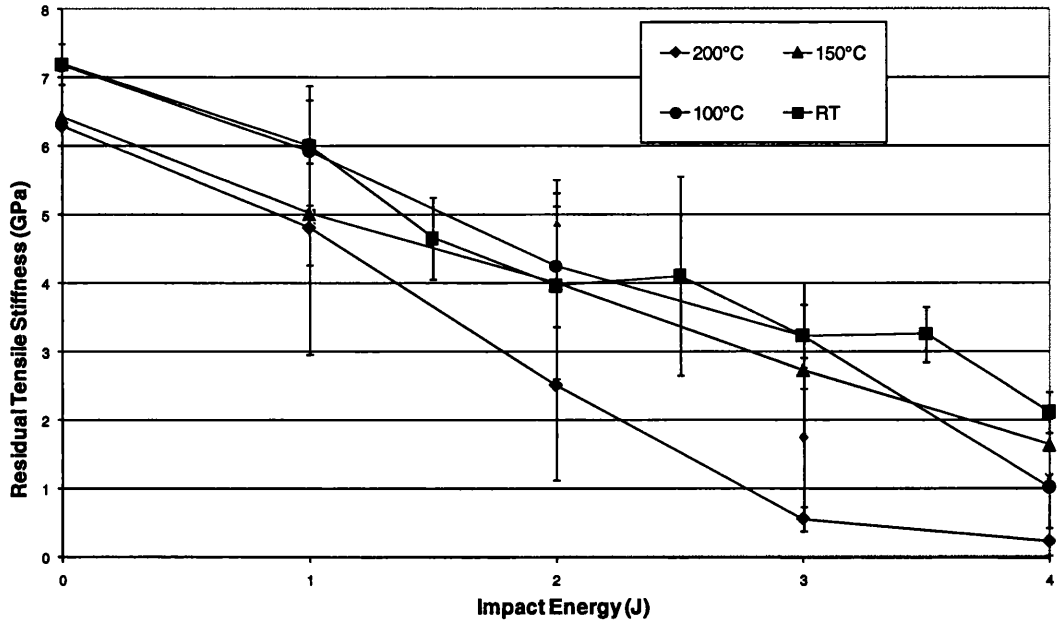

Fig. 6.6: Comparison of residual tensile stiffness of heat-treated and untreated fibre composites following low velocity impact

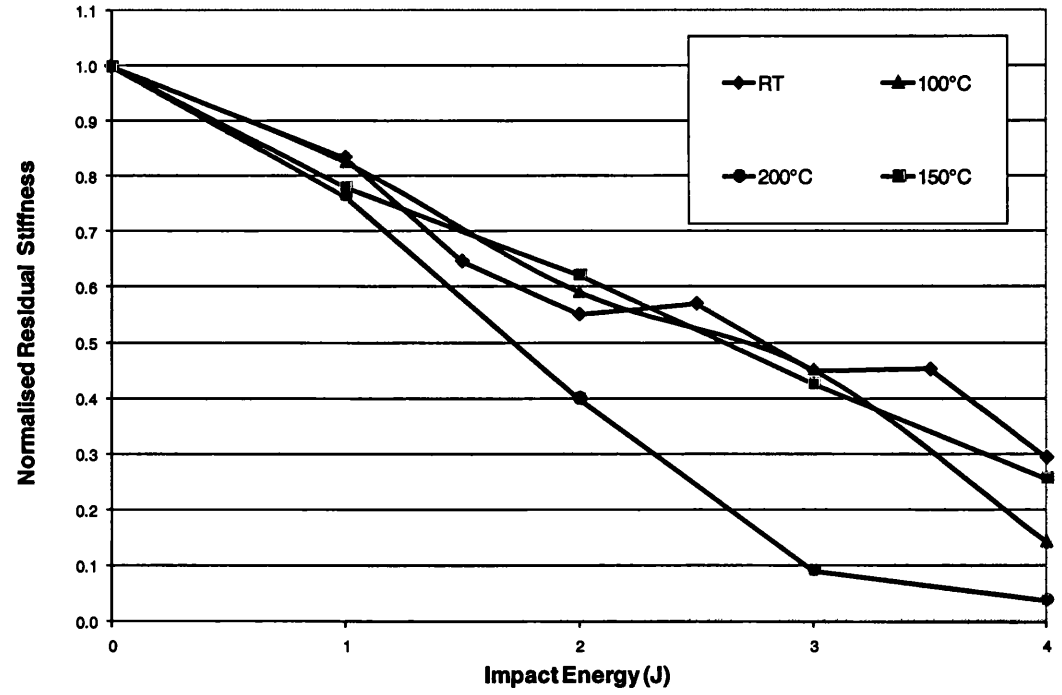

Fig. 6.7: Comparison of normalised residual stiffness of heat-treated and untreated fibre composites

The impact damage tolerance of composites in terms of normalised residual stiffness is shown in Fig. 6.7. Following impact at energy level of 4J, 100°C and 150°C treated fibre composites lost almost 80% of their original stiffness. The composites made from untreated fibres lost 70% of their original stiffness at impact energy of 4J. 200°C treated fibre composites lost almost all of their intrinsic stiffness following impact energy of 4J.

The comparison of strain to failure of heat-treated and untreated fibre composites following various impact energies is shown in Fig. 6.8.

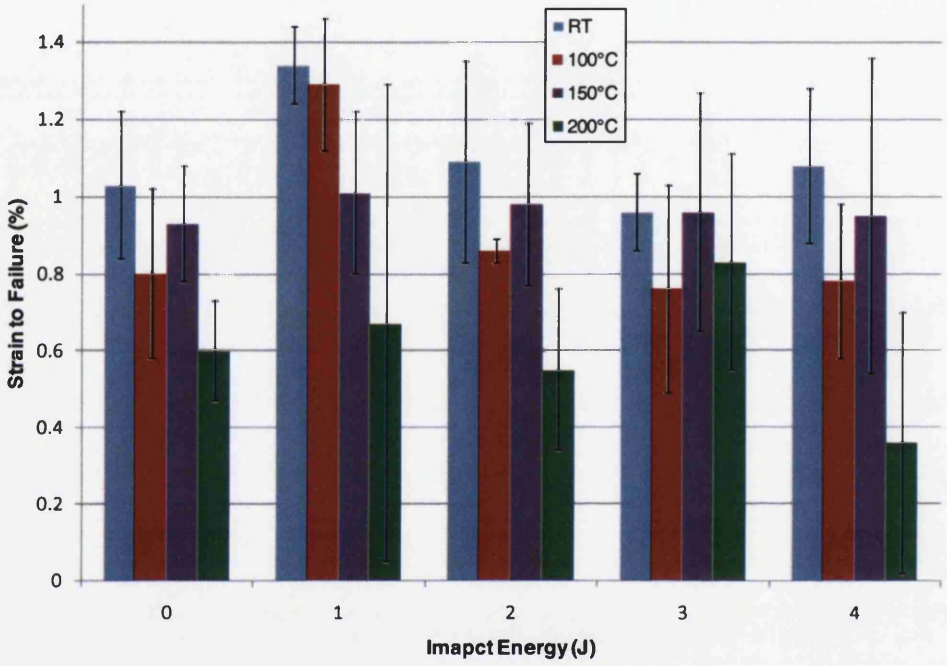

Fig. 6.8: Comparison of strain to failure of heat-treated and untreated fibre composites following low velocity impact

It is clear that at all energy levels the strain to failure of heat treated fibre composites is mostly reduced compared to non-treated fibre composites which points at increased brittleness of fibres following heat treatment. This also points at reduction in energy absorption capacity of composites following fibre heat treatment since it is proportional to area under the stress-strain curve. The decline in impact damage tolerance of composites impact can be mostly attributed to increase in brittleness of fibres, and hence decrease in strain to failure, as a result of heat treatment. The lower fibre weight fraction of the heat-treated fibre composites compared to non heat-treated fibre

composites can also be a factor in their reduced impact properties. It is thus concluded that heat treatment of hemp fibres does not result in any appreciable improvement in impact damage tolerance of hemp fibre composites.

6.1.3 Fatigue Properties

Composites made with pre-heat treated hemp fibres at 100°C were tested in tension-tension fatigue (R=0.1) at 1 Hz frequency. The comparison of S-N curves of heat-treated and untreated fibre composites is shown in Fig. 6.9. From the curves it can be seen that heat treated fibre composites have similar slope of curve and similar endurance limit of about 20 MPa to untreated fibre composites. Thus the fatigue strength of heat-treated fibre composites does not seem to show any measurable improvement compared to untreated fibre composites. However it should be appreciated that these composites had lower fibre weight fraction (47%) compared to untreated fibre composites (52%).

In order to compare the fatigue sensitivity of these composites with untreated fibre composites, their S-N curves were normalised by dividing their peak stress by static strength and the comparison of the curves is shown in Fig. 6.10. This curve also took into account their lower static strength because of lower fibre weight fraction. The figure shows slightly improved fatigue properties of heat-treated fibre composites which is also reflected in higher fatigue sensitivity coefficient value of 0.090 compared to non heat treated fibre composites, 0.097. However this does not represent a significant improvement in fatigue sensitivity. The fracture of heat treated fibre composites continued to be brittle in fatigue with no cracks visible on the surface of the samples during testing. Thus no appreciable improvement in fatigue properties of composites was observed for 100°C fibre treated composites.

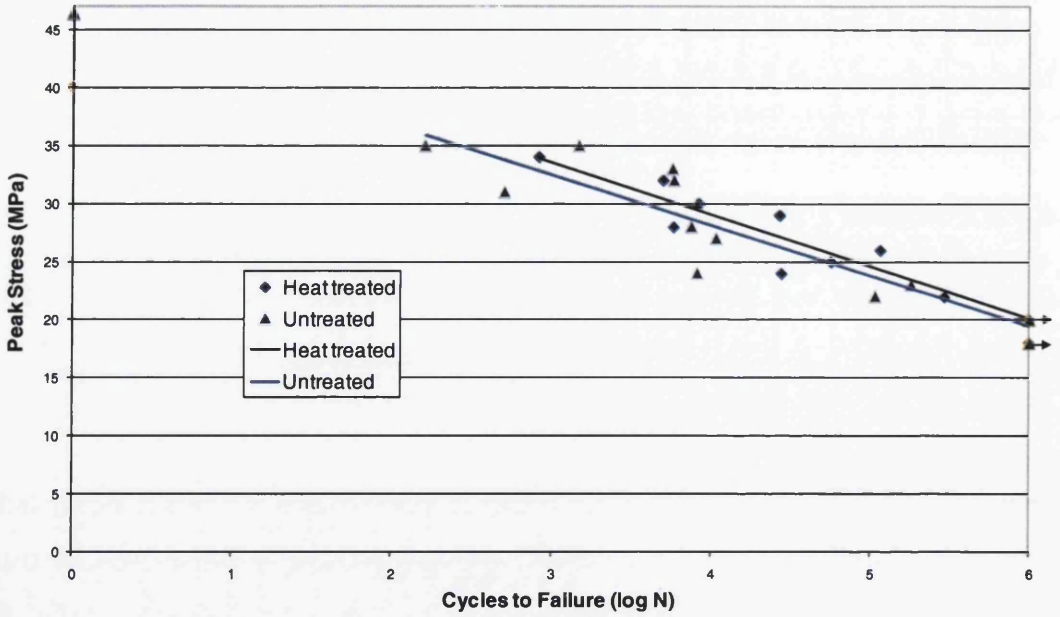

Fig. 6.9: Comparison of S-N curves of heat-treated and untreated fibre composites in tension-tension fatigue

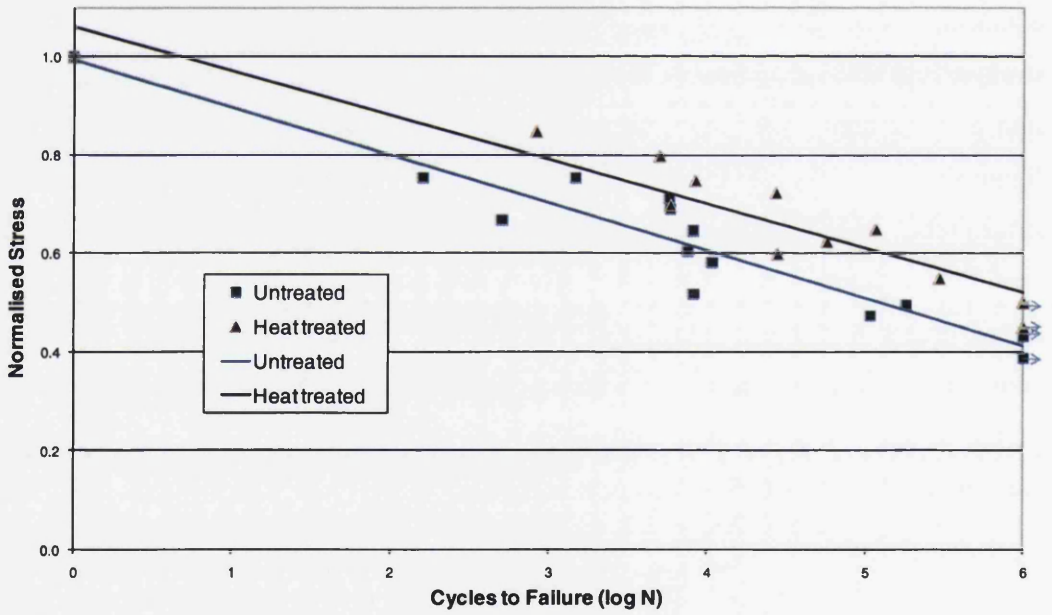

Fig. 6.10: Comparison of normalised S-N curves of heat-treated and untreated fibre composites

By comparing the tensile, impact, and fatigue properties of heat-treated fibre composites with those of untreated ones, it is clear that no appreciable improvement in mechanical properties can be gained by heat treatment of fibres. Some improvements in tensile and fatigue properties were observed for 100°C heat-treated fibre composites. The mechanical properties, especially post-impact residual properties, start to show deterioration for fibres heat treated at 150°C and above. The heat treatment will add up to the expense of making composites which does not seem to be justified when compared with the improvement gained in mechanical properties. So other methods of fibre surface treatment were explored to determine their effects on the mechanical properties of these composites.

6.2 ALKALISATION

Alkalisation is the most widely used process for the surface treatment of natural fibres because of its low cost, effectiveness, and convenience of use. A literature search reveals that it is the most common and efficient method of chemical modification and has been used to treat almost all natural fibres with successful results [46]. However the effect of this treatment on the impact and fatigue properties of hemp fibre composites has not been studied in detail.

There are two main parameters to be considered while carrying out the alkalisation process: NaOH concentration and treatment time. Unfortunately this process has not been standardised as yet and researchers have been using a range of concentration and treatment times in this process. In the initial stages of this research, 10% concentration of NaOH was used for 24 hours in this process. However, soon it became clear that this concentration was too high and was actually causing damage to the fibres and ultimately deterioration in properties of the composites made thereof. Therefore the concentration was reduced to 5% and 1% for making subsequent composites which resulted in considerable improvement in mechanical properties of these composites.

6.2.1 Properties of alkalised fibres

6.2.1.1 Surface morphology

One important aspect of the alkalisation process is the change in the surface morphology of the fibres. There are two distinct kinds of changes in the surface morphology of the fibres following alkalisation. The first is the removal of the waxy layer and other contaminations from the fibres surface, resulting in cleaner and rougher fibre surface. This is expected to result in better fibre/matrix adhesion. The other change is the defibrillation of the fibres, i.e., separating the fibre bundles into single fibres (ultimate fibres or cells), thus increasing the surface area of the fibres available for bonding with the matrix, and hence improving the fibre/matrix interfacial bonding.

However, as shown in Fig. 6.11, alkalisation at all the three concentrations used in this research did not result in defibrillation of fibre bundles and the fibres can still be seen to consist of five or more ultimate fibres as for non-alkalised fibres shown in Fig. 4.8. Thus alkalisation may not be an efficient method for defibrillation of fibres.

Another important effect was the change of colour of alkalised fibres. The colour of 10% alkalised fibres changed from light brown to dark brown. The change in colour was less noticeable for 1% and 5% alkalised fibres.

Perhaps the most important aspect of the 10% alkalisation process was the shrinkage of the hemp fibre mat. Following alkalisation the hemp fibre mat showed almost 30% reduction in surface area. An experiment was undertaken to study the effect of 10% alkalisation on individual hemp fibre bundles. The experiment confirmed that hemp fibre bundles experienced shrinkage from 10 to 50% following alkalisation. Alkalisation has a swelling effect on cellulose fibres, as discussed in Section 2.5.7.2, which may explain the shrinkage of these fibres. Hemp fibres treated to 1% and 5% solutions did not show any shrinkage of the mat following the treatment.

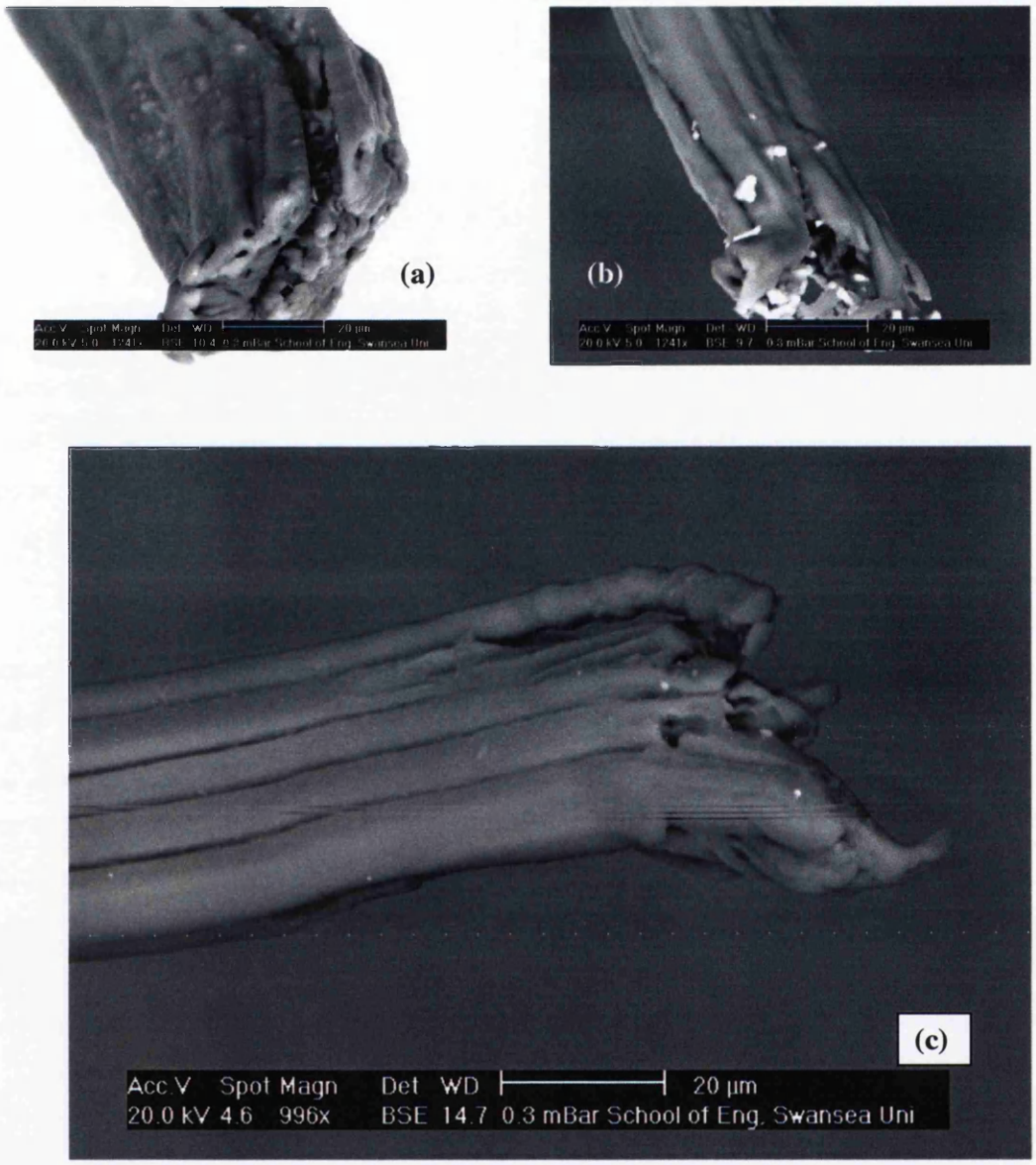

Fig. 6.11: SEM micrographs of (a) 1%, (b) 5%, and (c) 10% alkalised hemp fibres

Gassan and Bledzki [360] have shown that alkalisation can lead to significant shrinkage of jute fibres which can have detrimental effect on the composites made with them. They showed that an alkalisation treatment of 25% NaOH for 20 minutes led to almost 20% shrinkage in jute yarns. At 10% NaOH treatment the shrinkage was 8%. This resulted in considerable reduction in tensile strength and tensile modulus of fibres after alkalisation.

Rahman and Khan [361] reported shrinkage in coir fibres following treatment with various alkali concentrations (5-50%) at different temperatures (0-100°C). The shrinkage was higher at low temperatures and became insignificant at higher temperatures. The highest shrinkage (5.9%) was observed for fibres treated with 20% alkali at 0°C.

In order to determine if the duration of the alkalisation treatment had any effect on the fibres, some fibres were treated to 10% concentration for one hour instead of the usual 24 hours. It was observed that even after only one hour of exposure to NaOH, there was about 20% reduction in the surface area of the hemp mat. So the high concentration of NaOH started to have its effect as soon as the fibres were immersed in the solution and the chemical reaction of NaOH with the fibres was found to be quite rapid.

The hemp fibres used in this research were not woven but randomly oriented in the form of a mat. This meant that during washing up of fibres after alkalisation that already had been softened because of immersion in the solution, too vigorous rinsing and shaking was avoided since it would have led to loosening of the fabric of the fibres. In fact even with rinsing without too much shaking up, it was observed that some loosening of the mat fabric took place which led to further variation in the density of fibres across the mat. This introduced another possible source of variability in the properties of the composites.

6.2.1.2 Surface Energy

The surface energy of hemp fibres at the three alkali concentrations was evaluated and compared with that of non-alkalised fibres. The results are shown in Table 6.2. Following treatment at low concentration of 1% alkali solution, the surface energy does not seem to have changed much. This is consistent with the results reported by Park et al [328] who showed that 0.5% alkalisation of hemp fibres only resulted in a small increase in surface energy of hemp fibres from 35.3 mJ/m^2 to 37.3 mJ/m^2. At the higher concentrations of 5% and 10% alkali solution, the dispersive component seems to be decreasing which results in a decrease in total surface energy of fibres since the polar component of surface energy does not seem to change much. This makes the fibres more polar in nature following alkalisation at 5% and 10% solutions. This is consistent

with the fact that the removal of hemicellulose and pectin following alkalisation reduces the dispersive component of surface energy. This reduction in dispersive energy due to dissolution of hemicelluloses has also been reported for flax fibres following steam explosion treatment [33]. Thus the alkalisation treatment does not seem to have any positive effect on surface energy of hemp fibres, except possibly at low concentrations.

Table 6.2: Surface energy of alkalised hemp fibres

Concentration (%)	Polar (mJ/m^2)	Dispersive (mJ/m^2)	Total (mJ/m^2)
0	20.58 (4.83)	12.25 (6.57)	32.82 (4.38)
1	19.5 (14.1)	12.5 (12.3)	32.0 (7.8)
5	16.7 (10.6)	4.5 (6.3)	21.3 (8.8)
10	18.2 (6.6)	2.1 (1.9)	20.3 (7.2)

6.2.1.3 Tensile Properties

Tensile testing of alkalised hemp fibres was carried out to determine any effect of alkalisation treatment on the tensile properties of hemp fibres. This testing is vital because it will help to determine if the alkalisation of hemp fibres might result in any improvement in tensile properties of composites made from these fibres.

The results of tensile properties of hemp fibres compared to those of non-alkalised fibres are shown in Table 6.3. As shown in Fig. 6.11, alkalisation of fibres did not affect the fibre shapes and most of them were found to have polygonal cross section after treatment like non-alkalised fibres. Therefore calculations for tensile properties were done considering both circular and polygonal cross sections. However in most cases the values were within 10% of each other.

Table 6.3: Tensile properties of alkalised hemp fibres

Concent-ration (%)	Mean width (mm)	Tensile strength (MPa)		Tensile modulus (GPa)		Strain to failure (%)
		Circular	Polygonal	Circular	Polygonal	
0	67 (25)	277 (191)	244 (196)	9.5 (5.7)	8.6 (5.9)	2.3 (0.8)
1	72 (19)	311 (108)	285(120)	13.5(5.3)	12.1(4.4)	2.8 (1.0)
5	62 (15)	304 (136)	256(109)	14.9(6.8)	12.3(5.6)	2.3 (0.5)
10	61 (15)	262 (127)	220(114)	8.5(4.3)	7.1(3.8)	3.2 (0.6)

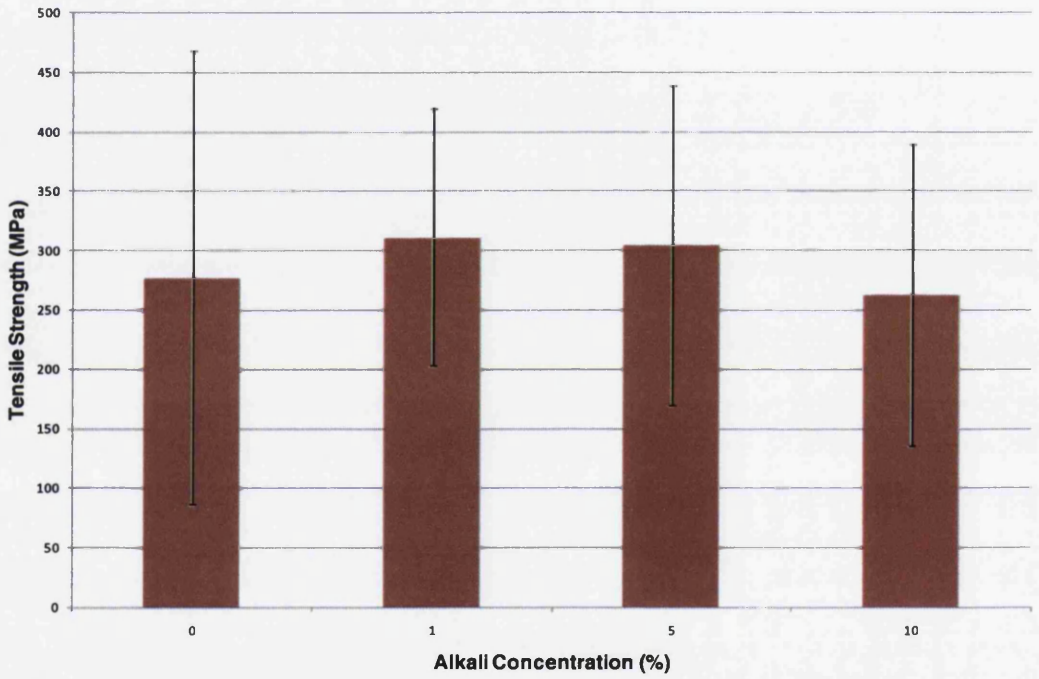

Fig. 6.12: Effect of alkalisation on tensile strength of hemp fibres

As shown in Figs. 6.12-13, some improvements in tensile properties, especially in modulus, were observed for 1% and 5% alkalised fibres, whereas 10% alkalised fibres showed a deterioration in tensile properties. This is to be expected because alkalisation at high concentration of 10% breaks hydrogen bonds within the fibres. However because of the large scatter in data, it is difficult to draw any conclusions.

The improvement in tensile properties at low alkali concentrations can be explained in terms of their increased crystallinity following the treatment. In the untreated fibres, cellulose chains are separated from each other by the inter-fibrillar region containing hemicellulose and lignin. Removal of hemicellulose and lignin following alkalisation means that fibrils can rearrange themselves in a more compact manner, leading to closer packing of cellulose chains. This results in increase in crystallinity of the fibres and its mechanical properties. At higher concentrations, the hydrogen bonds within the fibrils are broken, reducing their tensile properties.

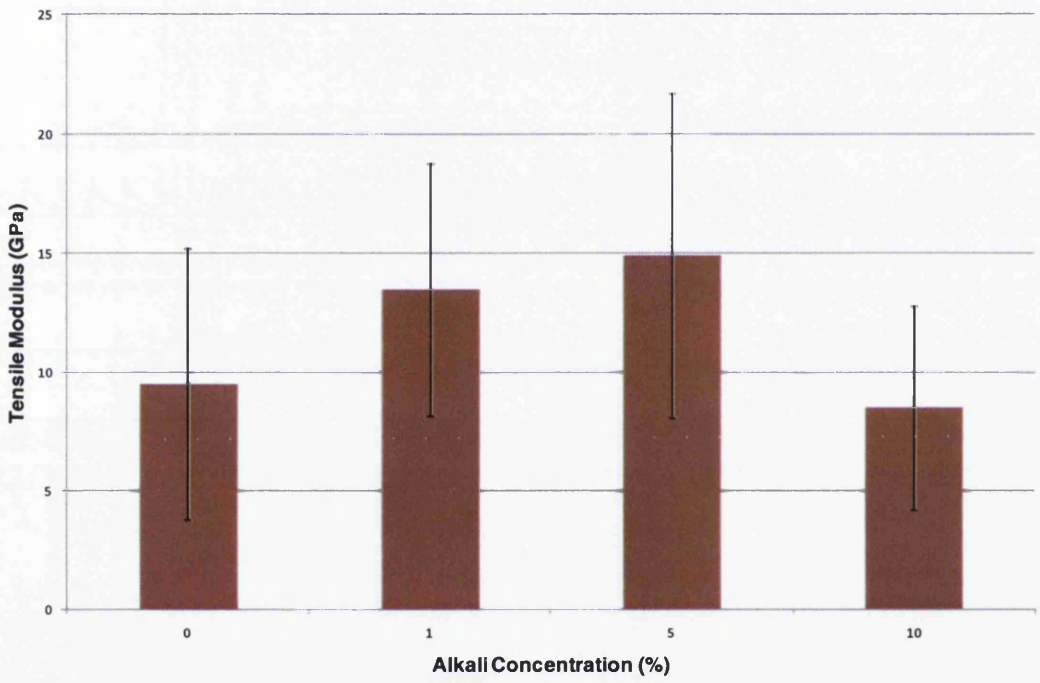

Fig. 6.13: Effect of alkalisation on tensile modulus of hemp fibres

A comparison of stress-strain curves of alkalised fibres and non-alkalised fibres is shown in Fig. 6.14. The graphs show no change in mechanical behaviour of fibres following treatment.

Deterioration of tensile properties of natural fibres following alkalisation at high concentrations is well documented. Mwaikambo and Ansell [147] reported that tensile strength of hemp fibres increased from 600 MPa to 1000 MPa following treatment with 6% concentration of NaOH for 48 hours. However the tensile strength began to decrease at concentration of greater than 6%. The increase in strength was linked to the rupture of

alkali sensitive bonds existing between different components in the fibre as a result of swelling and partial removal of hemicellulose. It was suggested the rupture of bonds made the fibres more homogeneous due to elimination of voids leading to improved stress transfer between ultimate fibre cells. Also new hydrogen bonds were formed as a result of removal of hemicellulose. At NaOH concentrations of greater than 6%, the molecular structure of the cellulose was disrupted and mechanical properties were reduced.

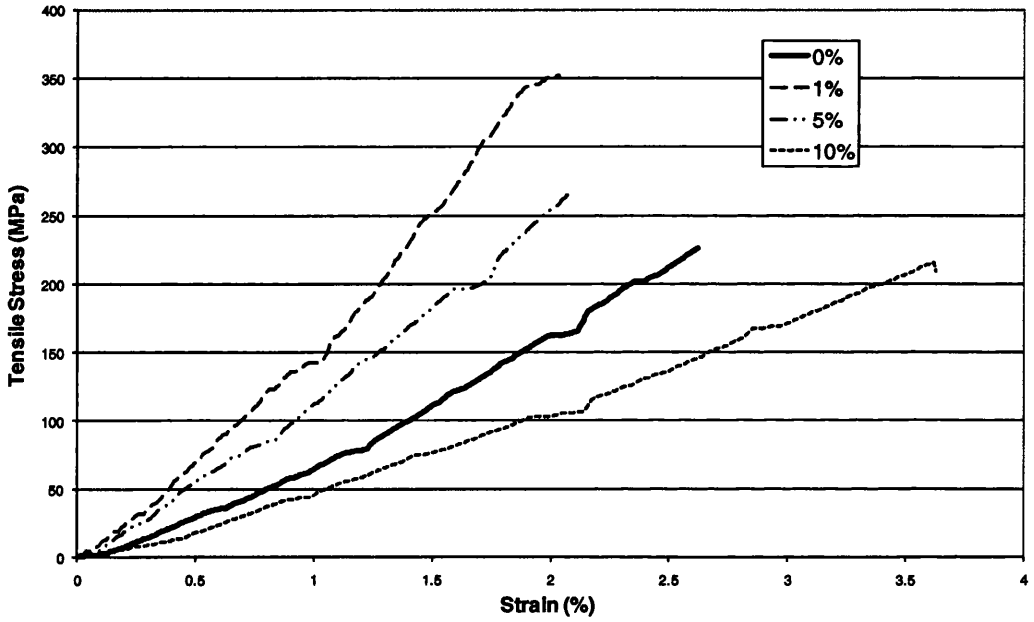

Fig. 6.14: Comparison of stress-strain curves of alkalised fibres and non-alkalised fibres

The tensile modulus of hemp fibres was found to drop slightly between 0.8% and 2% concentration of caustic soda. This was attributed to removal of inter-fibre binders which causes molecular relaxation. At higher concentration the modulus started to increase reaching the optimum value of about 60 GPa at 4-6% concentration. This was attributed to an increase in crystallite packing order along the fibre axis. At concentrations of greater than 6%, the modulus was again seen to be declining.

Deterioration in tensile properties of hemp fibres following alkalisation at high concentrations has also been reported by Ouajai et al [177], Bledzki et al [186], Pickering et al [329] ,[82] , and Kostic at al [73].

6.2.1.4 Hemp/Polyester Interfacial Shear Strength

The interfacial shear strength of alkalised fibres in polyester resin was determined in single fibre pull-out test and compared with non-alkalised fibres. The results are shown in Table 6.4 and Fig. 6.15. The error bars for alkalised fibres generally lie within the error bars for non-alkalised fibres and no appreciable improvement in interfacial shear strength was observed following alkalisation.

Table 6.4: Interfacial Shear Strength (IFSS) of Alkalised Hemp Fibres

NaOH concentration (%)	Force (N)	Fibre width (μm)	Embedded length (mm)	IFSS (MPa)
0	0.12(0.07)	33(7.5)	0.7(0.2)	1.9(1.3)
1	0.17(0.11)	46(13)	0.7(0.2)	2.1(1.7)
5	0.13(0.16)	29(8)	1.0(0.5)	1.4(2.1)
10	0.24(0.14)	45(13)	0.8(0.3)	2.4(1.6)

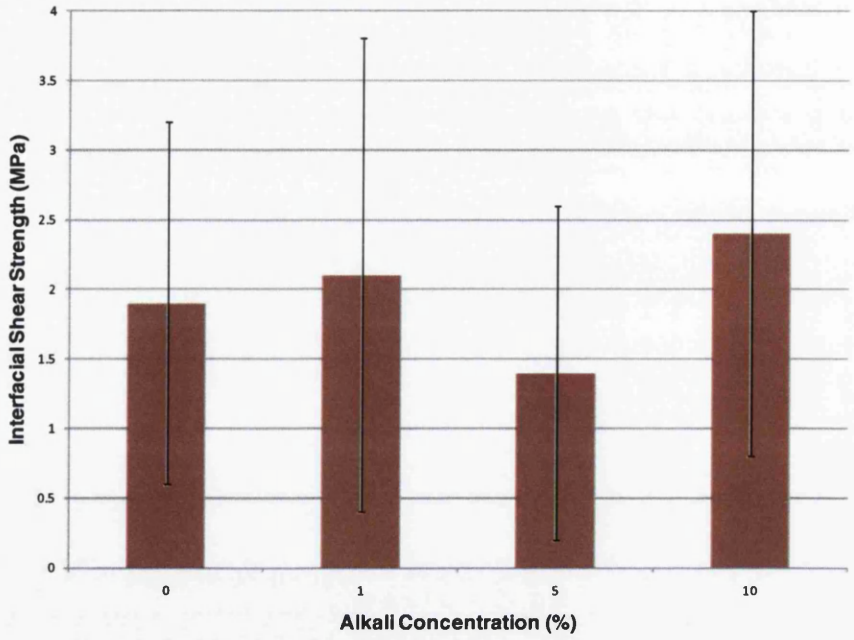

Fig. 6.15: Comparison of interfacial shear strength of alkalised and non-alkalised hemp fibres in polyester resin

6.2.1.5 Weight per unit area of alkalised fibre mat

As discussed in Section 6.2.1, alkalisation treatment resulted in shrinkage (particularly for 10% alkalised fibres) and rearrangement of the fibres within the mat. This meant that the weight per unit area of these fibres was different to that of non-alkalised fibres. So there was a need to determine the weight per unit area of alkalised fibre mats for use in calculations of fibre weight fraction of alkalised fibre composites. Samples of different dimensions were cut up from different parts of the 10%, 5%, and 1% alkalised hemp fibre mats. The weights of all samples were then measured. The comparison of weight per unit area of alkalised and non-alkalised hemp fibre mats is Fig. 6.16.

Alkalisation at 1% and 5% resulted in decrease of almost 20% weight per unit area compared to non-alkalised fibres, while that at 10% resulted in increase in almost 45% weight per unit area because of the increase in the thickness of the mat owing to shrinkage of the fibres. Two main reasons can be attributed to reduction in weight per unit area for 1% and 5% alkalised fibre mats. The first is the removal of moisture during

drying of fibre mats following alkalisation, and the second was that during rinsing of fibre mats following alkalisation some fibres were lost which lead to decrease in the weight per unit area of fibres. No shrinkage of fibres following 1% and 5% alkalisation was observed. This reduction in weight per unit area of the fibres was also reflected in the relatively lower fibre weight fraction of the composites made from these fibres which was 46%.

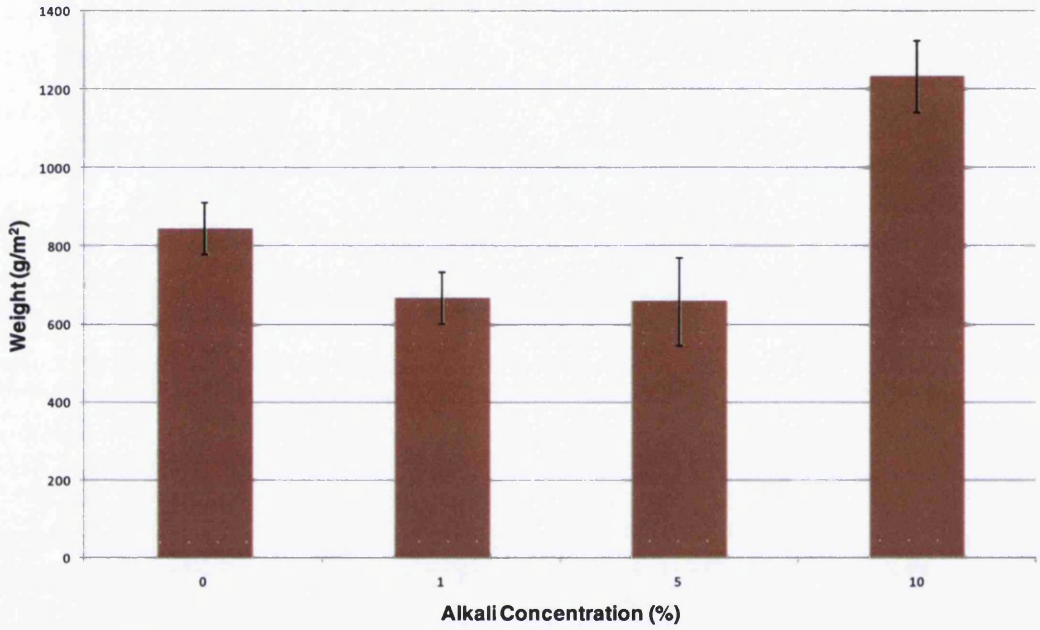

Fig. 6.16: Comparison of weight per unit area of alkalised and non-alkalised hemp fibre mats

6.2.2 Tensile Properties of Alkalised Fibre Composites

The tensile properties of alkalised hemp fibre reinforced polyester composites are shown in Table 6.5. The comparison of tensile properties of 10% alkalised and non-alkalised fibre composites is shown in Figs. 6.17-18.

Composites made with fibres treated for 24 hours in 10% alkalised solution had similar fibre weight fraction as the composites made with non-alkalised fibres. They had lower tensile strength but similar tensile modulus and strain to failure values. Reducing the treatment time to one hour at the same concentration did not result in any improvement in tensile properties. Treating the alkalised fibres with acetic acid to remove any residue of NaOH also did not result in any improvement in tensile properties. As shown

in Figs. 6.17-18, no overall improvement in tensile strength or modulus was observed for 10% alkalised fibre composites.

Table 6.5: Tensile Properties of Alkalised Fibre Composites

NaOH concentration & treatment duration	Fibre wt. fraction (%)	Tensile strength(MPa)	Tensile modulus(GPa)	Strain (%)
No treatment	56	46.4 (4.6)	7.2 (0.9)	1.03 (0.19)
	47	35.8 (4.2)	5.6 (0.7)	0.94 (0.19)
10% @ 24 hours	54	41.7 (4.9)	7.0 (0.7)	1.06 (0.4)
10% @ 1 hour	52	42.7 (5.0)	6.6 (0.9)	1.00 (0.3)
10%@ 24 hours, followed by acetic acid	54	43.3 (2.9)	6.6 (0.3)	1.30 (0.22)
5% @ 24 hours	46	46.4 (2.4)	7.5 (0.5)	0.93 (0.15)
1% @ 24 hours	47	51.5 (5.7)	7.3 (0.8)	1.19 (0.18)

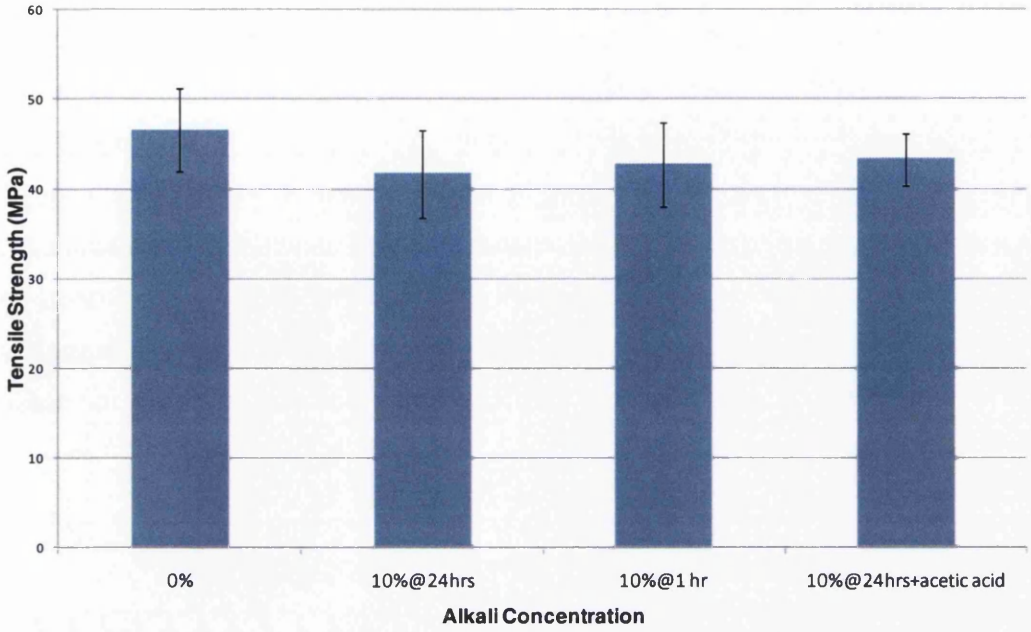

Fig. 6.17: Comparison of tensile strength of 10% alkalised and non-alkalised fibre composites

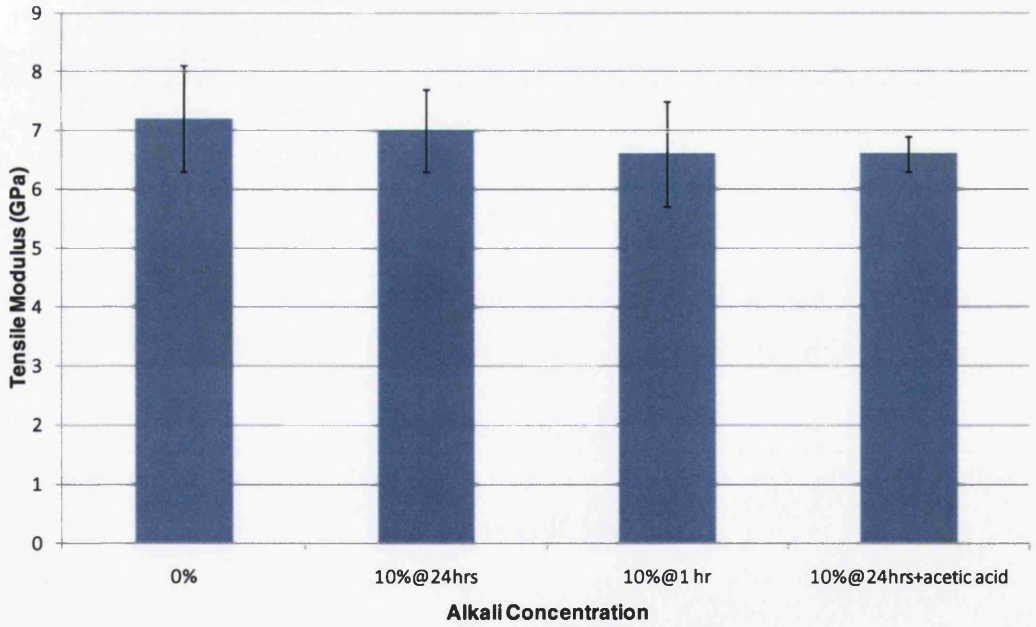

Fig. 6.18: Comparison of tensile modulus of 10% alkalised and non-alkalised fibre composites

The 5% alkalised fibre composites, despite having lower fibre weight fraction, showed comparable tensile properties to composites made with non-alkalised fibres at 3 MPa moulding pressure. However, as shown in Figs. 6.19-20, when their properties are compared with the composites made at moulding pressure of 1 MPa which had similar fibre weight fraction, the improvements in tensile properties become clear. For 5% alkalised fibre composites, the increase in tensile strength and modulus was about 30% compared to non-alkalised fibre composites. This is to be expected considering the improvement in tensile properties of hemp fibres following this treatment. This suggests that alkalisation at 5% concentration did have some positive effect on the tensile properties of the composites.

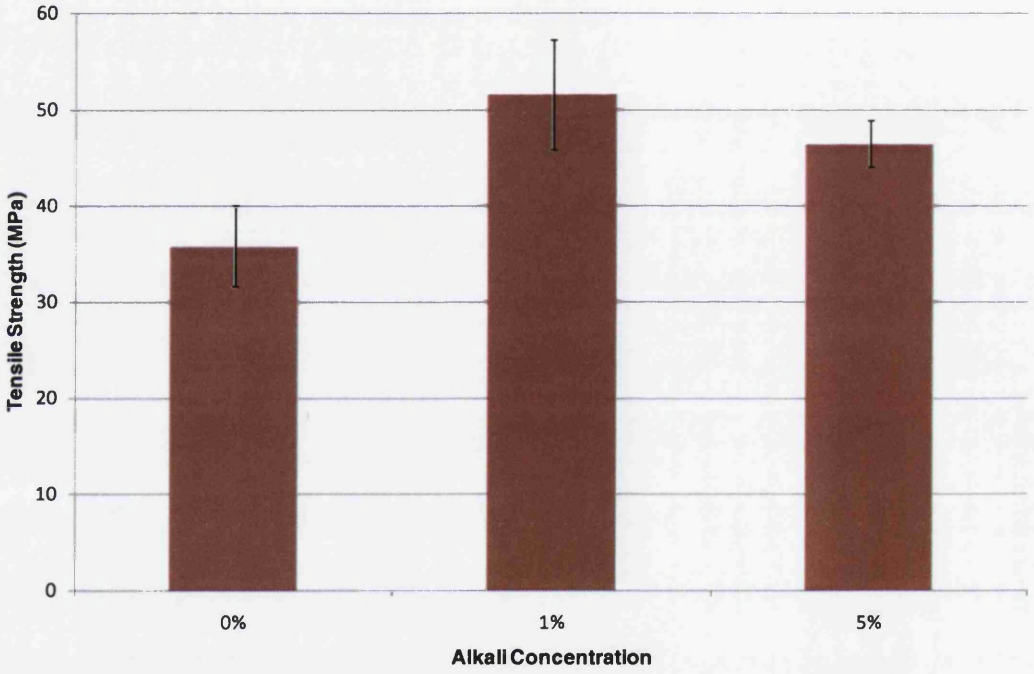

Fig. 6.19: Comparison of tensile strength of 1% and 5% alkalised and non-alkalised fibre composites

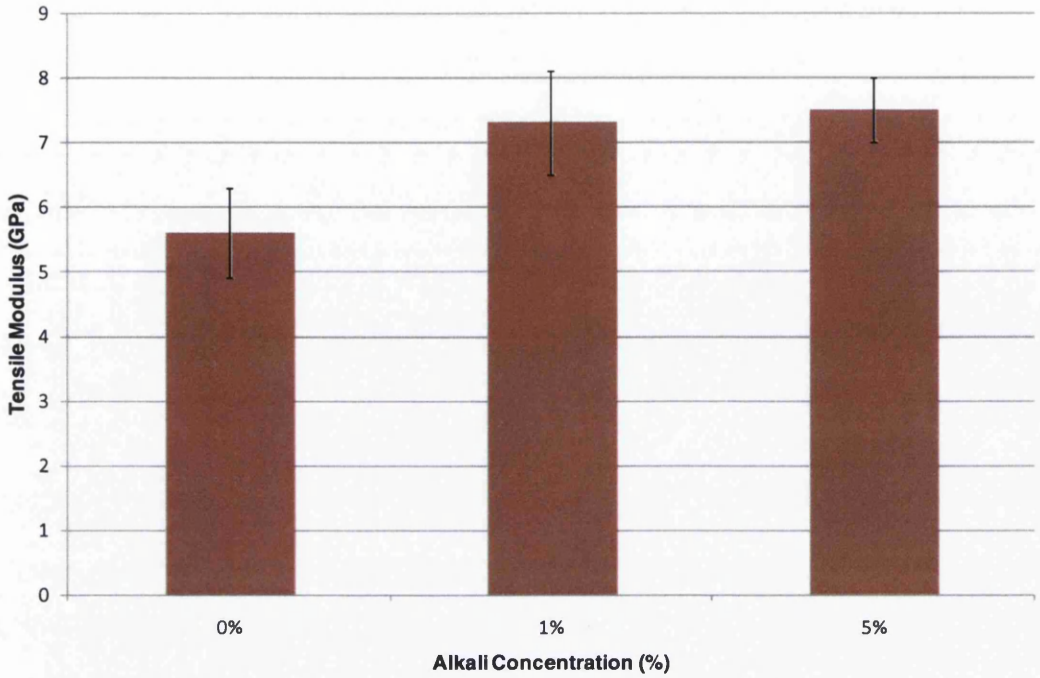

Fig. 6.20: Comparison of tensile modulus of 1% and 5% alkalized and non-alkalized fibre composites

The 1% alkalised fibre composites showed the greatest improvement in tensile properties. The increase in tensile strength was about 40% and that in tensile modulus was about 30% compared to non-alkalised fibre composites at similar fibre weight fraction. This is again consistent with the fact that the tensile properties and interfacial shear strength of hemp fibres showed some improvement following this treatment.

All the alkalised fibre samples failed in a brittle manner in tensile testing just like non-alkalised fibre samples and the fracture plane was normal to the applied load. The comparison of stress-strain curves of alkalised fibre samples with that of non-alkalised fibre sample is shown in Fig. 6.21. The figure shows that the alkalisation does not cause any significant change in the mechanical behaviour of the alkalised fibre composites in tensile testing. The position of 'knee' on the curves is quite similar, indicating the transfer of stress from matrix to fibres at the similar stress levels.

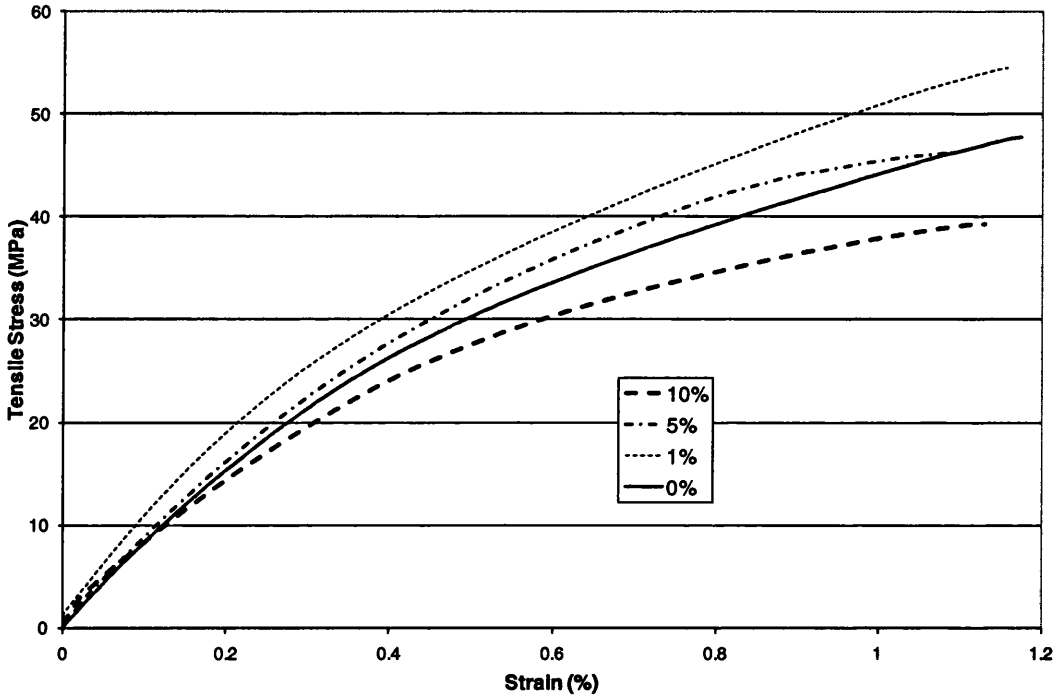

Fig. 6.21: Comparison of stress-strain curves of alkalised and non-alkalised fibre composites

Fig. 6.22 shows the SEM micrographs of fracture surfaces of 1% and 10% alkalised fibre samples that failed in tension. The figures show much improved wetting of the fibres with the matrix compared to non-alkalised samples (Fig. 5.9), evidenced by greater amount of polyester resin present in the fracture surface and sticking to fibres. This improvement in the fibre/matrix bonding and the improvement in tensile properties of fibres seem to be the major reasons for the increase in tensile properties of 1% alkalised fibre composites. For 10% alkalised fibre composites, two conflicting processes are taking place. Alkalisation at this concentration results in improvement in fibre/matrix interfacial bonding, also evidenced in improved interfacial shear strength in single fibre pull-out test, but also reduces the tensile properties of the fibres. This improved wetting does not seem to have resulted in any improvement in the tensile properties of the composites because the reduction of tensile properties of the fibres following 10% alkalisation treatment seems to have overridden any improvements in interfacial bonding. The improved interfacial bonding is also evidenced in less fibre pull-out in the fracture surfaces.

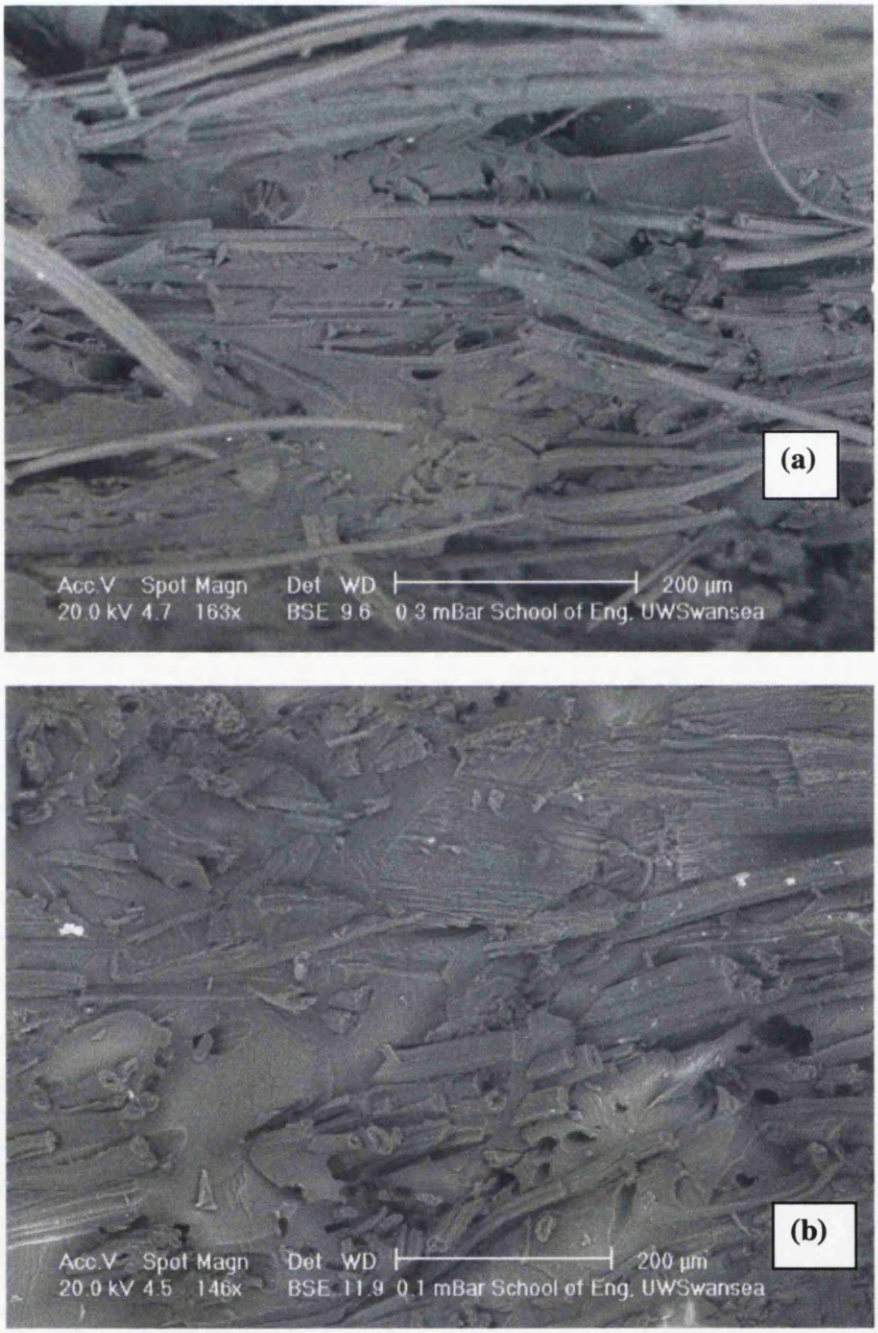

Fig. 6.22: SEM micrographs of fracture surfaces of (a) 1% alkalised and (b) 10% alkalised fibre composites after tensile testing

6.2.3 IMPACT PROPERTIES

6.2.3.1 Izod impact strength

Izod impact strength of 10% alkalised fibre composites was determined by using the standard testing procedure. A total of 17 samples with notches were used. The Izod impact strength was calculated to be 4.3 ± 0.9 kJ/m^2. This is considerably less than that of non-alkalised fibre composites which is 12.7 ± 2.8 kJ/m^2 for notched samples. Two factors can be attributed to this. One is the reduction in strength of fibres because of alkalisation. The second is the improved fibre/matrix interfacial bonding which results in less energy being absorbed through crack propagation and fibre pull-out from the matrix.

6.2.3.2. Low velocity impact properties

The alkalised fibre composites were subjected to low velocity impact testing and their residual tensile properties following impact were determined. The data for residual tensile strength of alkalised fibre composites is shown in Table 6.6. The comparison of residual tensile strength of 10% and 1% alkalised and non-alkalised fibre composites after low velocity impact is shown in Fig. 6.23.

Fig. 6.23 shows that alkalised fibre composites show no improvement in impact damage tolerance following the fibre treatment. There is gradual decline in the strength of alkalised fibre composites following impact. Unlike untreated fibre composites, alkalised fibre composites show no threshold energy level and decline in the strength is occurring even following impact of 1J. Even 1% alkalised composites that showed improved tensile strength compared to non-alkalised composites have lower residual strength following impact. The alkalisation process is thus seen to have had no positive effect on the impact damage tolerance of these composites.

Table 6.6: Residual tensile strength (MPa) of alkalised fibre composites following low velocity impact

Concen-tration (%)	Impact Energy (J) 0	1	2	3	4
0	46.4 (4.6)	46.0 (5.3)	26.2 (5.4)	22.7 (1.8)	15.2 (2.9)
1	51.5 (5.7)	36.5 (11.1)	23.9 (3.9)	13.2 (7.2)	9.9 (2.9)
10	41.7 (4.9)	-	22.8 (6.8)	17.0 (7.4)	12.9 (7.5)

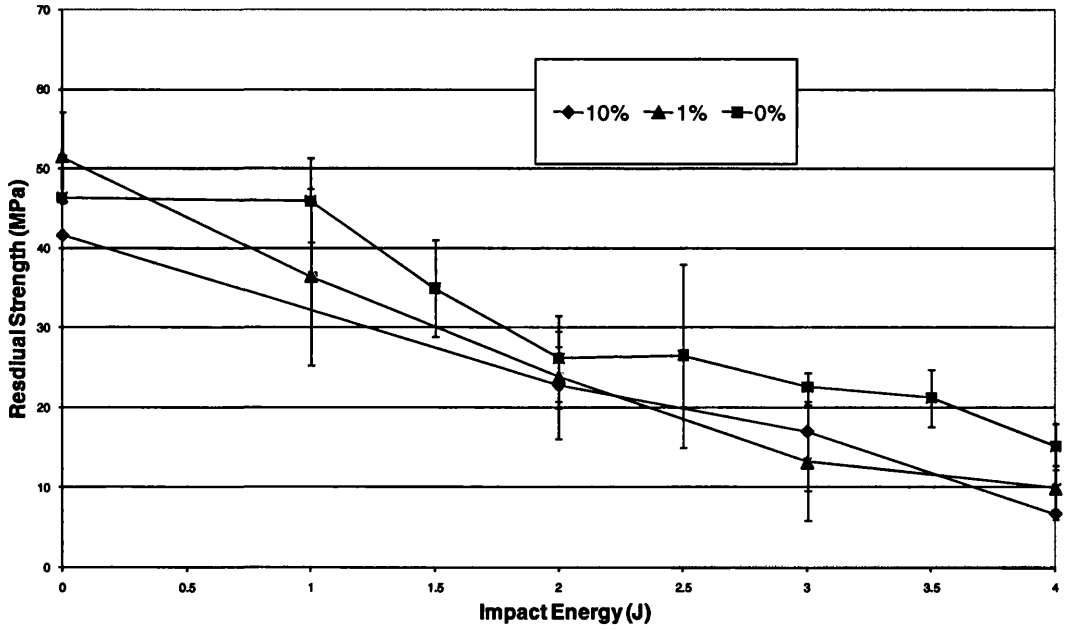

Fig. 6.23: Comparison of residual strength of 10% and 1% alkalised fibre composites with non-alkalised fibre composites after low velocity impact

Table 6.7: Residual tensile stiffness (GPa) of alkalised fibre composites following low velocity impact

Concen-tration (%)	Impact Energy (J) 0	1	2	3	4
0	7.2 (0.9)	6.0 (0.9)	4.0 (1.4)	3.2 (0.5)	2.1 (0.3)
1	7.3 (0.8)	6.1 (1.4)	3.9 (1.0)	2.6 (1.1)	1.9 (0.7)
10	7.0 (0.7)	-	5.6 (0.6)	3.7 (0.9)	2.4 (1.2)

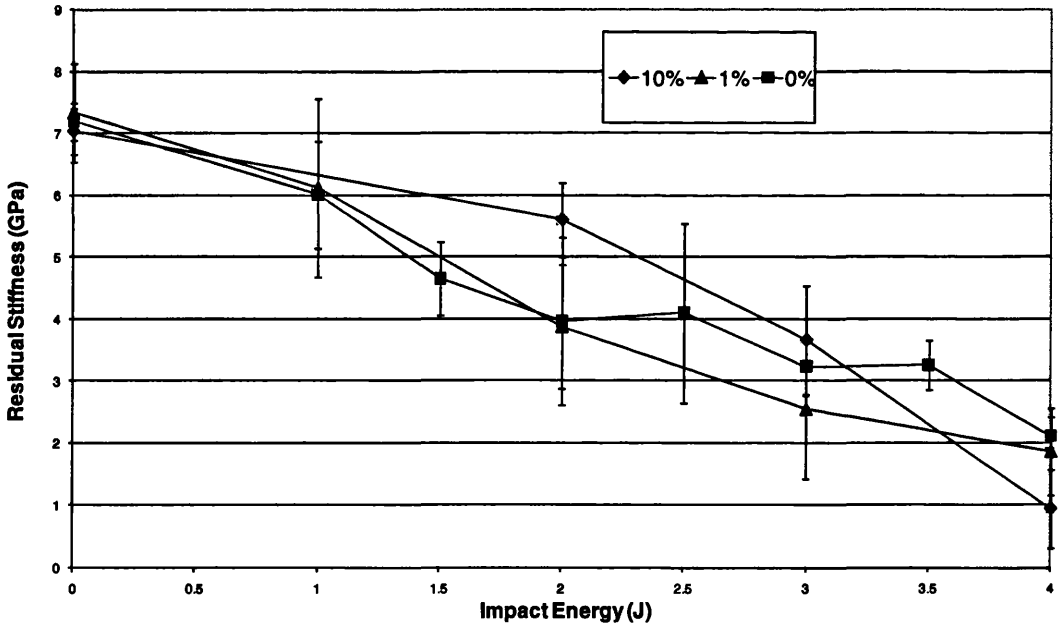

Fig. 6.24: Comparison of residual stiffness of 10% and 1% alkalised fibre composites with non-alkalised fibre composites after low velocity impact

The data for residual tensile stiffness of alkalised fibre composites is shown in Table 6.7. Fig. 6.24 compares the residual stiffness of alkalised fibre composited with non-

alkalised fibre composites. The decline in stiffness is gradual with increase in impact energy. No improvement in residual stiffness was observed for alkalised fibre composites for impact energies of up to 4J.

The comparison of strain to failure following impact of alkalised fibre composites with non-alkalised fibres composites is shown in Fig. 6.25. The alkalised fibre composites generally have lower strain to failure than non-alkalised composites following low velocity impact which can be attributed to increase in brittleness of fibres following the treatment.

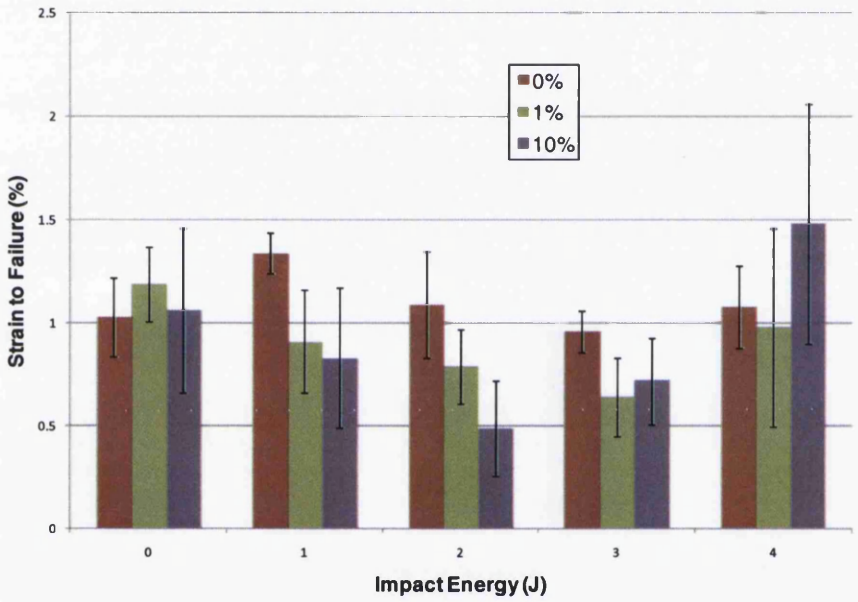

Fig. 6.25: Comparison of strain to failure of 10% and 1% alkalised fibre composites with non-alkalised fibre composites after low velocity impact

The impact damage tolerance of alkalised fibre composites can be best understood in terms of their normalised residual strength and stiffness curves following the impact. Fig. 6.26 shows the comparison of normalised residual strength following impact of alkalised and non-alkalised fibre composites. The figure shows the generally poor impact damage tolerance of alkalised fibre composites compared to non-alkalised fibre composites. Whereas non-alkalised fibre composites lost almost 70% of their original strength following impact at 4J, alkalised fibre composites lost almost 80% of their

original strength. The decline in strength of 1% alkalised fibre composites is greater at low energy levels compared to 10% alkalised fibre composites which is more gradual.

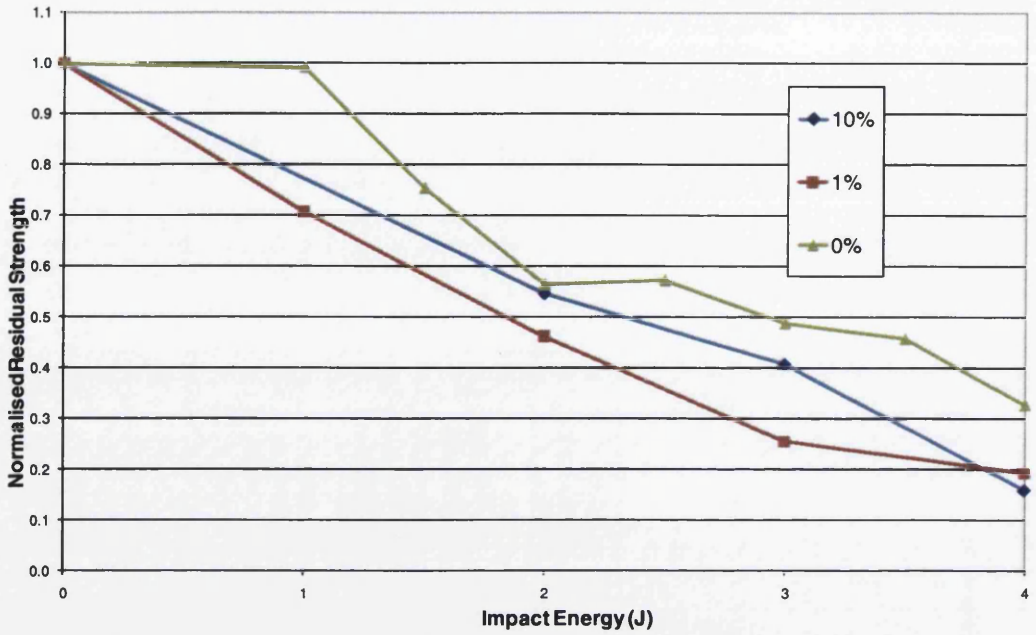

Fig. 6.26: Comparison of normalised residual strength of alkalised and non-alkalised fibre composites

Fig. 6.27 shows the comparison of normalised residual stiffness of alkalised fibre composites following impact with non-alkalised fibre composites. At low impact energy of up to 2J, 1% alkalised fibre composites have similar residual stiffness as non-alkalised fibre composites. 10% alkalised fibre composites show improved residual stiffness following impact energy of up to 3J. Following impact of 4J, 1% alkalised fibre composites have lost almost 75% of their original stiffness and 10% alkalised fibre composites have lost almost 85% of their original stiffness.

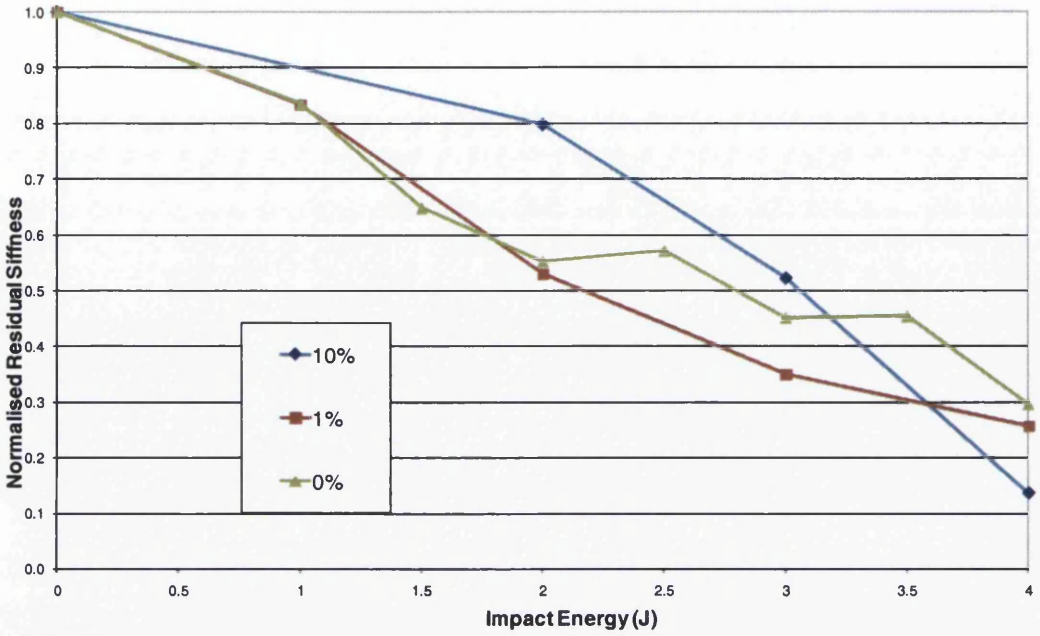

Fig. 6.27: Comparison of normalised residual stiffness of alkalised and non-alkalised fibre composites

Figs. 6.28-30 show macrographs of the impacted and distal faces of the 1% alkalised fibre samples following low velocity impact. 1% alkalised fibre composites have been selected because they exhibited greatest improvement in tensile properties following alkalisation. For impact energy of 1J, the impact is barely visible but it is still enough to cause damage to the sample resulting in 30% loss of residual strength and 17% of residual stiffness. As shown in Figs. 5.22-23, non-alkalised fibre composites were also able to resist an impact energy of 1J but without any loss in strength and the same loss of stiffness (17%) as 1% alkalised fibre composites. 1% alkalisation thus does not seem to result in any improvement in impact damage tolerance at this stage.

At impact energy level of 2J, the impact starts to become visible and considerable penetration, fibre/matrix debonding and matrix cracking is observed, shown by the arrowhead. This is also evidenced in the formation of the crater on the distal side of the samples because of the impact. At this stage the composites have lost almost 50% of their residual strength and stiffness. Non-alkalised fibre composites had also lost almost 50% of their intrinsic strength and stiffness following impact of 2J and evidence of considerable fibre fracture was found as shown in Fig. 5.24. A similar loss in strength

and stiffness shows that alkalisation does not seem to have any positive effect on impact damage tolerance at this stage as well.

Following impact at 3J, complete perforation of some samples was observed and considerable matrix cracking, debonding and fibre fracture was visible. The shape of the crater on the distal side was also more obvious with a characteristic triangular shaped cracks running across the crater. At this stage, the samples had lost almost 70% of their intrinsic strength and stiffness. Non-alkalised fibre composites had lost almost 50% of their intrinsic strength and stiffness at the same level of impact. Thus alkalisation seems to result in greater loss in impact damage tolerance at this level.

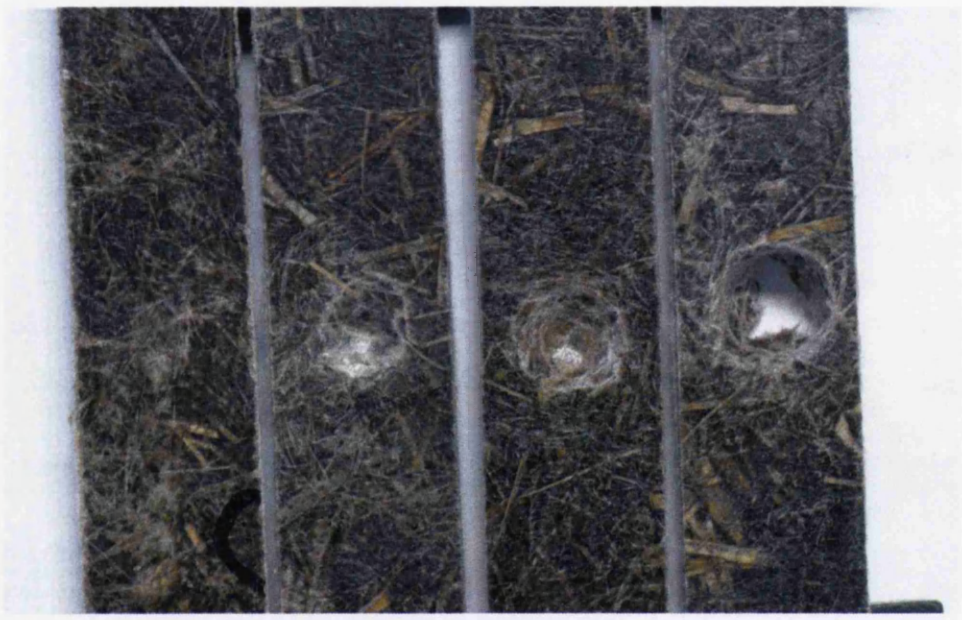

1J **2J** **3J** **4J**

Fig. 6.28: Macrographs of impacted face of 1% alkalised fibre composite samples with increasing impact energy levels from left to right

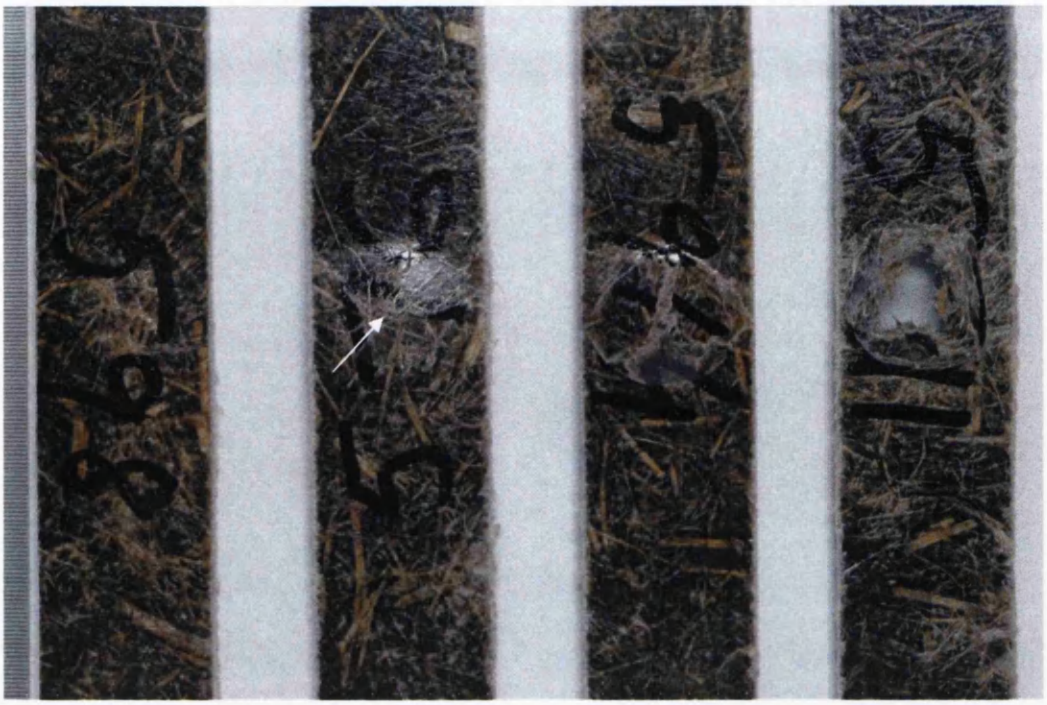

1J 2J 3J 4J

Fig. 6.29: Macrographs of distal face of 1% alkalised fibre composite samples with increasing impact energy levels from left to right

1J 2J 3J 4J

Fig. 6.30: Angled view of distal face of 1% alkalised fibre composite samples with increasing impact energy levels from left to right

At impact energy level of 4J, complete perforation for almost all samples was observed. The coupons at this point had lost almost 80% of their intrinsic strength and stiffness, compared to 70% loss for non-alkalised fibre composites. It was observed that diameter of the impact crater on the impacted face was 12.5 mm which was the same as the impactor diameter. The diameter of impact crater on the distal face was about 15 mm for non-perforated samples and about 18 mm for perforated samples.

Generally the alkalised fibre composites have shown no improvement in impact damage tolerance following low velocity impact. The most plausible reason for this is their improved fibre matrix adhesion due to alkalisation which hinders the crack propagation through the interface and the fibre pull-out from the matrix. Hence the contribution of these two main energy absorption mechanisms to total energy absorption is reduced for alkalised fibre composites. Even 1% alkalised fibre composites that had shown improved tensile properties do not seem to show any improvement in residual properties following impact. Just like non-alkalised composites, any impact of 2J or higher impact energy resulted in significant reduction in the strength and stiffness of alkalised fibre composites.

The poor impact properties of alkalised natural fibre composites have been reported by other authors. Work done on kenaf fibre composites by Aziz and Ansell [121] showed the tendency for the untreated fibre composites to be tougher in impact than caustic soda treated fibre composites. This was attributed to the fact that poorly bonded interfaces allowed the cracks to grow, thus increasing the energy absorption capacity of the composite. Oever van den et al [362] also reported that Charpy impact strength of flax fibre reinforced polypropylene composites decreased with increasing fibre internal bonding and enhanced fibre/matrix adhesion. They suggested that a high level of fibre/matrix adhesion results in shorter average fibre pull out lengths and therefore results in lower impact strengths. Towo [363] reported a 27% decease in impact strength of 0.06 M alkali treated sisal fibre reinforced polyester composites following the treatment.

Thus, unlike tensile properties, the alkalisation process has not proven to be advantageous to improving the impact properties of hemp fibre composites.

6.2.4 FATIGUE PROPERTIES

6.2.4.1 S-N Curves

The fatigue properties of alkalised fibre composites were evaluated in tension-tension mode (R=0.1) at 1 Hz frequency. The resulting S-N curves are shown in Figs 6.31-33.

Fig. 6.31 shows the S-N curve of 10% alkalised fibre composites. The composites have lower static strength than non-alkalised fibre composites but their fatigue strength is comparable to that of non-alkalised fibres composites. Following fatigue cycles of 10^6, their endurance limit is about 20 MPa, shown by arrowheads, the same as for non-alkalised fibre composites. Despite lower static strength, the improved fibre/matrix interfacial adhesion because of alkalisation seems to have resulted in comparable fatigue strength to that of non-alkalised fibre composites.

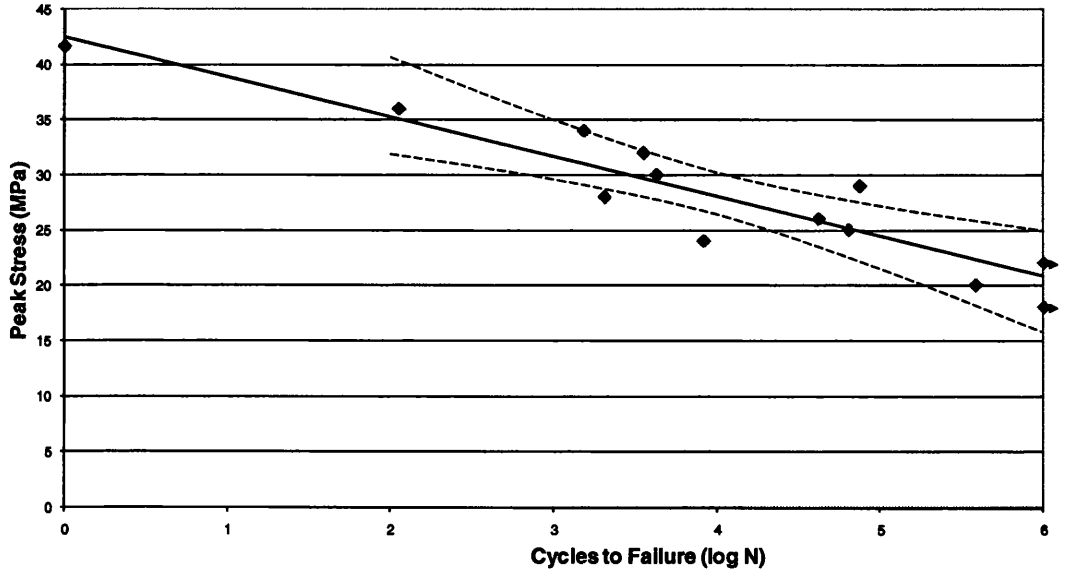

Fig. 6.31: S-N curve of 10% alkalised fibre composites

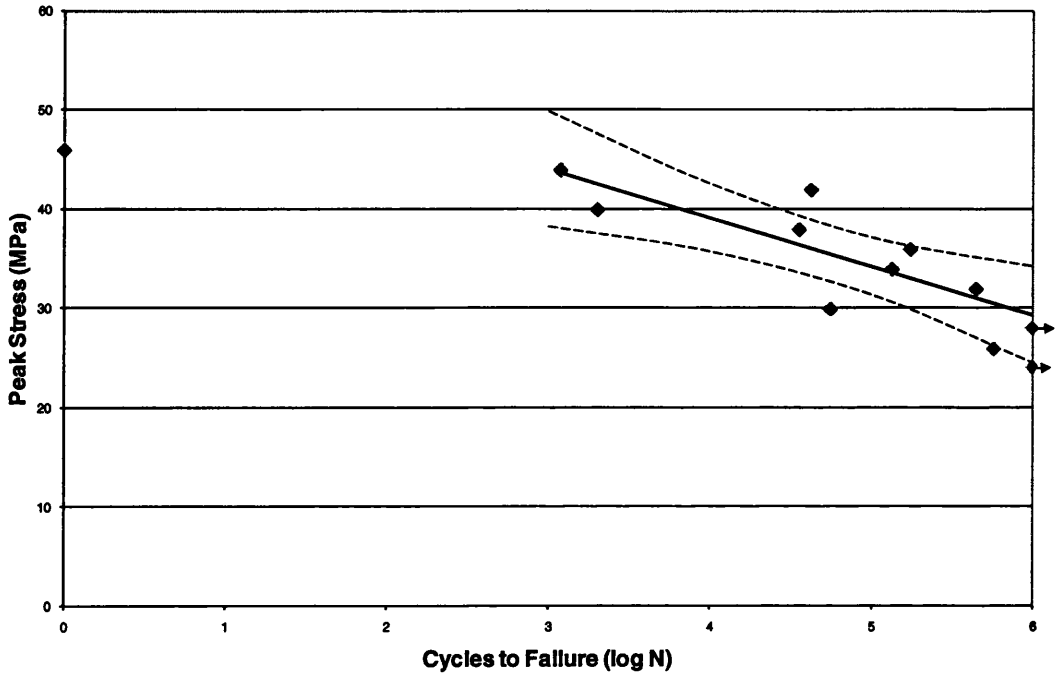

Fig. 6.32: S-N curve of 5% alkalised fibre composites

The S-N curve of 5% alkalised fibre composites is shown in Fig. 6.32. The figure shows considerable improvement in fatigue strength of the composites, also evidenced by increase in endurance limit of the composites to about 28 MPa, as shown by arrowheads, as against 20 MPa for non-alkalised fibre composites. As shown in Section 6.2.2, these composites had higher tensile strength and stiffness than non-alkalised fibre composites at similar fibre weight fraction. This coupled with the increase in interfacial adhesion seems to have contributed to the increase in fatigue strength of the composites.

The S-N curve of 1% alkalised fibre composites is shown in Fig. 6.33. This process also seems to have resulted in improvement in fatigue strength of composites. This is evidenced by increase in endurance limit of the composites to about 30 MPa, as shown by arrowheads, as against 20 MPa for non-alkalised fibre composites. As shown in Section 6.2.2 , these composites also had higher tensile strength than non-alkalised fibre composites at similar lower fibre weight fraction. This coupled with the increase in interfacial adhesion seems to have contributed to the increase in fatigue strength of the composites.

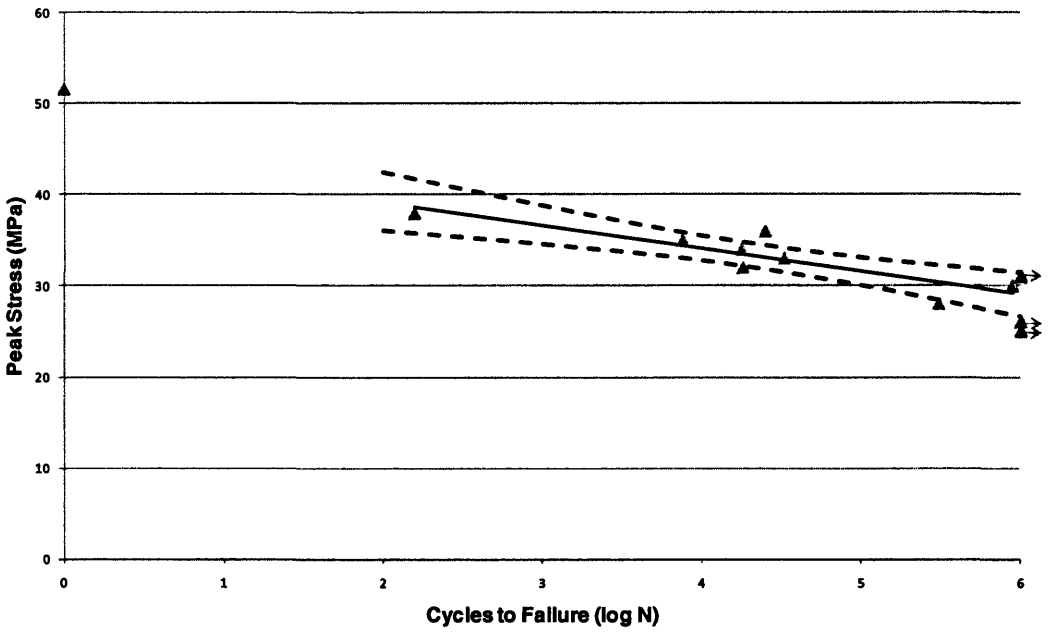

Fig. 6.33: S-N curve of 1% alkalised fibre composites

1% and 5% alkalisation processes seem to have had a positive effect on fatigue strength of composites as shown by the increase in the endurance limit of these composites. The endurance limit of these composites has increased to about 30 MPa for 1 % alkalised composites and to about 28 MPa for 5% alkalised composites. The mode of fracture for all alkalised fibre samples was still brittle.

6.2.4.2 Comparison of fatigue properties

The improvement in fatigue properties of alkalised fibre composites can be best understood in terms of their normalised S-N curves as shown in Fig. 6.34. The curves were obtained by dividing the peak stress with the static strength of the composites. The figure shows improvement in the fatigue sensitivity of all alkalised fibre composites, compared to non-alkalised fibre composites, by the improved slopes of the curves. The improvement in the slope of the curves is quantitatively represented by their fatigue sensitivity coefficients, as shown in Table 6.8.

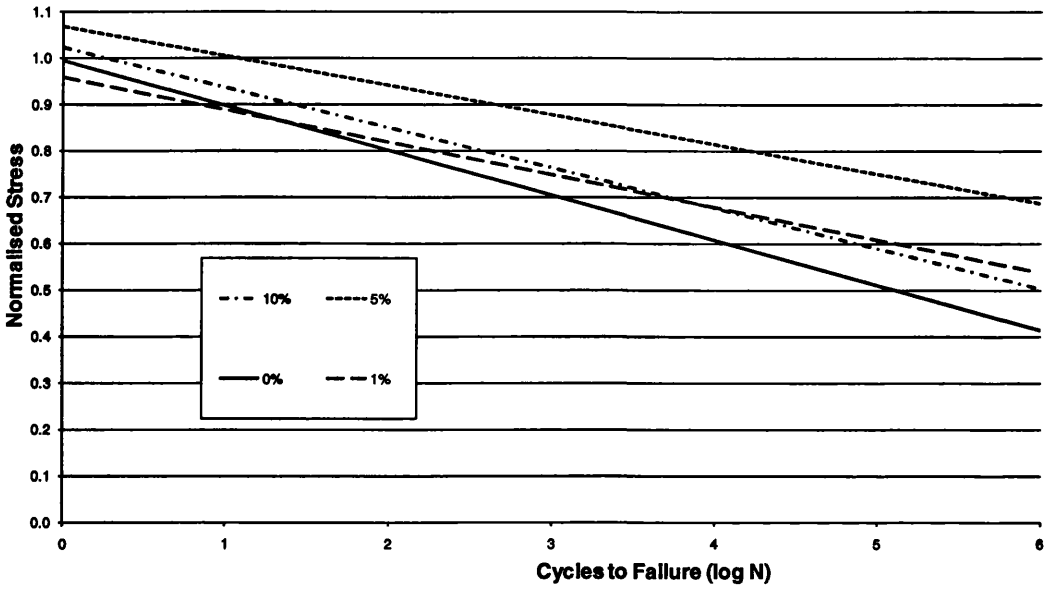

Fig. 6.34: Normalised S-N curves of alkalised fibre composites

Table 6.8: Fatigue sensitivity coefficients of alkalised fibre composites

Alkali concentration (%)	Fatigue sensitivity coefficient
0	0.097
1	0.070
5	0.063
10	0.087

Table 6.8 show that the biggest improvement in fatigue sensitivity was observed for 5% alkalised fibre composites, followed by 1% and 10% alkalised fibre composites. Alkalisation process resulted in improvement in fatigue sensitivity of composites at all three concentrations used in this research.

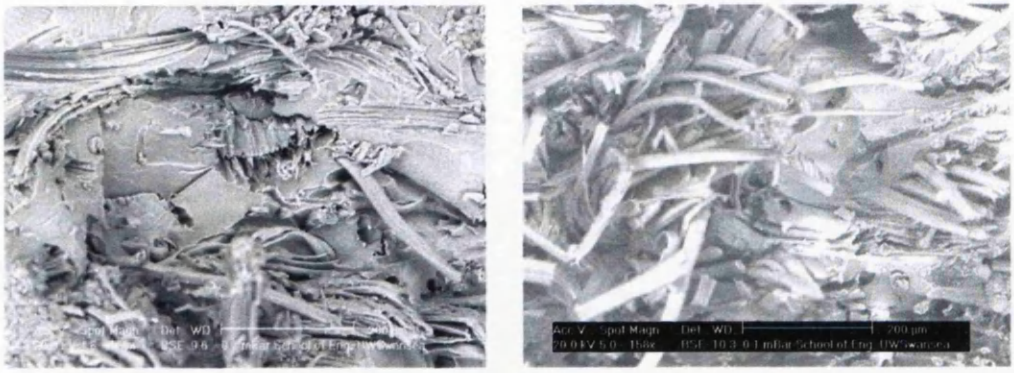

(a) (b)

Fig. 6.35: SEM micrographs of fracture surfaces of (a) 10% alkalised fibre composite, N=382000 cycles, σ=20 MPa, and (b) 1% alkalised fibre composites, N=890000 cycles, σ=30 MPa.

Fig. 6.36: SEM micrographs of the surface of 5% alkalised fibre composite sample that endured 10^6 cycles, σ= 34 MPa.

SEM micrographs of the fracture surface of alkalised fibre composites in fatigue testing are shown in Fig. 6.35. These micrographs show much improved interfacial adhesion of fibre/matrix, compared to non-alkalised fibre composites shown in Fig. 5.46, which could be the major reason of their improved fatigue strength and sensitivity. For comparison, the SEM micrograph of the 'fracture' surface of 5% alkalised sample that did not fail after 10^6 cycles of fatigue testing at tensile stress of 34 MPa (almost 70% of

static strength) is shown in Fig. 6.36. The sample was chosen because of all the alkalised fibre samples fatigue tested, this sample exhibited the highest endurance limit. These micrographs also show improved interfacial bonding evidenced by good wetting of fibre by the matrix. Application of a peak fatigue stress of 70% of the static strength did not weaken the interfacial bonding and the material was strong enough to stop the propagation of sub-surface cracks emanating in the material.

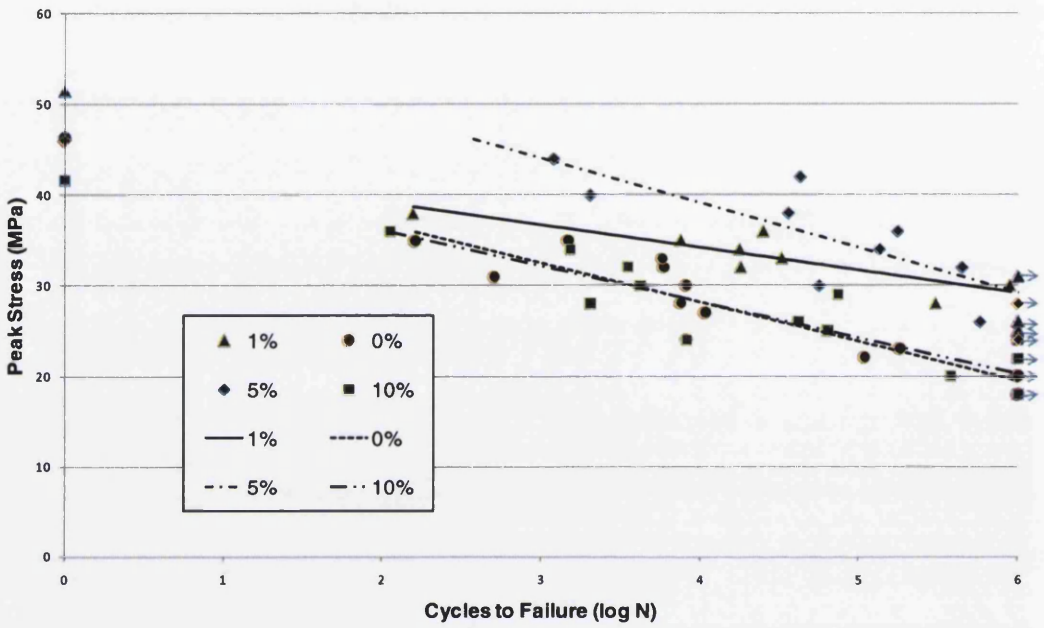

Fig. 6.37: Combined S-N curves of alkalised and non-alkalised fibre composites

The fatigue testing of the alkalised composites showed that the alkalisation process had the same positive effect on the dynamic tensile strength of the composites as for static tensile strength. The fatigue strength of alkalised fibre composites can be compared to their static strength. As shown in Fig. 6.37, 10% alkalised fibre composites showed no improvement in their fatigue strength compared to non-alkalised fibre composites which was consistent with the effect on their static tensile strength. 1% and 5% alkalised fibre composites showed considerable improvement in their fatigue strength, as was also observed in their static strength. This was reflected in about 35% increase in the endurance limit of 1% alkalised fibre composites and about 60% increase in the endurance limit of 5% alkalised fibre composites.

The positive effect of improved interfacial strength on glass and carbon fibre composites on their fatigue properties is well documented [269]. It is expected therefore that the improved interfacial strength because of fibre surface treatment should improve the fatigue properties of natural fibre composites as well.

Studies done by Gassan and Bledzki [269] have shown that the dynamic strength of MAH-PP modified jute-PP composites was increased by approximately 40%. The use of silane coupling agent for jute-polyester composites also resulted in improvement in dynamic strength. For both treatments, the critical load for damage initiation was higher and damage propagation less rapid than for non-treated fibre composites.

The positive effect of alkalisation on fatigue properties has also been confirmed by Towo and Ansell [187] for sisal-polyester composites. Composites made from 0.06M alkalised fibres and tested in tension-tension fatigue showed improvement in fatigue strength, although the effect was more pronounced at higher applied stresses. However no noticeable improvement in fatigue strength was observed for alkalised sisal-epoxy composites.

Alkalisation process was used to improve fibre-matrix adhesion and hence improve the mechanical properties of the composites in this research and it resulted in mixture of results for properties of the composites. These studies showed that a high NaOH concentration of 10% can have a detrimental effect on the properties of hemp fibres and the composites made from these fibres. Low concentrations of 1% and 5% of NaOH solution was found to result in improvement in tensile and fatigue properties of the composites. No improvement in impact damage tolerance of composites was observed for all three alkalisation treatments. From the present studies, the upper limit to the concentration of NaOH for it to have any beneficial effect on the fibres can be suggested to be 5%.

6.3 ACETYLATION

Acetylation of natural fibres has been proposed as a good method of improving the interfacial bonding of natural fibres with polymer resins. Various studies undertaken on acetylation of natural fibres have been discussed in Section 2.4.7. In this part of the study, hemp fibres were treated to acetylation process as described in Section 3.2.2.

However due to highly corrosive nature of the acetic anhydride used in this process, only one laminate could be made. Therefore the results obtained form these treatments are limited in scope. Because of this reason this process has obvious limitations for application in normal laboratory conditions.

6.3.1 TENSILE PROPERTIES

The comparison of the tensile properties of acetylated fibre composites with those of un-treated fibre composites are shown in Table 6.9. The figures in brackets are standard deviations. From the table, it is clear that no appreciable improvement in tensile properties of the acetylated composites was observed and the properties of both kinds of composites are similar. Thus any improvement in fibre/matrix interfacial bonding because of acetylation is not reflected in their tensile properties.

Table 6.9: Tensile properties of acetylated fibre composites

	Fibre weight fraction (%)	Tensile strength (MPa)	Tensile modulus (GPa)	Strain to failure (%)
Untreated	56	46.4 (4.6)	7.2 (0.9)	1.03 (0.19)
Acetylated	53	44.4 (6.0)	7.6 (0.8)	0.94 (0.20)

The acetylated fibre composites samples fractured in a brittle manner in tensile testing just like non-acetylated fibre samples. The comparison of stress-strain graphs of a typical acetylated sample in tensile testing with that of non-acetylated sample is shown in Fig. 6.38. The graph shows similarity in mechanical behaviour of the acetylated fibre composites with non-acetylated fibre composites in tensile testing. The shape of 'knee' portion of the curves is also quite similar suggesting the transfer of load from matrix to fibres at similar stress levels.

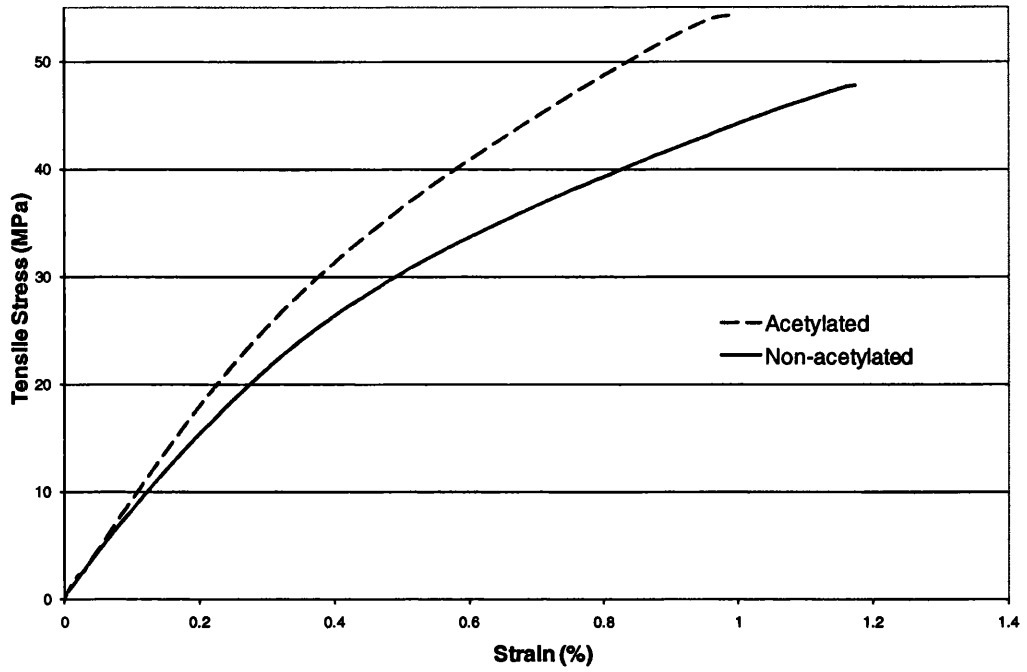

Fig. 6.38: Comparison of stress-strain curves of acetylated and non-acetylated fibre composites in tensile testing

6.2.2 IMPACT PROPERTIES

The acetylated fibre composites were subjected to low velocity impact testing. The comparisons of the residual tensile properties of acetylated fibre composites with non-acetylated fibre composites following low velocity impact are shown in Figs. 6.39-40.

The residual strength of the acetylated composites appears to decrease with increasing impact energy in the same proportion as for the non-acetylated composites as shown in Fig. 6.39. The residual strength of the acetylated fibre composites following impact at 2 and 3J is lower than the corresponding residual strength of the non-acetylated fibre composites. The acetylation process does not seem to have any positive effect on the impact damage tolerance of acetylated fibre composites.

The residual stiffness of the acetylated composites again has lower values than the corresponding values of non acetylated fibre composites following low velocity impact at 2 and 3 J, as shown in Fig. 6.40. This again shows the relatively poor impact damage tolerance of acetylated fibre composites.

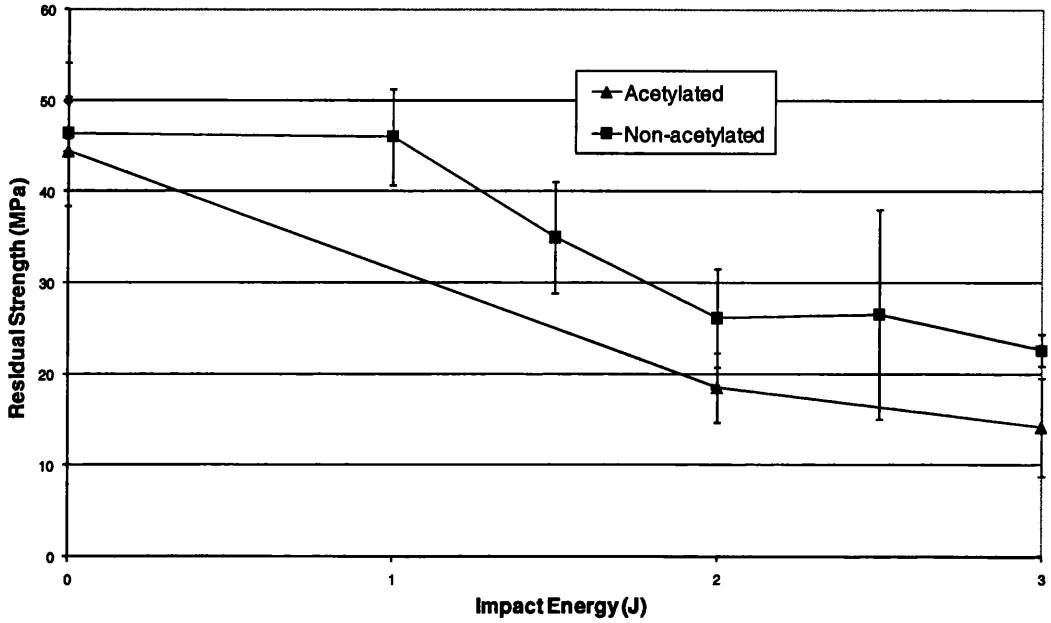

Fig 6.39: Comparison of residual strength of acetylated and non-acetylated fibre composites following low velocity impact

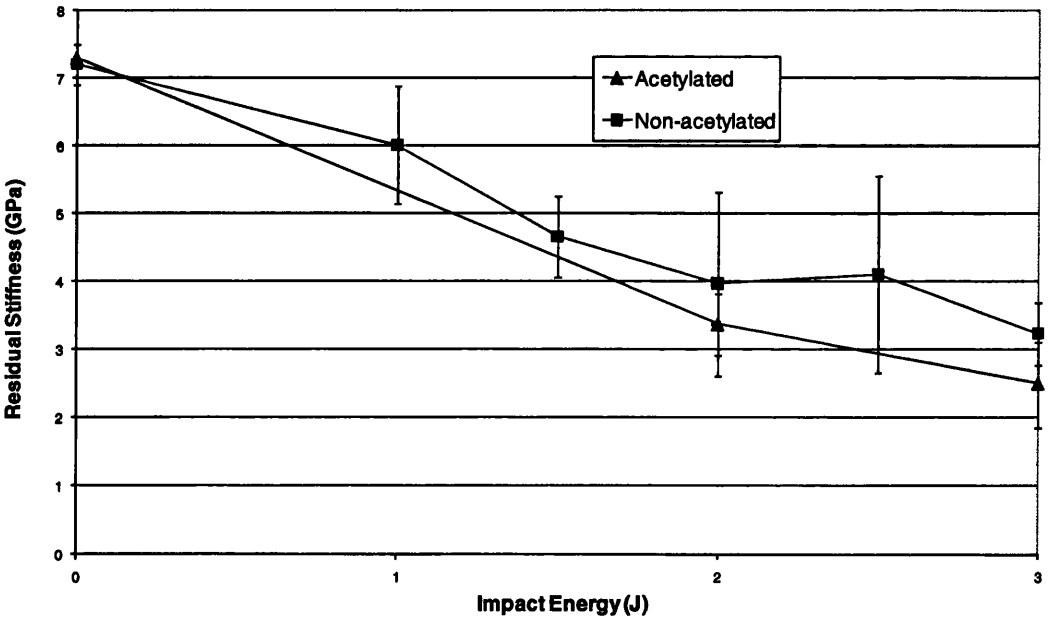

Fig 6.40: Comparison of residual stiffness of acetylated and non-acetylated fibre composites following low velocity impact

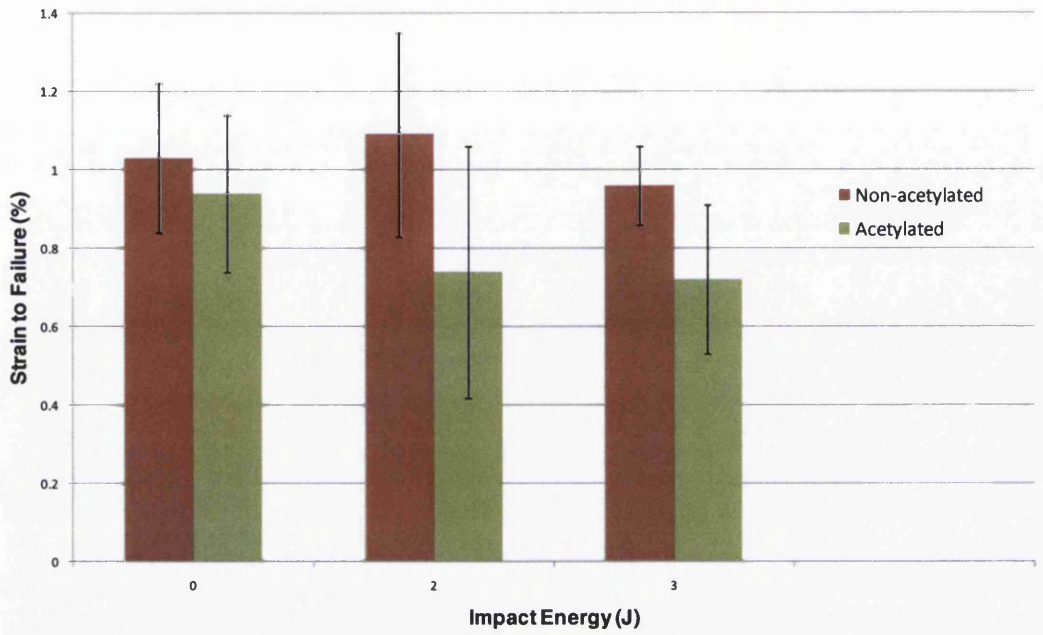

Fig. 6.41: Comparison of increasing impact energy level on the strain to failure of the acetylated and non-acetylated composites

The comparison of strain to failure of acetylated fibre composites with non acetylated fibre composites following low velocity impact is shown in Fig. 6.41. The strain to failure of acetylated composites is lower than the corresponding values of strain to failure of non-acetylated fibre composites following low velocity impact at 2J and 3 J but the differences are small when the error bars are taken into account. This however points at increase in brittleness of composites and decrease in energy absorption capacity in impact following the fibre treatment.

Generally no improvement in the tensile and impact properties of acetylated fibre composites were observed compared to non acetylated fibre composites. However, as stated earlier, the scope of these results is limited considering the low number of samples used in testing.

6.4 PLASMA TREATMENT

The fourth process used in the surface treatment of hemp fibres was plasma treatment. The plasma treatment of natural fibres has recently caught the attention of researchers as

a promising method for surface treatment of the fibres. Various studies undertaken on the plasma treatment of natural fibres have been discussed in Section 2.4.7. In this part of the study, hemp fibres were subjected to plasma treatment as described in Section 3.2.4 and the composites made from these fibres were tested for their tensile properties. The tensile properties of the plasma treated composites, compared with untreated fibre composites at similar fibre weight fraction, are shown in Table 6.10.

Table 6.10: Tensile Properties of Plasma Treated Fibre Composites

	Fibre weight fraction (%)	Tensile Strength (MPa)	Tensile Modulus (GPa)	Strain to failure (%)
Untreated	47	35.8 (4.2)	5.6 (0.7)	0.94 (0.19)
Plasma-treated	48	45.3 (5.7)	7.3 (1.2)	0.94 (0.1)

Improved reactivity of the fibres following the treatment was observed by less spillage of the resin in compression moulding compared to untreated fibre composites at same moulding pressure. This was also confirmed by lower fibre weight fraction of plasma treated fibre composites than untreated fibre composites at same moulding pressure. As shown in Table 6.10, the plasma treatment does seem to have resulted in improvement in tensile properties of the composites. Compared to untreated fibre composites at similar fibre weight fraction, the tensile strength has increased by about 25% and tensile modulus has increased by about 30%. The matrix/fibre interfacial adhesion was observed to have improved in this treatment as shown in SEM micrograph of the fracture surface of a sample in Fig. 6.42.

Fig. 6.42: SEM micrographs of fracture surface of tensile tested sample of plasma treated fibre composites

Further studies into the effects of this treatment on impact and fatigue properties of the composites could not be carried about because of shortage of time. This treatment has proved to be quite promising in improving the tensile properties of the composites. One study [364] has shown the effectiveness of this treatment in increasing the tensile properties of flax fibres because of increased crystallinity of fibres following the treatment. Considering that plasma treatment is a very high energy-consuming process, any advantages gained from this process will also have to be weighed against the cost of consumption of power in this process.

7. ENVIRONMENTAL PROPERTIES OF HEMP FIBRE REINFORCED POLYESTER COMPOSITES

One of the biggest advantages that composite materials made with synthetic fibres enjoy over other materials is their excellent environmental properties. Composites often find applications where they have to remain in water for long periods of time (e.g. boats, marine applications). Composites are also used extensively in outdoor applications (e.g. bridges, piping, building and automobile panels) where they are exposed to combinations of different environments like humidity, rain, and UV radiation. The composites are expected to have superior environmental properties for these applications.

The environmental properties of natural fibre reinforced composites have not been fully studied as yet. The hydrophilic nature of natural fibres means that these composites are susceptible to considerable water absorption which may lead to degradation of their mechanical properties. However it should also be noted that one of the main functions of these fibres is to transport moisture in the plant. The performance of these composites in various environments is vitally important from this point of view. Therefore this part of the research was devoted to studying the effects of different environments on mechanical properties of hemp fibre reinforced polyester composites.

Hemp fibre reinforced polyester composites were exposed to different types of environments for varying lengths of time and the effects of these environments on their mechanical properties were observed. These environments were: distilled water, salt water, and accelerated weathering conditions (UV radiation and a combination of UV radiation and condensation).

7.1 COMPOSITES IMMERSED IN DISTILLED WATER

7.1.1 Untreated fibre composites

Composite samples made from untreated hemp fibre were immersed in distilled water at 23°C, as described in Section 3.7.1, and their water absorption behaviour and the effect of water absorption on their mechanical properties was studied.

7.1.1.1 Water absorption

Water absorption behaviour of composites over 3700 hours immersion in water is shown in Fig 7.1. The average fibre weight fraction of these composites was 58% (equivalent to fibre volume fraction of 53%).

As anticipated the water absorption is quite rapid initially, reaching almost 15% after about 400 hours of immersion. Further immersion increases the weight gain to about 16% after 3700 hours of immersion but the error bars lie within the error bars of weight gain after 400 hours of immersion. This implies that the samples have reached their equilibrium water intake after about 400 hours of immersion.

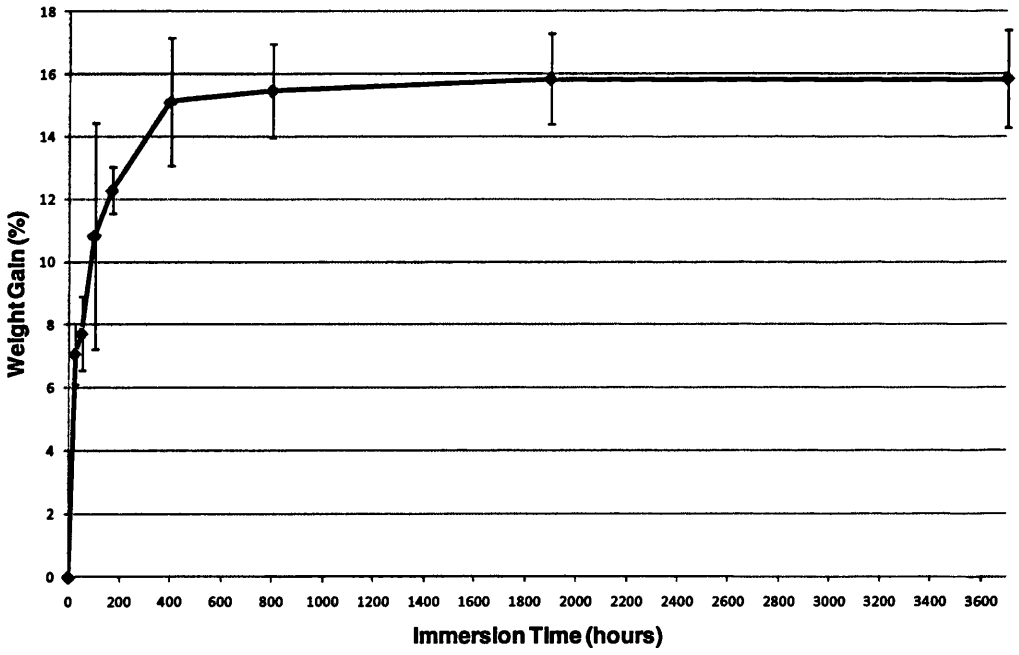

Fig. 7.1: Water absorption behaviour of hemp fibre reinforced polyester composites

The high value of equilibrium water uptake is consistent with that reported for other hemp fibre composites. In their studies on hemp fibre reinforced polyester composites, Dhakal et al [338] reported similar behaviour of water uptake for composites of fibre volume fraction of 26%. Their saturation water uptake value for these composites after 888 hours of immersion in water was 11%. These saturation values are less than the saturation value obtained in this research probably because of the higher fibre volume fraction of the composites used in this research. The water uptake and water saturation values in natural fibre composites have been shown, in various studies, to be strongly dependent on the fibre volume fraction of these composites (see Section 2. 7.6). Higher content of natural fibres results in higher absorption of water in these composites.

Compared to natural fibre composites, the saturation water intake for CSM glass fibre reinforced polyester composites has been reported to be 0.6% at fibre weight fraction of 44% [285] and 3.5% at fibre weight fraction of 65% [288].

7.1.1.2 Analysis of water absorption behaviour

Hemp fibres are hydrophilic in nature and so they have a great tendency to absorb water. As soon as the natural fibres are exposed to moisture, hydrogen bonds are formed between the hydroxyl groups (-CH_2OH) of the cellulose molecules and water as described in Section 2. 7.6. However in composites the surface layer of the resin provides protection against this tendency. On the other hand, natural fibres in the cut sides of samples have no resin protection so it is reasonable to expect that most of the water initially will be absorbed through them. Some water will also diffuse through the polyester resin and when this water reaches the natural fibres inside the sample it will lead to increase in the absorption rate of water. However after some time the material is expected to reach its saturation level and this is the point where the water absorption curve starts to level off.

The void content in the composite materials is also expected to contribute considerably to the water absorption where water can collect preferentially. In one study on carbon fibre reinforced epoxy composites, Hancox [365] reported that specimens containing more than 1 volume percent voids absorbed water more readily than those without any voids. The ratio of water taken up by the two types of specimen varied from approximately 2 at 40°C water to 2.5 at 95°C water. It was shown in Section 5.2.1 that the composites used in this research could contain voids up to 10% by weight. It is

therefore expected that this large content of voids may be an important contributor to water uptake in these composites.

Another possible mechanism of water absorption is poor fibre/matrix adhesion. The low interfacial shear strength of hemp fibres in polyester resin is indicative of their poor adhesion and this mechanism is also expected to contribute to water absorption. However its contribution is not expected to be as high as that due to hemp fibres absorption or the voids in the composites.

The overall solubility of water in these composites is a function of the water solubility in polyester matrix, the solubility in hemp fibres, the solubility in the interface region, and the amount of water present as a separate phase in voids, cracks, and debonded regions. Initially the water molecules will diffuse through the outer layer of polyester resin. They will also diffuse through the cut edges of the samples where hemp fibres and the interface region will be directly exposed to water. However the surface area of cut edges is only about 12% of the total surface area of each sample and it can be reasonably assumed that most of the water diffusion is through the polyester resin. In later studies done by immersing the samples in water with cut edges sealed with silicone sealant (see Section 7.1.3), it was found that water absorption because of sealed edges was only 1% less than that for non-sealed composites for immersion time of about 400 hours.

Water absorption in polyester resin

The solubility of liquid molecules in a polymer is generally expressed in terms of solubility parameter δ, which is defined as the square root of the cohesive energy density. Materials with similar solubility parameters have high solubility rates while those with different solubility parameters have low solubility. The values of δ for water and polyesters are 47.9 and 17.9 $MPa^{1/2}$ respectively [366]. This large difference in solubility parameters suggests that the solubility of water in polyesters is expected to be quite low.

This has been verified in various experimental studies. The moisture absorption and desorption behaviour of styrenated isophthalic unsaturated polyester resin, like the one used in this research, was studied by Jacobs and Jones [367] by using the model proposed by Shen and Springer [282]. They found that the resin had a two-phase

structure: dense and less-dense. They found the percentage moisture content of the resin to be about 0.9% at 75% RH, 1.4% at 96% RH, and about 1.6% following immersion in water at 50°C. The absorption curves for the resin specimens immersed in water and exposed to relative humidities of 96 and 75% showed two regions indicative of two-phase structure of the resin.

They reported that no visible deterioration was observed in the polyester resin in optical microscopy even for specimens immersed in water in excess of 80 days. Also there was no evidence of leaching during immersion in water. It was also noted that no correction factor was necessary for the samples exposed to different relative humidities, and this crucially demonstrated that in polyester resin, the diffusion was independent of concentration. The diffusion coefficient for the resin appeared to be dominated by the desorption of moisture from the less dense phase. This suggested that the two-phase structure of polyester resin is comprised of particles of the dense phase embedded in the less dense phase.

In general the solubility of a liquid in polymers increases with smaller liquid molecular volume, lower elastic modulus of polymer, reduced enthalpy of mixing, and increased free volume in polymer [366]. The polymers with greater levels of hydrogen bonding tend to have higher levels of equilibrium water solubility. Therefore unsaturated polyesters, with very few hydroxyl groups, have low water solubility of 1-1.5 wt. % [366]. Dyer [242] has reported a moisture saturation level of 0.67% for polyester resin immersed in distilled water. This saturation level was the same for polyester resin immersed in sea water. Compared to this, the saturation water uptake of hemp fibres at 23°C has been reported to be 66% [293].

Diffusion of water in the composite

The diffusion of a liquid into another material is commonly described by the well-known Fick's law [366],

$$\frac{dC}{dt} = D\frac{d^2C}{dx^2} \qquad \text{(7.1)}$$

where C is the concentration of the liquid, D is diffusion coefficient of the material absorbing the liquid, t is time, and x is a distance term.

For Fickian diffusion, mass uptake versus time is expressed as the following equation for thin plate samples like the one used in this research [366],

$$M_t = \left[\frac{M_\infty 16tD^{1/2}}{\pi h^2} \right]^{1/2} \quad \text{..... (7.2)}$$

where M_t is the mass uptake at time t, M_∞ is the equilibrium mass uptake, and h is the sample thickness. The mass uptake is therefore proportional to square root of time, and this fact is used to determine whether Fickian behaviour is observed or not.

Fujita [368] has observed that for true Fickian diffusion the absorption curve should exhibit the following features:

a) The curve should be linear up to and exceeding 60% of the equilibrium moisture content M_∞.
b) Above the linear portion the sorption curve should be concave to the abscissa, irrespective of any dependence of the diffusion coefficient on the moisture concentration.

The graph of weight uptake versus square root of time for these composites is shown in Fig 7.2 whereas Fig. 7.3 shows the normalised water uptake (instantaneous water uptake divided by equilibrium water uptake) against square root of time. The curves seem to obey the conditions set out by Fujita quite well. The diffusion of water in these composites is thus observed to be Fickian.

In order to correlate the experimental behaviour of water uptake of this material with the theoretical behaviour, computer modelling by 3D Finite Difference Method based on Fickian Diffusion [369] was used and compared with the experimental results. The results are shown in Figs.7.4-5. These figures show that absorption of water in this material is in excellent agreement with theoretical behaviour predicted by the model. So the water absorption behaviour is reaffirmed to be Fickian in this material.

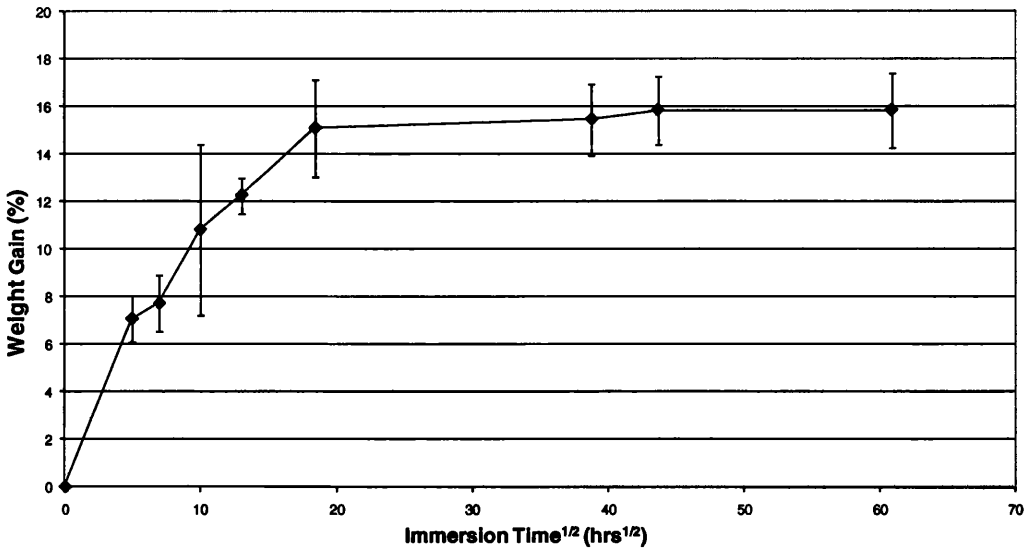

Fig. 7.2: Water uptake in hemp fibre reinforced polyester composites against square root of time

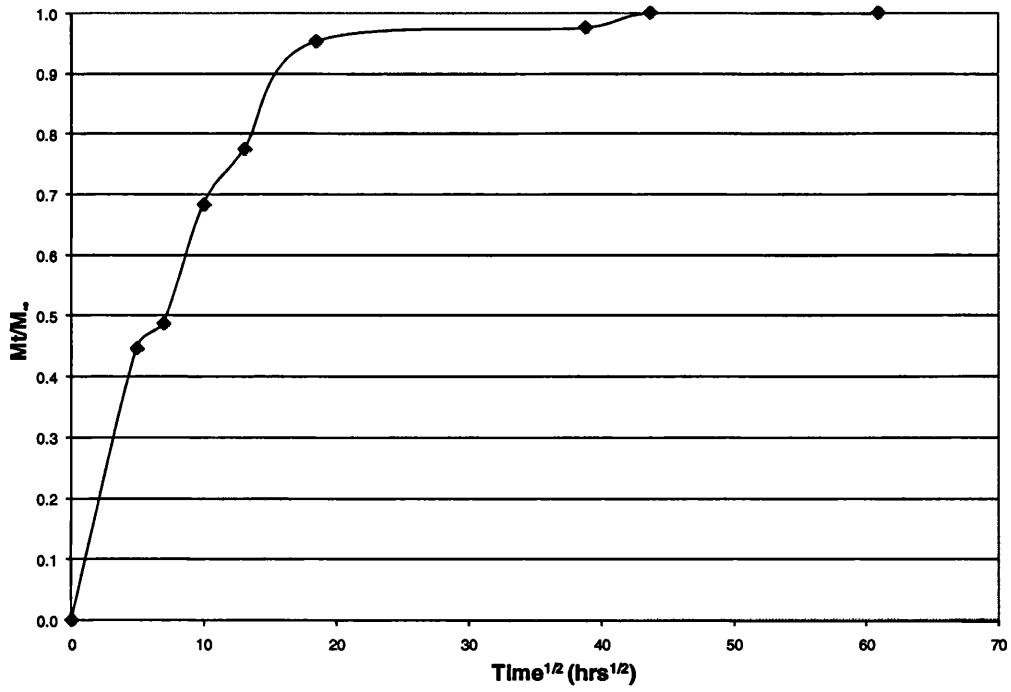

Fig. 7.3: Normalised water uptake of composites against square root of time

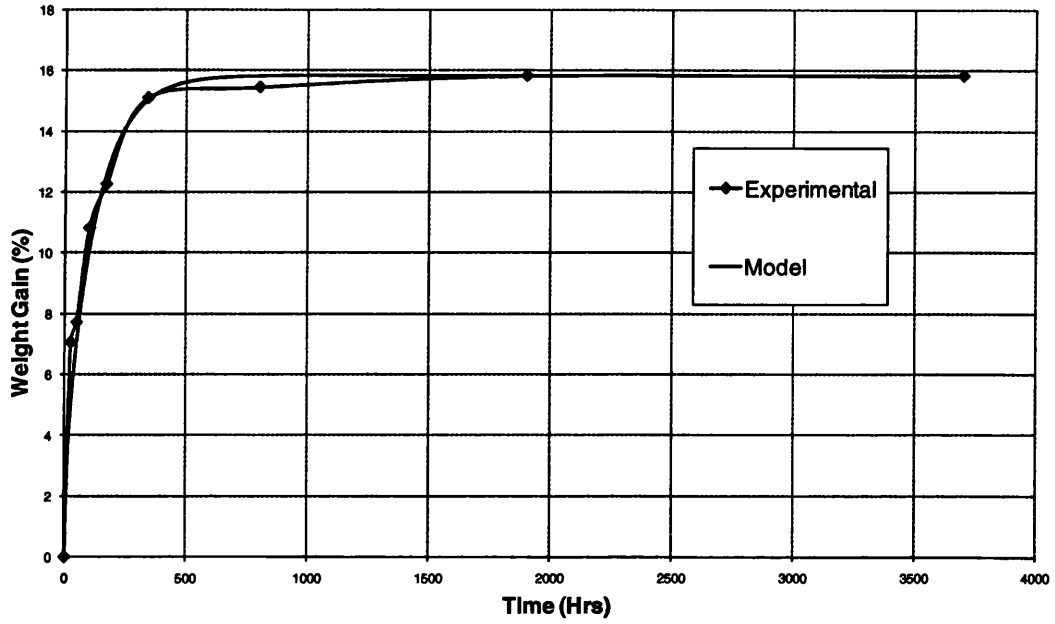

Fig. 7.4: Experimental and theoretical comparison of water uptake behaviour

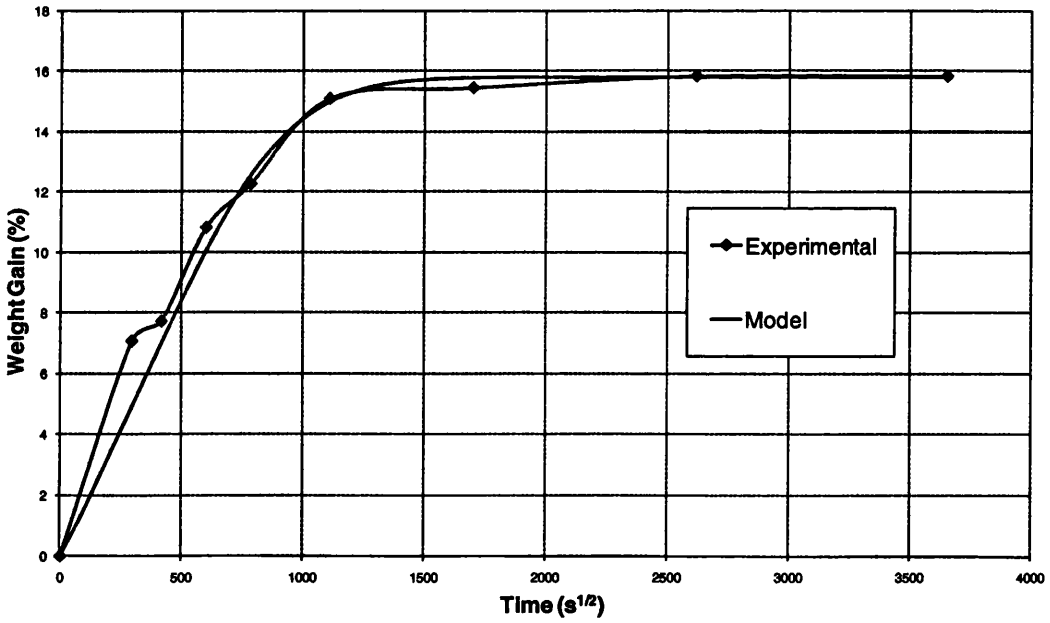

Fig. 7.5: Experimental and theoretical comparison of water uptake behaviour

The water diffusion in other natural fibre composites has been reported to be Fickian. Rao et. al. [370] reported the validity of the Fickian diffusion model for jute-epoxy

composites. The equilibrium moisture level in the composites with fibre volume fraction of 70% was 9.5 %. Giridhar et al [371] reported an equilibrium moisture level of as high as 40% for sisal-epoxy composites at fibre volume fraction of 70%. The high moisture absorption of sisal-epoxy composites was attributed to relatively high cellulose content of sisal fibres. The diffusion in these composites was also reported to follow Fick's law.

Absorption parameters:

Apart from determining whether the moisture absorption behaviour is Fickian or not, the moisture absorption graph is a very useful tool in determining various absorption parameters of the material. These are diffusion coefficient D, sorption coefficient S, and permeability coefficient P.

The value of diffusion coefficient D is obtained from the slope of weight gain versus square root of time curve, and is given by,

$$D = \pi \left[\frac{kh}{4M_\infty} \right]^2 \quad \text{..... (7.3)}$$

where k is the slope of the linear portion of the M_t versus $t^{1/2}$ curve, h is the sample thickness, 2.5 mm in this case, and M_∞ is the maximum weight gain due to water absorption. The slope of the linear portion of the curve was calculated to be 0.11 g/hour$^{1/2}$ from Fig. 7.2. The value of M_∞ was 2.18g. Using these values in equation (7.3) above, the value of the diffusion coefficient was calculated to be 8.7 x 10^{-13} m^2/s.

The sorption coefficient or solubility S is defined as

$$S = M_\infty / M_i \quad \text{..... (7.4)}$$

where M_∞ is the weight of water taken up at equilibrium and M_i is the initial weight of the sample. The values of S for individual samples were calculated and their average value was found to be 0.16.

Similarly permeability coefficient P, which represents the combined effects of sorption and diffusion, is defined as

$$P = DS \quad \text{..... (7.5)}$$

where D is diffusion coefficient and S is sorption coefficient. Using the values of D and S given in equation (7.5), the value of P was calculated to be 1.32 $x10^{-13}$ m^2/s. The values of absorption parameters determined for hemp-polyester composites in this research are comparable to the ones reported in literature for natural fibre composites as shown in Table 7.1. The fibre weight/volume fraction values are in parentheses.

Table 7.1: Water absorption parameters of natural fibre composites as reported by various researchers

Composite	D (m^2/s)	S	P (m^2/s)	Reference
Pineapple/polyester (40%wt)	$2.3x10^{-13}$	0.18	$3.6x10^{-14}$	[296]
Jute/epoxy (70% vol)	$4.5x10^{-13}$	-	-	[371]
Sisal/epoxy (70% vol)	$1.7x10^{-12}$	-	-	[371]
Sisal-polyester (50% vol)	$0.04x10^{-8}$	-	-	[138]
Banana/polyester (20% vol)	$7.7x10^{-8}$	-	-	[144]
Pandanus/polyester (20%)	$22.7x7x10^{-8}$	-	-	[144]
Sisal/polypropylene (30% wt)	$3.8x10^{-13}$	-	-	[304]
Coir/polypropylene (30% wt)	$10.9x10^{-13}$	-	-	[304]
Hemp/polyester (21% vol)	$3.8x10^{-11}$	-	-	[295]
Hemp/polyester (26% vol)	$4.4x10^{-3}$	-	-	[338]

7.1.1.3 Tensile properties

The hydrophilic nature of natural fibres can lead to considerable swelling in these fibres in water which in turn can have adverse effects on the mechanical properties of these composites. The swelling process is usually accompanied by a reduction in tensile modulus of composite through plasticisation. Swelling of fibres will also result in development of shear stress along the fibre-matrix interface which may lead to debonding. All these processes can result in degradation in mechanical properties of

composites. So the next stage of the research was to evaluate the effect of water absorption on mechanical properties of these composites.

The composites that had been immersed in distilled water were subjected to tensile testing following immersion at different lengths of time and the results are shown in Figs. 7.6-8. The horizontal axis has been chosen as hours$^{1/2}$ in these figures in order to highlight the properties at low immersion times. Fig. 7.6 shows that the strength of these composites increases slightly following immersion in water for 25 hours which can be attributed to the relaxation of residual stresses following immersion. However deterioration in tensile strength is quite rapid after that concurrent with rapid uptake of water. The composites have lost almost 15% of their intrinsic tensile strength after 100 hours at immersion. However the deterioration in strength seems to levels off after about 100 hours of immersion. Although the water uptake rate keeps increasing rapidly up to about 400 hours this does not seem to have further adverse effect on tensile strength of the composites. Further immersion in water, however, does result in further reduction in tensile strength.

As shown in Fig. 7.7, the decline in tensile modulus is also quite rapid initially, falling to about 50% of intrinsic tensile modulus after about 100 hours of immersion. The decline in tensile modulus is faster compared to decline in tensile strength which is expected because of the weakening of the fibre/matrix interface and the plasticization of the matrix. It has been shown [372] that moisture absorption in natural fibres results in greater reduction in modulus than strength, and the composites made of these fibres will also be expected to show similar behaviour. However, as in the case of tensile strength, the decline in tensile modulus tends to level off at about 400 hours of immersion and the error bars of modulus values lie within the error bar of the modulus after 400 hours of immersion.

The strain to failure of these composites, which is about 1% without water immersion, increased initially up to 100 hours of immersion, resulting in corresponding decrease in stiffness, and then levelled off to the value of 2% at about 2000 hours of immersion. The increase in strain to failure is again a manifestation of plasticization of the matrix and the reduction in modulus of the fibres following immersion in water.

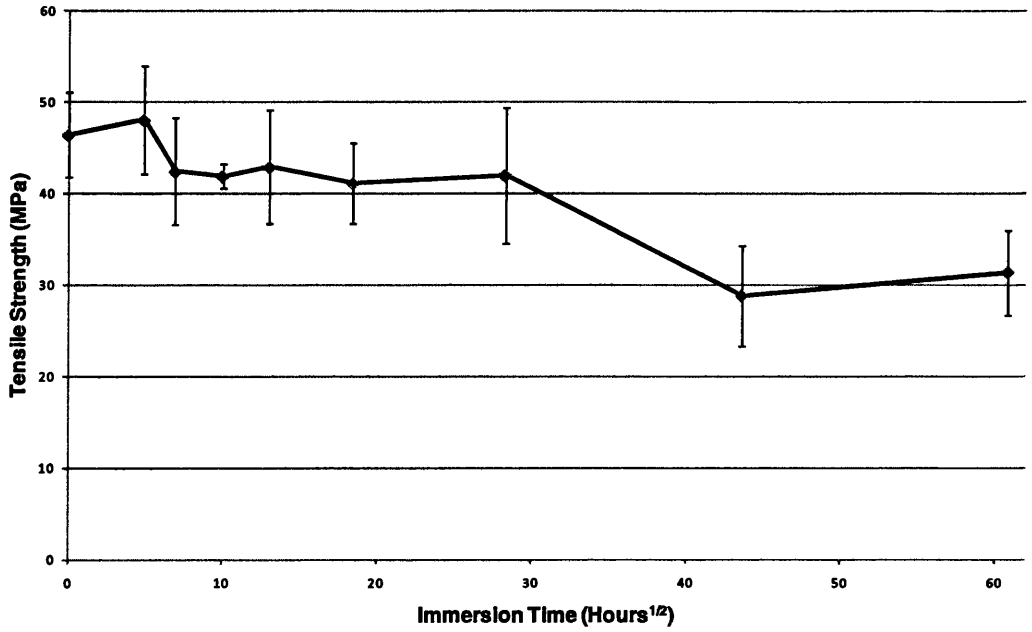

Fig. 7.6: Effect of water absorption on the tensile strength of composites

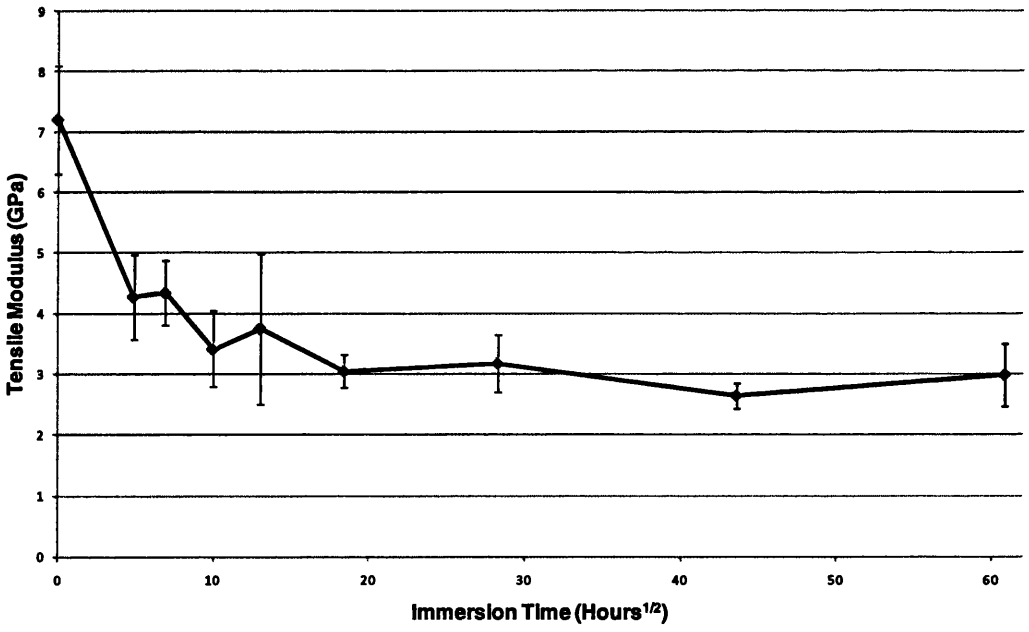

Fig. 7.7: Effect of water absorption on tensile modulus of composites

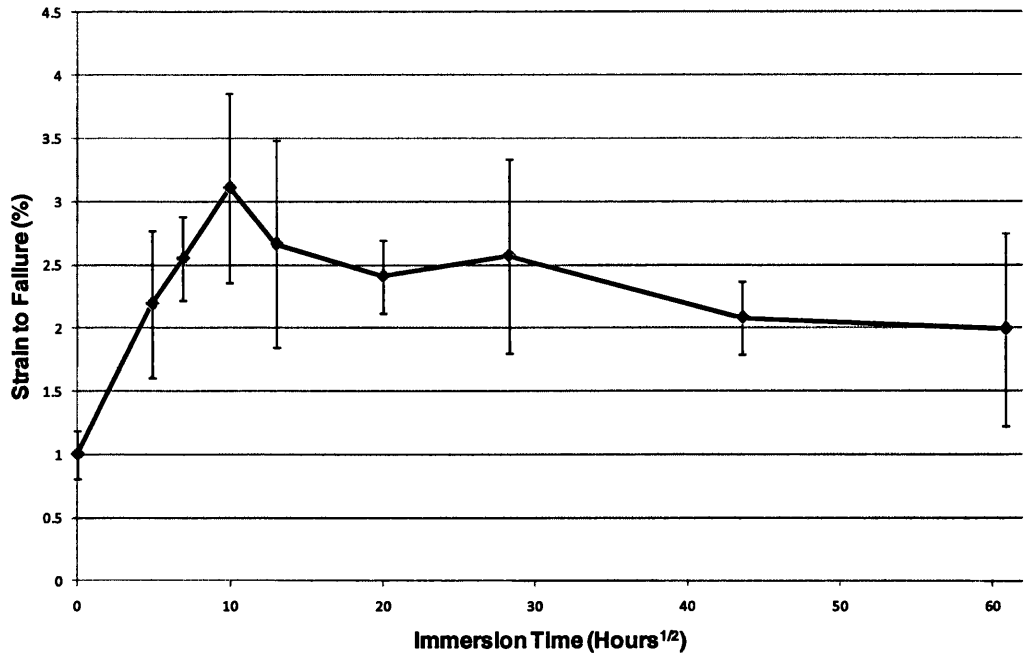

Fig. 7.8: Effect of water absorption on strain to failure of composites

7.1.1.4 Analysis of tensile properties

The effects of water immersion on the normalised tensile properties of the composites are shown in Fig. 7.9. The decline in tensile modulus is more pronounced than the decline in tensile strength following immersion in water. The loss in strength is only about 10% of the original strength following immersion for 800 hours whereas the loss in stiffness is almost 60% of the original stiffness following same time of immersion. However the loss in strength continues at further immersion times while the loss in stiffness stabilises and does not decline any further. The decline in tensile strength goes on increasing and only stabilises after about 2000 hours of immersion. Following immersion in water for 3700 hours, the loss in strength is about 35% of the original strength and the loss in stiffness is about 60% of the original stiffness. The loss in stiffness of fibres following immersion and the plasticisation of the matrix combine to result in greater loss in stiffness than strength for these composites.

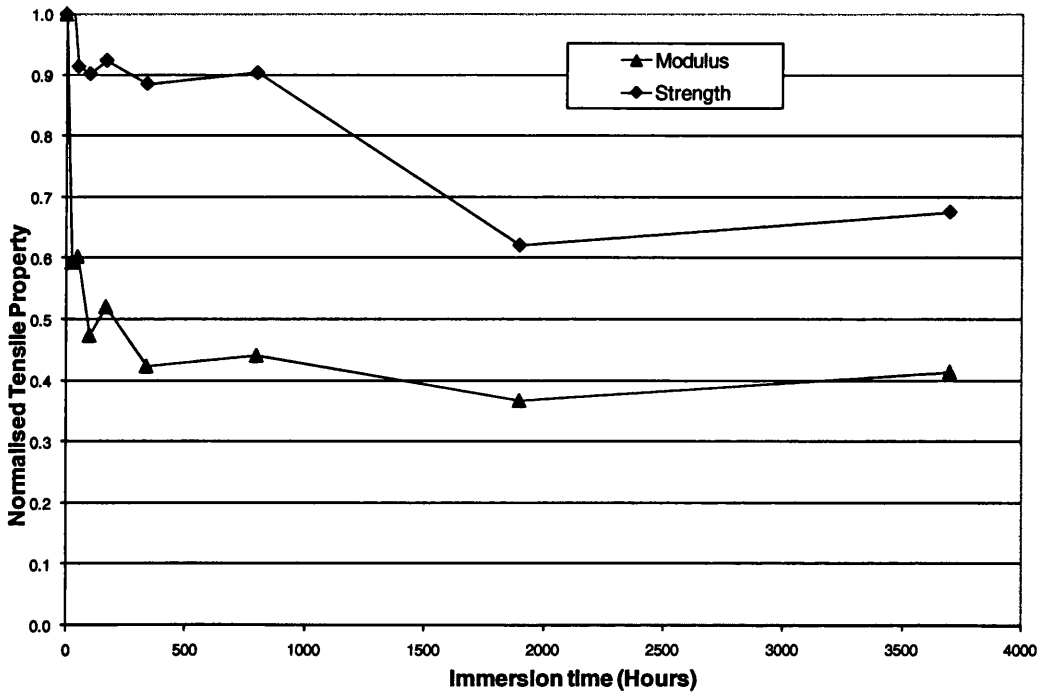

Fig. 7.9: Effects of water immersion on the normalised tensile properties of the composites

One important effect of immersion in water was the discolouring of the composites from dark brown to whitish brown. This fading can have implications with regard to aesthetic value of these composites.

A similar reduction in tensile properties of natural fibre composites has been reported by other researchers. Dhakal et al [338] reported tensile strength of hemp fibre reinforced polyester composites to decrease by 15% at fibre volume fraction of 21% following 888 hours of immersion in water. Tensile modulus was found to decrease by almost 50% following same immersion time.

Marais et al [135] reported that for flax fibre reinforced polyester composites immersed in water for 96 hours at 60°C, the tensile strength decreased form 115 MPa to 81 MPa while tensile modulus decreased from 11.5 GPa to 6.4 GPa.

Sindhu et al [290] studied the effect of water absorption on mechanical properties of coir fibre reinforced polyester composites. The composites with 30% fibre weight fraction gradually decreased their tensile properties. Following immersion in water for 2160 hours, the reduction in tensile strength was 18%, in tensile modulus of 2%, and in

strain to failure of 28%. The corresponding changes in CSM glass fibre/polyester composites (same fibre weight fraction) after 2160 hours in water were 20% reduction in tensile strength, 1% increase in tensile modulus, and 30% reduction in strain to failure.

Aghedo and Baillie [306] reported that mechanical properties of hemp fibre reinforced recycled linear low density polyethylene composites were not significantly affected by water absorption after eight weeks of immersion in water.

Thwe and Liao [105] reported no reduction in tensile strength and 19% reduction in tensile modulus of bamboo fibre reinforced polypropylene composites following immersion in water for 6 months. Espert et al [304] reported considerable decrease in tensile properties of cellulose-PP, sisal-PP, coir-PP and luffa-PP composites following immersion in water.

Fracture modes:

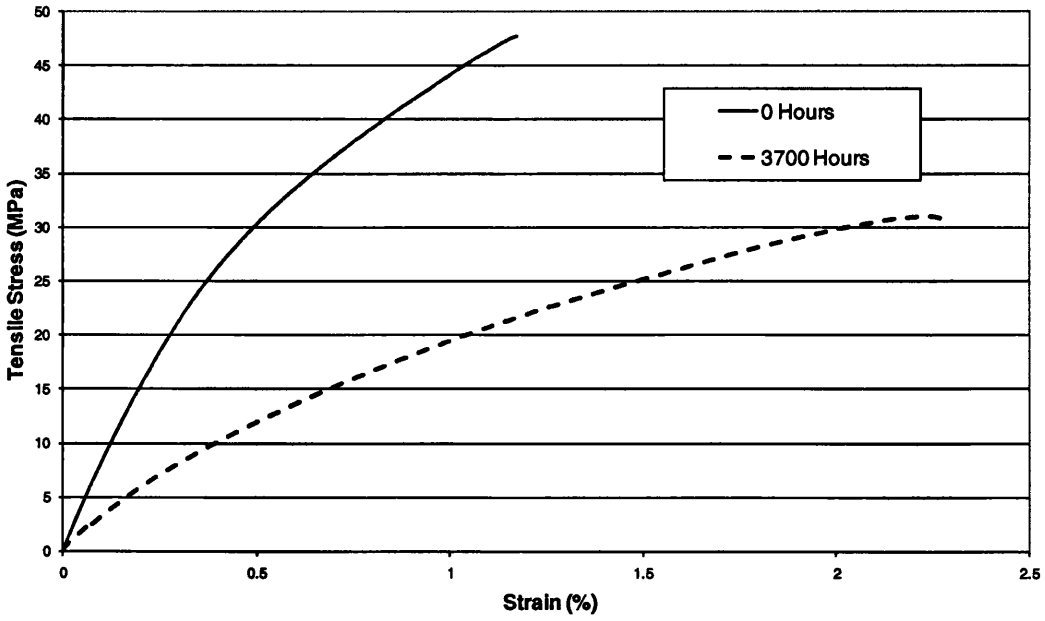

Fig. 7.10: Comparison of stress-strain graphs of a sample immersed in water with that of non-immersed sample

One significant effect of immersion water was the change of mode of fracture of these composites from brittle to more ductile failure even after about 50 hours of immersion.

For samples immersed in water for 100 hours and above, the mode of failure was almost entirely ductile.

The comparison of stress-strain graphs of one of the typical samples that failed in ductile mode after 3700 hours in water with that of non-immersed sample is shown in Fig. 7.10. The graph shows the increase in strain to failure and the corresponding decrease in stiffness of the composites following immersion in water. The 'knee' of the curve is also less prominent as the transfer of stress from matrix to the fibres becomes more uniform following immersion in water.

(a) (b)

Fig. 7.11: Transition from brittle (a) to more ductile (b) fracture in tensile tested composites following immersion in water for 3700 hours

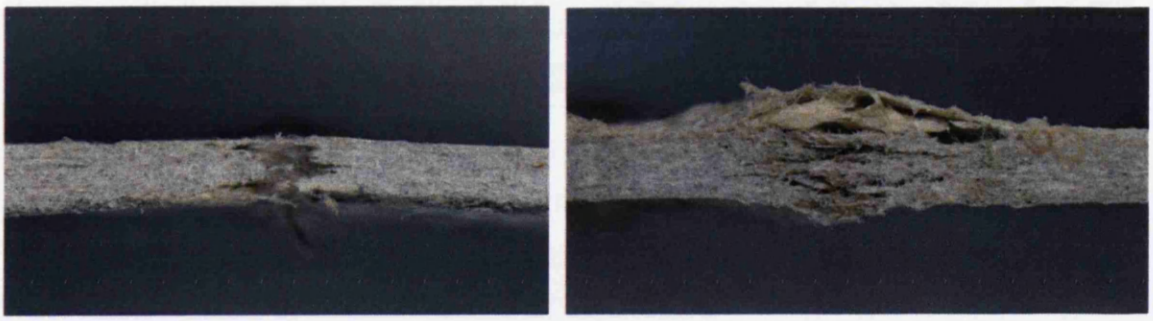

(a) (b)

Fig. 7.12: Sectional views of the samples fractured in brittle (a) and more ductile (b) modes in tensile testing following immersion in water for 3700 hours

This transition from brittle to more ductile fracture is also shown in Figs. 7.11 and 7.12. It was observed that for, most samples that failed in ductile mode, the fracture plane was inclined at an angle of typically about ±45° to the tensile axis as shown by the arrow in Fig. 7.11 (b). The absorption of water results in plasticisation of polyester resin that makes it more ductile. This and the swelling of fibres and weakening of fibre/matrix interface seem to have contributed to this transition from brittle to ductile fracture. The shear stresses induced because of these seem to have resulted in debonding and sliding of matrix and fibres resulting in ductile failure. The shear stress in any material in uniaxial tension is maximum at 45° plane and this is the plane at which these samples tend to fail. This suggests that, as against the samples not immersed in water where normal stresses were the dominant cause of fracture, shear stresses also become dominant following immersion in water and contribute significantly to the fracture of samples.

SEM micrographs:

Fig. 7.13 (a) and (b) show SEM micrographs of fracture surfaces of the tensile tested samples after 3700 hours of immersion in water. These samples surfaces had to be dried before their SEMs could be taken. The dried surfaces still showed the damage that immersion in water had done to the composites. The figure shows the normal modes of failure like matrix fracture and fibre fracture are present and there is evidence of increased fibre/matrix debonding, shown by the arrowheads, because of the weakening of the interfacial bonding.

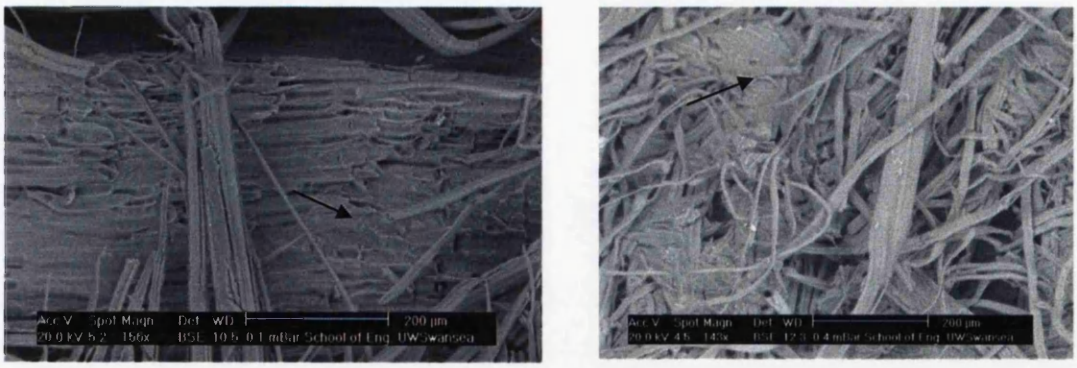

(a) **(b)**

Fig. 7.13: SEM micrographs of fracture surfaces of the tensile tested sample after 3700 hours immersion in water

7.1.1.5 Impact Properties

The effect of water immersion on impact damage tolerance of hemp fibre composites was evaluated. Since it was not possible to do the impact testing with the samples immersed in water, the samples were first subjected to impact testing and then immersed in water for up to 400 hours which is the average time these composites took to reach their saturation level.

The residual tensile properties of the impact-tested composites following immersion in water are shown in Figs. 7.14-16. The comparison of residual tensile strength of impacted samples following immersion in water for up to 400 hours is shown in Fig. 7.14. Immersion in water for non-impacted samples resulted in 10% reduction in tensile strength and 50% reduction in tensile modulus following immersion in water for 100 hours. Immersion in water of samples following impact for the same time period results in further degradation of residual tensile properties. The residual strength of 2J impacted samples is reduced by 30% and that of 3J impacted samples is reduced by 60% compared to non-impacted samples, following the same immersion time of 100 hours. As shown in Fig. 7.1 and 7.9, these composites attain their saturation water uptake following immersion in water for 400 hours and most of the degradation in tensile properties takes place by this time. However Figs. 7.14 shows that further immersion in water for up to 400 hours does not result in further degradation in residual strength. More importantly the graph shows that the composites do not suffer any appreciable deterioration in strength following impact and immersion in water for the same impact energy level.

The comparison of residual tensile stiffness of impacted samples following immersion in water for up to 400 hours is shown in Fig. 7.15. The graph shows similar deterioration in residual stiffness of composites following immersion in water to strength. The residual stiffness of 2J impacted samples is reduced by 30% and that of 3J impacted samples is reduced by 60% compared to non-impacted samples following immersion in water for 100 hours. Just like strength, the stiffness does not show further degradation following immersion in water for up to 400 hours at same impact energy level.

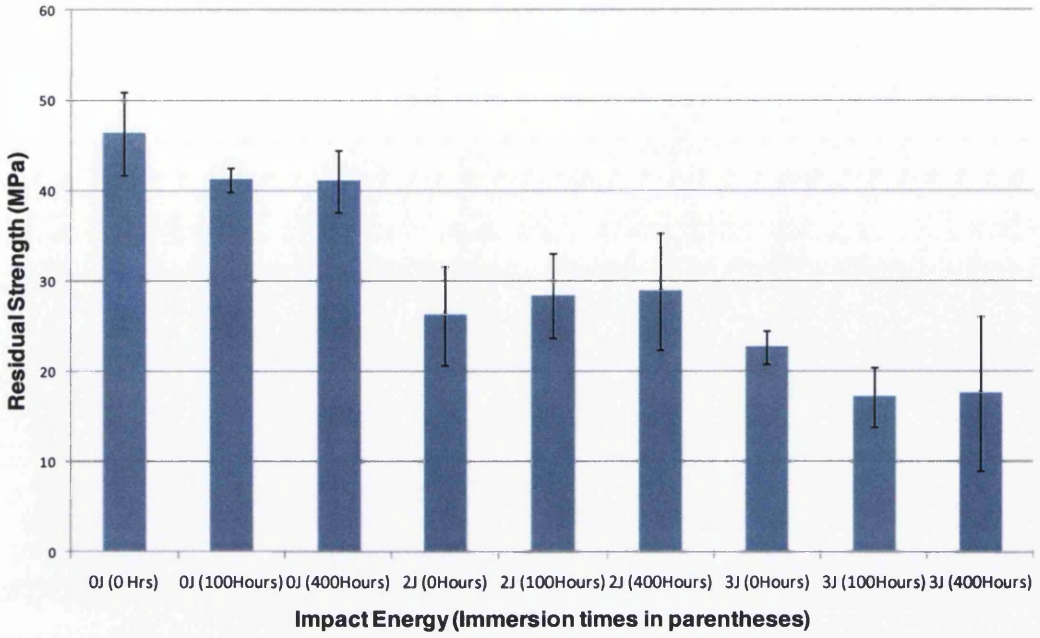

Fig. 7.14: Comparison of residual tensile strength of impacted samples following immersion in water for up to 400 hours

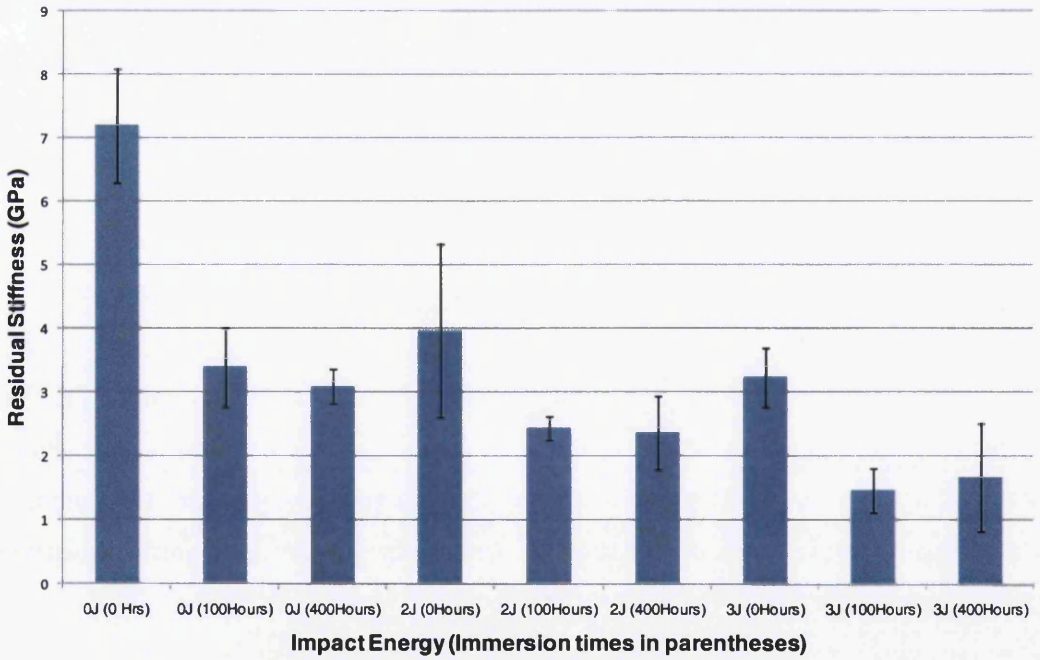

Fig. 7.15: Comparison of residual tensile stiffness of impacted samples following immersion in water for up to 400 hours

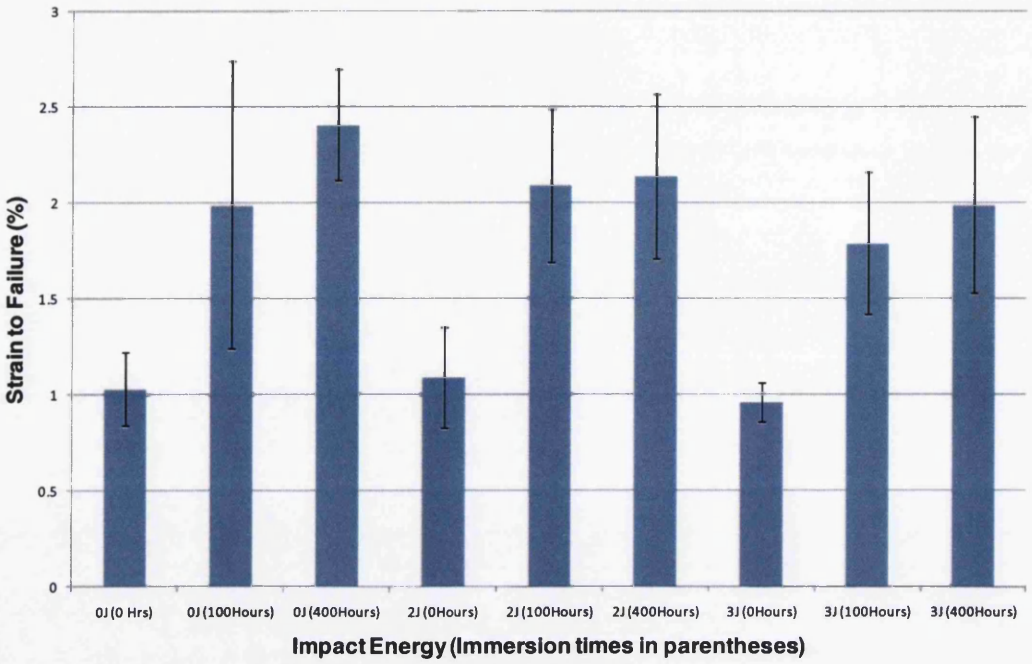

Fig. 7.16: Comparison of strain to failure of impacted samples following immersion in water for up to 400 hours

Fig. 7.16 shows the strain to failure of impacted samples following immersion in water for up to 400 hours. The strain to failure of all the samples increase following immersion in water. However most of the increase occurs within fist 100 hours of immersion and any further immersion does not result in any difference in strain to failure at same impact energy level.

These studies have shown that poor impact damage tolerance of these materials is further degraded when they are immersed in water. However, at same impact energy level, most of the degradation occurs within first 100 hours of immersion in water and further immersion in water for up to 400 hours does not result in any further degradation. Compared to non-impacted and non-immersed composites, the composites lost almost 62% of their intrinsic strength and almost 77% of their intrinsic stiffness following impact at 3J and immersion in water for 400 hours.

7.1.1.5 Fatigue Properties

The fatigue properties of the composites immersed in water were also investigated. The study of these properties is important because of widespread use of composite materials

in aqueous environments where they can be exposed to considerable fatigue loading. Generally the synthetic fibre composites have been found to show loss of fatigue strength when immersed in water ([373], [374], [375], [376], [377]). The reduction in strength has been attributed to ingress of moisture in cracks, and plasticisation of polymer matrix which reduces the stiffness of composites.

For fatigue testing in water, a specially designed water chamber was used as described in Section 3.6.3. The samples were almost completely immersed in water throughout the fatigue testing. The composites were tested in tension-tension mode (R=0.1) at a frequency of 1 Hz. Two different kinds of testing regimes were used. In the first, the composites were immersed in water straightaway without any pre-conditioning. In the second, the composite were first immersed in water for an average of 400 hours to allow the water to ingress the composites. As shown in Section 7.1, the water absorption in these composites is close to their equilibrium saturation level after about 400 hours of immersion in water. The mean fibre weight fraction of the samples used in these tests was 55%.

The S-N curve of the composites tested in water without pre-conditioning is shown in Fig. 7.17. The dashed lines represent 95% confidence interval of linear regression line. The curve shows very good fatigue properties of the composites in water because of the similar slope to S-N curve for composites fatigue tested in dry conditions. In particular there has been no change in the endurance limit of the composites which is about 20 MPa, shown by the arrowheads, the same as for dry composites.

The S-N curve for the composites pre-conditioned in water for about 15 days and then subjected to fatigue testing in water is shown in Fig. 7.18. The tensile strength of the composites following immersion in water for 400 hours has been used as static strength on this curve.

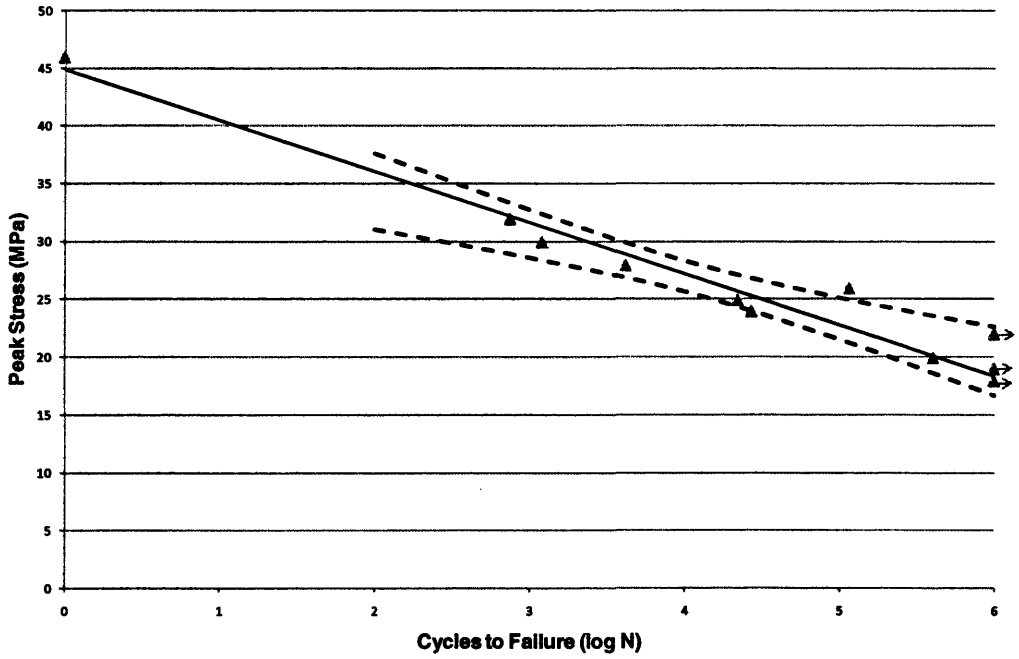

Fig. 7.17: S-N curve of composites in water without pre-conditioning

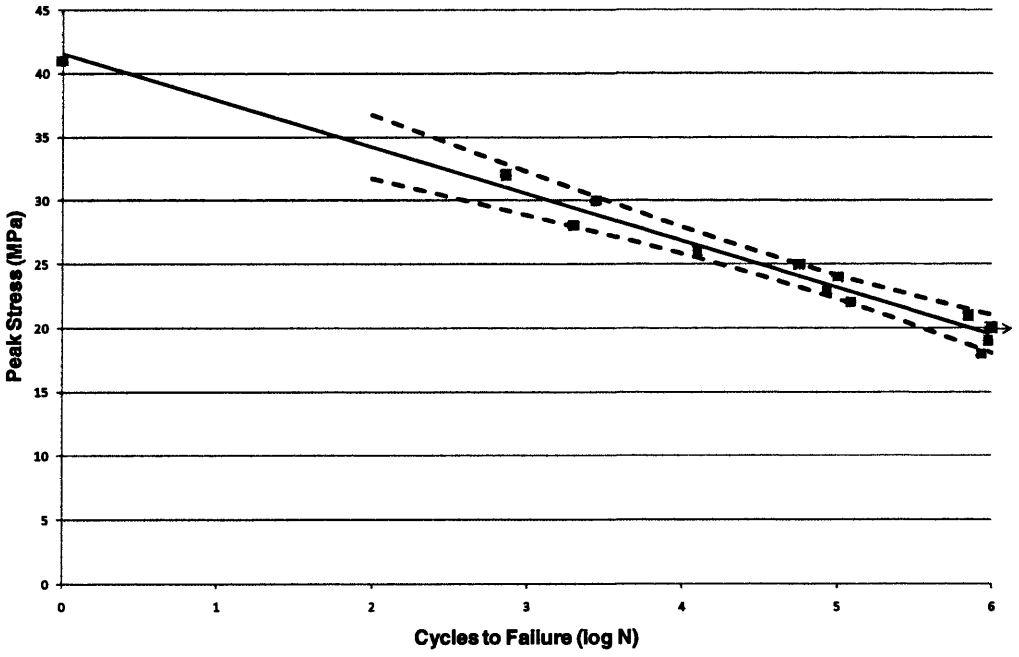

Fig. 7.18: S-N chart of composites in water with pre-conditioning

The S-N curve of the pre-conditioned composites again shows very good fatigue properties of the composites. The deterioration in tensile properties because of immersion in water does not seem to have any effect on their fatigue performance. Although these composites start with having lower tensile strength than dry composites because of immersion in water for 15 days, they seem to have the similar decline in fatigue strength with increase in fatigue cycles as those of dry composites or the composites immersed in water without pre-conditioning. The slope of the S-N curves is quite similar to the one for dry composites and composites immersed in water without pre-conditioning, as shown in Fig. 7.20. The endurance limit also remains unaffected at 20 MPa as shown by the arrowheads. These results seem to suggest that the fatigue strength of these composites is not affected by immersion in water. It was also observed that fracture surfaces of some samples were slanted rather than square just as in static tensile testing in water, as shown in Fig. 7.19. As discussed in Section 7.1.1.4, this points at shear stresses becoming dominant in fatigue testing in water.

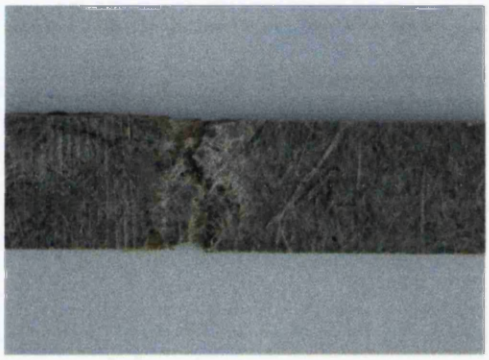

Fig. 7.19: Fracture surface of a sample in fatigue testing in water

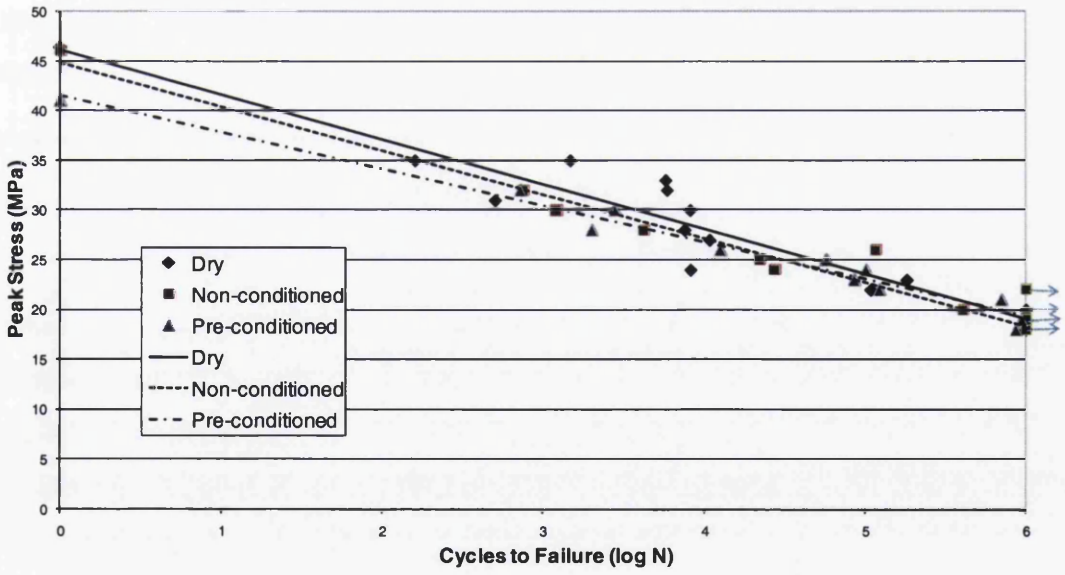

Fig. 7.20: Combined S-N curves of dry and water immersed composites

7.1.1.6 Analysis of fatigue properties

The comparison of fatigue properties of various composites in water can be done in on the basis of their fatigue sensitivity based on normalised S-N curves. The comparison of normalised S-N curves of dry and immersed composites is shown in Fig. 7.21.

The curves show that these composites perform very well in water in terms of their fatigue sensitivity. The data for the three kinds of composites is uniformly scattered and it should be possible to draw a single regression line through all data points. The composites that were immersed in water, with and without pre-conditioning, have almost similar slope to that of dry composites. This is expressed quantitatively in terms of their fatigue sensitivity coefficients as shown in Table 7.2.

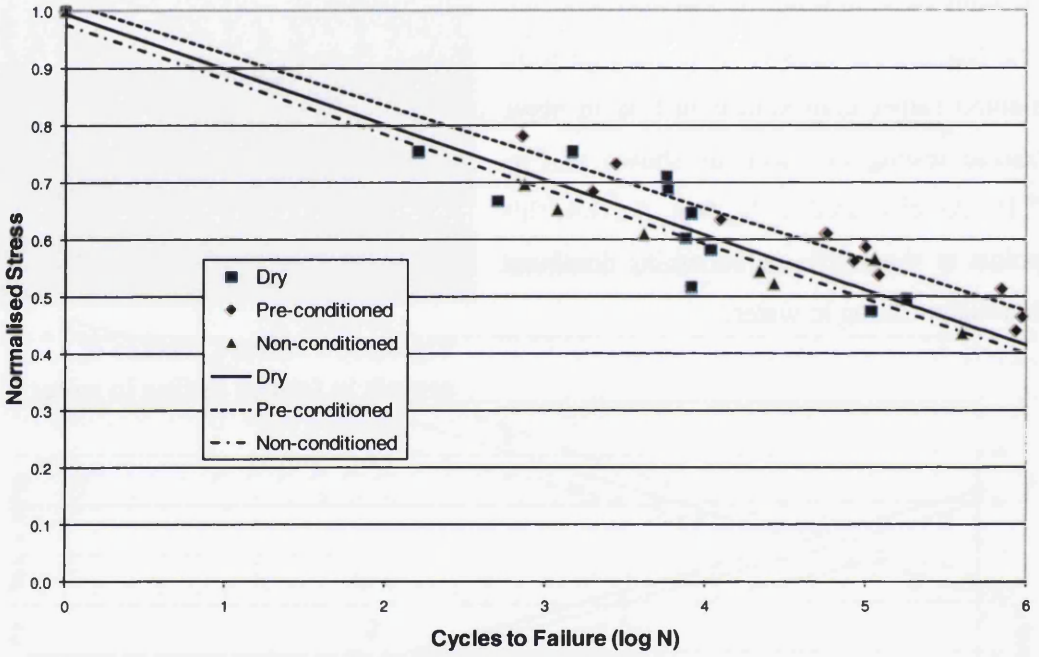

Fig. 7.21: Comparison of normalised S-N curves of composites

The fatigue sensitivity coefficients are similar in water as for dry composites. Immersion in water does not seem to have any appreciable effect on fatigue sensitivity of these composites. However it must be pointed out that the nature of the fatigue testing meant that the non-conditioned composites could only be immersed in water for a maximum of up to 277 hours (the time required to complete 10^6 fatigue cycles).

These results are still significant since, as shown in Fig. 7.9, after about 277 hours of immersion in water, these composites had lost almost 10% of their tensile strength and

almost 50% of their tensile modulus. However this degradation in tensile properties seems to have had no adverse effect on the fatigue properties of these composites. Fatigue is a fibre stiffness sensitive property and, despite losing almost half of their stiffness following immersion in water, the unaffected fatigue properties of these composites points at very good properties of these fibres in water.

Table 7.2: Fatigue sensitivity coefficients of composites in water

Composites	Fatigue sensitivity coefficient
Dry	0.097
Non-conditioned	0.096
Pre-conditioned	0.090

The pre-conditioning of the composites in water was considered to simulate the conditions of the composites more accurately since it is more likely that these composites would be immersed in water for some time before experiencing any fatigue conditions. The time period of 15 days was chosen because these composites were observed to have absorbed almost 90% of their saturation water absorption level after 15 days of absorption. Also most of the degradation in tensile properties occurs within this time period.

One possible reason for good fatigue resistance of these composites in water could be the closure of microcracks due to swelling of fibres. Natural fibres can swell considerably more than synthetic fibres and can help to close various microcracks developing in different parts of the composite because of fatigue loading.

This behaviour of fatigue resistance of natural fibre composites is unlike that reported for synthetic fibre composites. Dyer [242] studied fatigue properties of $[\pm 45]_4$ glass fibre reinforced-polyester and –polyurethane-vinylester composites in various aqueous media. The composite immersed in distilled water showed reduction in fatigue life for both types of composites. For composite immersed in sea water, polyurethane-vinyester composites showed reduction in strength only at higher applied stresses. The polyester composites showed gradual reduction in strength. For composites immersed in 10%

HCl solution, both types of composites showed reduction in strength only at lower applied stresses.

From their studies on zero-tension fatigue properties of CSM glass fibre reinforced polyester composites immersed in water, Ellis and Found [377] reported that the soaked samples had lower fatigue lives than dry samples at high stresses, but at lower stress range (of the order of 60 MPa) and fatigue cycles of the order of 10^5, the S-N curves of soaked and dry samples seemed to converge, indicating a lower effect of absorbed water on fatigue properties at these conditions.

It has been shown for some polymer matrices that water absorption raises their toughness and strain to failure, resulting in improved fatigue performance of the composites. Harris [378] has shown that the fatigue resistance of glass fibre reinforced epoxy can be raised by prior boiling in water.

Ellyin and Rohrbacher [289] undertook extensive studies of tension-tension fatigue performance of glass fibre-epoxy composites with different fibre configurations in distilled water at room temperature and at 90°C. The composites with cross-ply $[\pm 0_2, 90_3]_s$ configuration showed nominal reduction in fatigue strength when immersed at room temperature. However the reduction in fatigue strength of composites immersed at 90°C was significant. For the same number of cycles to failure, the room temperature specimens were able to bear a maximum stress which was 95% higher than that of the 90°C ones. Multi-directional $[\pm 45, 90_3]_s$ laminates also showed similar behaviour in the two environments, Angle ply $[\pm 45_2]_s$ laminates showed a less steep slope of strength reduction than dry ones, but similar increased reduction in life at 90°C.

SEM micrographs:

An SEM micrograph of the fracture surface of a sample fractured after 861000 cycles at tensile stress of 18 MPa that was pre-immersed in water for 400 hours is shown in Fig. 7.22. The figure shows that pre-immersion in water for 400 hours and subsequent fatigue loading in water for about 240 hours seems to have had little effect on fibre-matrix interfacial bonding. The fibres seem to be sticking to the matrix quite well. This structural integrity of the composites in water is also expected to be one of the reasons for their good fatigue performance in water.

Fig. 7.22: SEM micrograph of fracture surface of fatigue tested samples pre-immersed in water

These studies have shown good fatigue performance of hemp fibre composites in water despite the reduction in their tensile properties. The comparable fatigue properties of these composites to synthetic fibre composites in water can have useful implications for the use of these materials in aqueous media.

7.1.1.8 Flexural Properties

The flexural properties of the composites in water were determined by immersing them in water for varying lengths of time and evaluating their flexural properties using three point bending test. The average fibre weight fraction of these composites was 53%. The effect of water immersion on flexural strength is shown in Fig. 7.23. Similar to tensile behaviour, these composites lose some of their flexural strength after 50 hours immersion in water. However this reduction soon levels off and further immersion in water does not result in further reduction in flexural strength. After almost 2000 hours of exposure, the composites have lost about 30% of their intrinsic flexural strength.

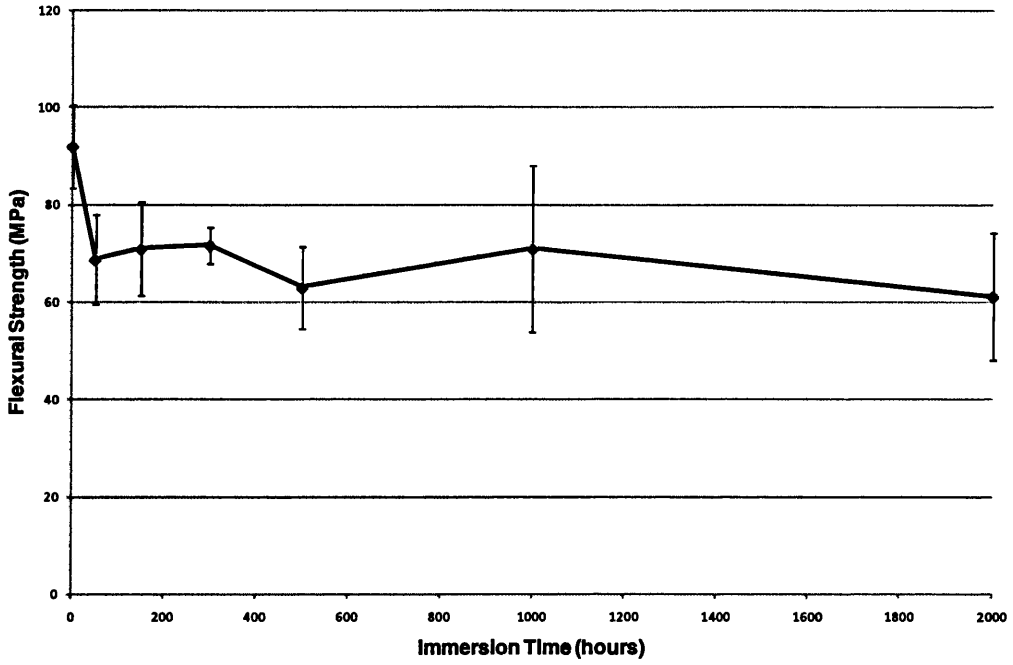

Fig. 7.23: Effect of water immersion on flexural strength of composites

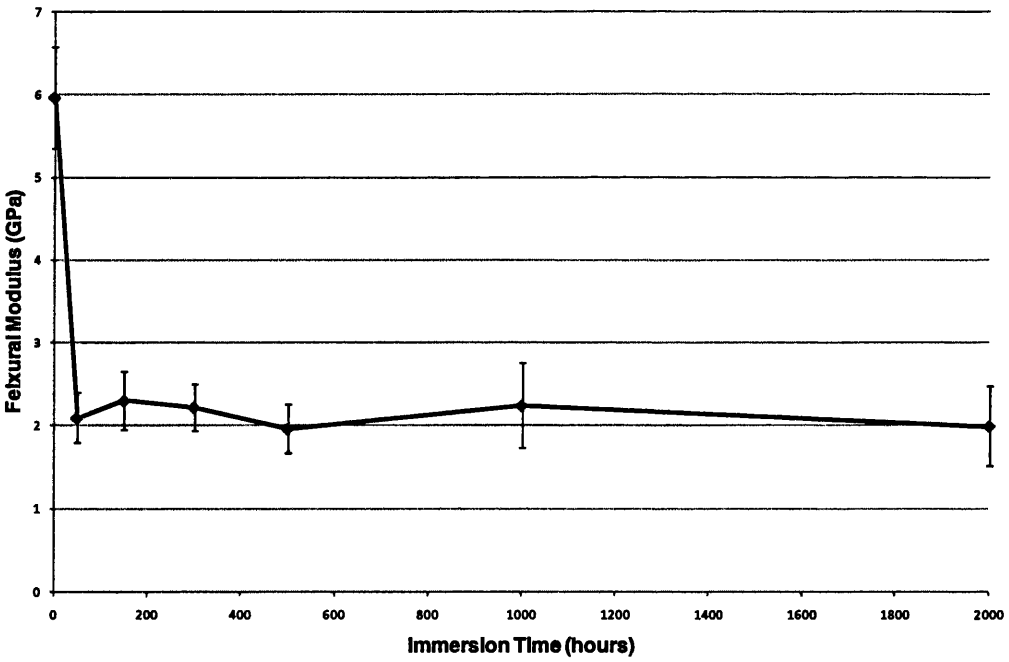

Fig. 7.24: Effect of water immersion on flexural modulus of the composites

The effect of water immersion on flexural modulus of the composites is shown in Fig. 7.24. Similar to tensile modulus, immersion in water seems to have had more adverse effect on flexural modulus than flexural strength of these composites. The decline in

flexural modulus is again quite rapid after 50 hours immersion in water and the composites have lost almost 70% of their intrinsic flexural modulus. However this loss in flexural modulus again levels off and no further appreciable decline in flexural modulus is observed after immersion for about 2000 hours in water.

Similar reduction in flexural properties has been reported by other researchers for natural fibre composites. Rouison et al [295] reported 11% reduction in flexural strength and 34% reduction in flexural modulus of hemp/polyester composites containing 19% fibres by volume following immersion in water for one month. Dhakal et al [338] also reported considerable reduction in flexural strength and modulus for hemp-polyester composites following immersion in water for 888days.

The images of flexural tested samples after 300 hours of immersion, Fig. 7.25, show the fracture on the surface in tension. They also show the curvature of samples after testing. Fig. 7.26 shows that no fracture is visible on the surface in tension, showing the transition to ductile behaviour for composites immersed for 1900 hours in water.

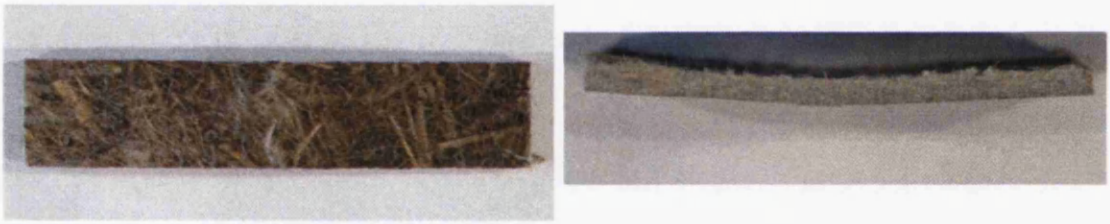

Fig. 7.25: Images showing fracture on tensile surface of the composites (left) and curvature (right) of the flexural tested samples after 300 hours in water

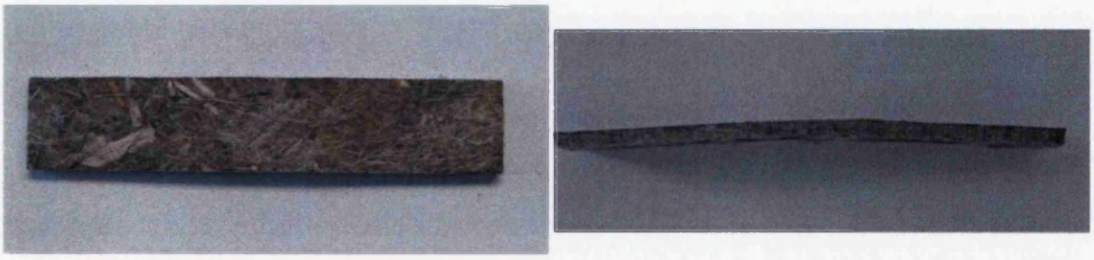

Fig. 7.26: Images showing transition to ductile fracture of the composites (left) and curvature (right) of the flexural tested samples after 1900 hours in water

7.1.2 ALKALISED FIBRE COMPOSITES

7.1.2.1 Water absorption

Hemicellulose in natural fibres is the primary source of water uptake and swelling in these fibres. Because of its open structure containing many hydroxyl and acetyl groups, hemicellulose is partly soluble in water and can absorb relatively large amounts of water [84]. One function of alkalisation of the fibres is the dissolution of hemicellulose, thus making them less hydrophilic. Reducing the amount of hemicellulose also reduces the swelling capacity of the fibre. However alkalisation also leads to transformation of cellulose I to cellulose II in fibre structure. Cellulose II has much greater water sorption and swelling capacity than cellulose I. This is because the average sorption energy for cellulose II is higher than that for cellulose I or amorphous cellulose. Therefore in cellulose II the water absorbs more readily and desorbs less readily than with other two forms of cellulose [84]. These two competing processes determine the moisture absorption behaviour of alkalised fibres depending on which of these processes is dominant. Another advantage of alkalisation process is that improved interfacial bonding between resin and the alkalised fibres is expected to prevent the ingress of water in the interface of the composites.

A mixture of results have been reported in literature for water absorption behaviour of alkalised hemp fibres. Pejic et al [379] studied the effect of 17.5% alkali solution and 0.7% sodium chlorite solution on water uptake behaviour of hemp fibres. Alkali solution was used to remove hemicelluloses and sodium chlorite was used to remove lignin. The fibres lost almost 70% of their original hemicellulose and almost 50% of their original lignin following the treatments. The coefficient of capillary diffusion was significantly higher for treated fibres than those of untreated fibres. The increase was more pronounced in case of lignin removal than for hemicellulose removal, implying that hemicellulose removal causes smaller changes in fibre structure than lignin removal. On the other hand hemicellulose removal increased the moisture sorption of hemp fibres while lignin removal decreased the moisture sorption of hemp fibres.

Kostic et al [73] reported that alkalisation can reduce the water holding capacity of hemp fibres. Fibre treated to alkali solutions of 5% and 18% concentration showed

lower water retention values compared to untreated fibres. Sgriccia [181] et al reported hemp fibre to be more hydrophobic following treatment with 5% alkali solution.

In order to study the behaviour of alkalised fibre composites in water, composites made from 1%, 5%, and 10% alkalised fibres were immersed in distilled water and their water uptake behaviour and its effect on their mechanical properties were investigated.

The water uptake behaviour of alkalised composites compared with non-alkalised composites is shown in Fig. 7.27.

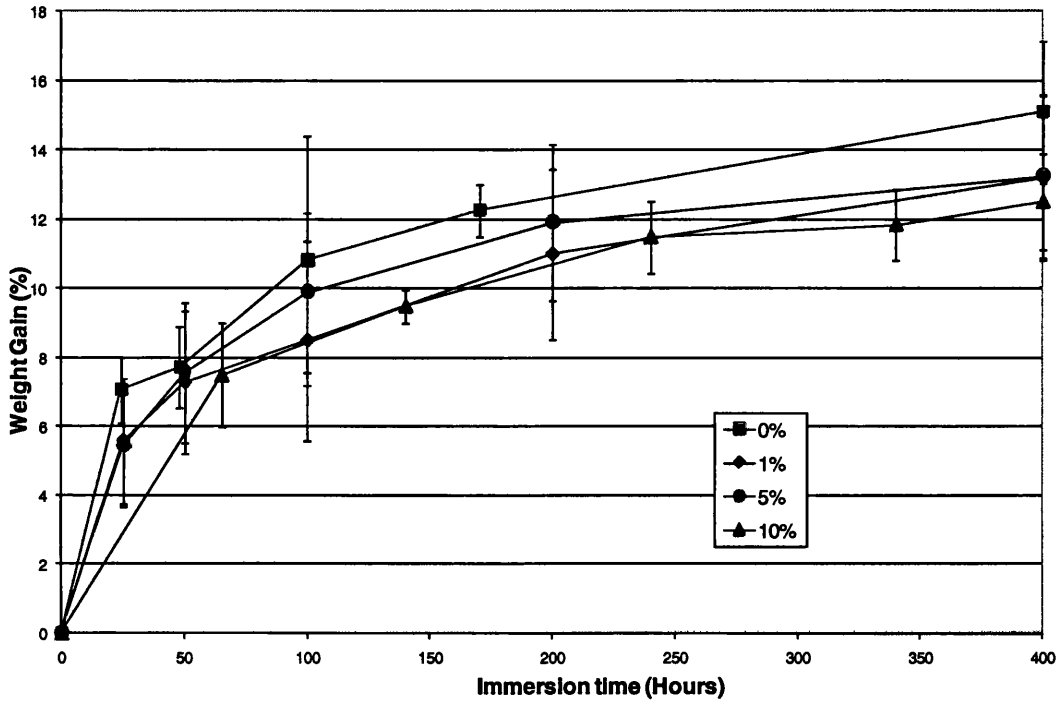

Fig. 7.27: Comparison of water uptake behaviour of non-alkalised and alkalised fibre composites in distilled water

Alkalised fibre composites seem to show greater resistance to absorption of water as against non-alkalised composites for up to 400 hours of immersion in water. On average, alkalised composites have absorbed almost 2% less water than non-alkalised composites after 400 hours of immersion in water. This suggests that removal of hemicellulose seems to be the dominant cause of resistance to water absorption which tends to increase with increase in NaOH concentration. The improved interfacial bonding following fibre alkalisation, confirmed by increase in interfacial shear strength

as shown in Section 6.2.1.4, is also expected to be the major reason for reduction in water absorption.

Rouison et al [295] reported some increase in water absorption of alkalised hemp fibre - polyester composites after immersion of 200 days. The fibres were treated to 2% solution. The increase was attributed to higher fibre volume fraction of 23% for treated fibre composites than untreated fibre composites at 20%. Sgriccia et al [181] found that for 5% alkalised hemp fibre reinforced epoxy composites immersed in water, the water absorption was greater than that for non-alkalised fibre composites.

7.1.2.2 Tensile Properties

The tensile strength of alkalised fibre composites compared to non-alkalised composites after immersion in water for up to 400 hours water is shown in Fig.7.28.

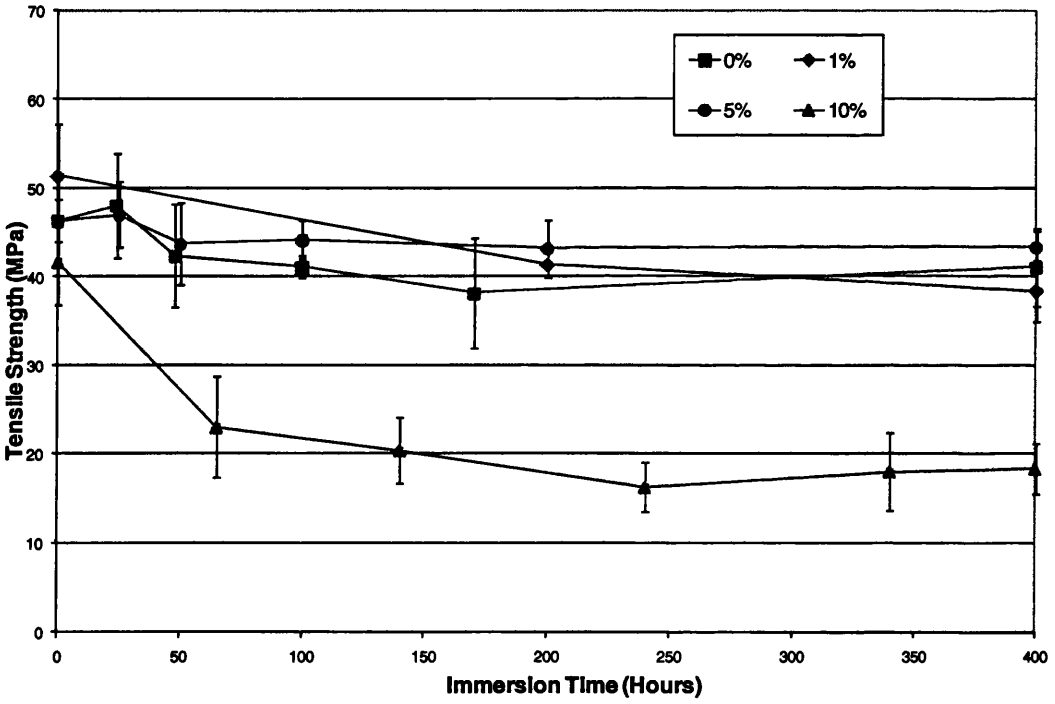

Fig. 7.28: Comparison of tensile strength of non-alkalised and alkalised fibre composites immersed in distilled water

The improved resistance of alkalised fibre composites to water absorption seems have had no positive effect on the tensile strength of the composites. It was previously shown in Section 6.2.2 that 10% alkalisation of hemp fibres had led to significant decline in

tensile strength of the composites made from them. A similar behaviour is seen here. The decline in tensile strength of 10% alkalised composites seems to have overridden any advantages gained by less absorption of water. On the other hand, 1% and 5% alkalised composites have almost similar decline in tensile strength as non-alkalised composites. Although 1% alkalised composites start off having higher tensile strength before immersion in water than non-alkalised and 5% alkalised composites, they end up with having lower tensile strength. Almost 25% reduction in tensile strength of 1% alkalised composites is observed compared to almost 7% for non-alkalised and 5% alkalised composites each for immersion of up to 400 hours. Overall reduction in water absorption does not necessarily mean greater resistance to decline in tensile strength in water.

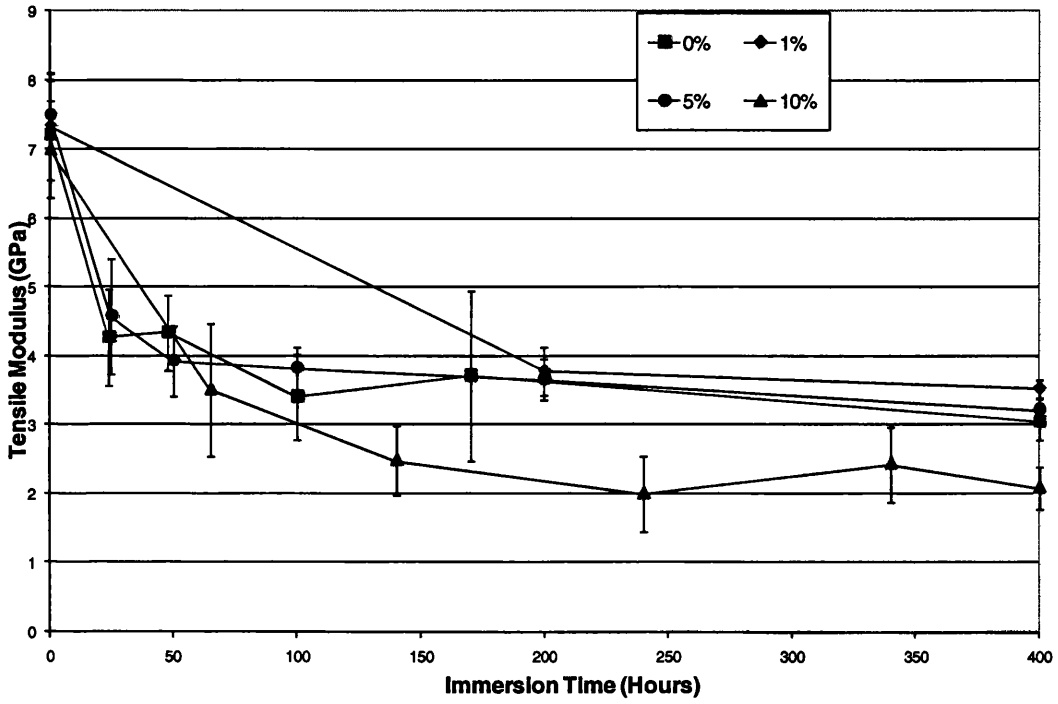

Fig. 7.29: Comparison of tensile modulus of non-alkalised and alkalised fibre composites immersed in distilled water

The effect of water absorption on tensile modulus of alkalised and non-alkalised fibre composites is shown in Fig. 7.29. Again the improved resistance of alkalised fibre composites to water absorption does not seem to have resulted in any improvement in modulus reduction following immersion in water. It is seen that decline in tensile modulus of 10% alkalised fibre composites is greater than other composites. These

composites have lost almost 70% of their intrinsic modulus after 400 hours of immersion in water. On the other hand the decline in 1% and 5% alkalised fibre composites is quite similar to non-alkalised composites. Like non-alkalised fibre composites, they have lost almost 50% of their intrinsic modulus after 400 hours of immersion. Hence less absorption of water does not result in any improvement in resistance to decline in modulus.

The strain to failure of alkalised fibre composites compared to that of non-alkalised fibre composites is shown in Fig. 7.30.

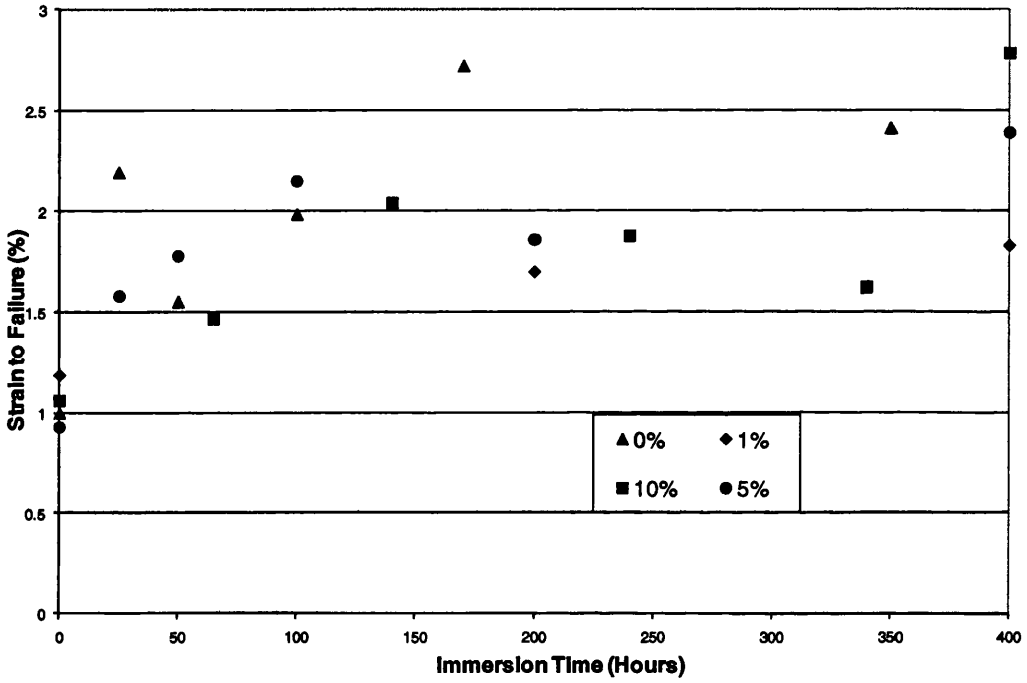

Fig. 7.30: Comparison of strain to failure of alkalised fibre composites compared to non-alkalised fibre composites after immersion in water

The strains to failure values of alkalised fibre composites are quite random and a non-uniform behaviour is observed. Strain to failure has increased for all alkalised fibre composites after immersion in water, but the increase is less compared to non-alkalised fibre composites. This can be attributed to increase in fibre/matrix interfacial strength following alkalisation of fibres.

7.1.2.3 Analysis of tensile properties

The effect of water immersion on tensile properties of alkalised fibre composites can be best understood in terms of their normalised properties. Fig. 7.31 shows the effect of water immersion on normalised tensile strength of alkalised fibre composites.

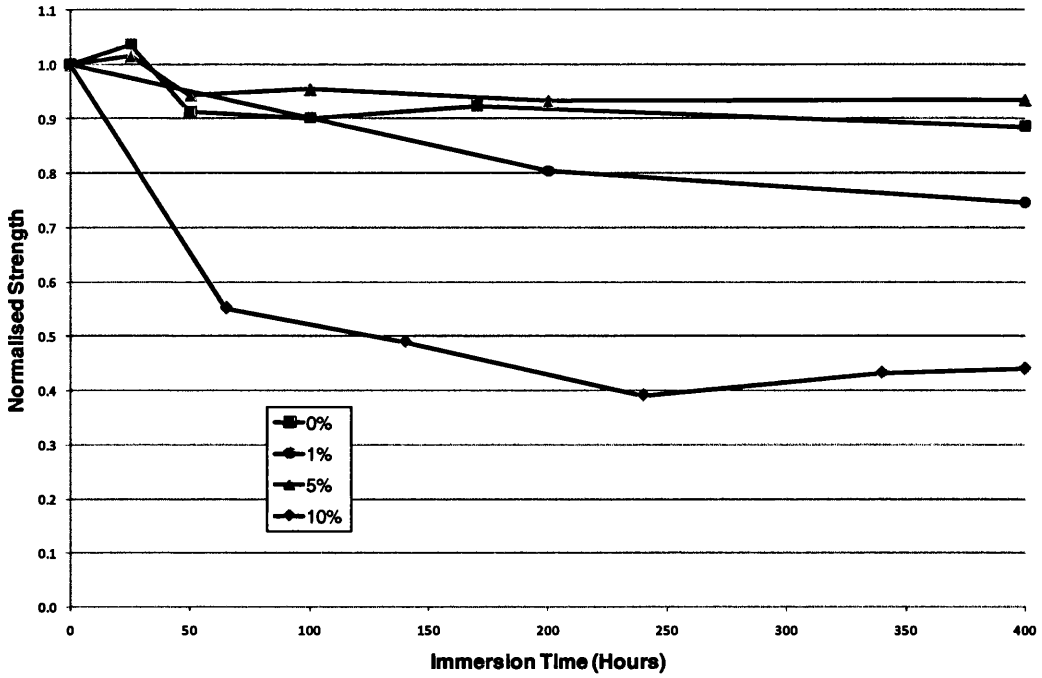

Fig. 7.31: Normalised strength of alkalised and non-alkalised fibre composites following immersion in water

The decline in strength of non-alkalised and 5% alkalised fibre composites is similar. Both show a decline in strength of almost 10% following immersion in water for 400 hours. 1% alkalised fibre composites show greater decline in strength and have lost almost 25% of their intrinsic strength following immersion in water for 400 hours. Despite having same level of water absorption as shown in Fig. 7.27, greater reduction in strength of 1% alkalised fibre composites suggests lower integrity of these composites following immersion in water. 10% alkalised fibre composites show the largest decrease in strength following immersion in water. The damage to the fibres following the treatments further deteriorates their properties in water, and despite showing good resistance to water absorption, their strength has declined by almost 60% following immersion in water.

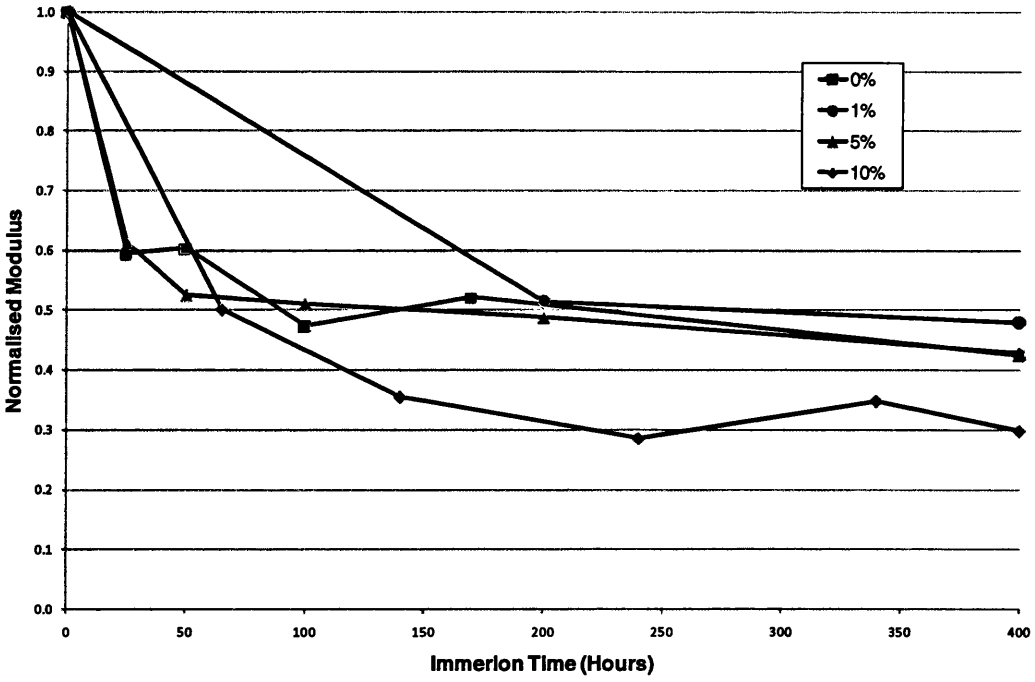

Fig. 7.32: Normalised modulus of alkalised and non-alkalised fibre composites following immersion in water

The comparison of normalised modulus of alkalised and non-alkalised fibre composites following immersion in water is shown in Fig. 7.32. Both 1% and 5% alkalised fibre composites show similar reduction in modulus to non-alkalised fibre composites following immersion in water. For immersion time of up to 400 hours, both kinds of composites have lost almost 50% of their intrinsic stiffness. 10% alkalised fibre composites again show greater reduction in modulus. For immersion time of up to 400 hours, these composites have lost almost 70% of their intrinsic stiffness.

As for non-alkalised fibre composites, the mode of fracture for alkalised fibre composites also started to change from brittle to ductile after about 100 hours of immersion. The comparison of stress-strain graphs of alkalised and non-alkalised fibre composites after immersion in water for 400 hours is shown in Fig. 7.33. The graphs show that alkalisation of fibres did not affect the mechanical behaviour of composites in water and the curves were found to be similar to those for non-alkalised fibre composites.

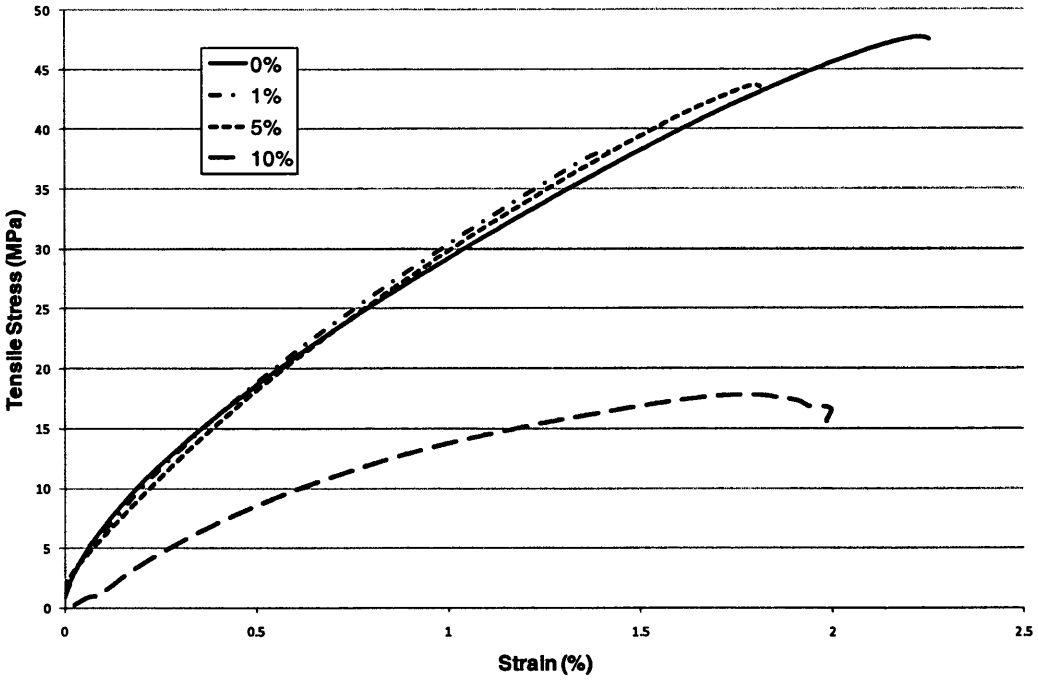

Fig. 7.33: Comparison of stress-strain graphs of alkalised fibre composites with non-alkalised fibre composites after 400 hours in water

Fig. 7.34 shows SEM micrographs of fracture surfaces of tensile tested alkalised fibre composites following immersion in water. The samples had to be dried before their micrographs could be taken. These micrographs show improved wetting of fibre/matrix and the interface seems to have retained its bonding following immersion in water, shown in Fig. (a). Some interfacial debonding can still be expected to take place as shown by the arrowhead in Fig. (b). Fig. (a) shows that although 10% alkalisation results in considerable damage to the fibres, they are still able to maintain their good interfacial bonding in water. Fig. (c) also shows good interfacial bonding for 5% alkalised fibre composites following immersion in water.

These studies have shown that although water absorption of alkalised fibre composites is reduced, this does not result in any improvement in reduction in their tensile properties. Thus alkalisation is not recommended if any improvement in tensile properties are required in water.

(a)

(b)

(c)

Fig. 7.34: SEM micrographs of fracture surface of 10% alkalised fibre sample after 340 hours (a), 1% alkalised fibre sample after 200 hours (b), and 5% alkalised fibre sample after 200 hours in water

7.1.3 Composites with Sealed Edges

The samples used in the study of water absorption behaviour had cut edges that resulted in direct exposure of fibres and the fibre/matrix interface to water. In order to determine the effect of preventing the ingress of water through cut edges, composite samples with their cut edges sealed with water-resistant silicone sealant were immersed in water and their water absorption and tensile properties were investigated. However, since silicone sealant is moderately permeable to water, this is not a real test of stopping water entering from the edges, but merely slowing it down.

7.1.3.1 Water absorption

The water absorption behaviour of the composites with sealed edges compared to samples with cut edges is shown in Fig. 7.35. There is only marginal difference in the absorption behaviour of composite with sealed edges with those of non-sealed edges.

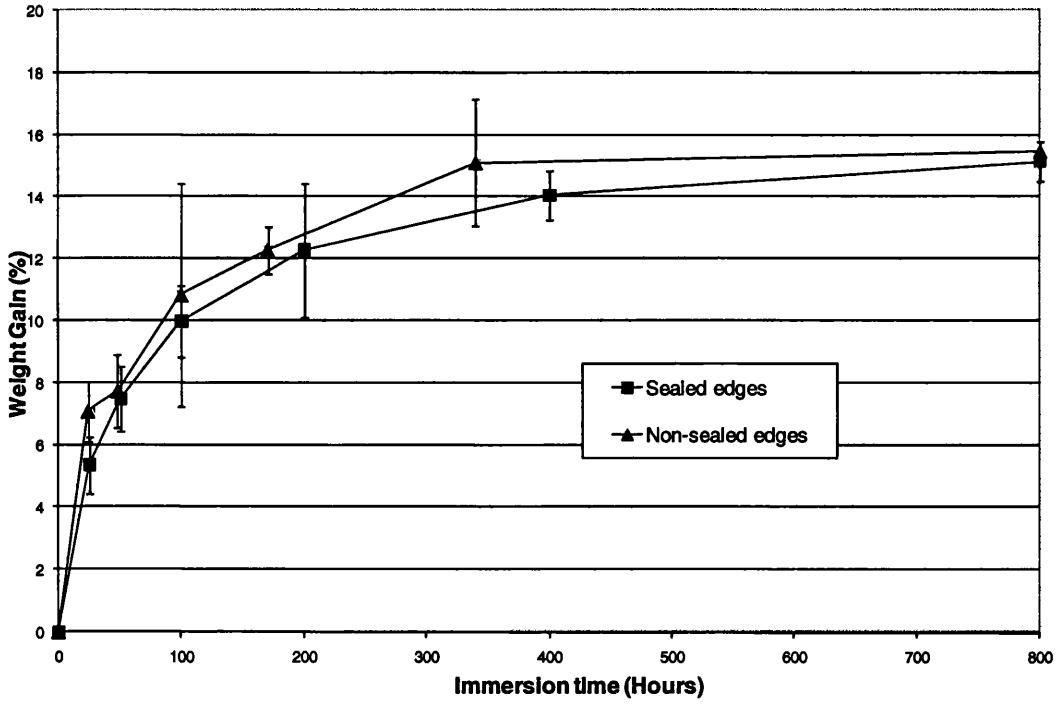

Fig. 7.35: Comparison of water absorption behaviour of composites with sealed and non-sealed edges

The water absorption in composites with sealed edges is slightly lower but within the error bars for non-sealed edges which shows that the difference is not significant. This is not unexpected because the surface of area of cut edges is only about 12% of the total

surface area of the samples. The maximum difference at any point in water absorption is only about 1.5%. However this difference is seen to be decreasing with increase in water immersion time.

7.1.3.2 Tensile properties

The effect of water immersion on tensile strength of composites with sealed edges compared with that of non-sealed edges is shown in Fig. 7.36. It is quite clear that the reduction in water absorption immediately after immersion due to sealed edges has no appreciable positive effect on tensile strength of these composites. The composites with non-sealed edges have slightly higher tensile strength than those with sealed edges for same immersion time in water, but the difference is within error bars of the two, indicating that the difference is not significant.

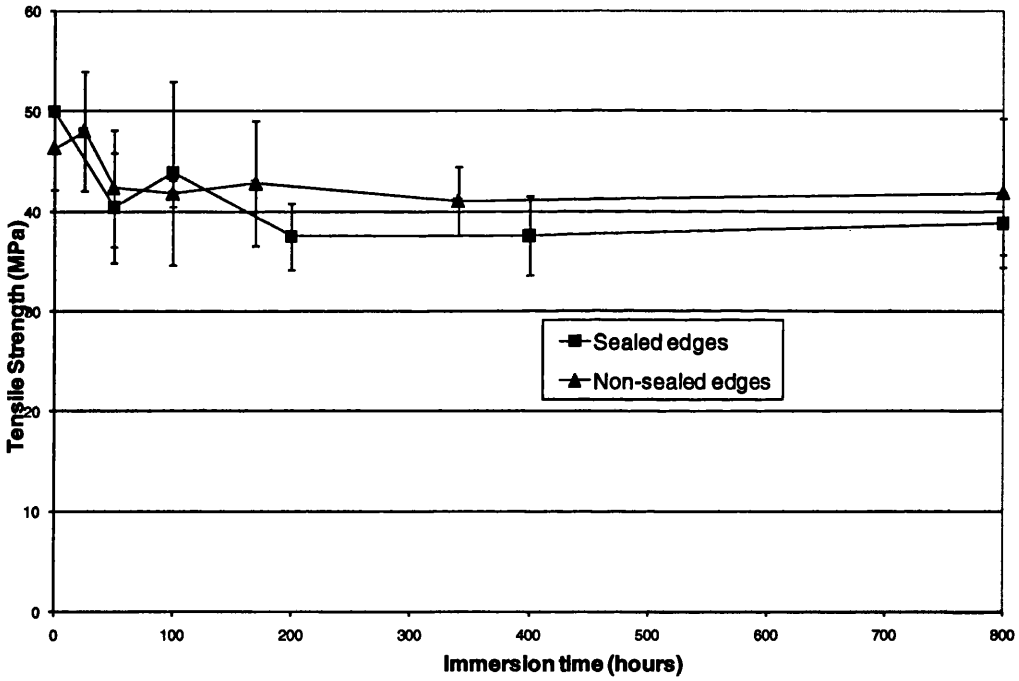

Fig. 7.36: Comparison of effect of water absorption on tensile strength of composites with sealed edges and non-sealed edges

The comparison of the effect of water immersion on tensile modulus of composites with sealed- and non-sealed edges is shown in Fig. 7.37. Again composites with sealed edges are seen to have similar reduction in their tensile modulus to composites with non-

sealed edges for same immersion time. The values of tensile modulus are within error bars at same water immersion times, indicating that the difference is not significant.

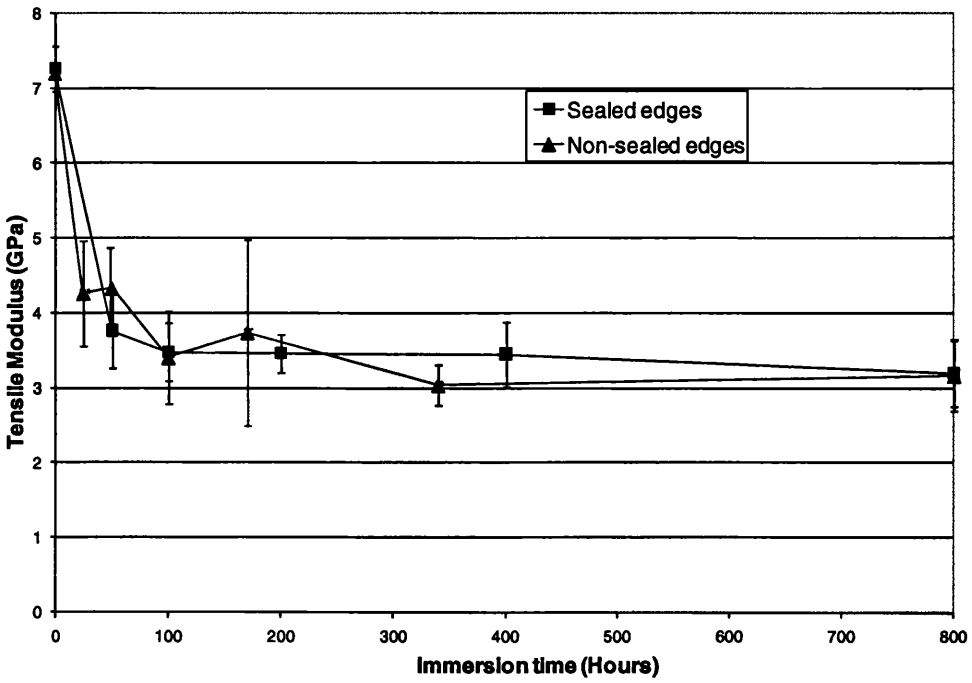

Fig. 7.37: Comparison of effect of water absorption on tensile modulus of composites with sealed and non-sealed edges

This part of the research has shown that sealing the cut edges of the samples does not lead to any significant reduction in water absorption of these composites. Therefore the reduction in tensile properties of composites with sealed and non-sealed edges following immersion in water is quite similar. It has been shown by Ellis and Found [377] for CSM glass fibre/ polyester composites that sealing the sample edges does not have significant effect on water absorption or tensile properties of the laminates. Hemp fibre composites are shown to behave similar to glass fibre composites in this respect. Therefore immersing the hemp fibre composite samples with exposed cut edges in water can give a good indication of their overall properties in water.

7.2 COMPOSITES IMMERSED IN SALT SOLUTION

Hemp fibre reinforced polyester composite samples were immersed in 5% Sodium Chloride salt solution for varying lengths of time to observe the effect of corrosive nature of this water on water absorption and tensile properties of these composites.

7.2.1 Water absorption

The water absorption behaviour of composites immersed in 5% salt water solution for up to 1900 hours compared with distilled water is shown in Fig. 7.38.

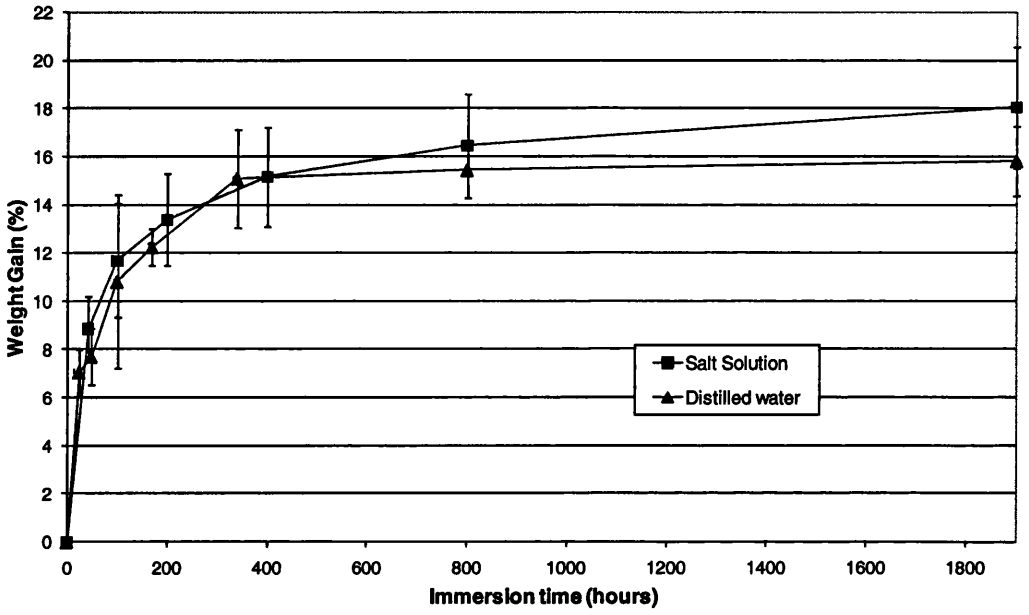

Fig. 7.38: Comparison of water absorption behaviour of composites in 5% salt solution and distilled water

From the graph, the water absorption pattern of composites in salt solution and distilled water is found to be similar at low immersion times. The aggressive nature of salt water does not seem to have resulted in any increase in water absorption and these composites seem to have coped fairly well in salt water. It is only at immersion times of greater than 600 hours that the water absorption seems to be slightly higher in salt water.

7.2.1. Tensile properties

The effect of immersion in salt solution on tensile strength of the composites is shown in Fig. 7.39. The decline in tensile strength of composites in salt water follows a similar pattern to the one in distilled water at low immersion times, consistent with similar water absorption behaviour. Increase in water absorption at high immersion times seems to have some effect in greater reduction in tensile properties salt solution. Following immersion in water for 1900 hours, the residual strength of composites in salt solution is slightly higher, although the effect is not significant. Again the aggressive nature of salt

water does not seem to have any increased deleterious effect on tensile strength of these composites compared to non-salt water.

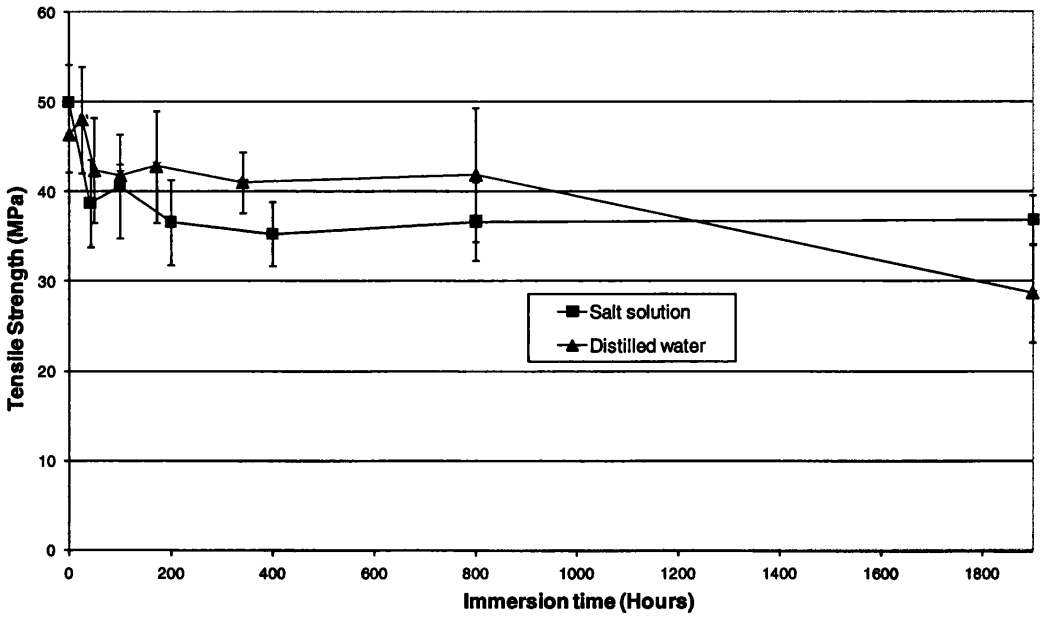

Fig. 7.39: Effect of immersion in 5% salt solution on tensile strength of composites

The effect of immersion in salt water on tensile modulus of composites is shown in Fig. 7.40. Once again similar patterns of decline in tensile modulus of the composites immersed in distilled water and salt solution are observed. The increased water uptake at higher immersion times in salt solution does not seem to have resulted in any increased reduction in tensile modulus and the values are within error bars at all immersion times. The aggressive nature of salt water has again had no additional deleterious effect on tensile modulus of these composites. This seems to suggest that interfacial bonding in these composites is strong enough to resist any corrosive attack from salt water.

The effect of immersion in salt solution on strain to failure of composites is shown in Fig. 7.41. The composites immersed in salt solution seem to have slightly higher strain to failure at higher immersion times which may be attributed to greater water absorption of these composites at these times but the differences are within statistical scatter.

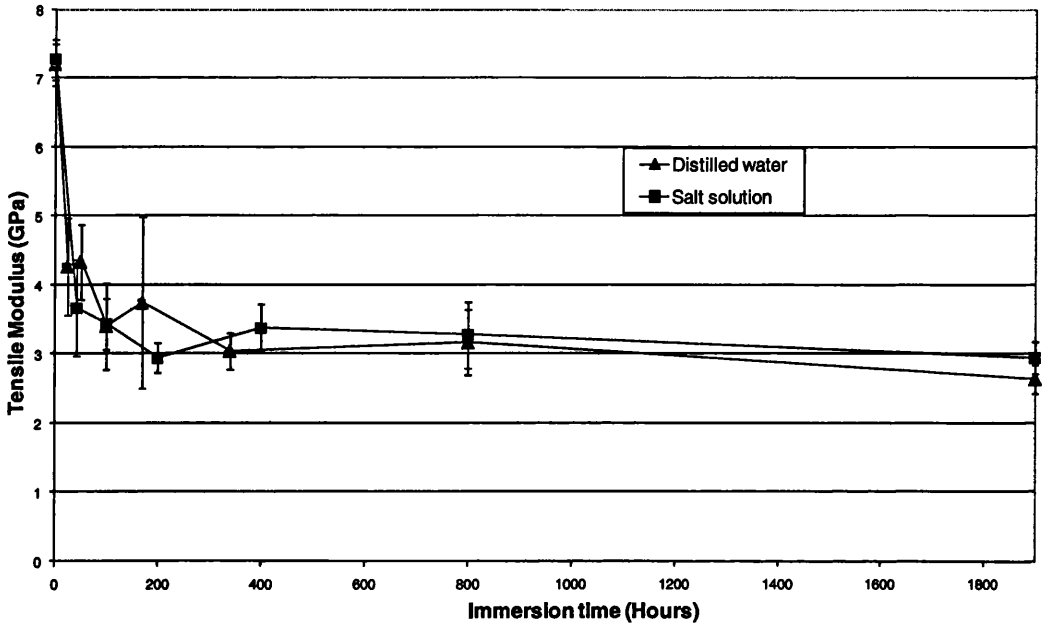

Fig. 7.40: Effect of immersion in 5% salt solution on tensile modulus of composites

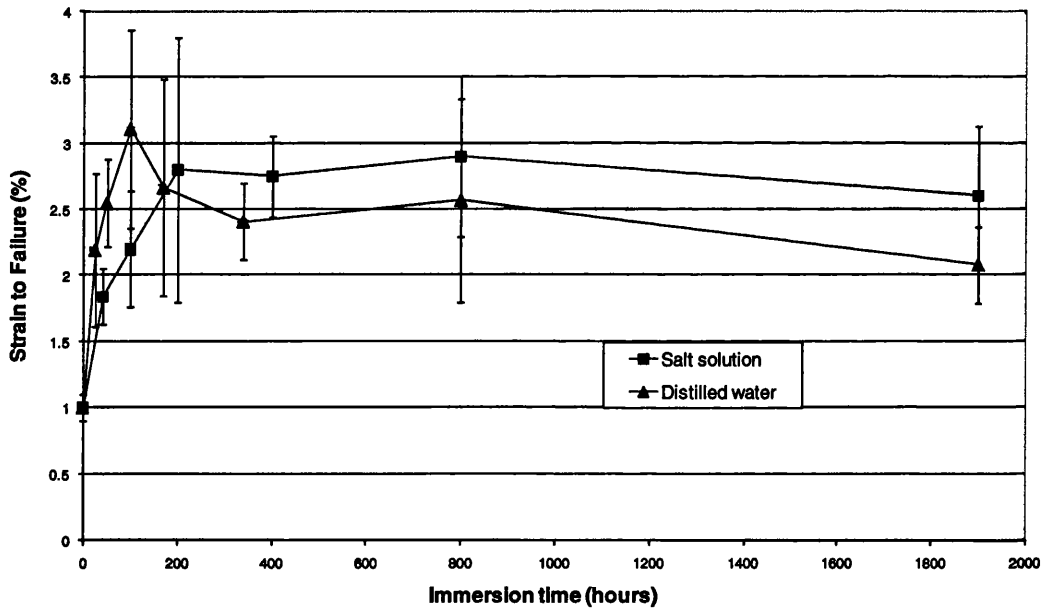

Fig. 7.41: Effect of immersion in salt solution on strain to failure of composites

This part of research has shown that the water absorption and reduction in tensile properties of these composites in salt solution is similar to that in distilled water. The deleterious effect of salt solution has been shown to have no significant effect on tensile

properties of these composites. The tensile properties of these composites in distilled water can therefore give a good indication of their properties in salt solution.

7.3 ACCELERATED WEATHERING CONDITIONS

Hemp fibre reinforced polyester composite samples were exposed to accelerated weathering conditions (UV radiation and a combination of UV radiation and condensation) for varying lengths of time and the effect of these environments on their weight and tensile properties was investigated. These conditions were designed to simulate the conditions experienced by the composites that are used in outdoor applications. The composites exposed to UV radiation only were continuously exposed to these conditions which simulated the conditions of constant exposure to sunlight. The composites exposed to UV radiation plus condensations were exposed to these conditions in cycles. Each cycle consisted of exposure of eight hours of UV light followed by four hours of condensation. This simulated the conditions of the composites that are exposed to sunlight in daytime and to moisture condensation at night.

The effects of accelerated weathering conditions on natural fibre composites have not been fully studied yet. Singh et al [309] studied the effect of UV radiation in accelerated weathering tester on mechanical properties of jute fibre reinforced phenolic composites. For composites exposed to 750 hours of aging, the tensile properties deteriorated and the tensile strength fell by 47%. There was also considerable reduction in flexural properties.

7.3.1 Weight loss

The effect of UV radiation only and UV radiation plus condensation on residual weight of these composites is shown in Fig. 7.42. It was observed that the composites started to lose weight soon after exposure to these conditions.

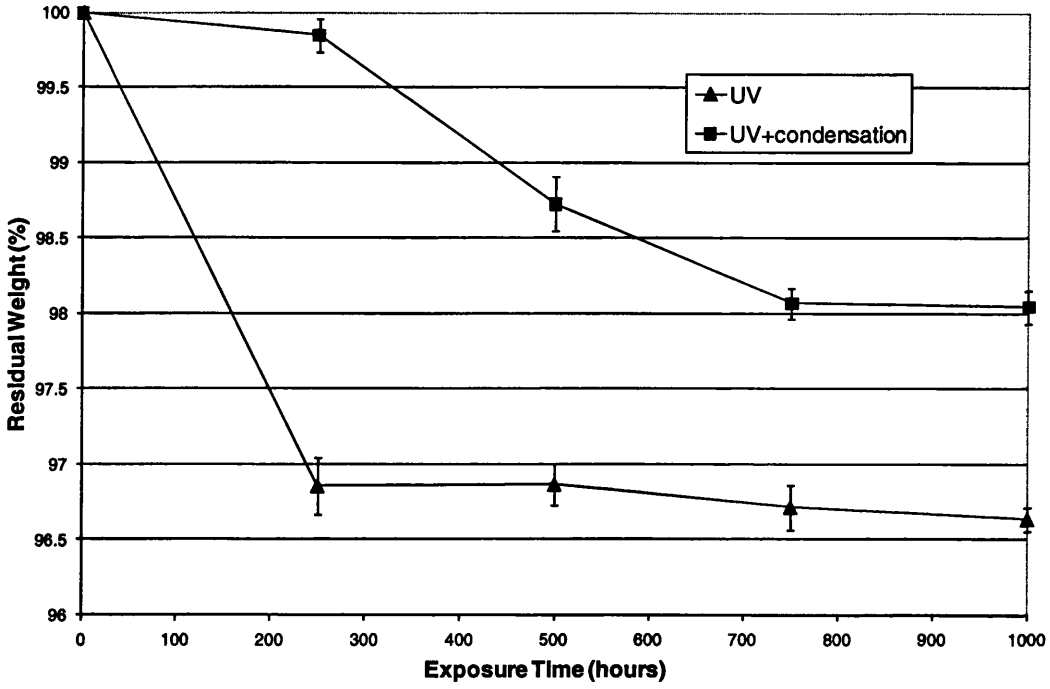

Fig. 7.42: Weight loss of composites exposed to UV light and condensation

The increase in weight loss for UV exposed composites was greater than for UV plus condensation exposed composites. It has been shown that when unsaturated polyester resins are heated, the polymer begins to dissociate chemically [273]. The temperatures at which this decomposition occurs and the fragments produced depend on the structure of the unsaturated polyester resin. It was shown that glass fibre reinforced isophthalic polyester resin composites, when exposed to 180° C, started to lose weight soon after exposure. The weight loss increased gradually with time, and after 720 hours of exposure the weight loss was 4.5% [273].

It has also been shown that polyesters have maximum photochemical sensitivity at wavelength of 325 nm. Since the UV radiation used in this study had a wavelength of 340 nm, it is not unexpected that this resulted in degradation of the upper polyester layer of the composites resulting in loss of weight. This degradation is a manifestation of chain scission and breaking of bonds between polymer molecules following exposure to UV radiation. However at increased exposure times, as the UV radiation is expected to interact with the hemp fibres, the fibres were able to resist the UV radiation. This resulted in reduced degradation of the samples for exposure time of greater than 250

hours. Further exposure of the sample to UV light did not result in any increased loss in weight which stabilised at about 3.2%.

However for composites exposed to UV plus condensation conditions, the loss in weight due to UV radiation was compensated by increase in weight due to moisture absorption during the condensation cycle. Therefore the loss in weight for composites exposed to UV plus condensation was considerably less than that for UV radiation only. The weight loss stabilised to a value of about 1.9% following exposure for 700 hours.

7.3.2 Tensile properties

The effect of UV radiation and condensation on tensile strength of the composites is shown in Fig. 7.43. The exposure to UV light and condensation leads to some loss in tensile strength initially but prolonged exposure to these conditions leads to some recovery in strength and does not lead to any further decline in tensile strength. The maximum reduction in strength is about 40% following exposure time of 500 hours. Following 1000 hours of exposure, the decline in strength is about 20% of intrinsic strength.

The decline in tensile strength is more gradual for composites exposed to UV radiation only but stabilises after about 450 hours of exposure. After 1000 hours of exposure to UV light, the composites have lost approximately 30% of their intrinsic tensile strength. Compared to this, the composites have lost only 10% of their strength following immersion in water for the same time period. Thus UV light results in greater degradation of tensile strength of composites than water. Chain scission and breaking of bonds in the upper resin layer, which can also expose the interface to radiation, appear to be the main cause of this reduction.

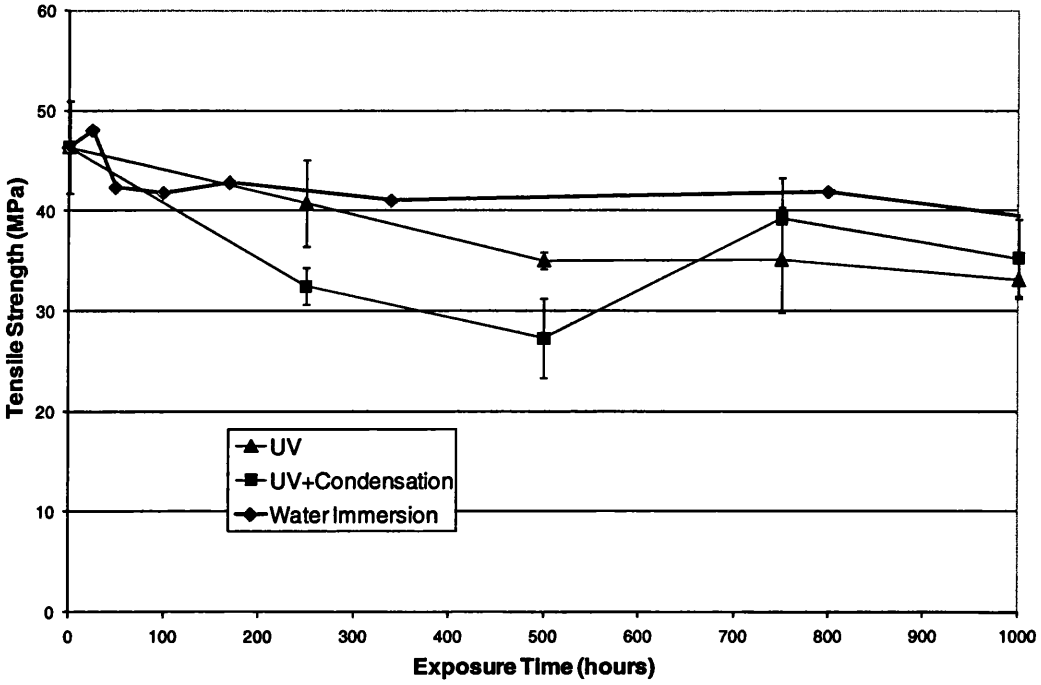

Fig. 7.43: Effect of UV light and condensation conditions on tensile strength of composites

The effect of UV radiation and condensation on tensile modulus of the composites is shown in Fig. 7.44. For composites exposed to UV radiation plus condensation the decline in modulus seems to follow the same pattern as for decline in strength. The decline in modulus is non uniform and after initial decline seems to recover for longer exposure times. The maximum decline is modulus is about 40% following exposure of 500 hours. After 1000 hours of exposure to UV radiation plus condensation, the composites have lost almost 30% of their intrinsic tensile modulus.

The reduction in tensile modulus is more gradual for composites exposed to UV radiation only. After 1000 hours of exposure to UV radiation, the composites have lost approximately 30% of their intrinsic modulus.

However the loss in modulus is less for composites exposed to UV and UV plus condensation conditions compared to immersion in water. This is to be expected since the diffusion of water into the composites affects the bulk properties of the material, plasticising the polyester matrix and fibres. UV and condensation mostly affect the

surface properties of the material only, thus having less effect on bulk properties of the material. Hence the greater reduction in modulus for composites immersed in water.

The effect of UV radiation and condensation on strain to failure of the composites is shown in Fig. 7.45. The strain to failure does not seem to have been affected very much by exposure to these conditions and stays close to the non-exposed value of 1%.

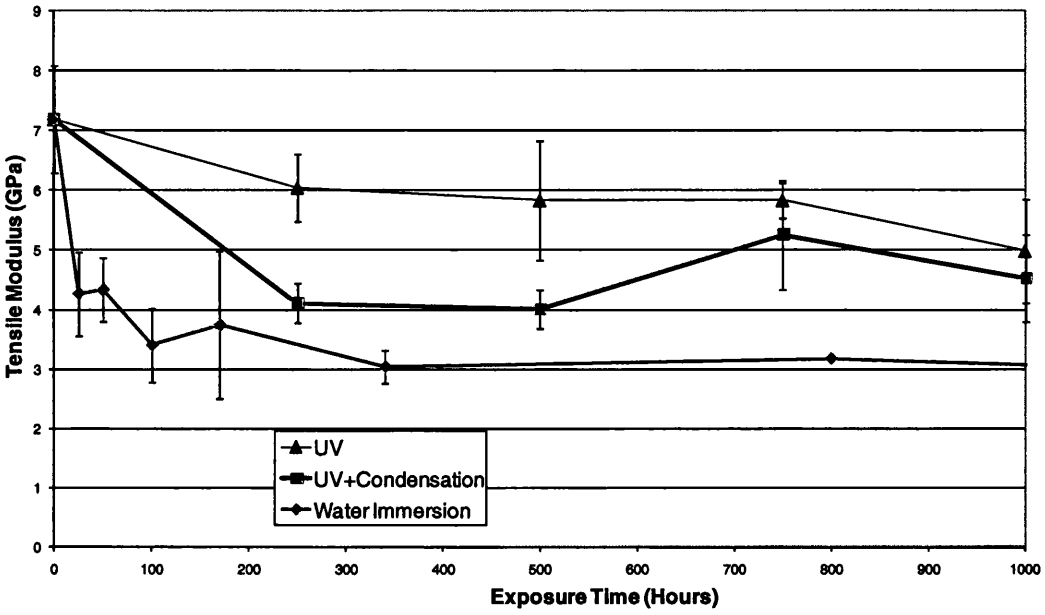

Fig. 7.44: Effect of UV light and condensation on tensile modulus of composites

However the strain to failure of composites immersed in water is considerably higher which can again be explained by the fact that the diffusion of water results in plasticisation of polyester resin and fibres, resulting in increase in strain to failure. UV and condensation affect the surface properties and hence the strain to failure is not affected.

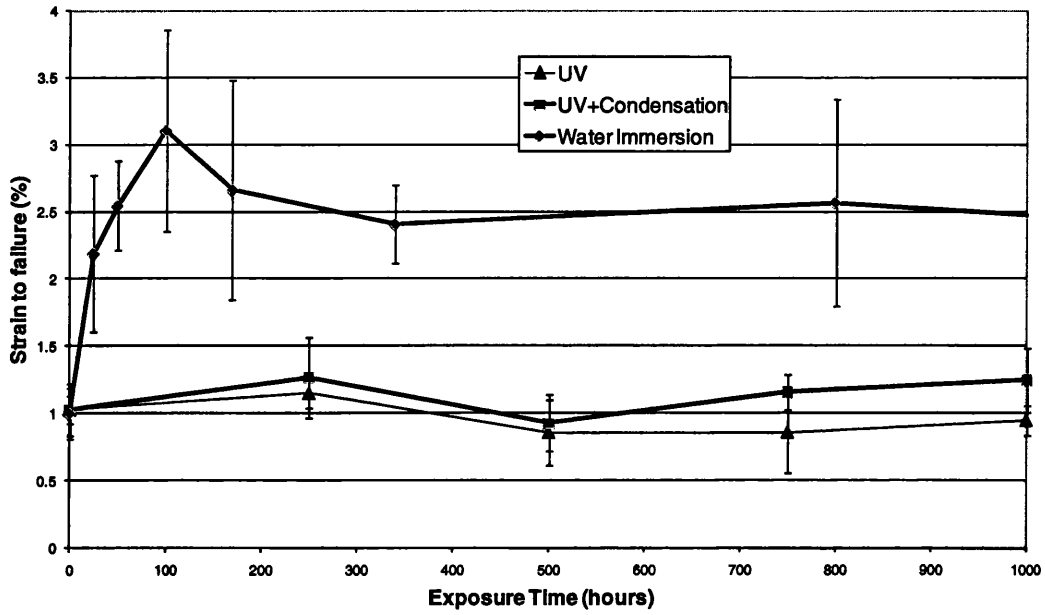

Fig. 7.45: Effect of UV light and condensation on strain to failure of composites

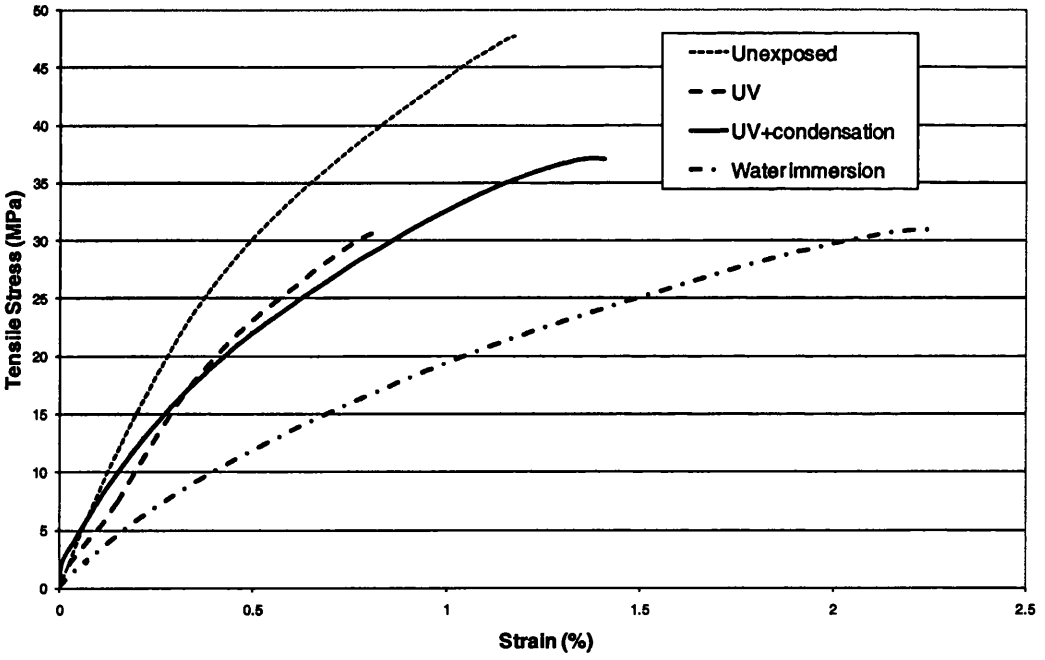

Fig. 7.46: Comparison of stress-strain graphs of composites exposed to weathering conditions

The exposure of composites to UV and condensation did not affect their fracture mode which was still brittle. Fig.7.46 shows the comparison of stress-strain graphs of

composites following exposure to both kinds of environments for 1000 hours with unexposed and water-immersed composites. The figure shows that the mechanical behaviour of the composites following exposure to weathering conditions did not change and the shape of the curve was found to be similar to that for unexposed composites.

One notable effect these conditions had was on the colour of these composites. The UV light can result in considerable yellowing of synthetic fibre composites also. The colour of these composites started to change from darkish brown to greyish brown. After 1000 hours of immersion it had changed to whitish brown as shown in Fig. 7.47. In each case, the top figure shows the hemp fibre sample without exposure to weathering conditions. The reaction of water, oxygen and UV radiation within the organic matter in the composites promote the change of colour. Mehta et al [307] studied the effect of accelerated weathering (UV+condensation+water spray) on colour change of natural fibre reinforced polyester composites by using reflectometer. The composites changed colour from greenish brown to white and the change in colour was more pronounced for hemp fibre composites than flax and big blue stem grass composites. Hence the interaction of hemp fibres with UV light and water can be expected to be the main reason for change in colour.

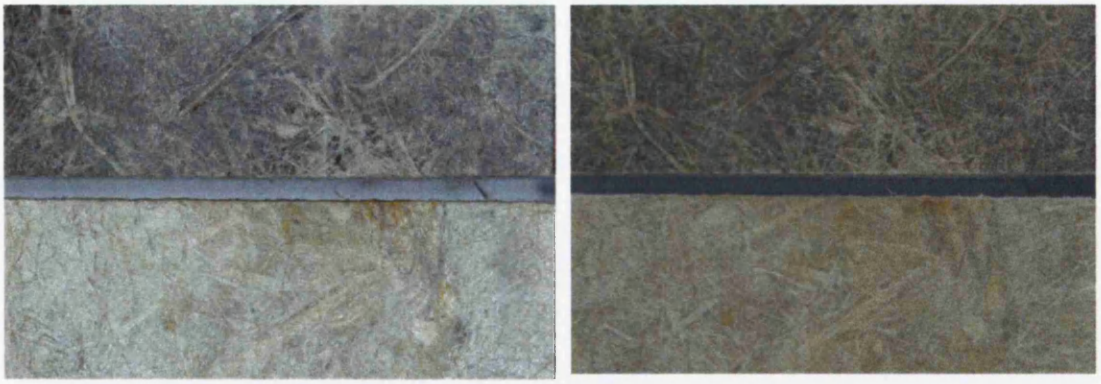

(a) **(b)**

Fig. 7.47: Discolouring and yellowness of the surface of the composites exposed to (a) UV radiation and condensation, and (b) UV radiation for 1000 hours

It has been shown [380] that the exposure of polyester to accelerated outdoor weathering can result in change in its colour, measured by yellowness index. Thus both

polyester resin and hemp fibres are expected to contribute to yellowness of the material. The discolouring and yellowness of the surface was more pronounced for composites exposed to UV radiation plus condensation because the moisture also contributed to the discolouring, also observed for composites immersed in distilled water. This fading of colour has important aesthetic implications when these composites are to be used in outdoor applications. Some kind of coating, paint or UV absorbing additives can be used on these composites to stop the fading effect.

This part of the research has shown that exposure to UV light and condensation leads to initial decline in the tensile properties of these composites, but the decline in properties does not seem to increase after prolonged exposure and these materials seem to have performed fairly well in these conditions. Also the reduction in strength and modulus is quite similar, contrary to immersion in water where the reduction in modulus was more pronounced than the reduction in strength.

8. CONCLUSIONS

8.1 CONCLUDING REMARKS

The use of natural fibres in composite materials has recently seen an increase in response to concerns about environmental pollution and recyclability of synthetic fibre composites. The mechanical properties of natural fibre composites have not yet been fully studied. This research focused on studying the impact and fatigue properties of natural fibre composites. Hemp fibres, one of the strongest natural fibres, were used with unsaturated polyester resin as matrix. For comparison with synthetic fibre composites, CSM glass fibre composites and glass/hemp fibre hybrid composites were also made using the same matrix. The impact properties were studied in terms of damage tolerance of composites following low velocity impact. Fatigue properties of composites were studied primarily in tension-tension fatigue. The effect of low velocity impact on fatigue properties was also studied.

The effects of various fibre surface treatments on the impact and fatigue properties of composites were studied. Alkalisation is the most widely used natural fibre surface treatment and this research also concentrated on this treatment. Finally the effects of some environments, primarily immersion in water, on the impact and fatigue properties of composites were studied.

8.1.1 Properties of Hemp Fibres

Various physical and mechanical properties of hemp fibres were evaluated to assess their suitability for use as reinforcement in composite materials. The moisture content of hemp fibres equilibrated at 23°C and 50%RH was found to be about 10%. This high moisture content was considered to be a major factor in relatively high void content of the composites made in this research. The thermal properties of hemp fibres at higher temperatures were consistent with the results reported in literature. Thermal degradation of hemp fibres started at just above 150°C. The decomposition of hemicelluloses and pectin occurred at around 260°C and that of cellulose occurred at around 360°C.

The cross-section of hemp fibres used in this research was found to be more polygonal than circular in shape. The tensile properties of hemp fibres with mean fibre width of 67±26μm were evaluated. The tensile strength was evaluated at 277±191 MPa, tensile modulus at 9.5±5.8 GPa and strain to failure at 2.3±0.8%. The large scatter in tensile properties underlined the variability in properties of hemp fibres which is one of their main weaknesses compared to synthetic fibres. The tensile properties of hemp fibres were found to be good enough to be used as reinforcement in composite materials.

The surface energy of hemp fibres was evaluated at 32.8 mJ/m^2, higher than that of glass fibres at 21.5 mJ/m^2, but lower than that of unsaturated polyester resin reported in the literature. The similarity in surface energies between hemp and polyester was expected to result in relatively poor interfacial bonding between them. This was confirmed in single fibre interfacial shear strength testing between hemp and polyester which was lower than that reported for glass fibre and polyester in the literature.

8.1.2 Hemp and Glass Fibre Composites

The average fibre weight fraction of hemp and glass fibre composites made in this research was about 55%. Additionally, hybrid composites were also made with two configurations of hemp skin-glass core and glass skin-hemp core. Both kinds of configurations represented the replacement of 11% of hemp fibres by glass fibres by volume.

Voids were identified as the primary source of imperfections in hemp fibre composites and their fraction was evaluated at about 10% by weight of composites. Other major sources of imperfections were identified as poor interfacial strength and residual stresses in laminates.

The tensile properties of hemp fibre composites were found to be comparable to the properties of glass fibre composites with woven and non-woven ±45° fibre configuration reported in the literature [262]. However they were much lower than the tensile properties of CSM glass fibre composites made in this research. Hybrid glass-hemp fibre composites showed almost 50% increase in tensile strength but only marginal increase in tensile modulus. The specific tensile properties of composites also confirmed the superiority of CSM glass fibre composites compared to hemp fibre composites.

The fracture properties of hemp and glass fibre composites in tensile testing were studied. The fracture of hemp fibre composites was brittle. The tensile stress-strain curve had a 'knee' which is a characteristic of short fibre composites. A closer examination of the fracture surface by SEM revealed the existence of matrix fracture, fibre/matrix debonding, fibre fracture and fibre pull-out as the major mechanisms of damage. No evidence of cracks on composite surfaces just before their fracture suggested most of damage processes taking place within the composites. Glass fibre composites, on the other hand, showed more evidence of cracks on the surface and considerable whitening of the samples before fracture showed the existence of damage processes taking place.

The impact damage tolerance of hemp fibre composites was very low. They lost almost half of their intrinsic strength and stiffness following an impact at 2J energy. Examination of impacted surface showed the existence of considerable matrix and fibre fracture having taken place at this impact level. An impact of 4J energy was enough to cause penetration of the impactor through the material. The brittle nature of hemp fibre and polyester resin, poor toughness of hemp fibre, combined with the imperfections in the laminates were considered to be the major reasons for poor impact properties of hemp fibre composites. Compared to this, CSM glass fibre composites showed vastly superior impact damage tolerance. They were able to endure an impact of up to 20J for 70% reduction in intrinsic strength and stiffness while hemp fibre composite showed similar reduction in intrinsic strength and stiffness following an impact of only 4J. Replacement of 11% of hemp fibres with glass fibres in hybrid composites increased their impact damage tolerance considerably. Following impact at 4J energy, hybrid composites lost only about 30% of their intrinsic strength and stiffness. However at this concentration of glass fibres in hemp fibres, the improvement in impact damage tolerance was limited to up to 15J impact at which level the hybrid composites lost almost 90% of their intrinsic strength and stiffness.

Hemp fibre composites had lower fatigue strength than CSM glass fibre composites. However their fatigue sensitivity was better than CSM glass fibre composites, shown by their less steep normalised S-N curve than glass fibre composites. This was also shown quantitatively in their lower fatigue sensitivity coefficient of 0.097 than 0.127 for glass fibre composites. Hybrid hemp-glass fibre composites showed improvement in fatigue

strength but no improvement in fatigue sensitivity was observed compared to hemp fibre composites.

Studies into stiffness degradation of composites during fatigue loading showed negligible reduction in stiffness for hemp fibre composites before sudden brittle fracture. This correlated well with little evidence of crack formation on the surface of these composites. Glass fibre composites showed gradual loss in stiffness with increase in fatigue cycles, which was accompanied with crack formation on the surface and whitening of the samples. This was consistent with lower fatigue sensitivity of hemp fibre composites than glass fibre composites.

Normalised S-N curves of hemp fibre composites following low velocity impact were divided into two different domains. S-N curve following impact at 1J had similar slope as non-impacted one, consistent with the fact that impact of 1J had negligible effect on their tensile properties. S-N curves following impact at 2J and 3J had similar slope, consistent with the fact that most of the damage had been done following impact at 2J. Normalised S-N curves of CSM glass fibre composites following impact at 5J and 10J had similar slopes. The fatigue strength and fatigue sensitivity of hemp fibre composites in tension-compression fatigue was poorer than in tension-tension.

8.1.3 Composites with Pre-treated Hemp Fibres

100°C and 150°C heat treated hemp fibre composites showed some improvement in tensile properties but no appreciable improvement was observed for 200°C heat treated hemp fibre composites. No improvement in impact damage tolerance was observed for all three heat treated fibre composites. 100°C heat treated fibre composites also showed no appreciable improvement in fatigue properties.

Alkalisation of hemp fibres with NaOH at concentrations of 1%, 5% and 10% showed no evidence of defibrillation. The surface energy of 1% alkalised fibres was similar to non-alkalised fibres but lower for 5% and 10% alkalised fibres. The tensile properties and interfacial shear strength of all alkalised fibres were found to lie within the range of non-alkalised fibres. The tensile properties of 1% and 5% alkalised fibre composites showed measurable improvement. For 1% alkalised fibre composites, about 40% improvement in tensile strength and about 30% in tensile modulus were observed. For 5% alkalised fibre composites, the improvement in strength and modulus was about

30% compared to untreated fibre composites. No overall improvement in tensile properties was observed for 10% alkalised fibres composites. Impact damage tolerance of all three alkalised fibre composites showed no improvement. Similarly fatigue strength and fatigue sensitivity of 1% and 5% alkalised fibre composites were improved but not for 10% alkalised fibre composites.

Acetylation of hemp fibres did not show measurable improvement in tensile properties or impact damage tolerance of composites made form these fibres. Plasma treatment of hemp fibres improved tensile properties of composites made from these fibres.

8.1.4 Environmental Properties of Hemp Fibre Composites

Hemp fibre composites showed a saturation water uptake of about 16% following immersion in water for 3700 hours. Most of the diffusion was found to be due to the presence of hemp fibres. The values of the diffusion coefficient, sorption coefficient and permeability coefficient were found to be 8.7×10^{-13} m^2/s, 0.16 and 1.32×10^{-13} m^2/s respectively. Alkalisation of hemp fibres resulted in about 2% less water being absorbed by composites following immersion in water for 400 hours.

Tensile properties of hemp fibre composites showed immediate decline following immersion in distilled water, the loss in modulus being more pronounced than the loss in strength. However the loss in properties stabilised following prolonged immersion. Following immersion in water for 3700 hours, the composites lost almost 35% of intrinsic strength and 60% of intrinsic modulus. Plasticisation of polyester matrix and loss in stiffness of hemp fibres following immersion in water were considered to be the major factors. Despite the reduction in water absorption for alkalised fibre composites, this did not result in any improvement in decline in their tensile properties following immersion in water for 400 hours.

Immersion in distilled water resulted in further degradation of impact damage tolerance of hemp fibre composites. Compared to non-impacted and non-immersed composites, the composites lost almost 62% of their intrinsic strength and almost 77% of their intrinsic stiffness following impact at 3J and immersion in water for 400 hours.

Hemp fibre composites showed no deterioration in fatigue properties following immersion in water. Composites fatigue tested in water without conditioning and those

pre-conditioned in water for 15 days and then fatigue tested showed similar fatigue strength and fatigue sensitivity as non-immersed composites.

Similar to the decline in tensile properties, hemp fibre composites showed immediate decline in flexural properties, the decline in modulus being more pronounced than decline in strength, following immersion in water which later stabilised for prolonged immersion times. The composites lost almost 30% of their intrinsic strength and 70% of their intrinsic modulus following immersion in water for 2000 hours.

Hemp fibre composites immersed in water with sealed edges showed similar water absorption behaviour and similar reduction in tensile properties to those with non-sealed edges.

Hemp fibre composites immersed in 5% sodium chloride salt solution showed similar water absorption behaviour and similar reduction in tensile properties to those immersed in distilled water.

Exposing hemp fibre composites to accelerated weathering conditions of UV light and UV light plus condensation resulted in immediate loss in weight which stabilised for prolonged exposure times. For composite exposed to these conditions for 1000 hours, the loss in weight was about 3.2% for composites exposed to UV light and about 1.9% for composites exposed to UV light plus condensation. Chemical dissociation of polyester resin due to exposure to UV light was considered to be the major reason for this loss in weight.

Exposure to UV light and UV light plus condensation led to initial decline in tensile properties of hemp fibre composites, but the decline in properties did not increase after prolonged exposure and these materials seemed to have performed fairly well in these conditions. Also the reduction in intrinsic strength and modulus was quite similar, unlike immersion in water where the reduction in modulus was more pronounced than the reduction in strength. Discolouring of composites following exposure to these conditions was also identified as an issue with these composites.

8.2 FINAL CONCLUSIONS

1. The properties of hemp fibres were found to be good enough to be used as reinforcement in composite materials. However the issues of relatively high equilibrium moisture content of fibres, variability in fibre properties and relatively poor fibre/matrix interfacial strength were identified as factors that can reduce the efficiency with which these composites can be utilised.

2. The absolute and specific tensile properties of CSM glass fibre composites were found to be much superior to hemp fibre composites even at lower fibre volume fractions. The application of tensile stress produced no visible signs of cracking on the surface of hemp fibre composites before fracture which suggested that most of the damage processes took place within the composites. In contrast, CSM glass fibre composites showed evidence of considerable cracking and whitening before eventual fracture.

3. The impact damage tolerance of hemp fibre composites was very low compared to CSM glass fibre composites. They lost almost half of their intrinsic strength and stiffness following impact at 2J energy. Considerable evidence of matrix fracture, interfacial debonding and fibre fracture was found in the fracture surface. Following an impact at 4J energy, hemp fibre composites lost almost 70% of their intrinsic strength and stiffness. CSM glass fibre composites were able to endure an impact of 20J energy for 70% reduction in their intrinsic strength and stiffness. However hybridisation of hemp with glass fibres even at low concentration increased their impact damage tolerance considerably and hence can be considered as a viable method for increasing the impact damage tolerance of hemp fibre composites.

4. Despite having poor absolute fatigue strength, hemp fibre composites exhibited better fatigue sensitivity than CSM glass fibre composites in tension-tension fatigue. This correlated well with lower stiffness degradation in hemp fibre composites than glass fibre composites at the same normalised stress level. Images taken during fatigue loading showed the better ability of hemp fibre composites at resisting crack formation and growth than glass fibre composites.

5. Alkalisation of hemp fibres at low concentrations of 1% and 5% resulted in improvement in tensile and fatigue properties of composites made from these fibres but

no such improvement was observed for 10% alkalised fibre composites. For 1% alkalised fibre composites, about 40% improvement in tensile strength and about 30% in tensile modulus were observed. For 5% alkalised fibre composites, the improvement in strength and modulus was about 30% compared to untreated fibre composite. This was mainly due to improvement in fibre/matrix bonding, also confirmed by SEM images. The fatigue strength and fatigue sensitivity of these composites were also improved considerably compared to untreated fibre composites. No improvement in impact damage tolerance was observed for all three alkalised fibre composites.

6. Environmental properties of hemp fibre composites following immersion in water were studied. Computer modelling of water absorption in these composites showed the diffusion to be Fickian in nature. The fracture of tensile tested hemp fibre composites following immersion in water was found to be more ductile which showed the evidence of shear stresses being more significant in these conditions. For impact damaged composites immersed in water, most of the degradation in tensile properties occurred within first 100 hours of immersion in water at same impact energy level and further immersion in water for up to 400 hours did not result in any further degradation. No deterioration in fatigue strength and fatigue sensitivity of hemp fibre composites following immersion in water reinforced good fatigue properties of these composites. Hemp fibre composites immersed in distilled water with sealed edges and those immersed in 5% sodium chloride salt solution did not show in any measurable difference in their water absorption behaviour and decline in tensile properties compared to those immersed in distilled water with non-sealed edges.

8.3 FUTURE WORK

Some of the issues regarding hemp fibre composites need more investigation. More research is required into ways of reducing the high void content in these composites. The improvement of fibre/matrix interfacial strength is also an issue that needs addressing. Using these fibres in woven form can also result in improvement in their properties and will make interesting comparison with woven synthetic fibre composites.

Hemp fibres, as a sustainable resource, are more environment friendly than glass fibres but the use of a fossil fuel derived thermoset resin makes composites less biodegradable. A lot of research is going on at the moment at developing biodegradable

resins based on plant oils. Their high cost is the main impediment in their widespread use. It is hoped that increase in awareness will eventually result in increase in their use that will bring down their cost. Although some exploratory work was done on hemp fibre composites with a biodegradable resin in this research, the results were not very promising. Nevertheless the study of mechanical properties of hemp fibre composites using a biodegradable resin will be an interesting project that will shed more light on the behaviour and lead to greater understanding of properties of natural fibre composites.

9. REFERENCES

1. Stern, N. *Stern Review: The Economics of Climate Change*. 2006; Available from: www.hm-treasury.gov.uk/stern_review_excetive_summary.html.
2. King, J. *The King Review of Low-Carbon Cars; Part1: The Potential for CO_2 Reduction*. October 2007; Available from: hm-treasury.gov.uk/king.
3. Mohanty, A.K., Misra, M., Drzal, L.T., Selke, S.E., Harte, B.R. and Hinrichsen, G., *Natural fibres, biopolymers and biocomposites: An introduction*, in *Natural Fibres, Biopolymers and Biocomposites*, A.K. Mohanty, Misra, M., and Drzal, L.T., Editor. 2005, Taylor & Francis. p. 1-36.
4. Peijs, T. *Composites turn green!* 2002; Available from: http://www.e-polymers.org.
5. Peijs, T., *Composites for recycling*. Materials Today, April 2003: p. 30-35.
6. Bismarck, A., Balatazar-y-Jimenez, A., and Sarikakis, K., *Green composites as panacea? Socio-economic aspects of green materials*. Environment, Development and Sustainability 2006. **8**: p. 445-463.
7. Mougin, G., *Natural fibre composites - problems and solutions*. JEC Composites, May-June 2006. **25**: p. 32-35.
8. Mohan, R., and Kishore, A., *Jute-glass sandwich composites*. Journal of Reinforced Plastics and Composites, 1985. **4**: p. 186-194.
9. Schloesser, T.P., *Natural fiber reinforced automotive parts*, in *Natural fibers, Plastics and Composites*, F.T. Wallenberger, and Weston, N., Editor. 2004, Kulwer Academic Publishers. p. 275-304.
10. Nishino, T., *Natural fibre sources*, in *Green Composites*, C. Baillie, Editor. 2004, Woodhead Publishing Ltd. p. 49-80.
11. Mathur, V.K., *Composite materials from local resources*. Construction and Building Materials, 2006. **20**(7): p. 470-477.
12. Wallenberger, F.T., and Weston, N., *Science and technology*, in *Natural fibers, plastics and composites*, F.T. Wallenberger, and Weston, N., Editor. 2004, Kulwer Academic Publishers. p. 3-7.
13. Chand, N., and Rohtagi, P.K., Journal of Materials Science Letters, 1986. **5**: p. 1181-1182.
14. Kelly, A., ed. *Concise Encyclopedia of Composite Materials*. 1994, Pergamon.
15. Matthews, F.L., and Rawlings, R.D., *Composite Materials: Engineering and Science*. 1999, Cambridge: Woodhead Publishing Limited.
16. Ashbee, K.H.G., *Fundamental Principles of Fibre Reinforced Composites*. 2nd ed. 1993, Lancaster: Technomic Publishing Co. Inc.
17. Kelly, A., *Very stiff fibres woven into engineering's future: a long-term perspsctive*. Journal of Materials Science, 2008. **43**: p. 6578-6585.
18. Gerdeen, J.C., Lord, H.W., Rorrer, R.A., *Engineering Design with Polymers and Composites*. 2006, Boca Raton: CRC.

19. *HC Bridge Company Completes First Composite Railroad Bridge* 02/12/2008]; Available from: www.netcomposites.com.
20. *Aircraft families/ A380 family.* 2008 02/12/2008]; Available from: www.airbus.com/en/aircraftfamilies/a380.
21. Hull, D., and Clyne, T.W., *An Introduction to Composite Materials.* Vol. 2nd. 1996, New York, USA: Cambridge University Press.
22. Agarwal, B.D., and Broutman, L.J., *Analysis and Performance of Fiber Composites.* Vol. 2nd. 1990: John Wiley & Sons.
23. Arnold, C.A., Hergenrother, P.M., and McGrath, J.E., *An overview of organic polymeric matrix resins for composites*, in *Composite Applications: The Role of Matrix, Fibre, and Interface*, T.L. Vigo, Kinzing, B.J., Editor. 1992, VCH: New York, USA.
24. Weatherhead, R.G., *FRP Technology.* 1980, London: Applied Science Publishers Ltd.
25. Rubin, M., *Polyester resins*, in *Handbook of fibreglass and advanced plastics composites*, G. Lubin, Editor. 1969, Van Nostrand Reinhold Co.
26. Harris, B., Beaumont, P.W., and De Ferren, E.M., Journal of Materials Science, 1971. **6**: p. 238.
27. Favre, J.P., and Merriene, M.C., International Journal of Adhesives, 1981. **1**: p. 311.
28. Ying, L. in *38th Annual Conference SPI* 1983.
29. Piggott, M.R., *Interface properties and their influence on fibre-reinforced polymers*, in *Composite Applications: The Role of Matrix, Fibre and Interface*, T.L. Vigo, Kinzing, B.J., Editor. 1992, VCH Publishers Inc. p. 221-265.
30. Van Krevelen, D.W., *Properties of Polymers.* 3rd ed. 1997: Elsevier.
31. Hoecker, F., and Karger-Kocsis, J., *Surface energetics of carbon fibres and its effects on the mechanical performance of CF/EP composites.* Journal of Applied Polymer Science, 1996. **59**: p. 139-153.
32. Owens, D.K., and Wendt, R.C., *Estimation of the surface free energy of polymers.* Journal of Applied Polymer Science, 1969. **13**: p. 1741-1747.
33. Heng, J.Y.Y., Pearse, D.F., Thielmann, F., Lampke, T., and Bismarck, A., *Methods to determine surface energies of natural fibres: a review.* Composite Interfaces, 2007. **14**(7-9): p. 581-604.
34. Daniel, I.M. and O. Ishi, *Engineering Mechanics of Composite Materials.* 1994: Oxford University Press.
35. Chou, T., *Microstructural design of fibre composites.* Cambridge solid state science series. 1992: Cambridge University Press.
36. Marom, G., and Fischer, S., *Hybrid effects in composites: conditions for positive or negative effects versus rule-of-mixtures behaviour.* Journal of Materials Science, 1978. **13**: p. 1419-1426.
37. Kretsis, G., *A review of the tensile, compressive, flexural and shear properties of hybrid fibre-reinforced plastics.* Composites, 1987. **18**: p. 13-23.
38. Aveston, J., and Kelly, A., *Tensile first cracking strain and strength of hybrid composites and laminates* Phil. Trans. Royal Soc. London, 1980. **A294**: p. 519-34.
39. Chamis, C.C., Hanson, M.P., and Serafini, T.T., *Impact resistance of unidirectional fibre composites.* Composite Materials: Testing and Design, 1972. **ASTM STP 497**: p. 324-49.

40. Beaumont, P.W.R., Riewald, ,P.G., and Zweben, C., *Methods for improving the impact resistance of composite materials.* Foreign Object Damage to Composites, 1974. **ASTM STP 568**: p. 134-58.
41. Dorey, G., Sidey, G.R., Hutchings, J., *Impact properties of carbon fibre/Kevlar 49 hybrid composites.* Composites, 1978. **9**: p. 25-32.
42. Adams, D.F., and Miller, A.K., *An analysis of impact behaviour of hybrid composite materials.* Materials Science and Engineering, 1975. **19**: p. 245-60.
43. Philips, L.N., *The hybrid effect - does it exist?* Composites, 1976. **7**: p. 7-8.
44. Bismarck, A., Mishra, S., and Lampke, T., *Plant fibres as reinforcement for green composites*, in *Natural Fibres, Biopolymers and Biocomposites*, A.K. Mohanty, Misra, M., and Drzal, L.T., Editor. 2005, Taylor & Francis: New York, USA. p. 37-108.
45. Bledzki, A.K., and Gassan, J., *Composites reinforced with cellulose based fibres.* Progress in Polymer Science, 1999. **24**: p. 221-274.
46. John, M.J., and Anandjiwala, R.D., *Recent developments in chemical modification and characterisation of natural fibre-reinforced composites.* Polymer Composites, 2008. **29**: p. 187-207.
47. *Natural Fibres*. 2009; Available from:www.naturalfibres2009.org/en/fibres.
48. Munder, F., Furl, C., and Hempel, H., *Processing of bast fibre plants for industrial applications*, in *Natural Fibres, Biopolymers and Biocomposites*, A.K. Mohanty, Misra, M., and Drzal, L.T., Editor. 2005, Taylor & Francis: New York, USA. p. 109-140.
49. Morvan, C., Andeme-Onzighi, C., Girault, R., Himmelsbach, D.S., Driouich, A., and Akin, D.E., *Building flax fibres: More than one brick in the walls.* Plant Physiology and Biochemistry, 2003. **41**: p. 935-944.
50. Catling, D., and Grayson, J., *Identification of Vegetable Fibres*. 1982, London: Chapman and Hall.
51. Olesen, P.O., and Plackett, D.V., *Perspectives on the performance of natural plant fibres* in *Plant Fibre Products - Essentials for the Future*. 1999: Copenhagen, Denmark.
52. Timell, T.E., *Some properties of native hemp, kapok and jute celluloses.* Textile Research Journal, 1957. **27**: p. 854-859.
53. Thygesen, A., Oddershede, J., Lilholt, H.,Thomsen, A.B., and Stahl, K., *On the determination of crystallinity and cellulose content in plant fibres.* Cellulose, 2005. **12**: p. 563-576.
54. Fink, H.P., Ganster, J., and Fraatz, J., in *Akzo-Nobel viskose chemistry seminar: Challenges in cellulosic man-made fibres*. 1994: Stockholm, Sweden.
55. Nilsson, T., and Gustafsson, P.J., *Influence of dislocations and plasticity on the tensile behaviour of flax and hemp fibres.* Composites: Part A, 2007. **38**: p. 1722-1728.
56. Keller, A., Leupin, M., Mediavilla, V., and Wintermantel, E., *Influence of the growth stage of industrial hemp on chemical and physical properties of the fibres.* Industrial Crops and Products, 2001. **13**: p. 35-48.
57. Prasad, B.M., Sain, M.M., and Roy, D.N., *Structure property correlation of thermally treated hemp fibre.* Macromolecular Materials and Engineering, 2004. **289**: p. 581-592.
58. Mukherjee, P.S., and Satyanarayana, K.G., *Structure and properties of some vegetable fibres.* Journal of Materials Science, 1986. **21**: p. 51-56.

59. Thygesen, A., *Quantification of dislocations in hemp fibres using acid hydrolysis and fibre segment length distributions.* Journal of Materials Science, 2008. **43**: p. 1311-1317.
60. Panaitescu, D.M., Donesco, D., Bercu, C., Vuluga, D.M., Iorga, M., and Ghiurea, M., *Polymer composites with cellulose microfibrils.* Polymer Engineeering and Science, 2007. **47**: p. 1128-1234.
61. Bos, H.L., Van den Oever, M.J.A., and Peters, O.C.J.J., *Tensile and compressive properties of flax fibres for natural fibre reinforced composites.* Journal of Materials Science, 2002. **37**(1683-1692).
62. Gassan, J., and Bledzki, A.K., *Effect of moisture content on the propeties of silanized jute-epoxy composites.* Polymer Composites, 1997. **18**(2): p. 179-184.
63. Kelly, A., *Hemp is at hand*, in *The Guradian, 27/09/2006*. p. 9.
64. Carpenter, J.E.P., *The Preparation and Properties of Composites Reinforced with Natural Fibres*, in *PhD thesis: School of Agricultural and Forest Sciences.* 2004, University of Wales: Bangor.
65. Thygesen, A., Daniel, G, F.T., Lilholt, H., and Thomsen, A.B., *Hemp fibre microstructure and use of fungal defibration to obtain fibres for composite materials.* Journal of Natural Fibres. **2**(4): p. 19-37.
66. Jarman, C., *Small Scale Textile: Plant Fibre Processing*. 1998: Intermediate Technology Publications.
67. Gassan, J., and Bledzki, A.K., Die Angnew Makromol Chem, 1996. **236**: p. 129-138.
68. Bolton, A.J., *The potential of crop fibres as crops for industrial use* Outlook on Agriculture, 1995. **24**(2): p. 85-89.
69. Garcia-Jaldon, C., Dupeyre, D., and Vignon M.R., *Fibres from semi-retted hemp bundles by steam explosion treatment.* Biomass and Bioenergy, 1998. **14**: p. 251-160.
70. Kozlowski, R., and Wladyka-Przybylak, M., *Uses of natural fibre reinforced plastics*, in *Natural fibers, Plastics and Composites*, F.T. Wallenberger, and Weston, N., Editor. 2004, Kluwer Academic Publishers. p. 249-274.
71. Baltazar-y-Jimenez, A., and Bismarck, A., *Wetting behaviour, moisture uptake and electrokinetic properties of lignocellulosic fibres.* Cellulose, 2007. **14**: p. 115-127.
72. Wang, B., Sain, M., and Oksman, K., *Study of structural morphology of hemp fibre from the micro to the nanoscale.* Applied Composite Materials, 2007. **14**: p. 89-103.
73. Kostic, M., Pejic, B., and Skundric, P., *Quality of chemically modified hemp fibres.* Bioresource Technology, 2008. **99**: p. 94-99.
74. Netravali, A.N., and Chabba, S., *Composites get greener.* Materials Today, April 2003: p. 22-29.
75. Ivens, J., Bos, H., and Verpoest, I., *The applicability of natural fibres as reinforcement for polymer composites*, in *Renewable Bioproducts - Industrial Outlets and Research for 21st Century*. 1997: International Agriculture Centre, Wegeningen, The Netherlands.
76. Brouwer, W.D., *Natural fibre composites - From upholstery to structural components*, in *Natural Fibres for Automotive Industry*. 2000: Manchester Conference Centre, Manchester.
77. Bledzki, A.K., Reihmane, S., and Gassan, J., *Properties and modification methods for vegetable fibres for natural fibre composites.* Journal of Applied Polymer Science, 1996. **59**: p. 1329-1336.

78. Berglund, L. *New concepts in natural fibre composites.* in *Proceedings of the 27th Riso International Symposium on Materials Science: Polymer Composite Materials for Wind Power Turbines.* 2006. Riso National Laboratory, Roskilde, Denmark.
79. Mueller, D.H., and Krobjilowski, A., *New discovery in the properties of composites reinforced with natural fibres.* Journal of Industrial Textiles, 2003. **33**(2): p. 111-130.
80. Bauccio, M., ed. *Engineering Materials Reference Book.* 2nd ed. 1994, ASM.
81. Bogoeva-Gaceva, G., Avella, M., Malinconico, M., Buzaovska, A., Grozdanov, A., Gentile, G., and Errico, M.E., *Natural fibre eco-composites.* Polymer Composites, 2007: p. 98-107.
82. Pickering, K.L., Beckermann, G.W., Alam, S.N., and Foreman, N.J., *Optimising industrial hemp fibre for composites.* Composites: Part A, 2007. **38**: p. 461-468.
83. George, J., Sreekala, M.S., and Thomas, S., *A review on interface modification and characterisation of natural fibre reinforced plastic composites.* Polymer Engineeering and Science, 2001. **41**(9): p. 1471-1485.
84. Pott, G.T., *Natural fibres with low moisture sensitivity* in *Natural Fibers, Plastics and Composites*, F.T. Wallenberger, and Weston, N., Editor. 2004, Springer. p. 105-122.
85. Van de Weyenberg, I., Chi Truong, T., B. Vangrimde, B., and Verpoest. I., *Improving the properties of UD flax fibre reinforced composites by applying an alkaline fibre treatment.* Composites: Part A, 2006. **37**: p. 1368-1376.
86. Wang, H.M., Postle, R., Kessler, R.W., and Kessler, W., *Removing pectin and lignin during chemical processing of hemp for textile applications.* Textile Research Journal, 2003. **8**: p. 664-669.
87. Gordon, J.E., *The New Science of Strong Materials.* 1976, London: Penguin Books.
88. McMullen, P., *Fibre/resin composites for aircraft primary structures: a short history, 1936-1984.* Composites, 1984. **15**(3): p. 222-230.
89. Hughes, M., *Applications*, in *Green Composites*, C. Baillie, Editor. 2004, Woodhead Publishing Ltd. p. 232-251.
90. Suddell, B.C., and Evans, W.J., *Natural fibre composites in automotive applications*, in *Natural Fibrs, Biopolymers and Biocomposites*, A.K. Mohanty, Misra, M., and Drzal, L.T., Editor. 2005, Taylor and Francis: New York, USA. p. 231-260.
91. Brown, W.J., *Fabric Reinforced Plastics.* 1947, London: Cleaver-Hume Press Ltd.
92. Karus, M., Ortmann, S., Gahle, C., and Pendarovski, C., *Use of natural fibres in composites for the German automotive production from 1999 till 2005.* 2006, Nova Institute GmbH: Hurth.
93. Karus, M., and Vogt, D., *European hemp industry: cultivation, processing and product lines.* Euphytica, 2004. **140**: p. 7-12.
94. *Hemp industry on global course of expansion.* 2007 23/12/2008; Available from: www.jeccomposites.com.
95. Nickel, J., and Reidel, U., *Activities in biocomposites.* Materials Today, April 2003.
96. Riedel, U., Nickel, J., and Herrmann, A.S., *High performance applications of plant fibres in areospace and related industries*, German Aerospace Centre (DLR), Germany.

97. Karus, M., and Gahle, C., *Injection moulding with natural fibres* in *Reinforced Plastics*. April 2008. p. 18-25.
98. *European Markets for Naturally Reinforced Plastic Composites*. 2008; Available from: http://www.researchandmarkets.com/reports/612781/.
99. Chand, N., and Rohtagi, P.K., Polymer Composites, 1987. **28**(5): p. 146-147.
100. Rowell, R.M., Sanadi, A.R., Caulfield, D.F., and Jacobson, R.E. *Utilisation of natural fibres in plastic composites: problems and opportunities*. 1997; Available from: www.fpl.fs.fed.us/documnets/pdf1997/rowel97d.ppf.
101. Mutje, P., Lopez,J.P., Lopez, A., Vallejos, M.E., and Vilaseca, F., *Full exploitation of cannabis sativa as reinforcment/filler of thermoplastic composite materials*. Composites: Part A, 2007. **38**: p. 369-377.
102. Wambua, P., Ivens, J., and Verpoest, I., *Natural fibres can they replace glass in fibre reinforced plastics?* Composites Science and Technology, 2003. **53**: p. 1259-1264.
103. Sain, M., Suhara, P., Law, S., and Bouillox, A. , *Interface modification and mechanical properties of natural fibre-polyolefin composite products*. Journal of Reinforced Plastics and Composites, 2005. **24**(2): p. 121-130.
104. Paul, S.A., Reussmann, T., Menning, G., Lampke, T., Pothen, L.A., Mathew, G.D.G., Joseph, K., and Thomas, S., *The role of interface modification on the mechanical properties of injection-moulded composites from commingled polypropylene/banana granules*. Composite Interfaces, 2007. **14**(7-9): p. 849-867.
105. Thwe, M.M., and Liao, K., *Durability of bamboo-glass fibre reinforced polymer matrix hybrid composites*. Composites Science and Technology, 2003. **63**: p. 375-387.
106. Thwe, M.M., and Liao, K., *Environmental effects on bamboo-glass/polypropylene hybrid composites*. Journal of Materials Science, 2003. **38**: p. 363-376.
107. Mechraoui, A., Riedl, B., and Rodrigue, D., *The effect of fibre and coupling agent content on the mechanical properties of hemp/polypropylene composites*. Composite Interfaces, 2007. **14**(7-9): p. 837-848.
108. Hargitai, H., Racz, I., and Anandjiwala, R.D., *Development of hemp fibre reinforced polypropylene composites*. Journal of Thermoplastic Composite Materials, 2008. **21**: p. 165-174.
109. Mutje, P., Girones, J., Lopez, A., Llop, M.F., and Vilaseca, F., *Hemp strands: PP composites by injection moulding: effect of low cost physio-chemical treatments*. Journal of Reinforced Plastics and Composites, 2006. **25**(3): p. 313-327.
110. Hargitai, H., Racz, I., and Anandjiwala, R.D., *Development of hemp fibre-PP nonwoven composites*. Macromolecular Symposium, 2006. **239**: p. 201-208.
111. Pervaiz, M., and Sain, M.M., *Carbon storage potential in natural fibre composites*. Resources Conservation and Recycling, 2003. **39**: p. 325-340.
112. Saleem, Z., Rennebaum, H., Pudel, F., and Grimm, E., *Treating bast fibres with pectinase improves mechanical characteristics of reinforced thermoplastic composites*. Composites Science and Technology, 2008. **68**: p. 471-476.
113. Siriwardena, S., Ismail, H., and Ishiaku, U.S., *A comparison of mechanical properties and water absorption behaviour of white rice husk ash and silica filled polypropylene composites*. Journal of Reinforced Plastics and Composites, 2003. **22**(18): p. 1645-1666.

114. Couto, E., Tan, I.H., Demarquette, N., Caraschi, J.C., and Leao, A., *Oxygen plasma treatment of sisal fibres and polypropylene: Effects on mechanical properties of composites.* Polymer Engineeering and Science, 2002. **42**(4): p. 790-797.
115. Sims, G.D., and Broughton. W. R., *Glass fibre reinforced plastics - properties,* in *Comprehensive Composite Materials* A. Kelly, and Zweben, C., Editor. 2000, Elsevier: London. p. 165.
116. Nabi Saheb, D., and Jog, J.P., *Natural fibre polymer composites: a review.* Advances in Polymer Technology, 1999. **18**(4): p. 351-363.
117. Ray, D., and Rout, J., *Thermoset Biocomposites,* in *Natural Fibres, Biopolymers and Biocomposites,* A.K. Mohanty, Misra, M., and Drzal, L.T., Editor. 2005, Taylor & Francis. p. 291-345.
118. Sanadi, A.R., Parsad, S.V., Rohtagi, P.K., *Sunhemp fibre reinforced polyester, Part 1: Analysis of tensile and impact results.* Journal of Materials Science, 1986. **21**: p. 4299-4304.
119. Hepworth, D.G., Bruce, D.M., Vincent, J.F.V., and Jeronimidis, G., *The manufacture and mechanical testing of thermosetting natural fibre composites.* Journal of Materials Science, 2000. **35**: p. 293-298.
120. Hautala, M., Pasila, A., and Pirila, J., *Use of hemp and flax in composite manufacture: a search for new production methods.* Composites: Part A, 2004. **35**: p. 11-16.
121. Aziz, S.H., and Ansell, M.P., *Optimising the properties of green composites,* in *Green Composites,* C. Baillie, Editor. 2004, Woodhead Publishing Ltd. p. 154-180.
122. Richardson, M., and Zhang, Z., *Nonwoven hemp reinforced composites.* Reinforced Plastics, 2001. **45**: p. 40-44.
123. Rouison, D., Couturier, and M., Sain., *Resin transfer moulding of hemp fibre composites: optimisation of the process and mechanical properties of the materials.* Composites Science and Technology, 2006. **66**: p. 895-906.
124. Sebe, G., Cetin, N.S., Hill, C.A.S., and Hughes, M., *RTM Hemp fibre reinforced polyester composites.* Applied Composite Materials, 2000. **7**: p. 341-349.
125. Yamamoto, T., Medina, L., and Schledjewski, R, *Tensile properties of natural fibre reinforced thermoset composites.* Advanced Composites Letters, 2005. **14**: p. 29-34.
126. Khoathane, M.C., Vorster, O.C., and Sadiku, E.R., *Hemp fibre reinforced 1-pentene/polypropylene copolymer: the effect of fibre loading on mechanical and thermal characteristics of the composites.* Journal of Reinforced Plastics and Composites, 2008. **27**(14): p. 1533-1544.
127. Roe, P.J., and Ansell, M.P., *Jute reinforced polyester composites.* Journal of Materials Science, 1985. **20**: p. 4015-4020.
128. Dash, B.N., Mishra, H.K., Rana, A.K., Mishra, M., Nayak, S.K. and Tripathy S.S., *Novel, low cost jute-polyester composites, Part1: processing, mechanical properties and SEM analysis.* Polymer Composites, 1999. **20**: p. 62.
129. Gowda, T.M., Naidu, A.C.B., and Chhaya, R., *Some mechanical properties of untreated jute fabric reinforced polyester composites.* Composites: Part A, 1999. **30**: p. 277-284.
130. Hughes, M., Hill, C.S.A., and Hague, J.R.B., *The fracture toughness of bast fibre reinforced polyester composites.* Journal of Materials Science, 2002. **37**: p. 4669-4676.

131. Santulli, C., *Post-impact damage characterisation of natural fibre reinforced composites using acoustic emission.* NDT&E International, 2001. **34**: p. 531-536.
132. Kiran, C.U., Reddy, G.R., Dabade, B.M., and Rajesham, S., *Tensile properties of sunhemp, banana and sisal fibre reinforced polyester composites.* Journal of Reinforced Plastics and Composites, 2007. **26**(10): p. 1043-1050.
133. Rout, J., Mishra, M., Tripathy, S.S., Nayak, S.K., and Mohanty, A.K., *The influence of fibre surface modification on the mechanical properties of coir-polyester composites.* Polymer Composites, 2001. **22**: p. 468.
134. Hill, C.S.A., and Abdul-Khalil, H.P.S., *Effect of fibre treatments on mechanical properties of coir or oil palm fibre reinforced polyester composites.* Journal of Applied Polymer Science, 2000. **78**: p. 1685-1697.
135. Marais, S., Gouanve, F., Bonnesoeur, A., Grenet, J., Poncin-Epaillard, F., Morvan, C., and Metayer, M., *Unsaturated polyester composites reinforced with flax fibres: effect of cold plasma and autoclave treatments on mechanical and permeation properties.* Composites: Part A, 2005. **36**: p. 975-986.
136. Singh, B., Gupta, M., and Verma, A., *Influence of fibre surface treatment on the properties of sisal-polyester composites.* Polymer Composites, 1996. **17**: p. 910.
137. Mishra, S., Naik, J.B., Misra, M., Tripathy, S.S., and Mohanty, A.K., *The influence of chemical surface modification on the performance of sisal-polyester biocomposites.* Polymer Composites, 2002. **23**: p. 164-170.
138. Sreekumar, P.A., Joseph, K., Unnikrishnan, G., and Thomas, S., *A comparative study on mechanical properties of sisal-leaf fibre reinforced polyester composites prepared by resin transfer and moulding techniques.* Composites Science and Technology, 2007. **67**: p. 453-461.
139. Joshy, M.K., Mathew, L., and Joseph, R., *Studies on interfacial adhesion in unidirectional isora fibre reinforced polyester composites.* Composite Interfaces, 2007. **14**(7-9): p. 631-646.
140. Mishra, S., Nayak, S.K., Misra, M., Tripathy, S.S., and Mohanty, A.K., *Potentiality of pineaple leaf fibre as reinforcement PALF-polyester composites: surface modification and mechanical properties* Journal of Reinforced Plastics and Composites, 2001. **2001**(20).
141. Devi, L.U., Bhagwan, S.S., and Thomas, S., *Mechanical properties of pineapple leaf fibre reinforced polyester composites.* Journal of Applied Polymer Science, 1998. **64**: p. 1739-1748.
142. White, N.M., and Ansell, M.P., Journal of Materials Science, 1983. **18**: p. 1549.
143. Rao, K.M.M., Prasad, A.V.R., Babu, M.N.V., Rao, K.M., and Gupta, A.V.S.S.K.S., *Tensile properties of elephant grass fibre reinforced polyester composites.* Journal of Materials Science, 2007. **42**: p. 3266-3272.
144. Mariatti, M., Jannah, M., Abu-Bakar, A., and Abdul-Khalil, H.P.S., *Properties of banana and pandanus woven fabric reinforced unsaturated polyester composites.* Journal of Composite Materials, 2008. **42**(9): p. 931-941.
145. Mehta, G., Mohanty, A.K., Drzal, L.T, and Misra, M., *Effect of fibre surface treatment on the properties of biocomposites from nonwoven industrial hemp fibre and unsaturated polyester resin.* Journal of Applied Polymer Science, 2006. **99**: p. 1055-1068.
146. Rouison, D., Couturier, and M., Sain., *The effect of surface modification on the mechanical properties of hemp fibre/polyester composites*, in *SAE 2004 World Congress and Exhibition* 2004: Detroit, MI, USA. p. 63-77.

147. Mwaikambo, L.Y., and Ansell, M.P., *Hemp fibre reinforced cashew nut shell liquid composites.* Composites Science and Technology, 2003. **63**: p. 1297-1305.
148. Akesson, D., Skrifvars, M., Seppala, J.V., and Walkenstrom, P. *Preparation of natural fibre composites from biobased thermoset resins.* in *Polymer Composite Materials for Wind Power Turbines.* 2006. Riso National Laboratory, Roskilde, Denmark.
149. Wollerdorfer, M., and Bader, H., *Influence of natural fibres on the mechanical properties of biodegradable polymers.* Industrial Crops and Products, 1998. **8**: p. 105-112.
150. Ochi, S., *Development of high strength biodegradable composites using Manila hemp fibre and starch-based biodegradable resin.* Composites: Part A, 2006. **37**: p. 1879-1883.
151. Williams, G.I., and Wool, R.P., *Composites from natural fibres and soy oil resins.* Applied Composite Materials, 2000. **7**: p. 421-432.
152. Mohanty, A.K., Wibowo, A., Misra, M., and Drzal, L.T., *Effect of process enginering on the performance of natural fibre reinforced celulose acetate biocomposites.* Composites: Part A, 2004. **35**: p. 363-370.
153. O'Donnell, A., Dweib, M.A., and Wool, R.P., *Natural fibre composites with plant oil-based resin.* Composites Science and Technology, 2004. **64**: p. 1135-1145.
154. Hu, R., and Lim, J., *Fabrication and mechanical properties of completely biodegradable hemp fibre reinforced polylactic acid composites.* Journal of Composite Materials, 2007. **41**(13): p. 1655-1669.
155. Mwaikambo, L.Y., Tucker, N., and Clark, A.J., *Mechanical properties of hemp fibre reinforced euphorbia composites.* Macromolecular Materials and Engineering, 2007. **292**: p. 993-1000.
156. Viviana, P., Iannace, S., Kenny, J.M., and Vazquez, A., *Relationship between processing and properties of biodegradable composites based on PCL/starch matrix and sisal fibres.* Polymer Composites, 2001. **22**(1): p. 104-110.
157. Alvarez, V., VA ´ ZQUEZ, A. and Bernal, C., *Effect of microstructure on the tensile and fracture properties of sisal fibre/starch-based composites.* Journal of Composite Materials, 2006. **40**(1): p. 21-35.
158. Dash, B.N., Sarkar, M., Rana, A.K., Mishra, M., Mohanty, A.K. and Tripathy S.S. , *A study on bidegradable composite prepared from jute felt and polyesteramide (BAK)* Journal of Reinforced Plastics and Composites, 2002. **21**(16): p. 1493-1503.
159. Santulli, C., *Impact properties of glass/plant fibre hybrid laminates.* Journal of Materials Science, 2007. **42**: p. 3699-3707.
160. Mohan, R., Shridhar, M.K., and Rao, R.M., Journal of Materials Science Letters, 1983. **2**: p. 99-102.
161. Clark, R.A., and Ansell, M.P., Journal of Materials Science, 1986. **21**: p. 269-276.
162. Aquino, E.M.F., Sarmento, L.P.S., and Oliveira, W. , *Moisture effect on degradation of jute/glass hybrid composites.* Journal of Reinforced Plastics and Composites, 2007. **26**: p. 219-233.
163. Reis, P.N.B., Ferreira, J.A.M., Antunes, F.V., and Costa, J.D.M., *Flexural behaviour of hybrid laminated composites.* Composites: Part A, 2007. **38**: p. 1612-1620.

164. Panthapulakkal, S., and Sain, M., *Studies on water absorption properties of short-hemp glass fibre hybrid polypropylene composites.* Journal of Composite Materials, 2007. **41**(15): p. 1871-1883.
165. Pavithran, C., Mukherjee, P.S., Brahamkumar, M., *Coir-glass intermingled fibre hybrid composites.* Journal of Reinforced Plastics and Composites, 1991. **10**: p. 91-101.
166. Pothan, L.A., Neelakantan, N.R., Rao, B., and Thomas, S., *Stress relaxation behaviour of banana fibre reinforced polyester composites.* Journal of Reinforced Plastics and Composites, 2004. **23**(2): p. 153-165.
167. Abdul-Khalil, H.P.S., Hanida, S., and Kang, C.W., *Agro-hybrid composite: the effects on mechanical and physical properties of oil palm fibre/glass hybrid reinforced polyester composites.* Journal of Reinforced Plastics and Composites, 2007. **26**: p. 203-218.
168. Hariharan, A.B.A., and Abdul-Khalil, H.P.S., *Lignocellulose based hybrid bilayer laminate composite: part1: studies on tensile and impact behaviour of oil palm fibre/glass fibre reinforced epoxy resin.* Journal of Composite Materials, 2004. **39**(8): p. 663-684.
169. John, K., and Naidu, S.V., *Sisal fibre/glass fibre hybrid composites: the impact and compressive properties.* Journal of Reinforced Plastics and Composites, 2004. **23**: p. 1253-1258.
170. Benevolenski, O.I., Karger-Kocsis, J., Mieck, K.P., and Reubmann, T., *Instrumented perforation impact response of polypropylene composites with hybrid reinforcement flax/glass and flax/cellulose fibres.* Journal of Thermoplastic Composite Materials, 2000. **13**: p. 481-496.
171. Idicula, M., Malhotra, S.K., Joseph, K., and Thomas, S., Composites Science and Technology, 2005. **65**: p. 1077.
172. de Medeioros, E.S., Agnelli, J.A.M., and Joseph, K., Polymer Composites, 2005. **26**: p. 1.
173. Jacob, M., Thomas, S., and Varughese, K.T., Applied Polymer Science, 2004. **93**: p. 2305.
174. Mwaikambo, L.Y., and Bisanda, E.T.N., Polymer Testing, 1999. **18**: p. 181.
175. Junior, C.Z.P., de Carvalho, L.H., and Fonseca., V.M., , Polymer Testing, 2004. **23**: p. 131.
176. Tserki, V., Zafeiropoulos, N.E., Simon, F., and Panayiotou, C., *A study of the effect of acetylation and propionylation surface treatments on natural fibres.* Composites: Part A 2005. **36**: p. 1110-1118.
177. Ouajai, S., Shanks, R.A., and Hodzic, A., *Morphological and grafting modifications of natural cellulose fibres.* Journal of Applied Polymer Science, 2004. **94**: p. 2456-2465.
178. Mwaikambo, L.Y., and Ansell, M.P., *Mechanical properties of alkali treated plant fibres and their potential as reinfrocement materials. 1. hemp fibres.* Journal of Materials Science, 2006. **41**: p. 2483-2496.
179. Ouajai, S., and Shanks, R.A., *Composition, structure and thermal degradation of hemp cellulose after chemical treatments.* Polymer Degradation and Stability, 2005. **89**: p. 327-335.
180. Gulati, D., and Sain, M., *Surface characteristics of untreated and modified hemp fibres.* Polymer Engineeering and Science, 2006: p. 269-273.
181. Sgriccia, N., Hawley, M.C., and Misra, M., *Characterisation of natural fibre surfaces and natural fibre composites.* Composites: Part A, 2008. **39**: p. 1632-1637.

182. Pietak, A., Korte, S., Tan, E., Downard, A., and Staiger, M.P., *Atomic force microscopy characterisation of the surface wettability of natural fibres.* Applied Surface Science, 2007. **253**: p. 3627-3635.
183. Sinha, E., and Rout, S.K. , *Influence of fibre-surface treatment on structural, thermal and mechanical properties of jute.* Journal of Materials Science, 2008. **43**: p. 2590-2601.
184. Taha, I., Steuernagel, L., and Ziegmann, G., *Optimisation of the alkali treatment process of date palm fibres for polymeric composites.* Composite Interfaces, 2007. **14**(7-9): p. 669-684.
185. Beckermann, G.W., and Pickering, K.L., *Engineering and evaluation of hemp fibre reinforced polypropylene composites: fibre treatment and matrix modification.* Composite : Part A, 2008. **39**: p. 979-988.
186. Bledzki, A.K., Fink, H.P., and Specht, K., *Unidirectional hemp and flax EP- and PP-composites: Influence of defined fibre treatments* Journal of Applied Polymer Science, 2004. **93**: p. 2150-2156.
187. Towo, A.N., and Ansell, M.P., *Fatigue evaluation and dynamic mechanical thermal analysis of sisal fibre-thermosetting resin composites.* Composites Science and Technology, 2008. **68**: p. 925-932.
188. Thygesen, A., Madsen, F.T., Lilholt, H., Felby, C., and Thomsen, A.B., *Changes in chemical composition, degree of crystallisation and polymersiation of cellulose in hemp fibres caused by pretreatment*, in *Proceedings of 23rd Riso International Symposium on Materials Science: Sustainable natural and polymeric composites- science and technology*, H. Lilholt, Madsen, B., and Mikkelsen, L.P., Editor. 2002: Riso National Laboratory, Roslikde, Denmark. p. 315-323.
189. Yuan, X., Jayaraman, K., and Bhattacharyya, D., *Effect of plamsa treatment in enhancing the performance of woodfibre-polypropylene composites.* Composites: Part A, 2004. **35**: p. 1363-1374.
190. George, J., Bhagwan, S.S., and Thomas, S., Composite Interfaces, 1998. **5**: p. 201.
191. Murkhejee, P.K., Ganguly, D., and Sur, J., Journal of Textile Institute, 1993. **84**: p. 348.
192. John, M.J., Francis, B., Varughese, K.T., Thomas, S., *Effect of Chemical Modification on Properties of Hybrid Fibre Composites.* Composites: Part A, 2008. **39**: p. 352-363.
193. Marsh, G., *Composites that grow in fields.* Reinforced Plastics, November 2008: p. 16-22.
194. Hogg, P.J., and Bibo, G.A., *Impact and damage tolerance*, in *Mechanical testing of advanced fibre composites*, M.J. Hodgkinson, Editor. 2000, CRC. p. 211-247.
195. Heida, J.H., Konijnenberg, P., Hart, and W.G.J. *Chracterisation of Impact Damage in Carbon-Epoxy Composites.* in *Impact and Dynamic Fracture of Polymers and Composites* 1993. Sardinia, Italy: ESIS.
196. Sjoblom, P.O., Hartness, J.T., and Cordell, T.M., *On low velocity impact testing of composite materials.* Journal of Composite Materials, 1988. **22**: p. 30-52.
197. Cantwell, W.J., and Morton, J., *The impact resistance of composite materials - a review.* Composites, 1991. **22**(5): p. 347-362.
198. Abrate, S., *Impact on laminated composite materials.* Applied Mechanics Review, 1991. **44**(4): p. 155-190.
199. Liu, D., and Malvern, L.E., *Matrix cracking in glass/epoxy plates.* Journal of Composite Materials, 1987. **21**: p. 594-609.

200. Robinson, P., and Davies, G.A.O., *Impactor mass and specimen geometry effects in low velocity impact of laminated composites.* International Journal of Impact Engineering, 1992. **12**: p. 189-207.
201. E. Demtus, R.S.S., and G.E. Maddux. *Barely visible damage threshold in graphite epoxy.* in *Proceedings of 8th International Conference on Composite Materials.* July 1981: SAMPE.
202. Richardson, M.O.W., and Wisheart, M.J., *Review of low-velocity impact properties of composite materials.* Composites: Part A, 1996. **27A**: p. 1123-1131.
203. Liu, D., *Impact induced delamination - a view of bending stiffness mismatching.* Journal of Composite Materials, 1988. **22**: p. 674-692.
204. Dorey, G., ed. *Damage tolerance and damage assessment.* Advanced Composites, ed. I.K. Partridge. 1989, Elsevier.
205. Cantwell, W.J., and Morton, J., *Geometrical effects in the low velocity impact response of CFRP.* Composite Structures, 1989. **12**: p. 39-59.
206. El-Habak, A.M., *Effect of impact perforation load on GFRP composites.* Composites, 1993. **24**: p. 341-345.
207. Agarwal, B.D., and Narang, J.N., *Strength and failure mechanisms of anisotropic composites.* Fibre Science and Technology, 1977. **10**(1): p. 37-52.
208. Mallick, P.K., and Broutman, L.J., *Impact properties of laminated angle ply composites*, in *SPI: 30th Annual Technical Conference.* 1975: Washington, USA.
209. Teh, K., and Morton, J. *Impact damage development and residual compression performance of advanced composite material systems.* in *34th AIAA Structure, Structural Dynamic and Materials Conference.* 1993. La Jolla, USA.
210. Yeung, P., and Broutman, L.J., *The effect of glass-resin interface strength on the impact strength of fibre reinforced plastics.* Polymer Engineeering and Science, 1978. **18**(2): p. 62-72.
211. Rydin, R.W., Bushman, M.B., and Karbhari, V.M. , *The influence of velocity in low-velocity impact testing of composites using drop-weight impact tower.* Journal of Reinforced Plastics and Composites, 1995. **14**: p. 113-127.
212. Matemilola, S.A., and Stronge, W.J. *Impact micro-damge in resin transfer moulded carbon fibre composite plates* in *Impact and Dynamic Fracture of Polymers and Composites.* 1993. Sardinia, Italy: ESIS.
213. Datta, S., Krishna, A.V., and Rao, R.M.V.J.K., *Low velocity impact damage tolerance studies on glass-epoxy laminates-effects of material, process and test parameters.* Journal of Reinforced Plastics and Composites, 2004. **23**(3): p. 327-345.
214. Sutherland, L.S., and Soares, C.G., *Effects of laminate thickness and reinforcement type on the impact behaviour of E-glass/polyester laminates.* Composites Science and Technology, 1999. **59**: p. 2243-2260.
215. Hancox, N.L., *An overview of the impact behaviour of fibre reinforced composites*, in *Impact Behaviour of Fibre Reinforced Composite Materials and Structures*, S.R. Reid, and Zhou, G., Editor. 2000, Woodhead Publishing Limited: Cambridge, UK. p. 1-32.
216. Awerbuch, J., and Hahn, H., *Hard object impact damage of metal matrix composites.* Journal of Composite Materials, 1976. **10**: p. 231.
217. Cairns, D.S., and Lagace, P.A., *Residual tensile strength of graphite/epoxy and Kevlar/epoxy laminates with impact damage*, in *Composite Materials:Testing and Design*, S.P. Garbo, Editor. 1990, ASTM: Philadelphia. p. 48-63.

218. Mall, S., *Laminated polymer matrix composites*, in *Composites Engineering Handbook*, P.K. Mallick, Editor. 1997, Marcel Dekker, Inc.
219. Caprino, G., *Residual strength prediction of impacted CFRP laminates.* Journal of Composite Materials, 1984. **18**: p. 508-518.
220. Found, M.S., Howard, I.C. *The modelling of damage in FRP composites.* in *Interfacial Phenomenon in Composite Materials.* 1989. Sheffield: Butterworths.
221. Sanulli, C., *Impact properties of glass/plant fibre hybrid laminates.* Journal of Materials Science, 2007. **42**: p. 3699-3707.
222. Parsad, S.V., *Natural fibre based composites*, in *Concise Encyclopedia of Composite Materials*, A. Kelly, Editor. 1994, Pergamon. p. 206-208.
223. Wambua, P., Ivens, J., and Verpoest, I., *The response of natural fibre composites to ballistic impact by fragment simulating projectiles* Composite Structures, 2007. **77**: p. 232-240.
224. Santulli, C., Janssen, M., and Jeronimidis, G., *Partial replacement of E-glass fibres with flax fibres in composites and effect on falling weight impact performance.* Journal of Materials Science, 2005. **40**: p. 3581-3585.
225. Ahmed, K.S., Vijayarangan, S., and Kumar, A., *Low velocity impact damage characterisation of woven jute glass fabric reinforced polyester hybrid composites.* Journal of Reinforced Plastics and Composites, 2007. **26**: p. 959-976.
226. Joffe. R., A., J., and Wallstrom, L., *Strength and adhesion characterisitics of elementary flax fibres with different surface treatments.* Composites Part A: Applied Science and Manufacturing 2003. **34**(7): p. 603-612.
227. Varma, I.K., Krishnan, S.R.A., and Krishnamoorthy, S., *Composites of glass/modified jute fabric and unsaturated polyester resin* Composites, 1989. **20**: p. 383-388.
228. Kalaparsad, G., Mathew, G., Pavithran, C. and Thomas, S., *Melt rheological behaviour of intimately mixed short sisal-glass hybrid fibre-reinforced low-density polypropylene composites.* Journal of Applied Polymer Science, 2003. **89**: p. 432-442.
229. Morye, S.S., and Wool, R.P., *Mechanical properties of glass/flax hybrid composites based on a novel modified soyabean oil matrix material.* Polymer Composites, 2005. **26**: p. 407-416.
230. Li, H.J., and Sain, M.M., *High stiffness natural fibre reinforced hybrid polypropylene composites.* Polymers and Plastics Technology and Engineering, 2003. **42**: p. 853-862.
231. Al-Kafi, A., Abedin, M.Z., Beg, M.D.H., Pickering, K.L., and Khan, M.A., *Study on mechanical properties of jute-glass fibre reinforced unsaturated polyester hybrid composites: effect of surface modification by ultraviolet radation.* Journal of Reinforced Plastics and Composites, 2006. **25**(6): p. 575-588.
232. Curtis, P.T., *Fatigue*, in *Mechanical testing of advanced fibre composites*, M.J. Hodgkinson, Editor. 2000, CRC. p. 249-267.
233. Salkind, M.J., *VTOL Aircraft*, in *Applications of Composite Materials* 1973, American Society for Testing and Materials p. 76-107.
234. Pinckney, R.L., *Helicopter Rotor Blades*, in *Applications of Composite Materials.* 1973, Amercican Society of Testing and Materials. p. 108-133.
235. Bathis, C., *Notch effect on fatigue of high performance composite materials: mechanisms and predictions*, in *Fracture of Composites*, E. Aramanios, Editor. 1996, Transtec Publuications. p. 389-404.

236. Hertzberg, R.W., and Manson, J.A., *Fatigue of Engineering Plastics*. 1980, London: Academic Press.
237. Reifsnider, K.L., Schulte, K., Duke, J.C. *Long Term Fatigue Behaviour of Composite Materials*. in *Long Term Behaviour of Composites*. 1983. Philadelphia, USA: ASTM.
238. Reifsnider, K.L., *Damage and damage mechanics*, in *Fatigue of Composite Materials*, K.L. Reifsnider, Editor. 1991, Elsevier: Amsterdam.
239. Talreja, R., *Damage models for fatigue of composite materials*, in *Fatigue of Composite Materials*. 1987, Technomic Publishing Co. Inc.: Lancaster.
240. Broutman, L.J., and Sahu, S., *Progressive damage of a glass reinforced plastic during fatigue*, in *SPI: 24th Annual Technical Conference*. 1969: Washington. USA.
241. Davis, J.W., McCarthy, J.A., and Schurb, J.N., *The fatigue resistance of reinforced plastics.* Materials Design and Engineering, 1964: p. 87-91.
242. Dyer, K.P., *Fatigue of Composite Materials*, in *PhD Thesis, Department of Materials Engineering*. 1996, University of Wales: Swansea.
243. Mandell, J.F., in *Developments in Reinforced Plastics-2, Applied Science*, G. Pritchard, Editor. 1982: New York. p. 67.
244. Tanimoto, T., and Amijima, S., *Progressive nature of fatigue damage of glass fibre reinforced plastics.* Journal of Composite Materials, 1975. **9**(4): p. 38-390.
245. Boller, K.H., *Fatigue characteristics of RP lamintes subjected to axial loading.* Modern Plastics, 1964. **41**: p. 145.
246. Hofer, K.E., Bennett, L.C., and Stander, M., *Effect of various fibre surface treatments on the fatigue behaviour of glass fabric composites in high humidity environments*, in *SPI: 31st Annual Technical Conference*. 1976: Washington, USA.
247. Dally, J.W., and Broutman, L.J., *Frequency effects on the fatigue of glass reinforced plastics.* Journal of Composite Materials, 1967. **1**: p. 424-442.
248. Mandell, J.F., and Meier, U. *Effects of stress ratio, frequency, and loading time on the tensile fatigue of glass-reinforced epoxy*. in *Long Term Behaviour of Composites*. 1982. Williamsburg, USA: ASTM.
249. Romans, J.B., Sands, A.G., Cowling, J.E., Industrial Engineering and Chemical Production Research and Development, 1972. **11**: p. 261.
250. Gauchel, J.V., Steg, I., and Cowling, J.E., ASTM STP 569, 1975: p. 45.
251. Beaumont, P.W.R., and Harris, B. in *International Conference on Carbon Fibres and their Composites Applications* 1971. Plastics Institute, London.
252. Talreja, R., *Stiffness based fatigue damage characterisation of fibrous composites*, in *Fatigue of Composite Materials*. 1987, Technomic Publishing Co. Inc.: Lancaster.
253. Nevadunsky, J.J., Lucas, J.J, and Salkind, M.J. , *Early fatigue damage detection in composite materials.* Journal of Composite Materials, 1975. **9**: p. 394-408.
254. Hahn, H.T., and Tsai, S.W., *On the behaviour of composite laminates after initial failures.* Journal of Composite Materials, 1974. **8**: p. 288-305.
255. Hahn, H.T., Kim, R.Y., *Fatigue behaviour of composite laminates.* Journal of Composite Materials, 1976. **10**: p. 156-180.
256. O'Brien, T.K., and Reifsnider, K.L., *Fatigue damage evaluation through stiffness measurments in boron-epoxy laminates.* Journal of Composite Materials, 1981. **15**: p. 55-70.

257. Stinchcomb, W.W., Bakis, C.E., *Fatigue Behaviour of Composite Laminates*, in *Fatigue of Composite Materials*, K.L. Reifsnider, Editor. 1990, Elsevier: Amsterdam.
258. Jamison, R.D., and Reifsnider, K.L., *Advanced fatigue damage development in graphite epoxy laminates*, in *AFWAL-TR-82-3103*. 1982, Air Force Wright Aeronautical Laboratories.
259. Sendeckyj, G.P., *Life Prediction of Resin-Matrix Composite Materials*, in *Fatigue of Composite Materials*, K.L. Reifsnider, Editor. 1991, Elsevier: Amsterdam.
260. Kim, H.C., Ebert, L.J., *Axial fatigue failure sequences and mechanisms in unidirectional fibreglass composites.* Journal of Composite Materials, 1978. **10**: p. 139.
261. Khan, Z., Al-Sulaiman, F.A., Farooqi, J.K., and Younas, M., *Fatigue life prediction in woven carbon fabric/polyester composites based on modulus degradation.* Journal of Reinforced Plastics and Composites, 2001. **20**(5): p. 377-398.
262. Yuanjian, T., *Low velocity impact, fatigue and stress relaxation behaviour of composite materials*, in *PhD thesis: Materials Research Centre*. 2004, University of Wales: Swansea.
263. Setiadi, Y., Jar, P.Y.B., Kuboki, T., and Cheng, J.J.R., *Comparison of damage development in random fibre-reinforced polymers under cyclic loading.* Journal of Composite Materials, 2006. **40**: p. 71-91.
264. Beaumont, P.W.R., *The failure of fibre composites: an overview*, in *The Failure of Reinforced Plastics* F.L. Matthews, Editor. 1990. p. 1-18.
265. Mandell, J.F., Huang, D.D., and McGarry, F.J., Composites Technology Review, 1981. **3**: p. 96.
266. Albrecht, C.O. *Statistical Evaluation of a Limited Number of Fatigue Test Specimens*. in *Fatigue Test of Aircraft Structures*. 1962: ASTM STP 338.
267. Sims, D.F., Brogdon, V.H., *Fatigue Behaviour of Composites under Different Loading Modes*, in *Fatigue of Elementary Composite Materials* K.L. Reifsnider, Lauraitis, K.N., Editor. 1977, ASTM STP 636. p. 185-205.
268. Reifsnider, K.L., and Jen, M.H.R., *Composite Flywheel Durability and Life. Part 2: Long Term Materials Data*, in *UCRL-1523 Part 2*. 1982, Lawrence Livermore National Laboratory Rep.
269. Gassan, J., *A study of fibre and interface parameters affecting the fatigue behaviour of natural fibre composites.* Composites: Part A, 2002. **33**: p. 369-374.
270. Pritchard, G., *Environmental testing of organic matrix composites*, in *Mechanical Testing of Advanced Fibre Composites*, M.J. Hodgkinson, Editor. 2000, CRC. p. 269-292.
271. Trojan, F., *Engineering materials and their applications*. 4th ed. 1990: Houghton Mifflin Company.
272. Kockott, D., *Weathering*, in *Handook of Polymer Testing*, R. Brown, Editor. 1999, Marcel Dekker, Inc.
273. Gauthier, M.M., ed. *Engineered Materials Handbook*. 1995, ASTM International.
274. Shokrieh, M.M., and Bayat, A., *Effects of ultraviolet radiation on mechanical properties of glass/polyester composites.* Journal of Composite Materials, 2007. **41**(20): p. 2443-2455.

275. Marom, G., *Environmental effects on fracture mechanical properties of polymer composites*, in *Application of fracture mechanics to composite materials*, K. Friedrich, Editor. 1989, Elsevier.
276. Harper, C.A., ed. *Handbook of plastics, elastomers, and composites*. 3rd ed. 1996, McGraw-Hill.
277. Appicella, A., Migiliaresi, C., Nicolais, L., Iaccarino, L., and Roccotelli, S., *The water ageing of unsaturated polyester based composites: influence of resin chemical structure.* Composite, 1983. **14**: p. 387-392.
278. Browning, C.E., Husman, G.E., Whitney, J.M. in *Composite materials testing and design, 4th conference*. 1977. Philadelphia: ASTM.
279. Pipes, R.B., Vinson, J.R., Chou, T., *On the hygrothermal response of laminated composite systems.* Journal of Composite Materials, 1976. **10**: p. 129-148.
280. Kawagoe, M., Doi, Y., Fuwa, N., Yasuda, T., and Takata, K., *Effects of absorbed water on the interfacial fracture between two layers of unsaturated polyester and glass.* Journal of Materials Science, 2001. **31**: p. 5161-67.
281. Pratt, B.A., Bradley, W.L. *Effect of moisture on interfacial shear strength: a study using the single fibre fragmentation test.* in *High Temperature and Environmental Effects on Polymeric Composites*. 1995. Norfolk, USA: ASTM.
282. Shen, C., and Springrer, G.S., *Moisture absorption and desorption of composite materials.* Journal of Composite Materials, 1976. **10**: p. 2-20.
283. Choqueuse, D., Davies, P., Mazeas, F., Baizeau, R. *Ageing of composites in water: comparison of five materials in terms of absorption kinetics and evolution of mechanical properties.* in *High Temperature and Environmantal Effects on Polymeric Composites*. 1995. Norfolk, USA: ASTM.
284. Dewimille, B., Bunsell, A.R., *Accelerated ageing of a glass fibre-reinforced epoxy resin in water.* Composites, 1983. **14**: p. 35-40.
285. Han, K.S., and Koutsky, J., *Effect of water on the interlaminar fracture behaviour of glass fibre reinforced polyester composite.* Composites, 1983. **14**: p. 67-70.
286. Philips, M.G., *Prediction of long term stress-rupture life for glass fibre reinforced polyester composites in air and in aqueous environments.* Composites, 1983. **14**: p. 270-275.
287. Jones, C.J., Dickson, R.F., Adam, T., and Harris, B., *Environmental fatigue of reinforced plastics.* Composites, 1983. **14**: p. 288-293.
288. Loos, A.C., and Springer, G.S., *Moisture absorption of polyester E-glass composites.* Journal of Composite Materials, 1980. **14**: p. 142-154.
289. Ellyin, F., and Rohrbacher, C., *The influence of aqueous environment, temperature and cyclic loading on glass fibre/epoxy composite laminates* Journal of Reinforced Plastics and Composites, 2003. **22**(7): p. 615-636.
290. Sindhu, K., Joseph, K., Joseph, J.M., and Mathew, T.V., *Degradation studies of coir fibre/polyester and glass fibre/polyester composites under different conditions.* Journal of Reinforced Plastics and Composites, 2007. **26**(15): p. 1571-1585.
291. Pritchard, G., Speake, S.D., *The use of water absorption kinetic data to predict laminate property changes.* Composites, 1987. **18**: p. 227-232.
292. Mohanty, A.K., Misra, M., and Hinrichsen, G., *Biofibres, biodegradable polymers and biocomposites: an overview.* Macromolecular Materials and Engineering, 2000. **276/277**: p. 1-24.

293. Ho, T.N., and Ngo, A.D., *Sorption of water in hemp and coir fibres*, in *8th International Conference on Woodfibre-Plastic Composites*. May 23-25, 2005: Madison, Wisconsin, USA.
294. Semsarzadeh, M.A., Polymer Composites, 1984. **7**(2): p. 23-25.
295. Rouison, D., Couturier, M., Sain, M., MacMillan, B., and Balcom, B.J., *Water absorption of hemp fibre/unsaturated polyester composites.* Polymer Composites, 2005. **26**: p. 509-525.
296. Devi, L.U., Joseph, K., Nair, K.C.M., and Thomas, S., *Ageing studies of pineapple leaf fibre reinforced polyester composites.* Journal of Applied Polymer Science, 2004. **94**: p. 503-510.
297. Pothan, L.A., and Thomas, S., *Effect of hybridisation and chemical modification on water absorption behaviour of banana fibre reinforced polyester composites* Journal of Applied Polymer Science, 2004. **91**: p. 3856-3865.
298. Marcovich, N.E., Rebordeo, M.M., and Aranguren, M.I., *Moisture diffusion in polyester-woodflour composites.* Polymer, 1999. **40**: p. 7313-7320.
299. Junior, C.Z.P., de Carvalho, L.H., Fonseca., V.M., Monteiro, S.N., and d'Almeida, J.R.M., *Accelerated ageing of hybrid ramie-cotton resin matrix composites in boiling water* Polymers and Plastics Technology and Engineering, 2004. **43**: p. 1365-1375.
300. Rong, M.Z., Zhang, M.Q., Liu, Y., Zhang, Z.W., Yang, G.C, and Zeng, H.M., *Mechanical properties of sisal reinforced composites in response to water absorption.* Polymer Composites, 2002. **10**: p. 407-426.
301. Joseph, P.V., Rabello, M.S., Mattoso, L.H.C., Joseph, K., and Thomas, S., *Environmental effects on the degradation behaviour of sisal fibre reinforced polypropylene composites* Composites Science and Technology, 2002. **62**: p. 1357-1372.
302. Ishak, Z.A.M., Yow, B.N., Ng, B.L., Abdul-Khalil, H.P.S., and Rozman, H.D., *Hygrothermal ageing and tensile behaviour of injection moulded rice husk-filled polypropylene composites.* Journal of Applied Polymer Science, 2001. **81**: p. 742-753.
303. George, J., Bhagwan, S.S., and Thomas, S., *Effects of environment on the properties of low-density polyethylene composites reinforced with pineapple leaf fibre.* Composites Science and Technology, 1998. **58**: p. 1471-1485.
304. Espert, A., Vilaplana, F., and Karlsson, S., *Comparison of water absorption in natural cellulosic fibres from wood and one-year crops in polypropylene composites and its influence on their mechanical properties.* Composites: Part A, 2004. **35**: p. 1267-1276.
305. Wang, B., Sain, M., and Cooper,P.A., *Study of moisture absorption in natural fibre plastic composites.* Composites Science and Technology, 2006. **66**: p. 379-386.
306. Aghedo, S., and Baillie, C., *The effect of pretreatment on the environmental durability of hemp fibre reinforced recycled linear low density polyethylene composites*, Queen's University, Canada: Ontario, Canada.
307. Mehta, G., Mohanty, A.K., Drzal, L.T, Kamdem, D.P., and Misra, M., *Effect of accelerated weathering on biocomposites processed by SMC and compression moulding.* Journal of Polymers and Environment, 2006. **14**: p. 359-368.
308. Mishra, S., Naik, J.B., and Patil, Y.P., *Studies on swelling properties of wood/polymer composites based on agro-waste and novolac.* Advances in Polymer Technology, 2004. **23**(1): p. 46-50.

309. Singh, B., Gupta, M., and Verma, A., *The durability of jute fibre-reinforced phenolic composites.* Composites Science and Technology, 2000. **60**: p. 581-589.
310. Summerscales, J., ed. *Microstructural Characterisation of Fibre-Reinforced Composites*. 1998, Woodhead Publishing Limited: Cambridge.
311. Engle, L., Klingele, H., Ehrenstien, G.T., and Schaper, H., *An Atlas of Polymer Damage: Surface Examination by Scanning Electron Microscope*. 1981, London: Wolfe Publishing Ltd. .
312. Czigany, T., Morlin, B., and Mezey, Z., *Interfacial adhesion in fully and partially biodegradable polymer composites examined with microdroplet test and acoustic emmission.* Composite Interfaces, 2007. **14**(7-9): p. 869-878.
313. Godwin, E.W., *Tension*, in *Mechanical testing of advanced fibre composites.* 2000, CRC. p. 43-73.
314. Prasad, B.M., Sain, M.M., and Roy, D.N., *Properties of ball milled thermally treated hemp fibres in an inert atmosphere for potential composite reinforcement.* Journal of Materials Science, 2005. **40**: p. 4271-4278.
315. Sain, M., Panthapulakkal, S. , *Green fibre thermoplastic composites*, in *Green Composites*, C. Baillie, Editor. 2004, Woodhead Publishing Ltd. p. 181-206.
316. Yang, P., and Kokot, S., *Thermal analysis of different cellulosic fabrics.* Journal of Applied Polymer Science 1996. **60**: p. 1137-1146.
317. Weilage, B., Lampke, Th., Marx, G., Nestler, K., Starke, D., *Thermogravimetric and Differential Scanning Calorimetric Analysis of Natural Fibres and Polypropylene.* Thermochimica Acta, 1999. **337**: p. 169-177.
318. Sridhar, M.K., Basavarajjappa, G., Kasturi, S.S., and Balsubramanian, N., Indian Journal of Textile Research, 1982. **7**.
319. Gonzalez, C., and Myers, G.E., International Journal of Polymer Materials, 1993. **23**: p. 67.
320. Mohanty, A.K., Patnaik, S., and Singh, B.C., Journal of Applied Polymer Science, 1989. **37**: p. 1171.
321. Sabaa, M.W., Polymer Degradation and Stability, 1991. **32**: p. 209.
322. Troedec, M., Sedan, D., Peyratout, C., Bonnet, J.P., Smith, A., Guinebretiere, R., Gloaguen, V., Krausz, P., *Influence of various chemical treatments on the composition and structure of hemp fibres.* Composite : Part A, 2008. **39**: p. 514-522.
323. Aziz, S.H., and Ansell, M.P., *The effect of alklisation and fibre alignment on the mechanical and thermal properties of kenaf and hemp bast fibre composites: Part1-polyester resin matrix.* Composites Science and Technology, 2004. **64**: p. 1219-1230.
324. Mwaikambo, L.Y., and Ansell, M.P., *Chemical modification of hemp, sisal, jute, and kapok fibres by alkalisation.* Journal of Applied Polymer Science, 2001. **84**: p. 2222-2234.
325. Prasad, B.M., and Sain, M.M., *Mechanical properties of thermally treated hemp fibres in inert atmospheres for potential composite reinforcement.* Materials Research and Innovation, 2003. **7**: p. 231-238.
326. Madsen, B., *Properties and Processing*, in *Bio-composites: The Next Generation of Composites*. September 2008: Shawbury, UK.
327. Silva, F.A., Chawla, N., and Filho, R.D.T., *Tensile behaviour of high performance natural (sisal) fibres.* Composites Science and Technology, 2008. **68**: p. 3438-3443.

328. Park, J., Quang, S.T., Hwang, B., and De Vries, K.L., *Interfacial evaluation of modified jute and hemp fibres/polypropylene-maleic anhydride polypropylene copolymers composites using micromechanical technique and nondestructive acoustic emission.* Composites Science and Technology, 2006. **66**: p. 2686-2699.
329. Pickering, K.L., Li, Y., and Farrell, R.L., *Fungal and alkali interfacial modification of hemp fibre reinforced composites.* Key Engineering Materials, 2007. **334-335**: p. 493-496.
330. Li, Y., and Pickering, K.L., *Hemp fibre reinforced composites using chelator and enzyme treatments.* Composites Science and Technology, 2008.
331. Baltazar-y-Jimenez, A., Bistritz, M, Schulz, E., and Bismarck, A., *Atmospheric air pressure plasma treatment of lignocellulosic fibres: impact on mechanical properties and adhesion to cellulose acetate butyrate.* Composites Science and Technology, 2008. **68**: p. 215-227.
332. Van de Velde, K., and Kiekens, P., *Wettability of natural fibres used as reinforcement for composites.* Die Angnew Makromol Chem, 1999. **272**: p. 87-93.
333. Zafeiropoulos, *On the use of single fibre composites testing to characterise the interface in natural fibre composites.* Composite Interfaces, 2007. **14**(7-9): p. 807-820.
334. Johnson, W., and Ghosh, S.K., *Review: Some Physical Defects Arising in Composite Material Fabrication.* Journal of Materials Science, 1981. **16**: p. 285-301.
335. Madsen, B., Thygesen, A., and Lilholt, H., *Plant fibre composites - porosity and volumetric interaction.* Composites Science and Technology, 2007. **67**: p. 1584-1600.
336. Mwaikambo, L.Y., and Ansell, M.P., *The determination of porosity and cellulose content of plant fibres by density methods.* Journal of Materials Science Letters, 2001. **20**: p. 2095-2096.
337. Bader, M.G., and Lekakou, C., *Processing for laminated structures*, in *Composites Engineering Handbook*, P.K. Mallick, Editor. 1997, Marcel Decker, Inc.
338. Dhakal, H.N., Zhang, Z.Y., and Richardson, M.O.W., *Effect of water absorption on the mechanical properties of hemp fibre reinforced unsaturated polyester composites.* Composites Science and Technology, 2007. **67**: p. 1674-1683.
339. Madsen, B., and Lilholt, H., *Physical and mechanical properties of unidirectional plant fibre composites - an evlauation of the influence of porosity.* Composites Science and Technology, 2003. **63**: p. 1265-1272.
340. Mallick, P.K., *Random fibre composites*, in *Composites Engineering Handbook*, P.K. Mallick, Editor. 1997, Marcel Dekker, Inc.
341. Johnson, A.F., *Engineering Design Properties of GRP*. 1978: British Plastics Federation Publication No. 215/1.
342. Owen, M.J., Tobias, A.M., and Rees, H.D., *Design limits for polyester SMCs.* Plastics and Rubber Processsing and Applications, 1984. **4**(4): p. 349-354.
343. Turner, S., *General Principles and Perspectives*, in *Mechanical Testing of Advanced Fibre Composites*, M.J. Hodgkinson, Editor. 2000, CRC Publishers. p. 5-35.
344. Broutman, L.J., and Krock, R.H., *Modern Composite Materials*. 1967, Reading, MA, USA: Addison Wesley.
345. Hirsch, Journal of American Construction Institute, 1962. **1**: p. 59,427.

346. Nielson, L.E., *Mechanical Properties of Polymers*. Vol. 2. 1974: Marcel Dekker.
347. Peponi, L., Biagiotti, J., Torre, L., Kenny, J.M., and Mondragon, I., *Statistical analysis of the mechanical properties of natural fibres and their composite materials. 2. Composite materials.* Polymer Composites, 2008: p. 321-325.
348. Callister, W.D., *Materials Science and Engineering*. 6th ed. 2003, New York: Wiley.
349. Crawford, R.J., *Plastics engineering*. 2nd ed. 1987: Pergamon Press.
350. Gaggar, S.K., and Broutman, L.J., *Effect of matrix ductility and interface treatment on mechanical properties of glass fibre mat composites.* Polymer Engineeering and Science, 1976. **16**: p. 537-543.
351. Facca, A.G., Kortschot, M.T, and Yan, N., *Predicting the tensile strength of natural fibre reinforced thermoplastics.* Composites Science and Technology, 2007. **67**: p. 2454-2466.
352. Mandell, J.F., *Fatigue Behaviour of Short Fibre Composite Materials*, in *Fatigue of Composite Materials*, K.L. Reifsnider, Editor. 1990, Elsevier: Amsterdam. p. 232-337.
353. John, K.a.N., S.V., *Tensile properties of unsaturated polyester based sisal fibre-glass fibre hybrid composites.* Journal of Reinforced Plastics and Composites, 2004. **23**(17): p. 1815-1819.
354. Towo, A.N., and Ansell, M.P., *Fatigue of sisal fibre reinforced composites: constant-life diagrams and hysteresis loop capture.* Composites Science and Technology, 2007.
355. Owen, M.J., and Dukes, R., *Fatigue of glass reinforced plastic under single and repeated loads.* Journal of Strain Analysis, 1967. **2**: p. 272-279.
356. Yuanjian, T., and Isaac, D.H., *Combined impact and fatigue of glass fibre reinforced composites.* Composites: Part B, 2008. **39**: p. 505-512.
357. Curtis, P.T., *The fatigue behaviour of fibrous composite materials.* Journal of Strain Analysis, 1989. **24**(4): p. 47-56.
358. Rong, M.Z., Zhang, M.Q., Liu, Y., Yang, G.C., and Zeng, H.M., *The effect of fiber treatment on the mechanical properties of unidirectional sisal-reinforced epoxy composites.* Composites Science and Technology, 2001. **61**: p. 1437-1447.
359. Peters, R., and Still, R., *Some aspects of degradation of polymers used in textile applications*, in *Applied Fibre Science 2*, F. Happey, Editor. 1979, Academic Press: London. p. 321-420.
360. Gassan, J., and Bledzki, A.K., *Possibilities for improving the mechanical properties of jute/epoxy composites by alkali treatment of fibres.* Composites Science and Technology, 1999. **59**: p. 1303-1309.
361. Rahman, M.M., and Khan, M.A. , *Surface treatment of coir fibres and its influence on the fibres' physio-mechanical properties* Composites Science and Technology, 2007. **67**: p. 2369-2376.
362. Oever van den, M.J.A., Bos, H.L., and Molenveld, K., *Flax fibre physical structure and its effect on composite properties: impact strength and thermo-mechanical properties.* Die Angnew Makromol Chem, 1999. **272**: p. 71-76.
363. Towo, A.N., *Fatigue of natural fibre composites*, in *PhD thesis*. 2006, Bath University: Bath.
364. Khammatova, V.V., *Effect of high frequency capacitive discharge plasma on the structure and properties of flax and lavsan materials.* Fibre Chemistry, 2005. **37**(4): p. 293-296.

365. Hancox, N.L., *The influence of voids on the hydrothermal response of carbon fibre reinforced plastics.* Journal of Materials Science, 1981. **16**: p. 627-632.
366. Arnold, J.C., *Environmental effects on crack growth in composites*, in *Comprehensive Structural Integrity*, I. Milne, Editor. 2007, Elsevier: New York. p. 428-470.
367. Jacobs, P.M., and Jones, F.R., *Diffusion of moisture in two-phase polymers; Part2: styrenated polyester resins.* Journal of Materials Science, 1989. **24**: p. 2343-2348.
368. Fujita, H., in *Diffusion in Polymers*, J. Crank, and Park, G.S., Editor. 1968, Academic Press: New York. p. 75.
369. Parkin, C.S., *Modelling moisture ingress in composite materials*, in *M.Res. Thesis, Materials Research Centre, School of Engineering*. 2004, Swansea University: Swansea.
370. Rao, R.M.V.K., Chanda, M., and Balasubramanian, N. , *A fickian diffusion model for permeable fibre polymer composites.* Jounrnal of Reinforced Plastics and Composites, 1982. **2**.
371. Giridhar, J., Kishore and Rao, R.M.V.J.K., *Moisture absorption characteristics of natural fibre composites.* Journal of Reinforced Plastics and Composites, 1986. **5**: p. 141-150.
372. Hearle, J.W.S., *The fine structure of fibres and crystalline polymers:interpretation of the mechanical properties of fibres.* Journal of Applied Polymer Science, 1963. **7**: p. 1207-23.
373. Hofer, K.E., Skaper, G.N., Rao, N., and Bennett, L.C. *Effect of moisture on fatigue and residual strength losses for various composites.* in *41st Annual Conference of Reinforced Plastics/Composites*. 1986. New York.
374. Demonet, C.M. *Interaction of moisture with resin matrix composites.* in *21st International SAMPE Technical Conference*. 1989. Atlantic City, NJ.
375. Lekatou, A., Qian, Y., Faidi, S.E., Lyon, S.B., Islam, N., and Newman, R.C., *Interfacial water transport and embrittlement in polymer matrix composites.* Polymer Interfaces, 1993. **34**: p. 27-32.
376. Jackson, S.P., and Weitsman, Y. , *Moisture effects and moisture induced defects in composites*, in *5th International Conference on Composite Materials*. 1985. p. 1435-1452.
377. Ellis, B., and Found, M.S., *The effect of water absorption on a polyester/chopped strand mat laminate.* Composites, 1983. **14**: p. 237-243.
378. Harris, B., *Fatigue-glass fibre reinforced plastics*, in *Handbook of Polymer Fibre Composites*, F.R. Jones, Editor. 1994, Longman. p. 309-316.
379. Pejic, B.M., Kostic, M.M., Skundric, P.D., and Praskalo, J.Z., *The effects of hemicelluloses and lignin removal on water uptake behaviour of hemp fibres* Bioresource Technology, 2008. **99**: p. 7152-7159.
380. *The effect of UV light and weather on plastics and elastomers.* 1994: Plastics Design Laboratory, USA.